

September 10, 2021

Mr. Gregory Beronja
SC&A, Inc.
2200 Wilson Blvd., Suite 300
Arlington, VA 22201

Subject: Technical Review of Major Liner Modification at Wayne Disposal Inc., Belleville, Michigan
TRC Project No. 430226.0000.0000

Dear Greg:

This letter presents the results of TRC's technical review of the proposed landfill liner design modifications for Wayne Disposal Inc. (WDI) Master Cell VI, Subcells F1-F4 and G4-G7. A Google Earth site location map is included in **Attachment 1**.

This review investigated the technical equivalency of the proposed GCL-based liner system and the technical adequacy of the proposed modifications compared to the permitted design. Conclusions of this review are based on information presented in WDI's 370-Page Modification Package, meetings with WDI and their contractors, and additional information provided by WDI. Appendices from the Modification Package that were of importance for this review are included in **Attachments 2-8**. Conformance with the Michigan Department of Environment, Great Lakes, and Energy (EGLE) regulations was considered.

This review began by determining how the proposed liner system differs from the permitted design. Based on our understanding, the four notable adjustments of the proposed system include:

- Use of a lower permeability soil drainage layer in the leachate collection system
- Replacement of the primary compacted clay layer with an Attenuation Layer
- Incorporation of two GCL layers both above and below the Attenuation Layer
- Removal of the secondary compacted clay layer

These proposed changes were the focus of this review and were further evaluated to determine the proposed design's suitability.

A summary of TRC's findings is presented below.

- **Permeability of Drainage Sand** – CTI's proposed leachate collection system includes a soil drainage layer with a permeability of 10^{-3} centimeters per second (cm/s) followed by a double-sided geocomposite. The Part 115 Rules R299.4423(2)(ii) states that 10^{-3} cm/s is an acceptable value for a soil drainage layer if used in conjunction with a geosynthetic drainage material with a permeability of 1 cm/s or greater.
- **Chemical Compatibility of Leachate and GCL** – A chemical compatibility analysis was performed by CETCO in 2018 using GCLs (Bentomat GCL and Resistex 200 GCL) contained in the proposed liner system and leachate from the WDI site. This analysis concluded that the Bentomat GCL would be incompatible with the site's leachate, however, the Resistex 200 GCL does meet the permeability performance requirements.

TRC requested additional information as to why Bentomat GCL was used in the proposed liner system. Further explanation from CTI is included in response number 13 on page 5 of **Attachment 6**. TRC agrees that installing Bentomat GCL in the secondary liner system results in a technically adequate design. The presence of the primary liner geosynthetics and 5-foot attenuation layer above the secondary liner system limit the amount of leachate that is able to impact the Bentomat GCL.

- **Technical Equivalency of Design** – The permeability of the Resistex 200 GCL measured by CETCO using leachate from the existing landfill was 1.6×10^{-9} cm/s. Comparing this to a five-foot clay compacted liner with an approximate permeability of 10^{-7} cm/s, the Resistex 200 GCL is superior, exhibiting a lower permeability.
- **Slope Stability** – CTI performed analyses to consider global stability failures through underlying soils, through the proposed waste, and along the proposed liner. The stability models examined cross sections of the proposed landfill design where the most critical conditions were determined based on-site geometry, including liner slopes and waste grades. TRC reviewed the final design drawings and agreed that these cross sections are representative of critical conditions. The models determined factors of safety against slope stability failure greater than the minimum allowable requirements, 1.5 for final conditions and 1.3 for interim conditions. Additionally, the soil and waste strength parameters assumed by CTI are considered suitable based on the information provided, referenced literatures, and TRC's experience on similar projects.

CTI varied the strengths of the interface between geosynthetics and soils, setting a minimum factor of safety to the regulatory requirements, to calculate a minimum allowable interface strength, with zero adhesion, for interfaces which include geosynthetic to geosynthetic, soil to geosynthetic, and internal strength of the GCL. The minimum allowable interface friction angle was determined to be 10.7 degrees. This value was compared to tests that have been performed for materials at the site. TRC recommends direct shear testing be performed, per ASTM D5321 and ASTM D6243, to confirm the soil to geosynthetic interface strength, geosynthetic to geosynthetic interface strength, and GCL internal strength for the materials proposed for construction. In Attachment B of the Modification Package, WDI commits to performing direct shear tests as part of the Construction Quality Assurance (CQA) scope of work.

WDI confirmed that direct shear testing will be performed on soil and geosynthetics proposed for liner construction in response number 14 on page 6 of **Attachment 6**. When testing is complete, results should be compared to the slope stability analyses to confirm the required strengths in the model are achieved.

Pore water pressure conditions were not considered in the initial analyses. Piezometric surfaces were not included at estimated groundwater levels or above the liner system simulating leachate on the liner. TRC recommended considering the maximum head on liner (calculated to be 11.94 inches in Attachment B-5.1), and the estimated groundwater conditions in the stability models. Additionally, global stability was not considered using the effective stress strength conditions of the underlying clays (drained conditions). Only undrained conditions were modelled. TRC recommended that slope stability be demonstrated under drained conditions.

Mr. Gregory Beronja
SC&A, Inc.
September 10, 2021
Page 3

CTI performed slope stability analyses considering a piezometric surface modeling 12 inches of leachate above the liner per TRC's request, in CTI's Attachments B1.10 and B1.11. The resulting factors of safety meet or exceed the required factor of safety (1.5) for final slope conditions.

TRC recommended that CTI analyze the foundation global stability conditions using parameters for drained soil conditions and the estimated groundwater conditions. In CTI's Attachments B1.8 and B1.9, titled Foundation Stability Under Drained Conditions, existing groundwater was modelled as a piezometric surface, but the soil parameters for the native clay soils the effective stress (drained) conditions match the parameters used in the total stress (undrained) conditions. TRC anticipated that the soil strength parameters of the clay would change in drained versus undrained conditions. For drained conditions, the effective friction angles would be expected to be non-zero and for the effective cohesions to be significantly lower than the values used in undrained analysis.

CTI submitted **Attachment 7** that clarified why the undrained soil parameters were used in the drained condition analyses in Attachment B-1 Slope Stability scenarios 8 through 11. CTI stated that undrained shear strength parameters used in the analyses are lower than shear strength values under drained conditions. TRC concurs with using the more conservative strength parameters to model the stability of the proposed landfill and requested that CTI provide the strength envelopes comparing the undrained and drained strengths for the upper clay, middle clay, and lower clay soils referenced in the stability analyses. This information was provided by CTI in **Attachment 8**. TRC agreed with the reasoning for using the selected approach and strength parameters provided in the attachment.

- **Leachate Collection Sump Addition** – The EGLE requested that each subcell contain its own leachate collection sumps to isolate detections. Construction drawings and additional information about this modification are now provided in **Attachment 6**.

Based on our review of the information, TRC believes the proposed design is technically adequate.

Sincerely,
TRC



Michael J. Amstadt, P.E.
Principal Project Manager

- Attachments:
1. Wayne Disposal Inc. Site Map
 2. 2021 WDI Attachment A – Technical Equivalency Information
 3. 2021 WDI Attachment A1 – Chemical Compatibility Evaluation Provided by CETCO
 4. Subset of 2021 WDI Attachment B – Slope Stability and Settlement Analysis
 5. 2021 WDI Attachment D – GCL Manufacturer Specifications, CQA Manual, and Installation Guidelines
 6. WDI Major Modification - Liner Design Upgrade Comments – April 13, 2021
 7. Additional Information - Ladd (1991) Stability During Staged Construction Terzaghi Lecture
 8. Additional Information - Response to Comments – August 18, 2021

cc: George Shereda – TRC

Attachment 1
Wayne Disposal Inc. Site Map

Wayne Disposal Inc.



F1-F4

G4-G7



Attachment 2

2021 WDI Attachment A – Technical Equivalency Information

Attachment A

Technical Equivalency Information

Proposed Liner System for MC VI-F and MC VI-G

WDI is proposing to install a polymer-treated geosynthetic clay liner (GCL) (Resistex[®] 200, manufactured by CETCO) immediately beneath the primary 80-mil HDPE geomembrane liner of Master Cell VI-F1 through Master Cell VI-F4 (MC VI-F) and Master Cell VI-G4 through Master Cell VI-G7 (MC VI-G) to maximize the barrier performance of the liner system. This proposed GCL liner system was approved by the agency in 2018 for MC VI-G2 and MC VI-G3, using the same information presented below. **Figure A-1** shows the proposed liner construction details. Note that the captions of other liner components (e.g., 80-mil HDPE geomembranes, double-sided geocomposite, geogrid, etc.) are omitted in **Figure A-1** for clarity. Please refer to **Attachment C**, 2020 Permit Engineering Drawings for more liner construction details.

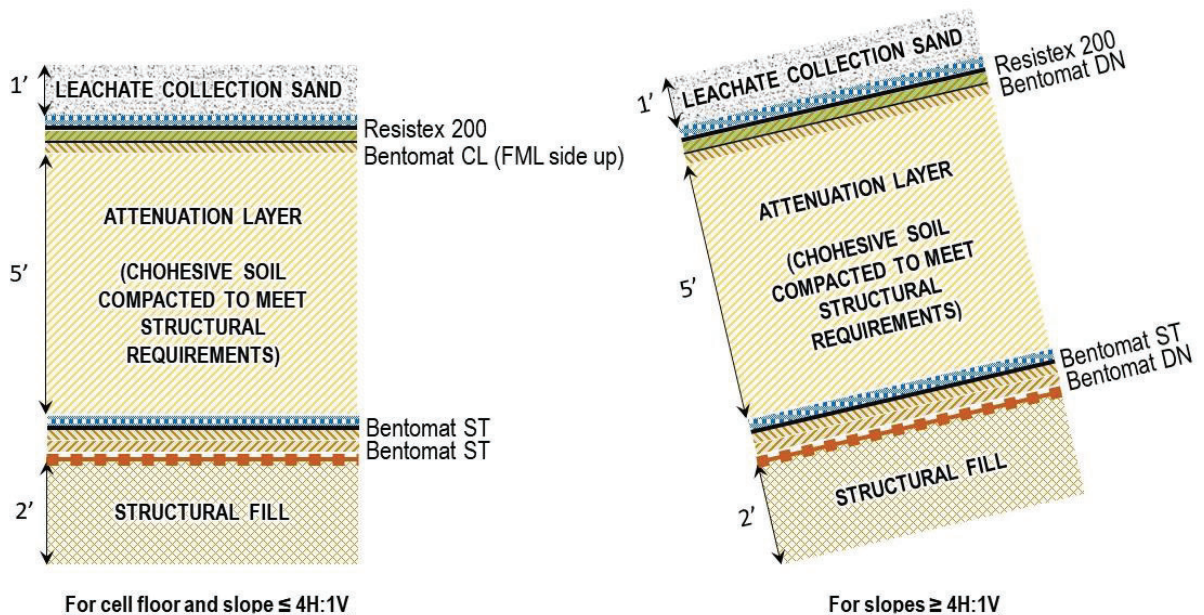


Figure A-1. Proposed MC VI-F and MC VI-G Base Liner Construction Detail.
(The geogrid and structure fill are only required on top of the existing waste within MC I and IV boundary)

To quantify the equivalency of the proposed liner system including GCL to the permitted liner system including CCL, WDI provided the GCL manufacturer (CETCO) with site-specific leachate test data for a conservative evaluation of GCL chemical compatibility. CETCO conducted a series of tests in their R&D laboratory on the supplied sample of leachate from WDI.

After 243 hours of permeation, CETCO measured an average permeability of 1.5×10^{-9} cm/sec with 0.7 pore volumes of leachate passing through the specimen. This means that the bentonite / polymer blend in the Resistex[®] 200 hydrated and cut off flow as designed. For the equivalency demonstration calculations (specifically, the steady-state solute flux), a conservative permeability of 1×10^{-8} cm/sec was used. In other words, an extra adjustment or safety factor of 6.7 was applied for additional conservatism. See **Attachment A-1** for CETCO's chemical evaluation report.

In addition to installing the polymer-treated GCL (Resistex[®] 200) immediately beneath the primary 80-mil HDPE geomembrane liner on the cell floor, WDI is also proposing to use another specialty GCL, Bentomat[®] CL, for enhanced protection. Bentomat[®] CL has an additional FML laminated on one side of the GCL to offer the highest level of hydraulic barrier performance. By installing this product with the FML side "facing

up” towards the cell as indicated in **Figure A-1**, Bentomat® CL provides another impervious layer to isolate its own bentonite layer from contacting moisture, if any, that may migrate through the primary HDPE geomembrane liner and the overlying GCL (Resistex® 200).

For sideslopes that are steeper than 4(H):1(V), WDI proposes to replace the FML-laminated GCL (Bentomat® CL) with a standard GCL product (Bentomat® DN) for slope stability purposes. Bentomat® DN consists of two layers of needle-punched, non-woven geotextiles on both sides of the bentonite interlayer. This configuration provides superior sideslope shear resistance. The FML-laminated GCL (Bentomat® DN) to be installed on the cell floor will be extended 5-ft vertically above the toe of the sideslopes for optimized performance.

Technical Equivalency

An equivalency assessment was conducted by the following steps allowing for a technically-sound, effective and project-focused equivalency demonstration.

1. Identify various technical criterion that are relevant to the proposed MC VI-F and G cell liners.
2. Divide the identified criterion into distinct categories to facilitate a direct technical comparison between GCLs (the proposed alternative) and CCLs (the approved design).
3. Identify criterion where technical equivalency between GCLs and CCLs has already been well-studied, demonstrated and documented by the lining industry (e.g., landfills, surface impoundments, mining, water-proofing of hydraulic structures, etc.), based on past tests and project experiences. No additional demonstration effort is needed for these items.
4. Identify criteria which are mainly site-, project-, or product-specific items, and demonstrate equivalency.

The results of Steps 1, 2 and 3 are summarized in **Table A-1** below. Both the format and content shown in the table is largely adapted from the well-referenced papers by Koerner and Daniel (1993), Bonaparte et. al. (2002), as well as from general liner engineering practice over the past two decades, with some site-specific modifications that are considered appropriate for the construction of the MC VI-F and MC VI-G liner.

Table A-1. Generalized Technical Equivalency Assessment for Liners Beneath Landfills

Category	Criterion for Evaluation	Equivalency of GCL to CCL			
		GCL is superior	GCL is equivalent	Equivalency is product-, design-, or site-specific	Category irrelevant to this project
Hydraulic	Steady state water flux	X			Evaluation will focus on site-specific leachate
	Breakthrough time - water	X			Evaluation will focus on site-specific leachate
	Horizontal flow in seams or lifts		X		-
	Horizontal flow beneath geomembranes	X			-
	Steady state solute flux			X	-
	Chemical adsorptive capacity / Solute breakthrough time			X	-
	Permeability to gases	-	-	-	A non-issue when GCL is installed under FML
Physical/ Mechanical	Generation of consolidation water	X			-
	Freeze-thaw behavior	X			-
	Wet-dry behavior	X			-
	Vulnerability to erosion	-	-	-	Erosion is irrelevant in the proposed liner
	Total settlement		X		-
	Differential settlement	X			-
	Stability on slopes			X	-
Construction	Bearing capacity			X	-
	Puncture resistance			X	-
	Ease of placement	X			-
	Speed of construction	X			-
	Availability of material	X			-
	Requirements of water	X			-
	Air pollution concerns	X			-
Quality assurance considerations		X		-	

Category of which GCL is superior than CCL	Category of which equivalency is product-, design-, or site-specific
Category of which GCL is equivalent to CCL	Category is irrelevant to this project

As shown in **Table A-1**, the following five items (criterion) are identified for Step 4 discussed above:

Hydraulic Properties

- Steady state solute flux
- Chemical adsorptive capacity / Solute breakthrough time

Physical/Mechanical Properties

- Stability of slopes
- Bearing capacity

Construction Properties

- Puncture resistance/subgrade condition

These items were subjected to detailed comparison between GCLs and CCLs as presented in the following sections.

Hydraulic Properties

Steady state solute flux

Past testing and experience have shown that sodium bentonite (the interlayer of GCL) is chemically compatible with many common waste streams, including leachate, some petroleum hydrocarbons, deicing fluids, livestock wastes, and dilute sodium cyanide mine waste.

In certain chemical environments, the sodium ions in bentonite can be replaced with cations dissolved in the water that comes in contact with the GCL, a process referred to as cation exchange. This type of

exchange reaction can reduce the amount of water that can be held in the interlayer, resulting in decreased swell.

With the design and installation configuration shown in **Figure A-1** in mind the steady state solute flux equivalency demonstration was prepared and presented in **Tables A-2a** and **A-2b**. Please note that the following assumptions were made in the demonstration for additional conservatism:

1. Comparisons were made as if the 80-mil HDPE primary geomembrane liner does not exist. In other words, GCL's superior swelling capability, which is capable of enhancing the performance in the overlying HDPE liner, is completely ignored.
2. Considering the evaluation performed by the GCL manufacturer of GCL chemical compatibility with site specific leachate data, the hydraulic conductivity of the upper GCL (Resistex[®] 200) is assumed at 1×10^{-8} cm/sec despite the tested results suggesting a permeability of 1.5×10^{-9} cm/sec. As discussed previously, this adjustment serves to conservatively address the concern of chemical compatibility associated with site-specific leachate. This adjustment is extremely conservative since this GCL layer will be completely covered by a layer of 80-mil HDPE geomembrane liner and hydration of GCL by leachate can only take place if it is exposed through liner imperfections. The chance of this assumed scenario does not practically exist.
3. Values of head-on-liner used in the evaluation were selected as 12.0 inches (30.5 cm) for the cell floor (per regulation) and 6.0 inches (15.2 cm) for sideslopes steeper than 4(H):1(V). Please note that the head-on-liner over both the floor and the sideslope is calculated as not to exceed 6 inches as shown in the "Maximum head-on-liner calculation" included in **Attachment B-5**. Moreover, while only the standard GCL product (Bentomat[®] DN) is used in the flux calculation, the calculated maximum head-on-liner will theoretically occur near the toe of the sideslope where the specialty GCL (Bentomat[®] CL) will be installed. This presents an additional conservative factor of safety.
4. Technically, an "apples-to-apples" comparison of steady state solute flux should be made by comparing flux that comes from the bottom of the 5-ft attenuation layer (in the proposed design case) and from the bottom of the 5-ft CCL layer (in the permitted design case). However, the equivalency evaluation was conservatively conducted by determining the flux that flows through the two layers of GCLs and comes out the bottom of the lower GCL layer (Bentomat[®] CL). In other words, any flow retardation capacity that could be provided by the underlying 5-ft thick cohesive attenuation layer is completely ignored in this evaluation.
5. Consequent to assumptions 3 and 4 discussed above, the hydraulic gradient (the driving force that causes flow to take place) selected for the proposed liner case is 14 times and 8 times greater than that selected for the permitted liner case for floor and sideslope liners, respectively. This represents another very conservative assumption.

The evaluation of the steady state solute flux criteria is made by dividing the calculated steady state solute flux of the proposed liner (GCL) by the number associated with the permitted liner (CCL). The resulting "ratio", if it is less than or equal to 100%, would indicate that the performance of the proposed liner system is acceptable, and therefore technical equivalency is demonstrated.

Input parameters, assumptions, and results of the steady state solute flux evaluation are presented in **Tables A-2a** and **A-2b** for cell floor and slopes that are steeper than 4(H):1(V), respectively.

**Table A-2a. Steady State Solute Flux Equivalency Demonstration
Liner over Cell Floor and Slopes ≤ 4(H):1(V)**

Layer	Thickness (cm)	K (cm/sec) (water)	K (cm/sec) (WDI leachate)	Additional adjustment	Adjusted K (cm/sec)	Thickness/Perm
Resistex 200	0.95	3E-09	1.5E-09	6.7	1.0E-08	47,625,000
Bentomat CL	0.95	5E-10	5E-10	1.0	5E-10	1,905,000,000

Saturated thickness of GCL = 0.375" (or 0.95 cm)

K equivalent	
1E-09	cm/sec

$$k_v = \frac{H}{\left(\frac{H_1}{k_1}\right) + \left(\frac{H_2}{k_2}\right) + \left(\frac{H_3}{k_3}\right) + \dots + \left(\frac{H_n}{k_n}\right)}$$

Demonstration is made by comparing the steady-state flux (Q's) using Darcy's Law $Q = kiA$ (assuming no geomembrane)

Clay Liner	K_{eq} (cm/sec)	head (cm)	thickness (cm)	gradient i	Flux, Q (gal/acre-day)
5-ft of CCL	1E-07	30.48	152.4	1.20	111
Resistex 200 / Bentomat CL	1E-09	30.48	1.91	17.0	15
Conversion: $1.0 \text{ cm}^3/\text{sec}/\text{cm}^2 = 9.237E+08 \text{ gal}/\text{acre}/\text{day}$					$Q_{GCL}/Q_{CCL} = 14\%$

**Table A-2b. Steady State Solute Flux Equivalency Demonstration
Liner on Slopes ≥ 4(H):1(V)**

Layer	Thickness (cm)	K (cm/sec) (water)	K (cm/sec) (WDI leachate)	Adjustment factor	Adjusted K (cm/sec)	Thickness/Perm
Resistex 200	0.95	3E-09	5E-09	2.0	1E-08	158,750,000
Bentomat DN	0.95	5E-09	5E-09	1.0	5E-09	190,500,000

Saturated thickness of GCL = 0.375" (or 0.95 cm)

K equivalent	
5.5E-09	cm/sec

$$k_v = \frac{H}{\left(\frac{H_1}{k_1}\right) + \left(\frac{H_2}{k_2}\right) + \left(\frac{H_3}{k_3}\right) + \dots + \left(\frac{H_n}{k_n}\right)}$$

Demonstration is made by comparing the steady-state flux (Q's) using Darcy's Law $Q = kiA$ (assuming no geomembrane)

Clay Liner	K_{eq} (cm/sec)	head (cm)	thickness (cm)	gradient i	Flux, Q (gal/acre-day)
5-ft of CCL	1E-07	15.2	152.4	1.10	102
Resistex 200 / Bentomat DN	5E-09	15.2	1.91	9.0	45
Conversion: $1.0 \text{ cm}^3/\text{sec}/\text{cm}^2 = 9.237E+08 \text{ gal}/\text{acre}/\text{day}$					$Q_{GCL}/Q_{CCL} = 45\%$

As shown in **Tables A-2a** and **A-2b**, the steady state solute flux “ratios” are 14% and 45% for the cell floor and sideslope, respectively. Both numbers are significantly less than 100% indicating the performance of the proposed liner system is superior. Therefore, technical equivalency is demonstrated and the proposed liner system is acceptable.

Chemical adsorptive capacity / Solute breakthrough time

Federal and State regulations focus on preventing contamination of groundwater (CFR 40 Part 264.301(b) and Michigan Part 111 R299.9620(4)(a)). Therefore, selecting a point in the subsoil that has the same hydrogeological characteristics and distance to groundwater and using that point as a reference for both liner systems would be an appropriate approach in demonstrating equivalency.

As shown in **Figure A-2**, two models were established according to the concept described above: (a) permitted and constructed MC VI-G Phase 1 liner and (b) proposed MC VI-F and MC VI-G liner. As shown in **Figure A-2**, the thickness of in-situ clayey subsoils under the existing waste where the proposed MC VI-F and MC VI-G cells will be constructed, is approximately the same as the combined thickness of the existing MC VI-G Phase 1 CCL liner and its in-situ clayey soil.

This is an important finding since numerical equivalency, in terms of chemical adsorptive capacity and solute breakthrough time, can already be achieved by the 10-ft in-situ clay present in the MC VI-F and MC VI-G subsoils since all clayey soils (e.g., CCL or in-situ clay) exhibit a similar diffusion coefficient (Lake and Rowe (2005)).

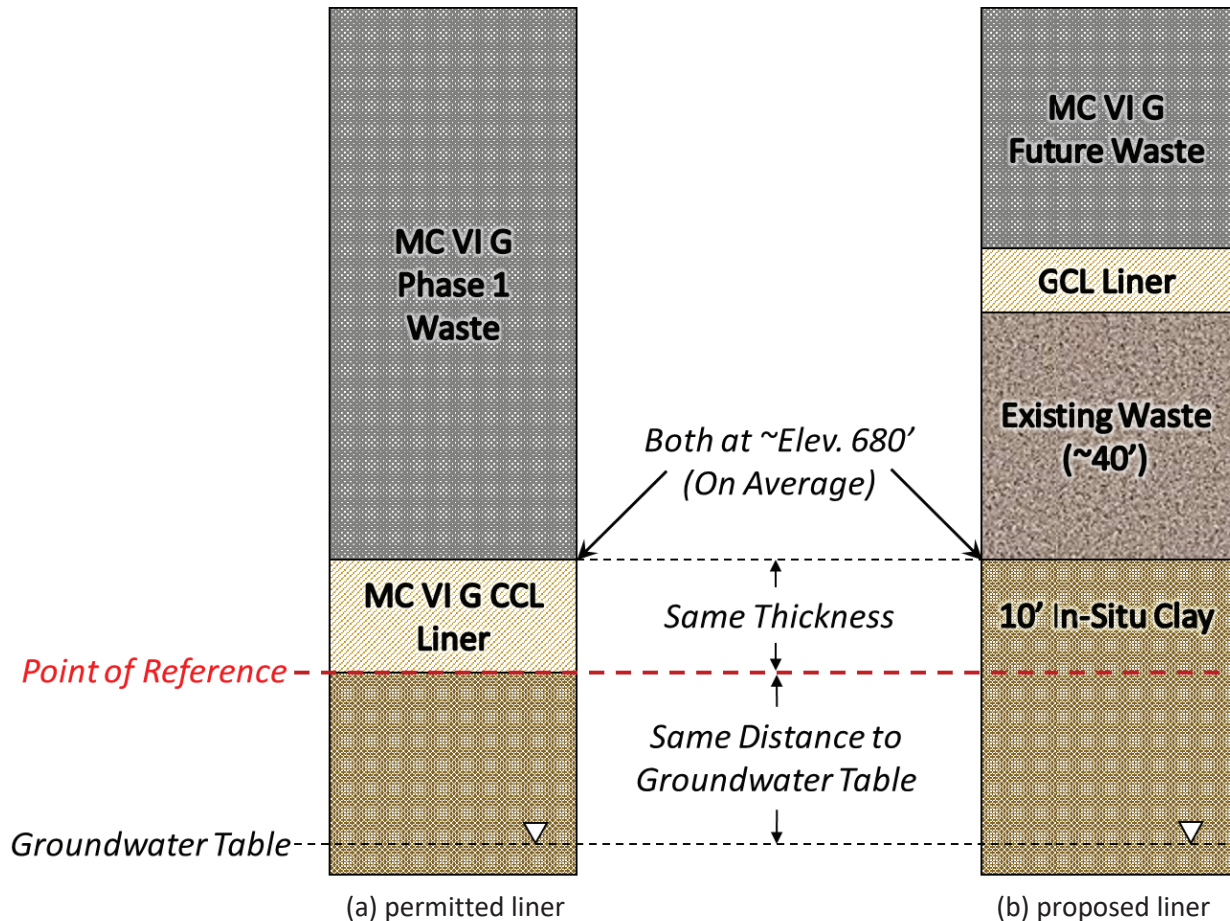


Figure A-2. Conceptual Model for Chemical Adsorptive Capacity and Breakthrough Time Comparison

In addition, as shown in **Figure A-1**, the proposed MC VI-F and MC VI-G liner system contains 7-ft of cohesive soil layers (5-ft attenuation layer and 2-ft structural fill). Since the distance between the contaminant source (leachate above the primary liner) and the point of reference is significantly thicker for the proposed MC VI-F and MC VI-G phases compared to the existing MC VI-G Phase 1, the breakthrough time will be significantly increased in the proposed system.

Another factor impacting the breakthrough time is the steady state flux passing through the liner system (higher flux would lead to shorter breakthrough time). Since it has already been demonstrated (see **Tables**

A-2a and **A-2b**) that the proposed GCL liner system will significantly reduce the steady state flux, the GCL liner system should also significantly increase the advective breakthrough time.

Additionally, as shown in **Figure A-2b**, approximately 40-ft of existing waste in the existing closed landfills further separates the new waste in MC VI-F and MC VI-G from the in-situ clay subsoil and groundwater. This existing waste layer provides additional chemical adsorptive capacity due to the following properties:

- Its anaerobic natural and high sulfide condition could bond heavy metals (Bhattacharyya et. al. (2006) and Robinson and Sum (1980))
- Non-degradable organic and other material provide additional adsorption and/or absorption capabilities for organic contaminants (De Gisi et. al. (2016) and Erses et. al. (2005))
- Additional biological activity reduces the half-life of organic pollutants and reduces potential breakthrough (Christensen et. al. (1994) and Guan et. al. (2014))
- Increases the mass transport distance and further reduces the concentration gradient (Shackelford (2013) and Xie (2015))
- Reduces the “concentration gradient” with the contaminants in the existing waste

Based on the above discussions, the performance of the proposed MC VI-F and MC VI-G liner system is superior in the criterion of chemical adsorptive capacity / solute breakthrough time than the reference case (MC VI-G Phase 1 liner system). Therefore, technical equivalency is demonstrated, and the proposed liner system is acceptable.

Conclusions

US Ecology Wayne Disposal, Inc. is proposing the use of GCL in the construction of MC VI-F and MC VI-G. The use of GCL was approved by the agencies in 2018 for the construction of MC VI-G2 and MC VI-G3 using the same equivalency demonstration presented above. WDI has presented this information again demonstrating that the proposed liner system is equivalent or superior to the currently permitted liner system and is capable of preventing the migration of hazardous constituents into the groundwater or surface water at least as effectively as the approved liner system.

List of References

- Koerner, R.M. and Daniel, D.E. (1993) "Technical Equivalency Assessment of GCLs to CCLs", Proceedings of the 7th GRI Seminar, Philadelphia, PA, December
- Bonaparte, R., Daniel, D.E., and Koerner, R.M. (2002) "Assessment and Recommendations for Improving the Performance of Waste Containment Systems", EPA/600/R-02/099, December
- Qian, X.D., Koerner, R.M., and Grey D.H. (2001) "Geotechnical aspects of landfill design and construction". New Jersey: Prentice Hall Inc.
- "Volume III – WDI Operating License Application, Master Cells VI F & G, Basis of Design Report", NTH Consultants, submitted in February 2011, revised in September 2011
- Lake, C.B., Rowe, R.K. (2005) "A Comparative Assessment of Volatile Organic Compound (VOC) Sorption to Various Types of Potential GCL Bentonites", *Geotextiles and Geomembranes*, 23, 323-347.
- Bhattacharyya, D., Jumawan, A.B., and Grieves, R.B. (2006) "Separation of Toxic Heavy Metals by Sulfide Precipitation", *Separation Science and Technology*, 14:5, 441-452.
- Robinson, A.K. and Sum, J.C. (1980) "Sulfide Precipitation of Heavy Metals", EPA-600/2-80-139, June.
- De Gisi, S., Lofrano, G., Grassi, M., and Notarnicola, M. (2016) "Characteristics and Adsorption Capacities of Low-Cost Sorbents for Wastewater Treatment: A Review.", *Sustainable Materials and Technologies*, 9, 10-40.
- Erses, A.S., Fazal, M.A., Onay, T.T., and Craig, W.H. (2005) "Determination of Solid Waste Sorption Capacity for Selected Heavy Metals in Landfills", *Journal of Hazardous Materials*, 121, 223-232.
- Christensen, T. H., Kjeldsen, P., Albrechtsen, H. J., Heron, G., Nielsen, P. H., Bjerg, P. L., and Holm, P. E. (1994) "Attenuation of Landfill Leachate Pollutants in Aquifers", *Critical Reviews in Environmental Science and Technology*, 24:2, 119-202.
- Guan, C., Xie, H. J., Wang, Y. Z., Chen, Y. M., Jiang, Y. S., and Tang, X. W. (2014) "An Analytical Model for Solute Transport through A GCL-Based Two-Layered Liner Considering Biodegradation", *Science of the Total Environment*, 466, 221-231.
- Shackelford, C. (2013) "Rowe Lecture: The Role of Diffusion in Environmental Geotechnics", Proceedings of the 18th International Conference on Soil Mechanics and Geotechnical Engineering, Paris, France, September.
- Xie, H.J., Thomas, H.R., Chen, Y.M., Sedighi, M., Zhan, T.L., and Tang, X.W. (2015) "Diffusion of Organic Contaminants in Triple-Layer Composite Liners: An Analytical Modeling Approach", *Acta Geotechnica*, 10, 255-262.
- "Upgrades to MC VI-G Phase 2 Liner Design", CTI and Associates, submitted on May 3, 2018, revised on May 16, 2018.

List of Supplemental Attachments

Attachment A-1: Chemical Compatibility Evaluation Report Provided by CETCO

Attachment 3

**2021 WDI Attachment A1 – Chemical Compatibility Evaluation
Provided by CETCO**

Attachment A-1

Chemical Compatibility Evaluation Report Provided by CETCO



May 1, 2018

Te-Yang Soong, Ph.D., P.E.
CTI and Associates, Inc.
28001 Cabot Drive, Ste. 250
Novi, MI 48377

RE: US Ecology's Wayne Disposal, Inc., Master Cell VI Sub-Cell G Phase 2
Geosynthetic Clay Liner – Tier I Report

Dear Mr. Soong:

The purpose of this letter is to present the results of compatibility testing of the CETCO® CG-50® bentonite used to make our Bentomat® products and the Resistex® geosynthetic clay liner (GCL) for the above mentioned project. This report is being made at the completion of the permeability testing for Resistex® 200 FLW9 GCL. All testing was performed by CETCO®'s in-house GAI-LAP accredited laboratory located in Hoffman Estates, Illinois.

Per your request, CETCO® initiated a geosynthetic clay liner (GCL) chemical compatibility evaluation as outlined in our Technical Reference (TR-345, attached) in April 2018 after receiving a representative sample of leachate. Completion of Tier I and II evaluations (see TR-345) indicated that a standard GCL (Bentomat®) in the presence of the leachate would likely not provide suitable performance as defined by permeability. CETCO®'s Resistex® 200 FLW9 GCL was also evaluated for its Tier II performance and is CETCO®'s recommended product for Tier III testing.

Permeability testing was completed in general accordance with ASTM D6766, Scenario II. For this testing, a cell pressure of 80 pounds per square inch (psi), 77 psi headwater pressure, and 75 psi tailwater pressure were utilized and represent test conditions that CETCO® utilizes in evaluating our GCL products. Permeability testing of the Resistex® 200 FLW9 product was terminated upon your request after 243.0 hours and 0.7 pore volumes of flow through the sample. The final average permeability for the Resistex® 200 FLW9 product was 1.5×10^{-9} cm/sec.

In addition to our Tier I & II results please find enclosed a copy of our Technical Data Sheet and Technical Reference. We appreciate your interest in CETCO® products. Please contact Tom Hauck, CETCO® Technical Sales Manager, at (248) 652-9274 if you have any further questions.

Table 1. Summary of final three measurements for the Resistex® 200 fLW9 product

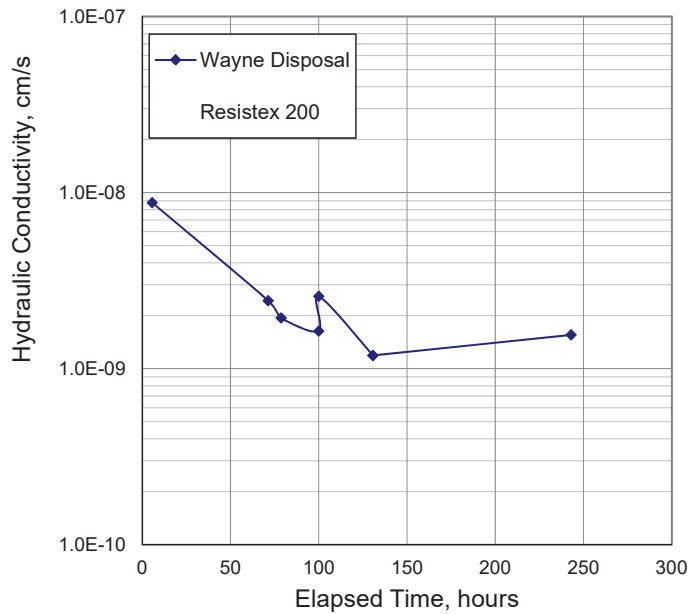
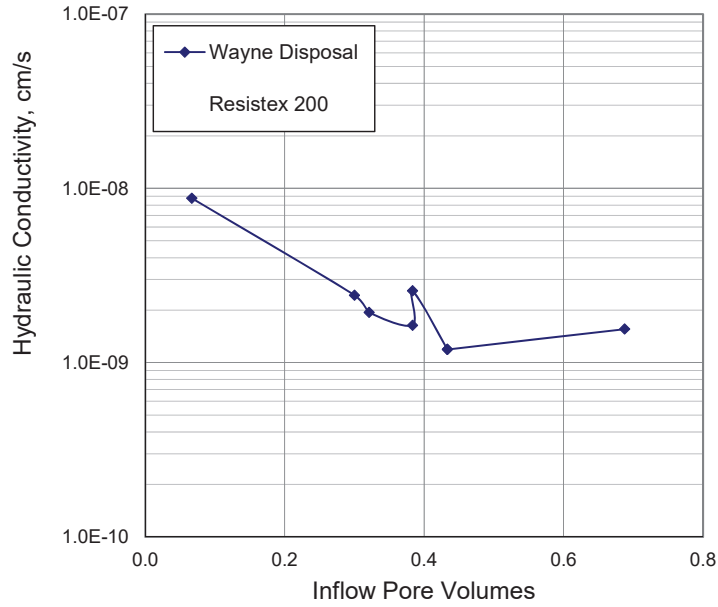
Elapsed Time (hr)	Pore Volumes	Inflow/Outflow	Permeability (cm/sec)
100.0	0.383	0.96	1.6×10^{-9}
130.7	0.433	0.96	1.2×10^{-9}
243.0	0.688	0.96	1.6×10^{-9}

Very truly yours,

John M. Allen, P.E.
Technical Services Manager
CETCO® Environmental Products

Attachments (3)





Permeability with pore volumes and time for the Resistex[®] 200 FLW9 GCL using site specific leachate per ASTM D6766, Scenario II, for the US Ecology's Wayne Disposal, Inc., Master Cell VI Sub-Cell G Phase 2

Analytical Results for the provided leachate for US Ecology's Wayne Disposal, Inc., Master Cell VI Sub-Cell G Phase 2 Project

Leachate Code Number	LT 18-1
Leachate Description	leachate
Leachate Type	leachate
Actual pH	9.250
Actual EC (uS/cm)	48,600
Calculations	LT 18-1
ICP Estimated EC (uS/cm) (Snoeyink Jenkins)	43281.45
Ionic Strength Estimated by ICP (mol/L)	0.693
RMD Estimated by ICP (M ^{0.5})	5.370
Ratio of SO ₄ /Cl	0.190

Cl ⁻	16400.000
Ag ⁺	0.169
Al ³⁺	
As ³⁺	2.816
B ₄ O ₅ (OH) ₄	51.462
Ba ²⁺	1.778
Ca ²⁺	47.013
Cd ²⁺	0.189
Cr ³⁺	0.211
Cu ²⁺	0.123
Fe ⁺²	3.859
Hg ²⁺	3.527
K ⁺	2231.718
Mg ²⁺	102.739
Mn ²⁺	1.216
Mo ²⁺	11.253
Na ⁺	9056.907
Ni ³⁺	1.473
P of PO ₄ -3	10.700
Pb ²⁺	1.359
S	2811.831
Sb ²⁺	0.968
Se ²⁺	0.754
Ti ⁴⁺	0.124
Zn ²⁺	0.532
Zr ⁴⁺	0.219
H+(Calculated)	0.000
OH- (Calculated)	0.302

EVALUATING GCL CHEMICAL COMPATIBILITY

Sodium bentonite is an effective barrier primarily because it can absorb water (i.e., hydrate and swell), producing a dense, uniform layer with extremely low hydraulic conductivity, on the order of 10^{-9} cm/sec. Water absorption occurs because of the unique physical structure of bentonite and the complementary presence of sodium ions in the interlayer region between the bentonite platelets. Sodium bentonite's exceptional hydraulic properties allow GCLs to be used in place of much thicker soil layers in composite liner systems.

Sodium bentonite which is hydrated and permeated with relatively "clean" water will perform as an effective barrier indefinitely. In addition, past testing and experience have shown that sodium bentonite is chemically compatible with many common waste streams, including Subtitle D municipal solid waste landfill leachate (TR-101 and TR-254), some petroleum hydrocarbons (TR-103), deicing fluids (TR-109), livestock waste (TR-107), and dilute sodium cyanide mine wastes (TR-105).

In certain chemical environments, the interlayer sodium ions in bentonite can be replaced with cations dissolved in the water that comes in contact with the GCL, a process referred to as ion exchange. This type of exchange reaction can reduce the amount of water that can be held in the interlayer, resulting in decreased swell. The loss of swell usually causes increased porosity and increased GCL hydraulic conductivity. Experience and research have shown that calcium and magnesium are the most common source of compatibility problems for GCLs (Jo et al, 2001, Shackelford et al, 2000, Meer and Benson, 2004, Kolstad et al, 2004/2006). Examples of liquids with potentially high calcium and magnesium concentrations include: leachates from lime-stabilized sludge, soil, or fly ash; extremely hard water; unusually harsh landfill leachates; and acidic drainage from calcareous soil or stone. Other cations (ammonium, potassium, and sodium) may contribute to compatibility problems, but they are generally not as prevalent or as concentrated as calcium (Alther et al, 1985), with the exception of brines and seawater. Even though these highly concentrated solutions do not necessarily contain high levels of calcium, their high ionic strength can reduce the amount of bentonite swelling, resulting in increased GCL hydraulic conductivity.

This reference discusses the tools that can be used by a design engineer to evaluate GCL chemical compatibility with a site-specific leachate or other liquid.

HOW IS GCL CHEMICAL COMPATIBILITY EVALUATED?

Ideally, concentration-based guidelines would be available for determining GCL compatibility with a site-specific waste. Unfortunately, considering the variety and chemical complexity of the liquids that may be evaluated, as well as the many variables that influence chemical compatibility (e.g., prehydration with subgrade moisture [TR-222], confining stress [TR-321], and repeated wet-dry cycling [TR-341]), it is not possible to establish such guidelines. Instead, a three-tiered approach to evaluating GCL chemical compatibility is recommended, as outlined below.

TR-345
03/09

800.527.9948 Fax 847.577.5566

For the most up-to-date product information, please visit our website, www.cetco.com.

A wholly owned subsidiary of AMCOL International Corporation. The information and data contained herein are believed to be accurate and reliable, CETCO makes no warranty of any kind and accepts no responsibility for the results obtained through application of this information.

Tier I

The first tier is a simple review of existing analytical data. The topic of GCL chemical compatibility has been the subject of much study in recent years, with several important references available in the literature. One of these references, Kolstad et al (2004/2006), reported the results of several long-term hydraulic conductivity tests involving GCLs in contact with various multivalent (i.e., containing both sodium and calcium) salt solutions. Based on the results of these tests, the researchers found that a GCL's long-term hydraulic conductivity (as determined by ASTM D6766) can be estimated if the ionic strength (I) and the ratio of monovalent to divalent ions (RMD) in the permeant solution are both known, using the following empirical expression:

$$\frac{\log K_c}{\log K_{DI}} = 0.965 - 0.976 \times I + 0.0797 \times RMD + 0.251 \times I^2 \times RMD$$

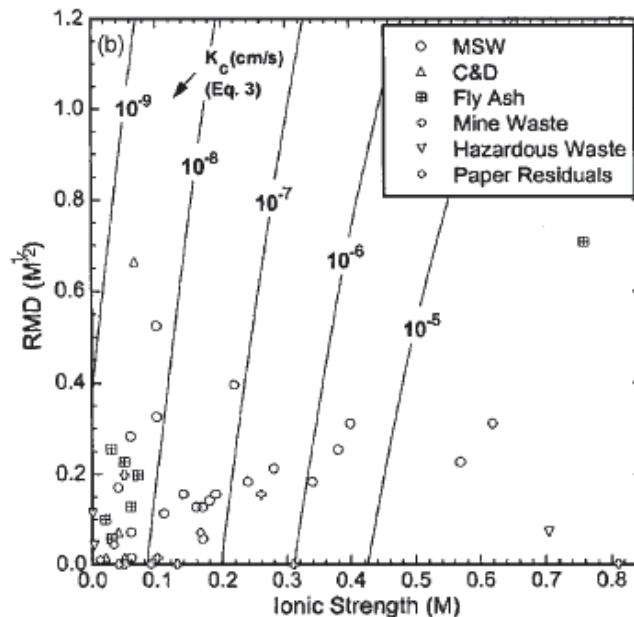
where:

I = ionic strength (M) of the site-specific leachate.

RMD = ratio of monovalent cation concentration to the square root of the divalent cation concentration ($M^{1/2}$) in the site-specific leachate.

K_c = GCL hydraulic conductivity when hydrated and permeated with site-specific leachate (cm/sec).

K_{DI} = GCL hydraulic conductivity with deionized water (cm/sec).



Using this tool, a Tier I compatibility evaluation can be performed if the major ion concentrations (typically, calcium, magnesium, sodium, and potassium) and ionic strength (estimated from either the total dissolved solids [TDS], or electrical conductivity [EC]) of the site leachate are known. For example, using the relationship above and MSW leachate data available in the literature, Kolstad et al. were able to conclude that high hydraulic conductivities (i.e., $>10^{-7}$ cm/sec) are unlikely for GCLs in base liners in many solid waste containment facilities.

In many cases, the Tier I evaluation is sufficient to show that a site-specific leachate should not pose compatibility problems. However, if the analytical data indicate a potential impact to GCL hydraulic performance, or if there is no analytical data available, then it is necessary to proceed to the second tier, involving bentonite "screening" tests, which are described below.

TR-345
03/09

800.527.9948 Fax 847.577.5566

For the most up-to-date product information, please visit our website, www.cetco.com.

A wholly owned subsidiary of AMCOL International Corporation. The information and data contained herein are believed to be accurate and reliable, CETCO makes no warranty of any kind and accepts no responsibility for the results obtained through application of this information.

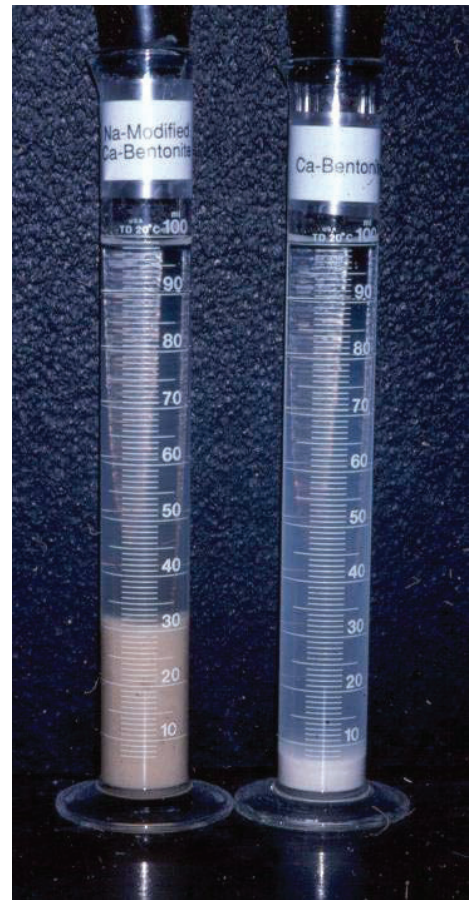
Tier II

The next tier of compatibility testing involves bentonite screening tests, performed in accordance with ASTM Method D6141. These tests are fairly straightforward, and can be performed at one of CETCO's R&D laboratories or at most commercial geosynthetics testing laboratories.

Liquid samples should be obtained very early in the project, such as during the site hydrogeological investigation. It is important that the sample collected is representative of actual site conditions. Synthetic leachate samples may also be considered for use in the compatibility tests. The objective is to create a liquid representative of that which will come in contact with the GCL. At least 1-gallon (4-Liter) of each sample should be submitted for testing. Samples should be accompanied by a chain-of-custody or information form. When a sample is received at the CETCO laboratory, the following screening tests are performed to assess compatibility:

- Fluid Loss (ASTM D5890) – A mixture of sodium bentonite and the site water/leachate is tested for fluid loss, an indicator of the bentonite's sealing ability.
- Swell Index (ASTM D5891) – Two grams of sodium bentonite are added to the site water/leachate and tested for swell index, the volumetric swelling of the bentonite.
- Water quality – The pH and EC of the site water/leachate are measured using bench-top water quality probes. pH will indicate if any strong acids (pH < 2) or bases (pH > 12) are present which might damage the bentonite clay. EC indicates the strength of dissolved salts in the water, which can hamper the swelling and sealing properties of bentonite if present at high concentrations.
- Chemistry – The site water/leachate is analyzed for major dissolved cations using ICP. The analytical results can then be used to perform a Tier I assessment, if one has not already been done.

As part of this testing, fluid loss and free swell tests are also performed on clean, deionized, or "DI" water for comparison to the results obtained with the site water/leachate sample. Sodium bentonite tested with DI water is expected to have a free swell of at least 24 mL/2g and a fluid loss less than 18 mL. Changes in bentonite swell and fluid loss indicate that the constituents dissolved in the site water may have an impact on GCL hydraulic conductivity. However, since it is only a screening tool, there are no specific values for the fluid loss and swell index tests that the clay must meet in order to be considered chemically compatible with the test liquid in question. Differences between the results of the baseline tests and those conducted with the site leachate may warrant further hydraulic testing.



TR-345
03/09

800.527.9948 Fax 847.577.5566

For the most up-to-date product information, please visit our website, www.cetco.com.

A wholly owned subsidiary of AMCOL International Corporation. The information and data contained herein are believed to be accurate and reliable, CETCO makes no warranty of any kind and accepts no responsibility for the results obtained through application of this information.

A major drawback of the D6141 tests is the potential for a false “negative” result, meaning that the bentonite swell index or fluid loss might predict no impact to hydraulic performance, where in reality, there may be a long-term adverse effect. This is primarily a concern with dilute calcium or magnesium solutions, which may slowly affect GCL hydraulic performance over months or years. Short-term (2-day) bentonite screening tests would not be able to capture this type of long-term effect. This is not expected to be a concern with strong calcium or magnesium or high ionic strength solutions, which have been shown to impact GCL hydraulic conductivity almost immediately, and whose effects would therefore be captured by the short-term bentonite screening tests. Another limitation of the bentonite screening tests is their inability to simulate site conditions, such as clean water prehydration, increased confining pressure, and wet/dry cycling. These limitations can be in part addressed by moving to the third tier, a long-term GCL hydraulic conductivity test, discussed below.



Tier III

The third-tier compatibility evaluation consists of an extended GCL hydraulic conductivity test performed in accordance with ASTM D6766. This test method is essentially a hydraulic conductivity test, but instead of permeating the GCL sample with DI water, the site-specific leachate is used. Since leachates can often be hazardous, corrosive, or volatile, the testing laboratory must have permeant interface devices, such as bladder accumulators, to contain the test liquid in a closed chamber, and prevent contamination of the flow measurement and pressure systems, or release of chemicals to the ambient air.

Method D6766 provides some flexibility in specifying the testing conditions so that certain site conditions can be simulated. For example, in situations where the GCL will be deployed on a subgrade soil that is compacted wet of optimum, the GCL will very likely hydrate from the relatively clean moisture in the subgrade (TR-222), long before it comes in contact with the potentially aggressive site leachate. Lee and Shackelford (2005) showed that a GCL which is pre-hydrated with clean water before being exposed to a harsh solution is expected to exhibit a lower hydraulic conductivity than one hydrated directly with the solution. Depending on the expected site conditions, the D6766 test can be specified to pre-hydrate the GCL with either water (Scenario 1) or the site liquid (Scenario 2).

Another site-specific consideration is confining pressure. Certain applications, such as landfill bottom liners and mine heap leach pads, involve up to several hundred feet of waste, resulting in high compressive loads on the liner systems. Although the standard confining pressure for the ASTM D6766 test is 5 psi (representing less than 10 feet of waste), the test method is flexible enough to allow greater confining pressures,

TR-345
03/09

800.527.9948 Fax 847.577.5566

For the most up-to-date product information, please visit our website, www.cetco.com.

A wholly owned subsidiary of AMCOL International Corporation. The information and data contained herein are believed to be accurate and reliable, CETCO makes no warranty of any kind and accepts no responsibility for the results obtained through application of this information.

thus mimicking conditions in a landfill bottom liner or heap leach pad. Petrov et al (1997) showed that higher confining pressures will decrease bentonite porosity, and tend to decrease GCL permeability. TR-321 shows that higher confining pressures will improve hydraulic conductivity even when the GCL is permeated with aggressive calcium solutions.

ASTM D6766 has two sets of termination criteria: hydraulic and chemical. To meet the hydraulic termination criterion, the ratio of inflow rate to outflow rate from the last three readings must be between 0.75 and 1.25. It normally takes between one week and one month to reach the hydraulic termination criterion. To meet the chemical termination criterion, the test must continue until at least two pore volumes of flow have passed through the sample and chemical equilibrium is established between the effluent and influent. The test method defines chemical equilibrium as effluent electrical conductivity within $\pm 10\%$ of the influent electrical conductivity. This requirement was put in place to ensure that a large enough volume of site liquid passes through the sample to allow slow ion exchange reactions to occur. Two pore volumes can take approximately a month to permeate through the GCL sample. However, reaching chemical equilibrium (effluent EC within 10% of influent EC), may take more than a year of testing, depending on the leachate characteristics.

ASTM D6766 is a very useful tool which provides a fairly conclusive assessment of GCL chemical compatibility with a site-specific leachate. However, the major drawback of the D6766 test is the potentially long period of time required to reach chemical equilibrium. This limitation reinforces the need for upfront compatibility testing early in the project. Clearly, requiring the contractor to perform this testing during the construction phase is not recommended.

WHAT DO THE ASTM D6766 COMPATIBILITY TEST RESULTS MEAN?

ASTM D6766 is currently the state-of-the-practice in the geosynthetics industry for evaluating long-term chemical compatibility of a GCL with a particular site waste stream. An ASTM D6766 test that is properly run until both the hydraulic (inflow and outflow within $\pm 25\%$ over three consecutive readings) and chemical (effluent EC within $\pm 10\%$ of influent EC) termination criteria are achieved, provides a good approximation of the GCL's long-term hydraulic conductivity when exposed to the site leachate. Jo et al (2005) conducted several GCL compatibility tests with weak calcium and magnesium solutions, with some tests running longer than 2.5 years, representing several hundred pore volumes of flow. The intent of this study was to run the tests until complete ion exchange had occurred, which required even stricter chemical equilibrium termination criteria than the D6766 test. The study found that the final GCL hydraulic conductivity values measured after complete ion exchange were fairly close to (within 2 to 13 times) the hydraulic conductivity values determined by ASTM D6766 tests, which took much less time to complete.

The laboratory that performs the chemical compatibility test, whether it is the CETCO R&D laboratory or an independent third-party laboratory, is only reporting the test results under the specified testing conditions, and is not making any guarantees about actual field performance or the suitability of a GCL for a particular project. It is the design engineer's responsibility to incorporate the D6766 results into their design to determine whether the GCL will meet the overall project objectives. Neither the testing laboratory nor the GCL manufacturer can make this determination.

TR-345
03/09

800.527.9948 Fax 847.577.5566

For the most up-to-date product information, please visit our website, www.cetco.com.

A wholly owned subsidiary of AMCOL International Corporation. The information and data contained herein are believed to be accurate and reliable, CETCO makes no warranty of any kind and accepts no responsibility for the results obtained through application of this information.

Also, it is important to note that the results of D6766 testing for a particular project are only applicable for that site, for the specific waste stream that is tested, and only for the specific conditions replicated by the test. For instance, D6766 testing performed at high normal loads representative of a landfill bottom liner should not be applied to a situation where the GCL will only be placed under a modest normal load, such as a landfill cover or pond. Similarly, the results of a D6766 test where the GCL was pre-hydrated with clean water should not be applied to sites located in extremely arid climates where little subgrade moisture is expected, unless water will be applied manually to the subgrade prior to deployment. And finally, since D6766 tests are normally performed on continuously hydrated GCL samples, the test results should not be applied to situations where repeated cycles of wetting and drying of the GCL are likely to occur, such as in some GCL-only landfill covers, as desiccation can worsen compatibility effects.

REFERENCES

1. Alther, G., Evans, J.C., Fang, H.-Y., and K. Witmer, (1985) "Influence of Inorganic Permeants Upon the Permeability of Bentonite," Hydraulic Barriers in Soil and Rock, ASTM STP 874, A.I. Johnson, R.K. Frobel, N.J. Cavalli, C.B. Peterson, Eds., American Society for Testing and Materials, Philadelphia, PA, pp. 64-73.
2. ASTM D 6141, Standard Guide for Screening Clay Portion of Geosynthetic Clay Liner for Chemical Compatibility to Liquids.
3. ASTM D 6766, Standard Test Method for Evaluation of Hydraulic Properties of Geosynthetic Clay Liners Permeated with Potentially Incompatible Liquids.
4. CETCO TR-101, "The Effects of Leachate on the Hydraulic Conductivity of Bentomat".
5. CETCO TR-103, "Compatibility Testing of Bentomat (Gasoline, Diesel and Jet Fuel)".
6. CETCO TR-105, "Bentomat Compatibility Testing with Dilute Sodium Cyanide".
7. CETCO TR-107, "GCL Compatibility with Livestock Waste".
8. CETCO TR-109, "GCL Compatibility with Airport De-Icing Fluid".
9. CETCO TR-222, "Hydration of GCLs Adjacent to Soil Layers".
10. CETCO TR-254, "Hydraulic Conductivity and Swell of Nonprehydrated GCLs Permeated with Multispecies Inorganic Solutions".
11. CETCO TR-321, "GCL Performance in a Concentrated Calcium Solution; Permeability vs. Confining Stress".
12. CETCO TR-341, "Addressing Ion Exchange in GCLs".
13. Jo, H., Katsumi, T., Benson, C., and Edil, T. (2001) "Hydraulic Conductivity and Swelling of Nonprehydrated GCLs with Single-Species Salt Solutions", *Journal of Geotechnical and Geoenvironmental Engineering*, ASCE, Vol. 127, No. 7, pp. 557-567.
14. Jo, H., Benson, C., Shackelford, C., Lee, J., and Edil, T. (2005) "Long-Term Hydraulic Conductivity of a GCL Permeated with Inorganic Salt Solutions", *Journal of Geotechnical and Geoenvironmental Engineering*, ASCE, Vol. 131, No. 4, pp. 405-417.

TR-345
03/09

800.527.9948 Fax 847.577.5566

For the most up-to-date product information, please visit our website, www.cetco.com.

A wholly owned subsidiary of AMCOL International Corporation. The information and data contained herein are believed to be accurate and reliable, CETCO makes no warranty of any kind and accepts no responsibility for the results obtained through application of this information.

15. Kolstad, D., Benson, C. and Edil, T., (2004) "Hydraulic Conductivity and Swell of Nonprehydrated GCLs Permeated with Multispecies Inorganic Solutions", *Journal of Geotechnical and Geoenvironmental Engineering*, ASCE, Vol. 130, No. 12, December 2004, pp.1236-1249.
16. Kolstad, D., Benson, C. and Edil, T., (2006) Errata for "Hydraulic Conductivity and Swell of Nonprehydrated GCLs Permeated with Multispecies Inorganic Solutions".
17. Lee, J. and Shackelford, C., (2005) "Concentration Dependency of the Prehydration Effect for a GCL", *Soils and Foundations*, Japanese Geotechnical Society, Vol. 45, No. 4.
18. Meer, S. and Benson, C., (2004) "In-Service Hydraulic Conductivity of GCLs Used in Landfill Covers – Laboratory and Field Studies", Geo Engineering Report No. 04-17, University of Wisconsin at Madison.
19. Petrov, R., Rowe, R.K., and Quigley, R., (1997) "Selected Factors Influencing GCL Hydraulic Conductivity", *Journal of Geotechnical and Geoenvironmental Engineering*, ASCE, Vol. 123, No. 8, pp. 683-695.
20. Shackelford, C., Benson, C., Katsumi, T., Edil, T., and Lin, L. (2000) "Evaluating the Hydraulic Conductivity of GCLs Permeated with Non-Standard Liquids." *Geotextiles and Geomembranes*, Vol. 18, pp. 133-162.

TR-345
03/09

800.527.9948 Fax 847.577.5566

For the most up-to-date product information, please visit our website, www.cetco.com.

A wholly owned subsidiary of AMCOL International Corporation. The information and data contained herein are believed to be accurate and reliable, CETCO makes no warranty of any kind and accepts no responsibility for the results obtained through application of this information.

Attachment 4

**Subset of 2021 WDI Attachment B – Slope Stability
and Settlement Analysis**

Attachment B-1

Slope Stability Analysis



Project Name:	<u>WDI MC6F Permit Modification</u>	Client:	<u>Wayne Disposal, Inc.</u>
Project Number:	<u>1208070039.004</u>	Project Manager:	<u>Chris Backus</u>
Project Location:	<u>Belleville, Michigan</u>	QA Manager:	<u></u>

Calculation Sheet Information

Calculation Medium: Electronic
 Hard copy Number of pages (including cover sheet): 53

Title of Calculation: Slope Stability Analyses

Calculation Originator: Andra Malburg, Mohammad Kabalan

Calculation Contributors: Mohammad Kabalan

Calculation Checker: Kevin Foye

Calculation Objective

This calculation evaluates the stability of the proposed MC6F at Wayne Disposal, Inc. (WDI) Landfill. The analyses include consideration of global slope stability for failures through the waste mass, along the liner system, and/or through the foundation soils at interim and final conditions. The analyses also determined the minimum required interface friction angle to attain a satisfactory factor of safety against failure at the liner system interface. Cross sections that are the most critical for analysis and design include cross sections with the steepest slopes and highest embankment (waste or soil) heights. The following critical cross sections were examined:

1. Cross Section B-B' oriented East-West and going through Cell F1.
2. Cross Section E-E' oriented North-South and going through Cell F4.

Assumptions and Open Items

1. Representative total stress shear strength parameters were used for all layers in the profile. Material properties were retrieved from existing site data (NTH 2012) and are presented in Table 1. Strength properties for the lower clay were modeled as a relationship of shear stress to normal stress (total vertical stress), whereas all other layers used the Mohr-Coulomb model with either an undrained shear strength or friction angle as input. A shear strength to total vertical stress ratio of 0.22 was applied for the lower clay in accordance with existing analyses (NTH 2012) to account for increases in shear strength resulting from increased overburden pressure within the lower clay layer.

Table 1: Material Properties

Material	Name	Color in Profile	Unit Wt(s) (pcf)	Strength ϕ or δ (deg.)	Strength C or Ca (psf)
1	Final Cover	Orange	130	0	1500
2	Existing Waste	Teal	86	34	0
3	New Waste	Light Green	103 ^[A]	26 ^[B]	300 ^[B]
4	Upper Clay	Brown	131	0	2150
5	Middle Clay	Yellow	136	0	3300
6	Lower Clay	Maroon	133	0.22 σ_v	
7	Silt	Blue	125	28	0
8	Sand	Red	115	32	0

Notes:

[A] unit weight of waste determined from site survey data reported in 2020.

[B] representative value of waste strength as reported by Qian et al. (2002)

All other properties obtained from NTH (2012)

2. For liner system stability cases, the domain of the slip surfaces are defined so that a portion of the failure surface conforms to the liner system.
3. Applicable data used in the analysis that was provided by third parties is assumed to be accurate.

Design Criteria/Design Basis (with Reference to Source of Data)

1. The minimum allowable factor-of-safety (FS) against slope stability failures is 1.50 for final conditions and 1.30 for interim conditions.
2. The analyses were conducted using the computer program SLOPE/W within the software package GeoStudio 2021 by GEOSLOPE International Ltd. This program performs an automatic search to identify a critical failure surface that has the lowest FS value.
3. The analyses were conducted using the Morgenstern-Price method, which considers both moment and force equilibrium.
4. The geometry of the cross sections was derived from the engineering drawing set submitted as part of the permit mod package.
5. The required/assumed interface friction angles shall be met by considering peak strength values for the cell floor and large-displacement strength values for the cell sideslopes.
6. The required minimum interface friction angle for the liner system components is determined under the final conditions (after final cover is installed).
7. Due to the complex nature of the waste fill phasing during operation, the liner stability shall be evaluated based on the actual measurements of the interface friction angle for the liner system components and the design waste filling geometry for each phase. An example of such a calculation was prepared to illustrate how to evaluate the required minimum interface friction angle for the liner system components. This example analysis was performed on cross section B-B' assuming an interim waste slope of 3.5H:1V.

Results/Conclusions

1. Global slope stability analyses of the waste and foundation for each cross section determined that filling to proposed final grades yields acceptable factors of safety.
 - a. Cross Section B-B': Factor of Safety = 1.84
 - b. Cross Section E-E': Factor of Safety = 2.23
2. Under the final conditions (after installation of final cover, the liner system analyses determined the minimum required interface friction angle for geosynthetics in the floor and slideslope liner systems to yield a factor of safety = 1.50. These values are **10.7 degrees for the floor (peak) and 7 degrees for the sideslope (large-displacement) with zero adhesion.**
 - a. Cross Section B-B': Factor of Safety = 1.50 (used to evaluate minimum friction angle)
 - b. Cross Section E-E': Factor of Safety = 1.77
3. The above values are minimum acceptable secant friction angles. Any combination of adhesion and friction angle resulting in comparable shear strength under representative normal stresses to final site conditions are also acceptable. Stability analysis using lab interface shear strength tests results from previous products used on site show that a combination of **$C_{\alpha, peak}=164 \text{ psf} / \phi_{peak}=11.1^\circ$ and $C_{\alpha, large displacement}=110 \text{ psf} / \phi_{large displacement}=7.3^\circ$** achieves an acceptable factor of safety. **Conformance testing of the selected geosynthetics shall be performed to confirm that the interface shear strength of the actual liner system components is sufficient to ensure the stability of the liner system.**
 - a. Cross Section B-B': Factor of Safety = 1.64
 - b. Cross Section E-E': Factor of Safety = 1.93
4. An example calculation of liner stability for an interim waste filling conditions is presented in Attachment 7. The required interface friction angle for the floor liner system was determined to be 12.7 degrees (peak). Actual interim phasing plan slopes and tested liner system interface properties shall be evaluated for each phase of fill per this example.

Source Documents and References

NTH (2012). WDI Operating License Application Master Cells VI F & G Volume III – Basis of Design Report

Qian, X., Gray, D.H., and Koerner, R.M. (2002) *Geotechnical Aspects of Landfill Design and Construction*.

Attachments

1. B-B' Foundation Stability
2. E-E' Foundation Stability
3. B-B' Liner Stability under Final Conditions with zero adhesion
4. E-E' Liner Stability under Final Conditions with zero adhesion
5. B-B' Liner Stability under Final Conditions with non-zero adhesion (previously tested values)
6. E-E' Liner Stability under Final Conditions with non-zero adhesion (previously tested values)
7. B-B' Liner Stability under Interim Conditions (example interim stability calculation)

Attachment B-1.1
B-B' Foundation Stability

SLOPE STABILITY ANALYSIS REPORT FORM

SLOPE STABILITY ANALYSIS REPORT FORM

Project Name:	WDI MC6F Permit Modification						
Project Number:	1208070039.004	Client:	Wayne Disposal, Inc.				
Analysis Short Name:	B-B' Foundation Stability			File name:	WDI Cross Section B Full_20201123_RevD_M K.gsz		
Revision:	1	Originated:	MK	Checked:	KF	Approved:	
Date:	11/23/20	Date:	11/23/20	Date:	11/23/20	Date:	

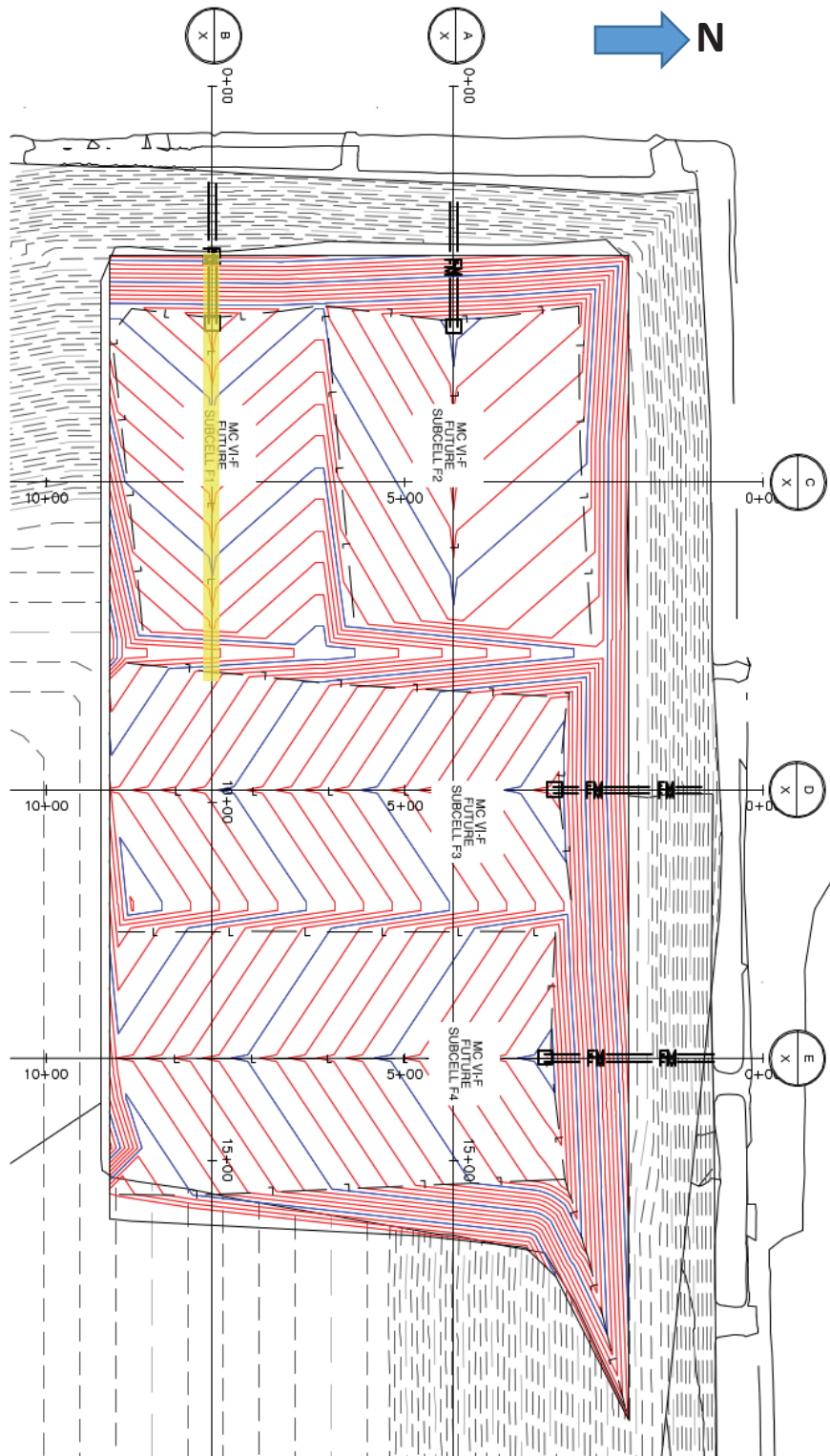
Purpose of Analysis:	To determine the factor of safety of the proposed final waste grades using cross-section B-B'. This case considers a west-facing slope, with fill to the final permitted grade elevations.		
<input type="checkbox"/> Effective Stress <input checked="" type="checkbox"/> Total Stress	<input checked="" type="checkbox"/> Static <input type="checkbox"/> Seismic	<input type="checkbox"/> Pore Pressure	<input checked="" type="checkbox"/> Optimized Surface
Additional Details:	The friction angle of the liner system was set equal to the required minimum interface friction angle determined from the liner stability analysis performed on Cross Section B.		

Material	Name	Color in Profile	Unit Wt(s) (pcf)	Strength ϕ or δ (deg.)	Strength C or Ca (psf)
1	Final Cover	Orange	130	0	1500
2	Existing Waste	Teal	86	34	0
3	New Waste	Light Green	103	26	300
4	Upper Clay	Brown	131	0	2150
5	Middle Clay	Yellow	136	0	3300
6	Lower Clay	Maroon	133	0.22 σ_v	
7	Silt	Blue	125	28	0
8	Sand	Red	115	32	0
9	Liner	Magenta	120	10.7	0

Source of Geometry:	Engineering Drawing Set
Source of Subsurface Profile:	Basis of Design Report - NTH (2012)
<input type="checkbox"/> Preconstruction <input type="checkbox"/> Construction <input type="checkbox"/> Interim <input checked="" type="checkbox"/> Final <input type="checkbox"/> Existing <input type="checkbox"/> Back-Analysis	
Construction Phase Represented:	Final Build out
Other Geometry Notes:	Cross Section B

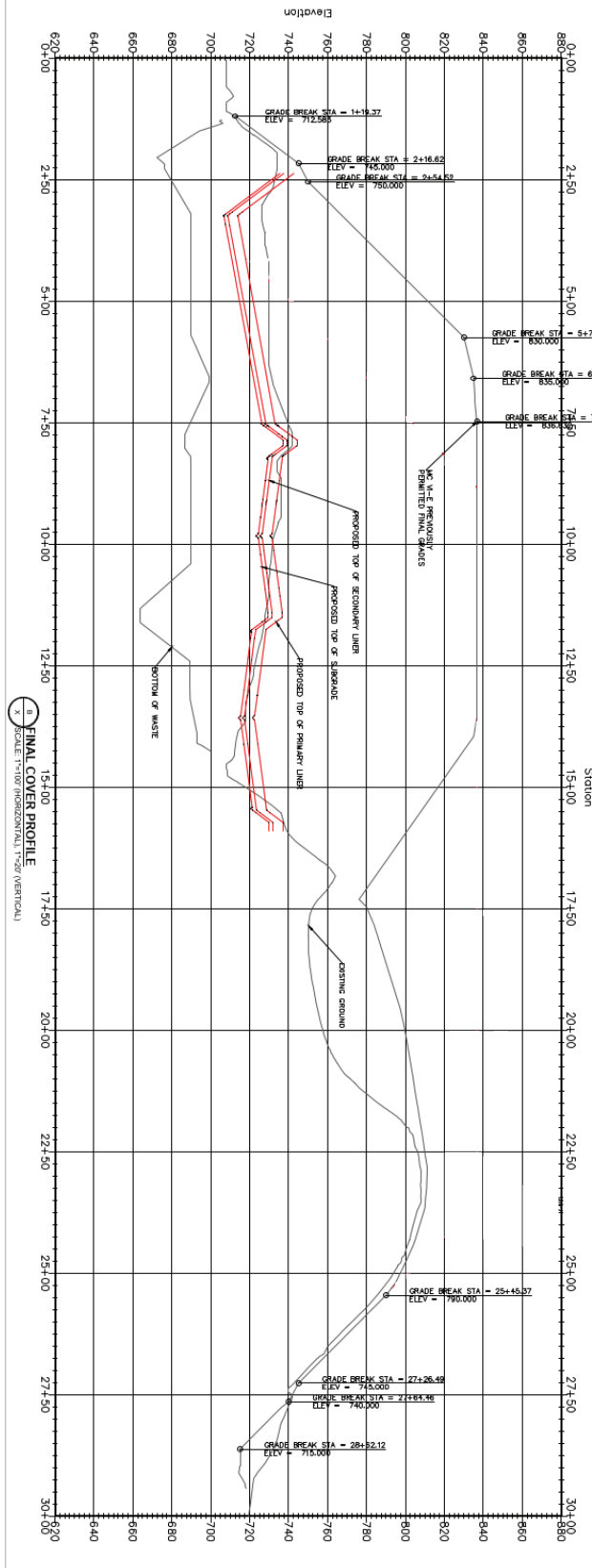
SLOPE STABILITY ANALYSIS REPORT FORM

Final Grades Cross-Section (plan):



SLOPE STABILITY ANALYSIS REPORT FORM

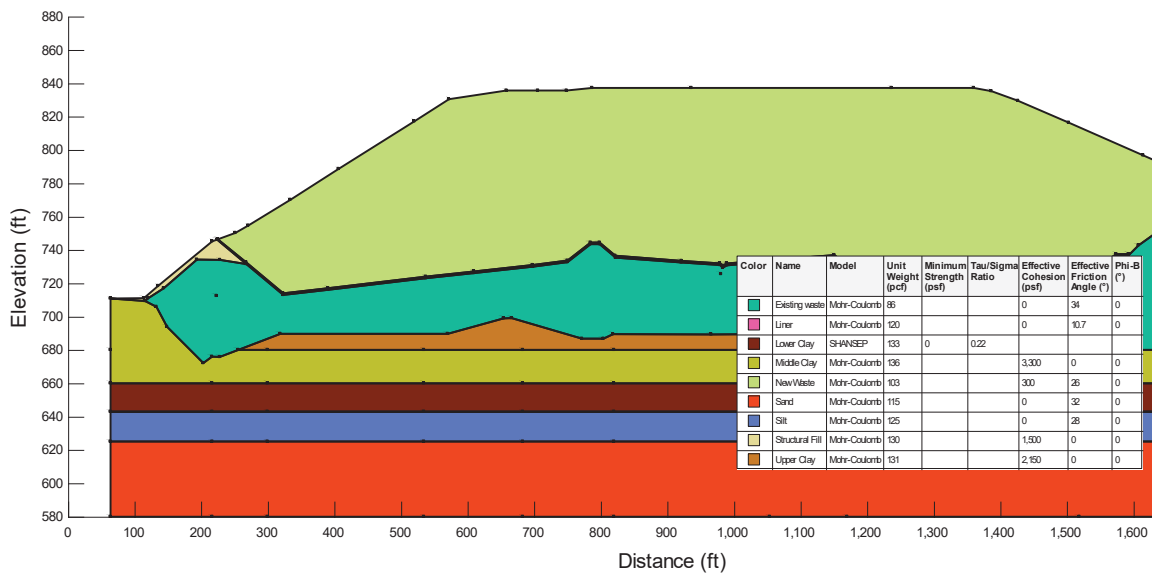
Final Grades Cross-Section (profile):



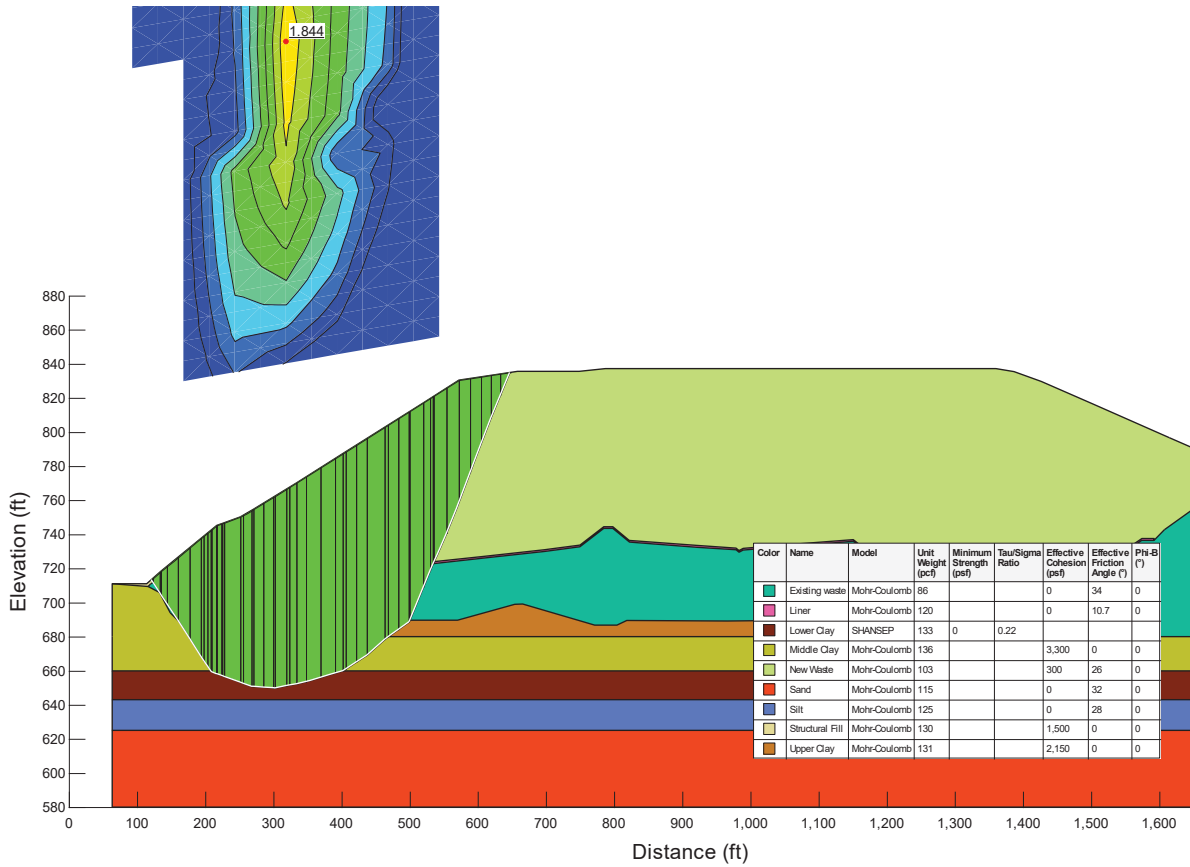
SLOPE STABILITY ANALYSIS REPORT FORM

Factor of Safety:	1.84	<input checked="" type="checkbox"/> Acceptable	<input type="checkbox"/> Not Acceptable	<input type="checkbox"/> Follow-up	<input type="checkbox"/> Superseded
Comments:					
Attachments:	Slope/W Cross Section and Results				

SLOPE STABILITY ANALYSIS REPORT FORM



SLOPE STABILITY ANALYSIS REPORT FORM



Attachment B-1.2
E-E' Foundation Stability

SLOPE STABILITY ANALYSIS REPORT FORM

SLOPE STABILITY ANALYSIS REPORT FORM

Project Name:	WDI MC6F Permit Modification						
Project Number:	1208070039.004	Client:	Wayne Disposal, Inc.				
Analysis Short Name:	E-E' Foundation Stability			File name:	WDI Cross Section E Full_20201123_RevD_M K.gsz		
Revision:	1	Originated:	MK	Checked:	KF	Approved:	
Date:	11/23/20	Date:	11/23/20	Date:	11/23/20	Date:	

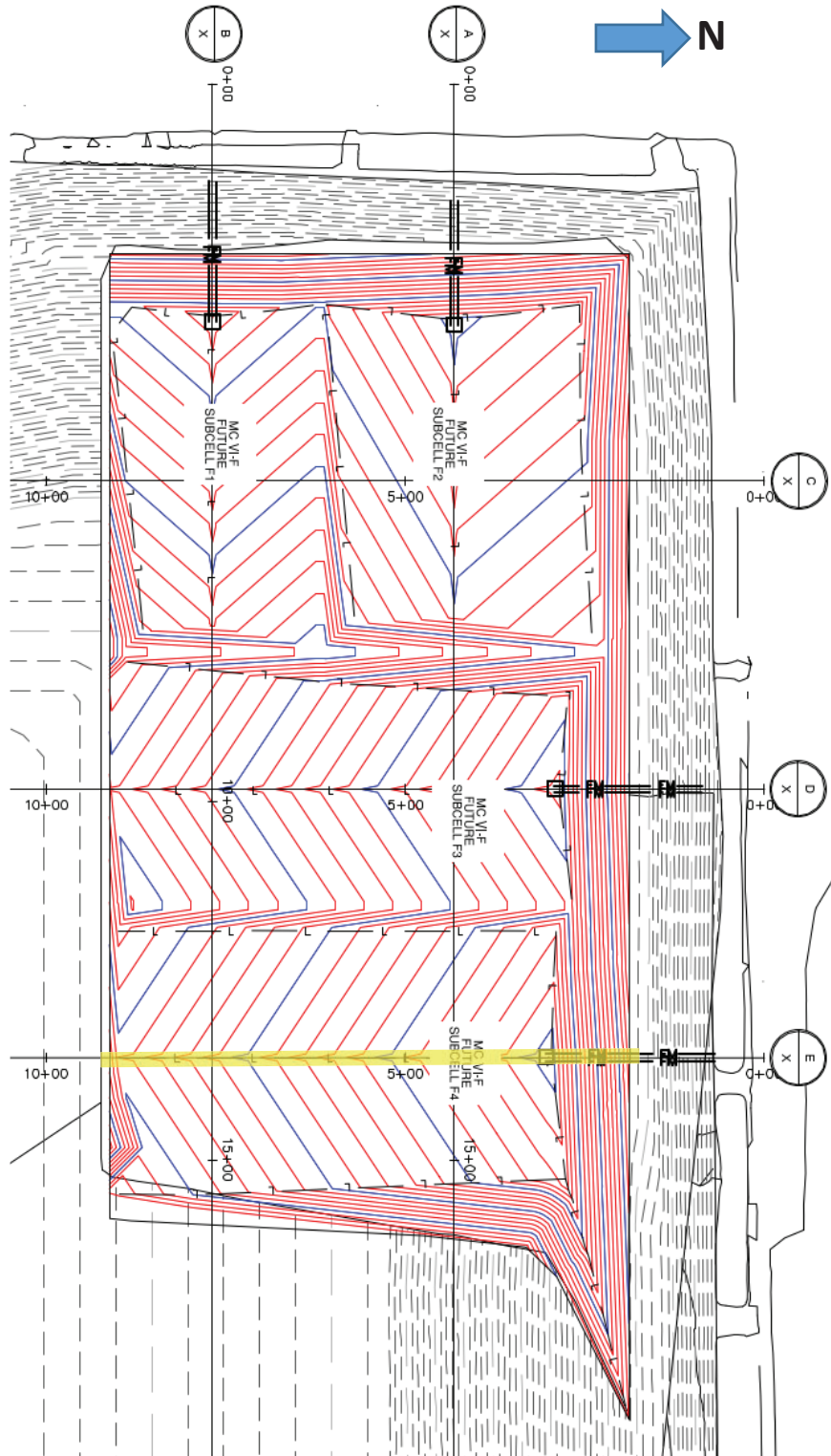
Purpose of Analysis:	To determine the factor of safety of the proposed final waste grades using cross-section E. This case considers a north-facing slope, with fill to the final grade elevations.		
<input type="checkbox"/> Effective Stress <input checked="" type="checkbox"/> Total Stress	<input checked="" type="checkbox"/> Static <input type="checkbox"/> Seismic	<input type="checkbox"/> Pore Pressure	<input checked="" type="checkbox"/> Optimized Surface
Additional Details:	The friction angle of the liner system was set equal to the required minimum interface friction angle determined from the liner stability analysis performed on Cross Section B		

Material	Name	Color in Profile	Unit Wt(s) (pcf)	Strength ϕ or δ (deg.)	Strength C or Ca (psf)
1	Final Cover	Orange	130	0	1500
2	Existing Waste	Teal	86	34	0
3	New Waste	Light Green	103	26	300
4	Upper Clay	Brown	131	0	2150
5	Middle Clay	Yellow	136	0	3300
6	Lower Clay	Maroon	133	0.22 σ_v	
7	Silt	Blue	125	28	0
8	Sand	Red	115	32	0
8	Liner System	Magenta	120	10.7	0

Source of Geometry:	Engineering Drawing Set
Source of Subsurface Profile:	Basis of Design Report - NTH (2012)
<input type="checkbox"/> Preconstruction <input type="checkbox"/> Construction <input type="checkbox"/> Interim <input checked="" type="checkbox"/> Final <input type="checkbox"/> Existing <input type="checkbox"/> Back-Analysis	
Construction Phase Represented:	Final build out
Other Geometry Notes:	Cross Section E-E'

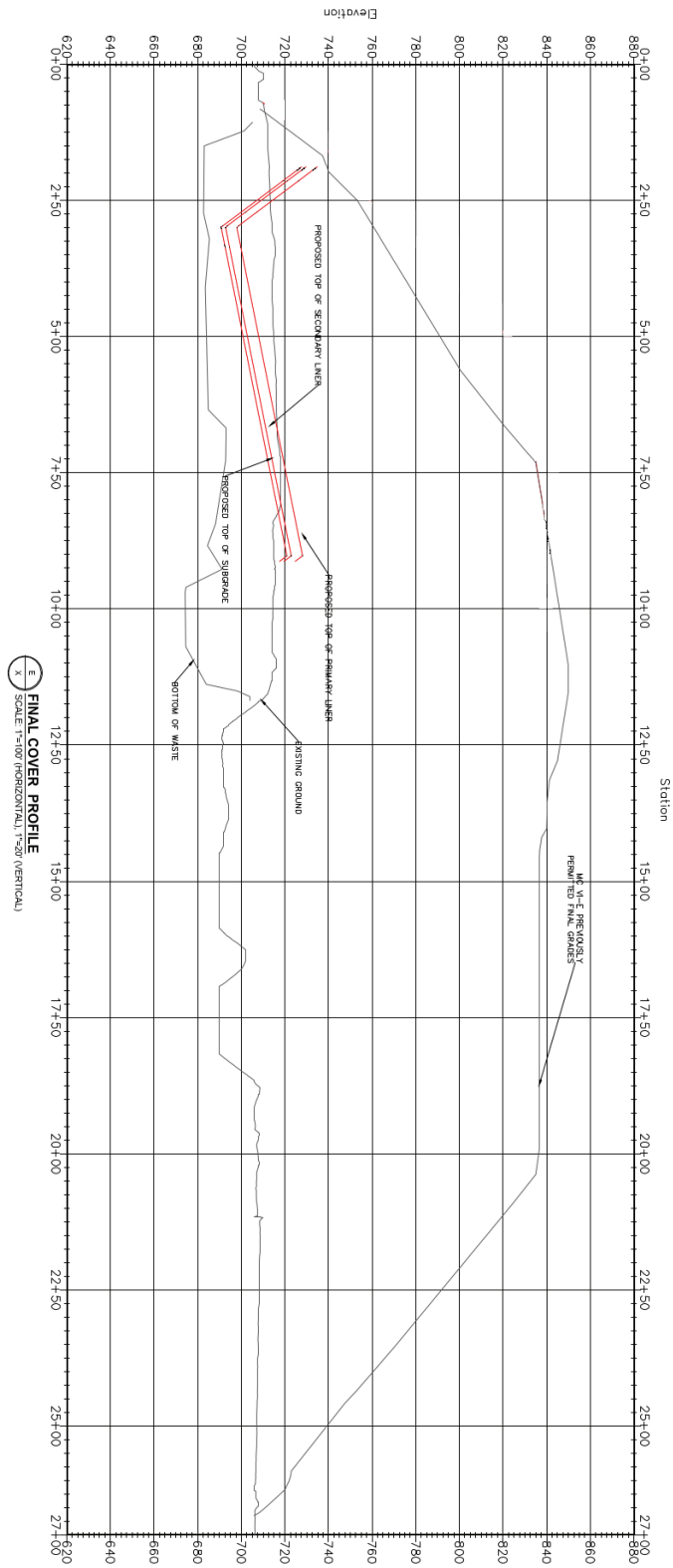
SLOPE STABILITY ANALYSIS REPORT FORM

Final Grades Cross-Section (plan):



SLOPE STABILITY ANALYSIS REPORT FORM

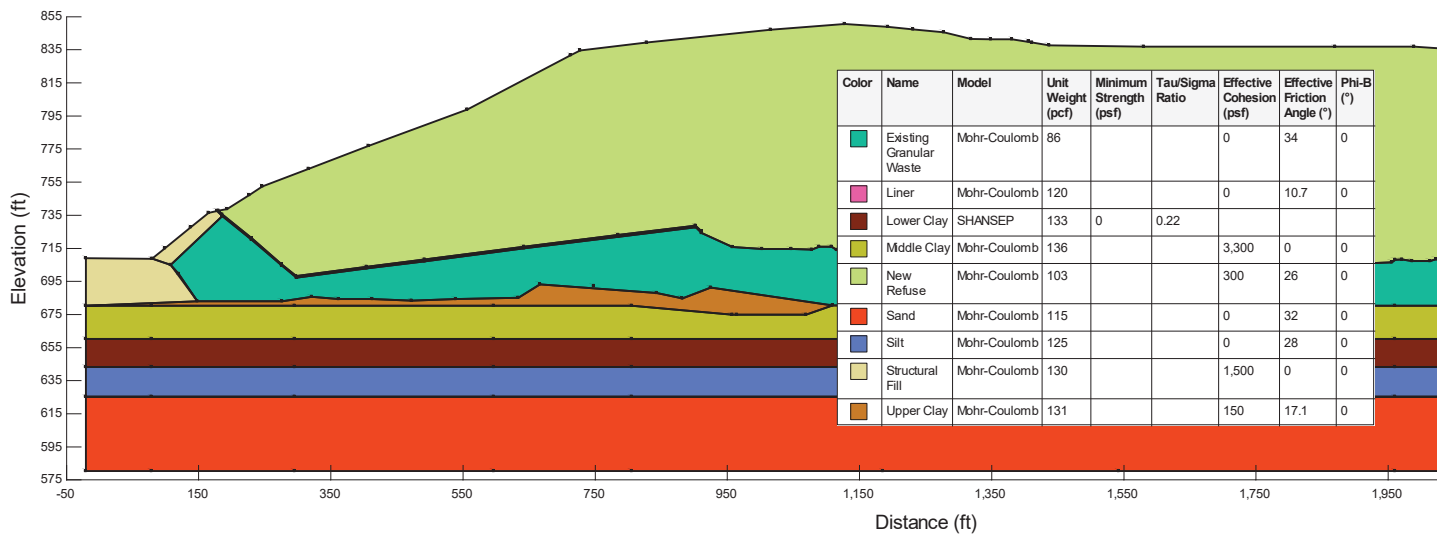
Final Grades Cross-Section (profile):



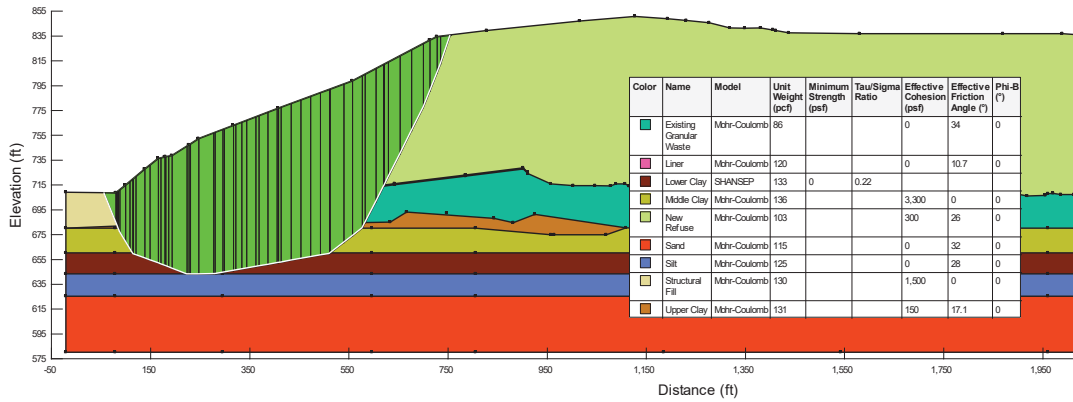
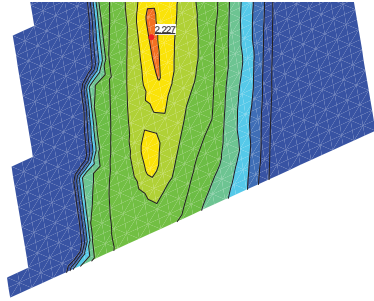
SLOPE STABILITY ANALYSIS REPORT FORM

Factor of Safety:	2.23	<input checked="" type="checkbox"/> Acceptable	<input type="checkbox"/> Not Acceptable	<input type="checkbox"/> Follow-up	<input type="checkbox"/> Superseded
Comments:					
Attachments:	Slope/W Cross Section and Results				

SLOPE STABILITY ANALYSIS REPORT FORM



SLOPE STABILITY ANALYSIS REPORT FORM



Attachment B-1.3

B-B' Liner Stability under Final Conditions with zero adhesion

SLOPE STABILITY ANALYSIS REPORT FORM

SLOPE STABILITY ANALYSIS REPORT FORM

Project Name:	WDI MC6F Permit Modification						
Project Number:	1208070039.004	Client:	Wayne Disposal, Inc.				
Analysis Short Name:	B-B' Liner Stability			File name:	WDI Cross Section B Liner_20201123_RevD_MK.gsz		
Revision:	1	Originated:	MK	Checked:	KF	Approved:	
Date:	11/23/20	Date:	11/23/20	Date:	11/23/20	Date:	

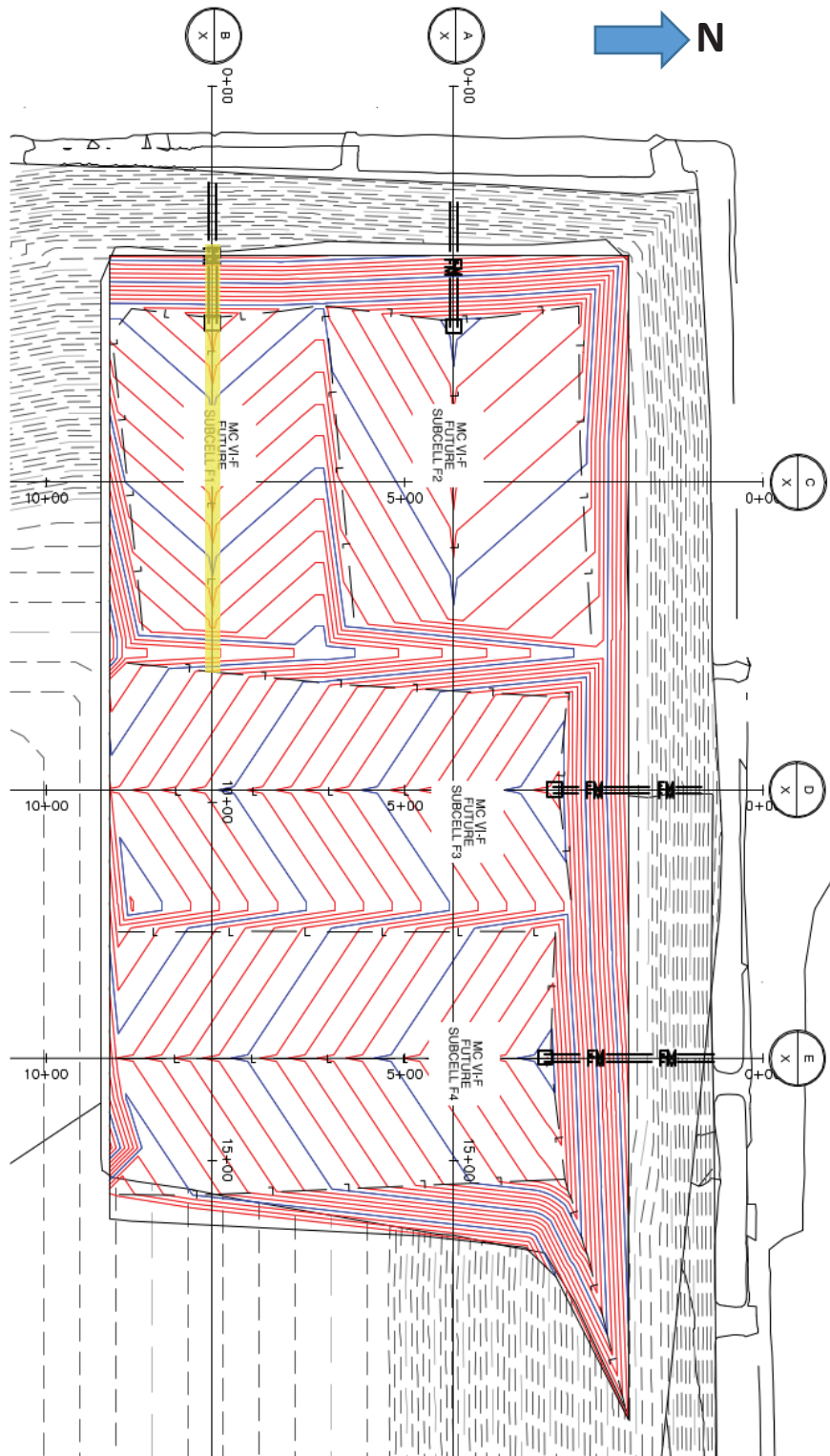
Purpose of Analysis:	To determine the required liner system interface strength to achieve an acceptable factor of safety of the proposed final waste grades using cross-section B. This case considers a west-facing slope, with fill to the final permitted grade elevations. The failure surface is defined such that failure occurs in the underlying liner in order to consider the stability of the liner.		
<input type="checkbox"/> Effective Stress <input checked="" type="checkbox"/> Total Stress	<input checked="" type="checkbox"/> Static <input type="checkbox"/> Seismic	<input type="checkbox"/> Pore Pressure	<input checked="" type="checkbox"/> Optimized Surface
Additional Details:	The liner system was modeled in 2 sections (floor and sideslope) to allow use of Peak and Large-Displacement strength parameters appropriately. The friction angle of the sideslope was set at 7° corresponding to commonly achievable large-displacement interface secant friction angle. The friction angle of the floor liner system was varied to determine the required peak interface secant friction angle to achieve the required factor of safety of 1.5.		

Material	Name	Color in Profile	Unit Wt(s) (pcf)	Strength ϕ or δ (deg.)	Strength C or Ca (psf)
1	Final Cover	Orange	130	0	1500
2	Existing Waste	Teal	86	34	0
3	New Waste	Light Green	103	26	300
4	Upper Clay	Brown	131	0	2150
5	Middle Clay	Yellow	136	0	3300
6	Lower Clay	Maroon	133	0.22 σ_v	
7	Silt	Blue	125	28	0
8	Sand	Red	115	32	0
9	Liner (Floor)	Magenta	120	TBD	0
10	Liner (Sideslope)	Purple	120	7	0

Source of Geometry:	Engineering Drawing Set
Source of Subsurface Profile:	Basis of Design Report - NTH (2012)
	<input type="checkbox"/> Preconstruction <input type="checkbox"/> Construction <input type="checkbox"/> Interim <input checked="" type="checkbox"/> Final <input type="checkbox"/> Existing <input type="checkbox"/> Back-Analysis
Construction Phase Represented:	Final build out
Other Geometry Notes:	Cross Section B

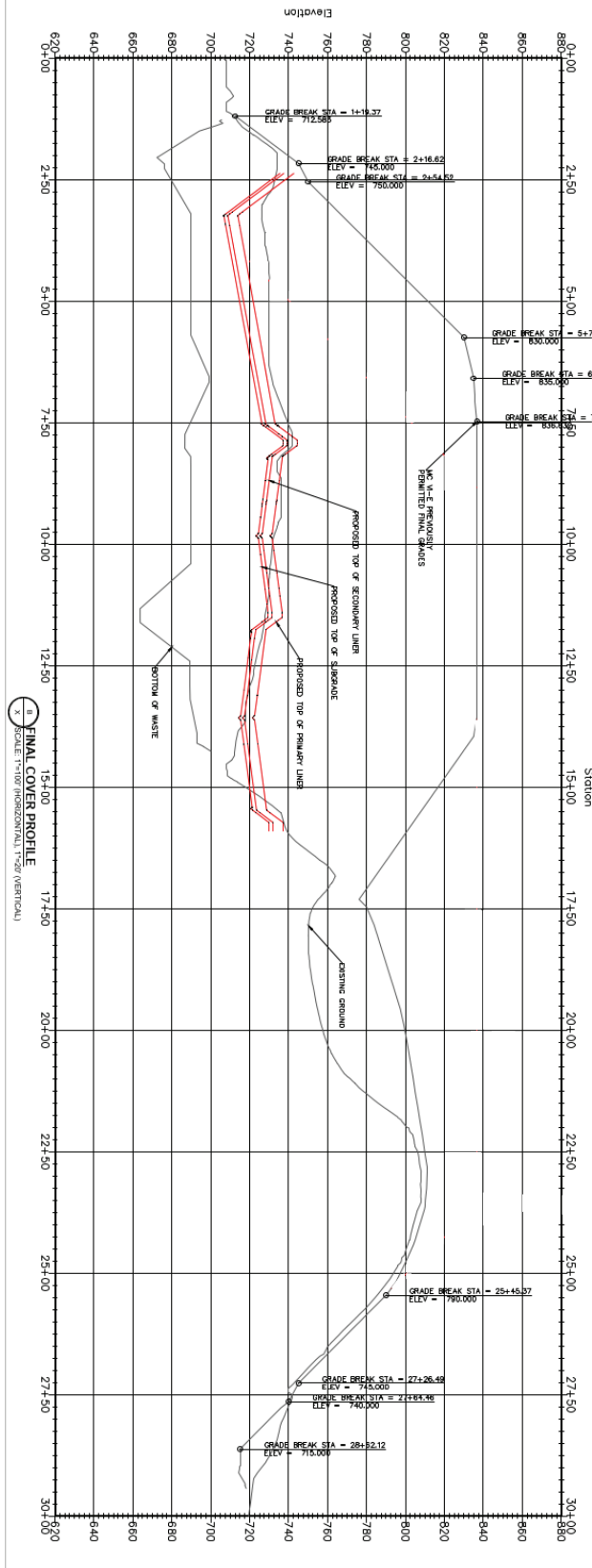
SLOPE STABILITY ANALYSIS REPORT FORM

Final Grades Cross-Section (plan):



SLOPE STABILITY ANALYSIS REPORT FORM

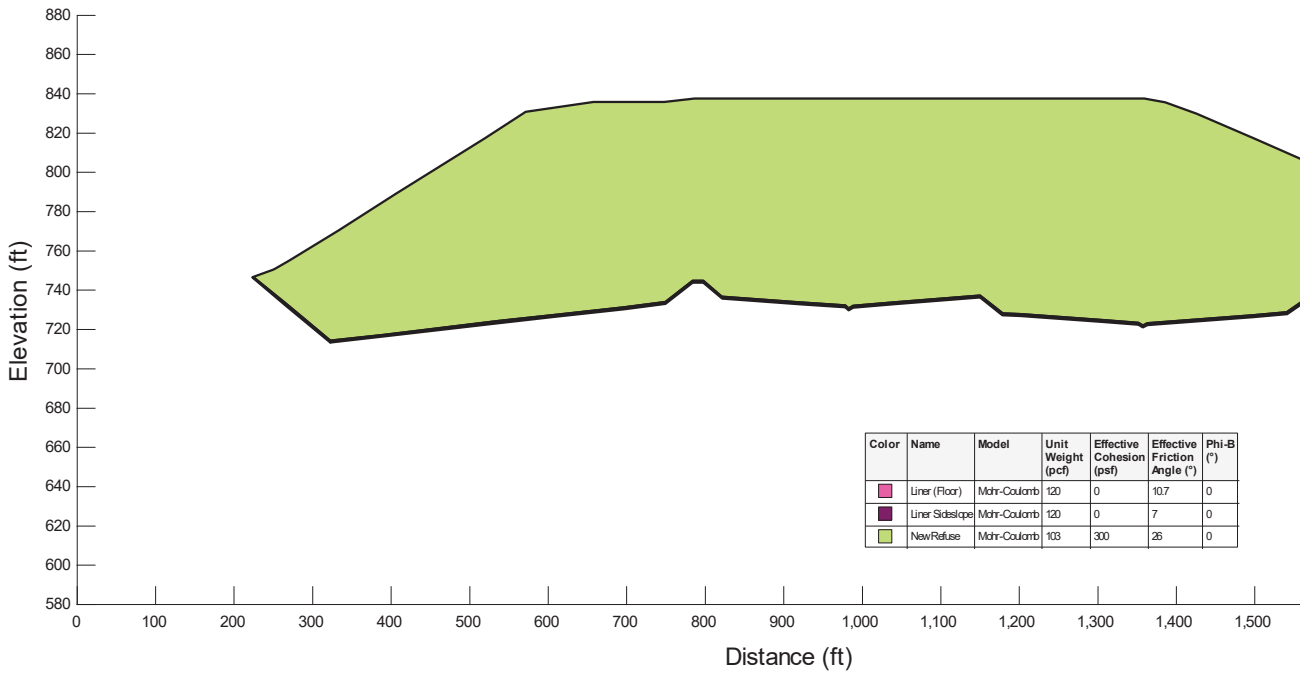
Final Grades Cross-Section (profile):



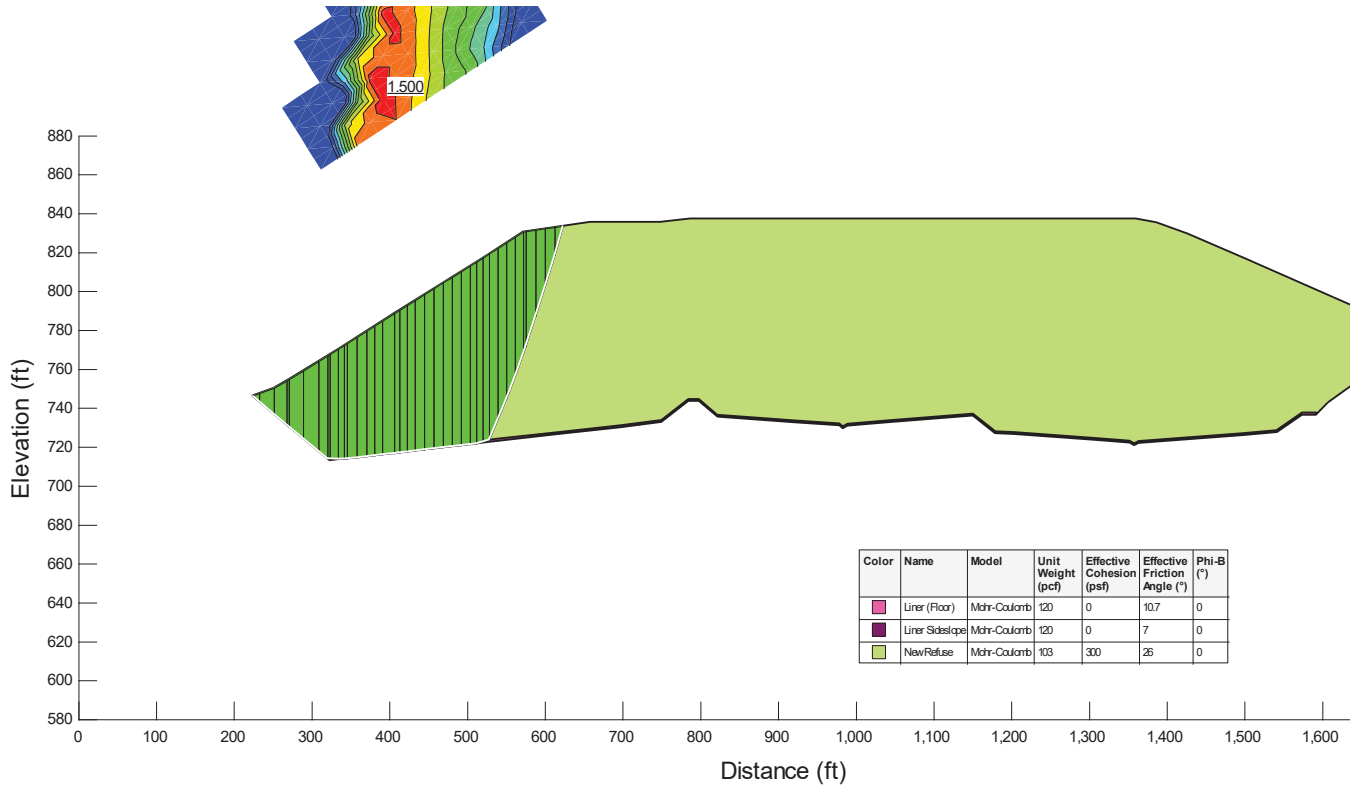
SLOPE STABILITY ANALYSIS REPORT FORM

Factor of Safety:	1.50	<input checked="" type="checkbox"/> Acceptable	<input type="checkbox"/> Not Acceptable	<input type="checkbox"/> Follow-up	<input type="checkbox"/> Superseded
Comments:	The required peak interface friction for the floor liner system was determined to be 10.7°.				
Attachments:	Slope/W Cross Section and Results				

SLOPE STABILITY ANALYSIS REPORT FORM



SLOPE STABILITY ANALYSIS REPORT FORM



Attachment B-1.4

E-E' Liner Stability under Final Conditions with zero adhesion

SLOPE STABILITY ANALYSIS REPORT FORM

SLOPE STABILITY ANALYSIS REPORT FORM

Project Name:	WDI MC6F Permit Modification						
Project Number:	1208070039.004	Client:	Wayne Disposal, Inc.				
Analysis Short Name:	E-E' Liner Stability			File name:	WDI Cross Section E Liner_20201123_RevC_MK.gsz		
Revision:	1	Originated:	MK	Checked:	KF	Approved:	
Date:	11/23/20	Date:	11/23/20	Date:	11/23/20	Date:	

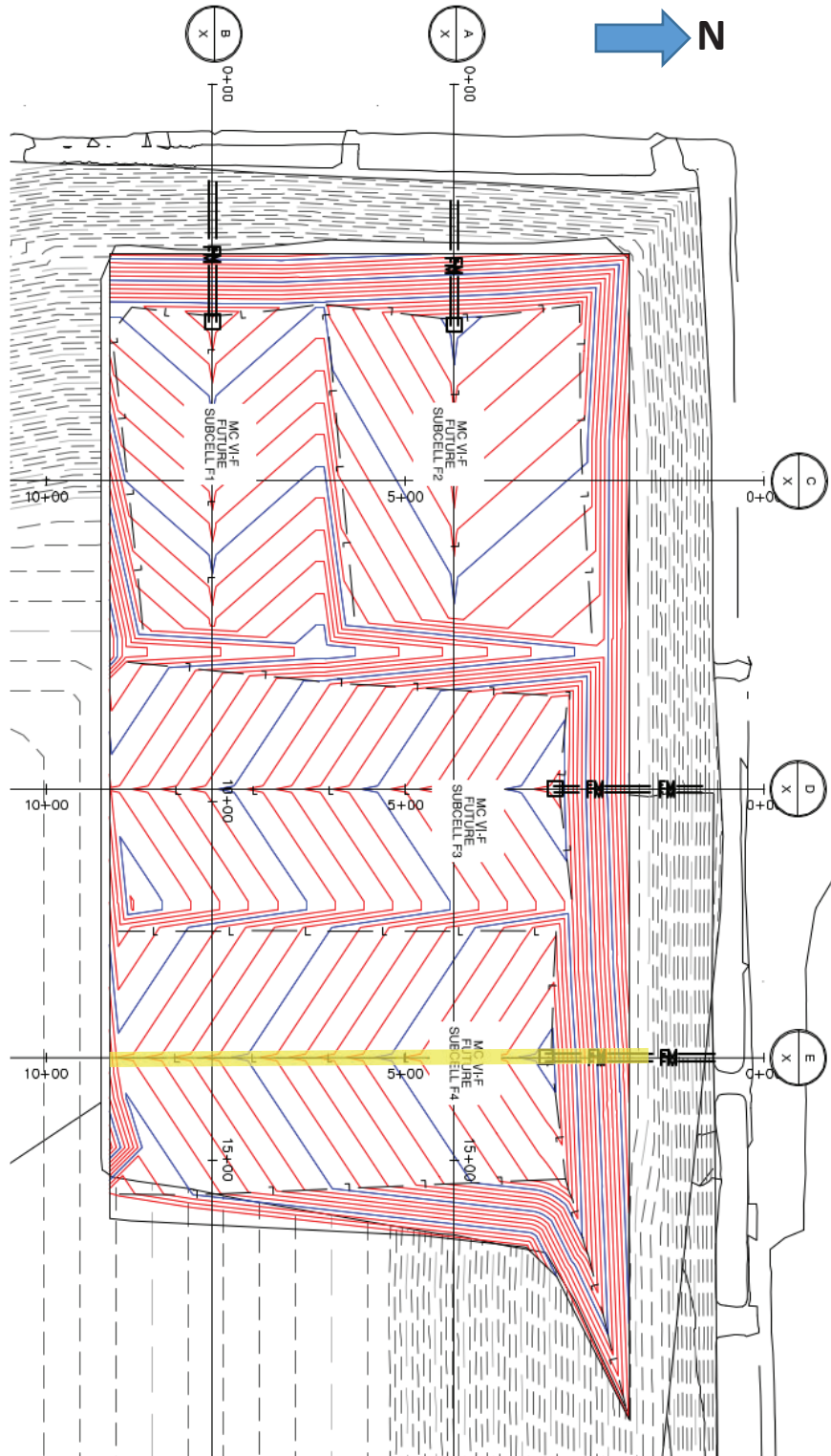
Purpose of Analysis:	To determine the factor of safety of the proposed final waste grades using cross-section E. This case considers a north-facing slope, with fill to the final grade elevations. The failure surface is defined such that failure occurs in the underlying liner in order to consider the stability of the liner.		
<input type="checkbox"/> Effective Stress <input checked="" type="checkbox"/> Total Stress	<input checked="" type="checkbox"/> Static <input type="checkbox"/> Seismic	<input type="checkbox"/> Pore Pressure	<input checked="" type="checkbox"/> Optimized Surface
Additional Details:	The friction angle of the liner system was set equal to the required minimum interface friction angle determined from the liner stability analysis performed on Cross Section B. The liner system was modeled in 2 sections (floor and sideslope) to allow use of Peak and Large-Displacement strength parameters appropriately.		

Material	Name	Color in Profile	Unit Wt(s) (pcf)	Strength ϕ or δ (deg.)	Strength C or Ca (psf)
1	Final Cover	Orange	130	0	1500
2	Existing Waste	Teal	86	34	0
3	New Waste	Light Green	103	26	300
4	Upper Clay	Brown	131	0	2150
5	Middle Clay	Yellow	136	0	3300
6	Lower Clay	Maroon	133	0.22 σ_v	
7	Silt	Blue	125	28	0
8	Sand	Red	115	32	0
9	Liner (Floor)	Magenta	120	10.7	0
10	Liner (Sideslope)	Purple	120	7	0

Source of Geometry:	Engineering Drawing Set
Source of Subsurface Profile:	Basis of Design Report - NTH (2012)
<input type="checkbox"/> Preconstruction <input type="checkbox"/> Construction <input type="checkbox"/> Interim <input checked="" type="checkbox"/> Final <input type="checkbox"/> Existing <input type="checkbox"/> Back-Analysis	
Construction Phase Represented:	Final build out
Other Geometry Notes:	Cross Section E

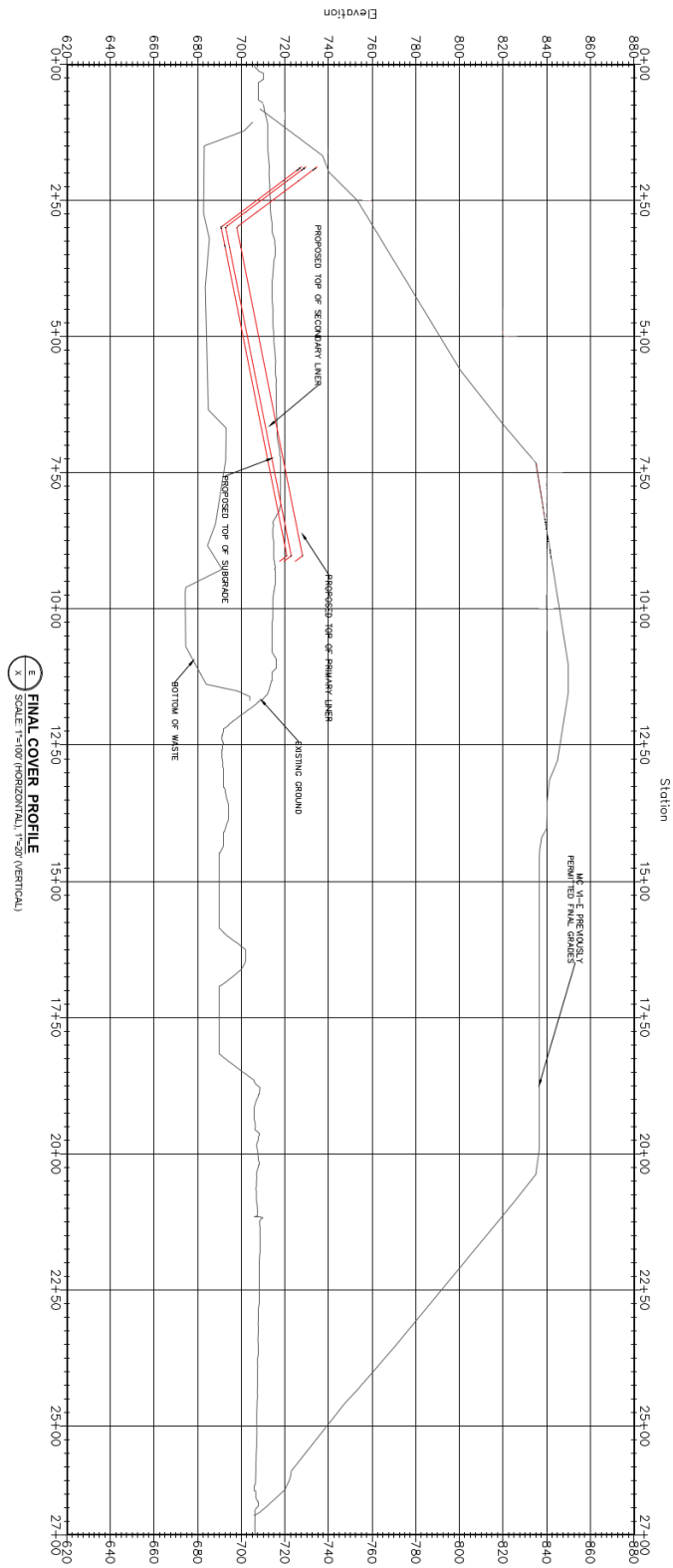
SLOPE STABILITY ANALYSIS REPORT FORM

Final Grades Cross-Section (plan):



SLOPE STABILITY ANALYSIS REPORT FORM

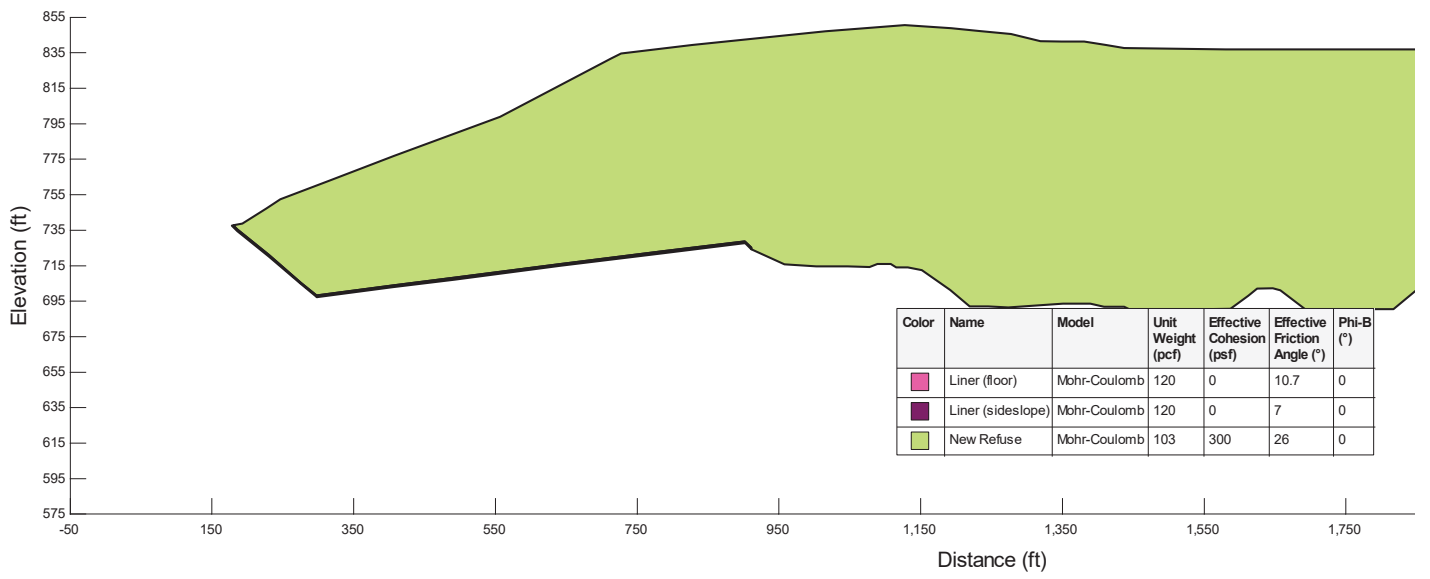
Final Grades Cross-Section (profile):



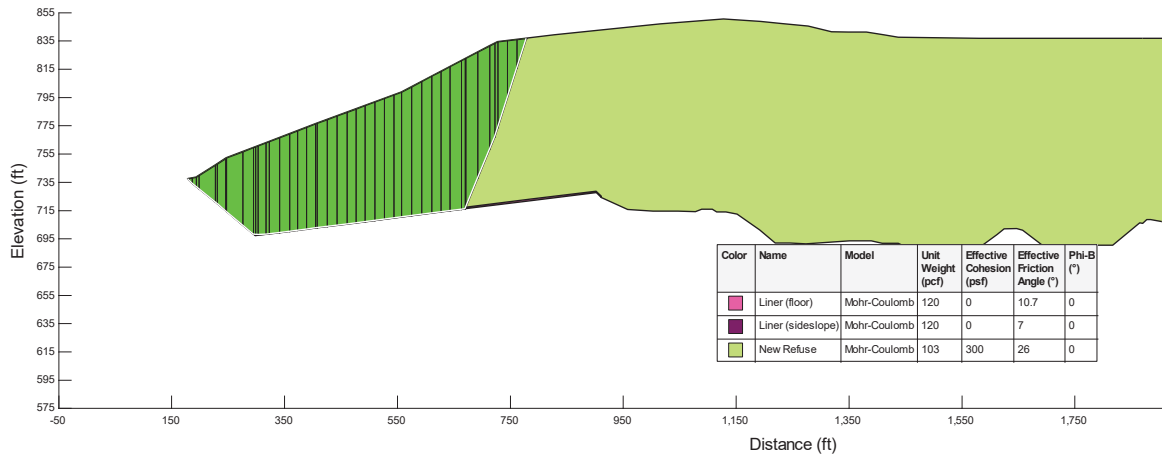
SLOPE STABILITY ANALYSIS REPORT FORM

Factor of Safety:	1.77	<input checked="" type="checkbox"/> Acceptable	<input type="checkbox"/> Not Acceptable	<input type="checkbox"/> Follow-up	<input type="checkbox"/> Superseded
Comments:					
Attachments:	Slope/W Cross Section and Results				

SLOPE STABILITY ANALYSIS REPORT FORM



SLOPE STABILITY ANALYSIS REPORT FORM



Attachment B-1.5

B-B' Liner Stability under Final Conditions with non-zero adhesion (previously tested values)

SLOPE STABILITY ANALYSIS REPORT FORM

SLOPE STABILITY ANALYSIS REPORT FORM

Project Name:	WDI MC6F Permit Modification						
Project Number:	1208070039.004		Client:	Wayne Disposal, Inc.			
Analysis Short Name:	B-B' Liner Stability with tested interface strength parameters			File name:	WDI Cross Section B Liner_20201123_RevC_MK_c_phi_combo		
Revision:	1	Originated:	MK	Checked:	KF	Approved:	
Date:	11/23/20	Date:	11/23/20	Date:	11/23/20	Date:	

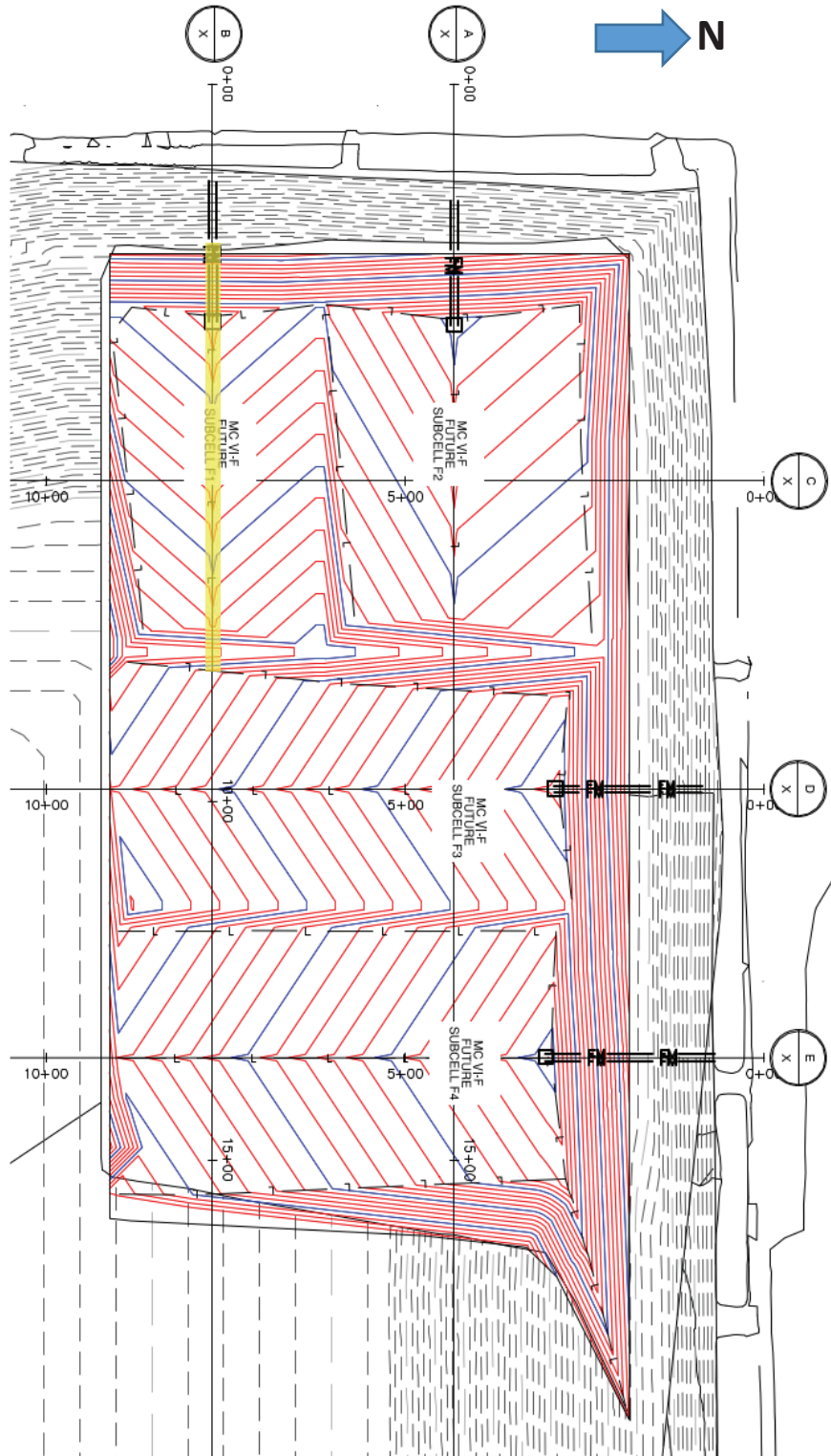
Purpose of Analysis:	To determine the factor of safety of the proposed final waste grades using cross-section B. This case considers a west-facing slope, with fill to the final permitted grade elevations. The failure surface is defined such that failure occurs in the underlying liner in order to consider the stability of the liner. The liner interface strength properties are based on interface strength test results of a similar liner system installed on site.		
<input type="checkbox"/> Effective Stress <input checked="" type="checkbox"/> Total Stress	<input checked="" type="checkbox"/> Static <input type="checkbox"/> Seismic	<input type="checkbox"/> Pore Pressure	<input checked="" type="checkbox"/> Optimized Surface
Additional Details:	The liner system was modeled in 2 sections (floor and sideslope) to allow use of Peak and Large-Displacement strength parameters appropriately. The required factor of safety is 1.5.		

Material	Name	Color in Profile	Unit Wt(s) (pcf)	Strength ϕ or δ (deg.)	Strength C or Ca (psf)
1	Final Cover	Orange	130	0	1500
2	Existing Waste	Teal	86	34	0
3	New Waste	Light Green	103	26	300
4	Upper Clay	Brown	131	0	2150
5	Middle Clay	Yellow	136	0	3300
6	Lower Clay	Maroon	133	$0.22\sigma_v$	
7	Silt	Blue	125	28	0
8	Sand	Red	115	32	0
9	Liner (Floor)	Magenta	120	11.1	164
10	Liner (Sideslope)	Purple	120	7.3	110

Source of Geometry:	Engineering Drawing Set
Source of Subsurface Profile:	Basis of Design Report - NTH (2012)
	<input type="checkbox"/> Preconstruction <input type="checkbox"/> Construction <input type="checkbox"/> Interim <input checked="" type="checkbox"/> Final <input type="checkbox"/> Existing <input type="checkbox"/> Back-Analysis
Construction Phase Represented:	Final build out
Other Geometry Notes:	Cross Section B

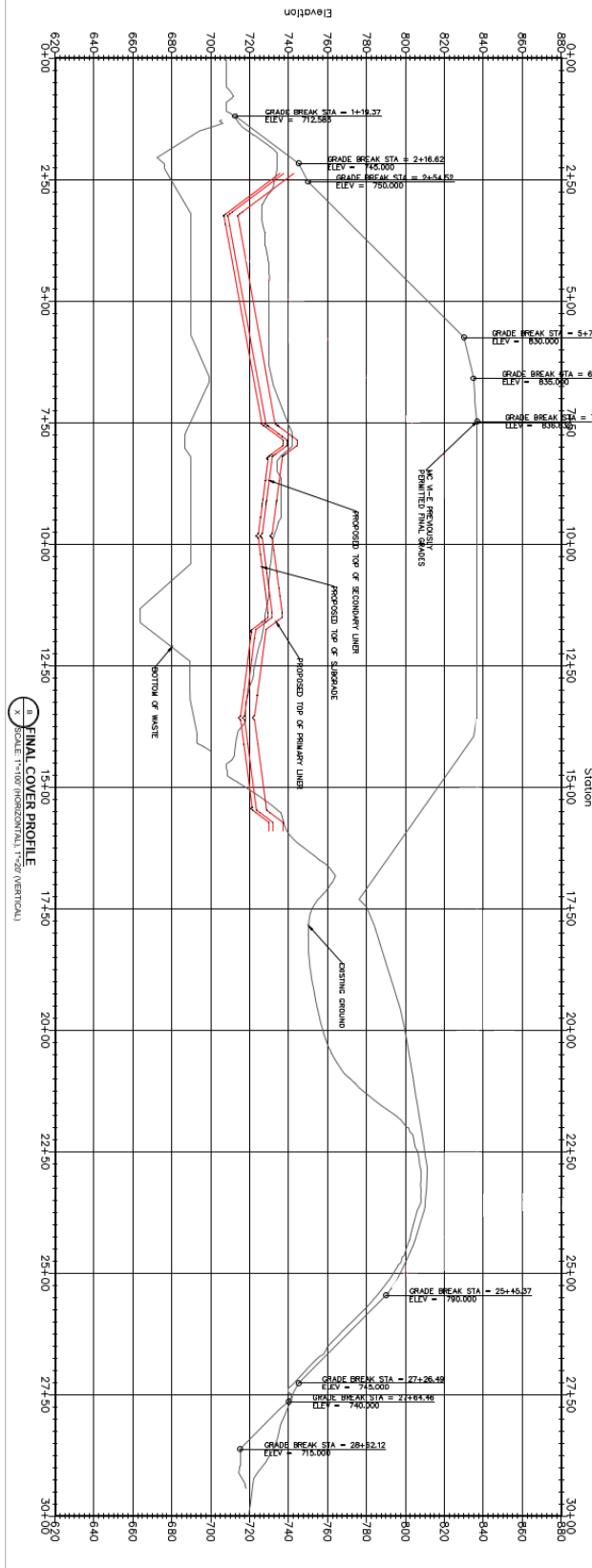
SLOPE STABILITY ANALYSIS REPORT FORM

Final Grades Cross-Section (plan):



SLOPE STABILITY ANALYSIS REPORT FORM

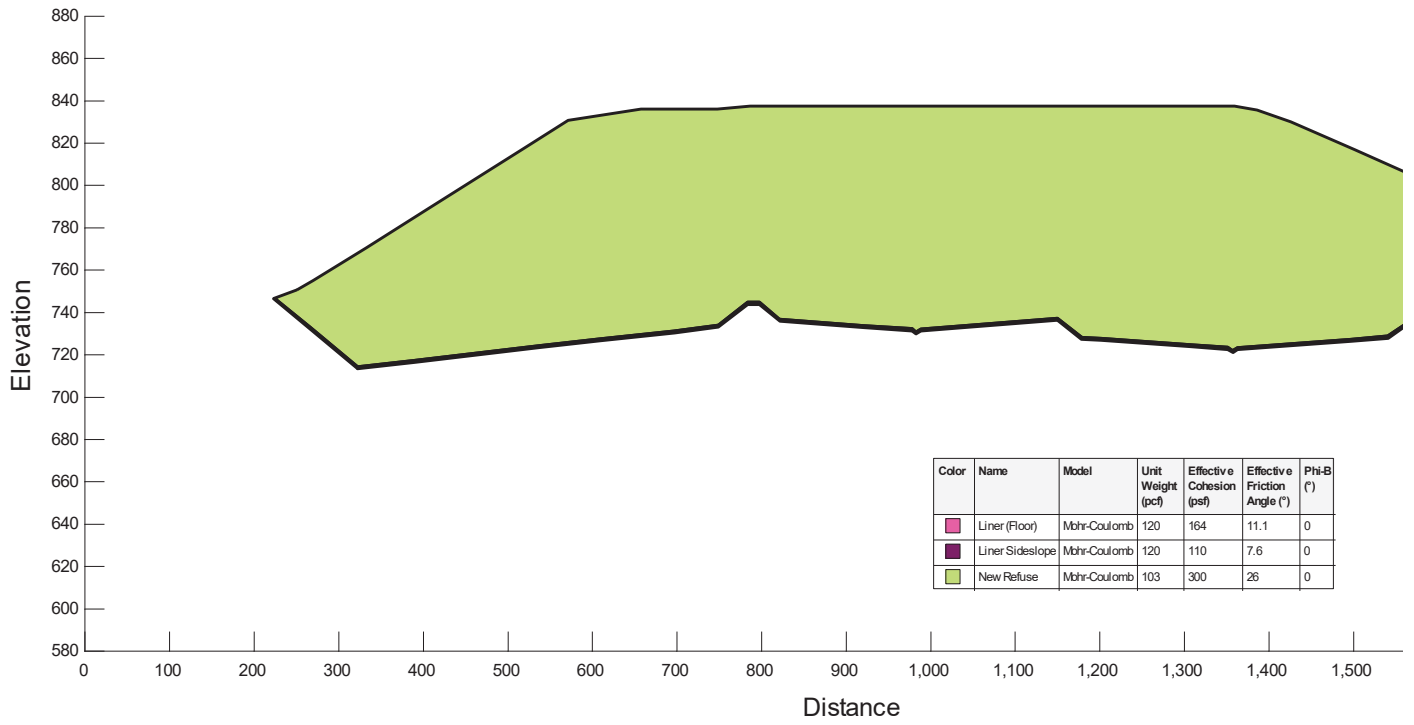
Final Grades Cross-Section (profile):



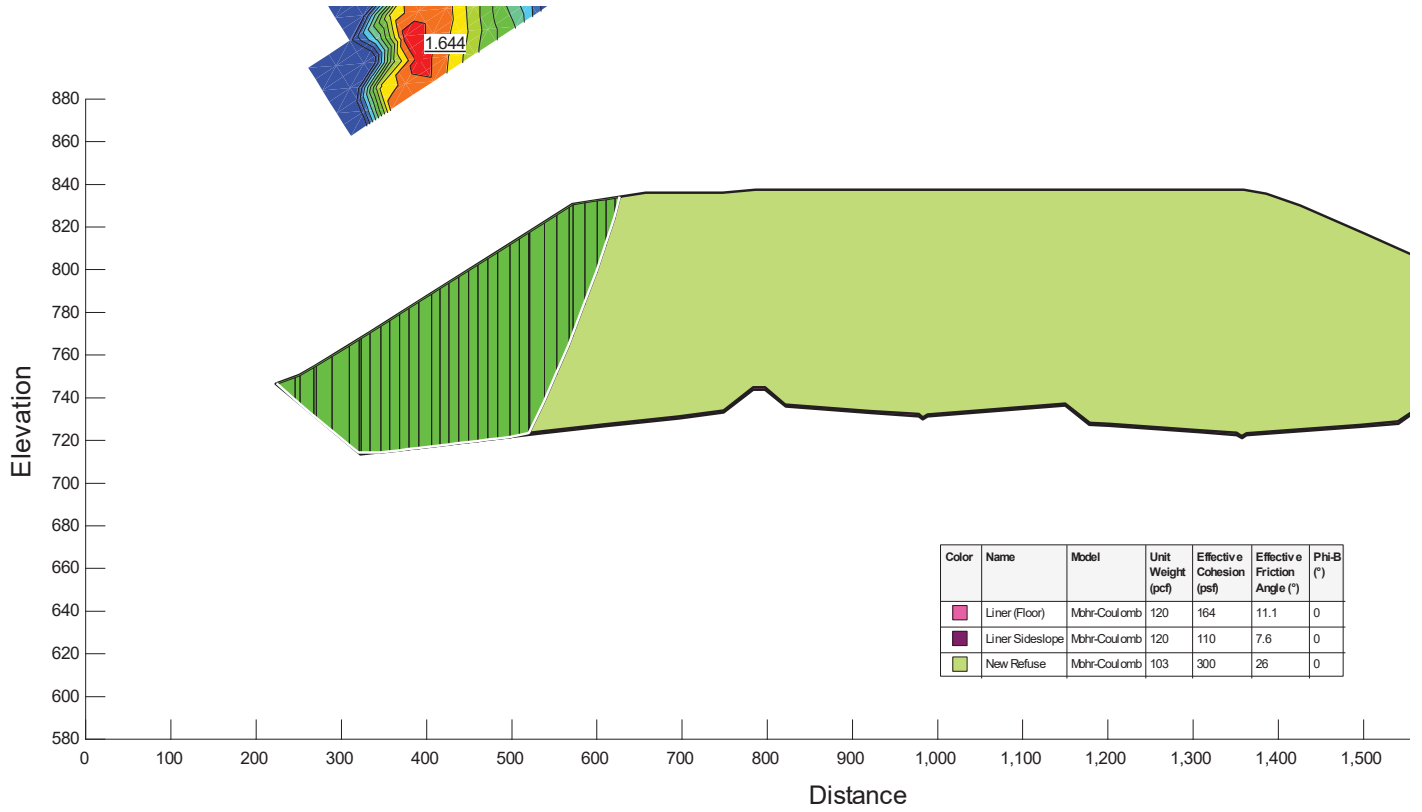
SLOPE STABILITY ANALYSIS REPORT FORM

Factor of Safety:	1.64	<input checked="" type="checkbox"/> Acceptable	<input type="checkbox"/> Not Acceptable	<input type="checkbox"/> Follow-up	<input type="checkbox"/> Superseded
Comments:					
Attachments:	Slope/W Cross Section and Results				

SLOPE STABILITY ANALYSIS REPORT FORM



SLOPE STABILITY ANALYSIS REPORT FORM



Attachment B-1.6

E-E' Liner Stability under Final Conditions with non-zero adhesion (previously tested values)

SLOPE STABILITY ANALYSIS REPORT FORM

SLOPE STABILITY ANALYSIS REPORT FORM

Project Name:	WDI MC6F Permit Modification						
Project Number:	1208070039.004	Client:	Wayne Disposal, Inc.				
Analysis Short Name:	E-E' Liner Stability			File name:	WDI Cross Section E Liner_20201123_RevC_MK_c_phi_combo.gsz		
Revision:	1	Originated:	MK	Checked:	KF	Approved:	
Date:	11/23/20	Date:	11/23/20	Date:	11/23/20	Date:	

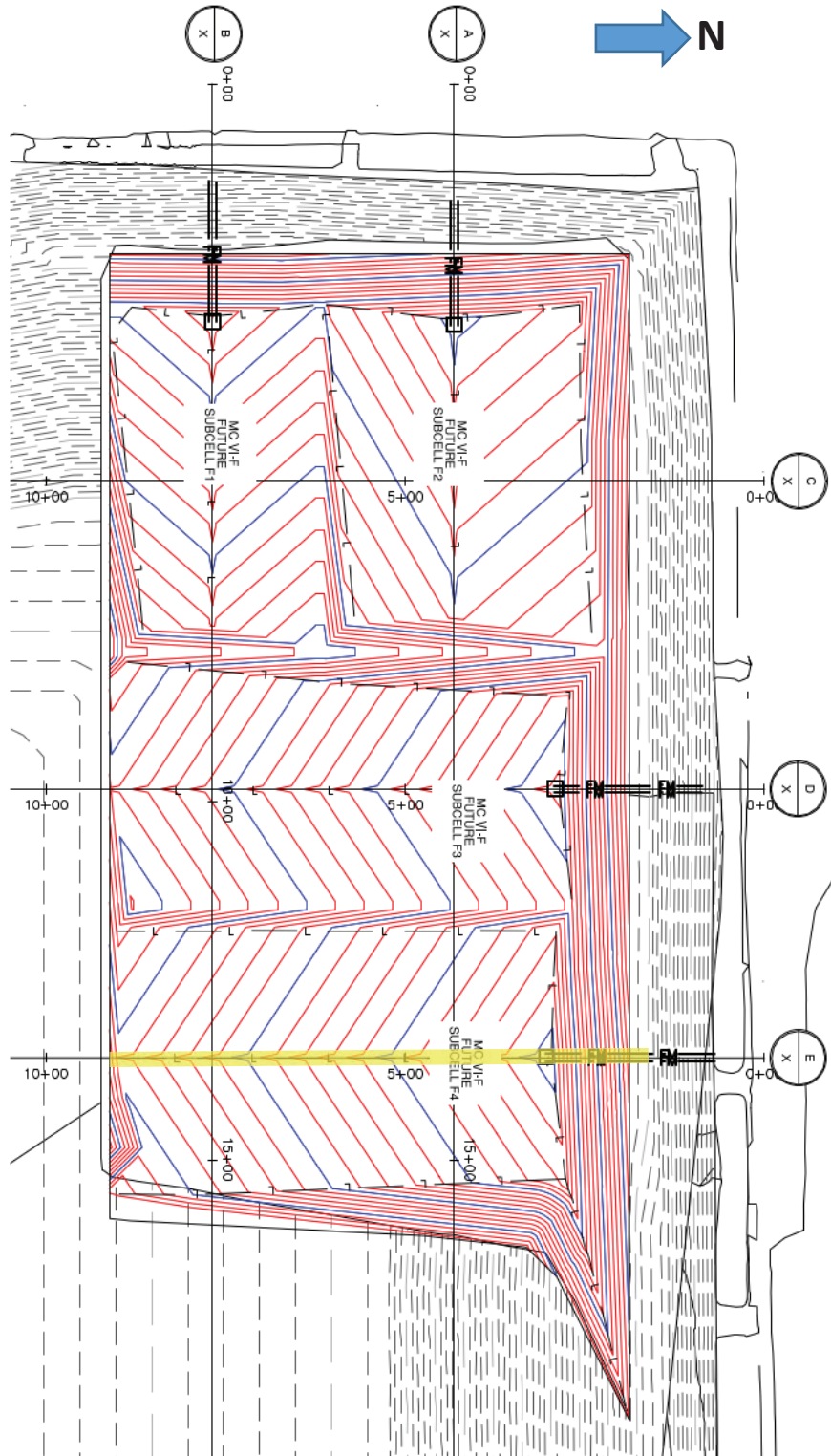
Purpose of Analysis:	To determine the factor of safety of the proposed final waste grades using cross-section E. This case considers a north-facing slope, with fill to the final grade elevations. The failure surface is defined such that failure occurs in the underlying liner in order to consider the stability of the liner. The liner interface strength properties are based on interface strength test results of a similar liner system installed on site.		
<input type="checkbox"/> Effective Stress <input checked="" type="checkbox"/> Total Stress	<input checked="" type="checkbox"/> Static <input type="checkbox"/> Seismic	<input type="checkbox"/> Pore Pressure	<input checked="" type="checkbox"/> Optimized Surface
Additional Details:	The liner system was modeled in 2 sections (floor and sideslope) to allow use of Peak and Large-Displacement strength parameters appropriately. The required factor of safety is 1.5.		

Material	Name	Color in Profile	Unit Wt(s) (pcf)	Strength ϕ or δ (deg.)	Strength C or Ca (psf)
1	Final Cover	Orange	130	0	1500
2	Existing Waste	Teal	86	34	0
3	New Waste	Light Green	103	26	300
4	Upper Clay	Brown	131	0	2150
5	Middle Clay	Yellow	136	0	3300
6	Lower Clay	Maroon	133	0.22 σ_v	
7	Silt	Blue	125	28	0
8	Sand	Red	115	32	0
9	Liner (Floor)	Magenta	120	11.1	164
10	Liner (Sideslope)	Purple	120	7.3	110

Source of Geometry:	Engineering Drawing Set
Source of Subsurface Profile:	Basis of Design Report - NTH (2012)
<input type="checkbox"/> Preconstruction <input type="checkbox"/> Construction <input type="checkbox"/> Interim <input checked="" type="checkbox"/> Final <input type="checkbox"/> Existing <input type="checkbox"/> Back-Analysis	
Construction Phase Represented:	Final build out
Other Geometry Notes:	Cross Section E

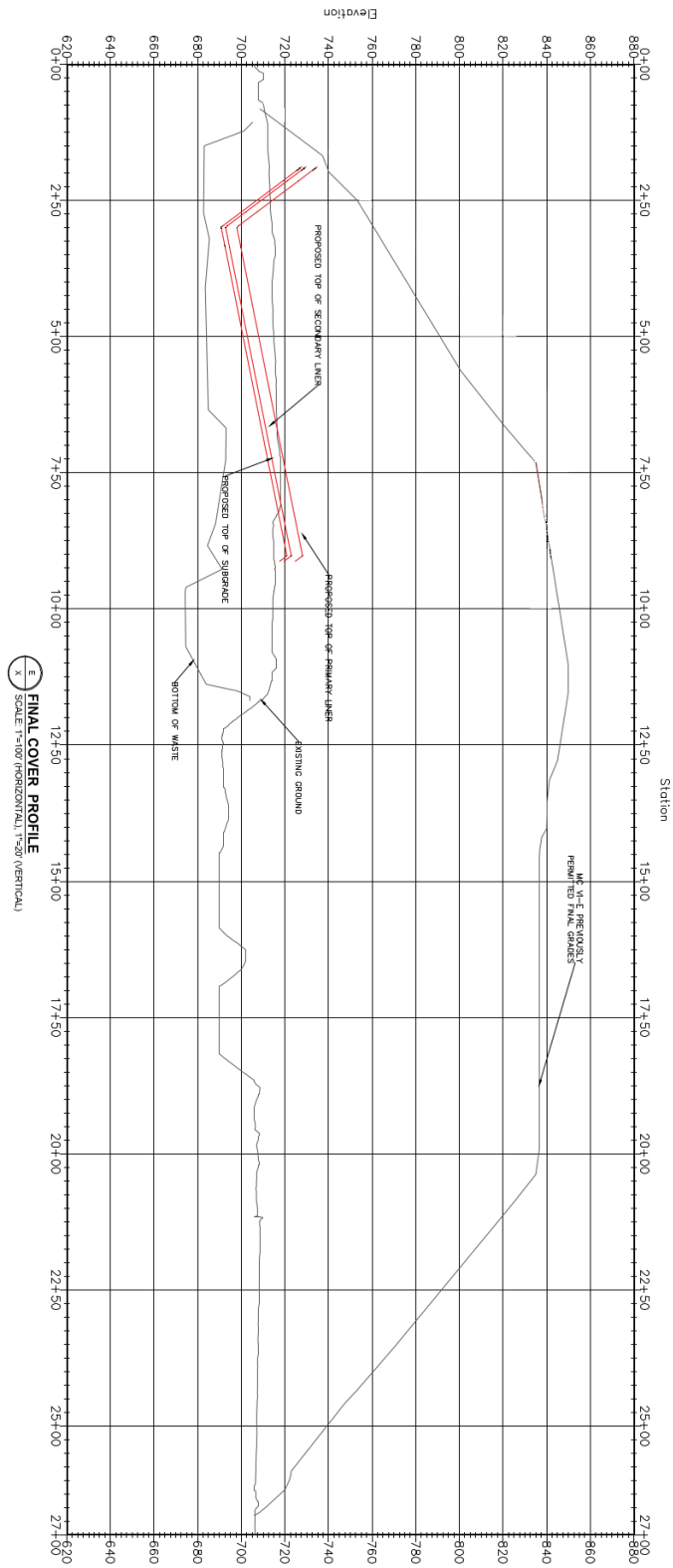
SLOPE STABILITY ANALYSIS REPORT FORM

Final Grades Cross-Section (plan):



SLOPE STABILITY ANALYSIS REPORT FORM

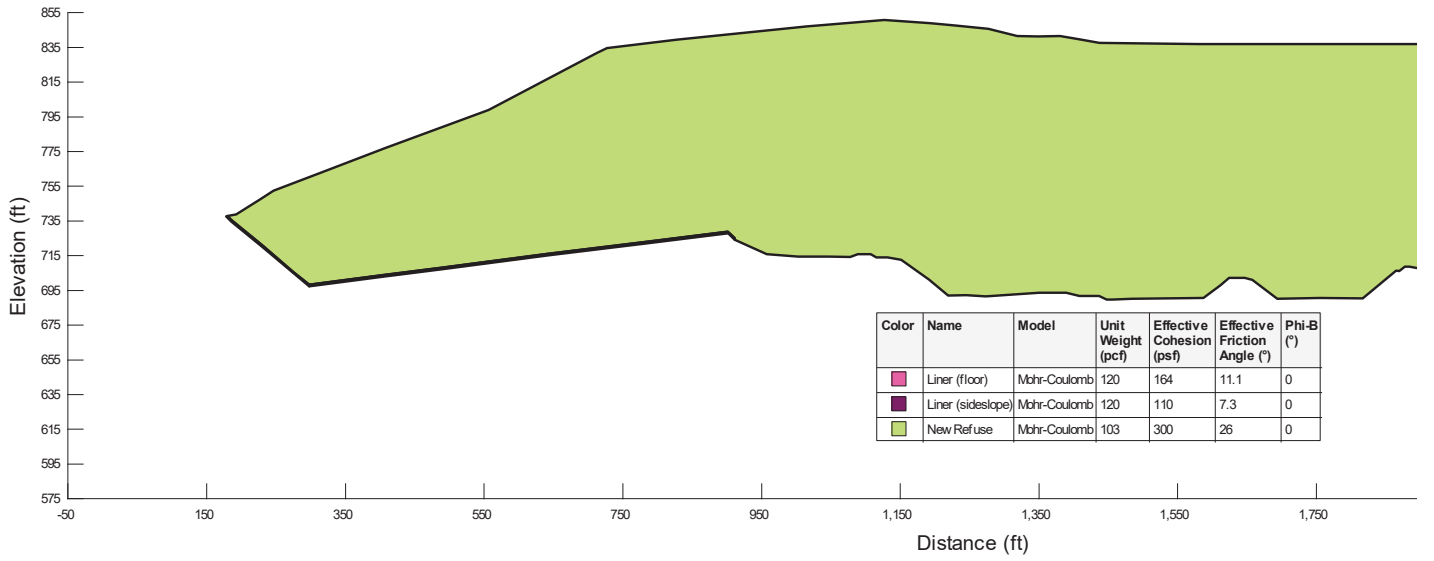
Final Grades Cross-Section (profile):



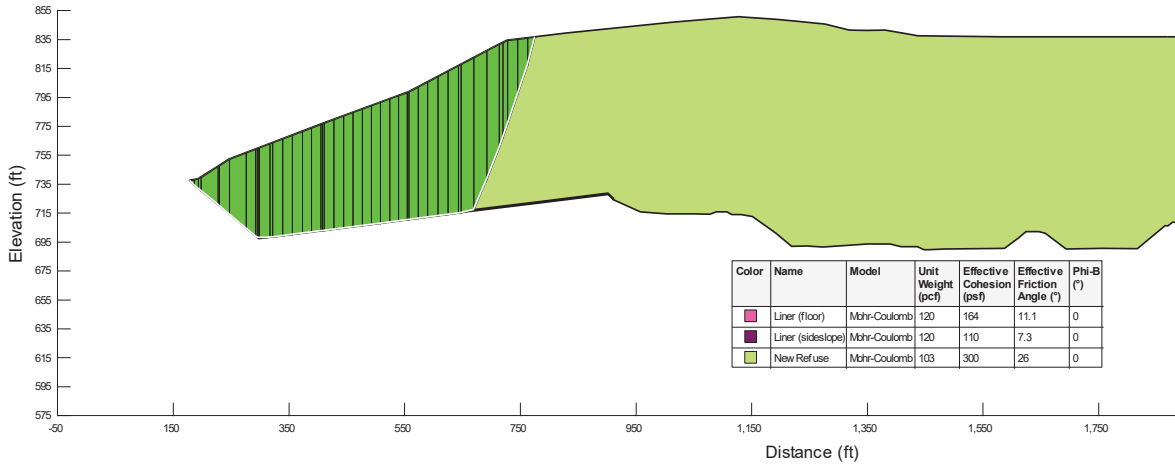
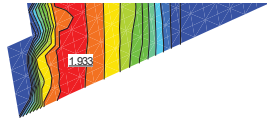
SLOPE STABILITY ANALYSIS REPORT FORM

Factor of Safety:	1.93	<input checked="" type="checkbox"/> Acceptable	<input type="checkbox"/> Not Acceptable	<input type="checkbox"/> Follow-up	<input type="checkbox"/> Superseded
Comments:					
Attachments:	Slope/W Cross Section and Results				

SLOPE STABILITY ANALYSIS REPORT FORM



SLOPE STABILITY ANALYSIS REPORT FORM



Color	Name	Model	Unit Weight (pcf)	Effective Cohesion (psf)	Effective Friction Angle (°)	Phi-B (°)
Light Green	Liner (floor)	Mohr-Coulomb	120	164	11.1	0
Dark Green	Liner (sideslope)	Mohr-Coulomb	120	110	7.3	0
Light Green	New Refuse	Mohr-Coulomb	103	300	26	0

Attachment B-1.7

B-B' Liner Stability under Interim Conditions (example interim stability calculation)

SLOPE STABILITY ANALYSIS REPORT FORM

SLOPE STABILITY ANALYSIS REPORT FORM

Project Name:	WDI MC6F Permit Modification						
Project Number:	1208070039.004	Client:	Wayne Disposal, Inc.				
Analysis Short Name:	B-B' Interim Liner Stability			File name:	WDI Cross Section B Interim_20201119_RevA_MK_3.5H1V.gsz		
Revision:	1	Originated:	MK	Checked:	KF	Approved:	
Date:	11/23/20	Date:	11/23/20	Date:	11/23/20	Date:	

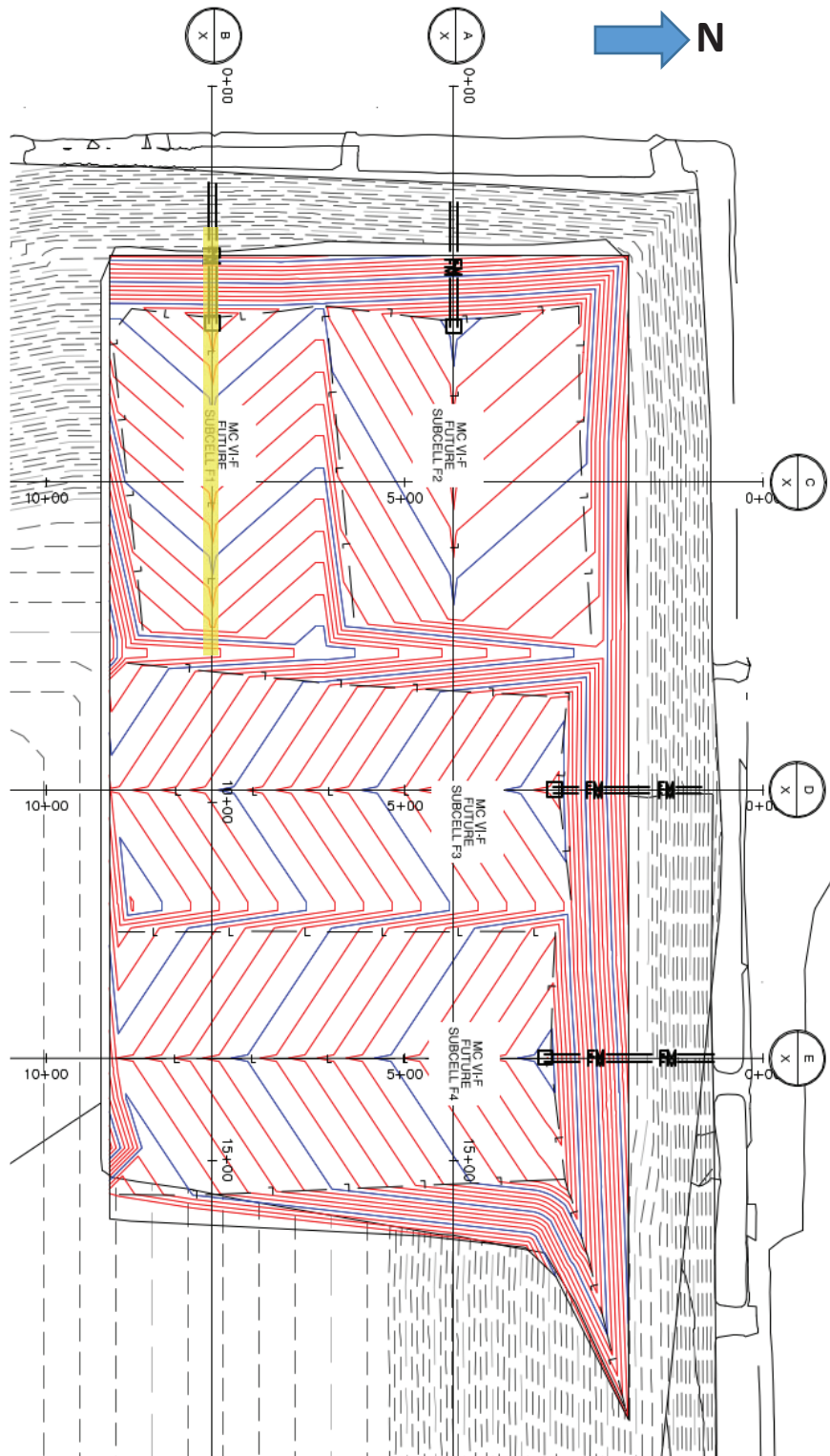
Purpose of Analysis:	To determine the required interface friction angle of the liner system to achieve an acceptable interim factor of safety of 1.3 using cross-section B. This case considers a west-facing slope and models an example interim fill case with waste fill up to the final permitted grade elevations at an interim slope of 3.5H:1V. The failure surface is defined such that failure occurs in the underlying liner in order to consider the stability of the liner.		
<input type="checkbox"/> Effective Stress <input checked="" type="checkbox"/> Total Stress	<input checked="" type="checkbox"/> Static <input type="checkbox"/> Seismic	<input type="checkbox"/> Pore Pressure	<input checked="" type="checkbox"/> Optimized Surface
Additional Details:			

Material	Name	Color in Profile	Unit Wt(s) (pcf)	Strength ϕ or δ (deg.)	Strength C or Ca (psf)
1	Final Cover	Orange	130	0	1500
2	Existing Waste	Teal	86	34	0
3	New Waste	Light Green	103	26	300
4	Upper Clay	Brown	131	0	2150
5	Middle Clay	Yellow	136	0	3300
6	Lower Clay	Maroon	133	0.22 σ_v	
7	Silt	Blue	125	28	0
8	Sand	Red	115	32	0

Source of Geometry:	Engineering Drawing Set
Source of Subsurface Profile:	Basis of Design Report - NTH (2012)
<input type="checkbox"/> Preconstruction <input type="checkbox"/> Construction <input checked="" type="checkbox"/> Interim <input type="checkbox"/> Final <input type="checkbox"/> Existing <input type="checkbox"/> Back-Analysis	
Construction Phase Represented:	Interim waste filling
Other Geometry Notes:	Cross Section B

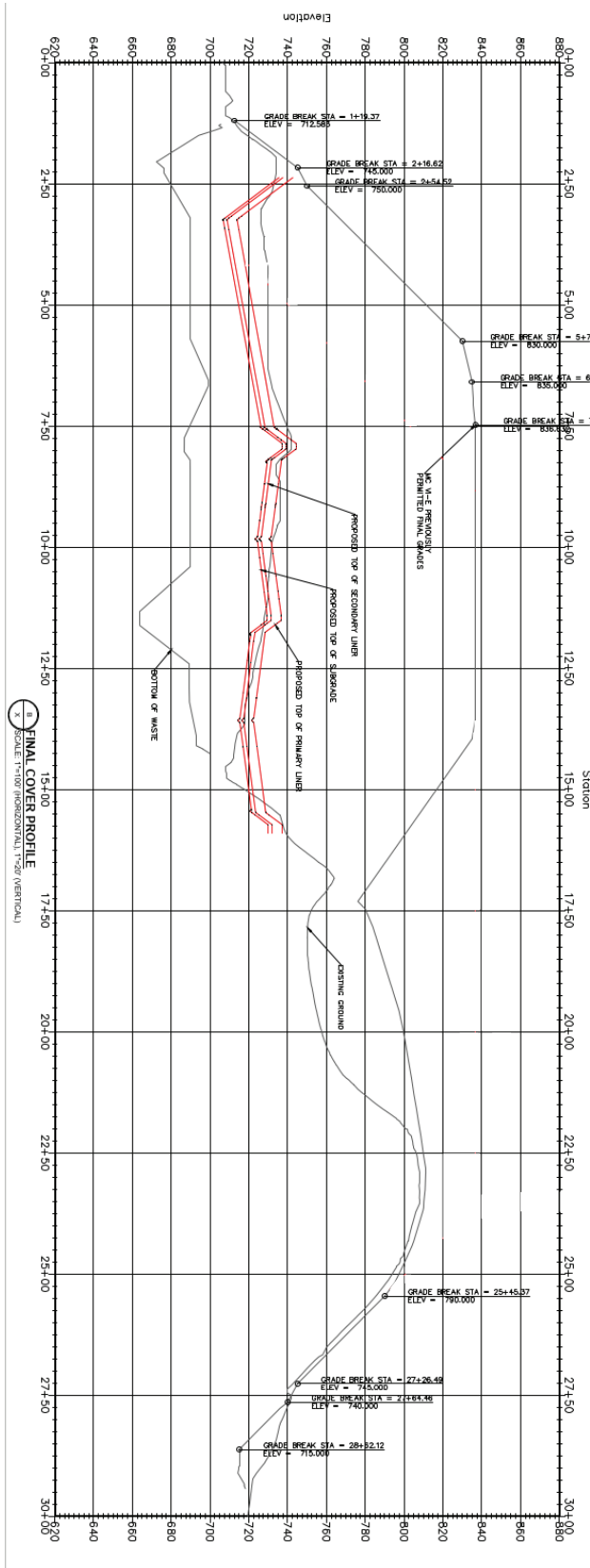
SLOPE STABILITY ANALYSIS REPORT FORM

Final Grades Cross-Section (plan):



SLOPE STABILITY ANALYSIS REPORT FORM

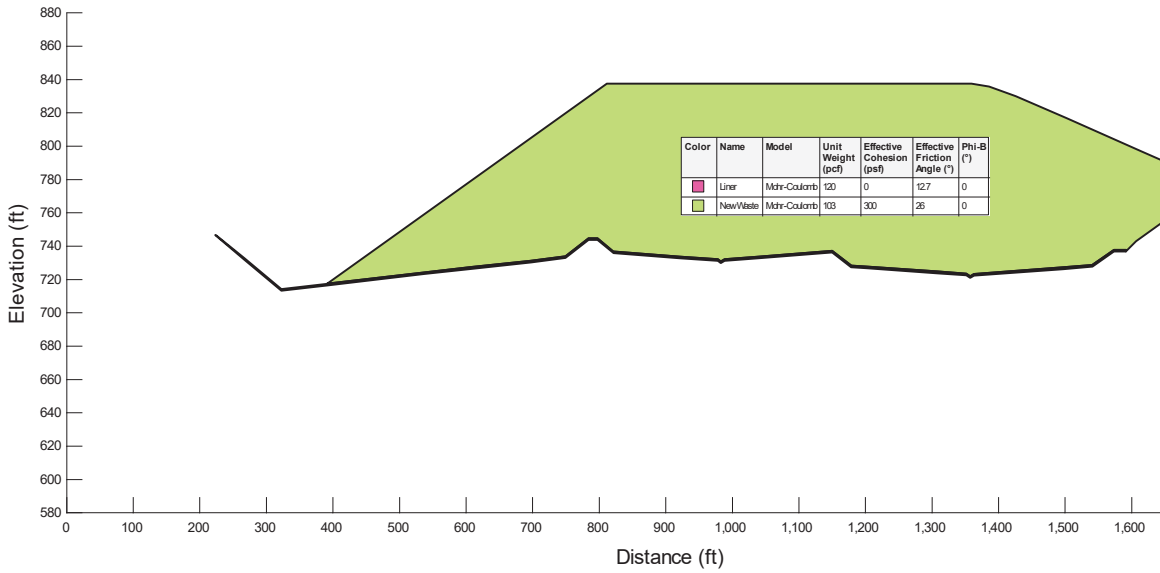
Final Grades Cross-Section (profile):



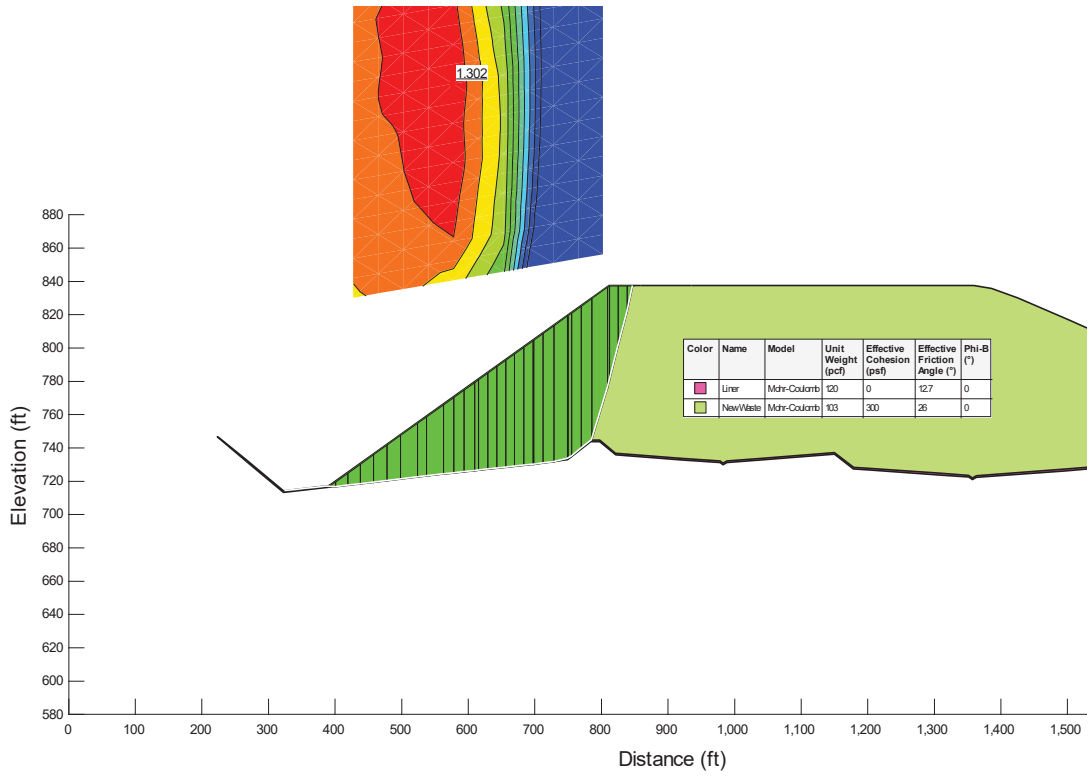
SLOPE STABILITY ANALYSIS REPORT FORM

Factor of Safety:	1.30	<input checked="" type="checkbox"/> Acceptable <input type="checkbox"/> Not Acceptable <input type="checkbox"/> Follow-up <input type="checkbox"/> Superseded
Comments:	Required friction angle of 12.7 degrees (peak). Any combination of adhesion and friction angle that yields a comparable shear strength under modeled site conditions is acceptable.	
Attachments:	Slope/W Cross Section and Results	

SLOPE STABILITY ANALYSIS REPORT FORM



SLOPE STABILITY ANALYSIS REPORT FORM



Attachment B-2

Settlement Calculations

**CALCULATION SHEET**Client: Wayne Disposal, Inc.Project: WDI MC6 F Permit ModificationCalculation: Leachate Collection Pipe Settlement Analysis MC6FProject No.: 1208070039.004Calculated By: KM Date: 11/16/2020Checked By: MK Date: 11/18/2020Approved By: KF Date: 11/19/2020

LEACHATE COLLECTION PIPE SETTLEMENT ANALYSIS

OBJECTIVE

This calculation evaluates the post-settlement slopes of the leachate collection pipes and cell floor cross slope for proposed Master Cell-VI (MC6) F1, F2, F3, and F4, at Wayne Disposal, Inc. (WDI). This evaluation is based on the estimated settlement of the existing waste and soil underlying the proposed cells due to additional overburden stresses induced by waste placement and the impact of such settlement on the post settlement cell floor slopes.

DESIGN CRITERIA AND ASSUMPTIONS

- The post-settlement slope of each proposed leachate collection pipe should be at least 1% and each cell floor cross slope should be at least 2% per Rule 299.9620 (4) (EGLE 2020).
- Pipe flowline analysis points were selected along the proposed leachate collection pipe flowlines within MC6-F (Attach. B-2.1). The specific locations of these points were selected to correspond to the cell floor high point, low point, changes in final cover slope and at regular intervals in between. Total settlement is estimated for each point, allowing an assessment of the post-settlement slope(s) along the flowline.
- Cross slope analysis points (Attach. B-2.1) were selected at the location of maximum fill height within each cell in order to evaluate post-settlement slopes under maximum load.
- Maximum settlement is expected to occur at the completion of the cap construction when the foundation is subjected to the maximum overburden pressure. Under the worst-case scenario, maximum load is applied (in full) to the foundation instantaneously during settlement analysis for a conservative (i.e., greater than anticipated) estimate of total settlement. In reality, loads would be applied incrementally as waste is placed gradually during the active life of the landfill. Additionally, the resulting settlement is assumed to occur immediately, conservatively accounting for the maximum settlement at the end of foundation soil consolidation.
- Table 1 Material properties used for the settlement analysis are listed in
- Table 2 summarizes the compressibility parameters used in the settlement analysis. The compacted clay liner is only very slightly compressible relative to the in-situ clay layer. Considering the insignificant magnitude of the settlement of the compacted clay liner, it was not included in the analysis.

**CALCULATION SHEET**

Client: Wayne Disposal, Inc.

Project: WDI MC6 F Permit Modification

Calculation: Leachate Collection Pipe Settlement Analysis MC6F

Project No.: 1208070039.004

Calculated By: KM Date: 11/16/2020

Checked By: MK Date: 11/18/2020

Approved By: KF Date: 11/19/2020

Table 1. Soil Properties for Settlement Analysis

Soil Type	Thickness [ft]	Moist Unit Weight [pcf]
Final cover soil	4	135
New waste	Varies	103*
Existing cover soil	Varies	135
Existing waste	Varies	82
Attenuation Layer	5	135
Structural Fill	2	135
Venting Layer	1	135
Leachate Collection Sand	1	135
In-situ middle clay	Varies	136
In-situ lower clay (moist)	5	128
In-situ lower clay (saturated)	12	128
In-situ silt (saturated)	18	125
In-situ sand (saturated)	45	115

* New waste unit weight obtained from email correspondence with WDI dated 11/18/2020

Table 2. Compressibility Parameters of Waste and Soils

Soil Type	Primary Compression Ratio $C_c/(1+e_0)$	Secondary Compression Ratio $C_\alpha/(1+e_0)$	Recompression Ratio $C_r/(1+e_0)$
Existing cover	0.102 ^[B]	0.005 ^[B]	0.017 ^[A]
Existing waste	0.147	0	0.0245 ^[A]
In-situ middle clay	0.102	0.005	0.017 ^[A]
In-situ lower clay	0.171	0.009	0.0285 ^[A]
In-situ silt	0.15 ^[B]	0 ^[B]	0 ^[B]
In-situ sand	0.1 ^[B]	0 ^[B]	0 ^[B]

^[A] Estimated from $C_r = C_c/6$.

^[B] Assumed values.

The information for subsurface soils is based on MCIV General Profiles (South), Appendix A Subsurface Soil/Waste Profiles & Corresponding Physical Properties, Volume III – WDI Operating License Application Master Cells VI F & G by NTH Consultants (2011a). Specifically, subsurface investigation boring logs, cross sectional profiles, and laboratory test results were used to assess the subgrade soil profile and its properties. Note that some uncertainty may exist in the interpretation of hydrogeological data due to natural soil's inherent variability, conservative assumptions have been applied to ensure a conservative estimate of settlement in this analysis.

METHODOLOGY

Total settlement is estimated using the 1-D consolidation equations (Coduto 1999), with primary consolidation being the critical component. Total settlement is calculated as:

$$S = S_c + S_s \quad (1)$$

Where:

S = total settlement [ft]

S_c = primary consolidation settlement due to load application [ft]

S_s = secondary compression settlement due to creep effects [ft]

Settlement caused by primary consolidation for a given layer of soil with uniform properties is calculated as:

$$S_c = \frac{h_0}{1 + e_0} \left(C_r \log \frac{\sigma_c}{\sigma_0} + C_c \log \frac{\sigma_i}{\sigma_c} \right) \quad (2)$$

Where:

C_c = primary compression index

C_r = recompression index

h_0 = initial compressible layer thickness [ft]

e_0 = initial void ratio of the clay subgrade

σ_0 = initial overburden pressure acting on the compressible layer [psf]

σ_i = final overburden pressure acting on the compressible layer [psf]

σ_c = preconsolidation stress [psf]

= $OCR \times \sigma_0$

OCR = overconsolidation ratio



CALCULATION SHEET

Client: Wayne Disposal, Inc.

Project: WDI MC6 F Permit Modification

Calculation: Leachate Collection Pipe Settlement Analysis MC6F

Project No.: 1208070039.004

Calculated By: KM Date: 11/16/2020

Checked By: MK Date: 11/18/2020

Approved By: KF Date: 11/19/2020

Settlement due to secondary compression is calculated using Equation 3 below:

$$S_s = h_0 \frac{C_\alpha}{1 + e_0} \log \left(\frac{t_2}{t_1} \right) \quad (3)$$

Where:

C_α = secondary compression index

H = layer thickness [ft]

t_2 = time after application of load (assumed 70 years)

t_1 = time required to complete primary consolidation (assumed 40 years)

- The elevations in this report are referenced to Mean Sea Level (MSL).
- The initial ground elevation (prior to initial development) was assumed to be approximately 705 ft. This value was inferred from the cross-sectional profile from Engineering Drawings, Wayne Disposal, Inc. Site No.2 MC VI-F&G by NTH Consultants (2011b).
- The preconsolidation pressure of the middle clay and lower clay, the major contributing compressible layers below the existing waste, was set equal to the initial effective overburden pressure acting on them prior to development. This value is used in Equation 2 to estimate settlement resulting from an initial load less than the preconsolidation pressure. Note that both layers have exhibited a higher overburden pressure since initial development of the site and placement of the now existing waste.
- Calculation of settlement following MC6-F construction accounts for changes in overburden pressure resulting from the excavation of existing materials, the placement of new liner system components, the placement of new MC6-F waste, and the placement of new MC6-F final cover.
- At each point selected along the leachate collection pipe system, the elevations for the existing ground, proposed overfill liner, final cover, and the foundation soils are determined and used to compute the initial and final overburden pressures for each layer within the analysis.
- Soil layers are identified using subsurface soil profiles provided in MCIV General Profiles (South), Appendix A Subsurface Soil/Waste Profiles & Corresponding Physical Properties, Volume III – WDI Operating License Application Master Cells VI F & G by NTH Consultants (2011a). These layers include in-situ clay with varying degrees of compressibility (see Table 2).
- Attachment B-2.1 presents plan locations of the settlement analysis points within MC6-F with respect to proposed cell floor grades and final grades. Leachate collection pipe cross section profiles are also presented in Attachment B-2.1.



Client: Wayne Disposal, Inc.
 Project: WDI MC6 F Permit Modification
 Calculation: Leachate Collection Pipe Settlement Analysis MC6F

Project No.: 1208070039.004
 Calculated By: KM Date: 11/16/2020
 Checked By: MK Date: 11/18/2020
 Approved By: KF Date: 11/19/2020

CALCULATIONS

Equations 1 through 3 were incorporated into a spreadsheet to conduct the settlement calculations. The settlement calculation output and resulting post-settlement slope(s) for each leachate collection pipe within MC6-F are presented in Table 3 through Table 6. The settlement calculation output and resulting post-settlement slope(s) for each analyzed cross slope within MC6-F are presented in Table 7 through Table 10.

Table 3. MC6-F1 Leachate Pipe Flowline Settlement Calculation Summary

Point			Elevation		Length [ft]	Liner Grade	Side Slope		Min. Slope [%]
	North [ft]	East [ft]	Flowline Elevation [ft]	Settlement [ft]		Post-Settlement [ft]	Pre-Settlement [%]	Post-Settlement [%]	
1	0.00	0.00	716.00	6.71	120	709.29	4.0%	2.4%	1%
2	120.00	0.00	720.80	8.66		712.14			
2	120.00	0.00	720.80	8.66	100	712.14	4.0%	3.0%	1%
3	220.00	0.00	724.80	9.70		715.10			
3	220.00	0.00	724.80	9.70	88	715.10	4.0%	3.4%	1%
4	308.00	0.00	728.32	10.20		718.12			
4	308.00	0.00	728.32	10.20	85	718.12	4.0%	3.9%	1%
5	393.00	0.00	731.72	10.29		721.43			

Table 4. MC6-F2 Leachate Pipe Flowline Settlement Calculation Summary

Point			Elevation		Length [ft]	Liner Grade	Side Slope		Min. Slope [%]
	North [ft]	East [ft]	Flowline Elevation [ft]	Settlement [ft]		Post-Settlement [ft]	Pre-Settlement [%]	Post-Settlement [%]	
1	0.00	0.00	710.00	6.21	72	703.79	3.0%	1.3%	1%
2	71.80	0.00	712.15	7.46		704.69			
2	71.80	0.00	712.15	7.46	65	704.69	3.0%	2.1%	1%
3	136.70	0.00	714.10	8.02		706.08			
3	136.70	0.00	714.10	8.02	131	706.08	3.0%	2.9%	1%
4	267.60	0.00	718.03	8.10		709.93			
4	267.60	0.00	718.03	8.10	124	709.93	3.0%	2.9%	1%
5	392.00	0.00	721.76	8.19		713.57			


CALCULATION SHEET

Client: Wayne Disposal, Inc.

Project: WDI MC6 F Permit Modification

Calculation: Leachate Collection Pipe Settlement Analysis MC6F

Project No.: 1208070039.004

Calculated By: KM Date: 11/16/2020

Checked By: MK Date: 11/18/2020

Approved By: KF Date: 11/19/2020

Table 5. MC6-F3 Leachate Pipe Flowline Settlement Calculation Summary

Point	North [ft]	East [ft]	Elevation		Length [ft]	Liner Grade Post-Settlement [ft]	Side Slope		Min. Slope [%]
			Flowline Elevation [ft]	Settlement [ft]			Pre-Settlement [%]	Post-Settlement [%]	
1	0.00	0.00	708.00	5.87	116	702.13	4.0%	2.2%	1%
2	116.00	0.00	712.64	7.99		704.65			
2	116.00	0.00	712.64	7.99	121	704.65	4.0%	2.7%	1%
3	237.00	0.00	717.48	9.58		707.90			
3	237.00	0.00	717.48	9.58	196	707.90	4.0%	4.3%	1%
4	433.00	0.00	725.32	8.93		716.39			
4	433.00	0.00	725.32	8.93	162	716.39	4.0%	3.6%	1%
5	595.00	0.00	731.80	9.52		722.28			

Table 6. MC6-F4 Leachate Pipe Flowline Settlement Calculation Summary

Point	North [ft]	East [ft]	Elevation		Length [ft]	Liner Grade Post-Settlement [ft]	Side Slope		Min. Slope [%]
			Flowline Elevation [ft]	Settlement [ft]			Pre-Settlement [%]	Post-Settlement [%]	
1	0.00	0.00	700.00	5.48	102	694.52	4.0%	3.0%	1%
2	102.00	0.00	704.08	6.51		697.57			
2	102.00	0.00	704.08	6.51	103	697.57	4.0%	3.1%	1%
3	205.00	0.00	708.20	7.42		700.78			
3	205.00	0.00	708.20	7.42	201	700.78	4.0%	3.0%	1%
4	406.00	0.00	716.24	9.52		706.72			
4	406.00	0.00	716.24	9.52	158	706.72	4.0%	3.4%	1%
5	564.00	0.00	722.56	10.53		712.03			

Table 7. MC6-F1 Cross Slope Settlement Calculation Summary

Point	North [ft]	East [ft]	Elevation		Length [ft]	Liner Grade Post-Settlement [ft]	Side Slope		Min. Slope [%]
			Floor Elevation [ft]	Settlement [ft]			Pre-Settlement [%]	Post-Settlement [%]	
5	0.00	0.00	734.00	10.16	142	723.84	4.5%	5.2%	2%
6	142.00	0.00	740.35	9.12		731.23			
5	0.00	0.00	734.00	10.16	101	723.84	4.5%	4.9%	2%
7	101.00	0.00	738.51	9.76		728.75			

Table 8. MC6-F2 Cross Slope Settlement Calculation Summary

Point	North [ft]	East [ft]	Elevation		Length [ft]	Liner Grade Post-Settlement [ft]	Side Slope		Min. Slope [%]
			Floor Elevation [ft]	Settlement [ft]			Pre-Settlement [%]	Post-Settlement [%]	
5	0.00	0.00	722.00	7.76	206	714.24	2.3%	4.2%	2%
6	206.00	0.00	726.64	3.78		722.86			
5	0.00	0.00	722.00	7.76	150	714.24	5.7%	5.0%	2%
7	150.00	0.00	730.48	8.67		721.81			

Table 9. MC6-F3 Cross Slope Settlement Calculation Summary

Point	North [ft]	East [ft]	Elevation		Length [ft]	Liner Grade Post-Settlement [ft]	Side Slope		Min. Slope [%]
			Floor Elevation [ft]	Settlement [ft]			Pre-Settlement [%]	Post-Settlement [%]	
5	0.00	0.00	738.00	9.02	105	728.98	4.5%	4.8%	2%
6	105.00	0.00	742.69	8.68		734.02			
5	0.00	0.00	738.00	9.02	163	728.98	4.5%	4.8%	2%
7	163.00	0.00	745.29	8.49		736.79			

**CALCULATION SHEET**Client: Wayne Disposal, Inc.Project: WDI MC6 F Permit ModificationCalculation: Leachate Collection Pipe Settlement Analysis MC6FProject No.: 1208070039.004Calculated By: KM Date: 11/16/2020Checked By: MK Date: 11/18/2020Approved By: KF Date: 11/19/2020**Table 10. MC6-F4 Cross Slope Settlement Calculation Summary**

Point	North [ft]	East [ft]	Elevation		Length [ft]	Liner Grade	Side Slope		Min. Slope [%]
			Floor Elevation [ft]	Settlement [ft]		Post-Settlement [ft]	Pre-Settlement [%]	Post-Settlement [%]	
5	0.00	0.00	728.00	10.09	187	717.91	4.5%	5.5%	2%
6	187.00	0.00	736.36	8.24		728.12			
5	0.00	0.00	728.00	10.09	180	717.91	4.5%	5.1%	2%
7	180.00	0.00	736.05	8.98		727.06			

CONCLUSIONS

The post-settlement slope of each proposed leachate collection pipe should be at least 1% and each cell floor cross slope should be at least 2% per Rule 299.9620 (4) (EGLE 2020). This calculation estimated the settlement at points along the leachate collection pipe and cross slopes within each subcell. The settlement of each of these points was used to calculate the post-settlement slopes of the MC6-F floor. This settlement analysis determined that all leachate collection pipes and cross slopes within MC6-F meet the required minimum post-settlement slopes.

REFERENCES

Coduto, D.P. (1999) *Geotechnical Engineering: Principles and Practices*, Prentice-Hall Inc., New Jersey

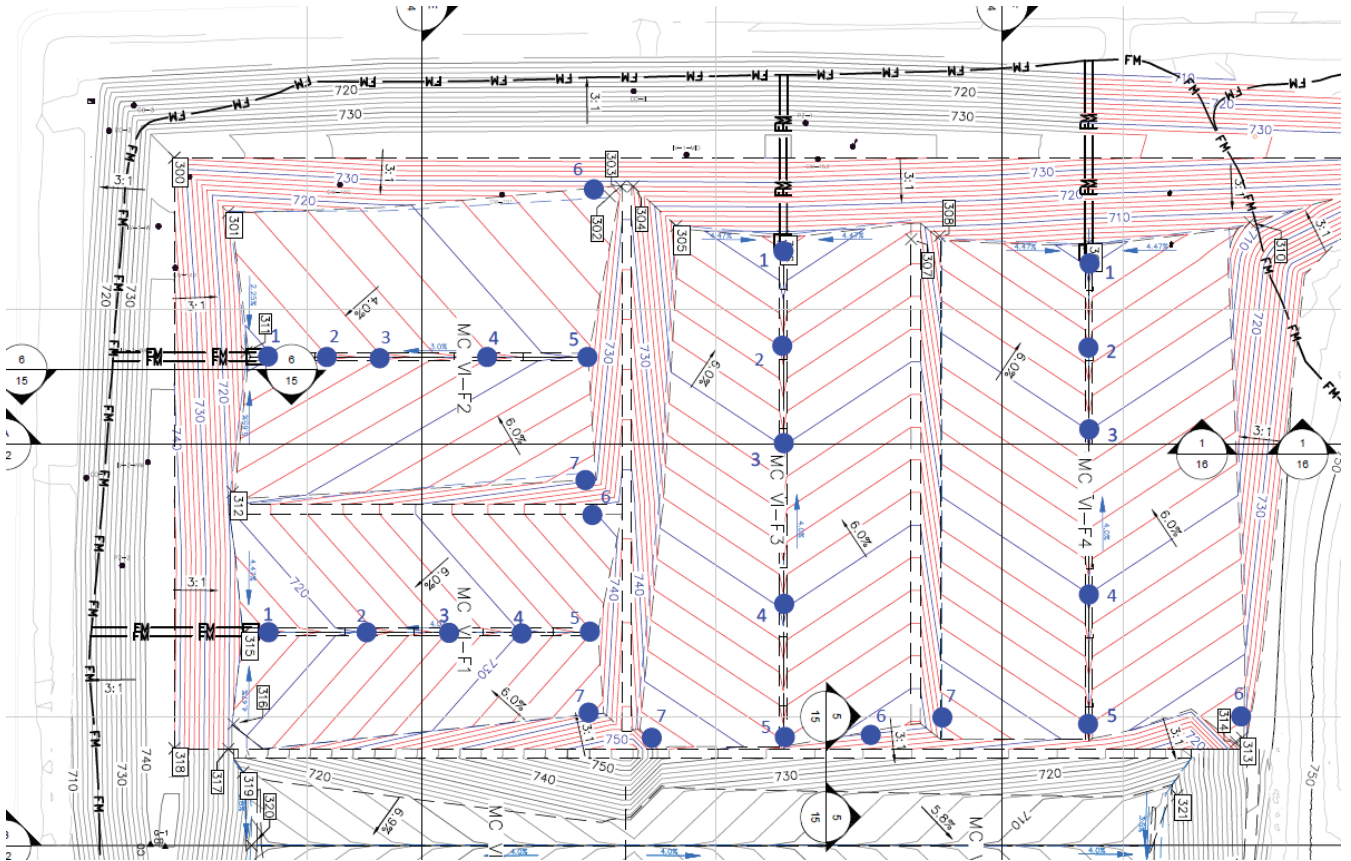
EGLE (2020) *Part 111 Administrative Rules*, Department of Environment, Great Lakes, and Energy Hazardous Waste Management, Materials Management Division.

NTH Consultants, Ltd. (2011a) *Volume III – WDI Operating License Application Master Cells VI F & G*.

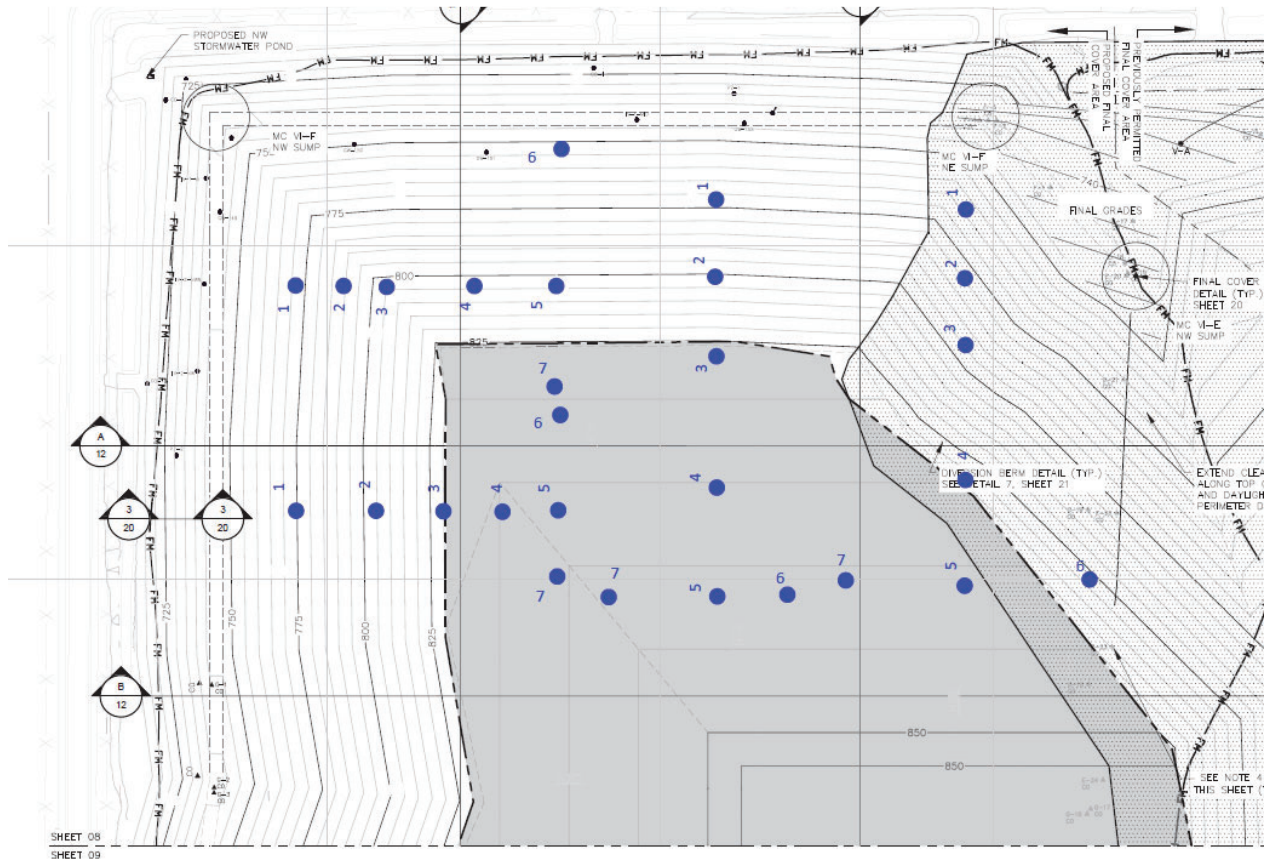
NTH Consultants, Ltd. (2011b) Engineering Drawings. *Wayne Disposal, Inc. Site No. 2 Master Cell VI-F&G*.

Attachment B-2.1

Plan View and Cross Sections of Leachate Flowlines

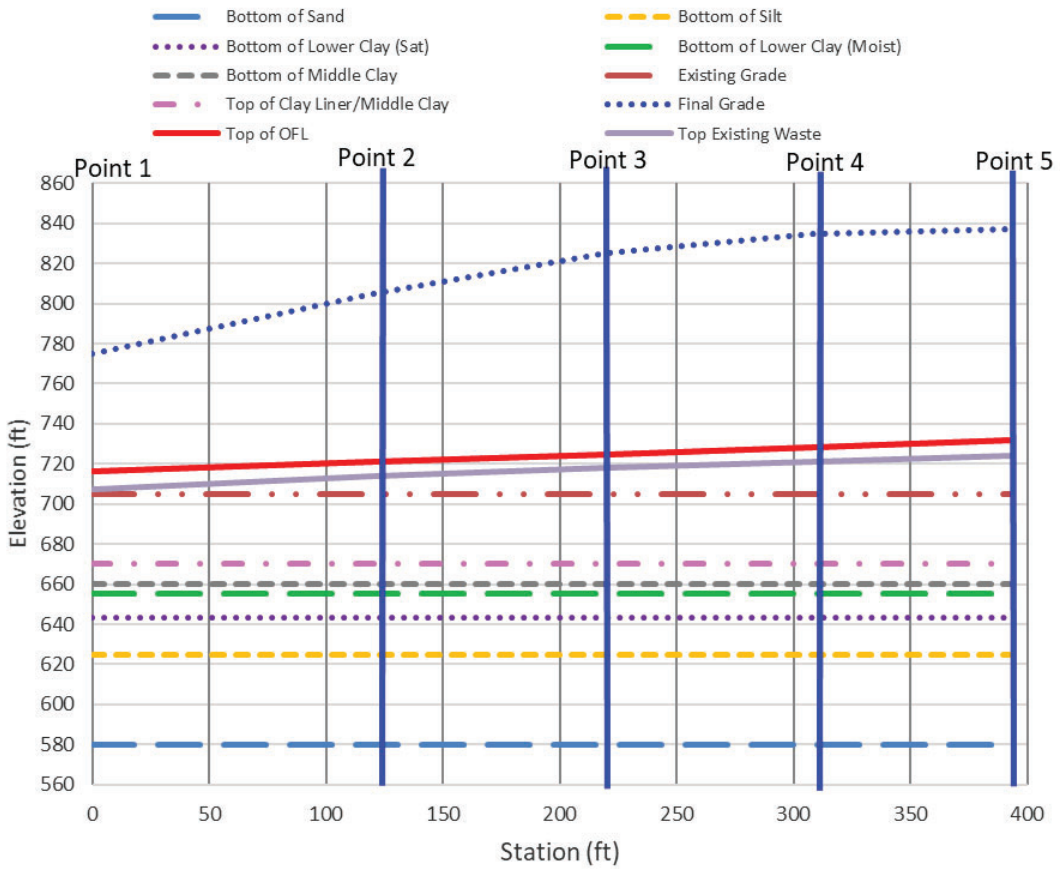


Plan View of Settlement Analysis Points Showing Top of Liner Grades

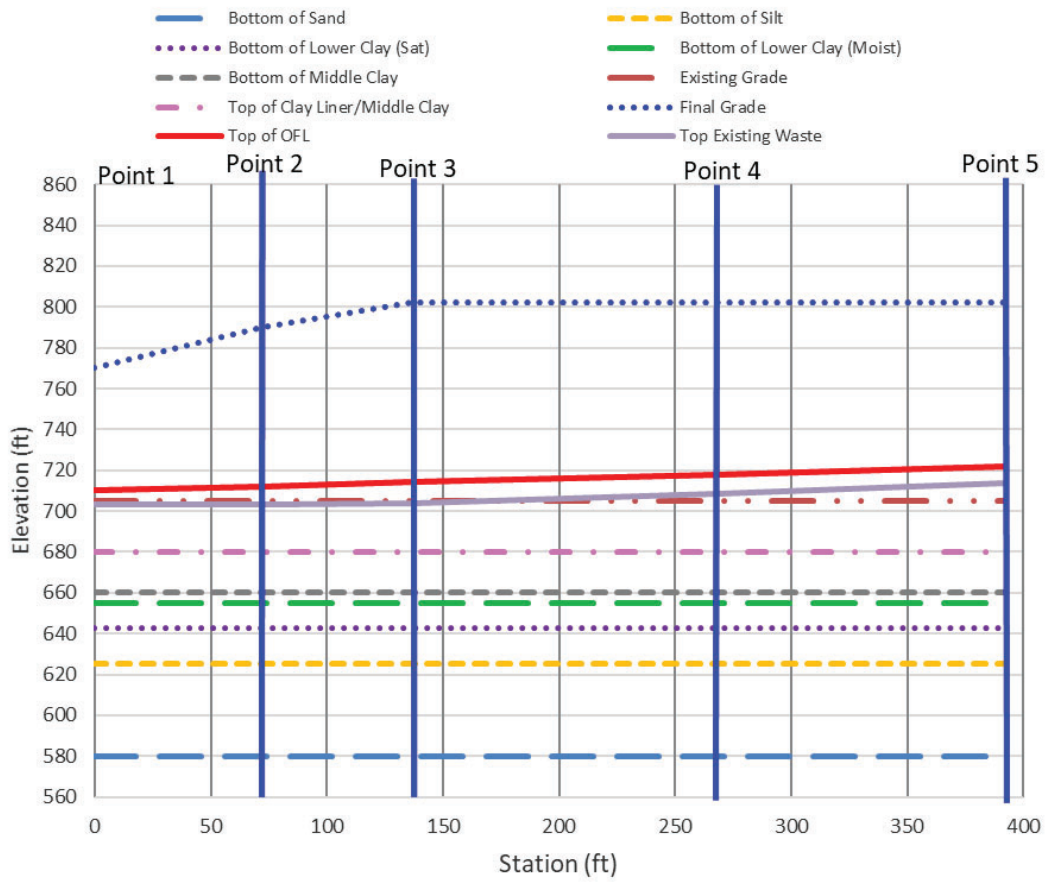


Plan View of Settlement Analysis Points Showing Final Grades

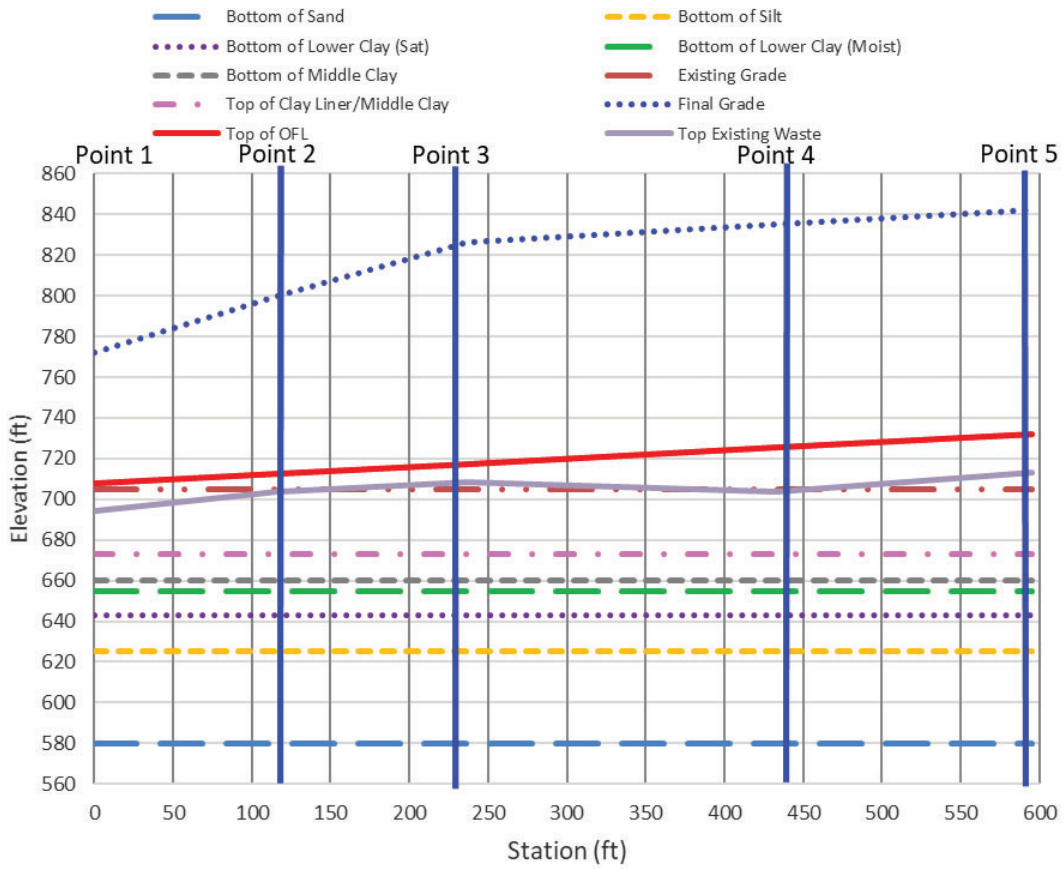
Cross Section Profile of MC6-F1 Leachate Pipe Flowline



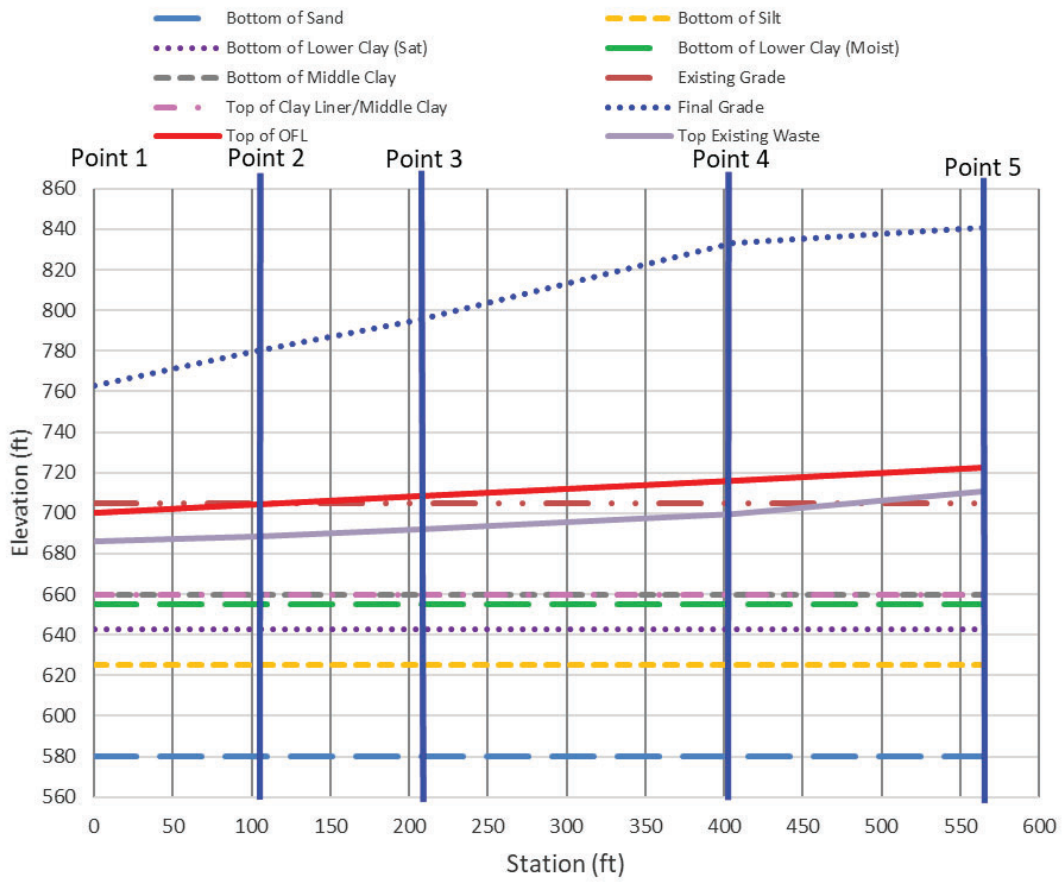
Cross Section Profile of MC6-F2 Leachate Pipe Flowline



Cross Section Profile of MC6-F3 Leachate Pipe Flowline



Cross Section Profile of MC6-F4 Leachate Pipe Flowline



Attachment 5

**2021 WDI Attachment D – GCL Manufacturer Specifications,
CQA Manual, and Installation Guidelines**

Attachment D

GCL Manufacturer Specifications, CQA Manual, and Installation Guidelines

RESISTEX® 200 FLW9 CERTIFIED PROPERTIES

CETCO® Resistex® geosynthetic clay liners are engineered to provide the highest level of chemical compatibility in extremely aggressive leachate environments such as some coal combustion product storage facilities, mining operations, and industrial waste storage facilities. Site-specific compatibility testing is strongly recommended.⁷

MATERIAL PROPERTY	TEST METHOD	TEST FREQUENCY	CERTIFIED VALUES
Scrim-reinforced Nonwoven Base Geotextile Mass/Area ¹	ASTM D5261	200,000 ft ² (20,000 m ²)	6.0 oz/yd ² (200 g/m ²) min.
Nonwoven Cap Geotextile Mass/Area ¹	ASTM D5261	200,000 ft ² (20,000 m ²)	9.0 oz/yd ² (300 g/m ²) min.
Bentonite Moisture Content ²	ASTM D2216	1 per 50 tonnes	12% max.
Bentonite Swell Index ²	ASTM D5890	1 per 50 tonnes	24 mL/2g min.
Bentonite Fluid Loss ²	ASTM D5891	1 per 50 tonnes	18 mL max.
Bentonite Mass/Area ³	ASTM D5993	40,000 ft ² (4,000 m ²)	0.75 lb/ft ² (3.7 kg/m ²) min.
Total Mass/Area ³	ASTM D5993	40,000 ft ² (4,000 m ²)	0.85 lb/ft ² (4.2 kg/m ²) min.
GCL Moisture Content	ASTM D5993	40,000 ft ² (4,000 m ²)	35% max.
GCL Grab Strength ⁴	ASTM D6768	200,000 ft ² (20,000 m ²)	50 lbs/in (8.8 kN/m) min.
GCL Peel Strength	ASTM D6496	40,000 ft ² (4,000 m ²)	3.5 lbs/in (610 N/m) min.
GCL Hydraulic Conductivity ⁵	ASTM D5887	250,000 ft ² (25,000 m ²)	3 x 10 ⁻¹¹ m/s max.
GCL Hydrated Internal Shear Strength ⁶	ASTM D6243	1,000,000 ft ² (100,000 m ²)	500 psf (24 kPa) typ.@ 200 psf (9.6 kPa)

Notes:

- ¹ Geotextile property tests performed on the geotextile components before they are incorporated into the finished GCL product.
- ² Bentonite property tests performed before the bentonite is incorporated into the finished GCL product.
- ³ Reported at 0 percent moisture content.
- ⁴ All tensile strength testing is performed in the machine direction using ASTM D6768.
- ⁵ Index flux and hydraulic conductivity testing with deaired distilled/deionized water at 80 psi (550 kPa) cell pressure, 77 psi (530 kPa) headwater pressure and 75 psi (515 kPa) tailwater pressure.
- ⁶ Peak values measured at 200 psf (9.6 kPa) normal stress for a specimen hydrated for 48 hours. Site-specific materials, GCL products, and test conditions must be used to verify internal and interface strength of the proposed design.

BENTOMAT® CL CERTIFIED PROPERTIES

CETCO® Bentomat® CL is a reinforced geosynthetic clay liner (GCL) consisting of a layer of sodium bentonite between a polypropylene woven geotextile and a polypropylene nonwoven geotextile, which are needle-punched together and laminated to a polyethylene geofilm.

MATERIAL PROPERTY	TEST METHOD	TEST FREQUENCY	CERTIFIED VALUES
Bentonite Moisture Content ²	ASTM D2216	1 per 50 tonnes	12% max.
Bentonite Swell Index ²	ASTM D5890	1 per 50 tonnes	24 mL/2g min.
Bentonite Fluid Loss ²	ASTM D5891	1 per 50 tonnes	18 mL max.
Bentonite Mass/Area ³	ASTM D5993	40,000 ft ² (4,000 m ²)	0.75 lb/ft ² (3.7 kg/m ²) min.
Geofilm Density ¹	ASTM D1505	200,000 ft ² (20,000 m ²)	0.92 g/cm ³
Geofilm Thickness ¹	ASTM D5199	200,000 ft ² (20,000 m ²)	5 mil (0.12 mm) min.
Geofilm Break Strength ^{1,4}	ASTM D882	200,000 ft ² (20,000 m ²)	14 lbs/in (2.5 kN/m) min.
Total Mass/Area ³	ASTM D5993	40,000 ft ² (4,000 m ²)	0.84 lb/ft ² (4.1 kg/m ²) min.
GCL Moisture Content	ASTM D5993	40,000 ft ² (4,000 m ²)	35% max.
GCL Grab Strength ⁵	ASTM D6768	200,000 ft ² (20,000 m ²)	30 lbs/in (5.3 kN/m) min.
GCL Peel Strength	ASTM D6496	40,000 ft ² (4,000 m ²)	3.5 lbs/in (610 N/m) min.
GCL Hydraulic Conductivity ⁶	ASTM D5887	250,000 ft ² (25,000 m ²)	5 x 10 ⁻¹² m/s max.
GCL Index Flux ⁶	ASTM D5887	250,000 ft ² (25,000 m ²)	1 x 10 ⁻⁹ m ³ /m ² /s max.
GCL Hydrated Internal Shear Strength ⁷	ASTM D6243	1,000,000 ft ² (100,000 m ²)	500 psf (24 kPa) typ.@ 200 psf (9.6 kPa)

Notes:

- ¹ Geosynthetic property tests performed on the geosynthetic components before they are incorporated into the finished GCL product.
- ² Bentonite property tests performed before the bentonite is incorporated into the finished GCL product.
- ³ Reported at 0 percent moisture content.
- ⁴ Geofilm tensile break strength performed in the machine and cross-machine directions using ASTM D882.
- ⁵ GCL tensile strength testing is performed in the machine direction using ASTM D6768.
- ⁶ ASTM D5887 is modified to include the laminated thin flexible membrane on the test specimen. Index flux and hydraulic conductivity testing with deaired distilled/deionized water at 80 psi (550 kPa) cell pressure, 77 psi (530 kPa) headwater pressure and 75 psi (515 kPa) tailwater pressure. ASTM D5887 (modified) testing is performed only on a periodic basis because the thin flexible membrane is essentially impermeable. The Bentomat® GCL core (without the flexible membrane) has a maximum hydraulic conductivity of 5 x 10⁻¹¹ m/s with deaired distilled/deionized water. For more information, see CETCO® Technical Reference (TR) Nos. 111 and 112.
- ⁷ Peak values measured at 200 psf (9.6 kPa) normal stress for a specimen hydrated for 48 hours. Site-specific materials, GCL products, and test conditions must be used to verify internal and interface strength of the proposed design.

BENTOMAT® DN CERTIFIED PROPERTIES

CETCO® Bentomat® DN is a reinforced geosynthetic clay liner (GCL) consisting of a layer of sodium bentonite between two polypropylene nonwoven geotextiles, which are needle-punched together.

MATERIAL PROPERTY	TEST METHOD	TEST FREQUENCY	CERTIFIED VALUES
Bentonite Moisture Content ¹	ASTM D2216	1 per 50 tonnes	12% max.
Bentonite Swell Index ¹	ASTM D5890	1 per 50 tonnes	24 mL/2g min.
Bentonite Fluid Loss ¹	ASTM D5891	1 per 50 tonnes	18 mL max.
Bentonite Mass/Area ²	ASTM D5993	40,000 ft ² (4,000 m ²)	0.75 lb/ft ² (3.7 kg/m ²) min.
Total Mass/Area ²	ASTM D5993	40,000 ft ² (4,000 m ²)	0.83 lb/ft ² (4.1 kg/m ²) min.
GCL Moisture Content	ASTM D5993	40,000 ft ² (4,000 m ²)	35% max.
GCL Grab Strength ³	ASTM D6768	200,000 ft ² (20,000 m ²)	50 lbs/in (8.8 kN/m) min.
GCL Peel Strength	ASTM D6496	40,000 ft ² (4,000 m ²)	3.5 lbs/in (610 N/m) min.
GCL Hydraulic Conductivity ⁴	ASTM D5887	250,000 ft ² (25,000 m ²)	5 x 10 ⁻¹¹ m/s max.
GCL Index Flux ⁴	ASTM D5887	250,000 ft ² (25,000 m ²)	1 x 10 ⁻⁸ m ³ /m ² /s max.
GCL Hydrated Internal Shear Strength ⁵	ASTM D6243	1,000,000 ft ² (100,000 m ²)	500 psf (24 kPa) typ. @ 200 psf (9.6 kPa)

Notes:

- ¹ Bentonite property tests performed before the bentonite is incorporated into the finished GCL product.
- ² Reported at 0 percent moisture content.
- ³ All tensile strength testing is performed in the machine direction using ASTM D6768.
- ⁴ Index flux and hydraulic conductivity testing with deaired distilled/deionized water at 80 psi (550 kPa) cell pressure, 77 psi (530 kPa) headwater pressure and 75 psi (515 kPa) tailwater pressure.
- ⁵ Peak values measured at 200 psf (9.6 kPa) normal stress for a specimen hydrated for 48 hours. Site-specific materials, GCL products, and test conditions must be used to verify internal and interface strength of the proposed design.

BENTOMAT® ST CERTIFIED PROPERTIES

CETCO® Bentomat® ST is a reinforced geosynthetic clay liner (GCL) consisting of a layer of sodium bentonite between a polypropylene woven geotextile and a polypropylene nonwoven geotextile, which are needle-punched together.

MATERIAL PROPERTY	TEST METHOD	TEST FREQUENCY	CERTIFIED VALUES
Bentonite Moisture Content ¹	ASTM D2216	1 per 50 tonnes	12% max.
Bentonite Swell Index ¹	ASTM D5890	1 per 50 tonnes	24 mL/2g min.
Bentonite Fluid Loss ¹	ASTM D5891	1 per 50 tonnes	18 mL max.
Bentonite Mass/Area ²	ASTM D5993	40,000 ft ² (4,000 m ²)	0.75 lb/ft ² (3.7 kg/m ²) min.
Total Mass/Area ²	ASTM D5993	40,000 ft ² (4,000 m ²)	0.81 lb/ft ² (4.0 kg/m ²) min.
GCL Moisture Content	ASTM D5993	40,000 ft ² (4,000 m ²)	35% max.
GCL Grab Strength ³	ASTM D6768	200,000 ft ² (20,000 m ²)	30 lbs/in (5.3 kN/m) min.
GCL Peel Strength	ASTM D6496	40,000 ft ² (4,000 m ²)	3.5 lbs/in (610 N/m) min.
GCL Hydraulic Conductivity ⁴	ASTM D5887	250,000 ft ² (25,000 m ²)	5 x 10 ⁻¹¹ m/s max.
GCL Index Flux ⁴	ASTM D5887	250,000 ft ² (25,000 m ²)	1 x 10 ⁻⁸ m ³ /m ² /s max.
GCL Hydrated Internal Shear Strength ⁵	ASTM D6243	1,000,000 ft ² (100,000 m ²)	500 psf (24 kPa) typ. @ 200 psf (9.6 kPa)

Notes:

- ¹ Bentonite property tests performed before the bentonite is incorporated into the finished GCL product.
- ² Reported at 0 percent moisture content.
- ³ All tensile strength testing is performed in the machine direction using ASTM D6768.
- ⁴ Index flux and hydraulic conductivity testing with deaired distilled/deionized water at 80 psi (550 kPa) cell pressure, 77 psi (530 kPa) headwater pressure and 75 psi (515 kPa) tailwater pressure.
- ⁵ Peak values measured at 200 psf (9.6 kPa) normal stress for a specimen hydrated for 48 hours. Site-specific materials, GCL products, and test conditions must be used to verify internal and interface strength of the proposed design.



LINING TECHNOLOGIES

Quality

CETCO GCL

CONSTRUCTION QUALITY ASSURANCE (CQA) MANUAL

Version 6.0, August 2008

TABLE OF CONTENTS

SECTION	PAGE
1. INTRODUCTION	4
1.1 Definitions	4
1.2 Scope and Purpose of the CQA Manual	4
2. PERSONNEL QUALIFICATIONS AND RESPONSIBILITIES	5
3. ON-SITE HANDLING	7
3.1 Unloading Procedures	7
3.1.1 Flatbed Truck Delivery	7
3.1.2 Trailer Delivery	8
3.2 Materials Handling	8
3.3 On-Site Storage	9
4. INSTALLATION	10
4.1 Start-Up Assistance	10
4.2 Equipment	10
4.3 Field Conditions	11
4.4 Site Inspection	11
4.5 Panel Deployment	11
4.6 Seaming	12
4.7 Detail Work	14
4.8 Damage and Damage Repair	14
4.8.1 Damage from Shipping and Handling	15
4.8.2 Damage from Installation Activities	15
5. PLACEMENT OF COVER MATERIALS	17
5.1 Soil/Stone Cover	17
5.2 Geosynthetic Cover	18
6. CONFORMANCE TESTING	19
6.1 Bentonite Mass per Unit Area	19
6.2 Bentonite Swell	19
6.3 Other Conformance Tests	19

TABLE OF CONTENTS (continued)

SECTION	PAGE
7. DOCUMENTATION	21

LIST OF APPENDICES

APPENDIX A List of Applicable ASTM Standards

APPENDIX B GCL Construction Quality Assurance Checklist

SECTION 1 INTRODUCTION

1.1 Definitions

Construction Quality Assurance. For the purposes of this manual, construction quality assurance (CQA) is defined as a planned system of activities that provides assurance that *installation* of the geosynthetic clay liner (GCL) proceeds in accordance with the project design drawings and specifications. In general, these activities include continuous inspection of the installation, testing of materials and procedures, and overall documentation.

Construction Quality Control. Again, for the purposes of this manual, construction quality control (CQC) is defined as a planned system of activities that provides assurance that the properties of the GCL *materials* meet the requirements of the project specifications. These activities primarily include materials testing and documentation.

There is a great deal of overlap in the nature of CQA and CQC, and from a practical standpoint, CQA and CQC activities are often performed by the same party. For this reason, we will use the term CQA to describe *all* of the quality-oriented tasks relating to the GCL and its installation.

1.2 Scope and Purpose of the CQA Manual

This manual is written to address third-party CQA activities and is *not* intended as a guide for GCL installation. Installation guidelines are available separately from CETCO (see Technical References TR-402). This manual is also not intended to describe the various *manufacturing* quality assurance and quality control (MQA/MQC) activities performed by CETCO at the GCL manufacturing facilities (see Technical Reference No. TR-403).

The purpose of the CQA Manual is provide the project CQA personnel with a general format for assuring that the GCL delivered to the job meets the requirements of the specifications and that this material is installed in accordance with the design drawings and specifications. This manual should be modified as necessary by the design or CQA engineer in order to account for site-specific or project-specific concerns and conditions. Any such changes, however, should be discussed with CETCO before they are introduced into the final version of the project CQA plan.

For the convenience of the CQA personnel, an overall CQA Checklist is provided in Appendix A. This checklist or a similar version thereof is designed to be used on a daily basis to document that all CQA activities are consistently executed throughout the project. The checklists should be maintained at the job site and should be included chronologically in the final CQA documentation package (Section 7).

SECTION 2

PERSONNEL QUALIFICATIONS AND RESPONSIBILITIES

It is vital that all parties involved in the installation of the GCL are in close communication with each other throughout the project, and that they fully understand the requirements of the project CQA plan. For the purposes of this manual, the qualifications and responsibilities of the various parties are delineated as follows:

Installing Contractor

Responsible for installing the GCL. The contractor should appoint an on-site Construction Supervisor to coordinate the installation effort and to interact with the other parties on the job site. The installing contractor should have prior experience in GCL installation and should staff the project with qualified technicians.

On-Site Engineer

Usually the design engineer or designee, this person is responsible for general oversight of the installation. Provides assurance that construction is performed as designed, although not formally responsible for CQA. Primary contact when the installing contractor is in need of clarification of design issues. Primary contact for dispute/problem resolution. This person should be a registered professional engineer.

CQA Engineer

Charged with CQA for Bentomat installation as well as for any other liner system components. Oversees all CQA inspection, testing, and documentation. This person should be a registered professional engineer or a certified geosynthetics installation technician. This person must also be independent of the other parties on site.

Manufacturer's Representative

CETCO may provide on-site start-up assistance, especially those in which the installer has little or no prior experience or where unusual site conditions exist. The on-site engineer or installer is responsible for notifying CETCO of the intended installation schedule such that CETCO may provide timely guidance during the start-up process. CETCO's GCL installation experience may provide valuable insights to the uninitiated engineer and/or installer.

CETCO also acts as the liaison between the manufacturing plant and the installer and coordinates the release of GCL from the plant in accordance with the installer's schedule. CETCO's *on-site* involvement is typically lessened when it is determined that the installer is sufficiently capable of installing GCL without CETCO's continuous assistance. CETCO remains available throughout the project should questions or problems arise.

CQA Laboratory

The GCL conformance tests in this manual are designed to be performed at the job site to facilitate real-time response as test results are generated. In some projects where additional testing is required, however, it may be necessary to utilize the services of an off-site laboratory. The on-site engineer should verify that the selected laboratory has ample experience in the testing of GCLs and is aware of the general content of the project CQA plan as well as its specific testing requirements. The CQA engineer should establish a key contact at the laboratory to coordinate sample delivery procedures, confirm testing parameters and methods, and arrange the timely reporting of test results.

It is recommended that a preconstruction meeting be held between the above parties in order to establish working relationships with one another and to review the design drawings and specifications prior to deployment of the GCL. Thereafter, regular meetings on a daily or weekly basis are recommended as the project continues.

SECTION 3 ON-SITE HANDLING

This section describes the procedures and equipment to be used in handling the GCL when it arrives at the job site. Proper execution of these procedures will ensure that the GCL is not damaged prior to installation. It should be noted that ASTM D 5888 also provides guidelines for GCL handling. The recommendations included herein are consistent with all ASTM guidelines.

CETCO's GCLs are produced in slightly different sizes depending upon the product selected. Weights and dimensions of these products and their corresponding core pipe sizes required for safe handling are provided in Table 1 below.

Product	Panel Size (m)	Roll Diam. (mm)	Typ. Roll Weight (kg)	Core Diam. (mm)	Core Pipe Diameter (mm)	Core Pipe Length (m)	Minimum Core Pipe Strength
Bentomat	4.57 x 45.7	610	1,200	100	89	6.1	XXH
Claymax	4.57 x 45.7	510	1,250	100	89	6.1	XXH

Table 1. GCL panel sizes and corresponding core pipe requirements.

It should be recognized that the weight of the GCL rolls will dictate what type of core pipe will be sufficiently strong for unloading and handling activities. Experience has shown that the type of steel from which the pipe was produced will influence its ability to sustain the weight of the roll. The strongest steel available should be used to prevent pipe bending. A core pipe that deflects more than 75 mm as measured from end to midpoint when the roll is lifted can cause damage to the GCL and is *not acceptable*. The pipes used to unload or deploy the GCL *must not bend* at any time.

3.1 Unloading Procedures

The GCL may be delivered to the job site in one of two ways: by flatbed truck or by closed trailer/container. Regardless of the delivery method, all unloading activities should take place away from main roadways and high-traffic areas at the site. The designated unloading area should be flat, dry, and stable, and should provide adequate peripheral access for the unloading equipment. Different techniques for unloading the GCL are used accordingly. Using the procedures and equipment described below will minimize unloading time.

3.1.1 Flatbed Truck Delivery

A front-end loader or backhoe is typically used to remove the rolls from the flatbed truck. Starting from the top rolls on the truck, the core pipe is inserted through the roll core. The core has an inside diameter of 100 mm but may be slightly bowed upon arrival to the job site. In this case, it may be necessary to assist the core pipe insertion process by using the back of the loader bucket to carefully

push the pipe through the core.

After the core pipe has been inserted, straps or chains are looped around each end of the pipe protruding from the roll. The other ends of the chains should be connected to a spreader bar (typically an I-beam) of equal length to the core pipe. The spreader bar itself is suspended from the loader bucket. The purpose of the spreader bar is to prevent the chains from chafing the ends of the roll as it is lifted. It is recommended that the chains or straps be secured by the placing a pin through each end of the pipe. The GCL roll should then be lifted and slowly carried from the flatbed to the temporary storage area.

GCL rolls can also be provided with a pair of slings to facilitate lifting and handling.

3.1.2 Trailer or Container Delivery

The GCL may also be delivered in closed trailers or shipping containers. In these cases, different unloading equipment and techniques must be employed. Because of limited access to the GCL rolls, it is usually necessary to utilize an extendable-boom forklift with a "stinger" attachment. The forklift dealer or manufacturer can provide details on selecting the proper stinger for the type of forklift used at the job site.

The rolls are placed inside the trailer or container in the same way that they are positioned on a flatbed truck. The rolls are removed by inserting the stinger through the roll cores and lifting/pulling the rolls from the trailer/container.

3.2 Materials Handling

The equipment used to unload the GCL from the delivery vehicle may also be used to handle the material on site and to convey it to work areas. All unloading and handling activities must be undertaken with great care to avoid damage to the GCL. The GCL should never be handled in ways that could affect its performance. Some activities to avoid:

- Dropping the rolls from the edge of the delivery truck or container.
- Pushing or pulling the rolls on the ground surface.
- Lifting the roll without a core pipe.
- Bending the rolls by using a core pipe that cannot bear the weight of the roll.
- Forcing a bent core pipe through the core.
- Carrying the GCL over excessively rutted, bumpy terrain, causing the roll to bend and bounce in transit.

Adherence to these common-sense precautions will prevent handling-related damage to the Bentomat.

The CQA engineer or designee should supervise the unloading and storage operations. It is the duty of the CQA engineer to maintain records of the shipments and to verify that the roll numbers on the labels match the roll numbers on the bills of lading. Any apparent discrepancies should be noted and reported to CETCO.

At this time, all of the rolls should also be visually inspected for damage. Damaged rolls should be clearly marked and set aside where they will not be immediately used. Major damage suspected to have occurred during shipment should *immediately* be reported to the carrier and to CETCO (see Section 4.8.1).

3.3 On-Site Storage

The GCL may be stored at a project site indefinitely, provided that proper storage procedures are followed. First, a dedicated storage area should be identified. This area should be level, dry, well drained, and located away from high-traffic areas of the job site.

For reasons of safety and material integrity, GCL rolls must never be stored on end. Rolls should be stored horizontally, in small stacks not to exceed four rolls in height. It is preferred that the bottom rolls be placed on plywood, on an arrangement of pallets, or on some other man-made surface, to promote drainage and to prevent damage by contact with the ground surface. If the rolls are to be placed directly on the ground, the local ground surface should be carefully prepared and proof-rolled to minimize the potential for damage. It is good practice to cover the stored rolls with a tarpaulin or plastic sheeting for supplemental protection from the elements.

The polyethylene sleeves of the GCL rolls should be examined for any obvious rips or tears. Sleeve damage should be repaired immediately with adhesive tape or additional plastic sheeting. At this time it is also recommended that the labels be examined and taped to the roll if they were displaced in transit.

SECTION 4 INSTALLATION

This section of the CETCO GCL CQA Manual covers the techniques and procedures to be used for ensuring the quality of a GCL installation. Although some installation techniques are described, this section is *not* an installation guide. Refer instead to CETCO GCL Technical Reference TR-402 for specific GCL installation guidelines. ASTM D 6102 also contains sound GCL installation guidelines.

4.1 Start-Up Assistance

CETCO or its representatives can provide on-site start-up assistance, especially where the installer has no prior GCL installation experience or in which the application is relatively unique. CETCO will work with the on-site engineer and CQA engineer in order to verify that the proper unloading, installation and conformance testing procedures are utilized. CETCO's input is based on extensive experience with GCL installation and on intimate knowledge of the physical characteristics of GCLs. It should be recognized, however, that it is the site engineer's responsibility to implement CETCO's recommendations.

4.2 Equipment

In many projects, the equipment used for unloading the GCL can also be used to install it. Most applications require a vehicle to lift and suspend the roll as it is deployed. Front-end loaders, bulldozers, boom cranes, forklifts, and tracked excavators all have been successfully used for this task. Other, more specialized equipment exists for these operations and may also be used. The equipment for unrolling the GCL should be able to lift the roll and suspend it *freely* such that it does not chafe against the vehicle or the ground. The vehicle must also have the ability to accommodate a spreader bar above the roll of GCL.

The spreader bar should be sufficiently strong to bear the full weight of the GCL roll without bending. Readily available I-beams or T-beams made of structural steel are typically used for this purpose, although steel pipes have also been successfully used. The chains or straps should be checked for their strength before the installation begins and should continually be inspected for wear as the installation continues.

The core pipe should be of the dimensions and strength indicated in Table 1. It has been CETCO's experience that the schedule of the core pipe is not always an accurate indicator of its strength. The type of steel from which the pipe is made, the presence of a longitudinal weld, and the overall length of the pipe all have an influence on its ability to sustain the weight of the GCL. It is essential that the core pipe *does not bend* when the full roll of GCL is suspended from it. Lastly, it is recommended that the core pipe have a means to prevent the chains or straps from slipping off the ends of the pipe. This can be accomplished by using pins or clamps.

It will often be necessary to cut the GCL before the end of the roll or to cut it to fit in certain confined areas. Cutting the GCL requires a *sharp* utility knife. It is very important to maintain the sharpness of the knife blades used for cutting the GCL, in order to prevent tearing its geosynthetic components and damaging the GCL where the cut is made. Frequent blade changes for the utility knives are strongly

recommended.

For construction of the bentonite enhanced overlapped seams of the Bentomat products, an acceptable fillet of bentonite can be poured directly from the bags of granular bentonite supplied with each roll of Bentomat, but a watering can (without a sprinkler head) is easier to use and produces a more controlled seam enhancement. A line chalker, such as those used for marking athletic fields, may also be used.

4.3 Field Conditions

At the beginning of each working day, the CQA engineer should confirm that there are no ambient site conditions which could affect the quality of the installation. Specifically, the presence at the job site of excessively high winds, rain, standing water, or snow may be construed as unsuitable weather for GCL installation. There are no temperature restrictions for installing the GCL, however.

Bentomat is not as susceptible as Claymax to damage due to "premature hydration" (i.e., hydration before a confining stress is applied). Although Bentomat will not delaminate when wetted, CETCO nevertheless recommends that it be installed in dry weather as with Claymax. This lessens the potential for damage to the material and ensures that its integrity is not compromised by the swelling of the bentonite. Should the GCL become prematurely hydrated, it urged that CETCO be contacted in order to recommend a project-specific and product-specific recommendation as to whether the GCL must be removed and replaced. CETCO's Technical Reference TR-312 provides a checklist for evaluating GCL that has been hydrated when no confining pressure is present.

4.4 Site Inspection

Prior to each day's installation activities, the site engineer and/or CQA engineer should inspect the work area to ensure that it has been prepared in accordance with the specification and design drawings. Specifically, the design grades should be verified, the slope length and steepness should be checked, the anchor trench dimensions should be measured, and the subgrade should be inspected and approved. Any deviations from the specifications or design drawings should be noted and rectified before the GCL is installed.

The anchor trench is especially important in applications where slopes are present. The anchor trench must meet or exceed the design dimensions but must also be free of any sharp corners or protrusions which could put excessive stress on the GCL. The CQA engineer must ensure that the anchor trench is as carefully prepared as the rest of the subgrade.

4.5 Panel Placement

The unrolling and placement of the GCL should be performed in such a way that the GCL is not damaged or unduly stretched, folded, or creased. The GCL rolls are typically suspended from the front of the vehicle while it travels backwards along the intended path of placement. During this activity, the roll should be able to rotate freely around the core pipe. Excessive friction due to a bent or large-diameter core pipe, or due to contact between the roll and the deployment equipment, may cause undesirable levels of tension to develop. It is necessary that the GCL be deployed in a fully

relaxed (but not wrinkled) state.

A common deployment technique when the GCL is placed on slopes is to suspend the roll at the top of the slope while several laborers unroll it as they walk downslope. This is an acceptable technique, but the CQA engineer should verify that excessive tension does not develop on the material and that the underside of the panel is not damaged by friction with the subgrade. Unless the subgrade is acceptably smooth, the GCL should be unrolled over an already-placed panel and then moved laterally into its correct position. Flat-bladed vise grips are very useful for handling and moving unrolled panels.

It is important to ensure that, at the top of a slope, the GCL is properly placed in the anchor trench. After confirming that the trench has been constructed according to the specifications, the GCL should be placed in the trench such that it extends across the trench floor but not up the rear wall of the trench. Excess material if any, should be cut off, *not* folded over on top of the existing material. Proper anchorage will be achieved if and only if the GCL is placed within the trench in this manner.

The orientation of the GCL panels is important. When working in sloping areas, the panels should be positioned such that their long dimension is parallel to the direction of the slope. Panels may only be placed across the slope when the slope is less steep than 4H:1V or when the slope length is very short (less than or equal to 3 m).

4.6 Seaming

Proper field seaming is vital for the liner to function to its maximum abilities. There are three elements of CQA for this important task:

- Verification of the minimum acceptable overlap.
- Verification of the continuity of the accessory bentonite (Bentomat only).
- Verification that there is no dirt in the overlap zone or on the bottom geotextile of the overlying GCL panel.

These elements for field seam CQA are straightforward and require only visual inspection by the CQA engineer. The upper surface of the GCL has two heavy dashed lines on both sides of the panel. The lap lines are 150 mm from the edges of the panel, and the match lines are 250 mm from the edges of the panel. The minimum acceptable overlap is 150 mm. Thus, the installer's objective is to place the overlying panel *between* the two lines of the underlying panel. The CQA engineer needs only to visually verify that the 150-mm lap line of the underlying panel is not visible. A properly executed seam, therefore, is verified when three dashed lines (not four) are visible at the overlap, as shown in Figure 1.

The hydraulic performance of Bentomat is maximized when the accessory bentonite is placed *continuously* within the overlap zone. Continuity is best achieved when a watering can or other similar device is used. Pouring the bentonite directly from the bag is less effective in this regard. Verification of continuity should be performed visually by the CQA engineer. The CQA engineer should observe the accessory bentonite as it is being placed within the overlap zone and should give verbal approval of the seam before the overlap is flipped back into place.

Bentomat ST, DN, and SDN with Supergroove® have self-seaming capabilities in their longitudinal overlaps (Figure 2) and do not require supplemental bentonite. For these Bentomat products, supplemental bentonite is required for the end-of-panel overlapped seams. For pond applications, supplemental bentonite must be used in longitudinal seams regardless of the CETCO GCL used.

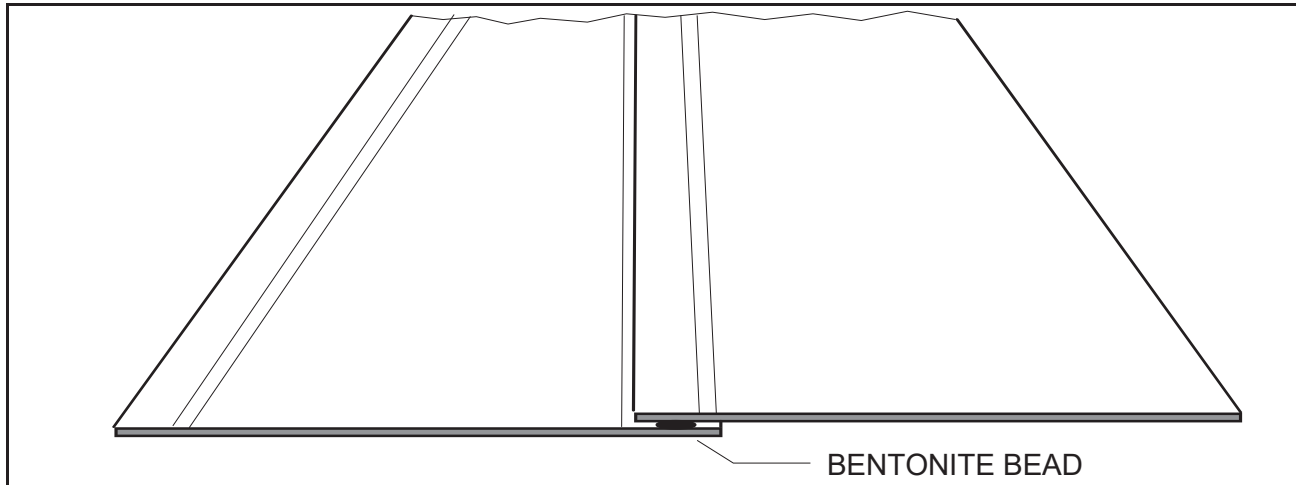


Figure 1. Schematic representation of a properly executed Bentomat field seam.

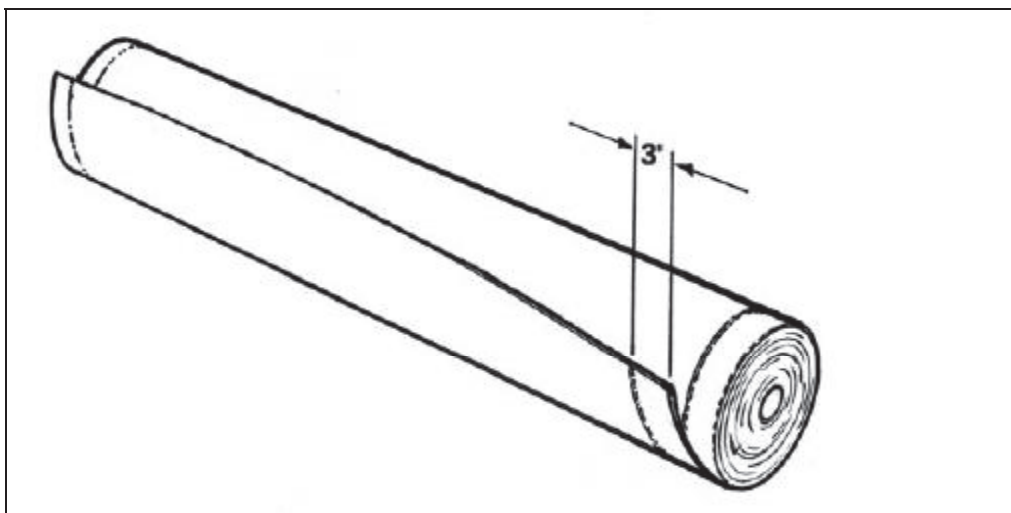


Figure 2. Supergroove Bentomat field seam.

Verification of the cleanliness of the overlap is also required, because dirt can enter the overlap and create a conduit for excessive lateral leakage. This is one reason CETCO recommends that the overlying panel is placed and then its edge flipped back to reveal the overlap zone. Exposing the overlap in this manner forces extra attention on the seam and reveals the presence of loose dirt that

may have inadvertently entered the overlap zone or may have become adhered to the bottom geotextile of the overlying panel. The CQA engineer should either verify that no dirt is present or ensure that the dirt is swept out of the overlap.

Verification of the *amount* of bentonite placed at the seam may be achieved by ensuring that one full 22.5 kg bag of granular bentonite is used for the lateral and longitudinal seaming of each roll of GCL. CETCO recommends that a minimum of 375 grams of granular bentonite be applied per lineal meter of seam. If the installer places bentonite at the rate of one bag per roll, this target application rate will be achieved.

The longitudinal overlap for the GCL should be at least 150 mm (Bentomat) and 300 mm (Claymax). Overlaps at the *ends* of the rolls, however, ("transverse" overlaps) should be at least 300 mm (Bentomat) and 600 mm (Claymax) to account for any incidental loss of bentonite that could occur due to excessive handling of this portion of the roll or to stress relaxation after placement. Overlap distances can be increased if unusual site conditions (such as a soft subgrade, or GCL covered only with geomembrane) exist.

4.7 Detail Work

The term "detail work" refers to the placement of GCL around structures such as vertical walls, gas vents, drainage basins, and pipe penetrations. In all of these cases, it is necessary to utilize granular bentonite or a bentonite mastic to create a seal between the GCL and the structure. CQA of these areas involves a visual inspection of the methods used to make the seal. Specific items requiring inspection include:

- Dimensions of the "notch" excavated around the structure.
- Amount of bentonite applied to the detail
- Condition of the GCL at its cut edge (the cut should be clean, not frayed, with little or no bentonite edge loss from the GCL)
- Integrity of the detail as cover material is placed over and around it.

When cutting the GCL, it is important to ensure that the cut is made where the GCL hangs from the roll or where it rests on the subgrade. The GCL cut should *never* be made on the roll itself or when it rests on any other liner system component.

4.8 Damage and Damage Repair

Even when all reasonable protective measures are taken, the GCL may still become damaged during shipping and handling or during installation. This section provides instructions on assessing and managing the damaged materials.

4.8.1 Damage From Shipping and Handling

Occasionally, a GCL roll will arrive at a job site with its protective plastic sleeve torn due to movement during transit. This roll should be inspected for damage in the area where the sleeve was torn. If the geotextile under the torn sleeve is also torn, the outermost wrap of GCL on the roll should be unwound and discarded when the roll is installed. It is not necessary to consider the entire roll unusable. It is important, however, to mark the roll in order to alert the installer that the initial wrap should be cut away and discarded, because the damaged geotextile may be hidden from view when the GCL is unrolled. It is remotely possible that further layers of GCL on the roll could be similarly damaged. If this happens, additional wraps may be unrolled and discarded prior to placement.

Damage due to poor handling may occur as a result of accidentally dropping a suspended roll onto the ground or using weak core pipes that bend when the GCL is lifted. These activities can cause damage not just to the outer wrap of GCL but to the entire roll. If such damage occurs, the rolls should be clearly marked and moved away from the storage area. The CQA engineer should ensure that procedures are immediately implemented in order to prevent the recurrence of this problem. The CQA engineer should also contact CETCO to help make a determination as to whether the mis-handled GCL is acceptable for use on the project.

4.8.2 Damage From Installation Activities

The more commonly observed incidents of damage occur during installation, as a result of inadvertent contact by heavy equipment. Because this type of damage will potentially have the largest overall effect on the integrity of the liner system, CETCO strongly recommends that equipment operating on or near the GCL *be monitored continuously*.

Equipment operators should be made fully aware of the importance of their actions and should be encouraged to notify the CQA engineer directly if they suspect at any time that the liner may have become damaged by their equipment. Close communication among everyone involved in the installation will help to ensure that this type of damage is reported and repaired.

Repeated passes by loaded dump trucks over GCL, which has minimal cover, can cause damage. It is therefore preferred to prevent potential for such damage by placing the GCL over these high-traffic areas *after* cover material delivery is largely completed. If this is not possible, then extra cover should be placed over high-traffic areas. At least 600-900 mm of screened, cohesive soil is recommended.

Should damage occur to the already-installed GCL, the following procedures should be followed:

1. Remove equipment from the damaged area and notify the CQA engineer.
2. *Manually* clean away all cover material within a 600-mm radius of the damaged area. Use a broom to sweep away the remaining dirt in order to make the area as clean as possible.
3. If necessary, repair the subgrade to its original conditions. Replace the torn/damaged GCL as closely as possible to its original position.
4. Place a bead of granular bentonite or bentonite paste at the minimum rate of 500 g per lineal meter around the damaged area.
5. Cut a patch of new GCL to fit over the damaged area and extending 600 mm beyond it.

6. Place the patch over the damaged area and carefully backfill over the patch.

Note that it is necessary only to repair the damaged portion of the GCL. It is usually not necessary to remove and replace the entire panel, unless the damage has occurred on a slope. In this case, slope stability may be compromised and the site engineer should be contacted to help determine whether a repair is acceptable.

SECTION 5

PLACEMENT OF COVER MATERIALS

As mentioned previously, the proper placement of cover on the GCL is crucial to the overall success of the installation. This section of the Bentomat CQA manual includes recommended materials and procedures, which will help to ensure that the integrity of the GCL is not compromised when it is covered.

Regardless of the nature of the cover material used, it should be placed as soon as possible after the GCL has been deployed. The efforts of placing the GCL and placing the final cover should be coordinated to the extent that only as much GCL as can be covered should be deployed in one working day. This will prevent premature hydration and will greatly reduce the chances for incidental damage to the GCL during other activities.

5.1 Soil/Stone Cover

When a GCL is the sole liner system component, soil or stone cover *must* be placed over it to provide protection from physical damage, erosional forces, and degradation by UV light. The presence of cover also provides a confining stress, which allows the overlapped seam to perform properly and enhances the long-term physical integrity of the material. Lastly, the cover may provide a base for vehicular traffic. Because it serves so many functions, proper placement and CQA of the soil/stone cover is essential.

Frequently used cover materials include sand, gravel, crushed stone, and common earth fill. Regardless of the type of material selected for the cover, it should be free of large stones (greater than 50 mm in diameter), sticks, and any other materials, which could cause puncture or tearing. The source of all cover material should be identified in order to ascertain its suitability well in advance of the installation.

In addition to particle size, the *angularity* of a crushed stone or gravel will impact the construction survivability of the GCL. It is preferred that relatively rounded materials be utilized. If these materials are not available, then extra caution must be taken during cover placement. Dumping the cover from a loader bucket positioned high above the GCL is unacceptable. The cover should be gently placed from as low a height as possible. Vehicular traffic should also be restricted if particularly angular or abrasive material is used. If there is some doubt as to the suitability of a potential cover material, a representative sample should be submitted to CETCO for analysis.

With respect to the equipment used to place the protective cover, it is strongly recommended that no heavy equipment come in direct contact with the GCL. Obviously, tracked equipment will damage the liner. In some cases, however it is necessary to drive equipment directly on the GCL. This can be accomplished with low-pressure, *rubber-tired* equipment. Permission to do so will be granted by CETCO through the CQA engineer on a case-by-case basis *only* and will include restrictions on the equipment itself and on the type of movements the vehicle may make on the GCL.

The chemical nature of the cover soil must also be considered. The use of fine-grained, calcareous soil or stone is strongly discouraged due to the potential for an adverse reaction with the sodium

bentonite contained in the GCL.

The cover material placed as backfill in the anchor trench should be of the same quality as the rest of the backfill. It is especially important that the anchor trench backfill be compacted either by hand tamping or by the use of a small walk-behind compactor. Compaction should be performed over each 150-mm lift of backfill placed in the anchor trench.

5.2 Geosynthetic Cover

A geomembrane or other geosynthetic liner system component is often placed over the GCL. Caution must be used during this activity to prevent GCL damage. Again, it is strongly recommended that no heavy equipment directly contact the GCL, but exceptions can be made on a project-specific basis.

A special precaution should be taken when textured geomembrane is installed directly over the GCL in a composite liner system. Because considerable friction may develop between the geomembrane and the GCL, it is difficult to pull the geomembrane into position for welding to adjacent sheets. A smooth "slip sheet" can be used to provide a low-friction sliding surface for the geomembrane until it is in position for welding.

SECTION 6 CONFORMANCE TESTING

Conformance testing is necessary in order to verify that the materials installed meet the requirements set forth in the specification. Although CETCO performs regular testing on its GCLs as part of its manufacturing QA/QC program, the engineer may require additional testing at the job site. This section lists several tests, which may be utilized to verify the quality of the delivered materials and the quality of the installation of those materials.

6.1 Bentonite Mass Per Unit Area

A relatively simple test to verify that the specified amount of bentonite has been encapsulated in the GCL is to measure the bentonite mass per unit area of representative samples cut from delivered rolls. The results of this test may be used in conjunction with the results of the bentonite swell test described in Section 6.2 to arrive at an indirect verification of the hydraulic performance of the GCL.

ASTM D 5993 provides procedures for performing the mass per unit area test. After the correction for geotextile mass is made, there should be at least 3,600 g of bentonite contained within the GCL per square meter. This is CETCO's minimum average roll value (MARV) for bentonite content of all of its GCLs. These values are always subject to change, so please refer to GCL Technical Reference No. TR-404 for the most recent list of certified physical GCL properties.

If for any reason the resulting mass per unit area values do not meet the required MARVs, the corresponding rolls should be set-aside for additional inspection and testing. CETCO should be notified to assist in resolving the problem if it persists.

6.2 Bentonite Swell Index and Fluid Loss

The swell index and fluid loss of the bentonite are two of the most important indicators of its ability to function as a barrier material. ASTM D 5890 provides a detailed free swell testing procedure used by CETCO. CETCO's MARV requirement for the bentonite is 24 mL/2g. ASTM D5891 provides a detailed fluid loss testing procedure. CETCO's maximum requirement for fluid loss of the bentonite is 18 ml. As with the mass per unit area test described in Section 6.1, if these values are not achieved in conformance testing, the corresponding rolls should be set aside for additional inspection and testing. CETCO should be notified to assist in resolving the problem if it persists.

6.3 Other Conformance Tests

Other conformance tests may be conducted at the request of the on-site engineer or the CQA engineer on a project specific basis. ASTM D6495 suggests grab tensile strength and index flux/permeability (as per ASTM D 5887), although it should be cautioned that rapid "real-time" results of index flux/permeability are not possible due to the time required to achieve steady-state permeability values. Thus, it is difficult to use permeability testing as a pass/fail criterion for GCL acceptance at the job site.

Also, the laminated GCLs are not easily tested for index flux/permeability due to potential sidewall leakage around the membrane. CETCO has a special setup procedure for its laminated GCLs in TR-302.

Lastly, it should be recognized that field-scale test pads and infiltrometer tests are typically *not* performed in GCL projects. This contrasts with compacted clay liner (CCL) projects, in which, for two reasons, field-scale data is almost always required. First, field data for CCL projects is necessary because there are many variables involved in their construction (compactor weight, speed, number of passes; soil type; moisture content; lift thickness; etc.). It is therefore necessary to build a test pad to ensure that the construction materials and methods intended for the project will provide the required level of performance. Second, laboratory test results and field test results may vary significantly with CCLs due to the difficulties in retrieving representative, undisturbed samples. This factor also warrants that field data be obtained for CCL projects.

With GCL installations, however, there are very few construction-related variables. Additionally, the GCL that is tested for permeability in the laboratory is the *same* material deployed in the field. For this reason, a GCL such as Bentomat or Claymax does not require a field permeability test.

SECTION 7 DOCUMENTATION

Thorough documentation of all CQA activities and tests is necessary in order to provide a written record that the GCL has been properly installed. The CQA documentation package for a GCL installation should include the following items:

- Bills of lading and corresponding packing list confirming receipt of all GCL installed at the site.
- A panel layout drawing in which the GCL roll numbers are keyed to their location in the field. Locations where damage was encountered and repaired should also be marked.
- The roll numbers from which samples were taken for conformance tests, along with the results of those tests.
- A daily report or diary of the activities undertaken at the site during construction.
- Certification that the requirements for the subgrade and for the cover material were achieved.
- A compilation of all CQA checklists completed during the installation.
- The manufacturing quality control (MQC) certification and accompanying test data.
- A description of deviations, if any, made to the original CQA plan during the installation.
- Photographs of the GCL during installation.

CETCO provides the MQC certification. All other items on the above list are the responsibility of the CQA engineer.

APPENDIX A

List of Applicable ASTM Standards

ASTM D 5887, “Standard Test Method for Measurement of the Index Flux Through Saturated Geosynthetic Clay Liner Specimens Using a Flexible Wall Permeameter,” *Annual Book of ASTM Standards, Vol. 4.09*, American Society for Testing and Materials, W. Conshohocken, PA.

This method describes the specimen preparation, stress and gradient conditions, and testing procedures to be used for determining the flux (flow per unit area) through GCLs. Adherence to the specimen preparation procedures presented will help to minimize sidewall leakage, a common problem when testing thin barriers. This is an index test designed to determine product acceptability and uses a maximum confining stress of 35 kPa (5 psi) and a hydraulic gradient of 14 kPa (2 psi).

ASTM D 5888, “Standard Guide for Storage and Handling of Geosynthetic Clay Liners,” *Annual Book of ASTM Standards, Vol. 4.09*, American Society for Testing and Materials, W. Conshohocken, PA.

This is a guide for the safe handling of GCL rolls at a job site, identifying the equipment and techniques typically employed to unload the material from delivery trucks and to place it in a dedicated storage area. Procedures are also presented for proper storage of the GCL in order to minimize the potential for product damage while in storage.

ASTM D 5889, “Standard Practice for Quality Control of Geosynthetic Clay Liners,” *Annual Book of ASTM Standards, Vol. 4.09*, American Society for Testing and Materials, W. Conshohocken, PA.

Test methods and testing frequencies are presented for manufacturing quality control (MQC) of GCLs. This standard practice includes conformance tests to be performed on the GCL components (bentonite and geotextiles and/or geomembranes) as well as tests to be performed on the finished GCL product. Special procedures for GCL permeability/flux testing require the manufacturer to provide an historical database to demonstrate the consistency of the hydraulic performance of the finished product and to justify the reduced need for frequent MQA permeability testing.

ASTM D 5890, “Standard Test Method for Swell Index Measurement of Clay Mineral Component of Geosynthetic Clay Liners,” *Annual Book of ASTM Standards, Vol. 4.09*, American Society for Testing and Materials, W. Conshohocken, PA.

This test method was adapted from the basic elements of a swell test presented in the USP/NF (United States Pharmacopeia/National Formulary). Two grams of dried and powdered bentonite are slowly dropped into a graduate cylinder containing 100 mL of distilled water. The swell value in mL is recorded after 24 hours, by reading the value on the graduate cylinder at the clay/water interface.

APPENDIX A (continued)

List of Applicable ASTM Standards

ASTM D 5891, “Standard Test Method for Measurement of Fluid Loss of Clay Mineral Component of Geosynthetic Clay Liners.”

This test method was adapted from the API (American Petroleum Institute) Procedure 13A/13B for bentonite. A bentonite slurry is created, aged, and then filtered in a pressurized cell. The amount of water passing through the filter cake in a specified time interval is recorded as the filtrate loss or fluid loss. The test indicates the clay’s general ability to function as a barrier to liquids.

ASTM D 5993, “Standard Test Method for Measuring the Mass per Unit Area of Geosynthetic Clay Liners.”

This test method describes how to measure the bentonite mass per unit area of a GCL sample. A GCL specimen of a certain minimum area is weighed, oven-dried, and weighed again. The dry weight of the specimen, minus the nominal weight of the geosynthetic component(s), is then divided by the area of the specimen. The moisture content of the specimen is determined by subtracting the dry weight from the wet weight.

ASTM D 6072, “Standard Guide for Obtaining Samples of Geosynthetic Clay Liners.”

Presents procedures for obtaining representative samples of GCL material for laboratory testing purposes. These samples may be obtained either at the factory or in the field. Procedures for packaging and protecting the sample are also included to prevent the possibility of damage in transit to the laboratory.

ASTM D 6102, “Standard Guide for Installation of Geosynthetic Clay Liners.”

Provides detailed recommendations for the proper installation of GCLs. Discusses the necessary site conditions, equipment, and techniques for installing GCLs without damaging them. Includes recommendations on panel placement, overlaps, and special considerations for slopes. Also discusses the preferred types of soil cover and equipment used to apply this cover.

ASTM D 6243, “Standard Test Method for Determining the Internal and Interface Shear Resistance of Geosynthetic Clay Liner by the Direct Shear Method.”

This test method covers a procedure for determining the internal shear resistance of a GCL or the interface shear resistance between the GCL and an adjacent material under a constant rate of displacement or constant stress.

ASTM D 6496, “Standard Test Method for Determining Average Bonding Peel Strength Between Top and Bottom Layers of Needle-Punched Geosynthetic Clay Liners.”

This test method was adapted from ASTM D 4632 for grab strength testing of geotextiles. The method covers the laboratory determination of the average bonding strength between the top and bottom layers of a sample of a GCL. These results provide an indication of a GCL’s internal reinforcement and internal shear strength.

APPENDIX A (continued)
List of Applicable ASTM Standards

ASTM D 6768, “Standard Test Method for Tensile Strength of Geosynthetic Clay Liners.”

This test method was adapted from ASTM D 4632 for grab strength testing of geotextiles. The test method establishes the procedures for the measurement of tensile strength of a GCL. This test method is strictly an index test method to be used to verify the tensile strength of GCLs. Results from this test method should not be considered as an indication of actual or long-term performance of the geosynthetic in field applications.

ASTM D 6495, “Standard Guide for Acceptance Testing Requirements for Geosynthetic Clay Liners”.

Provides guidelines for acceptance testing requirements for GCLs, including test methods and verifications.

APPENDIX B CETCO GCL Construction Quality Assurance Checklist

Project Name/Number: _____

CQA Inspector: _____

Date: _____ Weather: _____

STORAGE AREA	
<input type="checkbox"/>	Rolls covered/tarped
<input type="checkbox"/>	Rolls labeled
<input type="checkbox"/>	No standing water present
<input type="checkbox"/>	Packaging intact/repaired
<input type="checkbox"/>	Accessory bentonite protected

MATERIALS RECEIVED TODAY	
<input type="checkbox"/>	Packaging intact
<input type="checkbox"/>	Rolls inspected for damage-- none found
<input type="checkbox"/>	Damage suspected (indicate roll numbers and nature of damage _____)

SITE INSPECTION	
<input type="checkbox"/>	Subgrade surface acceptable
<input type="checkbox"/>	Installation area dry
<input type="checkbox"/>	Anchor trenches acceptable
<input type="checkbox"/>	Design grades achieved
<input type="checkbox"/>	Cover soil acceptable (as applicable)

INSTALLATION	
<input type="checkbox"/>	Number of rolls deployed today (attach list of roll numbers)
<input type="checkbox"/>	Anchor trench fill compacted
<input type="checkbox"/>	Min. seam overlap achieved
<input type="checkbox"/>	All seams visually inspected
<input type="checkbox"/>	Seam bentonite added (as applicable)
<input type="checkbox"/>	All detail work inspected
<input type="checkbox"/>	Downslope panel orientation
<input type="checkbox"/>	All mat covered at end of day
<input type="checkbox"/>	Storage area maintained

INSTALLATION EQUIPMENT	
<input type="checkbox"/>	Core pipe straight
<input type="checkbox"/>	Spreader bar straight
<input type="checkbox"/>	Chains/Straps inspected
<input type="checkbox"/>	Knife blades replaced
<input type="checkbox"/>	Seaming clay supply available

CONFORMANCE TESTING		
<i>Bentonite Mass/Area:</i>		
Bentomat Roll No. _____	Bentonite (g/sm) _____	Pass/ Fail? _____
_____	_____	_____
_____	_____	_____
<i>Bentonite Swell:</i>		
Bentomat Roll No. _____	Final Swell Value (mL/2g) _____	Pass/ Fail? _____
_____	_____	_____
_____	_____	_____
_____	_____	_____
_____	_____	_____
_____	_____	_____

NOTES/OBSERVATIONS	
<div style="border-bottom: 1px solid black; margin-bottom: 5px;"></div> <div style="border-bottom: 1px solid black; margin-bottom: 5px;"></div> <div style="border-bottom: 1px solid black;"></div>	

NOTE:

This checklist is intended to serve as a *guideline* for the CQA engineer to use in the development of a project-specific or company-specific CQA plan. The checklist is not all-inclusive. The items presented in this list are those that CETCO feels are the most important for the proper installation of Bentomat.

BENTOMAT[®] INSTALLATION GUIDELINES

GEOSYNTHETIC CLAY LINERS



BENTOMAT®

GEOSYNTHETIC CLAY LINERS

CONTENTS

1.	Introduction	Page 3
2.	Equipment Requirements	Page 3
3.	Shipping, Unloading, and Storage	Page 5
4.	Subgrade Preparation	Page 5
5.	Installation	Page 6
6.	Anchorage	Page 8
7.	Seaming	Page 8
8.	Sealing Around Penetrations and Structures	Page 9
9.	Damage Repair	Page 10
10.	Cover Placement	Page 12
11.	Hydration	Page 12

NOTICE: THIS DOCUMENT IS INTENDED FOR USE AS A GENERAL GUIDELINE FOR THE INSTALLATION OF CETCO GCLS. THE INFORMATION AND DATA CONTAINED HEREIN ARE BELIEVED TO BE ACCURATE AND RELIABLE. CETCO MAKES NO WARRANTY OF ANY KIND AND ACCEPTS NO RESPONSIBILITY FOR THE RESULTS OBTAINED THROUGH APPLICATION OF THIS INFORMATION. INSTALLATION GUIDELINES ARE SUBJECT TO PERIODIC CHANGES. PLEASE CONSULT OUR WEBSITE @ WWW.CETCO.COM/LT FOR THE MOST RECENT VERSION.

SECTION 1 INTRODUCTION

1.1

This document provides procedures for the installation of CETCO GCLs in a manner that maximizes safety, efficiency, and the physical integrity of the GCL.

1.2

These guidelines are based upon many years of experience at a variety of sites and should be generally applicable to any type of lining project using CETCO GCLs. Variance from these guidelines is at the engineer's discretion.

1.3

The performance of the GCL is wholly dependent on the quality of its installation. It is the installer's responsibility to adhere to these guidelines, and to the project specifications and drawings as closely as possible. It is the engineer's and owner's responsibility to provide construction quality assurance (CQA) for the installation. This will ensure that the installation has been executed properly. This document covers only installation procedures.

1.4

For additional guidance, refer to ASTM D5888 (Standard Guide For Storage and Handling of Geosynthetic Clay Liners) and ASTM D 6102 (Standard Guide For Installation of Geosynthetic Clay Liners).

SECTION 2 EQUIPMENT REQUIREMENTS

2.1

CETCO GCLs are delivered in rolls typically 2,600-2,950 lbs (1180-1340 kg). Roll dimensions and weights will vary with the dimensions of the product ordered. It is necessary to support this weight using an appropriate core pipe, as indicated in Table 1. For any installation, the core pipe must not deflect more than 3 inches (75 mm), as measured from end to midpoint when a full GCL roll is lifted.

2.2

Lifting chains or straps appropriately rated should be used in combination with a spreader bar made from an I-beam, as shown in Figure 1.

2.3

The spreader bar ensures that lifting chains or straps do not chafe against the ends of the GCL roll, allowing it to rotate freely during installation. Spreader bar and core pipe kits are available through CETCO.

2.4

A front end loader, backhoe, dozer, or other equipment can be utilized with the spreader bar and core pipe or slings. Alternatively, a forklift with a "stinger" attachment may be used for on-site handling. A forklift without a stinger attachment should not be used to lift or handle the GCL rolls. Stinger attachments (Figures 2-4) are specially fabricated to fit various forklift makes and models.

Table 1: Core Requirements

Product	Nominal GCL Roll Size Length X Diameter	Typical GCL Roll Weight	Interior Core Size	Core Pipe Length x Diameter	Minimum Core Pipe Strength
BENTOMAT DN, SDN	16' x 24" (4.9 m x 610 mm)	2,650 lbs. (1204 kg)	3 3/4" (100 mm)	20' x 3.5" O.D. (6.1 m x 89 mm)	XXH
BENTOMAT ST	16' x 24" (4.9 m x 610 mm)	2,650 lbs. (1204 kg)	3 3/4" (100 mm)	20' x 3.5" O.D. (6.1 m x 89 mm)	XXH
BENTOMAT STM	16' x 32" (4.9 m x 814 mm)	2,500 lbs. (1130 kg)	3 3/4" (100 mm)	20' x 3.5" O.D. (6.1 m x 89 mm)	XXH
BENTOMAT 200R	16' x 24" (4.9 m x 610 mm)	2,650 lbs. (1204 kg)	3 3/4" (100 mm)	20' x 3.5" O.D. (6.1 m x 89 mm)	XXH
BENTOMAT CLT	16' x 26" (4.9 m x 660 mm)	2,650 lbs. (1204 kg)	3 3/4" (100 mm)	20' x 3.5" O.D. (6.1 m x 89 mm)	XXH
BENTOMAT CL	16' x 25" (4.9 m x 635 mm)	2,650 lbs. (1204 kg)	3 3/4" (100 mm)	20' x 3.5" O.D. (6.1 m x 89 mm)	XXH
BENTOMAT 600 CL	16' x 25" (4.9 m x 635 mm)	2,700 lbs. (1227 kg)	3 3/4" (100 mm)	20' x 3.5" O.D. (6.1 m x 89 mm)	XXH

BENTOMAT®

GEOSYNTHETIC CLAY LINERS

FIGURE 1 -SPREADER BAR ASSEMBLY

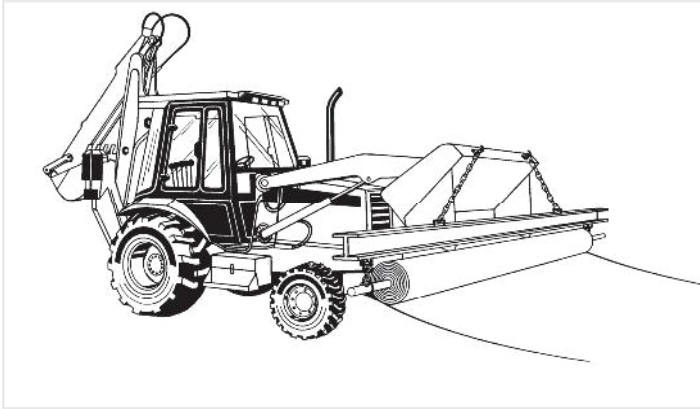
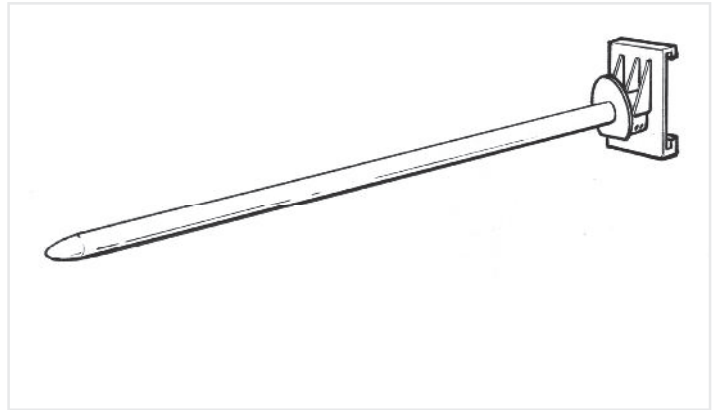


FIGURE 2 - HOOK MOUNT



2.5

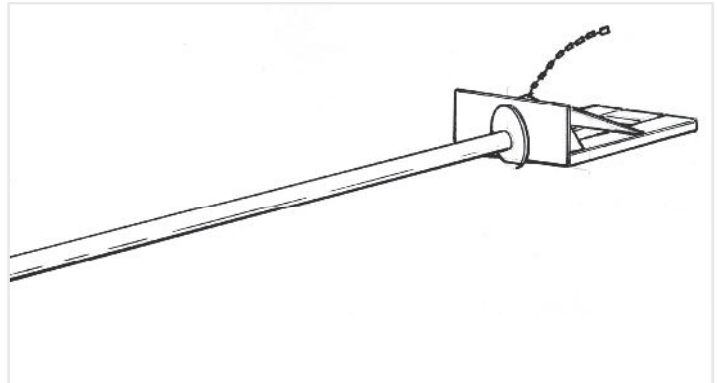
When installing over certain geosynthetic materials, a 4 wheel, all-terrain vehicle (ATV) can be used to deploy the GCL. An ATV can be driven directly on the GCL provided that no sudden stops, starts, or turns are made.

2.6

Additional equipment needed for installation of CETCO GCLs includes:

- ▶ Utility knife and spare blades (for cutting the GCL)
- ▶ Granular bentonite for end-of-roll GCL seams and for sealing around structures and details
- ▶ Waterproof tarpaulins (for temporary cover on installed material as well as for stockpiled rolls)
- ▶ Optional flat-bladed vise grips (for positioning the GCL panel by hand)

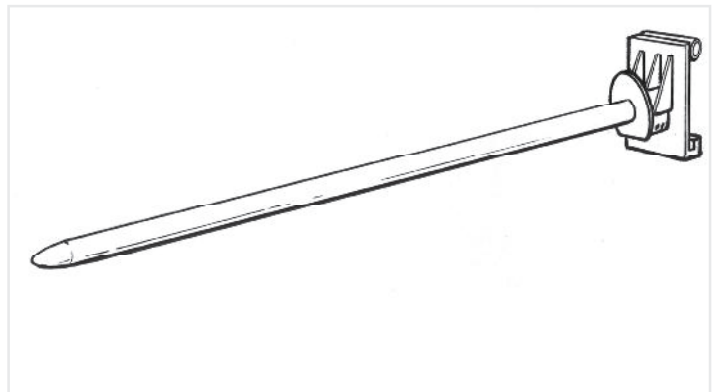
FIGURE 3 - FORK MOUNT (WITH FORK POCKETS)



2.7

The CETCO EASY ROLLER™ GCL Deployment System is a preferred method of installing geosynthetic clay liners. Use of the EASY ROLLER system eliminates the need for spreader bars and heavy core pipes. Installation speed and worker safety are also significantly increased. For further details, contact CETCO.

FIGURE 4 - PIN MOUNT



SECTION 3 SHIPPING, UNLOADING, & STORAGE

3.1

All lot and roll numbers should be recorded and compared to the packing list. Each roll of GCL should also be visually inspected during unloading to determine if any packaging has been damaged. Damage, whether obvious or suspected, should be recorded and the affected rolls marked.

3.2

Major damage suspected to have occurred during transit should be reported to the carrier and to CETCO immediately. The nature of the damage should also be indicated on the bill of lading, with specific lot and roll numbers noted. Accumulation of some moisture within roll packaging is normal and does not damage the product.

3.3

The party directly responsible for unloading the GCL should refer to this manual prior to shipment to ascertain the appropriateness of their unloading equipment and procedures. Unloading and on-site handling of the GCL should be supervised.

3.4

In most cases, CETCO GCLs are delivered on flatbed trucks. There are three methods of unloading: core pipe and spreader bar, slings, or stinger bar. To unload the rolls from the flat-bed using a core pipe and spreader bar, first insert the core pipe through the core tube. Secure the lifting chains or straps to each end of the core pipe and to the spreader bar mounted on the lifting equipment. Hoist the roll straight up and make sure its weight is evenly distributed so that it does not tilt or sway when lifted.

3.5

All CETCO GCLs are delivered with two 2'x 12' (50 mm x 3.65 mm) Type V polyester endless slings on each roll. Before lifting, check the position of the slings. Each sling should be tied off in the choke position, approximately one third (1/3) from the end of the roll. Hoist the roll straight up so that it does not tilt or sway when lifted.

3.6

In some cases, GCL rolls will be stacked in three pyramids on flatbed trucks. If slings are not used, rolls will require unloading with a stinger bar and extendible boom fork lift. Spreader bars will not work in this situation because of the limited access

between the stacks of GCL. Three types of stingers are available from CETCO, a hook mount, fork mount and pin mount (Figures 2-4). To unload, guide the stinger through the core tube before lifting the GCL roll and removing the truck.

3.7

An extendible boom fork lift with a stinger bar is required for unloading vans. Rolls in the nose and center of the van should first be carefully pulled toward the door using the slings provided on the rolls.

3.8

Rolls should be stored at the job site away from high-traffic areas but sufficiently close to the active work area to minimize handling. The designated storage area should be flat, dry, and stable. Moisture protection of the GCL is provided by its packaging; however, based on expected weather conditions, an additional tarpaulin or plastic sheet may be required for added protection during prolonged outdoor storage.

3.9

Rolls should be stacked in a manner that prevents them from sliding or rolling. This can be accomplished by chocking the bottom layer of rolls. Rolls should be stacked no higher than the height at which they can be safely handled by laborers (typically no higher than four layers of rolls). Rolls should never be stacked on end.

SECTION 4 SUBGRADE PREPARATION

4.1

Subgrade surfaces consisting of granular soils or gravels are not acceptable due to their large void fraction and puncture potential. In applications where the GCL is the only barrier, subgrade soils should have a particle-size distribution of at least 80 percent finer than the #60 sieve (0.25 mm). In other applications, subgrade soils should range between fines and 1 inch (25 mm). In high-head applications (greater than 1 foot or 30.48 cm), CETCO recommends a membrane-laminated GCL (BENTOMAT CLT, BENTOMAT CL, or BENTOMAT 600 CL).

4.2

When the GCL is placed over an earthen subgrade, the subgrade surface must be prepared in accordance with the project specifications. The engineer's approval of the subgrade must be obtained prior to installation. The finished surface should be firm and unyielding, without abrupt elevation changes, voids, cracks, ice, or standing water.

BENTOMAT®

GEOSYNTHETIC CLAY LINERS

4.3

The subgrade surface must be smooth and free of vegetation, sharp-edged rocks, stones, sticks, construction debris, and other foreign matter that could contact the GCL. The subgrade should be rolled with a smooth-drum compactor to remove any wheel ruts greater than 1 inch in depth, footprints, or other abrupt grade changes. Furthermore, all protrusions extending more than 0.5 inch (12 mm) from the subgrade surface shall be removed, crushed, or pushed into the surface with a smooth-drum compactor. The GCL may be installed on a frozen subgrade, but the subgrade soil in the unfrozen state should meet the above requirements.

SECTION 5 INSTALLATION

5.1

GCL rolls should be taken to the work area of the site in their original packaging. The orientation of the GCL (i.e., which side faces up) may be important if the GCL has two different types of geosynthetics. Check with the project engineer to determine if there is a preferred installation orientation for the GCL. If no specific orientation is required, allow the roll to unwind from the bottom rather than pulling from the top (Figure 5A). The arrow sticker on the plastic sleeve indicates the direction that the GCL will naturally unroll when placed on the ground (Figure 6). Prior to deployment, the packaging should be carefully removed without damaging the GCL.

5.2

Equipment which could damage the GCL should not be allowed to travel directly on it. Therefore, acceptable installation may be accomplished whereby the GCL is unrolled in front of backwards-moving equipment (Figure 7). If the installation equipment causes rutting of the subgrade, the subgrade must be restored to its originally accepted condition before placement continues.

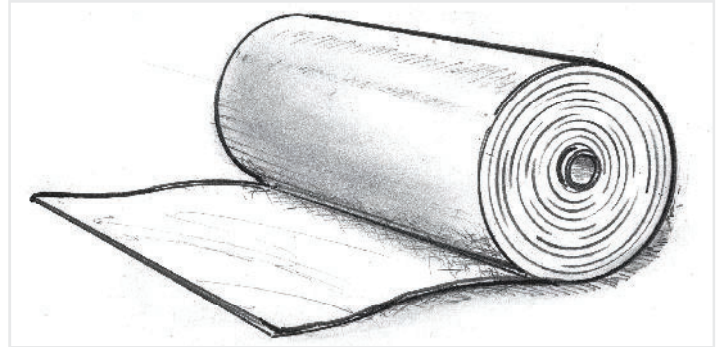
5.3

If sufficient access is available, GCL may be deployed by suspending the roll at the top of the slope, with a group of laborers pulling the material off of the roll, and down the slope (Figure 8).

5.4

GCL rolls should not be released on the slope and allowed to unroll freely by gravity.

FIGURE 5 A & B
"NATURAL' ORIENTATION (5A)



TOP OF THE ROLL (5B)

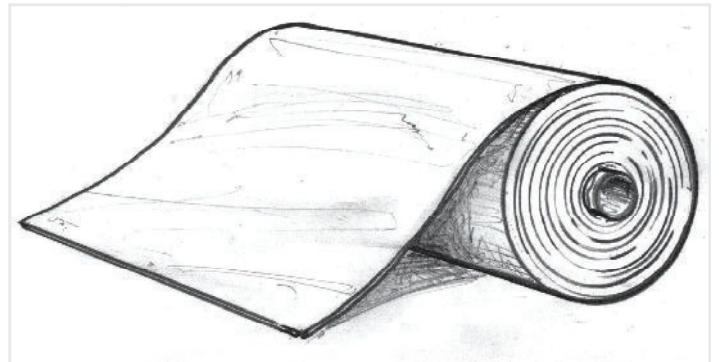


FIGURE 6 - DIRECTION TO UNROLL GCL ON GROUND PER FIGURE 5A

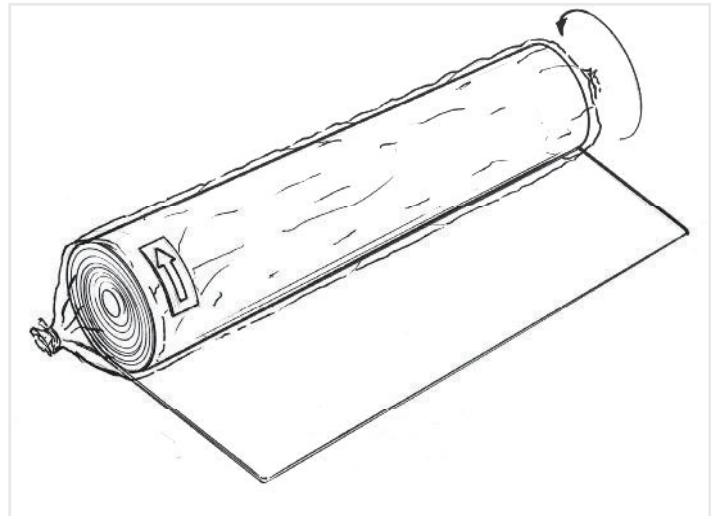


FIGURE 7 - TYPICAL BENTOMAT® INSTALLATION TECHNIQUE

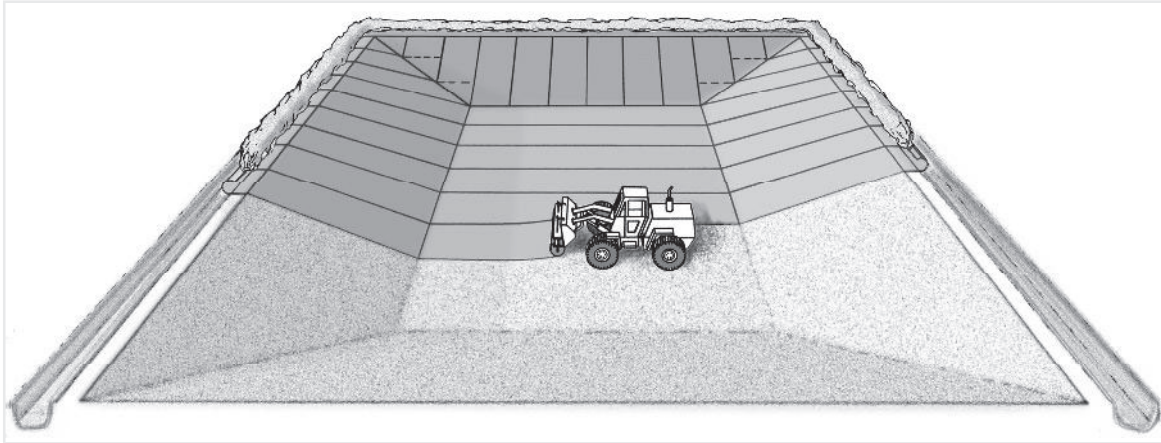
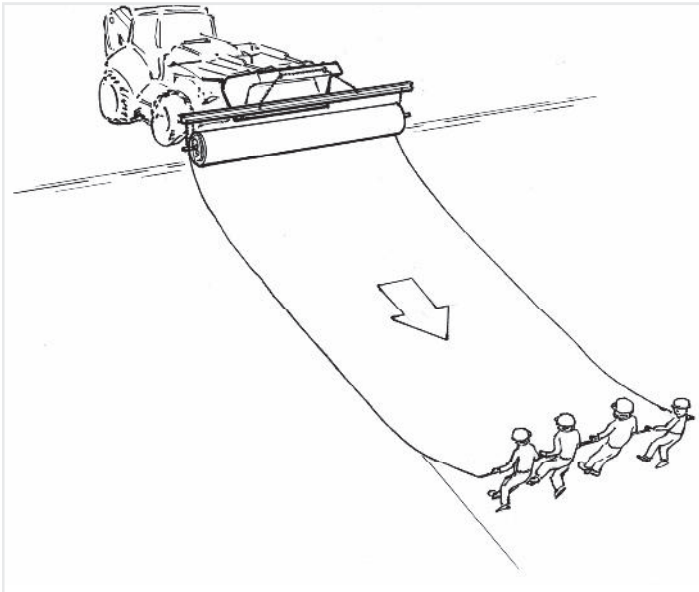


FIGURE 8 - UNROLLING BENTOMAT



5.5

Care must be taken to minimize the extent to which the GCL is dragged across the subgrade to avoid damage to the bottom surface of the GCL. Care must also be taken when adjusting BENTOMAT CLT panels to avoid damage to the geotextile surface of one panel of GCL by the textured sheet of another panel of GCL. A temporary geosynthetic subgrade cover commonly known as a slip sheet or rub sheet may be used to reduce friction damage during placement.

5.6

The GCL should be placed so that seams are parallel to the direction of the slope. End-of-panel seams should also be located at least 3 ft (1 m) from the toe and crest of slopes steeper than 4H:1V. End-of-roll seams on slopes should be used only if the liner is not expected to be in tension.

5.7

All GCL panels should lie flat, with no wrinkles or folds, especially at the exposed edges of the panels. When BENTOMAT geosynthetic clay liners with SUPERGROOVE® is repositioned, it should be gripped inside the SUPERGROOVE by folding the edge.

5.8

The GCL should not be installed in standing water or during rainy weather. Only as much GCL shall be deployed as can be covered at the end of the working day with soil, geomembrane, or a temporary waterproof tarpaulin. The GCL shall not be left uncovered overnight. If the GCL is hydrated when no confining stress is present, it may be necessary to remove and replace the hydrated material. CETCO recommends that premature hydration be evaluated on a case-by-case basis. The project engineer, CQA inspector, and CETCO TR-312 should be consulted for specific guidance if premature hydration occurs. The type of GCL, duration of exposure, degree of hydration, location in the liner system, and expected bearing loads should all be considered.

BENTOMAT®

GEOSYNTHETIC CLAY LINERS

In many instances, a needlepunch reinforced GCL may not require removal/replacement if the following are true:

- ▶ The geotextiles have not been separated, torn, or otherwise damaged
- ▶ There is no evidence that the needlepunching between the two geotextiles has been compromised
- ▶ The GCL does not leave deep indentations when stepped upon
- ▶ Overlapped seams with bentonite enhancement (see Section 7) are intact

5.9

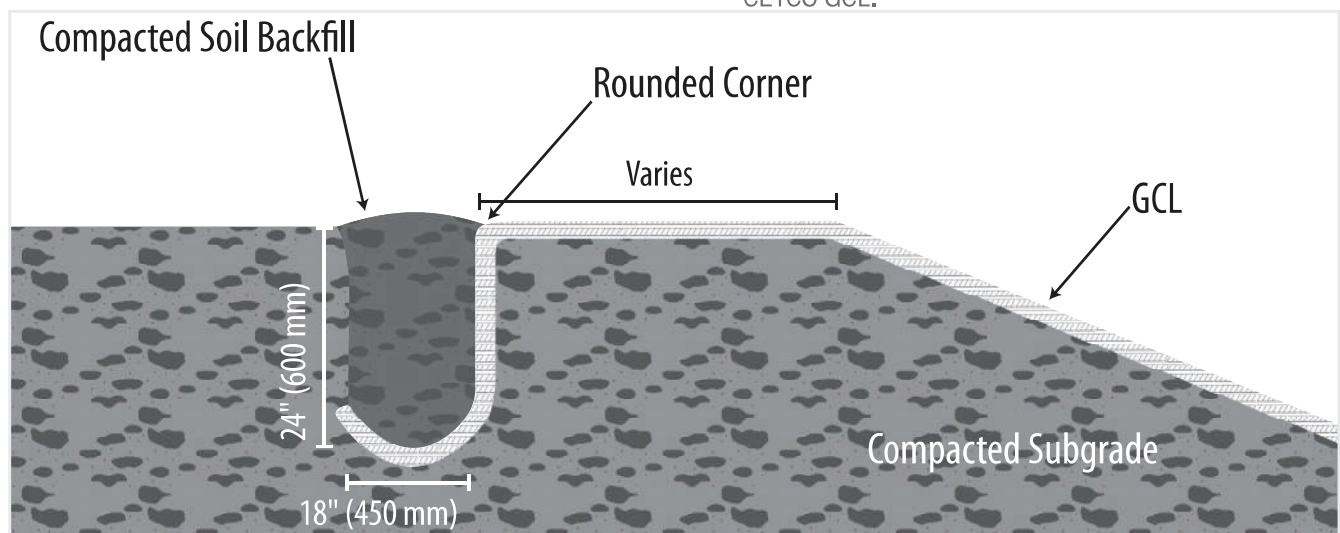
For the convenience of the installer, hash marks are placed on BENTOMAT geosynthetic clay liners every 5' (1.5 m) of length.

SECTION 6 ANCHORAGE

6.1

If required by the project drawings, the end of the GCL roll should be placed in an anchor trench at the top of a slope. The front edge of the trench should be rounded to eliminate any sharp corners that could cause excessive stress on the GCL. Loose soil should be removed or compacted into the floor of the trench.

FIGURE 9 - TYPICAL ANCHOR TRENCH DESIGN



6.2

If a trench is used for anchoring the end of the GCL, soil backfill should be placed in the trench to provide resistance against pullout. The size and shape of the trench, as well as the appropriate backfill procedures should be in accordance with the project drawings and specifications. Typical dimensions are shown in Figure 9.

6.3

The GCL should be placed in the anchor trench such that it covers the entire trench floor but does not extend up the rear trench wall.

6.4

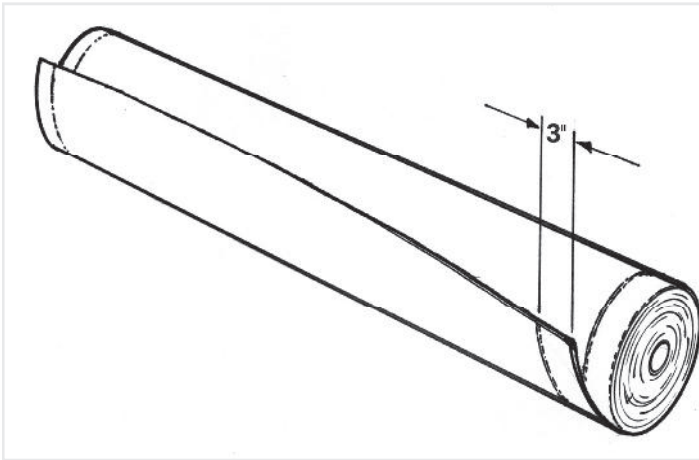
Sufficient anchorage may alternately be obtained by extending the end of the GCL roll back from the crest of the slope, and placing cover soil. The length of this “runout” anchor should be prepared in accordance with project drawings and specifications.

SECTION 7 SEAMING

7.1

GCL seams are constructed by overlapping adjacent panel edges and ends. Care should be taken to ensure that the overlap zone is not contaminated with loose soil or other debris. BENTOMAT 200R, BENTOMAT ST, BENTOMAT DN, and BENTOMAT SDN have SUPERGROOVE® which provides self-seaming capabilities in their longitudinal overlaps, and therefore do not require supplemental bentonite. However, for pond applications, supplemental bentonite must be used in longitudinal seams, regardless of the CETCO GCL.

FIGURE 10 - SUPERGROOVE®



7.2

Longitudinal seams should be overlapped a minimum of 6 inches (150 mm) for BENTOMAT geosynthetic clay liners. For high-head applications (greater than 1 foot or 20.48 cm) involving BENTOMAT CL, BENTOMAT CLT, or BENTOMAT 600 CL, a minimum longitudinal seam overlap of 12 inches (300 mm) and supplemental bentonite (per Section 7.6) is recommended.

7.3

End-of-panel overlapped seams should be overlapped 24 inches (600 mm) for BENTOMAT geosynthetic clay liners.

7.4

End-of-panel overlapped seams are constructed such that they are shingled in the direction of the grade to prevent runoff from entering the overlap zone. End-of-panel seams on slopes are permissible, provided adequate slope stability analysis has been conducted (i.e., the GCL is not expected to be in tension). Bentonite-enhanced seams are required for all BENTOMAT end-of-panel overlapped seams.

7.5

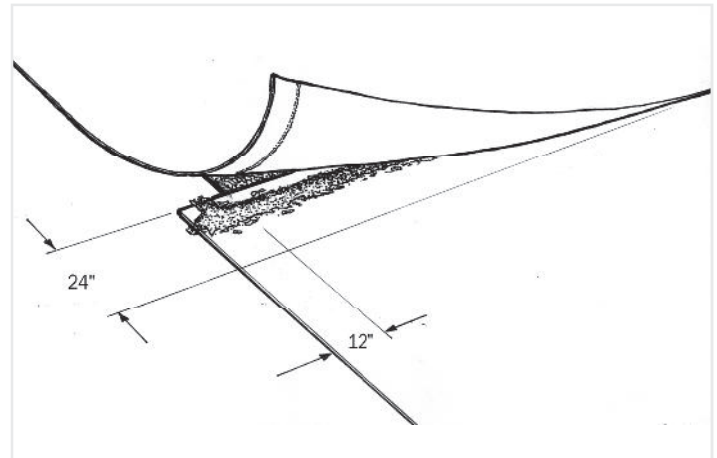
BENTOMAT end-of-panel, bentonite-enhanced, overlapped seams are constructed first by overlapping the adjacent panels, exposing the underlying panel, and then applying a continuous bead or fillet of granular sodium bentonite 12" from the edge of the underlying panel (Figure 11). The minimum application rate at which the bentonite is applied is one-quarter pound per linear foot (0.4 kg/m).

7.6

If longitudinal bentonite enhanced seams are required for BENTOMAT 200R, BENTOMAT ST, BENTOMAT DN, or BENTOMAT SDN, they are constructed by overlapping the adjacent panels a minimum 6 inches (150 mm), exposing the underlying edge, and

applying a continuous bead of granular bentonite approximately 3 inches (75 mm) from the edge. For pond applications involving BENTOMAT CL or BENTOMAT CLT, longitudinal seams are constructed by overlapping adjacent panels by 12 inches (300 mm), exposing the underlying edge, and applying a continuous bead of bentonite approximately 6 inches (150 mm) from the edge. The minimum application rate for the granular bentonite is one quarter pound per linear foot (0.4 kg/m).

**FIGURE 11
BENTOMAT END-OF-PANEL OVERLAPPED SEAM**



SECTION 8 SEALING AROUND PENETRATIONS AND STRUCTURES

8.1

Cutting the GCL should be performed using a sharp utility knife. Frequent blade changes are recommended to avoid irregular tearing of the geotextile components of the GCL during the cutting process.

8.2

The GCL should be sealed around penetrations and structures embedded in the subgrade in accordance with Figures 12 through 14. Granular bentonite shall be used liberally (approximately 0.25 lbs/ln. ft. or 0.4 kg/m) to seal the GCL to these structures.

BENTOMAT®

GEOSYNTHETIC CLAY LINERS

FIGURE 12 A CROSS-SECTION OF A HORIZONTAL PIPE PENETRATION

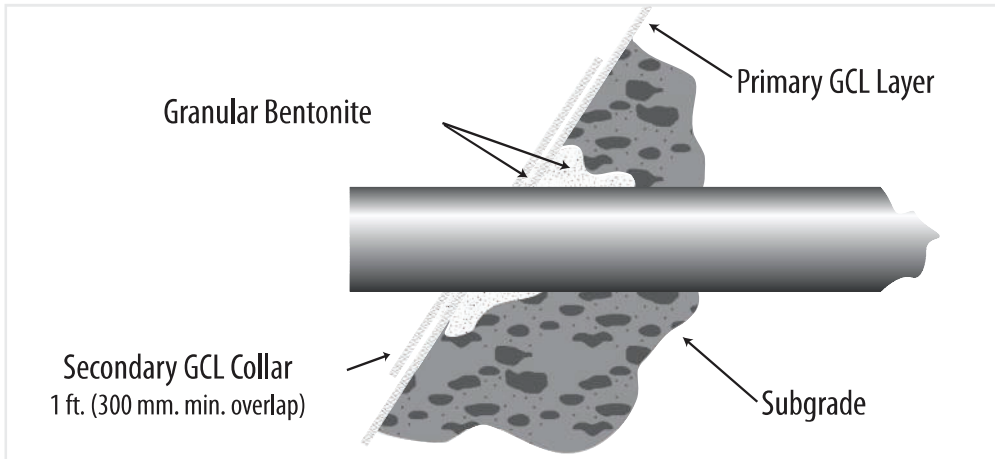


FIGURE 12 B ISOMETRIC VIEW OF A COMPLETED HORIZONTAL PIPE PENETRATION

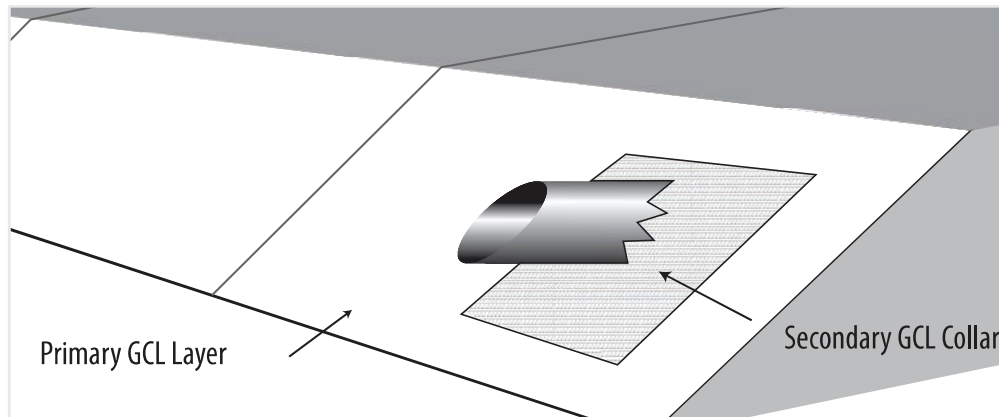


FIGURE 13 A CROSS-SECTION OF A VERTICAL PENETRATION

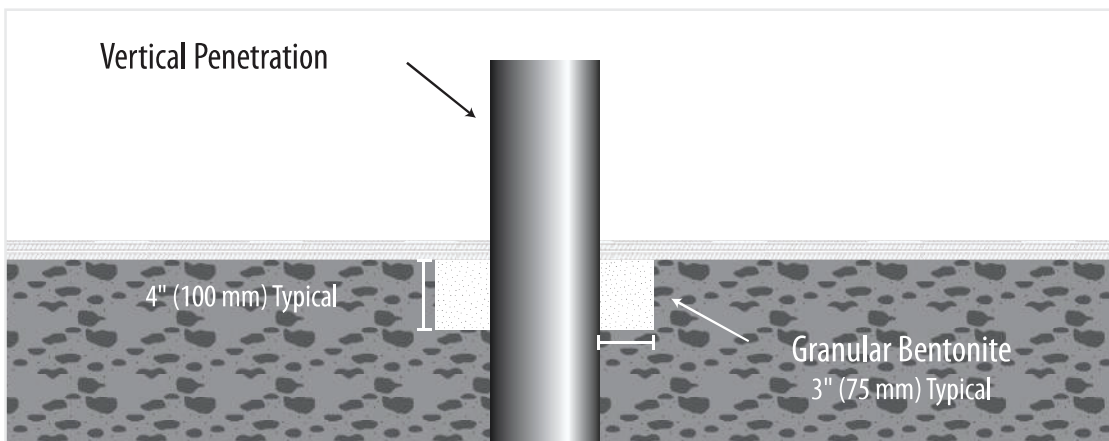


FIGURE 13B ISOMETRIC VIEW OF THE COMPLETED VERTICAL PENETRATION

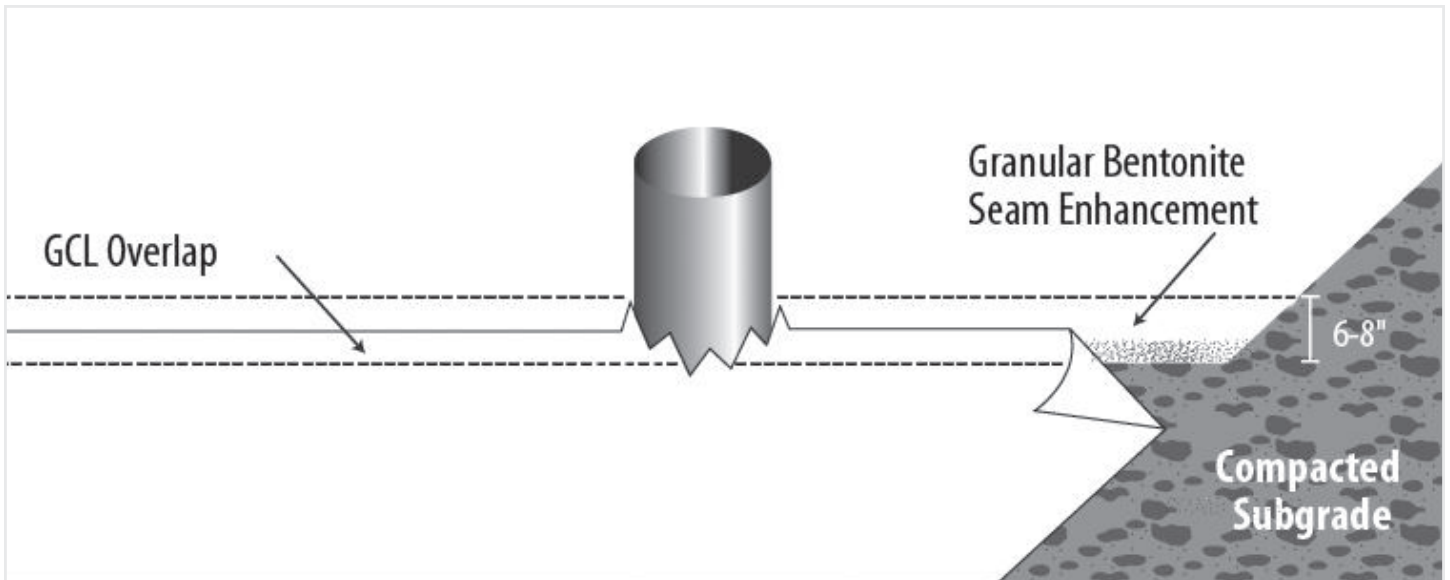
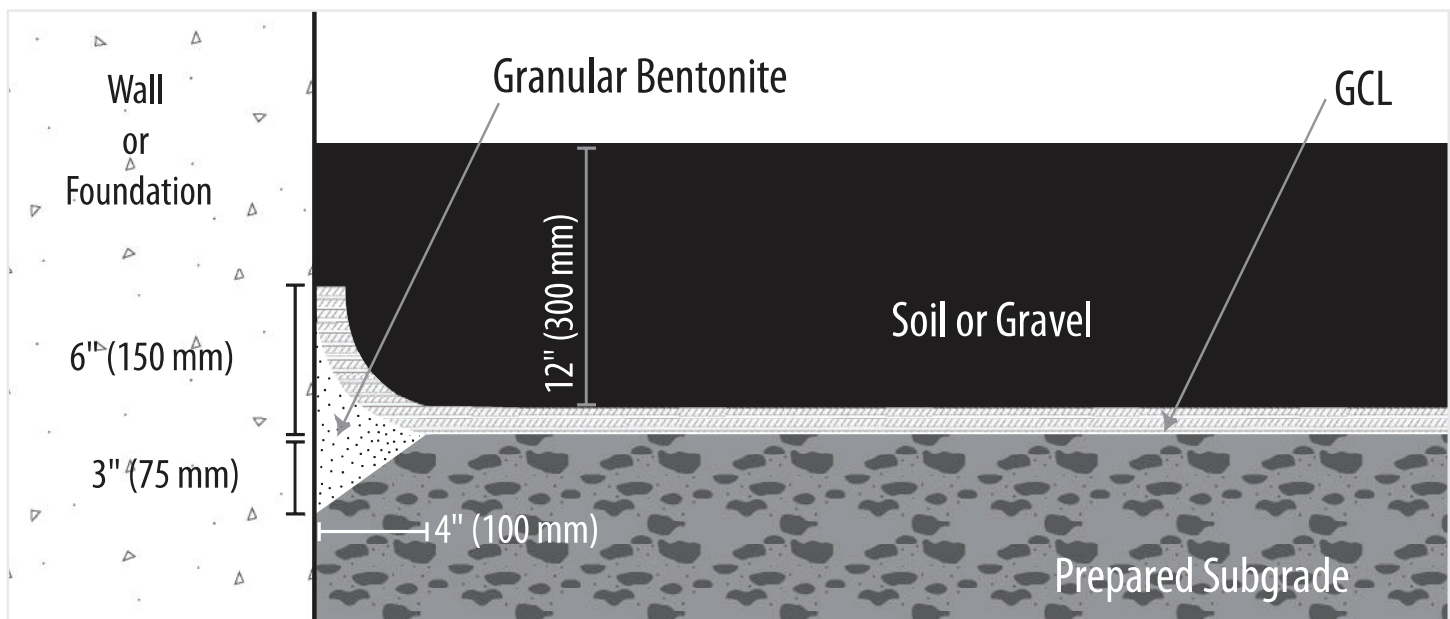


FIGURE 14 CROSS-SECTION OF GCL SEAL AGAINST AN EMBEDDED STRUCTURE OR WALL



BENTOMAT®

GEOSYNTHETIC CLAY LINERS

8.3

When the GCL is placed over a horizontal pipe penetration, a “notch” should be excavated into the subgrade around the penetration (Figure 12a). The notch should then be backfilled with granular bentonite. A secondary collar of GCL should be placed around the penetration, as shown in Figure 12b. It is helpful to first trace an outline of the penetration on the GCL and then cut a “star” pattern in the collar to enhance the collar’s fit to the penetration. Granular bentonite should be applied between the primary GCL layer and the secondary GCL collar.

8.4

Vertical penetrations are prepared by notching into the subgrade as shown in Figure 13a. The penetration can be completed with two separate pieces of GCL as shown in Figure 13b. Alternatively, a secondary collar can be placed as shown in Figure 12a or 12b.

8.5

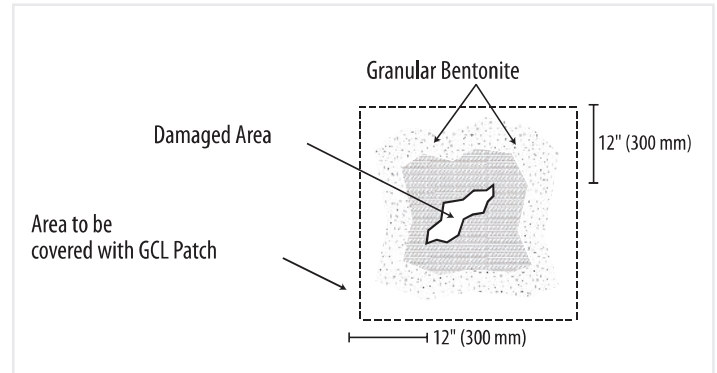
When the GCL is terminated at a structure or wall that is embedded into the subgrade on the floor of the containment area, the subgrade should be notched, as described in Sections 8.3 and 8.4. The notch is filled with granular bentonite; the GCL should be placed over the notch and up against the structure (Figure 14). Connection to the structure can be accomplished by placement of soil or stone backfill in this area. When structures or walls are at the top of a slope, additional detailing may be required. Contact CETCO for specific guidance.

SECTION 9 DAMAGE REPAIR

9.1

If the GCL is damaged (torn, punctured, perforated, etc.) during installation, it may be possible to repair it by cutting a patch to fit over the damaged area (Figure 15). The patch should be cut to size such that a minimum overlap of 12 inches (300 mm) is achieved around all parts of the damaged area. Granular bentonite should be applied around the damaged area prior to placement of the patch. It may be necessary to use an adhesive such as wood glue to affix the patch in place so that it is not displaced during cover placement. Smaller patches may be tucked under the damaged area to prevent patch movement.

FIGURE 15 DAMAGE REPAIR BY PATCHING



SECTION 10 COVER PLACEMENT

10.1

The final thickness of soil cover on the GCL varies with the application. A minimum cover layer must be at least 1 foot (300 mm) thick to provide confining stress to the GCL, eliminate the potential for seam separation and prevent damage by equipment, erosion, etc.

10.2

Cover soils should be free of angular stones or other foreign matter that could damage the GCL. Cover soils should be approved by the engineer with respect to particle size, uniformity, and chemical compatibility. Consult CETCO if cover soils have high concentrations of calcium (e.g. limestone, dolomite, gypsum, seashell fragments).

10.3

Recommended cover soils should have a particle size distribution ranging between fines and 1 inch (25 mm), unless a cushioning geotextile is specified.

10.4

Soil cover shall be placed over the GCL using construction equipment that minimizes stresses on the GCL. A minimum thickness of 1 foot (300 mm) of cover soil should be maintained between the equipment tires/tracks and the GCL at all times during the covering process. In high-traffic areas such as on roadways, a minimum thickness of 2 feet (600 mm) is required.

10.5

Soil cover should be placed in a manner that prevents the soil from entering the GCL overlap zones. Soil cover should be pushed up on slopes, not down slopes, to minimize tensile forces on the GCL.

10.6

When a textured geomembrane is installed over the GCL, a temporary geosynthetic covering known as a slip sheet or rub sheet should be used to minimize friction during placement and to allow the textured geomembranes to be more easily moved into its final position.

10.7

Cyclical wetting and drying of GCL covered only with geomembrane can cause overlap separation. Soil cover should be placed promptly whenever possible. Geomembranes should be covered with a white geotextile and/or operations layer without delay to minimize the intensity of wet-dry cycling. If there is the potential for unconfined cyclic wetting and drying over an extended period of time, the longitudinal seam overlaps should be increased based on the project engineer's recommendation.

10.8

To avoid seam separation, the GCL should not be put in excessive tension by the weight or movement of textured geomembrane on steep slopes. If there is the potential for unconfined geomembrane expansion and contraction over an extended period of time, the longitudinal seam overlaps should be increased based upon the project engineer's recommendation.

SECTION 11 HYDRATION

11.1

Hydration is usually accomplished by natural rainfall and/or absorption of moisture from soil. However, in cases where the containment of non-aqueous liquid is required, it may be necessary to hydrate the covered GCL with water prior to use.

11.2

If manual hydration is necessary, water can be introduced by flooding the covered lined area or using a sprinkler system. If flooding, care must be taken to diffuse the energy of the water discharge so that the cover material is not displaced.

11.3

If the GCL is hydrated when no confining stress is present, it may be necessary to remove and replace the hydrated material.

As discussed in Section 5.8, in many instances a needlepunch reinforced GCL may not require removal/replacement if the following are true:

- ▶ The geotextiles have not been separated, torn or otherwise damaged
- ▶ There is no evidence that the needlepunching between the two geotextiles has been compromised
- ▶ The GCL does not leave deep indentations when stepped upon
- ▶ Any overlapped seams with bentonite enhancement (see Section 7) are intact

BENTOMAT®

GEOSYNTHETIC CLAY LINERS



AMCOL® INTERNATIONAL HEADQUARTERS



Headquartered in Hoffman Estates, IL, AMCOL International Corporation (AMCOL) operates over 68 facilities in Africa, Asia, Australia, Europe, North America and South America. AMCOL employs more than 1,750 employees in 26 countries. The company, established in 1927, currently trades on the New York Stock Exchange under the symbol "ACO". AMCOL produces and markets a wide range of specialty mineral products used for industrial, environmental and consumer-related applications. With more than 68 world-wide locations, AMCOL manages a global supply chain to deliver world-class quality. Our full range of products and services allow us to bring value to our customers, but ultimately, our commitment to understanding customer's needs is what sets us apart in our industry.

DECEMBER 2010

IMPORTANT: The information contained herein is believed to be accurate and reliable. This document supersedes all previous printed versions. For the most up-to-date information, please visit www.CETCO.com. CETCO accepts no responsibility for the results obtained throughout application of this product. CETCO reserves the right to update information without notice.

© 2010 CETCO | PRINTED IN THE USA ON RECYCLED PAPER

2870 Forbs Avenue, Hoffman Estates, IL 60192
847.851.1800 | 800.527.9948 | cetco.com



CETCO, a wholly owned subsidiary of AMCOL International Corp.

Attachment 6

**WDI Major Modification - Liner Design Upgrade Comments
April 13, 2021**

WDI Major Modification - Liner Design Upgrade Comments

EGLE Comments April 13, 2021

Attachment B-1: Slope Stability Analysis

1. Why was the liner stability analysis under interim condition for the E-E' Cross Section not conducted and was conducted only for the B-B' Cross Section?

Response

As stated in the calculation sheet (Point 5 on Page 2 of Attachment B-1), the B-B' cross section is used as an example to demonstrate the methodology for the calculation of what is the acceptable interim waste slope based on the interim filling geometry (slope and height - both of which are controllable by the site) and minimum interface friction angle (or friction/adhesion combination). As part of the geosynthetic acceptance before each construction phase, direct shear testing will be performed on materials proposed for construction per ASTM D5321 and ASTM D6243 and will cover all critical soil/geosynthetic and geosynthetic/geosynthetic interfaces. The maximum allowed waste filling slope will be determined using the method demonstrated in this calculation.

Attachment B-2: Settlement Calculations

2. From the Document "WDI 2021 Permit Modification _ Final – Combined," "Attachment B-2 Settlement Calculations," CTI did not explain what the values of σ_v , σ_c , σ_i , and OCR are, which are used in Equation (2) (see below) for the settlement calculations and how these values were determined?

Settlement caused by primary consolidation for a given layer of soil with uniform properties is calculated as:

$$S_c = \frac{h_0}{1 + e_0} \left(C_r \log \frac{\sigma_c}{\sigma_0} + C_c \log \frac{\sigma_i}{\sigma_c} \right) \quad (2)$$

Where:

C_c = primary compression index

C_r = recompression index

h_0 = initial compressible layer thickness [ft]

e_0 = initial void ratio of the clay subgrade

σ_0 = initial overburden pressure acting on the compressible layer [psf]

σ_i = final overburden pressure acting on the compressible layer [psf]

σ_c = preconsolidation stress [psf]

= OCR \times σ_0

OCR = overconsolidation ratio

Response

Additional details were added to the calculation sheet to help clarify the analysis showing sample calculations for two points along the pipe alignment. The method for determining initial and final stresses is described on page 4 of 7 of Attachment B-2 and implemented in the detailed calculation presented in Attachment B-2.2 (new attachment).

3. CTI only listed the calculation results in Tables 3 to 10 and did not present the values of these original parameters used in calculations and explain how to determine these parameters. The calculation examples for at least two adjacent settlement points should be included in the Report, including total settlement, differential settlement and grade change after settlement between two adjacent settlement points.

Response

Detailed calculation of settlement at two adjacent points were added to the calculation sheet (Attachment B-2.2).

4. What is the full name of OFL shown in Cross Section of MC6-F1 Leachate Pipe Flowline (Page 12 of Attachment B-2 Settlement Calculations) and other cross sections? Does this represent the elevation of the leachate collection pipe before settlement?

Response

The acronym OFL is used to refer to the proposed MC6 top of liner elevations that occur above the existing waste and soil foundation. This also represents the elevation of the bottom of the leachate collection pipe before settlement. This definition was also added to Page 4 of 7 of the Attachment B-2 calculation sheet.

Attachment C: Permit Drawings

5. Please update the Title Sheet to include the following comments.

Response

The Title Sheet has been updated to reflect the following comments.

6. Drawing 02 – Please identify the boundaries of the closed cells as they are shown in the current drawing located in Attachment 17 of WDI’s License.

Response

Closed cell solid waste boundaries have been added.

7. Please include both drawings for the Existing Utility Plan as they are shown in Attachment 17 of the License.

Response

The original MC VI and MC I utility drawings have been added. It should be noted that these utilities are not relevant to the design as they have been or will be removed prior to construction of MC VI-G/F.

8. Drawing 03 – Please include the table showing the footprint area, permit volume, revised volume, and volume adjustment similar to Drawing 05 in Attachment 17 of the License.

Response

A table with the requested theoretical information has been included on Sheet 03 of the permit drawings. Errors in the Table on the 2018 drawing Sheet 05 were also corrected. WDI is approved to dispose of 22.45 million cubic yards of hazardous waste. WDI is not requesting the ability to accept volumes beyond its permitted 22.45 million cubic yards. As we have previously discussed and agreed to with EGLE WDI intends to modify the variations in volumes from grade changes at a later date

once all grade modification can be combined including changes that may occur as a result of the leachate collection sump additions in G4 through G7.

9. Drawing 05 – The leachate collection system is only revised for MC VI-G. Please confirm that the leachate collection system will not be revised for MC VI-F.

Response

At EGLE's request, the leachate collection system for MC VI-F has been modified in order to improve the leachate management operations and provide additional leak detection capabilities. The leachate collection system for MC VI-G has not been revised. WDI is working on evaluating the placement and grade requirements in order to incorporate leachate collection sumps into MC VI-G4 through G7 (if possible), but it is not being requested at this time. Those cells are approximately 10 years away from needing to be constructed and as a result WDI has focused on MC VI-F.

10. Drawings 08 & 09 – Please identify cover areas that were previously permitted vs. proposed.

Response

All cover areas have been previously permitted. This reference in old drawings was made prior to MC VI-F and G cells being permitted and is therefore no longer relevant.

11. Drawings 08, 09, 10, and 11 – In order to clearly understand the relationship between cell locations and final cover contours, the locations of the old and new cell areas should be indicated by color dashed lines.

Response

Colored cell boundary lines have been added to Sheets 08, 09, 10, and 11.

12. Drawings 12, 13, and 14 – Please identify the orientation of the cross sections with arrows on the Overview of Cross Sections.

Response

Arrows have been added to the cross sections on Sheets 12, 13, and 14.

EPA Comments April 22, 2021

13. A chemical compatibility analysis was performed by CETCO in 2018 using GCLs (Bentomat GCL and Resistex 200 GCL) contained in the proposed liner system and leachate from the WDI site. This analysis concluded that the Bentomat GCL would be incompatible with the site’s leachate, however, the Resistex 200 GCL does meet the permeability performance requirements. Since the Bentomat GCLs were incompatible, please provide information on why these GCLs were used in the proposed liner system.

Response

Resistex 200 GCL is the first layer of GCL directly beneath the primary geomembrane. Additional GCL types were included under the Resistex 200 as described below.

WDI believes using standard Bentomat GCL products, under the Resistex 200 in the proposed design, is technically adequate. These products, along with the reasons that they were selected, are summarized in the table below:

Primary/ Secondary Liner	Primary Function	Cell Floor or Side Slope	Design Focus	Upper or Lower GCL	Key Selection Criterion	Proposed Product
Primary	Seepage control	Cell floor	Permeability	Upper	Chemical resistance	Resistex 200
				Lower	Permeant isolation*	Bentomat CL
		Side slope	Slope stability	Upper	Chemical resistance	Resistex 200
				Lower	Shear resistance	Bentomat DN
Secondary	Form a witness zone for leakage detection	Cell floor	Permeability	Upper	Typical application	Bentomat ST
				Lower	Typical application	Bentomat ST
		Side slope	Slope stability	Upper	Typical application	Bentomat ST
				Lower	Shear resistance	Bentomat DN

* To further impede leakage from migrating downwardly

The chemical compatibility analysis performed by CETCO in 2018 using standard Bentomat GCL was an “initial screening” assessment. This assessment was initiated by WDI to see if the standard Bentomat GCL products are adequate for the primary, cell floor liner system, which has the highest potential to be directly impacted by the site leachate - if a leakage should occur.

Once the Tier I and Tier II chemical compatibility analysis reports became available, WDI immediately and conservatively decided to incorporate “specialty” GCL products (i.e., Resistex 200 and Bentomat CL) in the primary liner system when possible.

The only “standard” GCL product that was proposed for the primary liner system is Bentomat DN - to be used as the lower primary GCL layer on side slopes. This standard GCL product was selected due to its superior shear resistance since it consists of

needed-punched, non-woven geotextiles on both sides of the bentonite clay layer. This design recommendation was a result of focusing on maximizing the overall liner shear resistance (therefore the stability) on side slopes as indicated in the table above.

It is also very important to note that steady leachate head (which is needed for any leakage to happen) is very unlikely to exist on 3(H):1(V) side slopes. To incorporate additional conservatism in the proposed design, WDI decided to extend the specialty GCL primary cell floor systems (i.e., Resistex 200/Bentomat CL combination) above the cell floor footprint and extended 5-ft vertically above the toe of side slopes. This is equivalent to more than 15 feet of extra protection on the lower portion of the side slopes. Only at that elevation, the lower GCL layer in the primary liner system on the side slopes is transitioned from Bentomat CL to Bentomat DN for the purpose of maximizing shear resistance as discussed above.

Unlike the primary liner system, the secondary liner system is intended to allow a “detection zone” or “witness zone” to be formed so that any potential leakage caused by defects in the primary liner system, if occurred, can be detected and proper measure can be taken. In other words, the secondary liner system is intended for leak detection only and not intended to continuously contain a large volume of leachate.

Additionally, the secondary GCL layers will be isolated from the leachate by the entire primary liner system, a 5 foot compacted clay attenuation layer, plus the secondary 80-mil HDPE geomembrane. It is therefore deemed extremely unlikely for the secondary GCL products to directly interact with site leachate in any meaningful way.

For the above reasons, WDI selected and proposed the use of some standard GCL products (Bentomat ST and DN) in the proposed secondary liner system. The decision was made for standard containment and for slope stability reasons and WDI believes it is technically adequate.

14. TRC recommends direct shear testing be performed, per ASTM D5321 and ASTM D6243, to confirm the soil to geosynthetic interface strength, geosynthetic to geosynthetic interface strength, and GCL internal strength for the materials proposed for construction. In Attachment B of the Modification Package, WDI commits to performing direct shear tests as part of the Construction Quality Assurance scope of work. Confirm that shear testing will be performed and what standard(s) that will be followed.

Response

Direct shear testing will be performed on materials proposed for construction per ASTM D5321 and ASTM D6243 and will cover all critical soil/geosynthetic and geosynthetic/geosynthetic interfaces.

15. Pore water pressure conditions were not considered in the analyses. Piezometric surfaces were not included at estimated groundwater levels or above the liner system simulating leachate on the liner.

TRC recommends considering the maximum head on liner (calculated to be 11.94 inches in Attachment B-5.1), and the estimated groundwater conditions in the stability models. Additionally, global stability was not considered using the effective stress strength conditions of the underlying clays (drained conditions). Only undrained conditions were modelled, TRC recommends that slope stability be demonstrated under drained conditions.

Response

The undrained strength assumptions for the underlying clay is both applicable and conservative for the slope stability calculations.

Additional analyses of the cross sections under drained conditions, including the long term groundwater table and a leachate head build up scenario, were added to the calculation sheet as applicable and as requested and are presented in Attachment B-1 (pages 1-4 and Attachments B1.8-B1.11). The analyses showed that the factor of safety is acceptable under those conditions.

16. As requested by MEGLE, leachate collection sumps are to be added to isolate detections in each subcell. Please provide construction drawings and additional information about this modification. Drawing 7, 18 and 9 include the details.

Response

Riser locations for the leachate management system are shown on Sheet 08 of the permit drawings. Details for the design of the leachate management system are shown on Sheets 18 and 19 of the permit drawings.

Attachment B-1

Slope Stability Analysis

Table 1: Material Properties

Material	Name	Color in Profile	Unit Wt(s) (pcf)	Strength ϕ or δ (deg.)	Strength C or Ca (psf)
1	Final Cover	Orange	130	0	1500
2	Existing Waste	Teal	86	34	0
3	New Waste	Light Green	103 ^[A]	26 ^[B]	300 ^[B]
4	Upper Clay	Brown	131	0	2150
5	Middle Clay	Yellow	136	0	3300
6	Lower Clay	Maroon	133	0.22 σ_v	
7	Silt	Blue	125	28	0
8	Sand	Red	115	32	0

Notes:

[A] unit weight of waste determined from site survey data reported in 2020.

[B] representative value of waste strength as reported by Qian et al. (2002)

All other properties obtained from NTH (2012)

2. For liner system stability cases, the domain of the slip surfaces are defined so that a portion of the failure surface conforms to the liner system.
3. Applicable data used in the analysis that was provided by third parties is assumed to be accurate.

Design Criteria/Design Basis (with Reference to Source of Data)

1. The minimum allowable factor-of-safety (FS) against slope stability failures is 1.50 for final conditions and 1.30 for interim conditions.
2. The analyses were conducted using the computer program SLOPE/W within the software package GeoStudio 2021 by GEOSLOPE International Ltd. This program performs an automatic search to identify a critical failure surface that has the lowest FS value.
3. The analyses were conducted using the Morgenstern-Price method, which considers both moment and force equilibrium.
4. The geometry of the cross sections was derived from the engineering drawing set submitted as part of the permit mod package.
5. The required/assumed interface friction angles shall be met by considering peak strength values for the cell floor and large-displacement strength values for the cell sideslopes.
6. The required minimum interface friction angle for the liner system components is determined under the final conditions (after final cover is installed).
7. Due to the complex nature of the waste fill phasing during operation, the liner stability shall be evaluated based on the actual measurements of the interface friction angle for the liner system components and the design waste filling geometry for each phase. An example of such a calculation was prepared to illustrate how to evaluate the required minimum interface friction angle for the liner system components. This example analysis was performed on cross section B-B' assuming an interim waste slope of 3.5H:1V.

Results/Conclusions

1. Global slope stability analyses of the waste and foundation for each cross section determined that filling to proposed final grades yields acceptable factors of safety.
 - a. Undrained Conditions:
 - i. Cross Section B-B': Factor of Safety = 1.84
 - ii. Cross Section E-E': Factor of Safety = 2.23
 - b. Drained Conditions:
 - i. Cross Section B-B': Factor of Safety = 1.83
 - ii. Cross Section E-E': Factor of Safety = 2.19
2. Under the final conditions (after installation of final cover, the liner system analyses determined the minimum required interface friction angle for geosynthetics in the floor and slideslope liner systems to yield a factor of safety = 1.50. These values are **10.7 degrees for the floor (peak) and 7 degrees for the sideslope (large-displacement) with zero adhesion**. These values were also confirmed for an analysis of a case with a leachate head buildup of 12 inches in the leachate collection layer.
 - a. Cross Section B-B': Factor of Safety = 1.50 (used to evaluate minimum friction angle)
 - b. Cross Section E-E': Factor of Safety = 1.77
3. The above values are minimum acceptable secant friction angles. Any combination of adhesion and friction angle resulting in comparable shear strength under representative normal stresses to final site conditions are also acceptable. Stability analysis using lab interface shear strength tests results from previous products used on site show that a combination of **$C_{\alpha, peak} = 164 \text{ psf} / \phi_{peak} = 11.1^\circ$ and $C_{\alpha, large displacement} = 110 \text{ psf} / \phi_{large displacement} = 7.3^\circ$** achieves an acceptable factor of safety. **Conformance testing of the selected geosynthetics shall be performed to confirm that the interface shear strength of the actual liner system components is sufficient to ensure the stability of the liner system.**
 - a. Cross Section B-B': Factor of Safety = 1.64
 - b. Cross Section E-E': Factor of Safety = 1.93
4. An example calculation of liner stability for an interim waste filling conditions is presented in Attachment 7. The required interface friction angle for the floor liner system was determined to be 12.7 degrees (peak). Actual interim phasing plan slopes and tested liner system interface properties shall be evaluated for each phase of fill per this example.

Source Documents and References

- NTH (2012). WDI Operating License Application Master Cells VI F & G Volume III – Basis of Design Report
- Qian, X., Gray, D.H., and Koerner, R.M. (2002) *Geotechnical Aspects of Landfill Design and Construction*.

Attachments

1. B-B' Foundation Stability
2. E-E' Foundation Stability
3. B-B' Liner Stability under Final Conditions with zero adhesion
4. E-E' Liner Stability under Final Conditions with zero adhesion
5. B-B' Liner Stability under Final Conditions with non-zero adhesion (previously tested values)
6. E-E' Liner Stability under Final Conditions with non-zero adhesion (previously tested values)
7. B-B' Liner Stability under Interim Conditions (example interim stability calculation)
8. B-B' Foundation Stability under drained conditions
9. E-E' Foundation Stability under drained conditions
10. B-B' Liner Stability under Final Conditions with zero adhesion and leachate head build up
11. E-E' Liner Stability under Final Conditions with zero adhesion and leachate head build up

Attachment 1

B-B' Foundation Stability

SLOPE STABILITY ANALYSIS REPORT FORM

SLOPE STABILITY ANALYSIS REPORT FORM

Project Name:	WDI MC6F Permit Modification						
Project Number:	1208070039.004	Client:	Wayne Disposal, Inc.				
Analysis Short Name:	B-B' Foundation Stability			File name:	WDI Cross Section B Full_20201123_RevD_M K.gsz		
Revision:	1	Originated:	MK	Checked:	KF	Approved:	
Date:	11/23/20	Date:	11/23/20	Date:	11/23/20	Date:	

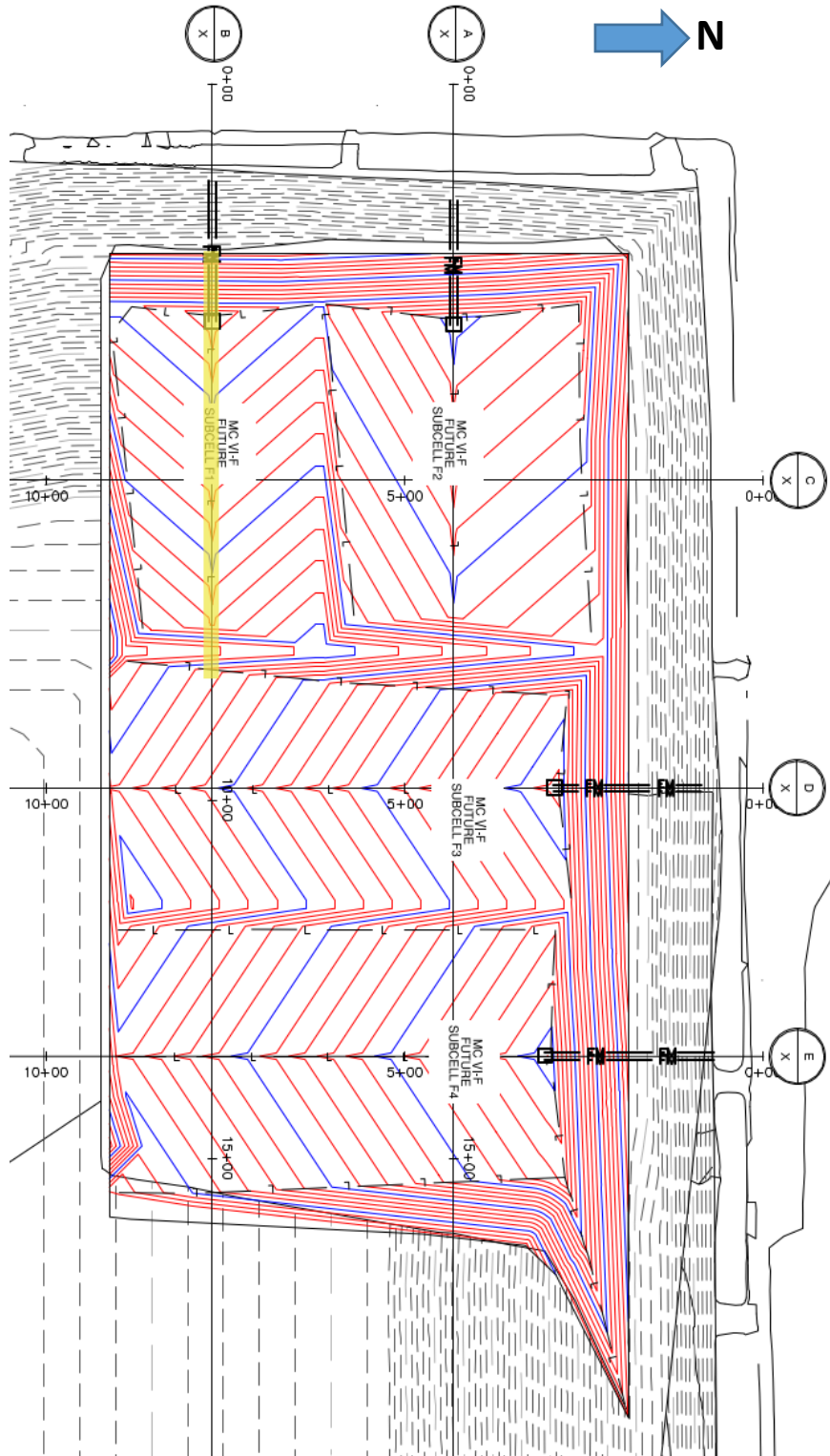
Purpose of Analysis:	To determine the factor of safety of the proposed final waste grades using cross-section B-B'. This case considers a west-facing slope, with fill to the final permitted grade elevations.		
<input type="checkbox"/> Effective Stress <input checked="" type="checkbox"/> Total Stress	<input checked="" type="checkbox"/> Static <input type="checkbox"/> Seismic	<input type="checkbox"/> Pore Pressure	<input checked="" type="checkbox"/> Optimized Surface
Additional Details:	The friction angle of the liner system was set equal to the required minimum interface friction angle determined from the liner stability analysis performed on Cross Section B.		

Material	Name	Color in Profile	Unit Wt(s) (pcf)	Strength ϕ or δ (deg.)	Strength C or Ca (psf)
1	Final Cover	Orange	130	0	1500
2	Existing Waste	Teal	86	34	0
3	New Waste	Light Green	103	26	300
4	Upper Clay	Brown	131	0	2150
5	Middle Clay	Yellow	136	0	3300
6	Lower Clay	Maroon	133	0.22 σ_v	
7	Silt	Blue	125	28	0
8	Sand	Red	115	32	0
9	Liner	Magenta	120	10.7	0

Source of Geometry:	Engineering Drawing Set
Source of Subsurface Profile:	Basis of Design Report - NTH (2012)
<input type="checkbox"/> Preconstruction <input type="checkbox"/> Construction <input type="checkbox"/> Interim <input checked="" type="checkbox"/> Final <input type="checkbox"/> Existing <input type="checkbox"/> Back-Analysis	
Construction Phase Represented:	Final Build out
Other Geometry Notes:	Cross Section B

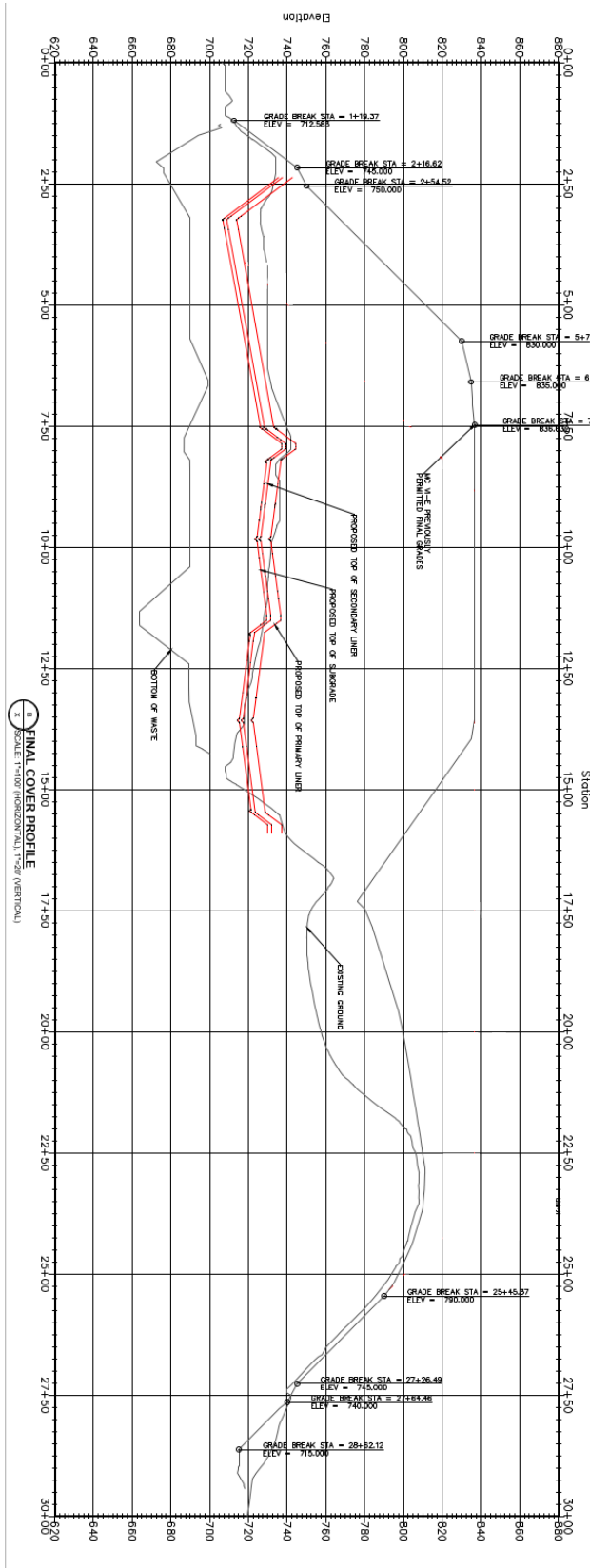
SLOPE STABILITY ANALYSIS REPORT FORM

Final Grades Cross-Section (plan):



SLOPE STABILITY ANALYSIS REPORT FORM

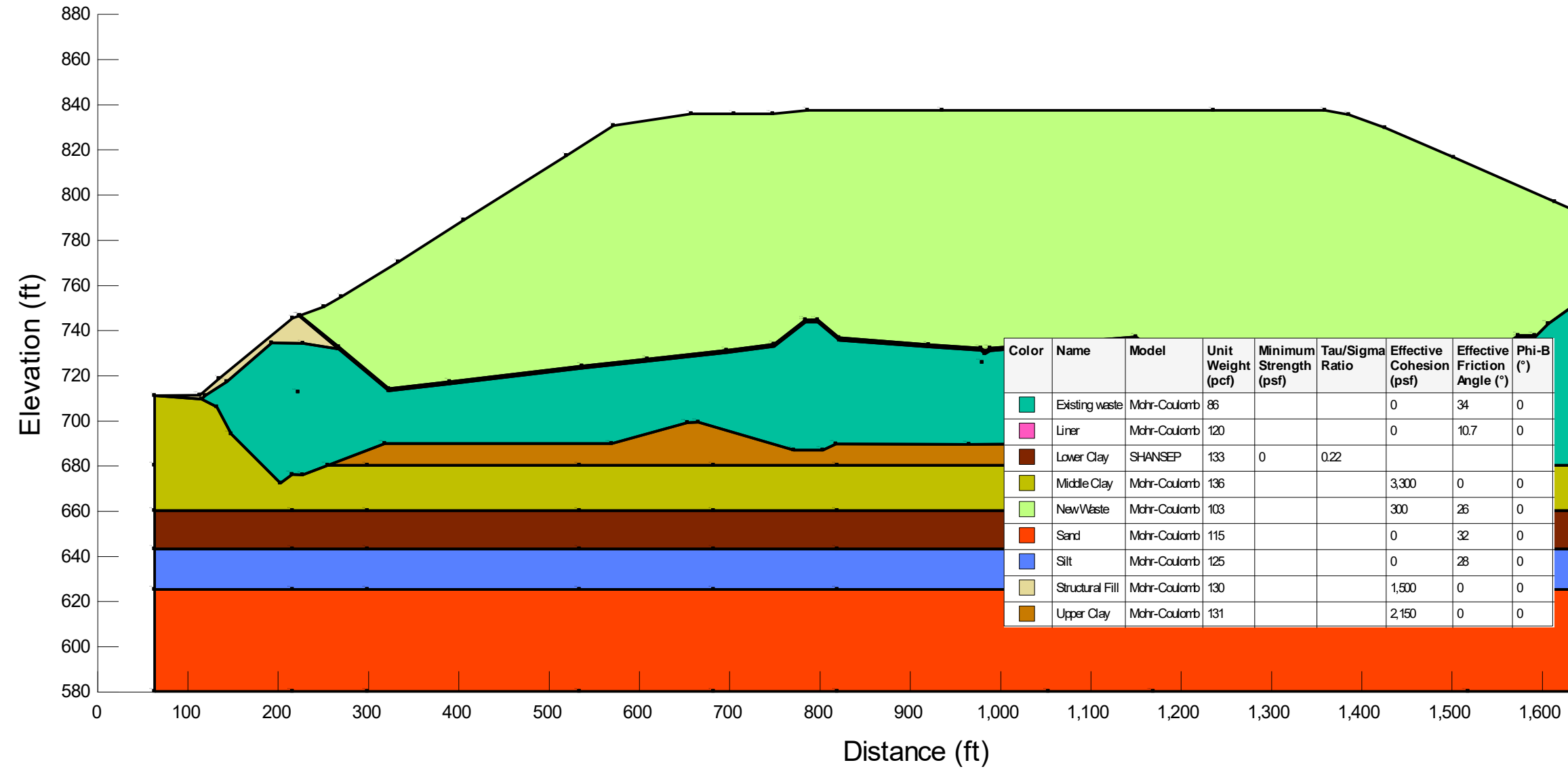
Final Grades Cross-Section (profile):



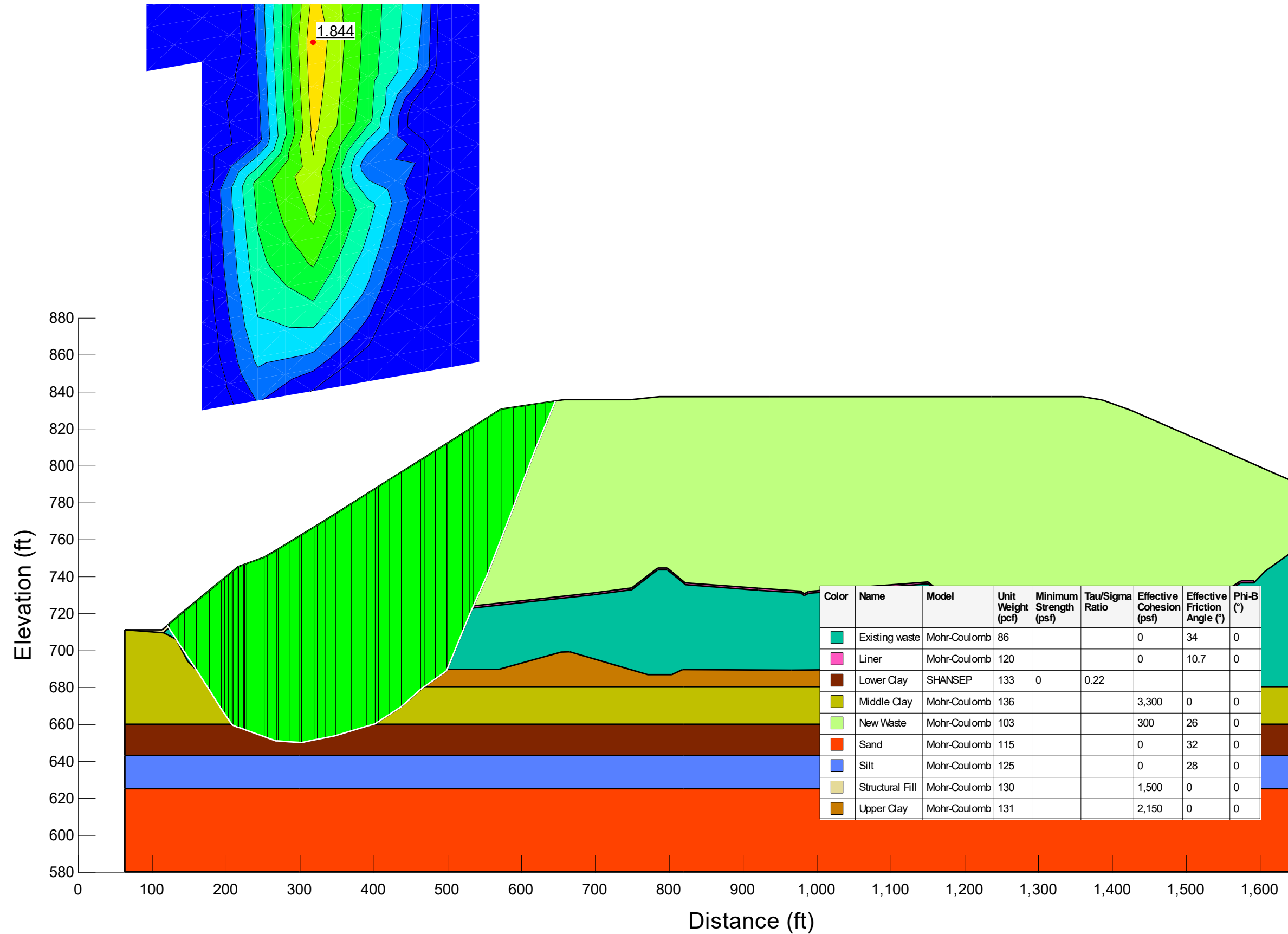
SLOPE STABILITY ANALYSIS REPORT FORM

Factor of Safety:	1.84	<input checked="" type="checkbox"/> Acceptable	<input type="checkbox"/> Not Acceptable	<input type="checkbox"/> Follow-up	<input type="checkbox"/> Superseded
Comments:					
Attachments:	Slope/W Cross Section and Results				

SLOPE STABILITY ANALYSIS REPORT FORM



SLOPE STABILITY ANALYSIS REPORT FORM



Attachment 2

E-E' Foundation Stability

SLOPE STABILITY ANALYSIS REPORT FORM

SLOPE STABILITY ANALYSIS REPORT FORM

Project Name:	WDI MC6F Permit Modification						
Project Number:	1208070039.004		Client:	Wayne Disposal, Inc.			
Analysis Short Name:	E-E' Foundation Stability			File name:	WDI Cross Section E Full_20201123_RevD_M K.gsz		
Revision:	1	Originated:	MK	Checked:	KF	Approved:	
Date:	11/23/20	Date:	11/23/20	Date:	11/23/20	Date:	

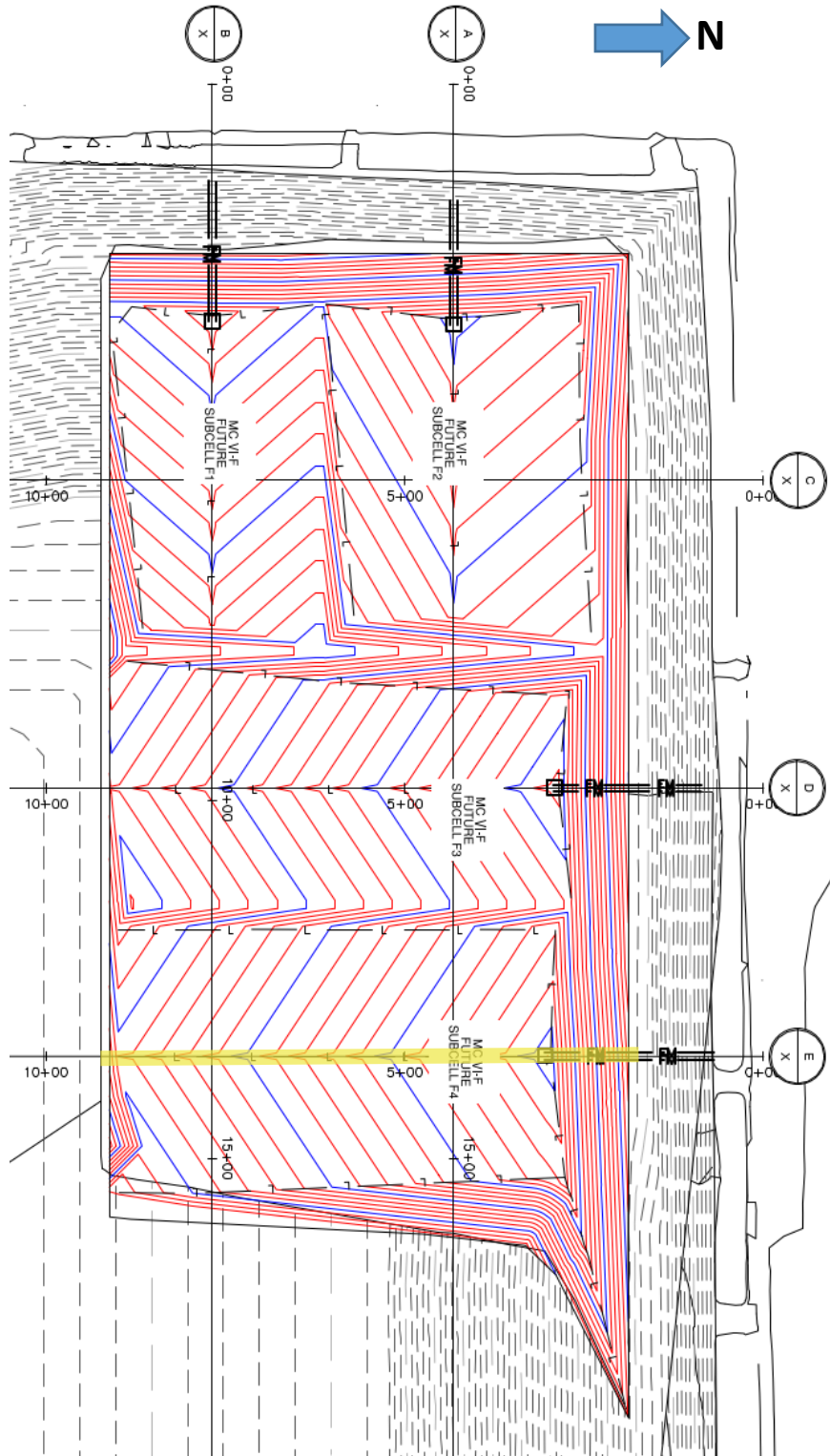
Purpose of Analysis:	To determine the factor of safety of the proposed final waste grades using cross-section E. This case considers a north-facing slope, with fill to the final grade elevations.		
<input type="checkbox"/> Effective Stress <input checked="" type="checkbox"/> Total Stress	<input checked="" type="checkbox"/> Static <input type="checkbox"/> Seismic	<input type="checkbox"/> Pore Pressure	<input checked="" type="checkbox"/> Optimized Surface
Additional Details:	The friction angle of the liner system was set equal to the required minimum interface friction angle determined from the liner stability analysis performed on Cross Section B		

Material	Name	Color in Profile	Unit Wt(s) (pcf)	Strength ϕ or δ (deg.)	Strength C or Ca (psf)
1	Final Cover	Orange	130	0	1500
2	Existing Waste	Teal	86	34	0
3	New Waste	Light Green	103	26	300
4	Upper Clay	Brown	131	0	2150
5	Middle Clay	Yellow	136	0	3300
6	Lower Clay	Maroon	133	0.22 σ_v	
7	Silt	Blue	125	28	0
8	Sand	Red	115	32	0
8	Liner System	Magenta	120	10.7	0

Source of Geometry:	Engineering Drawing Set
Source of Subsurface Profile:	Basis of Design Report - NTH (2012)
	<input type="checkbox"/> Preconstruction <input type="checkbox"/> Construction <input type="checkbox"/> Interim <input checked="" type="checkbox"/> Final <input type="checkbox"/> Existing <input type="checkbox"/> Back-Analysis
Construction Phase Represented:	Final build out
Other Geometry Notes:	Cross Section E-E'

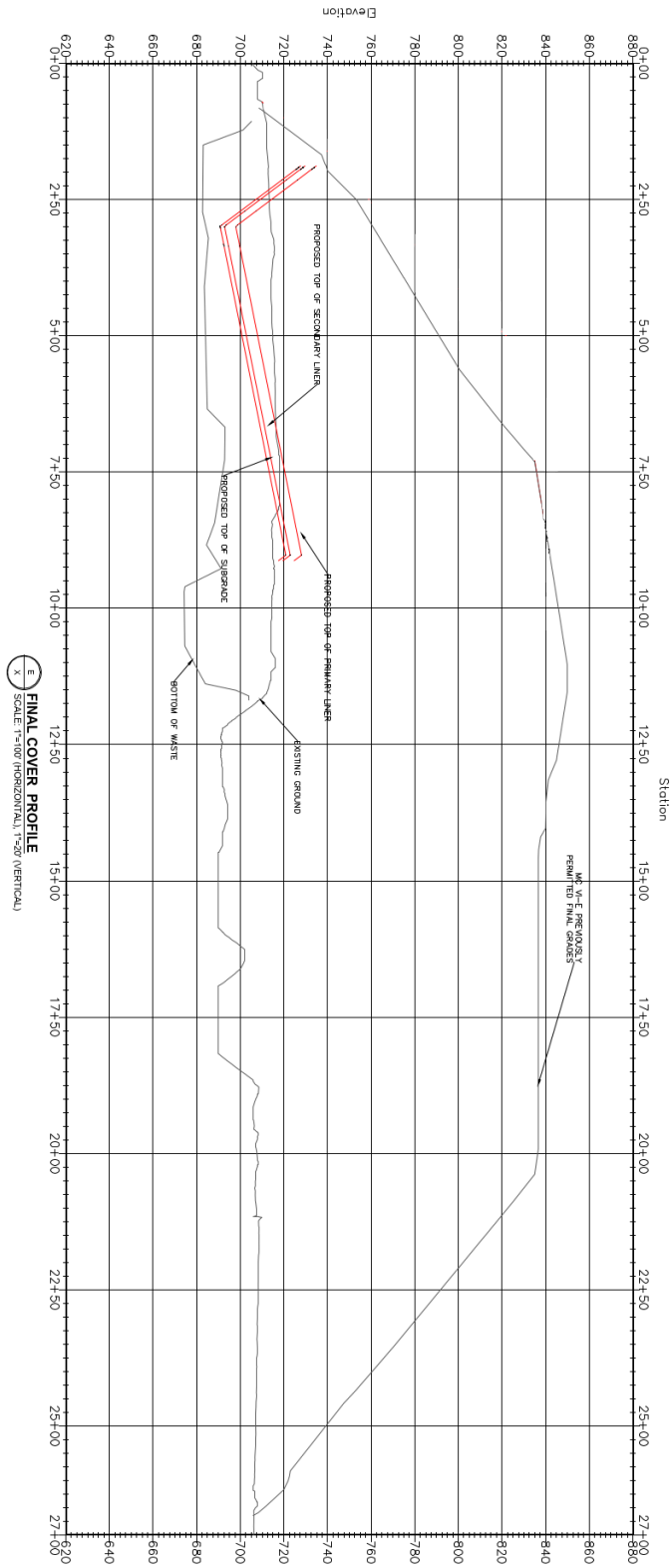
SLOPE STABILITY ANALYSIS REPORT FORM

Final Grades Cross-Section (plan):



SLOPE STABILITY ANALYSIS REPORT FORM

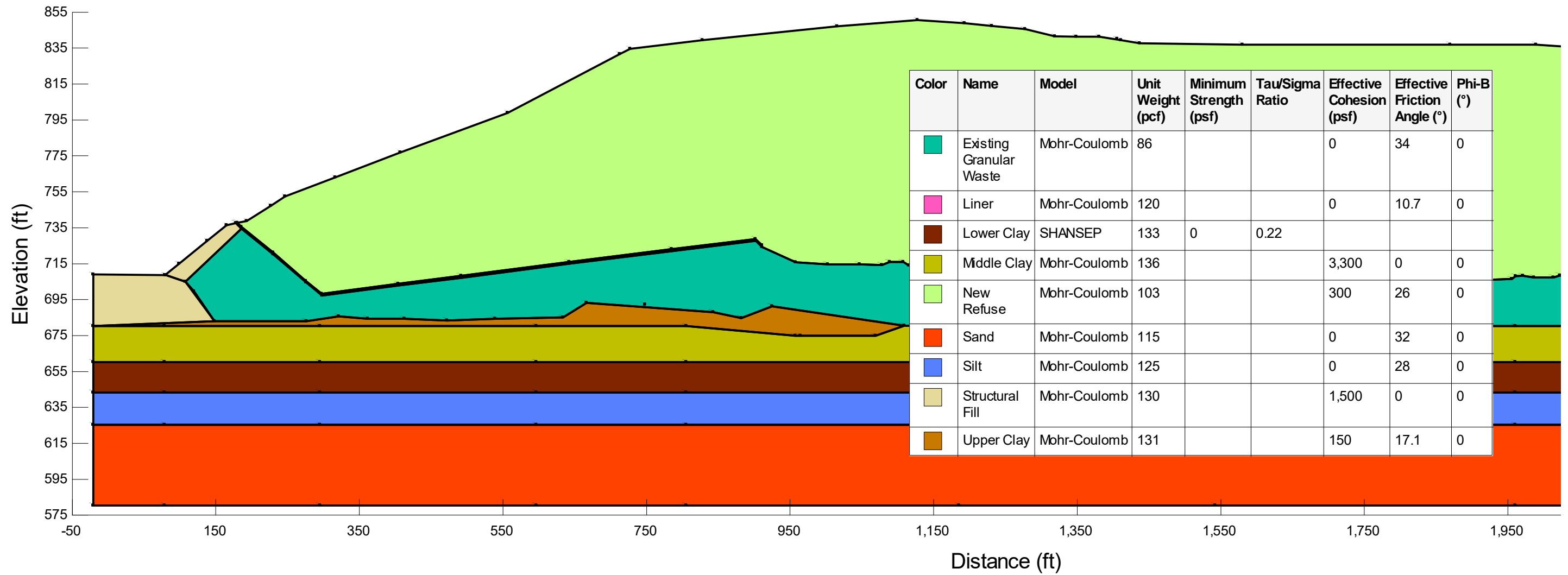
Final Grades Cross-Section (profile):



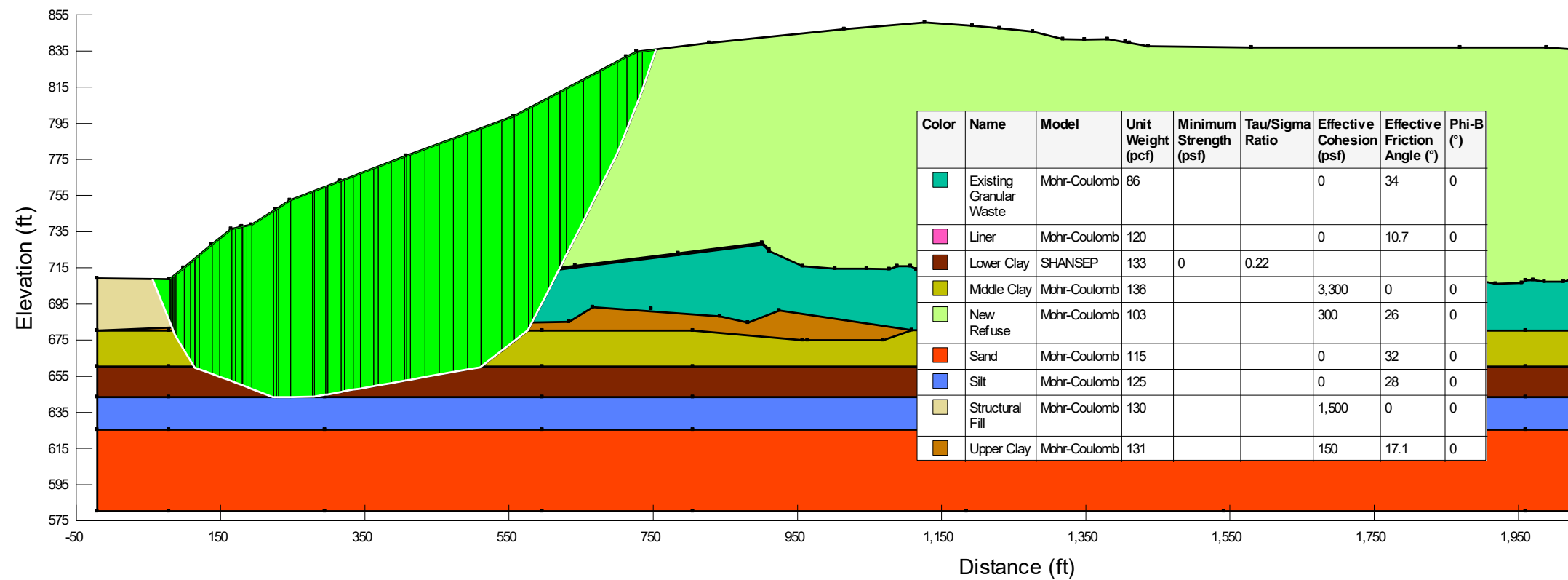
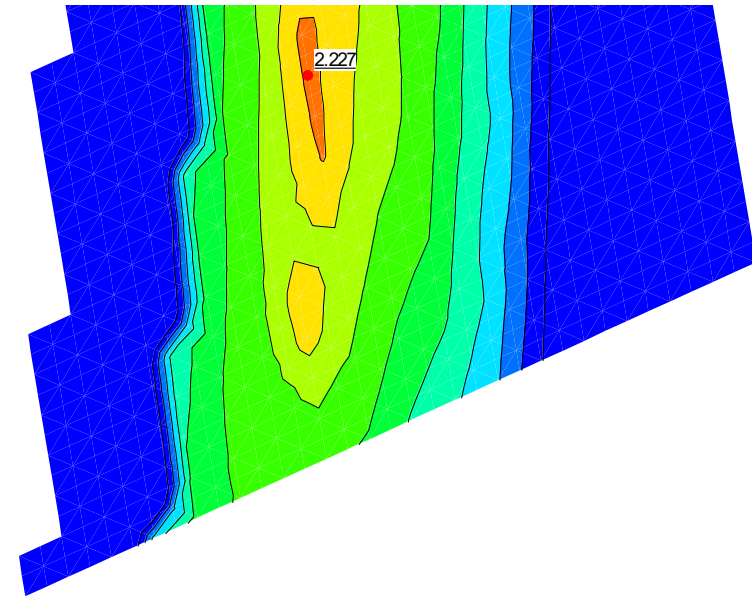
SLOPE STABILITY ANALYSIS REPORT FORM

Factor of Safety:	2.23	<input checked="" type="checkbox"/> Acceptable	<input type="checkbox"/> Not Acceptable	<input type="checkbox"/> Follow-up	<input type="checkbox"/> Superseded
Comments:					
Attachments:	Slope/W Cross Section and Results				

SLOPE STABILITY ANALYSIS REPORT FORM



SLOPE STABILITY ANALYSIS REPORT FORM



Attachment 3

B-B' Liner Stability under Final Conditions with zero adhesion

SLOPE STABILITY ANALYSIS REPORT FORM

SLOPE STABILITY ANALYSIS REPORT FORM

Project Name:	WDI MC6F Permit Modification						
Project Number:	1208070039.004	Client:	Wayne Disposal, Inc.				
Analysis Short Name:	B-B' Liner Stability			File name:	WDI Cross Section B Liner_20201123_RevD_MK.gsz		
Revision:	1	Originated:	MK	Checked:	KF	Approved:	
Date:	11/23/20	Date:	11/23/20	Date:	11/23/20	Date:	

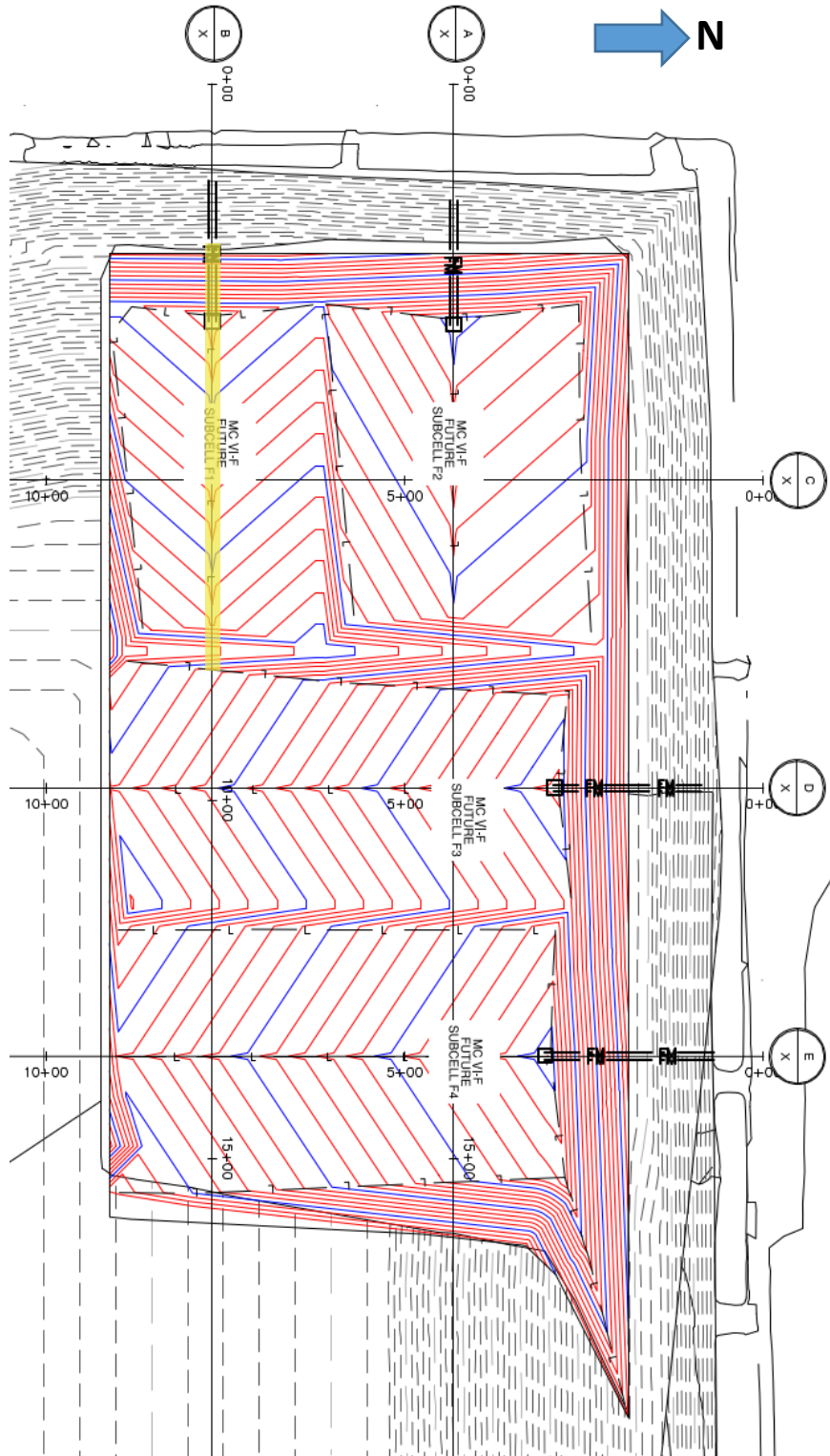
Purpose of Analysis:	To determine the required liner system interface strength to achieve an acceptable factor of safety of the proposed final waste grades using cross-section B. This case considers a west-facing slope, with fill to the final permitted grade elevations. The failure surface is defined such that failure occurs in the underlying liner in order to consider the stability of the liner.		
<input type="checkbox"/> Effective Stress <input checked="" type="checkbox"/> Total Stress	<input checked="" type="checkbox"/> Static <input type="checkbox"/> Seismic	<input type="checkbox"/> Pore Pressure	<input checked="" type="checkbox"/> Optimized Surface
Additional Details:	The liner system was modeled in 2 sections (floor and sideslope) to allow use of Peak and Large-Displacement strength parameters appropriately. The friction angle of the sideslope was set at 7° corresponding to commonly achievable large-displacement interface secant friction angle. The friction angle of the floor liner system was varied to determine the required peak interface secant friction angle to achieve the required factor of safety of 1.5.		

Material	Name	Color in Profile	Unit Wt(s) (pcf)	Strength ϕ or δ (deg.)	Strength C or Ca (psf)
1	Final Cover	Orange	130	0	1500
2	Existing Waste	Teal	86	34	0
3	New Waste	Light Green	103	26	300
4	Upper Clay	Brown	131	0	2150
5	Middle Clay	Yellow	136	0	3300
6	Lower Clay	Maroon	133	0.22 σ_v	
7	Silt	Blue	125	28	0
8	Sand	Red	115	32	0
9	Liner (Floor)	Magenta	120	TBD	0
10	Liner (Sideslope)	Purple	120	7	0

Source of Geometry:	Engineering Drawing Set
Source of Subsurface Profile:	Basis of Design Report - NTH (2012)
	<input type="checkbox"/> Preconstruction <input type="checkbox"/> Construction <input type="checkbox"/> Interim <input checked="" type="checkbox"/> Final <input type="checkbox"/> Existing <input type="checkbox"/> Back-Analysis
Construction Phase Represented:	Final build out
Other Geometry Notes:	Cross Section B

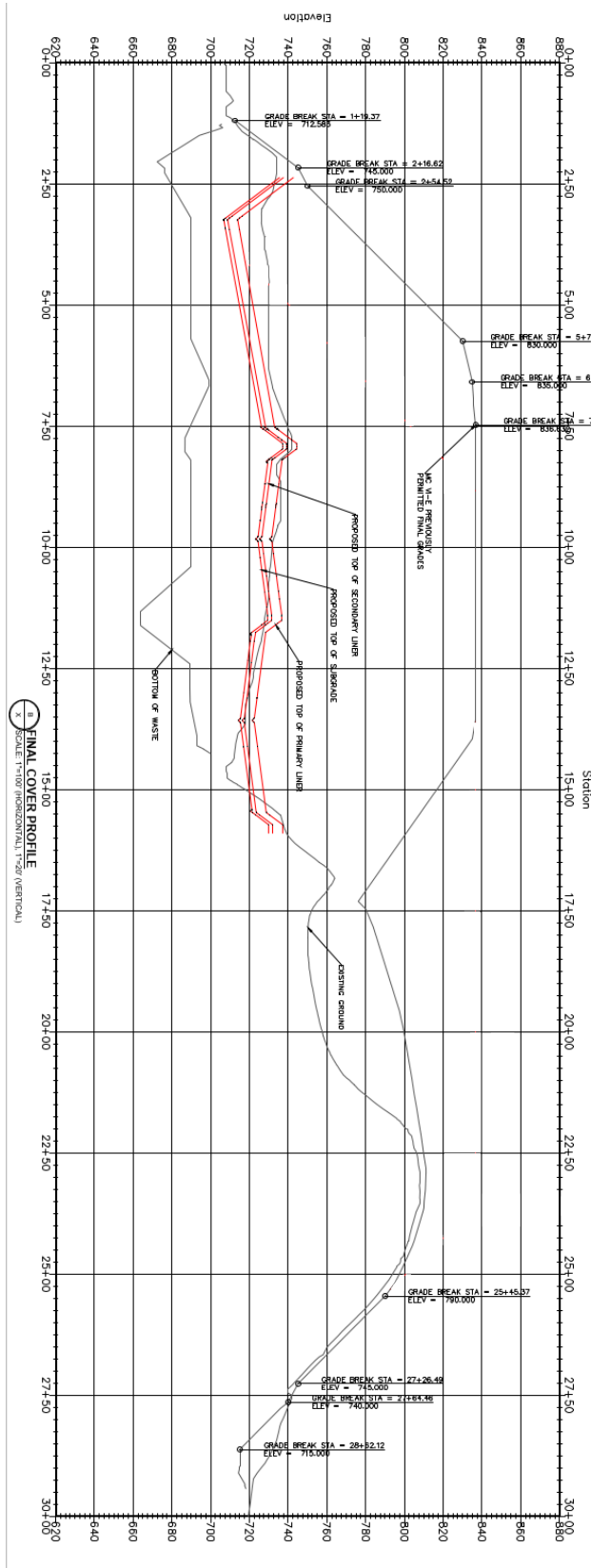
SLOPE STABILITY ANALYSIS REPORT FORM

Final Grades Cross-Section (plan):



SLOPE STABILITY ANALYSIS REPORT FORM

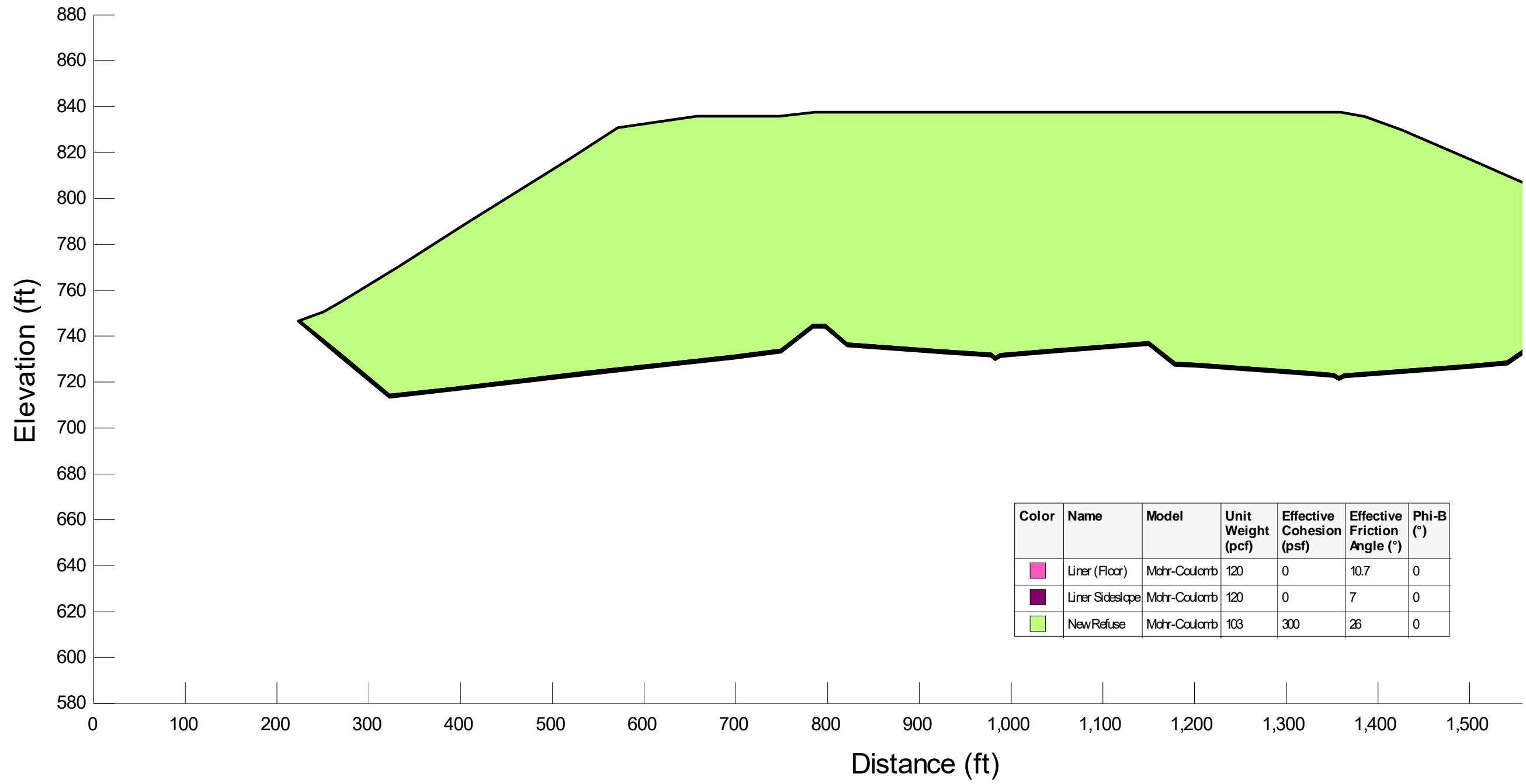
Final Grades Cross-Section (profile):



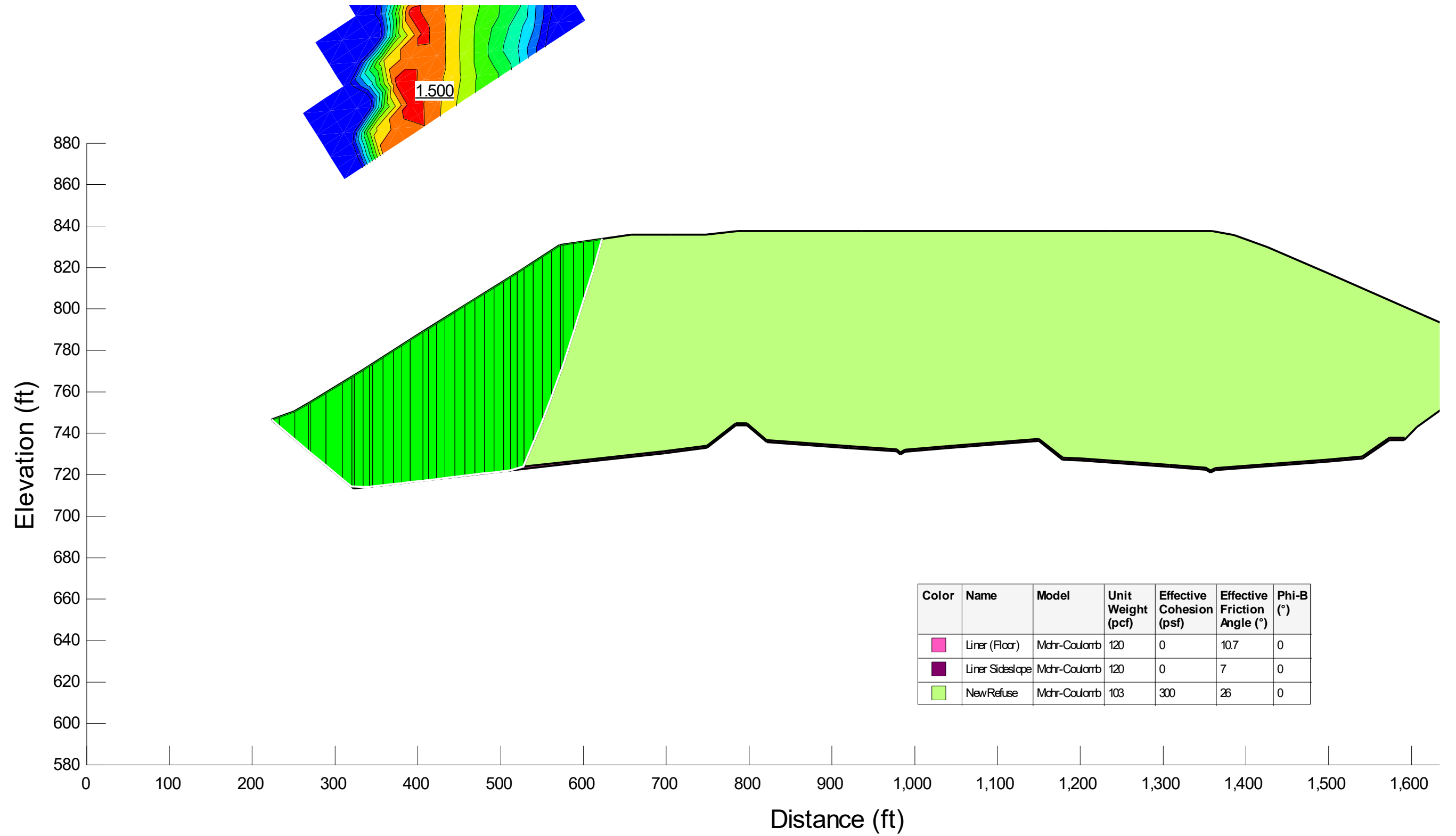
SLOPE STABILITY ANALYSIS REPORT FORM

Factor of Safety:	1.50	<input checked="" type="checkbox"/> Acceptable	<input type="checkbox"/> Not Acceptable	<input type="checkbox"/> Follow-up	<input type="checkbox"/> Superseded
Comments:	The required peak interface friction for the floor liner system was determined to be 10.7°.				
Attachments:	Slope/W Cross Section and Results				

SLOPE STABILITY ANALYSIS REPORT FORM



SLOPE STABILITY ANALYSIS REPORT FORM



Attachment 4

E-E' Liner Stability under Final Conditions with zero adhesion

SLOPE STABILITY ANALYSIS REPORT FORM

SLOPE STABILITY ANALYSIS REPORT FORM

Project Name:	WDI MC6F Permit Modification						
Project Number:	1208070039.004	Client:	Wayne Disposal, Inc.				
Analysis Short Name:	E-E' Liner Stability			File name:	WDI Cross Section E Liner_20201123_RevC_MK.gsz		
Revision:	1	Originated:	MK	Checked:	KF	Approved:	
Date:	11/23/20	Date:	11/23/20	Date:	11/23/20	Date:	

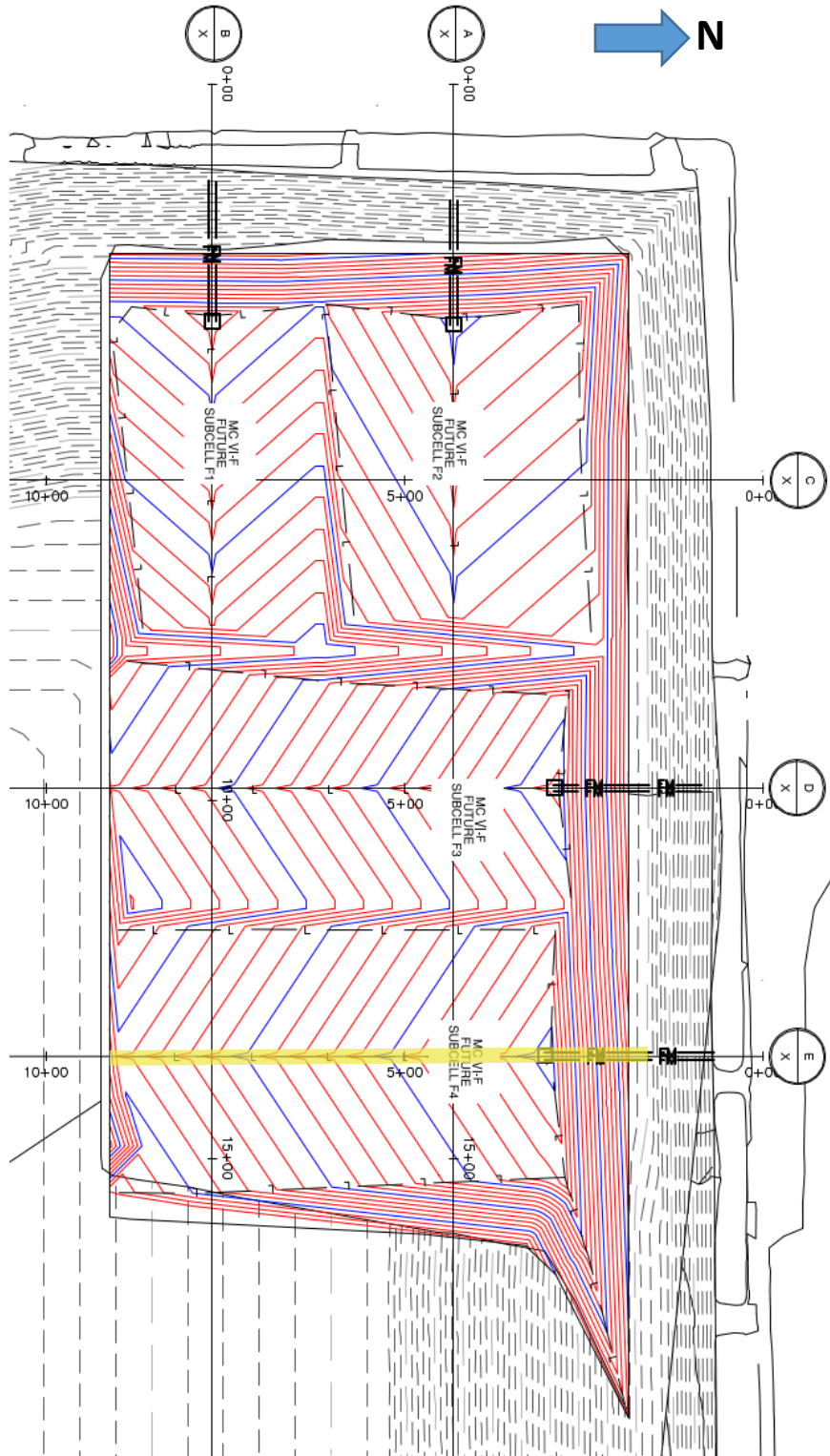
Purpose of Analysis:	To determine the factor of safety of the proposed final waste grades using cross-section E. This case considers a north-facing slope, with fill to the final grade elevations. The failure surface is defined such that failure occurs in the underlying liner in order to consider the stability of the liner.		
<input type="checkbox"/> Effective Stress <input checked="" type="checkbox"/> Total Stress	<input checked="" type="checkbox"/> Static <input type="checkbox"/> Seismic	<input type="checkbox"/> Pore Pressure	<input checked="" type="checkbox"/> Optimized Surface
Additional Details:	The friction angle of the liner system was set equal to the required minimum interface friction angle determined from the liner stability analysis performed on Cross Section B. The liner system was modeled in 2 sections (floor and sideslope) to allow use of Peak and Large-Displacement strength parameters appropriately.		

Material	Name	Color in Profile	Unit Wt(s) (pcf)	Strength ϕ or δ (deg.)	Strength C or Ca (psf)
1	Final Cover	Orange	130	0	1500
2	Existing Waste	Teal	86	34	0
3	New Waste	Light Green	103	26	300
4	Upper Clay	Brown	131	0	2150
5	Middle Clay	Yellow	136	0	3300
6	Lower Clay	Maroon	133	0.22 σ_v	
7	Silt	Blue	125	28	0
8	Sand	Red	115	32	0
9	Liner (Floor)	Magenta	120	10.7	0
10	Liner (Sideslope)	Purple	120	7	0

Source of Geometry:	Engineering Drawing Set
Source of Subsurface Profile:	Basis of Design Report - NTH (2012)
<input type="checkbox"/> Preconstruction <input type="checkbox"/> Construction <input type="checkbox"/> Interim <input checked="" type="checkbox"/> Final <input type="checkbox"/> Existing <input type="checkbox"/> Back-Analysis	
Construction Phase Represented:	Final build out
Other Geometry Notes:	Cross Section E

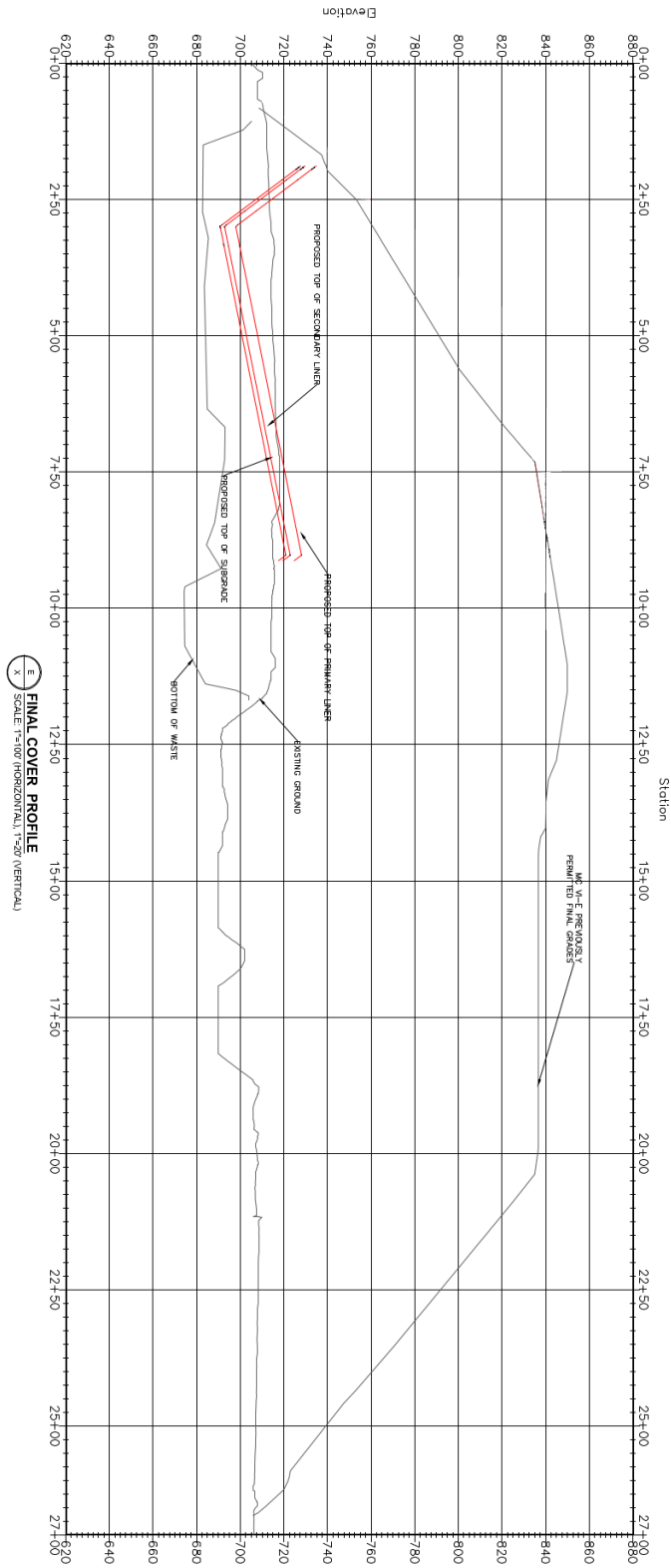
SLOPE STABILITY ANALYSIS REPORT FORM

Final Grades Cross-Section (plan):



SLOPE STABILITY ANALYSIS REPORT FORM

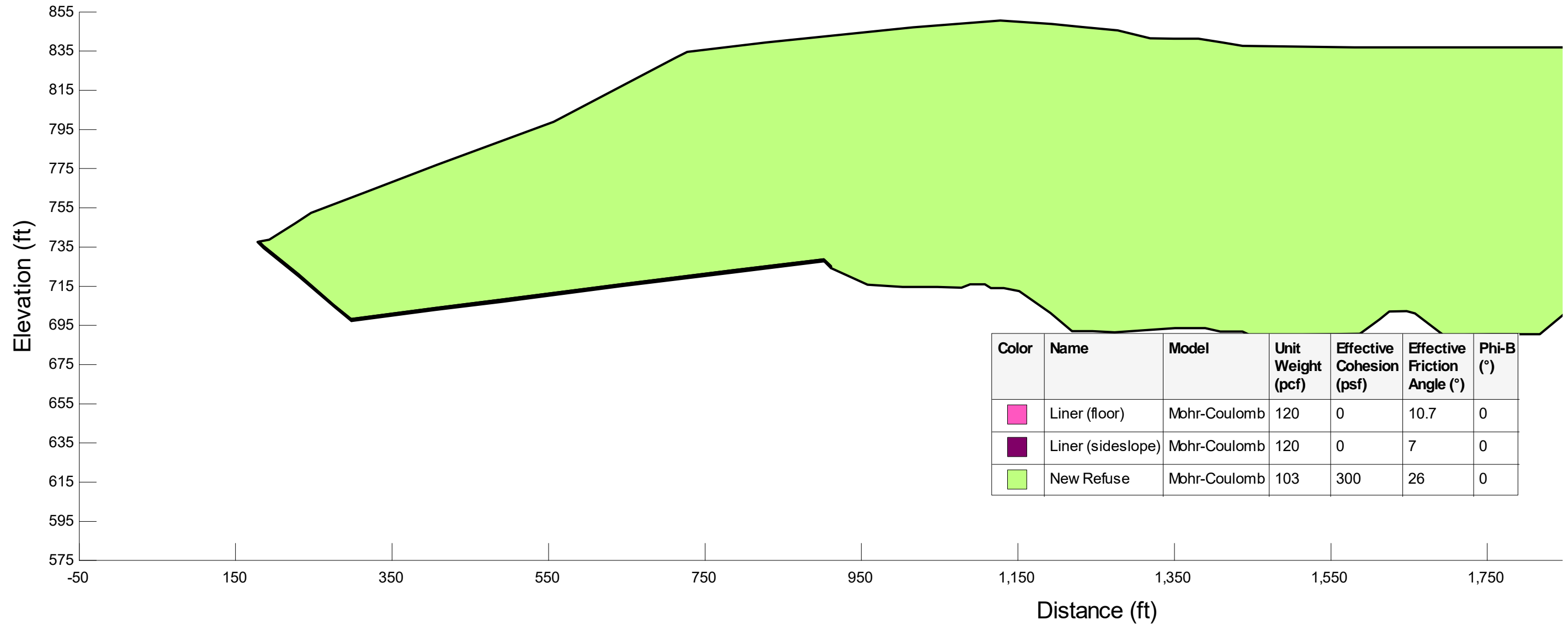
Final Grades Cross-Section (profile):



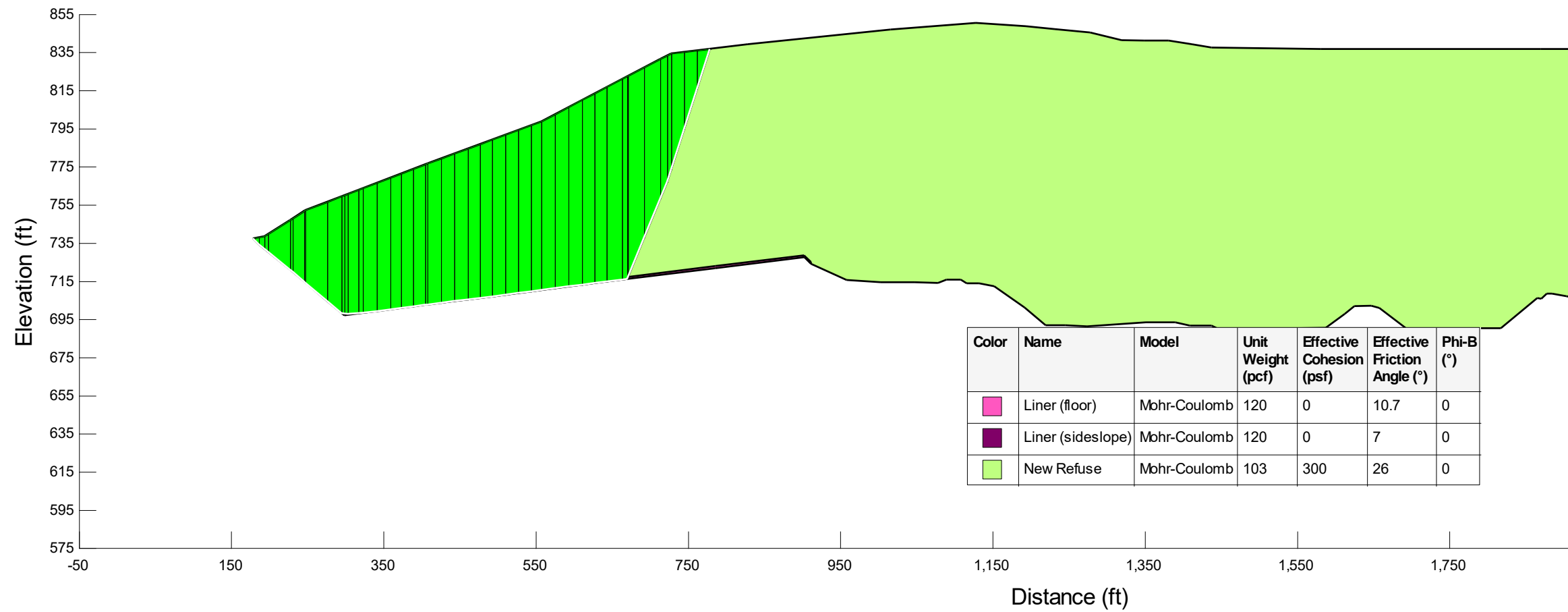
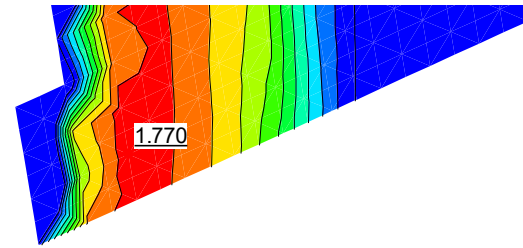
SLOPE STABILITY ANALYSIS REPORT FORM

Factor of Safety:	1.77	<input checked="" type="checkbox"/> Acceptable	<input type="checkbox"/> Not Acceptable	<input type="checkbox"/> Follow-up	<input type="checkbox"/> Superseded
Comments:					
Attachments:	Slope/W Cross Section and Results				

SLOPE STABILITY ANALYSIS REPORT FORM



SLOPE STABILITY ANALYSIS REPORT FORM



Attachment 5

B-B' Liner Stability under Final Conditions with non-zero adhesion (previously tested values)

SLOPE STABILITY ANALYSIS REPORT FORM

SLOPE STABILITY ANALYSIS REPORT FORM

Project Name:	WDI MC6F Permit Modification					
Project Number:	1208070039.004		Client:	Wayne Disposal, Inc.		
Analysis Short Name:	B-B' Liner Stability with tested interface strength parameters			File name:	WDI Cross Section B Liner_20201123_RevC_MK_c_phi_combo	
Revision:	1	Originated:	MK	Checked:	KF	Approved:
Date:	11/23/20	Date:	11/23/20	Date:	11/23/20	Date:

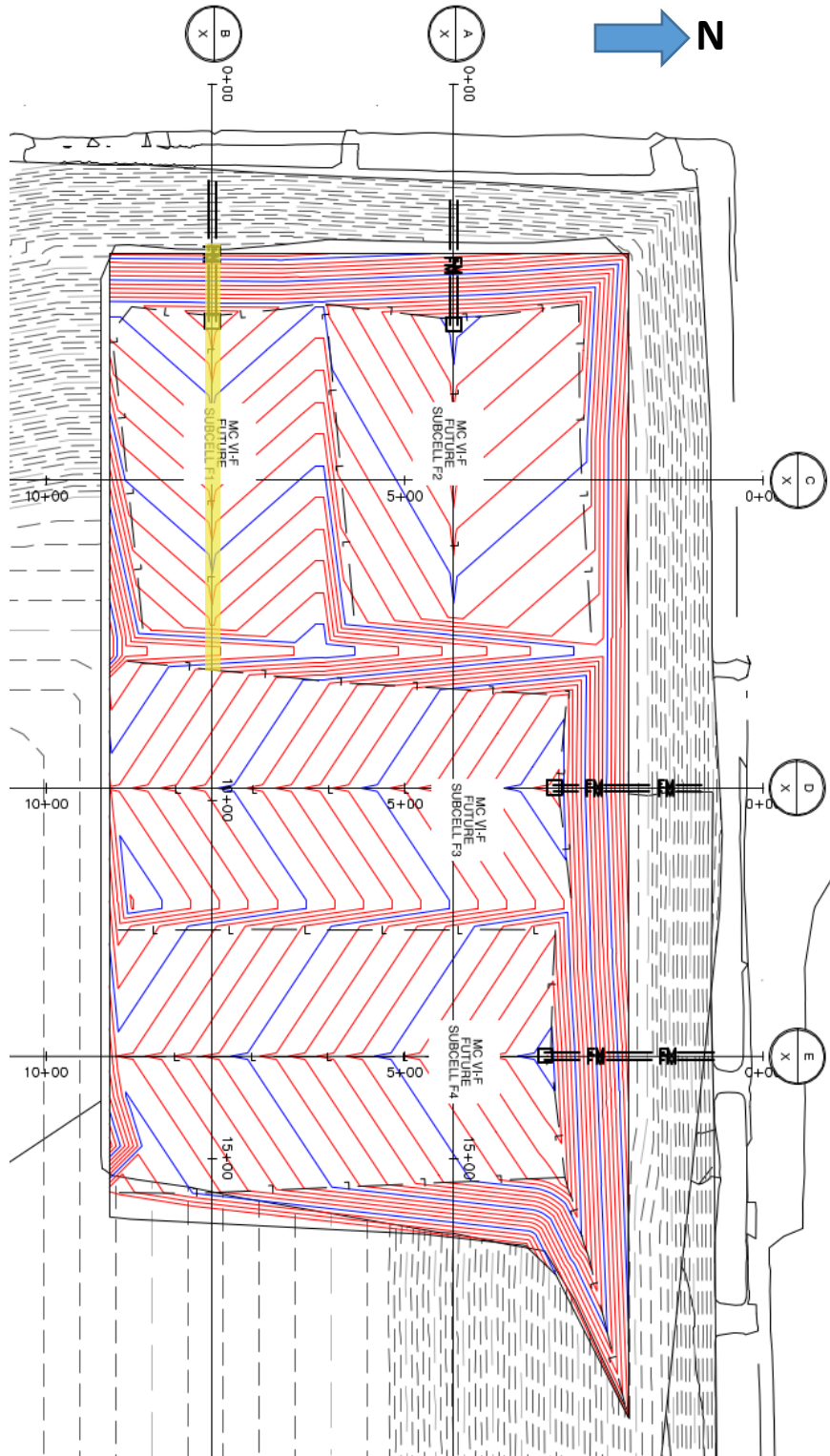
Purpose of Analysis:	To determine the factor of safety of the proposed final waste grades using cross-section B. This case considers a west-facing slope, with fill to the final permitted grade elevations. The failure surface is defined such that failure occurs in the underlying liner in order to consider the stability of the liner. The liner interface strength properties are based on interface strength test results of a similar liner system installed on site.		
<input type="checkbox"/> Effective Stress <input checked="" type="checkbox"/> Total Stress	<input checked="" type="checkbox"/> Static <input type="checkbox"/> Seismic	<input type="checkbox"/> Pore Pressure	<input checked="" type="checkbox"/> Optimized Surface
Additional Details:	The liner system was modeled in 2 sections (floor and sideslope) to allow use of Peak and Large-Displacement strength parameters appropriately. The required factor of safety is 1.5.		

Material	Name	Color in Profile	Unit Wt(s) (pcf)	Strength ϕ or δ (deg.)	Strength C or C_a (psf)
1	Final Cover	Orange	130	0	1500
2	Existing Waste	Teal	86	34	0
3	New Waste	Light Green	103	26	300
4	Upper Clay	Brown	131	0	2150
5	Middle Clay	Yellow	136	0	3300
6	Lower Clay	Maroon	133	0.22 σ_v	
7	Silt	Blue	125	28	0
8	Sand	Red	115	32	0
9	Liner (Floor)	Magenta	120	11.1	164
10	Liner (Sideslope)	Purple	120	7.3	110

Source of Geometry:	Engineering Drawing Set
Source of Subsurface Profile:	Basis of Design Report - NTH (2012)
<input type="checkbox"/> Preconstruction <input type="checkbox"/> Construction <input type="checkbox"/> Interim <input checked="" type="checkbox"/> Final <input type="checkbox"/> Existing <input type="checkbox"/> Back-Analysis	
Construction Phase Represented:	Final build out
Other Geometry Notes:	Cross Section B

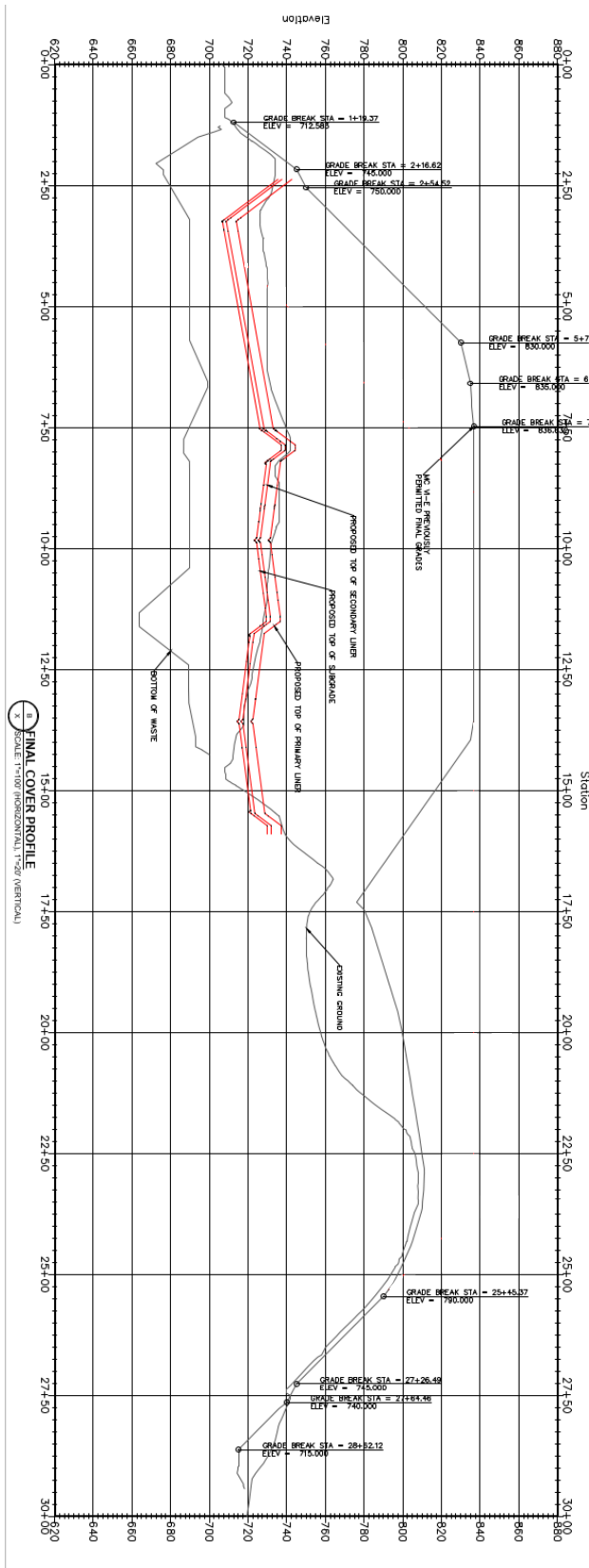
SLOPE STABILITY ANALYSIS REPORT FORM

Final Grades Cross-Section (plan):



SLOPE STABILITY ANALYSIS REPORT FORM

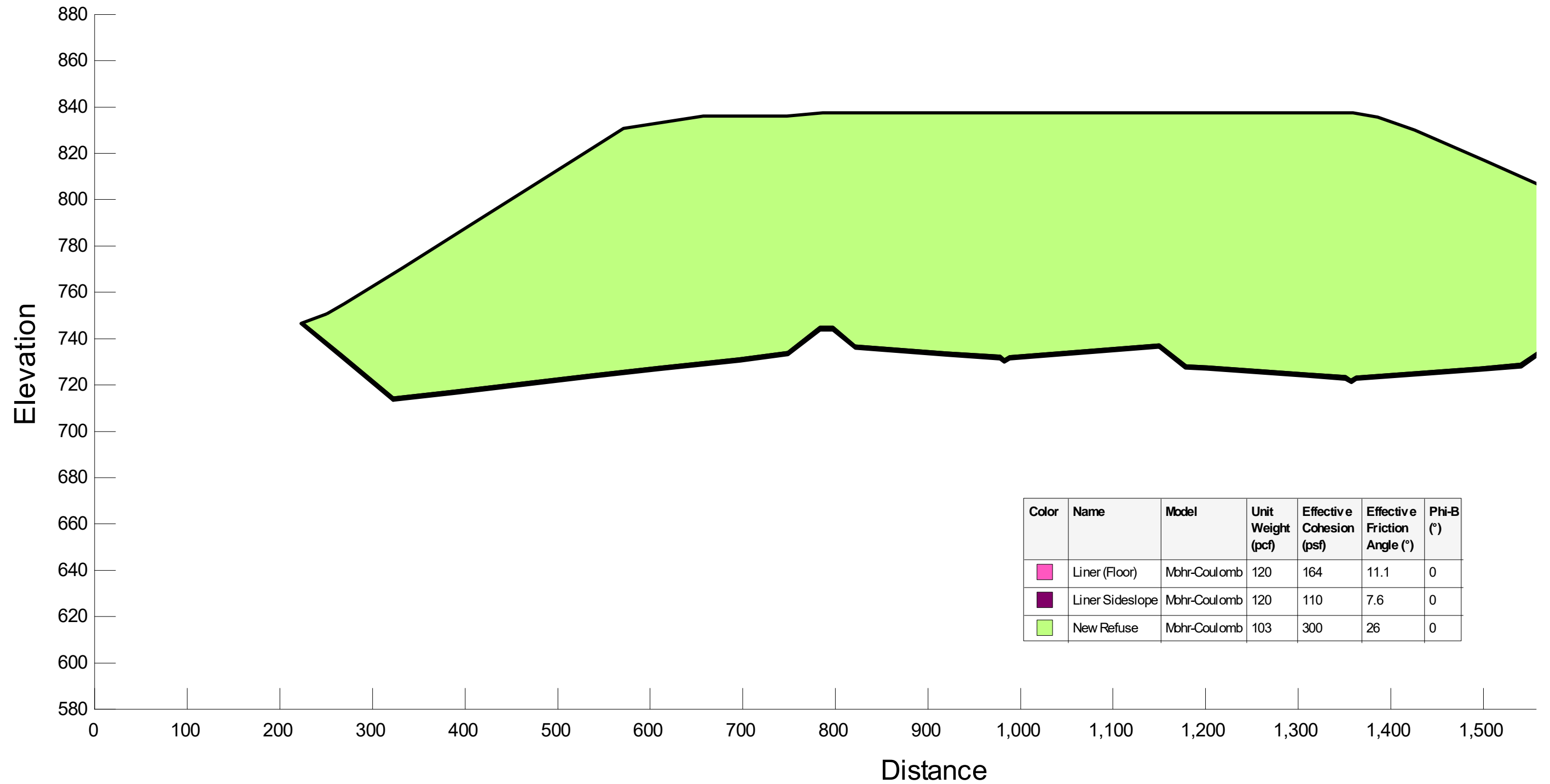
Final Grades Cross-Section (profile):



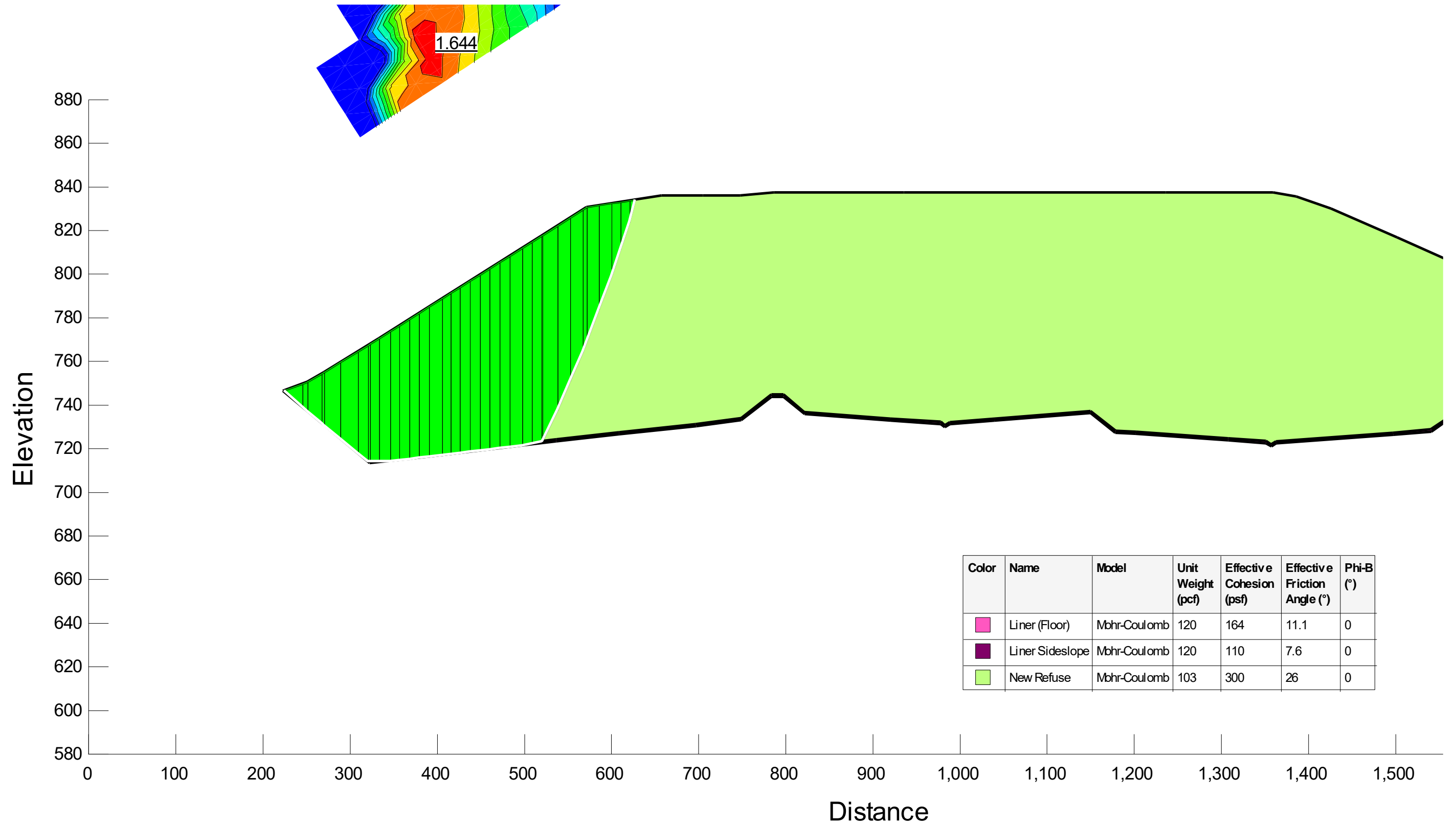
SLOPE STABILITY ANALYSIS REPORT FORM

Factor of Safety:	1.64	<input checked="" type="checkbox"/> Acceptable	<input type="checkbox"/> Not Acceptable	<input type="checkbox"/> Follow-up	<input type="checkbox"/> Superseded
Comments:					
Attachments:	Slope/W Cross Section and Results				

SLOPE STABILITY ANALYSIS REPORT FORM



SLOPE STABILITY ANALYSIS REPORT FORM



Attachment 6

E-E' Liner Stability under Final Conditions with non-zero adhesion (previously tested values)

SLOPE STABILITY ANALYSIS REPORT FORM

SLOPE STABILITY ANALYSIS REPORT FORM

Project Name:	WDI MC6F Permit Modification						
Project Number:	1208070039.004	Client:	Wayne Disposal, Inc.				
Analysis Short Name:	E-E' Liner Stability			File name:	WDI Cross Section E Liner_20201123_RevC_MK_c_phi_combo.gsz		
Revision:	1	Originated:	MK	Checked:	KF	Approved:	
Date:	11/23/20	Date:	11/23/20	Date:	11/23/20	Date:	

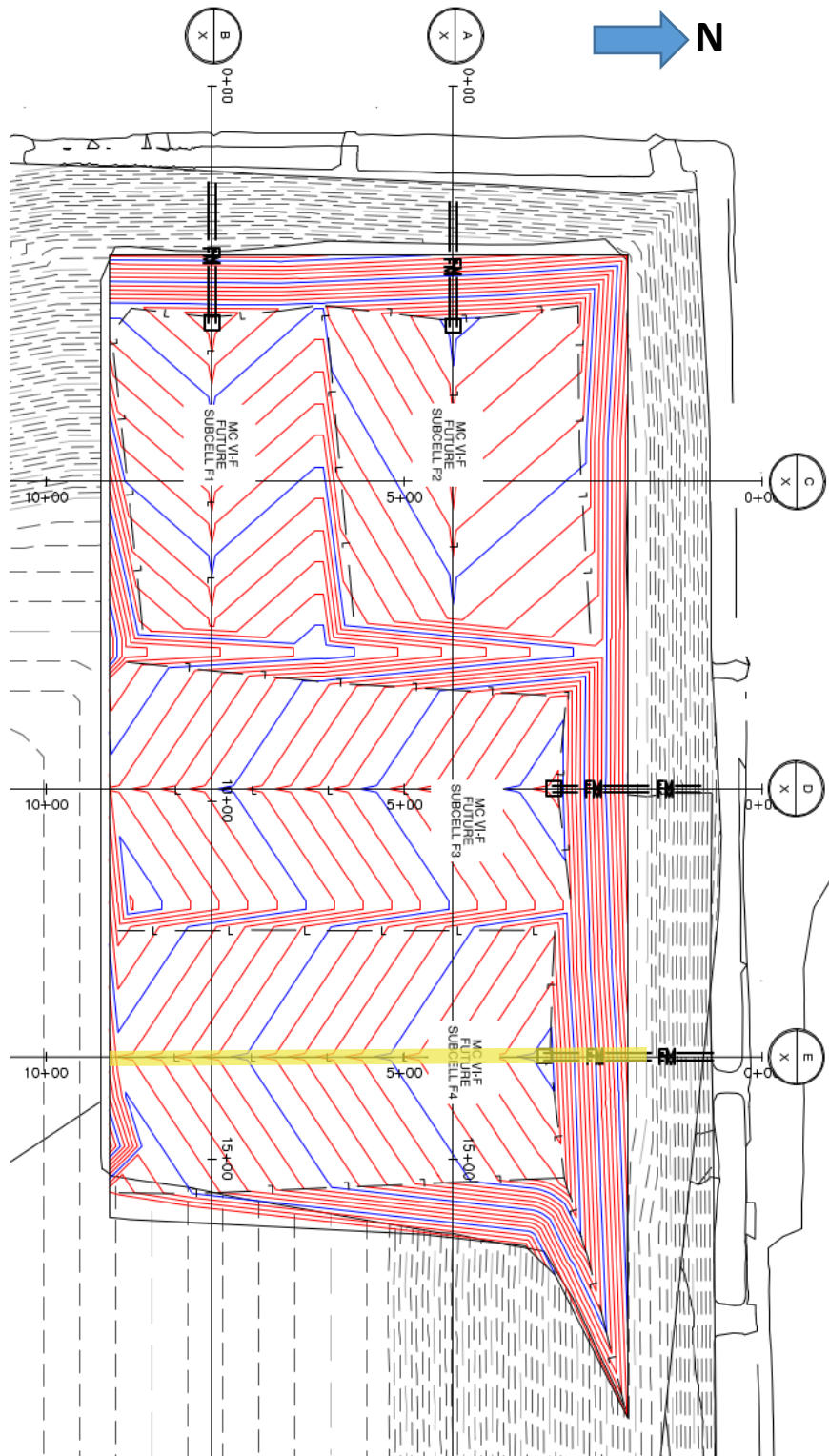
Purpose of Analysis:	To determine the factor of safety of the proposed final waste grades using cross-section E. This case considers a north-facing slope, with fill to the final grade elevations. The failure surface is defined such that failure occurs in the underlying liner in order to consider the stability of the liner. The liner interface strength properties are based on interface strength test results of a similar liner system installed on site.		
<input type="checkbox"/> Effective Stress <input checked="" type="checkbox"/> Total Stress	<input checked="" type="checkbox"/> Static <input type="checkbox"/> Seismic	<input type="checkbox"/> Pore Pressure	<input checked="" type="checkbox"/> Optimized Surface
Additional Details:	The liner system was modeled in 2 sections (floor and sideslope) to allow use of Peak and Large-Displacement strength parameters appropriately. The required factor of safety is 1.5.		

Material	Name	Color in Profile	Unit Wt(s) (pcf)	Strength ϕ or δ (deg.)	Strength C or Ca (psf)
1	Final Cover	Orange	130	0	1500
2	Existing Waste	Teal	86	34	0
3	New Waste	Light Green	103	26	300
4	Upper Clay	Brown	131	0	2150
5	Middle Clay	Yellow	136	0	3300
6	Lower Clay	Maroon	133	0.22 σ_v	
7	Silt	Blue	125	28	0
8	Sand	Red	115	32	0
9	Liner (Floor)	Magenta	120	11.1	164
10	Liner (Sideslope)	Purple	120	7.3	110

Source of Geometry:	Engineering Drawing Set
Source of Subsurface Profile:	Basis of Design Report - NTH (2012)
<input type="checkbox"/> Preconstruction <input type="checkbox"/> Construction <input type="checkbox"/> Interim <input checked="" type="checkbox"/> Final <input type="checkbox"/> Existing <input type="checkbox"/> Back-Analysis	
Construction Phase Represented:	Final build out
Other Geometry Notes:	Cross Section E

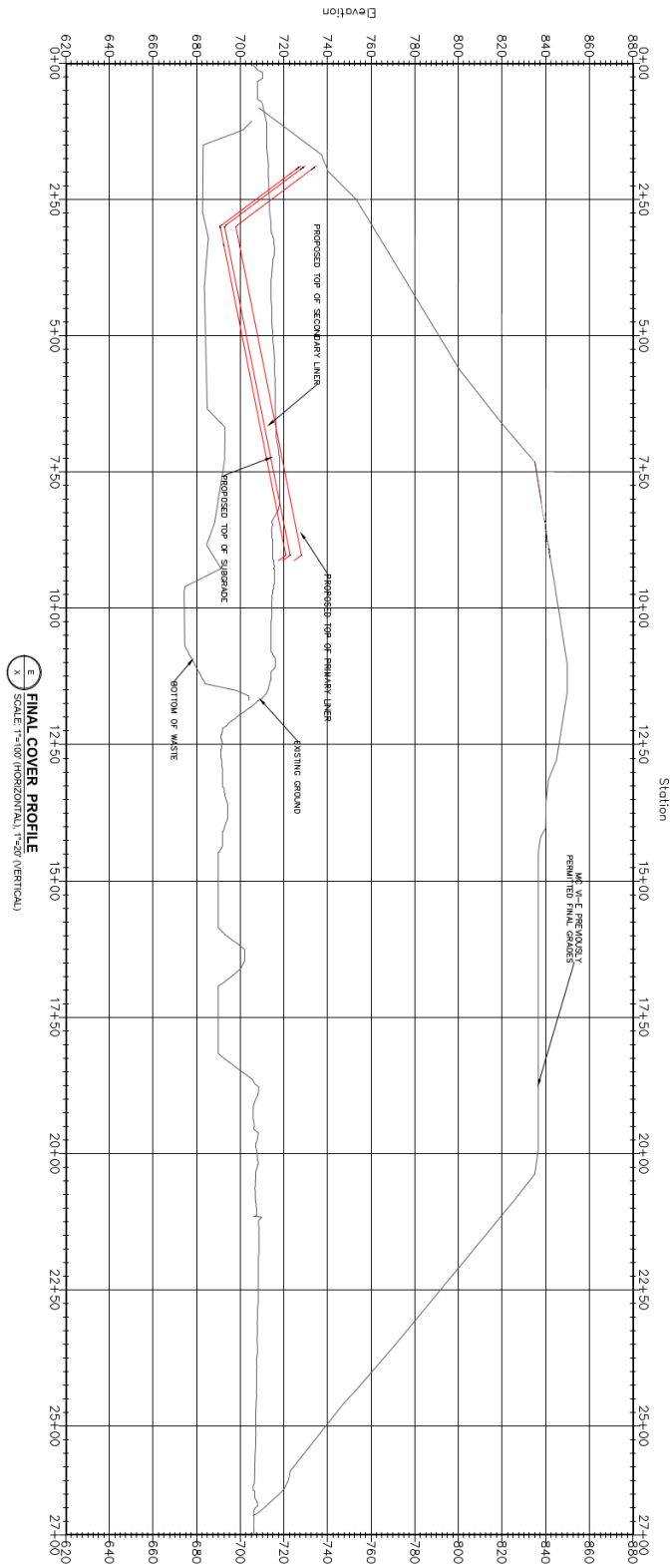
SLOPE STABILITY ANALYSIS REPORT FORM

Final Grades Cross-Section (plan):



SLOPE STABILITY ANALYSIS REPORT FORM

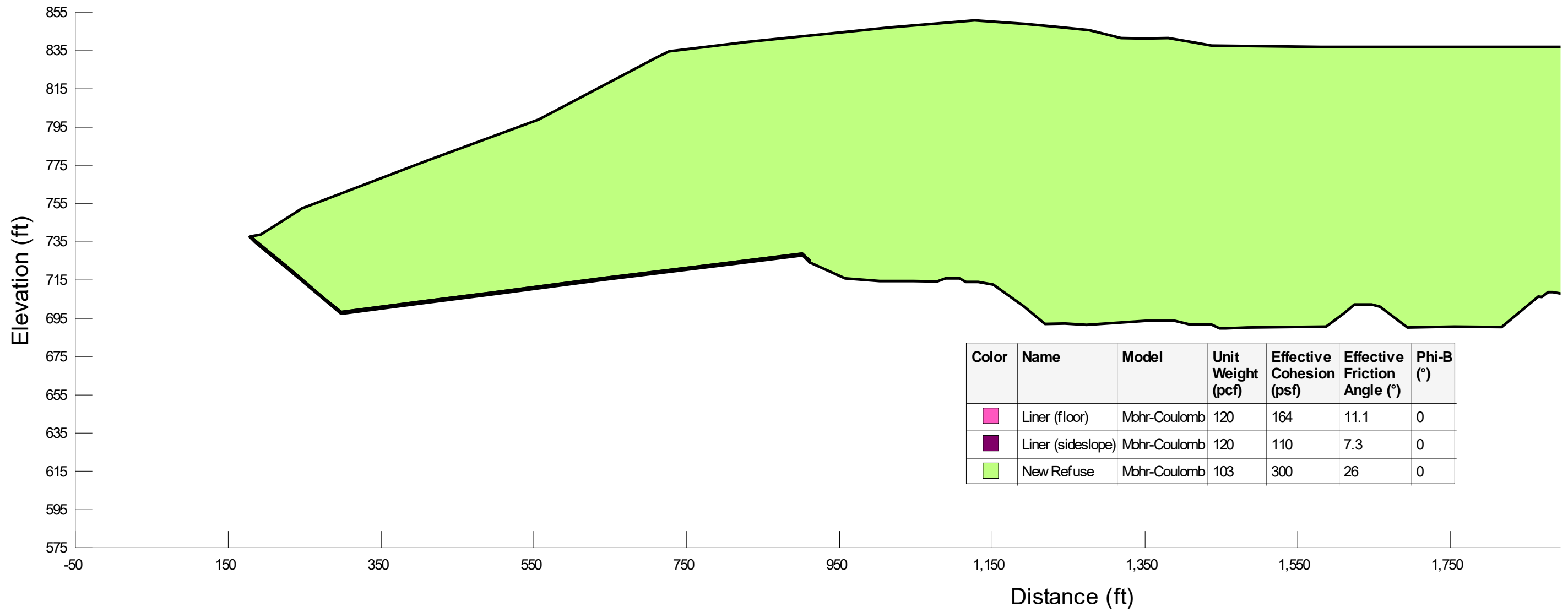
Final Grades Cross-Section (profile):



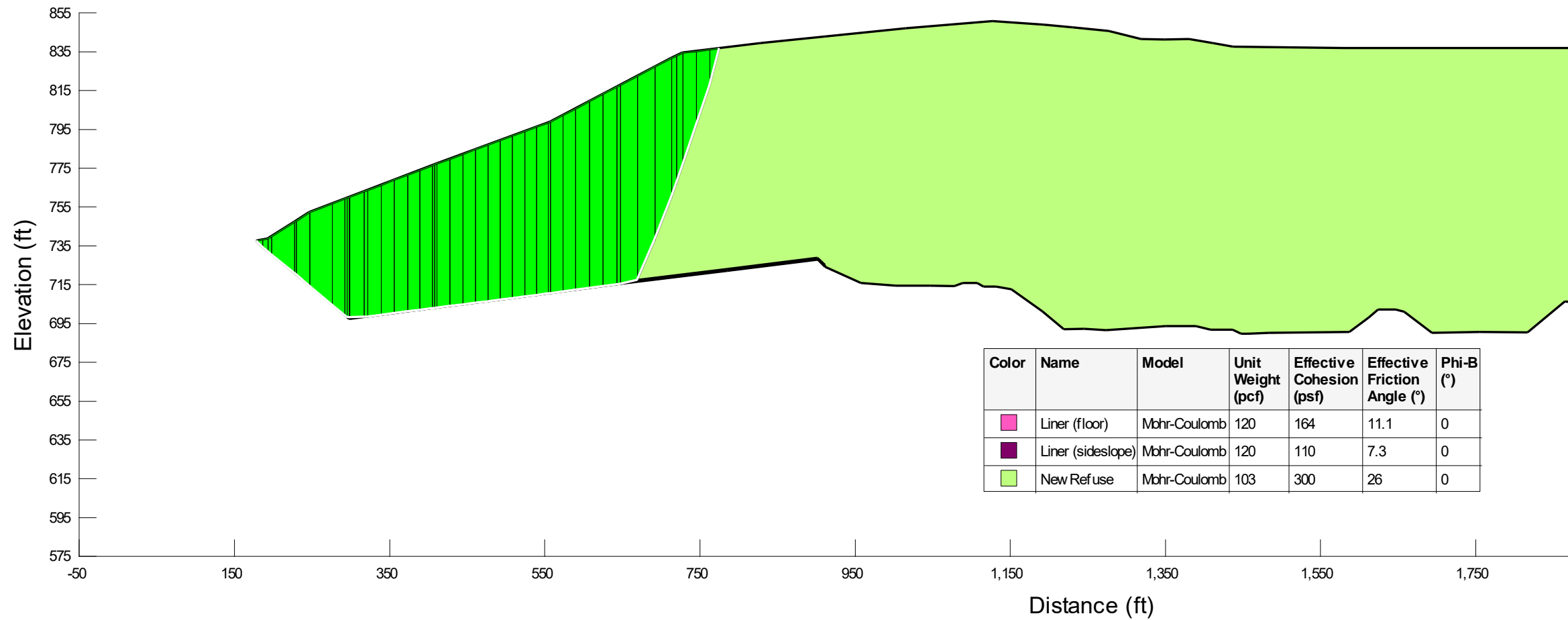
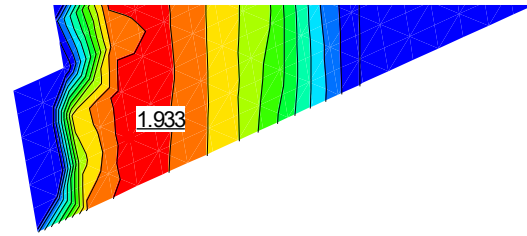
SLOPE STABILITY ANALYSIS REPORT FORM

Factor of Safety:	1.93	<input checked="" type="checkbox"/> Acceptable	<input type="checkbox"/> Not Acceptable	<input type="checkbox"/> Follow-up	<input type="checkbox"/> Superseded
Comments:					
Attachments:	Slope/W Cross Section and Results				

SLOPE STABILITY ANALYSIS REPORT FORM



SLOPE STABILITY ANALYSIS REPORT FORM



Attachment 7

B-B' Liner Stability under Interim Conditions (example interim stability calculation)

SLOPE STABILITY ANALYSIS REPORT FORM

SLOPE STABILITY ANALYSIS REPORT FORM

Project Name:	WDI MC6F Permit Modification						
Project Number:	1208070039.004			Client:	Wayne Disposal, Inc.		
Analysis Short Name:	B-B' Interim Liner Stability			File name:	WDI Cross Section B Interim_20201119_RevA_MK_3.5H1V.gsz		
Revision:	1	Originated:	MK	Checked:	KF	Approved:	
Date:	11/23/20	Date:	11/23/20	Date:	11/23/20	Date:	

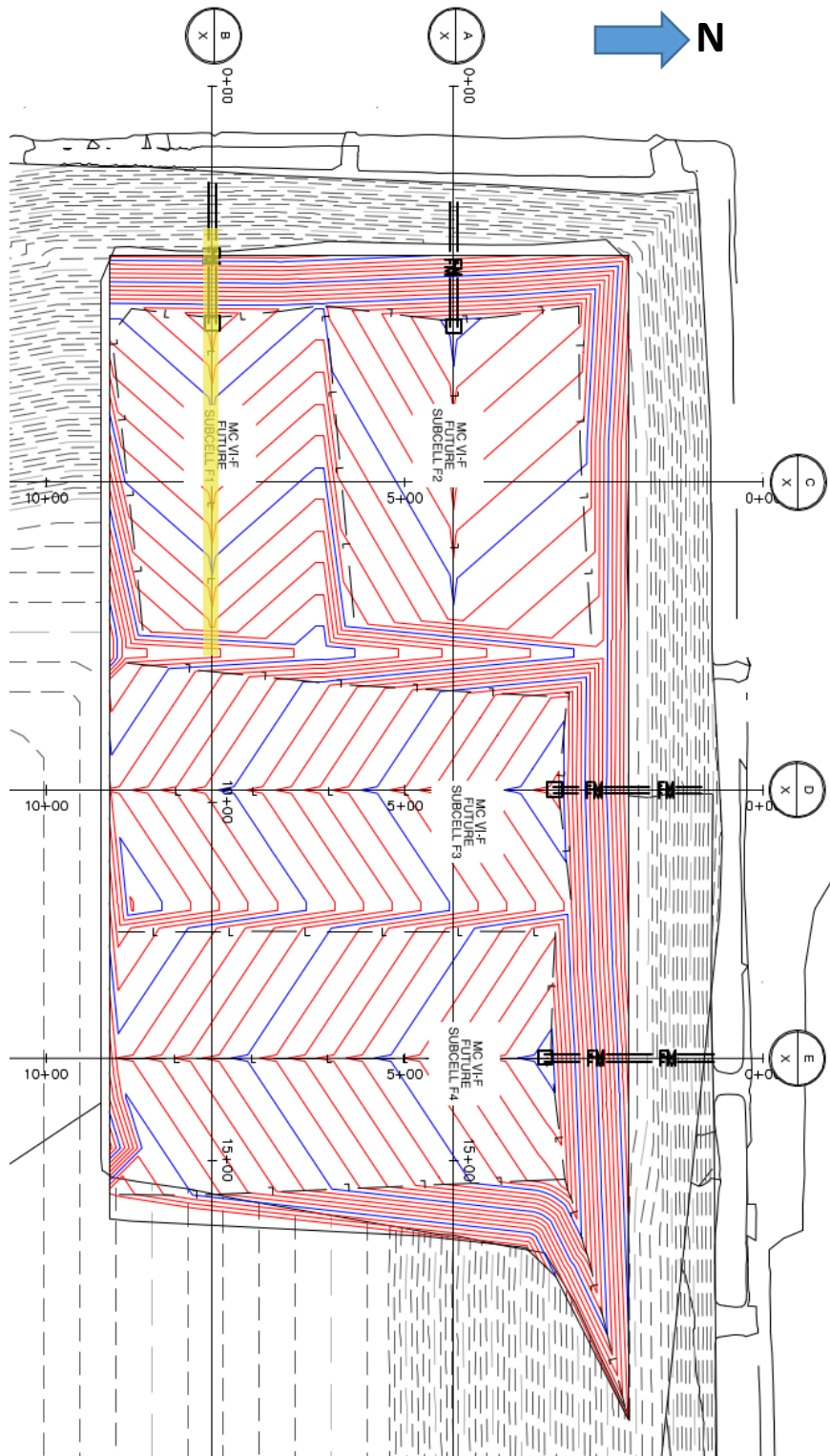
Purpose of Analysis:	To determine the required interface friction angle of the liner system to achieve an acceptable interim factor of safety of 1.3 using cross-section B. This case considers a west-facing slope and models an example interim fill case with waste fill up to the final permitted grade elevations at an interim slope of 3.5H:1V. The failure surface is defined such that failure occurs in the underlying liner in order to consider the stability of the liner.		
<input type="checkbox"/> Effective Stress <input checked="" type="checkbox"/> Total Stress	<input checked="" type="checkbox"/> Static <input type="checkbox"/> Seismic	<input type="checkbox"/> Pore Pressure	<input checked="" type="checkbox"/> Optimized Surface
Additional Details:			

Material	Name	Color in Profile	Unit Wt(s) (pcf)	Strength ϕ or δ (deg.)	Strength C or Ca (psf)
1	Final Cover	Orange	130	0	1500
2	Existing Waste	Teal	86	34	0
3	New Waste	Light Green	103	26	300
4	Upper Clay	Brown	131	0	2150
5	Middle Clay	Yellow	136	0	3300
6	Lower Clay	Maroon	133	0.22 σ_v	
7	Silt	Blue	125	28	0
8	Sand	Red	115	32	0

Source of Geometry:	Engineering Drawing Set
Source of Subsurface Profile:	Basis of Design Report - NTH (2012)
<input type="checkbox"/> Preconstruction <input type="checkbox"/> Construction <input checked="" type="checkbox"/> Interim <input type="checkbox"/> Final <input type="checkbox"/> Existing <input type="checkbox"/> Back-Analysis	
Construction Phase Represented:	Interim waste filling
Other Geometry Notes:	Cross Section B

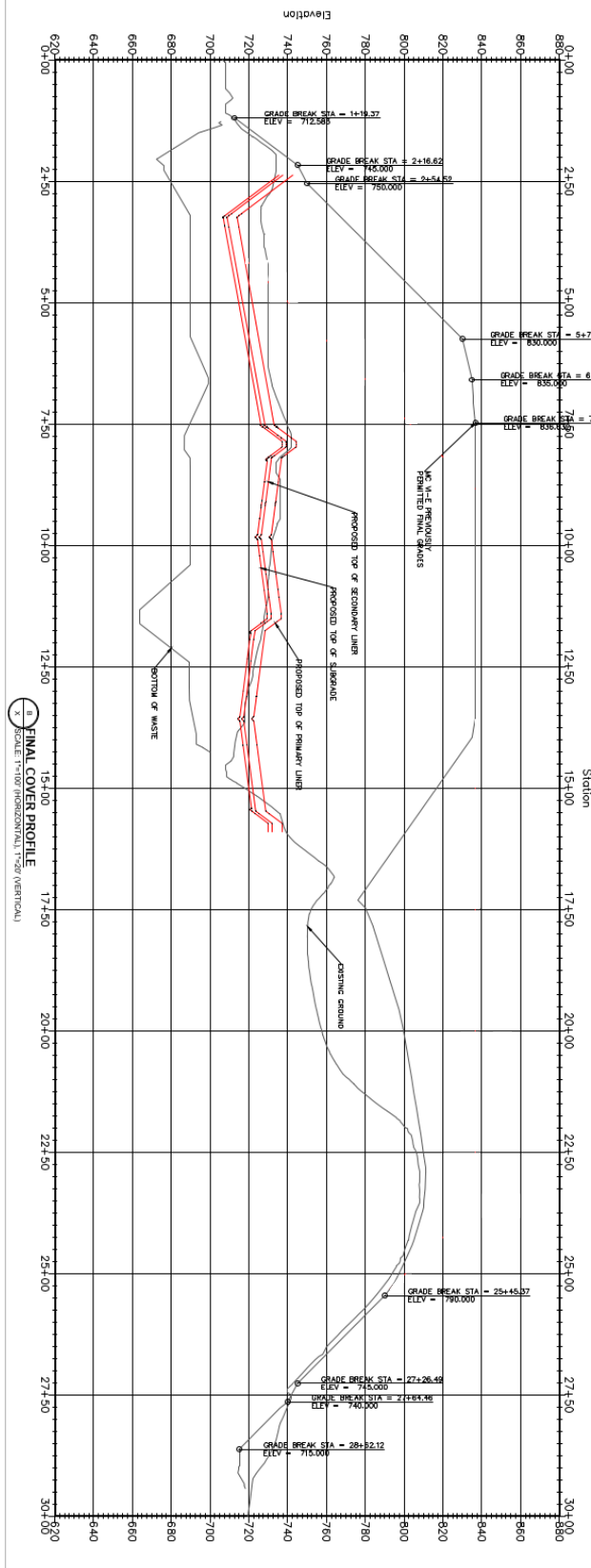
SLOPE STABILITY ANALYSIS REPORT FORM

Final Grades Cross-Section (plan):



SLOPE STABILITY ANALYSIS REPORT FORM

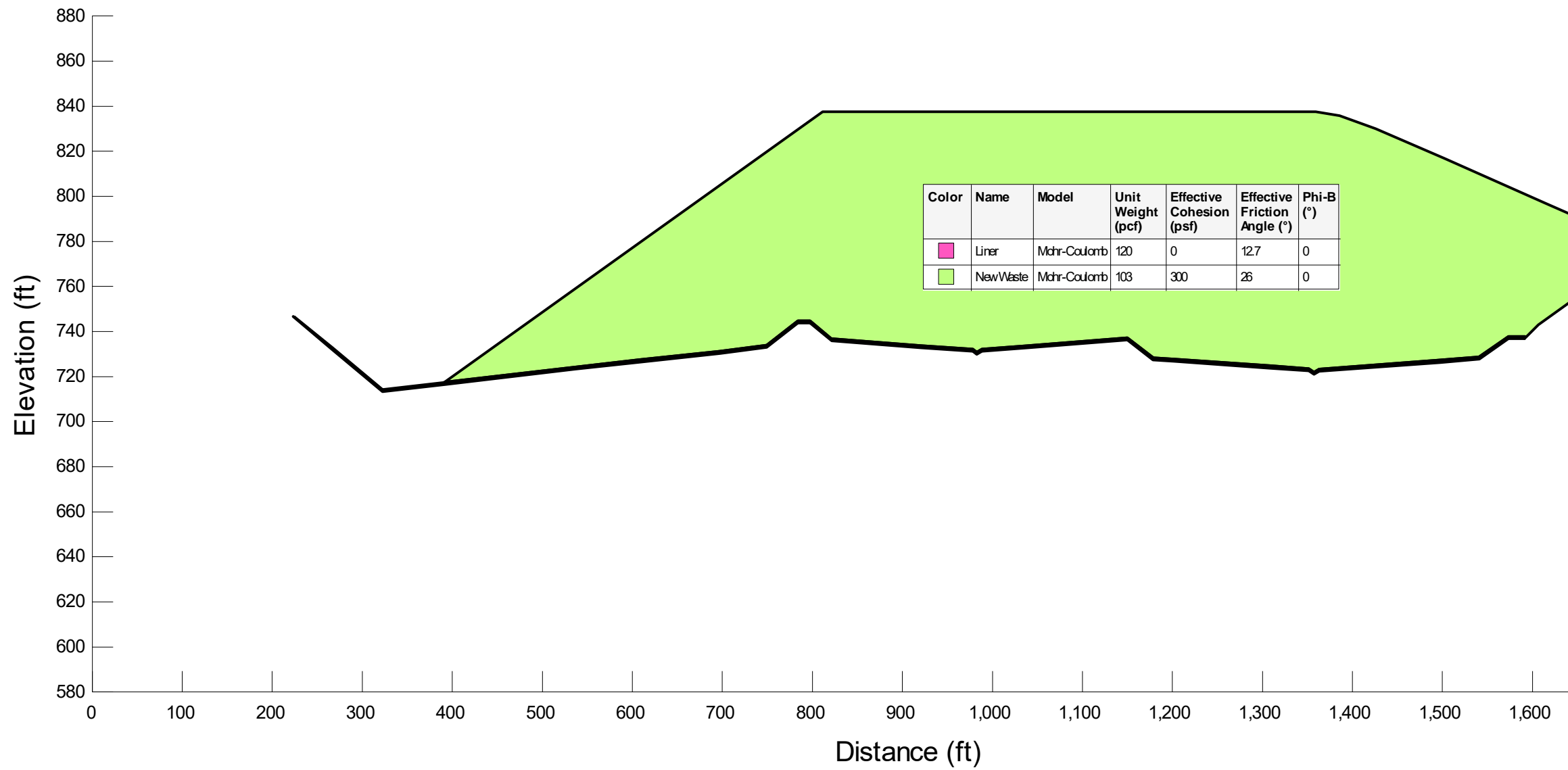
Final Grades Cross-Section (profile):



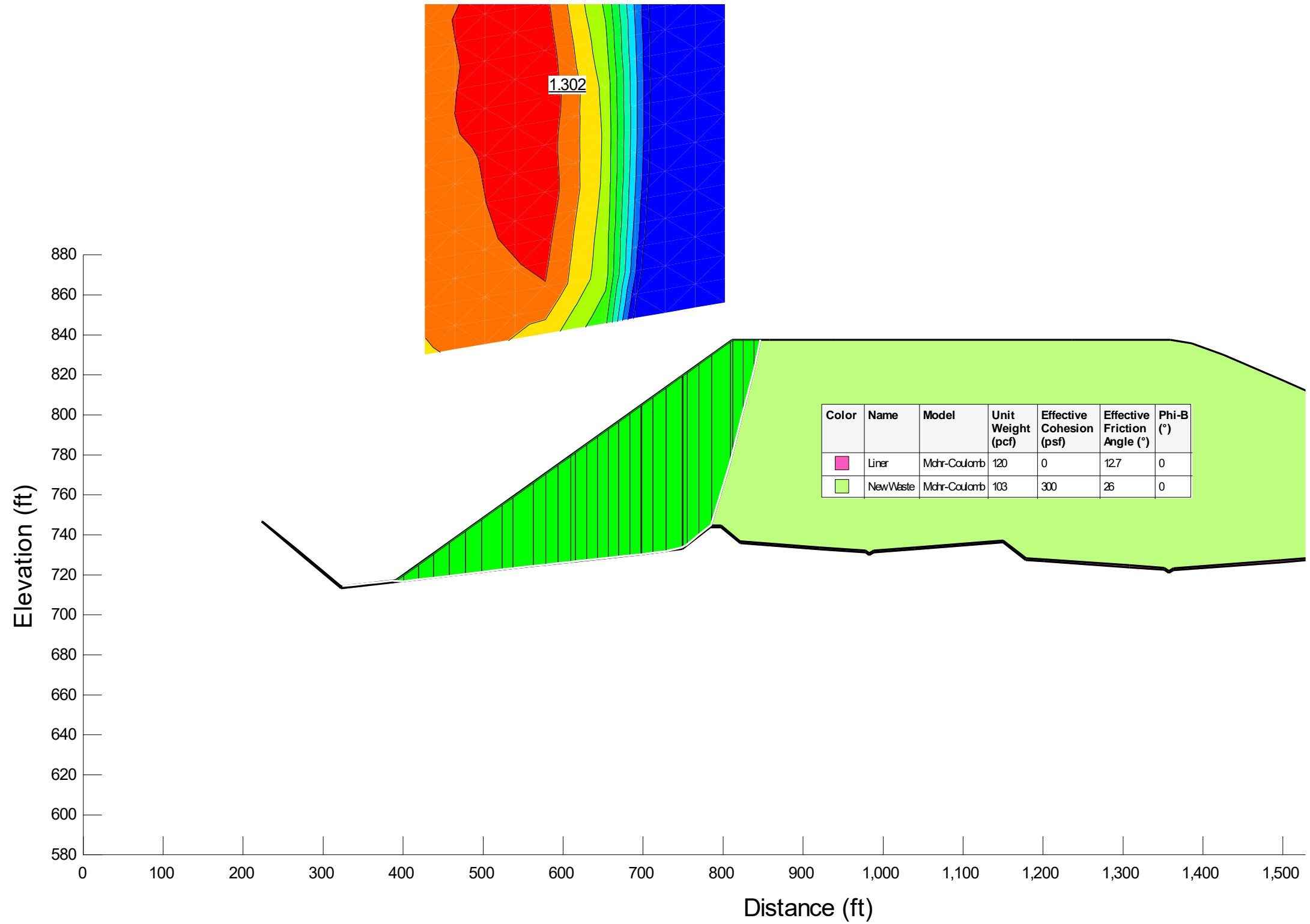
SLOPE STABILITY ANALYSIS REPORT FORM

Factor of Safety:	1.30	<input checked="" type="checkbox"/> Acceptable <input type="checkbox"/> Not Acceptable <input type="checkbox"/> Follow-up <input type="checkbox"/> Superseded
Comments:	Required friction angle of 12.7 degrees (peak). Any combination of adhesion and friction angle that yields a comparable shear strength under modeled site conditions is acceptable.	
Attachments:	Slope/W Cross Section and Results	

SLOPE STABILITY ANALYSIS REPORT FORM



SLOPE STABILITY ANALYSIS REPORT FORM



Attachment B-1.8

B-B' Foundation Stability under drained conditions

SLOPE STABILITY ANALYSIS REPORT FORM

SLOPE STABILITY ANALYSIS REPORT FORM

Project Name:	WDI MC6F Permit Modification						
Project Number:	1208070039.004			Client:	Wayne Disposal, Inc.		
Analysis Short Name:	B-B' Foundation Stability			File name:	WDI Cross Section B Full_20210428_Drained_RevA_MK.gsz		
Revision:	0	Originated:	MK	Checked:	KF	Approved:	
Date:	04/28/21	Date:	04/28/21	Date:		Date:	

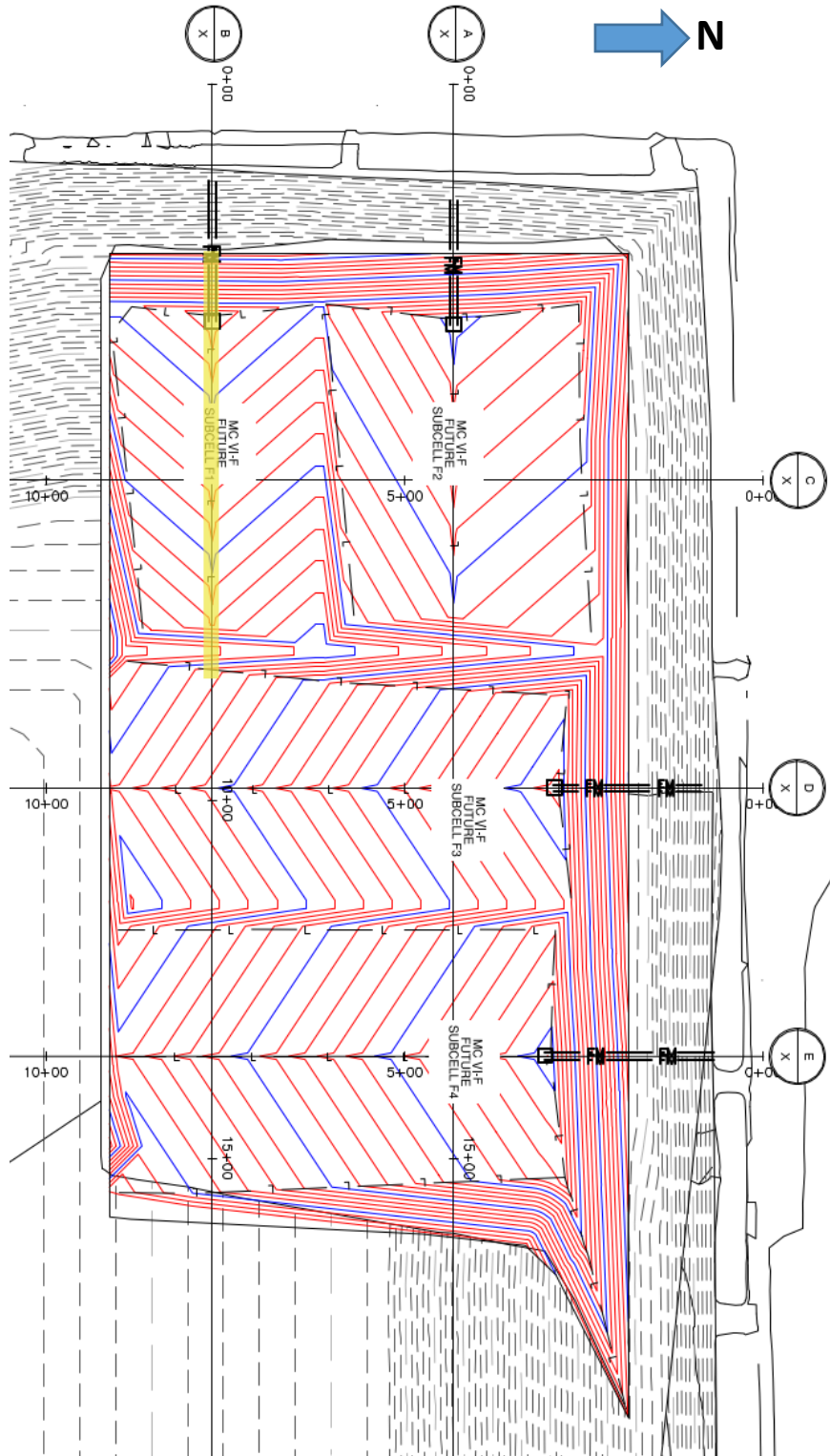
Purpose of Analysis:	To determine the factor of safety of the proposed final waste grades using cross-section B-B'. This case considers a west-facing slope, with fill to the final permitted grade elevations under drained conditions.		
<input checked="" type="checkbox"/> Effective Stress <input type="checkbox"/> Total Stress	<input checked="" type="checkbox"/> Static <input type="checkbox"/> Seismic	<input checked="" type="checkbox"/> Pore Pressure	<input checked="" type="checkbox"/> Optimized Surface
Additional Details:	The friction angle of the liner system was set equal to the required minimum interface friction angle determined from the liner stability analysis performed on Cross Section B. The groundwater level was set at elevation 655ft based on historical borings in MC-IV as documented in the Basis of Design Report (NTH 2012).		

Material	Name	Color in Profile	Unit Wt(s) (pcf)	Strength ϕ or δ (deg.)	Strength C or Ca (psf)
1	Final Cover	Orange	130	0	1500
2	Existing Waste	Teal	86	34	0
3	New Waste	Light Green	103	26	300
4	Upper Clay	Brown	131	0	2150
5	Middle Clay	Yellow	136	0	3300
6	Lower Clay	Maroon	133	0.22 σ_v	
7	Silt	Blue	125	28	0
8	Sand	Red	115	32	0
9	Liner	Magenta	120	10.7	0

Source of Geometry:	Engineering Drawing Set
Source of Subsurface Profile:	Basis of Design Report - NTH (2012)
	<input type="checkbox"/> Preconstruction <input type="checkbox"/> Construction <input type="checkbox"/> Interim <input checked="" type="checkbox"/> Final <input type="checkbox"/> Existing <input type="checkbox"/> Back-Analysis
Construction Phase Represented:	Final Build out
Other Geometry Notes:	Cross Section B

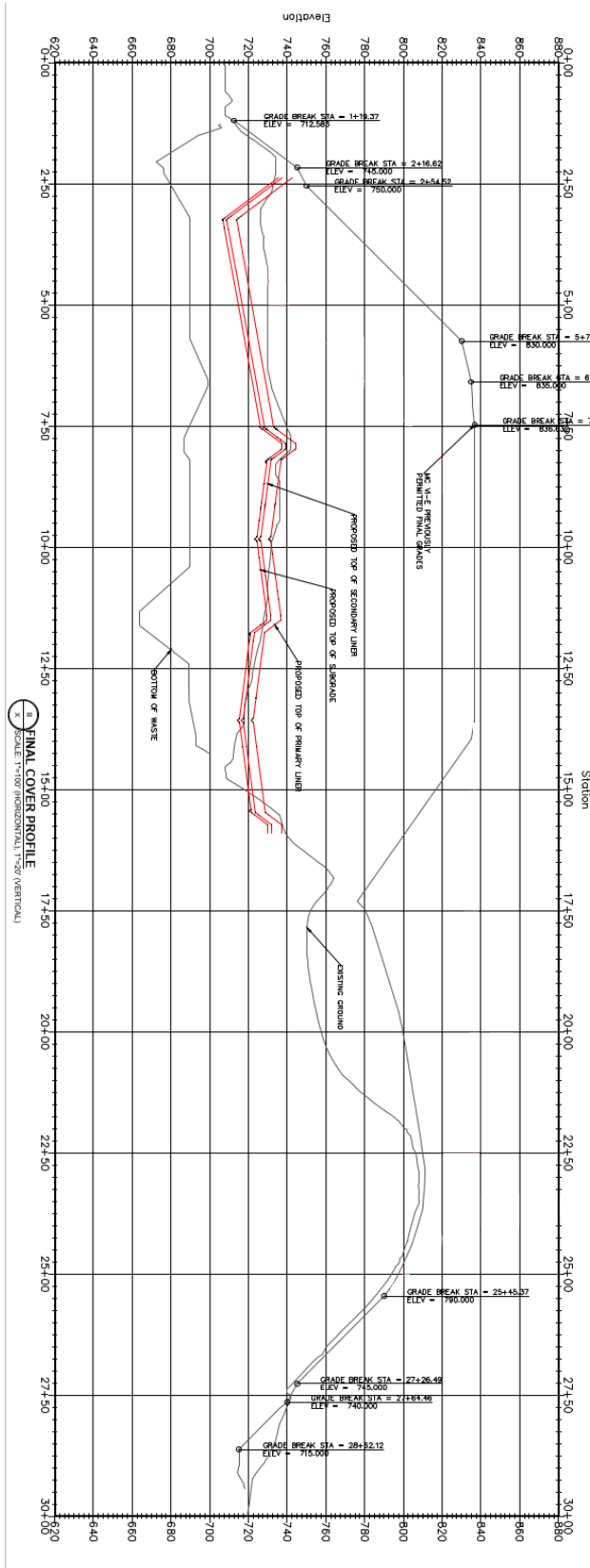
SLOPE STABILITY ANALYSIS REPORT FORM

Final Grades Cross-Section (plan):



SLOPE STABILITY ANALYSIS REPORT FORM

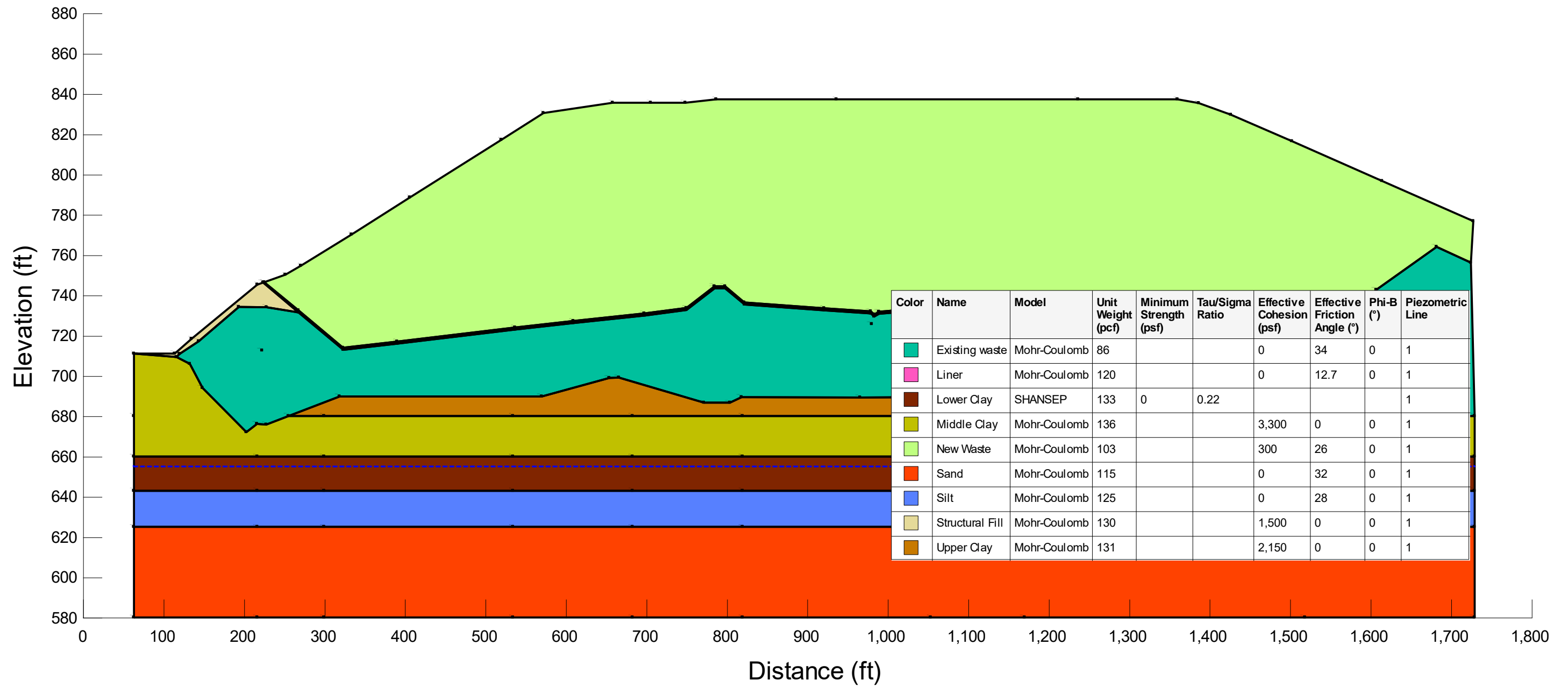
Final Grades Cross-Section (profile):



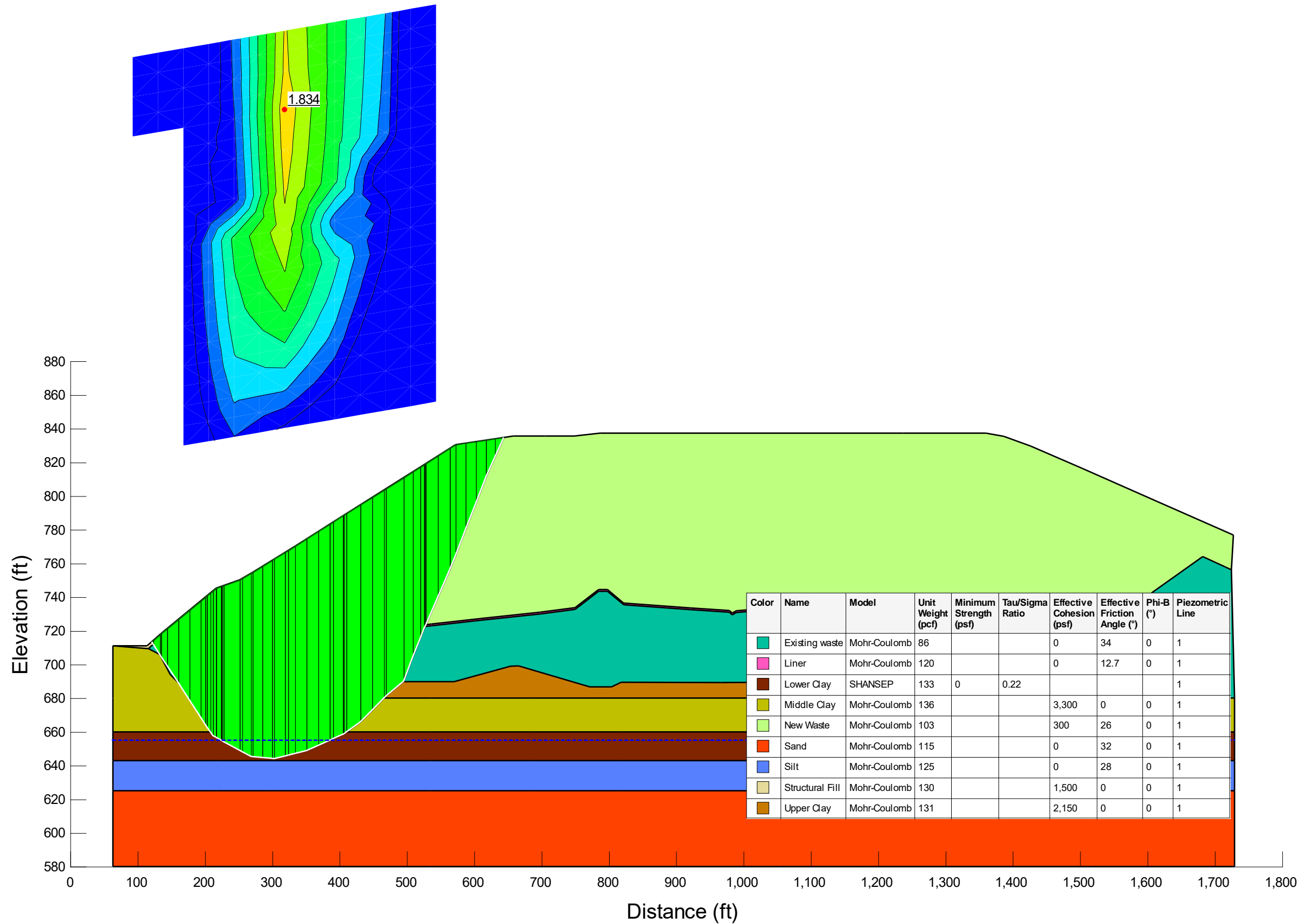
SLOPE STABILITY ANALYSIS REPORT FORM

Factor of Safety:	1.83	<input checked="" type="checkbox"/> Acceptable	<input type="checkbox"/> Not Acceptable	<input type="checkbox"/> Follow-up	<input type="checkbox"/> Superseded
Comments:					
Attachments:	Slope/W Cross Section and Results				

SLOPE STABILITY ANALYSIS REPORT FORM



SLOPE STABILITY ANALYSIS REPORT FORM



Attachment B-1.9

E-E' Foundation Stability under drained conditions

SLOPE STABILITY ANALYSIS REPORT FORM

SLOPE STABILITY ANALYSIS REPORT FORM

Project Name:	WDI MC6F Permit Modification						
Project Number:	1208070039.004			Client:	Wayne Disposal, Inc.		
Analysis Short Name:	E-E' Foundation Stability			File name:	WDI Cross Section E Full_20210428_Drained_RevA_MK.gsz		
Revision:	0	Originated:	MK	Checked:	KF	Approved:	
Date:	04/28/21	Date:	04/28/21	Date:		Date:	

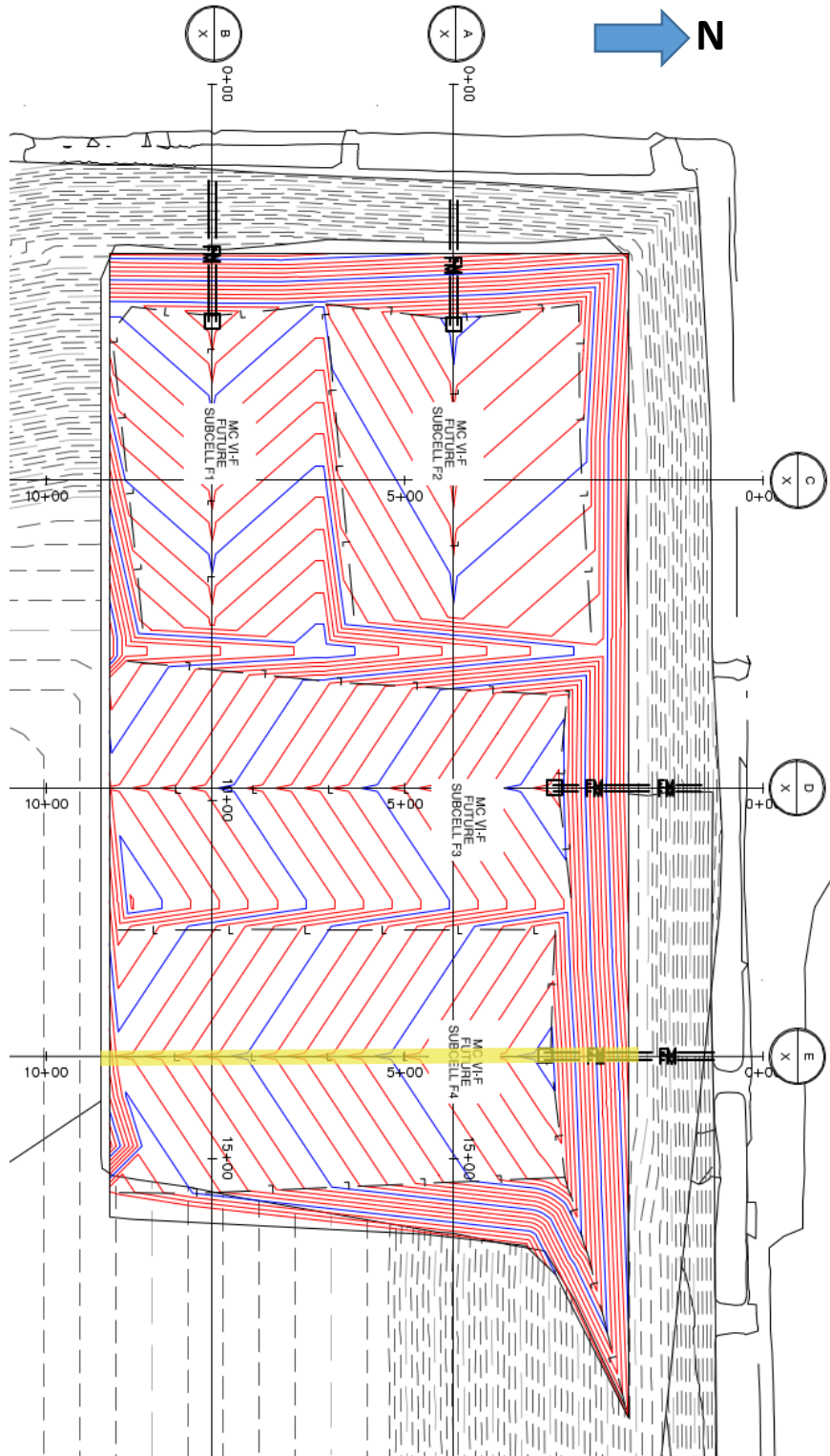
Purpose of Analysis:	To determine the factor of safety of the proposed final waste grades using cross-section E. This case considers a north-facing slope, with fill to the final permitted grade elevations under drained conditions.		
<input checked="" type="checkbox"/> Effective Stress <input type="checkbox"/> Total Stress	<input checked="" type="checkbox"/> Static <input type="checkbox"/> Seismic	<input checked="" type="checkbox"/> Pore Pressure	<input checked="" type="checkbox"/> Optimized Surface
Additional Details:	The friction angle of the liner system was set equal to the required minimum interface friction angle determined from the liner stability analysis performed on Cross Section B. The groundwater level was set at elevation 655ft based on historical borings in MC-IV as documented in the Basis of Design Report (NTH 2012).		

Material	Name	Color in Profile	Unit Wt(s) (pcf)	Strength ϕ or δ (deg.)	Strength C or Ca (psf)
1	Final Cover	Orange	130	0	1500
2	Existing Waste	Teal	86	34	0
3	New Waste	Light Green	103	26	300
4	Upper Clay	Brown	131	0	2150
5	Middle Clay	Yellow	136	0	3300
6	Lower Clay	Maroon	133	0.22 σ_v	
7	Silt	Blue	125	28	0
8	Sand	Red	115	32	0
8	Liner System	Magenta	120	10.7	0

Source of Geometry:	Engineering Drawing Set
Source of Subsurface Profile:	Basis of Design Report - NTH (2012)
	<input type="checkbox"/> Preconstruction <input type="checkbox"/> Construction <input type="checkbox"/> Interim <input checked="" type="checkbox"/> Final <input type="checkbox"/> Existing <input type="checkbox"/> Back-Analysis
Construction Phase Represented:	Final build out
Other Geometry Notes:	Cross Section E-E'

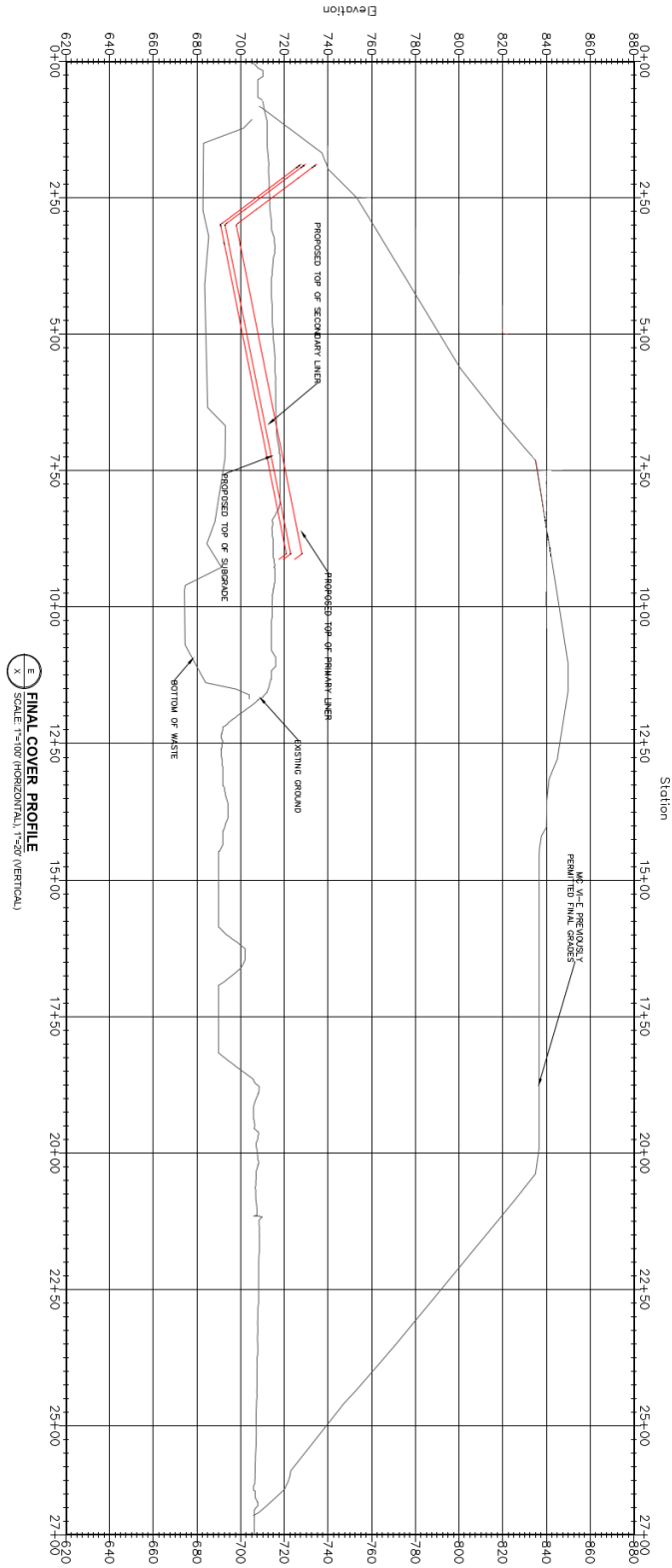
SLOPE STABILITY ANALYSIS REPORT FORM

Final Grades Cross-Section (plan):



SLOPE STABILITY ANALYSIS REPORT FORM

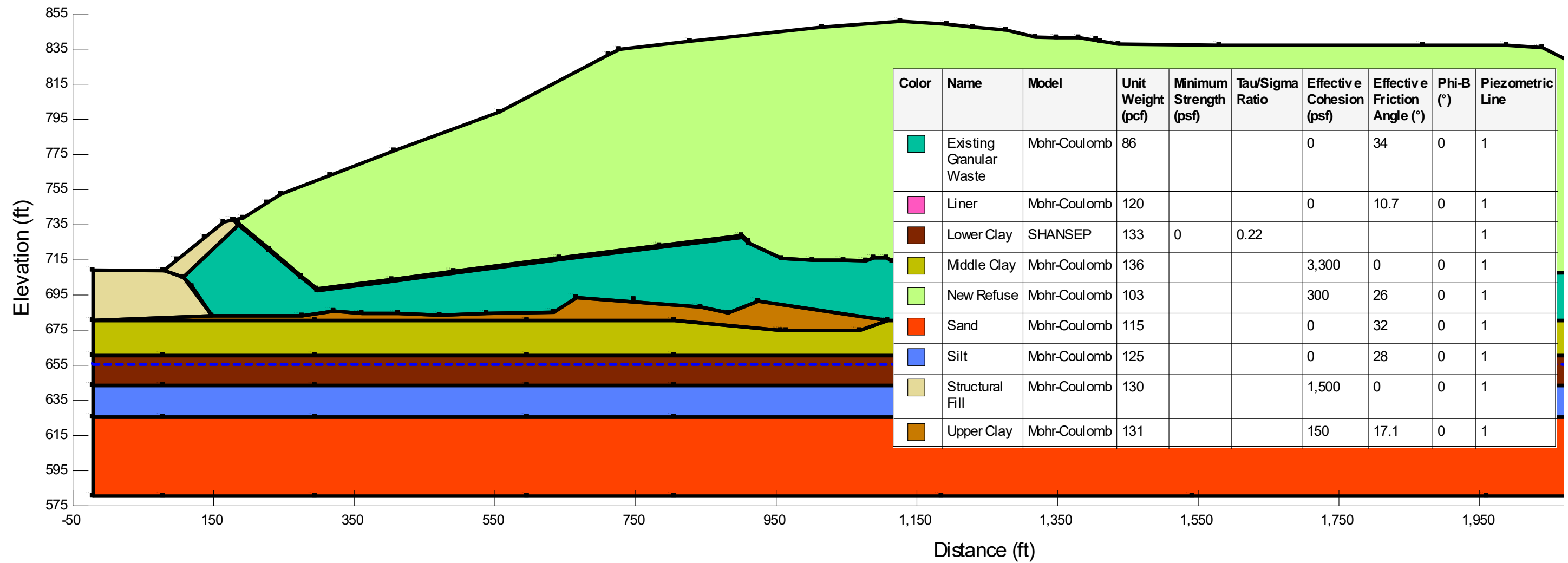
Final Grades Cross-Section (profile):



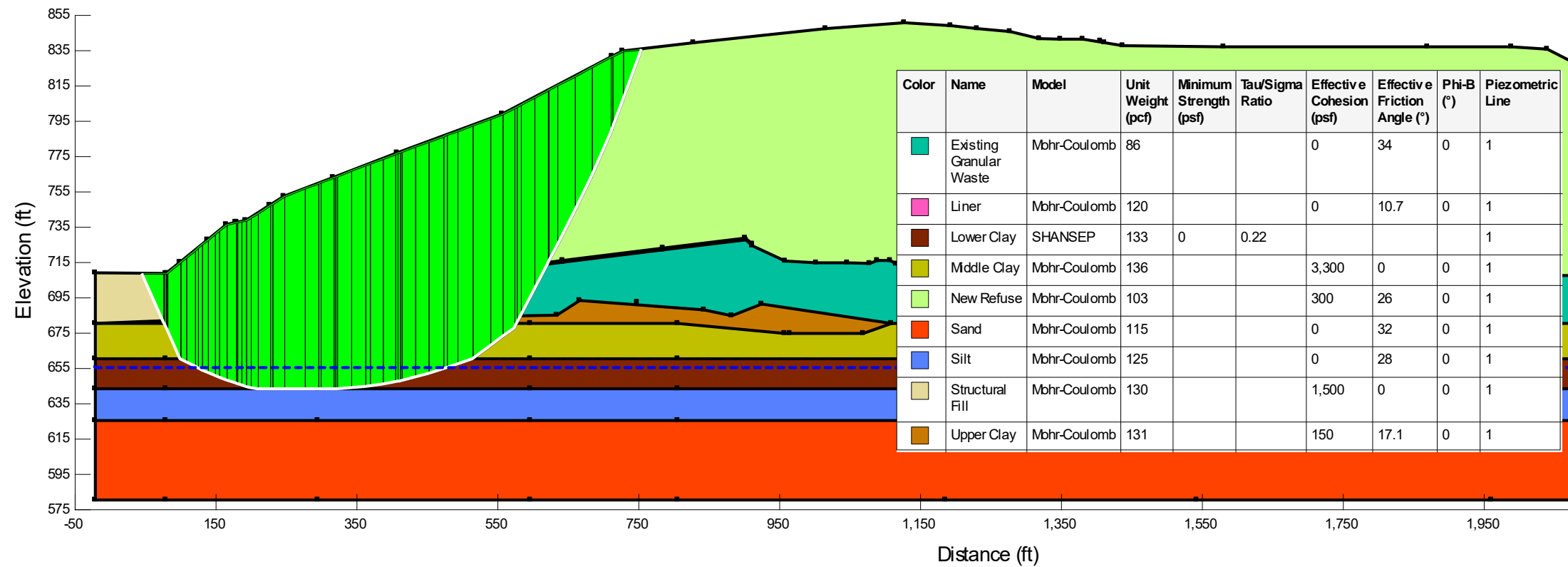
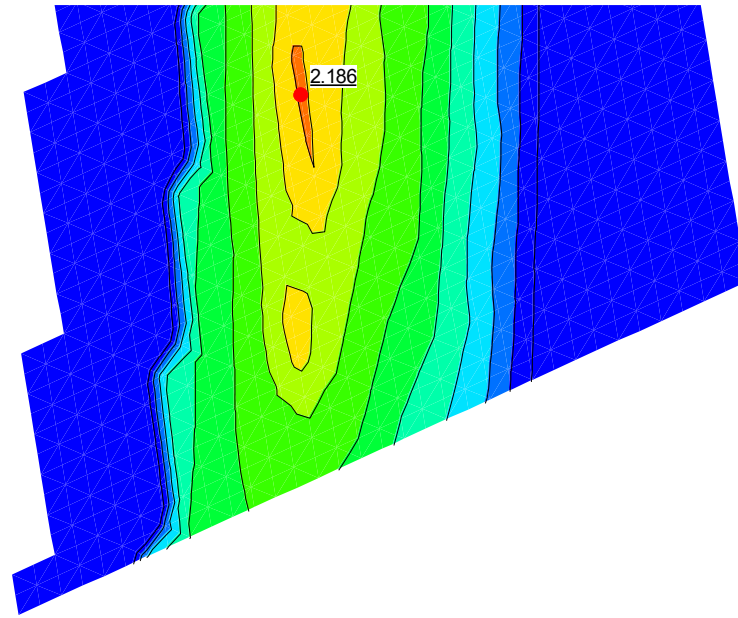
SLOPE STABILITY ANALYSIS REPORT FORM

Factor of Safety:	2.2	<input checked="" type="checkbox"/> Acceptable	<input type="checkbox"/> Not Acceptable	<input type="checkbox"/> Follow-up	<input type="checkbox"/> Superseded
Comments:					
Attachments:	Slope/W Cross Section and Results				

SLOPE STABILITY ANALYSIS REPORT FORM



SLOPE STABILITY ANALYSIS REPORT FORM



Attachment B-1.10

B-B'' Liner Stability under Final Conditions with zero adhesion and leachate head build up

SLOPE STABILITY ANALYSIS REPORT FORM

SLOPE STABILITY ANALYSIS REPORT FORM

Project Name:	WDI MC6F Permit Modification					
Project Number:	1208070039.004		Client:	Wayne Disposal, Inc.		
Analysis Short Name:	B-B' Liner Stability			File name:	WDI Cross Section B Liner_20201123_RevD_MK.gsz	
Revision:	0	Originated:	MK	Checked:	KF	Approved:
Date:	04/28/21	Date:	04/28/21	Date:		Date:

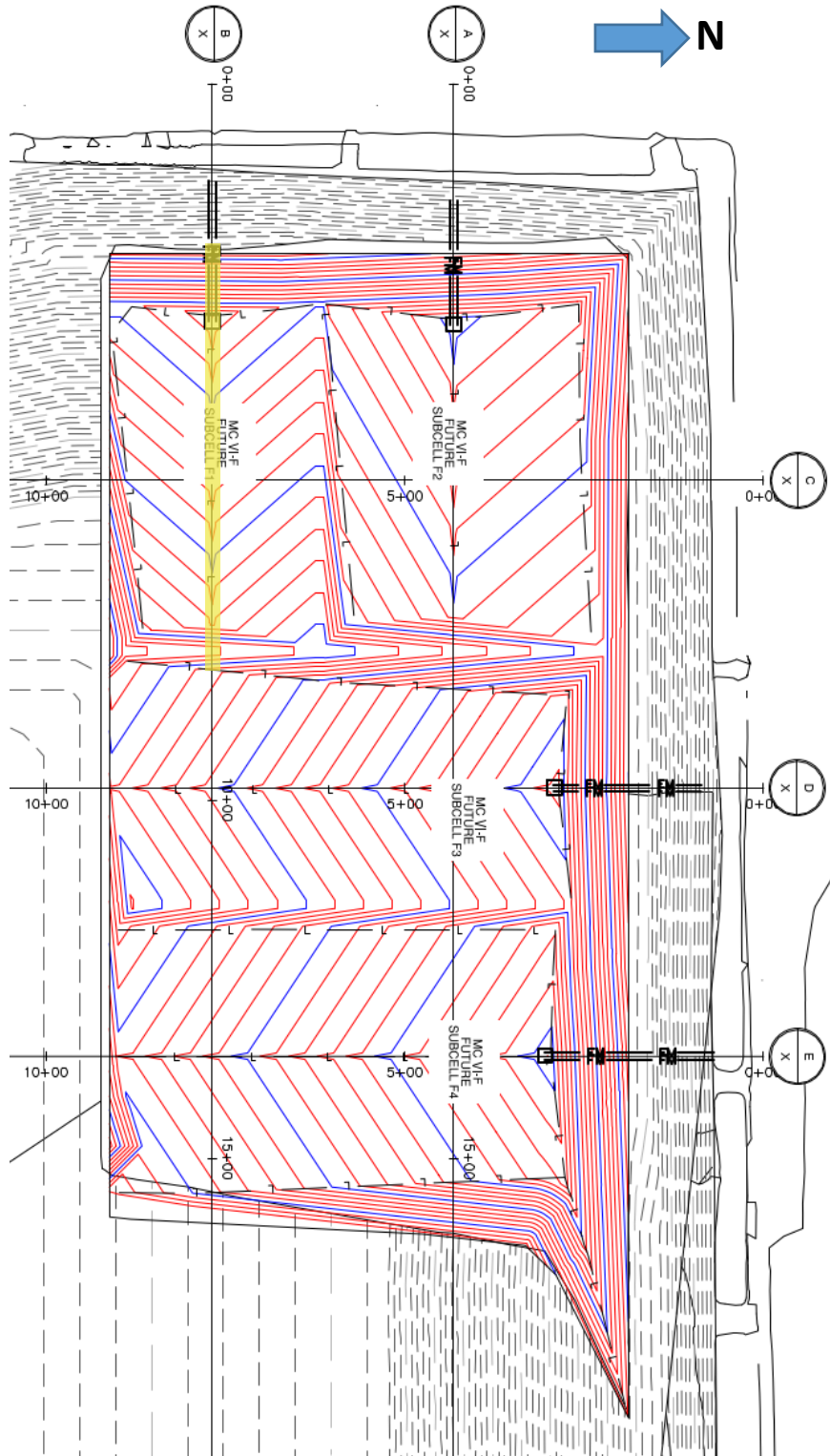
Purpose of Analysis:	To determine the required liner system interface strength to achieve an acceptable factor of safety of the proposed final waste grades using cross-section B. This case considers a west-facing slope, with fill to the final permitted grade elevations. The failure surface is defined such that failure occurs in the underlying liner in order to consider the stability of the liner.		
<input checked="" type="checkbox"/> Effective Stress <input type="checkbox"/> Total Stress	<input checked="" type="checkbox"/> Static <input type="checkbox"/> Seismic	<input checked="" type="checkbox"/> Pore Pressure	<input checked="" type="checkbox"/> Optimized Surface
Additional Details:	The liner system was modeled in 2 sections (floor and sideslope) to allow use of Peak and Large-Displacement strength parameters appropriately. The friction angle of the sideslope was set at 7° corresponding to commonly achievable large-displacement interface secant friction angle. The friction angle of the floor liner system was varied to determine the required peak interface secant friction angle to achieve the required factor of safety of 1.5. A scenario of leachate build up in the leachate collection layer (to a height of 12 inches) is modeled in this analysis.		

Material	Name	Color in Profile	Unit Wt(s) (pcf)	Strength ϕ or δ (deg.)	Strength C or Ca (psf)
1	Final Cover	Orange	130	0	1500
2	Existing Waste	Teal	86	34	0
3	New Waste	Light Green	103	26	300
4	Upper Clay	Brown	131	0	2150
5	Middle Clay	Yellow	136	0	3300
6	Lower Clay	Maroon	133	0.22 σ_v	
7	Silt	Blue	125	28	0
8	Sand	Red	115	32	0
9	Liner (Floor)	Magenta	120	TBD	0
10	Liner (Sideslope)	Purple	120	7	0

Source of Geometry:	Engineering Drawing Set
Source of Subsurface Profile:	Basis of Design Report - NTH (2012)
	<input type="checkbox"/> Preconstruction <input type="checkbox"/> Construction <input type="checkbox"/> Interim <input checked="" type="checkbox"/> Final <input type="checkbox"/> Existing <input type="checkbox"/> Back-Analysis
Construction Phase Represented:	Final build out
Other Geometry Notes:	Cross Section B

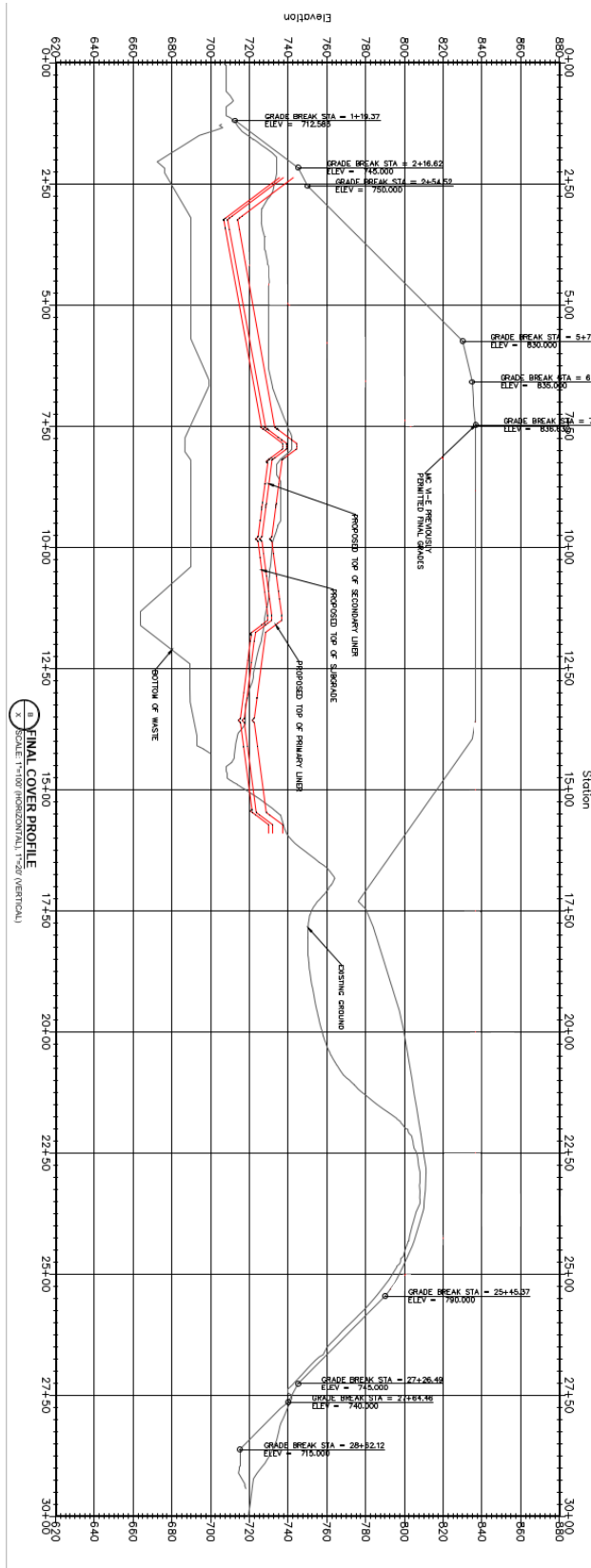
SLOPE STABILITY ANALYSIS REPORT FORM

Final Grades Cross-Section (plan):



SLOPE STABILITY ANALYSIS REPORT FORM

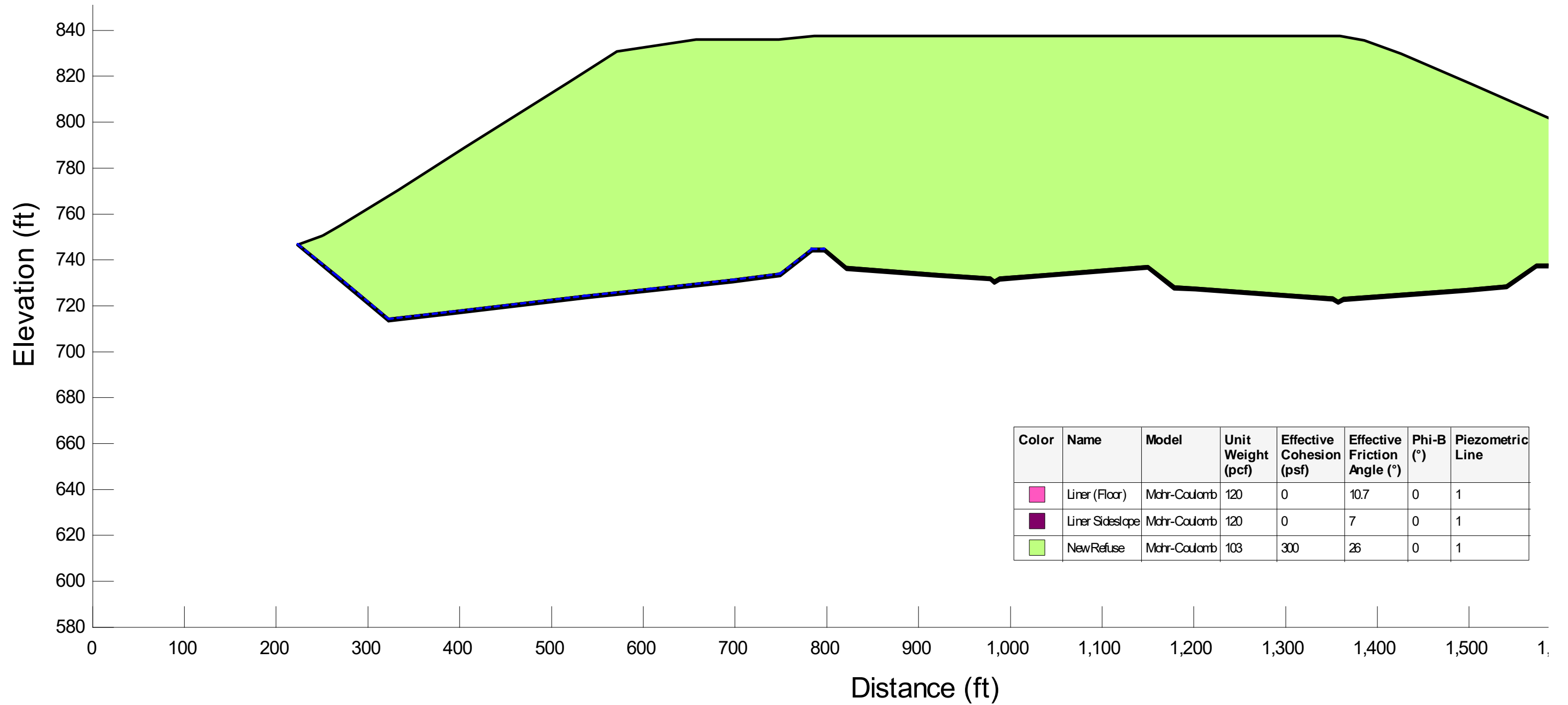
Final Grades Cross-Section (profile):



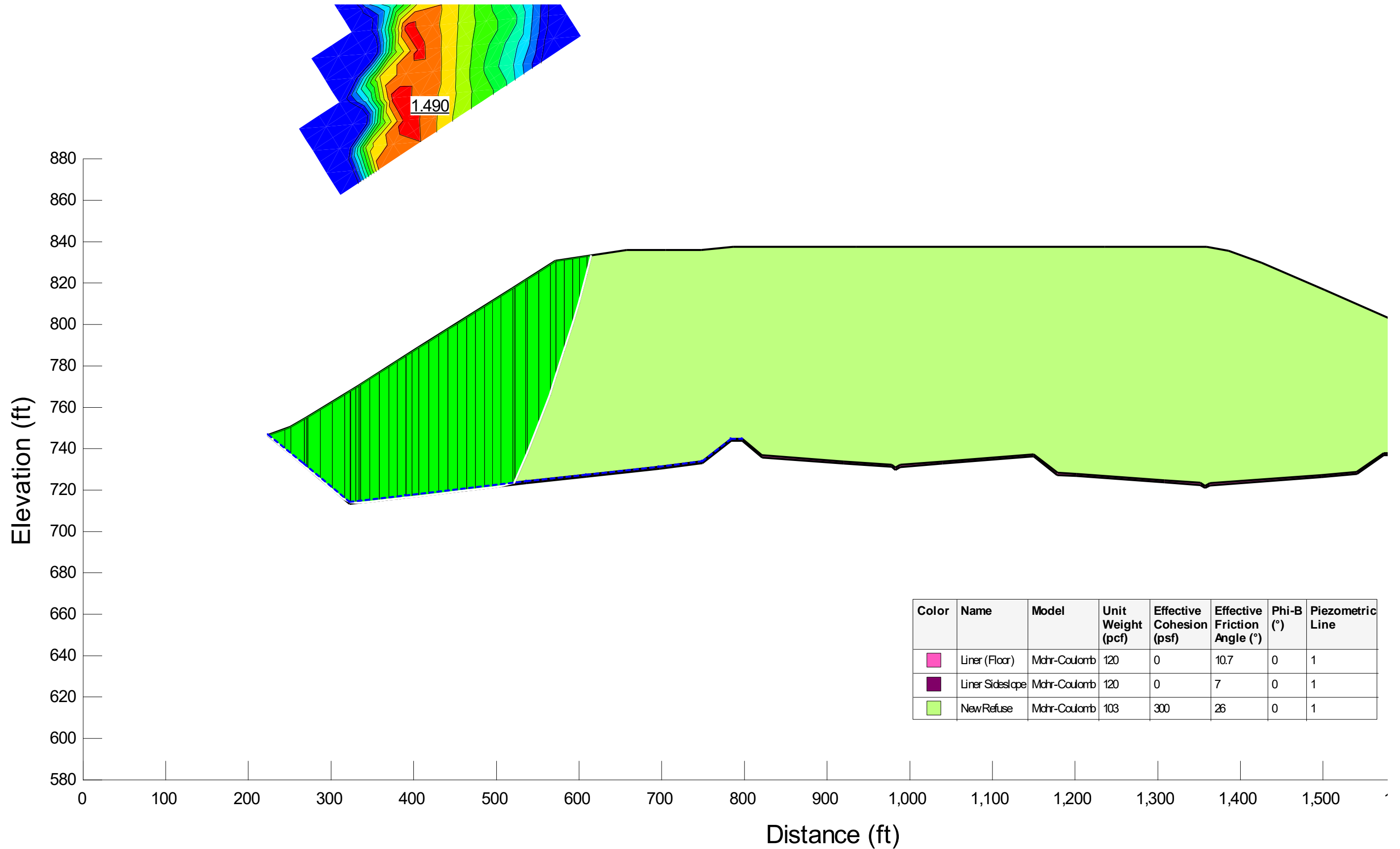
SLOPE STABILITY ANALYSIS REPORT FORM

Factor of Safety:	1.5	<input checked="" type="checkbox"/> Acceptable <input type="checkbox"/> Not Acceptable <input type="checkbox"/> Follow-up <input type="checkbox"/> Superseded
Comments:	The required peak interface friction for the floor liner system was determined to be 10.7°.	
Attachments:	Slope/W Cross Section and Results	

SLOPE STABILITY ANALYSIS REPORT FORM



SLOPE STABILITY ANALYSIS REPORT FORM



Attachment B-1.11

E-E' Liner Stability under Final Conditions with zero adhesion and leachate head build up

SLOPE STABILITY ANALYSIS REPORT FORM

SLOPE STABILITY ANALYSIS REPORT FORM

Project Name:	WDI MC6F Permit Modification					
Project Number:	1208070039.004		Client:	Wayne Disposal, Inc.		
Analysis Short Name:	E-E' Liner Stability			File name:	WDI Cross Section E Liner_20210428_HeadOn Liner_RevA_MK.gsz	
Revision:	0	Originated:	MK	Checked:	KF	Approved:
Date:	04/28/21	Date:	04/28/21	Date:		Date:

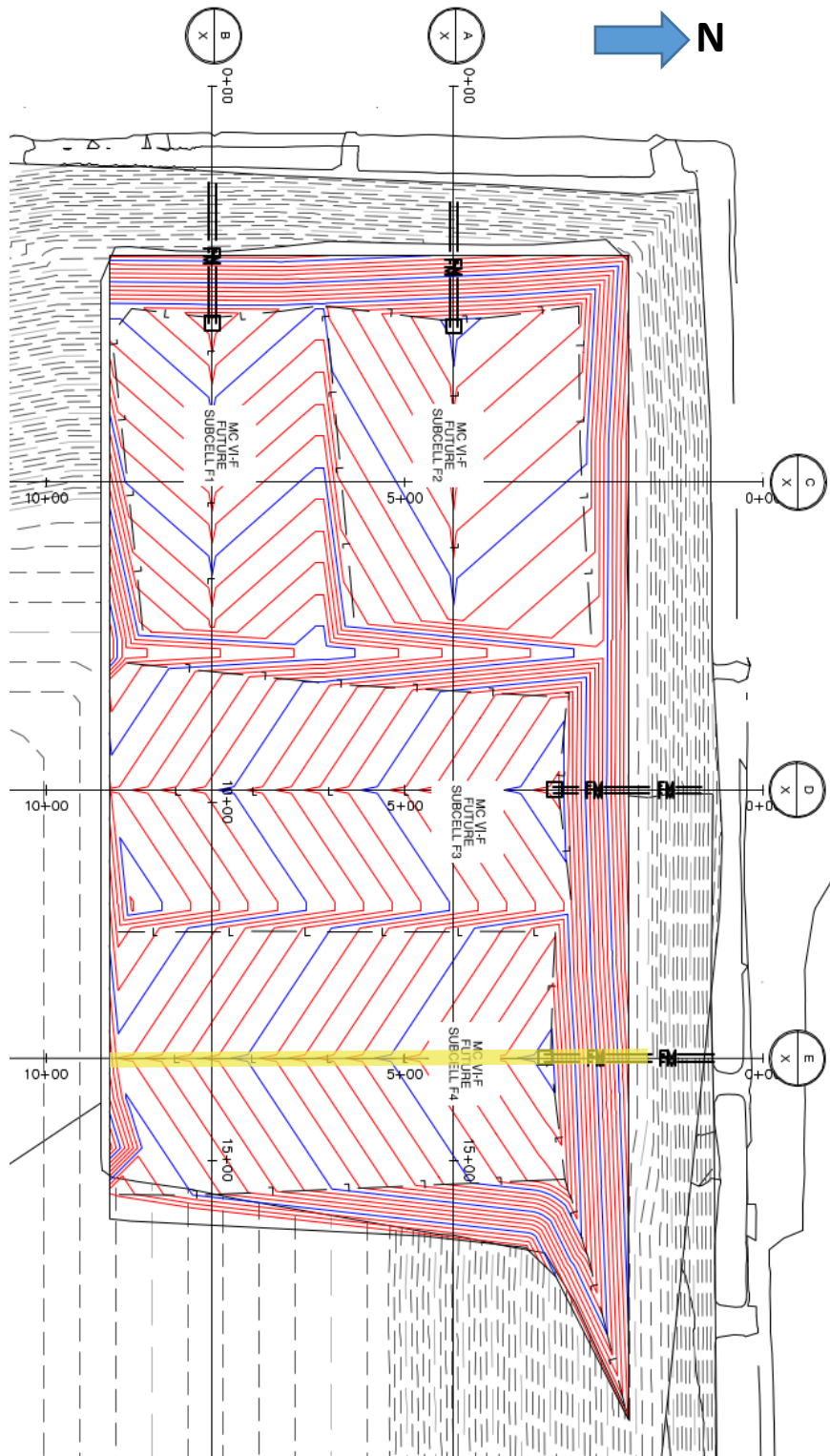
Purpose of Analysis:	To determine the factor of safety of the proposed final waste grades using cross-section E. This case considers a north-facing slope, with fill to the final grade elevations. The failure surface is defined such that failure occurs in the underlying liner in order to consider the stability of the liner.		
<input checked="" type="checkbox"/> Effective Stress <input type="checkbox"/> Total Stress	<input checked="" type="checkbox"/> Static <input type="checkbox"/> Seismic	<input checked="" type="checkbox"/> Pore Pressure	<input checked="" type="checkbox"/> Optimized Surface
Additional Details:	The friction angle of the liner system was set equal to the required minimum interface friction angle determined from the liner stability analysis performed on Cross Section B. The liner system was modeled in 2 sections (floor and sideslope) to allow use of Peak and Large-Displacement strength parameters appropriately. A scenario of leachate build up in the leachate collection layer (to a height of 12 inches) is modeled in this analysis.		

Material	Name	Color in Profile	Unit Wt(s) (pcf)	Strength ϕ or δ (deg.)	Strength C or Ca (psf)
1	Final Cover	Orange	130	0	1500
2	Existing Waste	Teal	86	34	0
3	New Waste	Light Green	103	26	300
4	Upper Clay	Brown	131	0	2150
5	Middle Clay	Yellow	136	0	3300
6	Lower Clay	Maroon	133	0.22 σ_v	
7	Silt	Blue	125	28	0
8	Sand	Red	115	32	0
9	Liner (Floor)	Magenta	120	10.7	0
10	Liner (Sideslope)	Purple	120	7	0

Source of Geometry:	Engineering Drawing Set
Source of Subsurface Profile:	Basis of Design Report - NTH (2012)
	<input type="checkbox"/> Preconstruction <input type="checkbox"/> Construction <input type="checkbox"/> Interim <input checked="" type="checkbox"/> Final <input type="checkbox"/> Existing <input type="checkbox"/> Back-Analysis
Construction Phase Represented:	Final build out
Other Geometry Notes:	Cross Section E

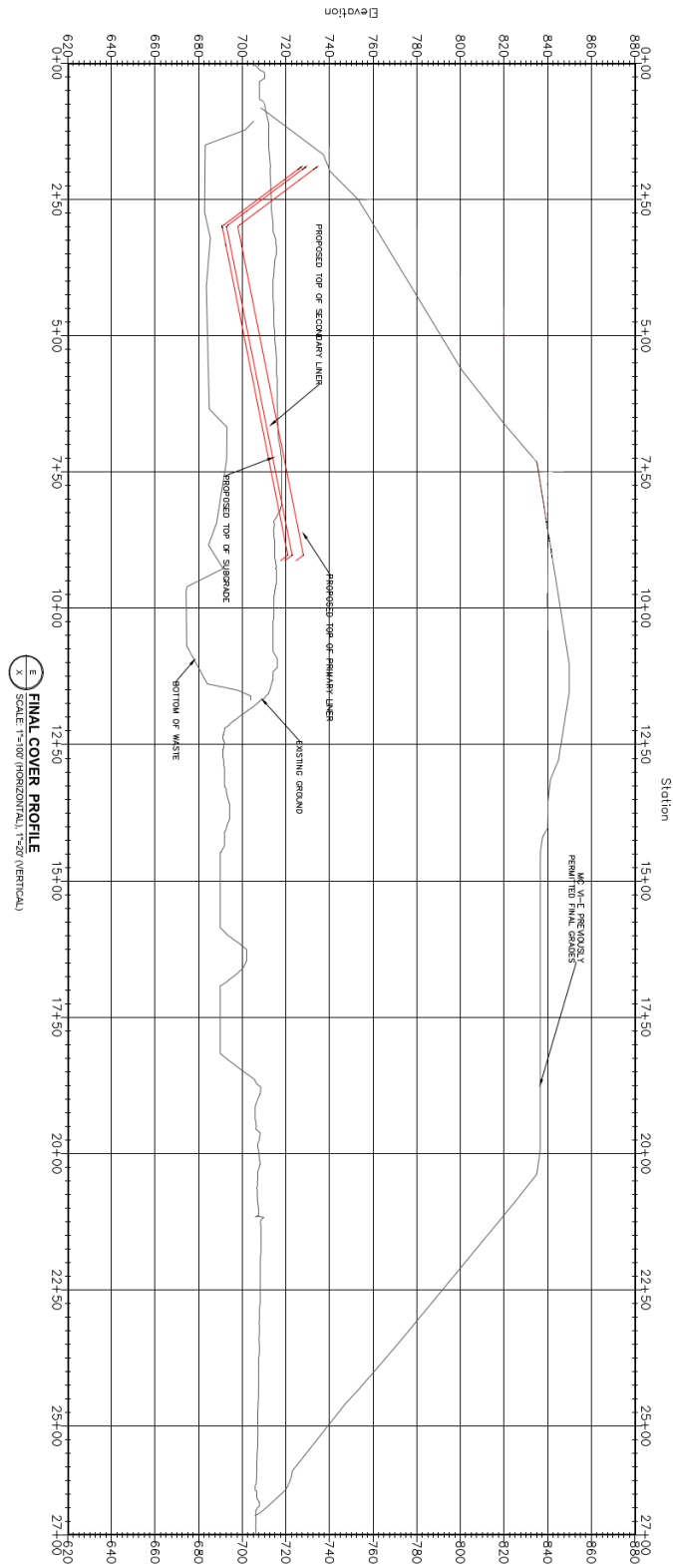
SLOPE STABILITY ANALYSIS REPORT FORM

Final Grades Cross-Section (plan):



SLOPE STABILITY ANALYSIS REPORT FORM

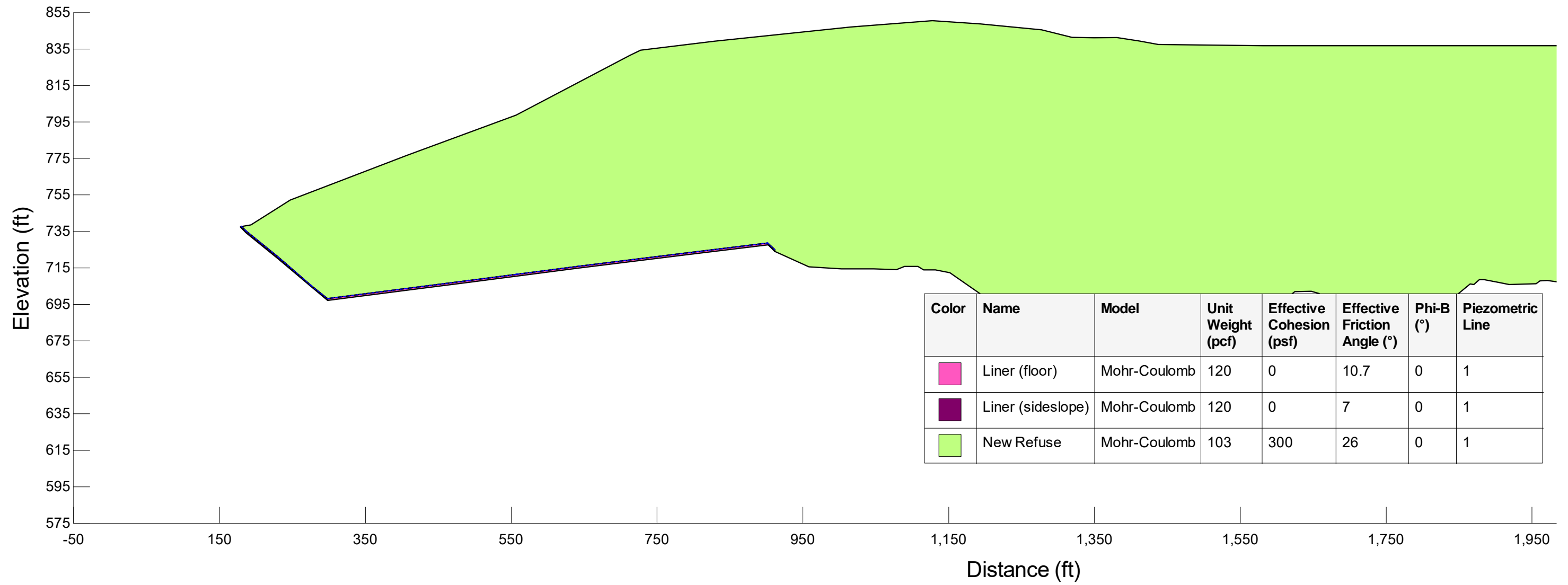
Final Grades Cross-Section (profile):



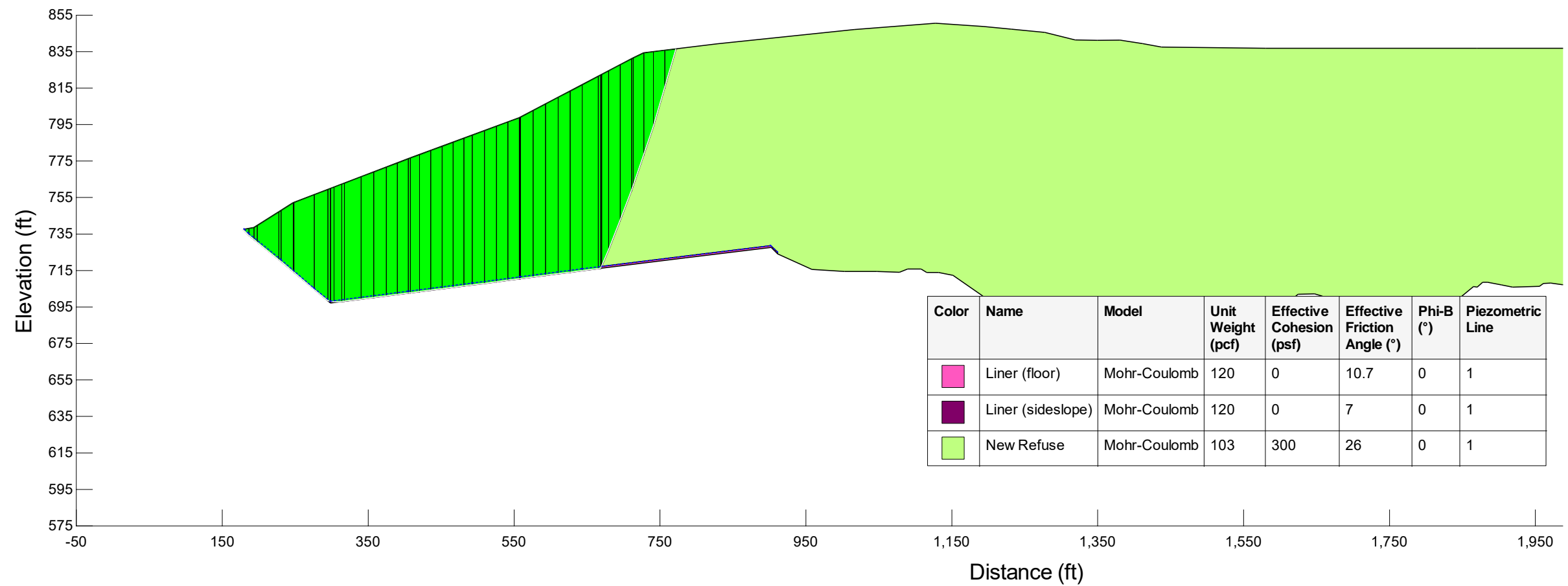
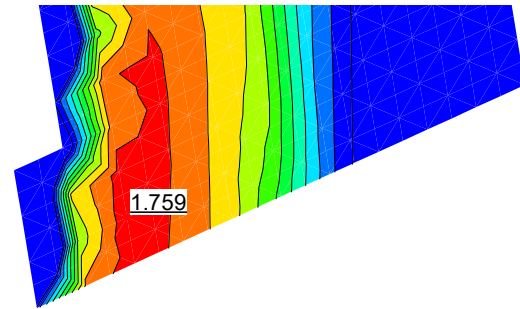
SLOPE STABILITY ANALYSIS REPORT FORM

Factor of Safety:	1.76	<input checked="" type="checkbox"/> Acceptable	<input type="checkbox"/> Not Acceptable	<input type="checkbox"/> Follow-up	<input type="checkbox"/> Superseded
Comments:					
Attachments:	Slope/W Cross Section and Results				

SLOPE STABILITY ANALYSIS REPORT FORM



SLOPE STABILITY ANALYSIS REPORT FORM



Attachment B-2

Settlement Calculations

**CALCULATION SHEET**Client: Wayne Disposal, Inc.Project: WDI MC6 F Permit ModificationCalculation: Leachate Collection Pipe Settlement Analysis MC6FProject No.: 1208070039.004Calculated By: KM Date: 11/16/2020Checked By: MK Date: 11/18/2020Approved By: KF Date: 11/19/2020

LEACHATE COLLECTION PIPE SETTLEMENT ANALYSIS

OBJECTIVE

This calculation evaluates the post-settlement slopes of the leachate collection pipes and cell floor cross slope for proposed Master Cell-VI (MC6) F1, F2, F3, and F4, at Wayne Disposal, Inc. (WDI). This evaluation is based on the estimated settlement of the existing waste and soil underlying the proposed cells due to additional overburden stresses induced by waste placement and the impact of such settlement on the post settlement cell floor slopes.

DESIGN CRITERIA AND ASSUMPTIONS

- The post-settlement slope of each proposed leachate collection pipe should be at least 1% and each cell floor cross slope should be at least 2% per Rule 299.9620 (4) (EGLE 2020).
- Pipe flowline analysis points were selected along the proposed leachate collection pipe flowlines within MC6-F (Attachment A). The specific locations of these points were selected to correspond to the cell floor high point, low point, changes in final cover slope and at regular intervals in between. Total settlement is estimated for each point, allowing an assessment of the post-settlement slope(s) along the flowline.
- Cross slope analysis points (Attachment A) were selected at the location of maximum fill height within each cell in order to evaluate post-settlement slopes under maximum load.
- Maximum settlement is expected to occur at the completion of the cap construction when the foundation is subjected to the maximum overburden pressure. Under the worst-case scenario, maximum load is applied (in full) to the foundation instantaneously during settlement analysis for a conservative (i.e., greater than anticipated) estimate of total settlement. In reality, loads would be applied incrementally as waste is placed gradually during the active life of the landfill. Additionally, the resulting settlement is assumed to occur immediately, conservatively accounting for the maximum settlement at the end of foundation soil consolidation.
- **Table 1** Material properties used for the settlement analysis are listed in Table 1.
- Table 2 summarizes the compressibility parameters used in the settlement analysis. The compacted clay liner is only very slightly compressible relative to the in-situ clay layer. Considering the insignificant magnitude of the settlement of the compacted clay liner, it was not included in the analysis.

**CALCULATION SHEET**

Client: Wayne Disposal, Inc.
 Project: WDI MC6 F Permit Modification
 Calculation: Leachate Collection Pipe Settlement Analysis MC6F

Project No.: 1208070039.004
 Calculated By: KM Date: 11/16/2020
 Checked By: MK Date: 11/18/2020
 Approved By: KF Date: 11/19/2020

Table 1. Soil Properties for Settlement Analysis

Soil Type	Thickness [ft]	Moist Unit Weight [pcf]
Final cover soil	4	135
New waste	Varies	103*
Existing cover soil	Varies	135
Existing waste	Varies	82
Attenuation Layer	5	135
Structural Fill	2	135
Venting Layer	1	135
Leachate Collection Sand	1	135
In-situ middle clay	Varies	136
In-situ lower clay (moist)	5	128
In-situ lower clay (saturated)	12	128
In-situ silt (saturated)	18	125
In-situ sand (saturated)	45	115

* New waste unit weight obtained from email correspondence with WDI dated 11/18/2020

Table 2. Compressibility Parameters of Waste and Soils

Soil Type	Primary Compression Ratio $C_c/(1+e_0)$	Secondary Compression Ratio $C_\alpha/(1+e_0)$	Recompression Ratio $C_r/(1+e_0)$
Existing cover	0.102 ^[B]	0.005 ^[B]	0.017 ^[A]
Existing waste	0.147	0	0.0245 ^[A]
In-situ middle clay	0.102	0.005	0.017 ^[A]
In-situ lower clay	0.171	0.009	0.0285 ^[A]
In-situ silt	0.15 ^[B]	0 ^[B]	0 ^[B]
In-situ sand	0.1 ^[B]	0 ^[B]	0 ^[B]

^[A] Estimated from $C_r = C_c/6$.

^[B] Assumed values.

The information for subsurface soils is based on MCIV General Profiles (South), Appendix A Subsurface Soil/Waste Profiles & Corresponding Physical Properties, Volume III – WDI Operating License Application Master Cells VI F & G by NTH Consultants (2011a). Specifically, subsurface investigation boring logs, cross sectional profiles, and laboratory test results were used to assess the subgrade soil profile and its properties. Note that some uncertainty may exist in the interpretation of

**CALCULATION SHEET**Client: Wayne Disposal, Inc.Project: WDI MC6 F Permit ModificationCalculation: Leachate Collection Pipe Settlement Analysis MC6FProject No.: 1208070039.004Calculated By: KM Date: 11/16/2020Checked By: MK Date: 11/18/2020Approved By: KF Date: 11/19/2020

hydrogeological data due to natural soil's inherent variability, conservative assumptions have been applied to ensure a conservative estimate of settlement in this analysis.

METHODOLOGY

Total settlement is estimated using the 1-D consolidation equations (Coduto 1999), with primary consolidation being the critical component. Total settlement is calculated as:

$$S = S_c + S_s \quad (1)$$

Where:

S = total settlement [ft]

S_c = primary consolidation settlement due to load application [ft]

S_s = secondary compression settlement due to creep effects [ft]

Settlement caused by primary consolidation for a given layer of soil with uniform properties is calculated as:

$$S_c = \frac{h_0}{1 + e_0} \left(C_r \log \frac{\sigma_c}{\sigma_0} + C_c \log \frac{\sigma_i}{\sigma_c} \right) \quad (2)$$

Where:

C_c = primary compression index

C_r = recompression index

h_0 = initial compressible layer thickness [ft]

e_0 = initial void ratio of the clay subgrade

σ_0 = initial overburden pressure acting on the compressible layer [psf]

σ_i = final overburden pressure acting on the compressible layer [psf]

σ_c = preconsolidation stress [psf], calculated using Equation 4.

Settlement due to secondary compression is calculated using Equation 3 below:

$$S_s = h_0 \frac{C_\alpha}{1 + e_0} \log \left(\frac{t_2}{t_1} \right) \quad (3)$$

Where:

C_α = secondary compression index



CALCULATION SHEET

Client: Wayne Disposal, Inc.Project: WDI MC6 F Permit ModificationCalculation: Leachate Collection Pipe Settlement Analysis MC6FProject No.: 1208070039.004Calculated By: KM Date: 11/16/2020Checked By: MK Date: 11/18/2020Approved By: KF Date: 11/19/2020

H = layer thickness [ft]

t_2 = time after application of load (assumed 70 years)

t_1 = time required to complete primary consolidation (assumed 40 years)

- The elevations in this report are referenced to Mean Sea Level (MSL).
- The initial ground elevation (prior to initial development) was assumed to be approximately 705 ft. This value was inferred from the cross-sectional profile from Engineering Drawings, Wayne Disposal, Inc. Site No.2 MC VI-F&G by NTH Consultants (2011b).
- The preconsolidation pressure of the middle clay and lower clay, the major contributing compressible layers below the existing waste, was set equal to the initial effective overburden pressure acting on them prior to development. This value is used in Equation 2 to estimate settlement resulting from an initial load less than the preconsolidation pressure. Note that both layers have exhibited a higher overburden pressure since initial development of the site and placement of the now existing waste. This value is calculated using Equation 4.
- Calculation of settlement following MC6-F construction accounts for changes in overburden pressure resulting from the excavation of existing materials, the placement of new liner system components, the placement of new MC6-F waste, and the placement of new MC6-F final cover.
- At each point selected along the leachate collection pipe system, the elevations for the existing ground, proposed MC6-F liner system (OFL), final cover, and the foundation soils are determined and used to compute the initial and final overburden pressures at each settlement point within the analysis using Equation 4 similarly to the preconsolidation pressure. An example calculation at 2 adjacent settlement points along MC6-F1 is presented in Attachment B-2.2.

$$\sigma_{c,0,f} = \sum_{i=0}^n \gamma_i \times h_i \quad (4)$$

Where:

σ_c : preconsolidation stress [psf]

$\sigma_{c,0,f} = \sigma_0$: initial stress [psf]

σ_f : final stress [psf]

γ_i = Unit weight of soil layer i [psf]

Thickness of layer i [ft] at settlement point as follows:

For σ_c use thicknesses of layers prior to development

h_i = For σ_0 use thicknesses of layers up to existing elevations

For σ_f use thicknesses of layers up to proposed final elevations

- Soil layers are identified using subsurface soil profiles provided in MCIV General Profiles (South), Appendix A Subsurface Soil/Waste Profiles & Corresponding Physical Properties, Volume III – WDI Operating License Application Master Cells VI F & G by NTH Consultants (2011a). These layers include in-situ clay with varying degrees of compressibility (see Table 2).



Client: Wayne Disposal, Inc.
 Project: WDI MC6 F Permit Modification
 Calculation: Leachate Collection Pipe Settlement Analysis MC6F

Project No.: 1208070039.004
 Calculated By: KM Date: 11/16/2020
 Checked By: MK Date: 11/18/2020
 Approved By: KF Date: 11/19/2020

- Attachment A presents the plan locations of the settlement analysis points within MC6-F with respect to proposed cell floor grades and final grades. Leachate collection pipe cross section profiles are also presented in Attachment A.

CALCULATIONS

Equations 1 through 4 were incorporated into a spreadsheet to conduct the settlement calculations. The settlement calculation output and resulting post-settlement slope(s) for each leachate collection pipe within MC6-F are presented in Table 3 through Table 6. The settlement calculation output and resulting post-settlement slope(s) for each analyzed cross slope within MC6-F are presented in Table 7 through Table 10. A sample settlement calculation of points 1 and 2 along the leachate pipe flowline in MC6-F1 is presented in Attachment B-2.2.

Table 3. MC6-F1 Leachate Pipe Flowline Settlement Calculation Summary

Point			Elevation		Length	Liner Grade	Side Slope		Min. Slope
	North	East	Flowline Elevation	Settlement		Post-Settlement	Pre-Settlement	Post-Settlement	
	[ft]	[ft]	[ft]	[ft]	[ft]	[ft]	[%]	[%]	[%]
1	0.00	0.00	716.00	6.71	120	709.29	4.0%	2.4%	1%
2	120.00	0.00	720.80	8.66		712.14			
2	120.00	0.00	720.80	8.66	100	712.14	4.0%	3.0%	1%
3	220.00	0.00	724.80	9.70		715.10			
3	220.00	0.00	724.80	9.70	88	715.10	4.0%	3.4%	1%
4	308.00	0.00	728.32	10.20		718.12			
4	308.00	0.00	728.32	10.20	85	718.12	4.0%	3.9%	1%
5	393.00	0.00	731.72	10.29		721.43			

Table 4. MC6-F2 Leachate Pipe Flowline Settlement Calculation Summary

Point			Elevation		Length	Liner Grade	Side Slope		Min. Slope
	North	East	Flowline Elevation	Settlement		Post-Settlement	Pre-Settlement	Post-Settlement	
	[ft]	[ft]	[ft]	[ft]	[ft]	[ft]	[%]	[%]	[%]
1	0.00	0.00	710.00	6.21	72	703.79	3.0%	1.3%	1%
2	71.80	0.00	712.15	7.46		704.69			
2	71.80	0.00	712.15	7.46	65	704.69	3.0%	2.1%	1%
3	136.70	0.00	714.10	8.02		706.08			
3	136.70	0.00	714.10	8.02	131	706.08	3.0%	2.9%	1%
4	267.60	0.00	718.03	8.10		709.93			
4	267.60	0.00	718.03	8.10	124	709.93	3.0%	2.9%	1%
5	392.00	0.00	721.76	8.19		713.57			

Table 5. MC6-F3 Leachate Pipe Flowline Settlement Calculation Summary

Point			Elevation		Length	Liner Grade	Side Slope		Min. Slope
	North	East	Flowline Elevation	Settlement		Post-Settlement	Pre-Settlement	Post-Settlement	
	[ft]	[ft]	[ft]	[ft]	[ft]	[ft]	[%]	[%]	[%]
1	0.00	0.00	708.00	5.87	116	702.13	4.0%	2.2%	1%
2	116.00	0.00	712.64	7.99		704.65			
2	116.00	0.00	712.64	7.99	121	704.65	4.0%	2.7%	1%
3	237.00	0.00	717.48	9.58		707.90			
3	237.00	0.00	717.48	9.58	196	707.90	4.0%	4.3%	1%
4	433.00	0.00	725.32	8.93		716.39			
4	433.00	0.00	725.32	8.93	162	716.39	4.0%	3.6%	1%
5	595.00	0.00	731.80	9.52		722.28			


CALCULATION SHEET

Client: Wayne Disposal, Inc.

Project: WDI MC6 F Permit Modification

Calculation: Leachate Collection Pipe Settlement Analysis MC6F

Project No.: 1208070039.004

Calculated By: KM Date: 11/16/2020

Checked By: MK Date: 11/18/2020

Approved By: KF Date: 11/19/2020

Table 6. MC6-F4 Leachate Pipe Flowline Settlement Calculation Summary

Point	North [ft]	East [ft]	Elevation		Length [ft]	Liner Grade	Side Slope		Min. Slope [%]
			Flowline Elevation [ft]	Settlement [ft]		Post-Settlement [ft]	Pre-Settlement [%]	Post-Settlement [%]	
1	0.00	0.00	700.00	5.48	102	694.52	4.0%	3.0%	1%
2	102.00	0.00	704.08	6.51		697.57			
2	102.00	0.00	704.08	6.51	103	697.57	4.0%	3.1%	1%
3	205.00	0.00	708.20	7.42		700.78			
3	205.00	0.00	708.20	7.42	201	700.78	4.0%	3.0%	1%
4	406.00	0.00	716.24	9.52		706.72			
4	406.00	0.00	716.24	9.52	158	706.72	4.0%	3.4%	1%
5	564.00	0.00	722.56	10.53		712.03			

Table 7. MC6-F1 Cross Slope Settlement Calculation Summary

Point	North [ft]	East [ft]	Elevation		Length [ft]	Liner Grade	Side Slope		Min. Slope [%]
			Floor Elevation [ft]	Settlement [ft]		Post-Settlement [ft]	Pre-Settlement [%]	Post-Settlement [%]	
5	0.00	0.00	734.00	10.16	142	723.84	4.5%	5.2%	2%
6	142.00	0.00	740.35	9.12		731.23			
5	0.00	0.00	734.00	10.16	101	723.84	4.5%	4.9%	2%
7	101.00	0.00	738.51	9.76		728.75			

Table 8. MC6-F2 Cross Slope Settlement Calculation Summary

Point	North [ft]	East [ft]	Elevation		Length [ft]	Liner Grade	Side Slope		Min. Slope [%]
			Floor Elevation [ft]	Settlement [ft]		Post-Settlement [ft]	Pre-Settlement [%]	Post-Settlement [%]	
5	0.00	0.00	722.00	7.76	206	714.24	2.3%	4.2%	2%
6	206.00	0.00	726.64	3.78		722.86			
5	0.00	0.00	722.00	7.76	150	714.24	5.7%	5.0%	2%
7	150.00	0.00	730.48	8.67		721.81			

Table 9. MC6-F3 Cross Slope Settlement Calculation Summary

Point	North [ft]	East [ft]	Elevation		Length [ft]	Liner Grade	Side Slope		Min. Slope [%]
			Floor Elevation [ft]	Settlement [ft]		Post-Settlement [ft]	Pre-Settlement [%]	Post-Settlement [%]	
5	0.00	0.00	738.00	9.02	105	728.98	4.5%	4.8%	2%
6	105.00	0.00	742.69	8.68		734.02			
5	0.00	0.00	738.00	9.02	163	728.98	4.5%	4.8%	2%
7	163.00	0.00	745.29	8.49		736.79			

Table 10. MC6-F4 Cross Slope Settlement Calculation Summary

Point	North [ft]	East [ft]	Elevation		Length [ft]	Liner Grade	Side Slope		Min. Slope [%]
			Floor Elevation [ft]	Settlement [ft]		Post-Settlement [ft]	Pre-Settlement [%]	Post-Settlement [%]	
5	0.00	0.00	728.00	10.09	187	717.91	4.5%	5.5%	2%
6	187.00	0.00	736.36	8.24		728.12			
5	0.00	0.00	728.00	10.09	180	717.91	4.5%	5.1%	2%
7	180.00	0.00	736.05	8.98		727.06			

**CALCULATION SHEET**Client: Wayne Disposal, Inc.Project: WDI MC6 F Permit ModificationCalculation: Leachate Collection Pipe Settlement Analysis MC6FProject No.: 1208070039.004Calculated By: KM Date: 11/16/2020Checked By: MK Date: 11/18/2020Approved By: KF Date: 11/19/2020**CONCLUSIONS**

The post-settlement slope of each proposed leachate collection pipe should be at least 1% and each cell floor cross slope should be at least 2% per Rule 299.9620 (4) (EGLE 2020). This calculation estimated the settlement at points along the leachate collection pipe and cross slopes within each subcell. The settlement of each of these points was used to calculate the post-settlement slopes of the MC6-F floor. This settlement analysis determined that all leachate collection pipes and cross slopes within MC6-F meet the required minimum post-settlement slopes.

REFERENCES

Coduto, D.P. (1999) *Geotechnical Engineering: Principles and Practices*, Prentice-Hall Inc., New Jersey

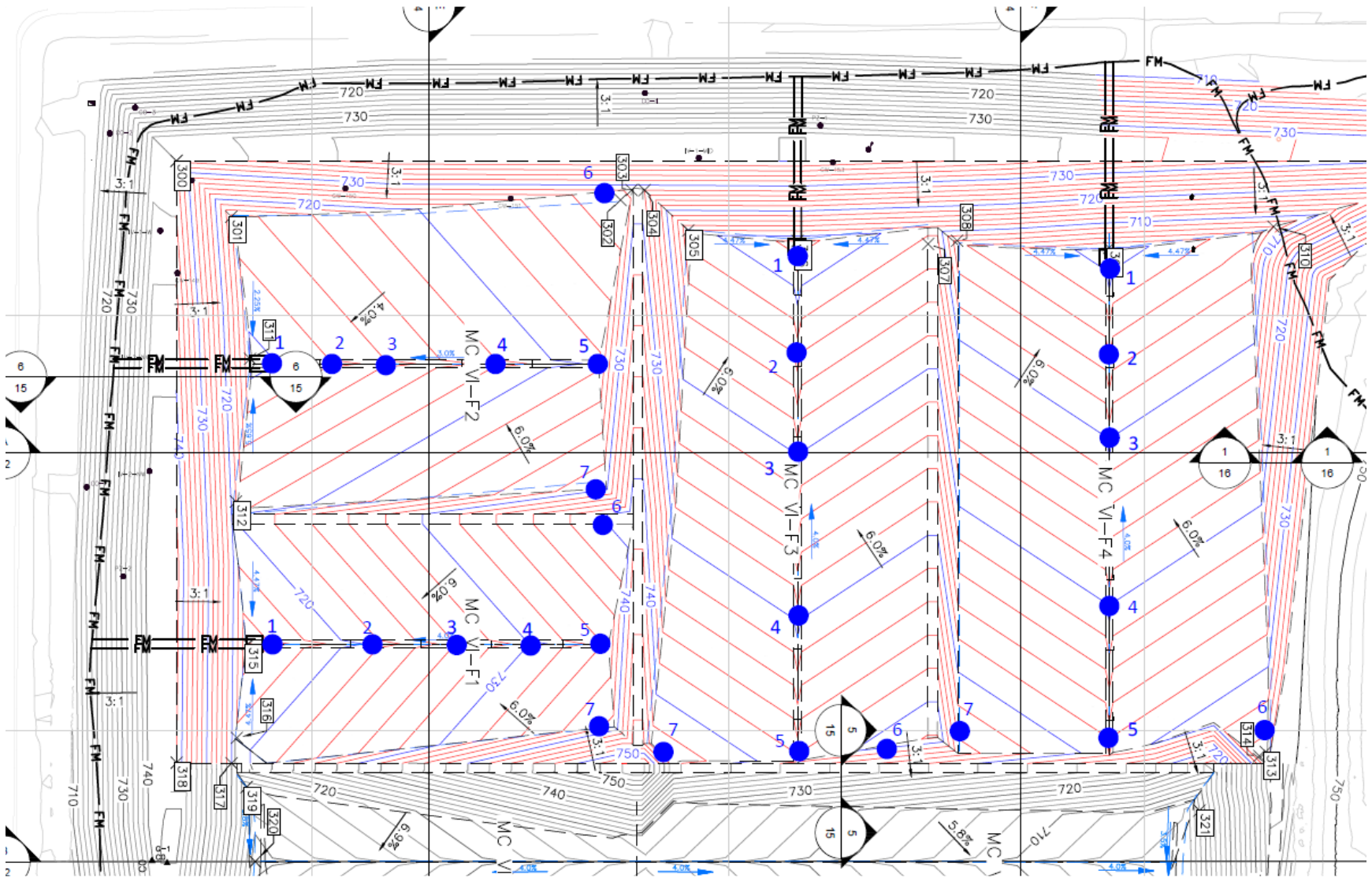
EGLE (2020) *Part 111 Administrative Rules*, Department of Environment, Great Lakes, and Energy
Hazardous Waste Management, Materials Management Division.

NTH Consultants, Ltd. (2011a) *Volume III – WDI Operating License Application Master Cells VI F & G*.

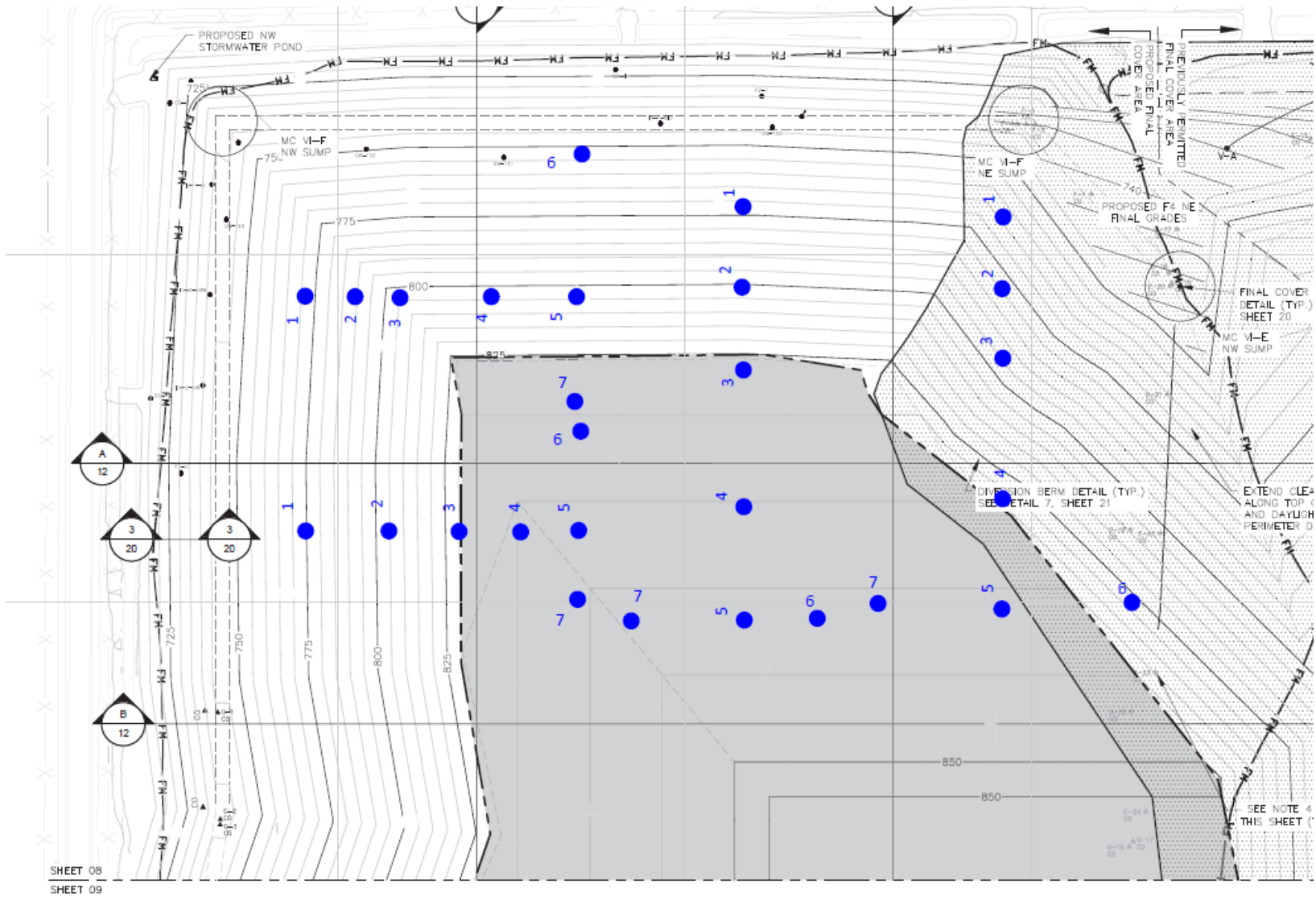
NTH Consultants, Ltd. (2011b) Engineering Drawings. *Wayne Disposal, Inc. Site No. 2 Master Cell VI-F&G*.

Attachment B-2.1

Plan View and Cross Sections of Leachate Flowlines

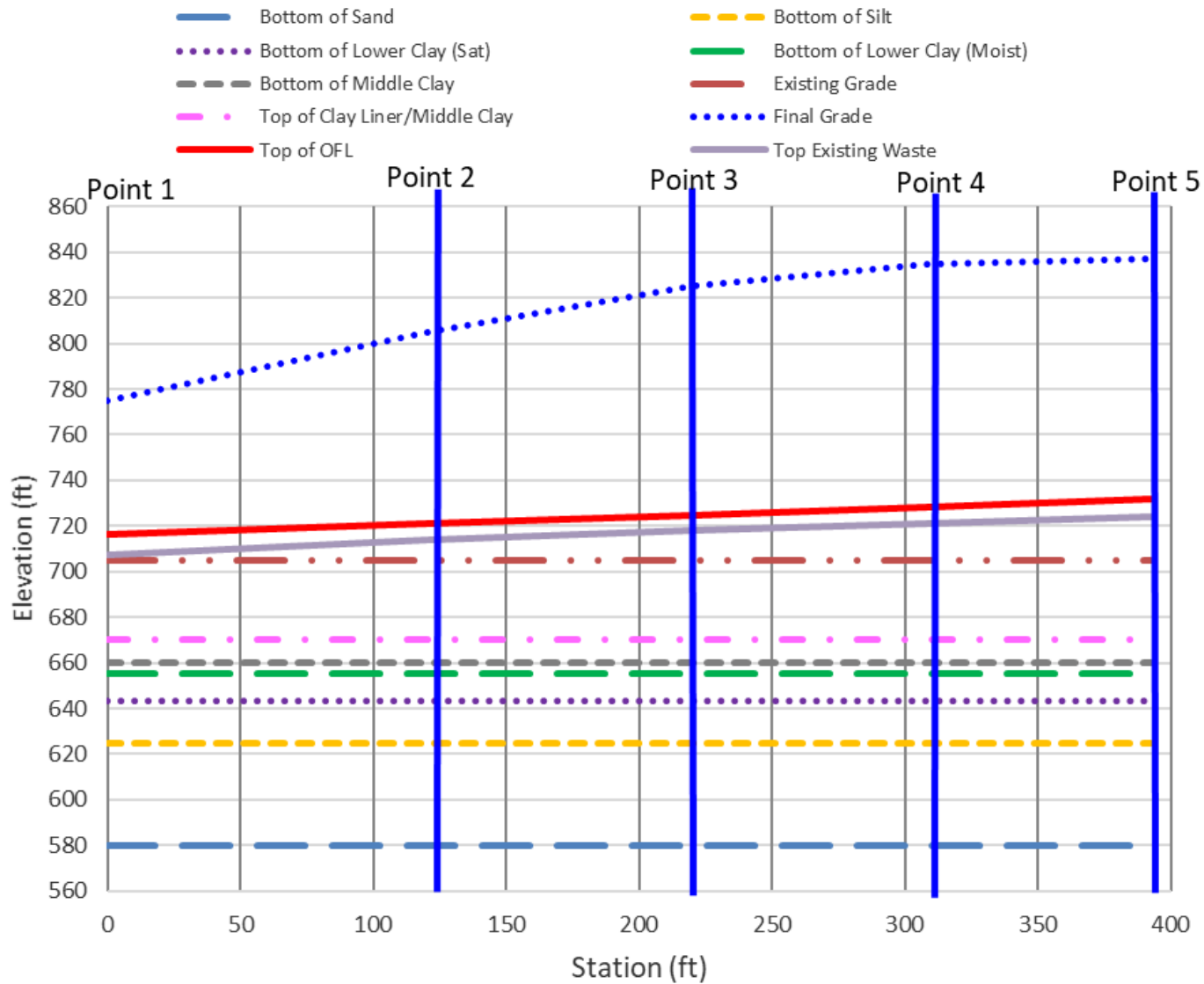


Plan View of Settlement Analysis Points Showing Top of Liner Grades

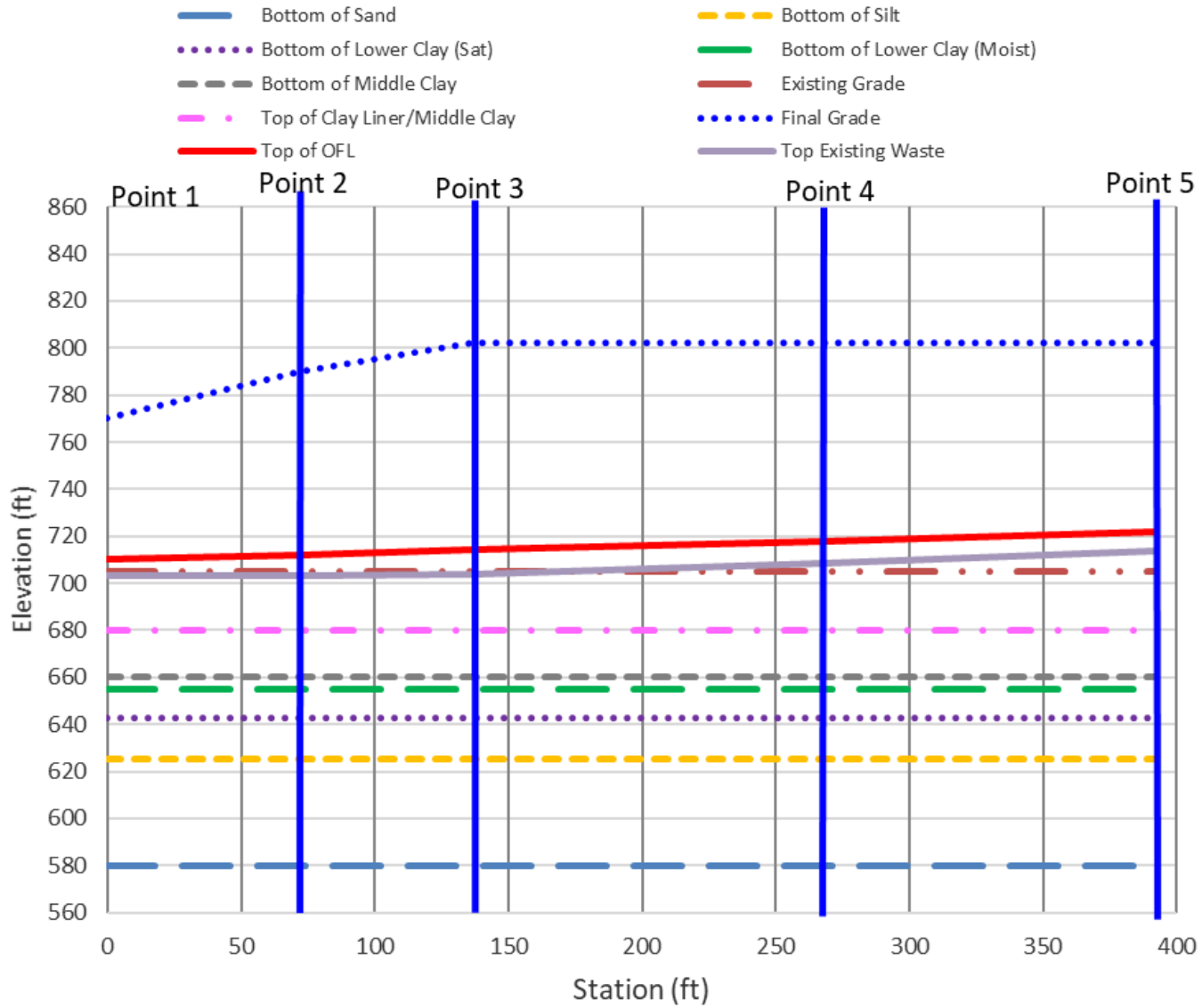


Plan View of Settlement Analysis Points Showing Final Grades

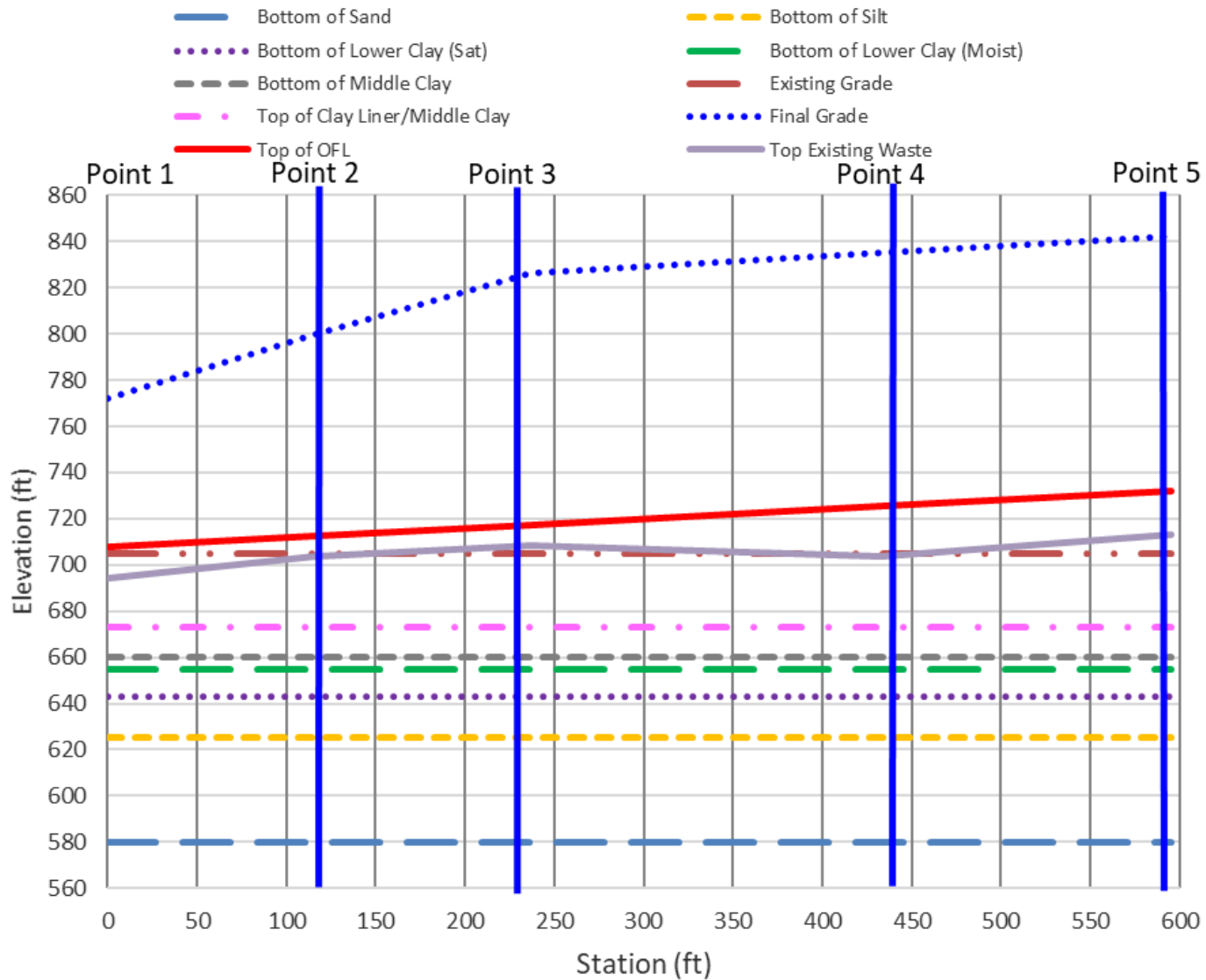
Cross Section Profile of MC6-F1 Leachate Pipe Flowline



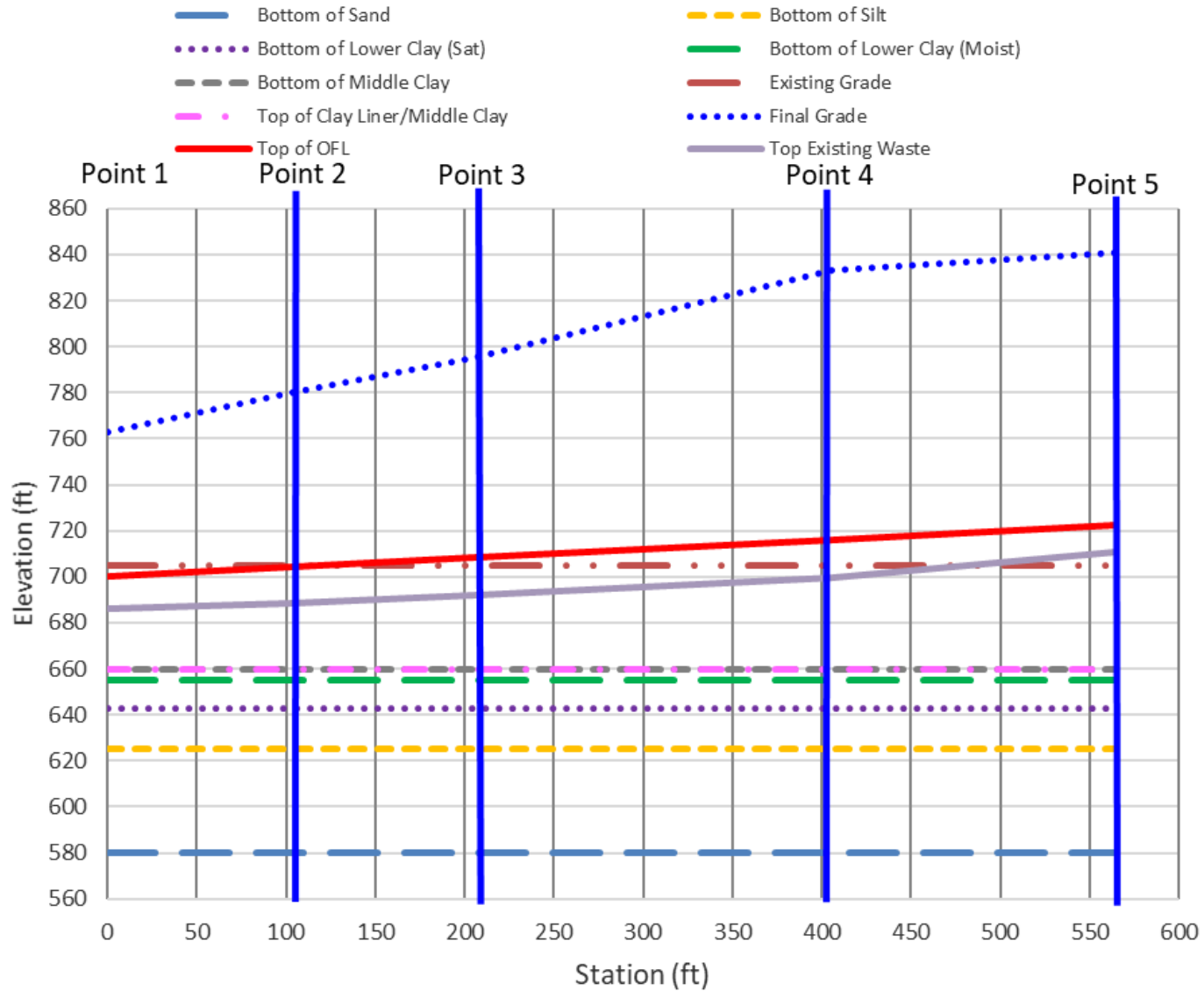
Cross Section Profile of MC6-F2 Leachate Pipe Flowline



Cross Section Profile of MC6-F3 Leachate Pipe Flowline



Cross Section Profile of MC6-F4 Leachate Pipe Flowline



Attachment B-2.2

Sample Settlement Calculation

SETTLEMENT POINT 1	Coordinates		Elevations									
	North	East	OFL	Final	Existing	BOTTOM MC	BOTTOM LC (DRY)	BOTTOM LC (SAT)	BOTTOM SILT	BOTTOM SAND	TOP CLAY	TOP EXISTING WASTE
	[ft]	[ft]	[ft MSL]	[ft MSL]	[ft MSL]	[ft MSL]	[ft MSL]	[ft MSL]	[ft MSL]	[ft MSL]	[ft MSL]	[ft MSL]
	0.00	0.00	716.00	775.00	705.00	660.00	655.00	643.00	625.00	580.00	670.00	707.50

Layer Type	Layer	Layer Height	Eff. Unit Weight	Cut Layer	Inc. Layer Stress	Compression Parameters			Initial Stress	Consolidation Stress	Final Stress	Consolidation Case	Primary Settlement	Secondary Settlement	
		H [ft]	γ' [pcf]	1 = yes 0 = no	σ_i [psf]	$\frac{C_c}{1+e_0}$	$\frac{C_r}{1+e_0}$	$\frac{C_\alpha}{1+e_0}$	(midpoint of layer)			-	S_c [ft]	S_s [ft]	
									σ_0' [psf]	σ_c' [psf]	σ_f' [psf]				
Overburden	1	Cover	4.00	135.0	0	540.0									
	2	New Waste	55.00	103.0	0	5665.0									
	3	OFL	0.50	135.0	0	67.5									
	4	Existing Waste	0.50	82.0	1	-41.0									
		<none>		-	0	-									
		<none>		-	0	-									
Consolidation		<none>		-	0	-									
	3	OFL	4.25	135.0	0	573.8	0.102	0.017	0.005	327.9	327.9	6559.4	NC	0.564	0.005
	3	OFL	4.25	135.0	0	573.8	0.102	0.017	0.005	901.6	901.6	7133.1	NC	0.389	0.005
	4	Existing Waste	4.69	82.0	0	384.4	0.147	0.025	-	1380.7	1380.7	7612.2	NC	0.511	-
	4	Existing Waste	4.69	82.0	0	384.4	0.147	0.025	-	1765.1	1765.1	7996.6	NC	0.452	-
	4	Existing Waste	4.69	82.0	0	384.4	0.147	0.025	-	2149.4	2149.4	8380.9	NC	0.407	-
	4	Existing Waste	4.69	82.0	0	384.4	0.147	0.025	-	2533.8	2533.8	8765.3	NC	0.371	-
	4	Existing Waste	4.69	82.0	0	384.4	0.147	0.025	-	2918.2	2918.2	9149.7	NC	0.342	-
	4	Existing Waste	4.69	82.0	0	384.4	0.147	0.025	-	3302.6	3302.6	9534.1	NC	0.317	-
	4	Existing Waste	4.69	82.0	0	384.4	0.147	0.025	-	3686.9	3686.9	9918.4	NC	0.296	-
	4	Existing Waste	4.69	82.0	0	384.4	0.147	0.025	-	4071.3	4071.3	10302.8	NC	0.278	-
	6	Middle Clay	5.00	136.0	0	680.0	0.102	0.017	0.005	4603.5	4950.0	10835.0	OC-2	0.176	0.006
	6	Middle Clay	5.00	136.0	0	680.0	0.102	0.017	0.005	5283.5	5630.0	11515.0	OC-2	0.161	0.006
	7	Lower Clay (Moist)	5.00	128.0	0	640.0	0.171	0.029	0.009	5943.5	6290.0	12175.0	OC-2	0.249	0.011
	8	Lower Clay (Sat)	6.00	65.6	0	393.6	0.171	0.029	0.009	6460.3	6806.8	12691.8	OC-2	0.281	0.014
	8	Lower Clay (Sat)	6.00	65.6	0	393.6	0.171	0.029	0.009	6853.9	7200.4	13085.4	OC-2	0.270	0.014
	9	Silt	9.00	62.6	0	563.4	0.150	-	-	7332.4	7678.9	13563.9	OC-2	0.334	-
	9	Silt	9.00	62.6	0	563.4	0.150	-	-	7895.8	8242.3	14127.3	OC-2	0.316	-
10	Sand	9.00	52.6	0	473.4	0.100	-	-	8414.2	8760.7	14645.7	OC-2	0.201	-	
10	Sand	9.00	52.6	0	473.4	0.100	-	-	8887.6	9234.1	15119.1	OC-2	0.193	-	
10	Sand	9.00	52.6	0	473.4	0.100	-	-	9361.0	9707.5	15592.5	OC-2	0.185	-	
10	Sand	9.00	52.6	0	473.4	0.100	-	-	9834.4	10180.9	16065.9	OC-2	0.178	-	
10	Sand	9.00	52.6	0	473.4	0.100	-	-	10307.8	10654.3	16539.3	OC-2	0.172	-	
													6.644	0.063	
														6.71	

Variables & Constants	
Point Name	1
Settlement Layer [ft]	136.0
ERROR	0.0
# of Layers	22
t / t_p [ratio]	1.8

- Use the master "Material Properties" sheet to input the correct "Layer Type" into column C. This will auto-populate the density and compression parameters. Coordinates and elevations are referenced from the "Points" sheet for comparison to the total consolidation layer.

- Split layers greater than 10 feet thick.

- Existing layers that are to be removed are to be marked with a "1" in the "Cut Layer" column.

Total Settlement [ft]

6.71

SETTLEMENT POINT 2	Coordinates		Elevations									
	North	East	OFL	Final	Existing	BOTTOM MC	BOTTOM LC (DRY)	BOTTOM LC (SAT)	BOTTOM SILT	BOTTOM SAND	TOP CLAY	TOP EXISTING WASTE
	[ft]	[ft]	[ft MSL]	[ft MSL]	[ft MSL]	[ft MSL]	[ft MSL]	[ft MSL]	[ft MSL]	[ft MSL]	[ft MSL]	[ft MSL]
	120.00	0.00	719.60	805.00	705.00	660.00	655.00	643.00	625.00	580.00	670.00	713.70

Layer Type	Layer	Layer Height H [ft]	Eff. Unit Weight γ' [pcf]	Cut Layer 1 = yes 0 = no	Inc. Layer Stress σ_i [psf]	Compression Parameters			Initial Stress σ'_0 [psf]	Consolidation Stress σ'_c [psf]	Final Stress σ'_f [psf]	Consolidation Case -	Primary Settlement S_c [ft]	Secondary Settlement S_s [ft]	
						$\frac{C_c}{1+e_0}$	$\frac{C_r}{1+e_0}$	$\frac{C_\alpha}{1+e_0}$							
						(midpoint of layer)									
Overburden	1	Cover	4.00	135.0	0	540.0									
	2	New Waste	81.40	103.0	0	8384.2									
	3	OFL	3.10	135.0	0	418.5									
	4	Existing Waste	3.10	82.0	1	-254.2									
		<none>		-	0	-									
		<none>		-	0	-									
Consolidation		<none>		-	0	-									
	3	OFL	2.95	135.0	0	398.2	0.102	0.017	0.005	453.3	453.3	9541.8	NC	0.398	0.004
	3	OFL	2.95	135.0	0	398.2	0.102	0.017	0.005	851.6	851.6	9940.1	NC	0.321	0.004
	4	Existing Waste	5.46	82.0	0	447.9	0.147	0.025	-	1274.7	1274.7	10363.2	NC	0.731	-
	4	Existing Waste	5.46	82.0	0	447.9	0.147	0.025	-	1722.6	1722.6	10811.1	NC	0.641	-
	4	Existing Waste	5.46	82.0	0	447.9	0.147	0.025	-	2170.5	2170.5	11259.0	NC	0.574	-
	4	Existing Waste	5.46	82.0	0	447.9	0.147	0.025	-	2618.4	2618.4	11706.9	NC	0.522	-
	4	Existing Waste	5.46	82.0	0	447.9	0.147	0.025	-	3066.4	3066.4	12154.9	NC	0.480	-
	4	Existing Waste	5.46	82.0	0	447.9	0.147	0.025	-	3514.3	3514.3	12602.8	NC	0.445	-
	4	Existing Waste	5.46	82.0	0	447.9	0.147	0.025	-	3962.2	3962.2	13050.7	NC	0.416	-
	4	Existing Waste	5.46	82.0	0	447.9	0.147	0.025	-	4410.1	4410.1	13498.6	NC	0.390	-
	6	Middle Clay	5.00	136.0	0	680.0	0.102	0.017	0.005	4974.1	4950.0	14062.6	NC	0.230	0.006
	6	Middle Clay	5.00	136.0	0	680.0	0.102	0.017	0.005	5654.1	5630.0	14742.6	NC	0.212	0.006
	7	Lower Clay (Moist)	5.00	128.0	0	640.0	0.171	0.029	0.009	6314.1	6290.0	15402.6	NC	0.331	0.011
	8	Lower Clay (Sat)	6.00	65.6	0	393.6	0.171	0.029	0.009	6830.9	6806.8	15919.4	NC	0.377	0.014
	8	Lower Clay (Sat)	6.00	65.6	0	393.6	0.171	0.029	0.009	7224.5	7200.4	16313.0	NC	0.363	0.014
	9	Silt	9.00	62.6	0	563.4	0.150	-	-	7703.0	7678.9	16791.5	NC	0.457	-
	9	Silt	9.00	62.6	0	563.4	0.150	-	-	8266.4	8242.3	17354.9	NC	0.435	-
	10	Sand	9.00	52.6	0	473.4	0.100	-	-	8784.8	8760.7	17873.3	NC	0.278	-
	10	Sand	9.00	52.6	0	473.4	0.100	-	-	9258.2	9234.1	18346.7	NC	0.267	-
10	Sand	9.00	52.6	0	473.4	0.100	-	-	9731.6	9707.5	18820.1	NC	0.258	-	
10	Sand	9.00	52.6	0	473.4	0.100	-	-	10205.0	10180.9	19293.5	NC	0.249	-	
10	Sand	9.00	52.6	0	473.4	0.100	-	-	10678.4	10654.3	19766.9	NC	0.241	-	
													8.616	0.059	
														8.68	

Variables & Constants	
Point Name	2
Settlement Layer [ft]	139.6
ERROR	0.0
# of Layers	22
t / t_p [ratio]	1.8

- Use the master "Material Properties" sheet to input the correct "Layer Type" into column C. This will auto-populate the density and compression parameters. Coordinates and elevations are referenced from the "Points" sheet for comparison to the total consolidation layer.

- Split layers greater than 10 feet thick.

- Existing layers that are to be removed are to be marked with a "1" in the "Cut Layer" column.

Total Settlement [ft]

8.68

Attachment C
Permit Drawings

WAYNE DISPOSAL, INC. SITE NO. 2 MASTER CELL VI-F&G

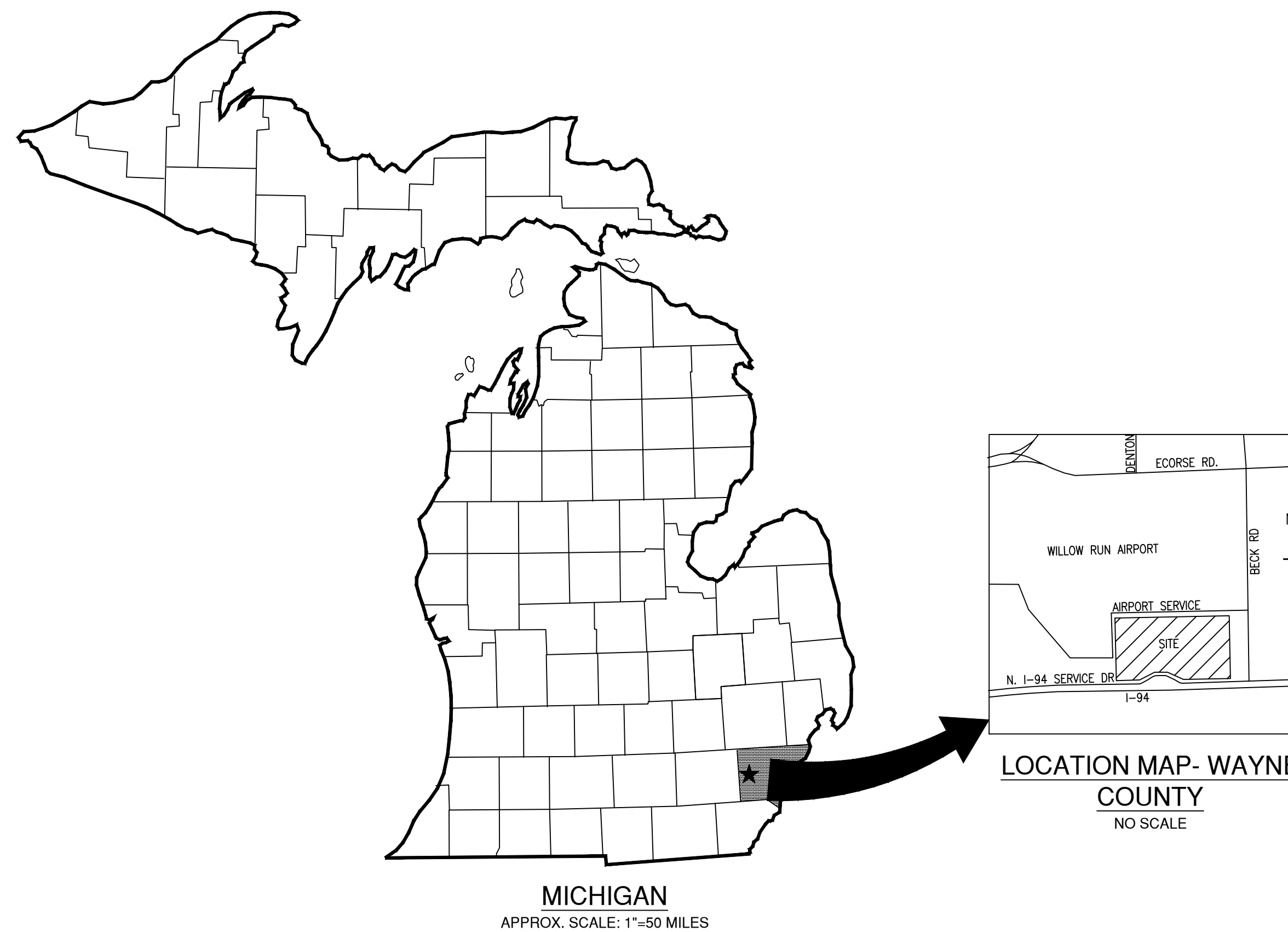
VAN BUREN TOWNSHIP, WAYNE COUNTY, MICHIGAN

CTI PROJECT NO.1208070039

FEBRUARY 2011
REVISED: SEPTEMBER 2011
REVISED: MAY 2018
REVISED: MAY 2021

OWNER:
Wayne Disposal, Inc.
49350 N. I-94 Service Drive
Belleville, Michigan 48111

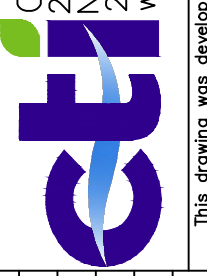
ENGINEER:
CTI and Associates, Inc.
28001 Cabot Drive, Ste. 250
Novi, Michigan 48377

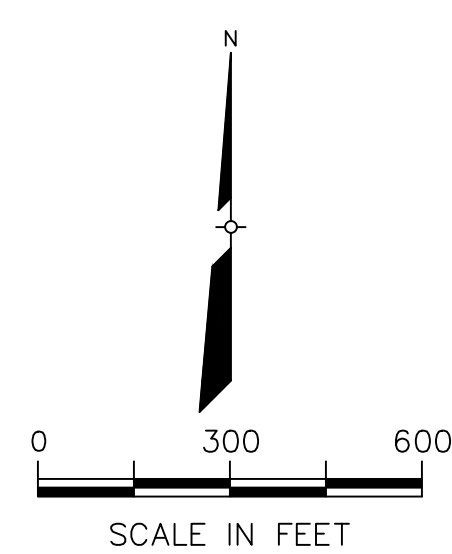


SHEET INDEX

- △△△△ 01 TITLE SHEET
- △ 02 GENERAL SITE PLAN
- △△△△ 03 CONSTRUCTION PHASING
- △△△△ 04 TOP OF SUBGRADE GRADING PLAN
- △△△△ 05 TOP OF SECONDARY LINER GRADING PLAN
- △△△△△ 06 TOP OF PRIMARY LINER GRADING PLAN
- △△ 07 LEACHATE MANAGEMENT PLAN
- △△ 08 FINAL COVER GRADING PLAN (1 OF 2)
- △△△ 09 FINAL COVER GRADING PLAN (2 OF 2)
- △ 10 STORMWATER MANAGEMENT AND SEDIMENTATION PLAN (1 OF 2)
- △ 11 STORMWATER MANAGEMENT AND SEDIMENTATION PLAN (2 OF 2)
- △△△△ 12 CROSS SECTIONS (1 OF 3)
- △△ 13 CROSS SECTIONS (2 OF 3)
- △△ 14 CROSS SECTIONS (3 OF 3)
- △△△△ 15 LINER SYSTEM DETAILS (1 OF 3)
- △△△△ 16 LINER SYSTEM DETAILS (2 OF 3)
- △△△△ 17 LINER SYSTEM DETAILS (3 OF 3)
- △△△△ 18 LEACHATE COLLECTION SYSTEM DETAILS (1 OF 2)
- △△△△ 19 LEACHATE COLLECTION SYSTEM DETAILS (2 OF 2)
- △ 20 FINAL COVER DETAILS
- △ 21 STORMWATER MANAGEMENT SYSTEM DETAILS
- △△△ 22 CONCEPTUAL GAS VENTING SYSTEM

**ADDITIONAL SHEETS 3&4 INCLUDED FROM THE 2011 NTH PERMIT TO SHOW UTILITIES IN MCI AND MCIV

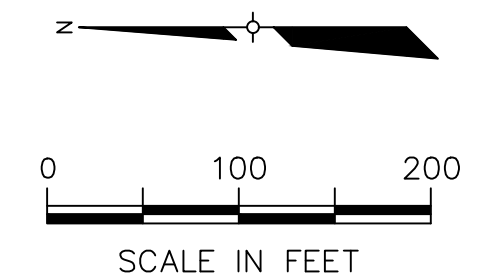
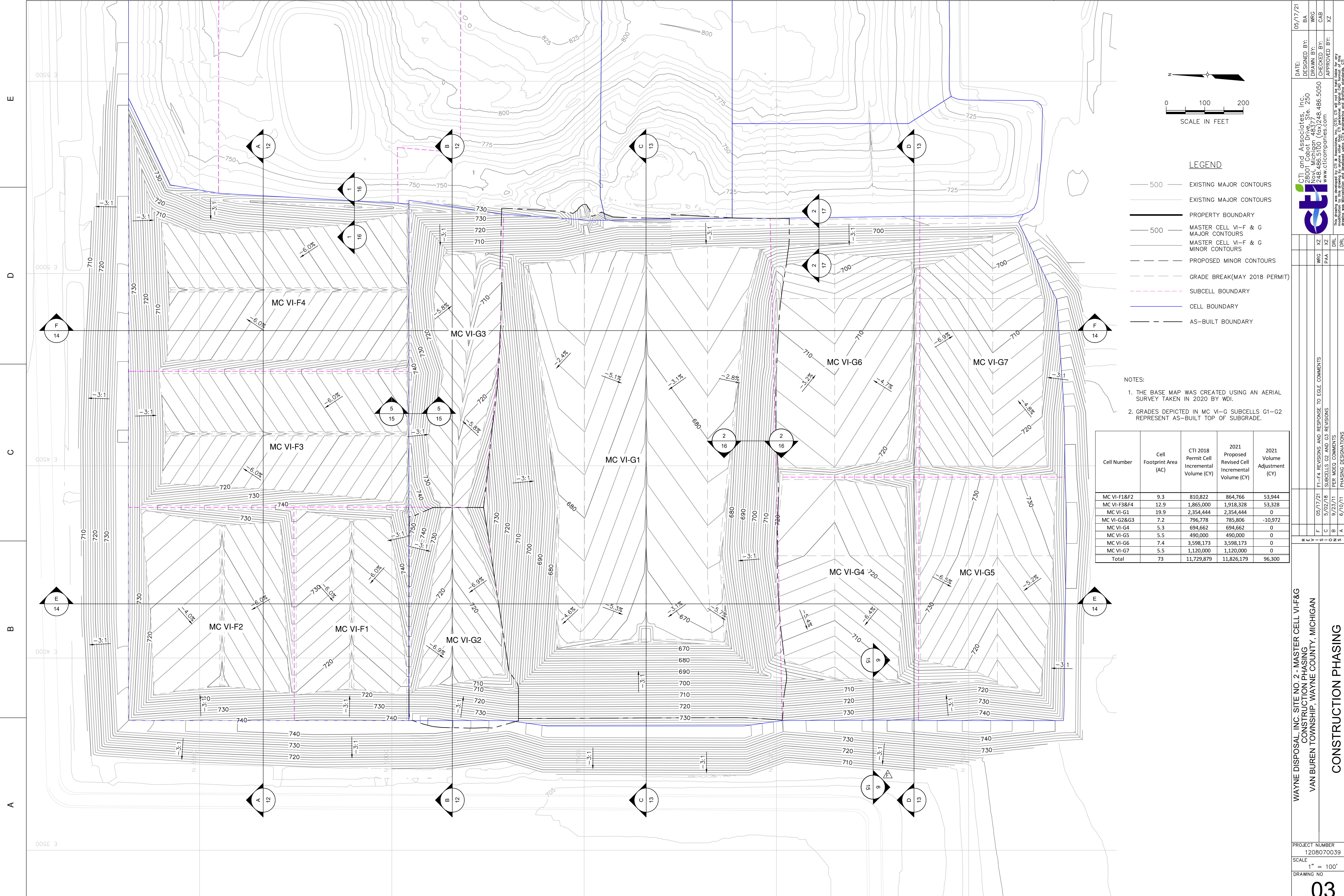
		DATE: 05/17/21 DESIGNED BY: BA DRAWN BY: WRG CHECKED BY: CAB APPROVED BY: XZ
CTI and Associates, Inc. 28001 Cabot Drive, Ste. 250 Novi, Michigan 48377 248.486.5100 (fax) 248.486.5050 www.cticompanies.com		The sheets were prepared by CTI and Associates, Inc. (CAI) and are intended for use only in the project for which they were prepared. No other use or reproduction of these sheets without the written consent of CAI is permitted. CAI does not warrant the accuracy of the information contained herein and does not assume any liability for errors or omissions.
PROJECT NUMBER 1208070039	SCALE NONE	DRAWING NO 01
WAYNE DISPOSAL, INC. SITE NO. 2 - MASTER CELL VI-F&G TITLE SHEET VAN BUREN TOWNSHIP, WAYNE COUNTY, MICHIGAN		
TITLE SHEET		



- LEGEND**
- 500 — EXISTING MAJOR CONTOURS
 - — — EXISTING MINOR CONTOURS
 - - - - PREVIOUSLY PERMITTED HAZARDOUS WASTE BOUNDARY
 - — — PROPERTY BOUNDARY
 - - - - SUBCELL BOUNDARY
 - — — CELL BOUNDARY
 - — — CELL BOUNDARY (CLOSED)

NOTES:
1. THE BASE MAP WAS CREATED USING AN AERIAL SURVEY TAKEN IN DECEMBER, 2020 BY WDI.

WAYNE DISPOSAL, INC. SITE NO. 2 - MASTER CELL VI-F&G GENERAL SITE PLAN VAN BUREN TOWNSHIP, WAYNE COUNTY, MICHIGAN			DATE: 05/17/21 DESIGNED BY: BA DRAWN BY: WRC CHECKED BY: CAB APPROVED BY: XZ
PROJECT NUMBER: 1208070039 SCALE: 1" = 300' DRAWING NO: 02			C.T.I. and Associates, Inc. 2800 Chubbuck Ave., 230 Novi, Michigan 48377 248.486.5100 (fax) 248.486.5050 www.cticompanies.com
REVISION DESCRIPTION F 05/17/21 F1-F4 REVISIONS AND RESPONSE TO EGLE COMMENTS		This drawing was developed by C.T.I. & Associates, Inc. (CTI). CTI will not be held liable for any modification to this drawing by anyone other than CTI personnel. Original CAD format of this drawing, including all files, shall be maintained in the project folder.	REV DATE F 05/17/21



LEGEND

- 500 — EXISTING MAJOR CONTOURS
- 500 — EXISTING MAJOR CONTOURS
- 500 — MASTER CELL VI-F & G MAJOR CONTOURS
- 500 — MASTER CELL VI-F & G MINOR CONTOURS
- PROPOSED MINOR CONTOURS
- - - GRADE BREAK(MAY 2018 PERMIT)
- - - SUBCELL BOUNDARY
- CELL BOUNDARY
- - - AS-BUILT BOUNDARY

- NOTES:**
1. THE BASE MAP WAS CREATED USING AN AERIAL SURVEY TAKEN IN 2020 BY WDI.
 2. GRADES DEPICTED IN MC VI-G SUBCELLS G1-G2 REPRESENT AS-BUILT TOP OF SUBGRADE.

Cell Number	Cell Footprint Area (AC)	CTI 2018 Permit Cell Incremental Volume (CY)	2021 Proposed Revised Cell Incremental Volume (CY)	2021 Volume Adjustment (CY)
MC VI-F1&F2	9.3	810,822	864,766	53,944
MC VI-F3&F4	12.9	1,865,000	1,918,328	53,328
MC VI-G1	19.9	2,354,444	2,354,444	0
MC VI-G2&G3	7.2	796,778	785,806	-10,972
MC VI-G4	5.3	694,662	694,662	0
MC VI-G5	5.5	490,000	490,000	0
MC VI-G6	7.4	3,598,173	3,598,173	0
MC VI-G7	5.5	1,120,000	1,120,000	0
Total	73	11,729,879	11,826,179	96,300

DATE: 05/17/21
DESIGNED BY: BA
DRAWN BY: WRG
CHECKED BY: CAB
APPROVED BY: XZ

CTI and Associates, Inc.
7200 N. 28th St., Ste. 250
Farmington Hills, MI 48334
248.486.5100 (fax) 248.486.5050
www.cticompanies.com

This drawing was prepared by CTI & Associates, Inc. (CTI) and shall be used only for the project and location specifically identified on the drawing. Any other use of this drawing without the written consent of CTI is prohibited. Original data format of any information used in this drawing shall be maintained and made available to the client upon request. CTI does not warrant the accuracy or completeness of the information provided and does not assume any liability for errors or omissions. The user of this drawing shall be responsible for verifying the accuracy and completeness of the information provided and for obtaining any necessary permits or approvals from the appropriate authorities.

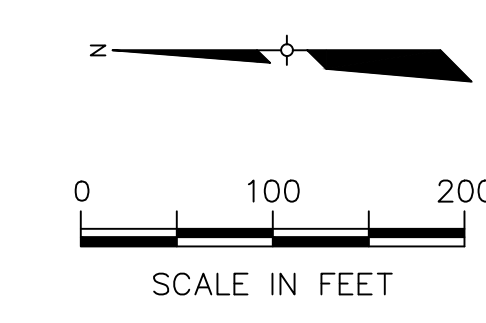
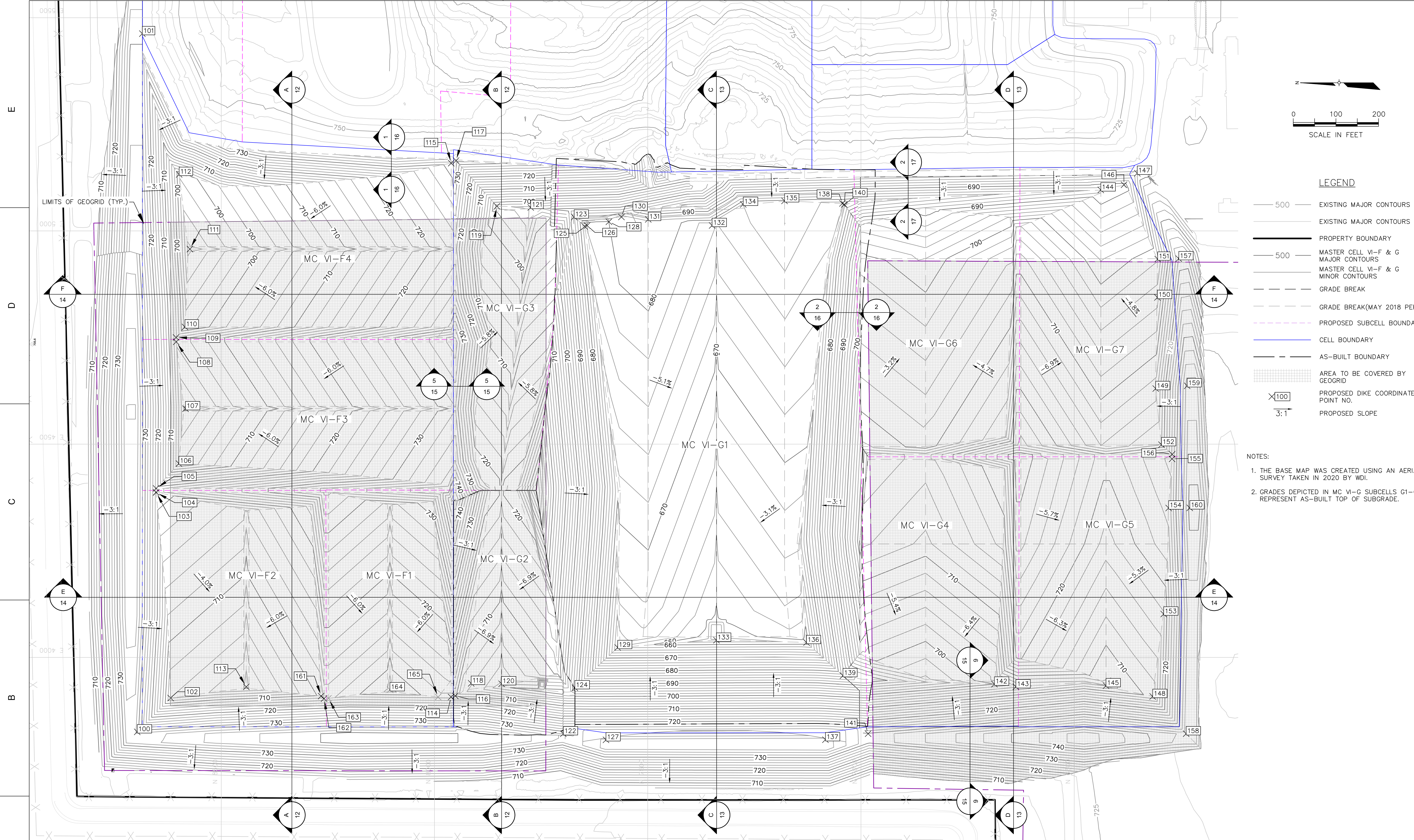
PROJECT NUMBER: 1208070039
SCALE: 1" = 100'
DRAWING NO: 03

REVISIONS AND RESPONSE TO EGLE COMMENTS

REV	DATE	REVISION DESCRIPTION
1	05/17/21	F1-F4 REVISIONS AND RESPONSE TO EGLE COMMENTS
2	05/20/21	SUBCELLS G2 AND G3 REVISIONS
3	5/23/21	PER WDC COMMENTS
4	6/10/21	PHASING DESIGNATIONS

WAYNE DISPOSAL, INC. SITE NO. 2 - MASTER CELL VI-F&G
CONSTRUCTION PHASING
VAN BUREN TOWNSHIP, WAYNE COUNTY, MICHIGAN

CONSTRUCTION PHASING



- LEGEND**
- 500 — EXISTING MAJOR CONTOURS
 - 500 — EXISTING MAJOR CONTOURS
 - — PROPERTY BOUNDARY
 - 500 — MASTER CELL VI-F & G MAJOR CONTOURS
 - — MASTER CELL VI-F & G MINOR CONTOURS
 - - - GRADE BREAK
 - - - GRADE BREAK(MAY 2018 PERMIT)
 - - - PROPOSED SUBCELL BOUNDARY
 - — CELL BOUNDARY
 - - - AS-BUILT BOUNDARY
 - ▨ AREA TO BE COVERED BY GEOGRID
 - ⊗100 PROPOSED DIKE COORDINATE POINT NO.
 - 3:1 PROPOSED SLOPE

- NOTES:**
- THE BASE MAP WAS CREATED USING AN AERIAL SURVEY TAKEN IN 2020 BY WDI.
 - GRADES DEPICTED IN MC VI-G SUBCELLS G1-G2 REPRESENT AS-BUILT TOP OF SUBGRADE.

DATE: 05/17/21
DESIGNED BY: BA
DRAWN BY: WRG
CHECKED BY: CAB
APPROVED BY: XZ

CTI and Associates, Inc.
2800 N. Lapeer Ave., Ste. 250
Farmington Hills, MI 48334
248.466.5100 (fax) 248.466.5050
www.cticompanies.com

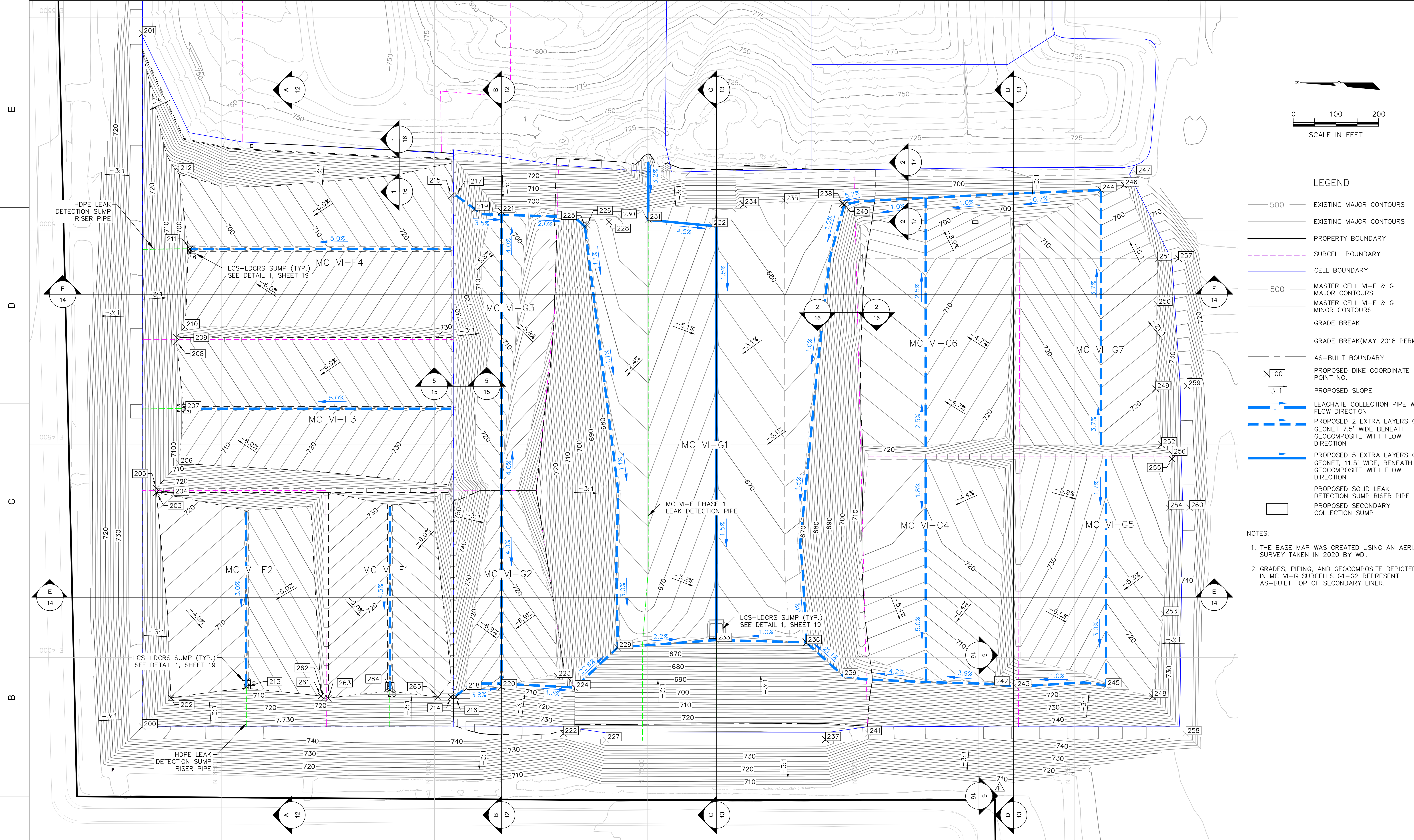
PROJECT NUMBER: 1208070039
SCALE: 1" = 100'
DRAWING NO: 04

WAYNE DISPOSAL, INC. SITE NO. 2 - MASTER CELL VI-F&G
TOP SUBGRADE LAYER
VAN BUREN TOWNSHIP, WAYNE COUNTY, MICHIGAN
TOP OF SUBGRADE GRADING PLAN

REV	DATE	REVISION DESCRIPTION
F	05/17/21	FI-F4 REVISIONS AND RESPONSE TO EGLE COMMENTS
E	9/23/11	PER MDCO COMMENTS
B	6/10/11	PHASING DESIGNATIONS

DRN	APP	REVISION DESCRIPTION
WRG	XZ	
DRL		

SUBGRADE PERIMETER DIKE COORDINATES				SUBGRADE PERIMETER DIKE COORDINATES				SUBGRADE PERIMETER DIKE COORDINATES				SUBGRADE PERIMETER DIKE COORDINATES				SUBGRADE PERIMETER DIKE COORDINATES				SUBGRADE PERIMETER DIKE COORDINATES				SUBGRADE PERIMETER DIKE COORDINATES				SUBGRADE PERIMETER DIKE COORDINATES							
Point #	Northing	Easting	Elevation (ft)	Point #	Northing	Easting	Elevation (ft)	Point #	Northing	Easting	Elevation (ft)	Point #	Northing	Easting	Elevation (ft)	Point #	Northing	Easting	Elevation (ft)	Point #	Northing	Easting	Elevation (ft)	Point #	Northing	Easting	Elevation (ft)	Point #	Northing	Easting	Elevation (ft)	Point #	Northing	Easting	Elevation (ft)
100	8696.95	3825.42	730.00	109	8605.88	4750.21	704.32	118	7913.92	3939.16	700.65	127	7597.89	3806.80	735.60	136	7127.70	4034.87	660.23	145	6425.37	3933.71	704.74	154	6278.55	4350.36	723.66	162	8258.95	3903.52	712.50				
101	8685.01	5462.64	720.71	110	8585.05	4774.98	697.17	119	7853.52	5057.82	0.00	128	7591.06	5021.51	682.01	137	7083.24	3807.01	736.24	146	6383.17	5108.23	687.81	155	6270.50	4465.41	725.70	162	8258.95	3903.52	712.50				
102	8618.63	3904.74	705.98	111	8573.54	4957.47	690.49	120	7842.73	3938.19	697.92	129	7570.41	4023.20	663.24	138	7043.49	5064.48	678.89	147	6352.10	5135.27	696.41	156	6270.26	4476.27	725.42	163	8248.62	3904.19	712.53				
103	8652.59	4386.81	721.34	112	8598.69	5132.62	698.35	121	7774.33	5054.99	702.31	130	7561.67	5032.75	683.13	139	7042.16	3957.20	684.60	148	6316.02	3908.50	709.72	157	6254.80	4935.00	717.24	164	8104.44	3924.15	706.44				
104	8652.83	4387.08	721.42	113	8441.35	3930.96	700.80	122	7697.89	3821.03	730.74	131	7498.71	5027.05	685.09	140	7039.03	5062.00	677.47	149	6308.86	4630.41	711.90	158	6237.41	3821.03	736.23	165	7991.56	3907.10	711.41				
105	8652.78	4396.24	721.42	114	7961.13	3907.15	711.29	123	7672.54	5032.68	686.26	132	7349.00	5012.85	678.14	141	6983.25	3821.03	729.35	150	6304.89	4844.00	704.12	159	6235.06	4636.89	736.17								
106	8599.35	4454.59	703.72	115	7960.81	5158.83	731.11	124	7670.81	3928.84	694.50	133	7338.74	4040.41	658.10	142	6687.01	3937.42	698.98	151	6304.21	4934.01	700.81	160	6228.94	4350.65	739.90								
107	8583.77	4583.16	699.09	116	7951.05	3909.68	709.54	125	7647.66	5010.45	678.68	134	7276.06	5062.38	679.69	143	6636.63	3931.13	702.62	152	6295.30	4498.77	717.18	161	8265.78	3909.28	710.49								
108	8605.58	4739.88	704.33	117	7949.45	5164.97	0.00	126	7641.99	5012.71	680.19	135	7179.18	5070.45	681.75	144	6437.61	5096.19	685.31	153	6290.14	4101.64	716.79	161	8265.78	3909.28	710.49								



LEGEND

- 500 — EXISTING MAJOR CONTOURS
- 500 — EXISTING MAJOR CONTOURS
- — PROPERTY BOUNDARY
- — SUBCELL BOUNDARY
- — CELL BOUNDARY
- 500 — MASTER CELL VI-F & G MAJOR CONTOURS
- — MASTER CELL VI-F & G MINOR CONTOURS
- - - GRADE BREAK
- - - GRADE BREAK (MAY 2018 PERMIT)
- - - AS-BUILT BOUNDARY
- X100 PROPOSED DIKE COORDINATE POINT NO.
- 3:1 PROPOSED SLOPE
- — LEACHATE COLLECTION PIPE WITH FLOW DIRECTION
- — PROPOSED 2 EXTRA LAYERS OF GEONET, 7.5' WIDE BENEATH GEOCOMPOSITE WITH FLOW DIRECTION
- — PROPOSED 5 EXTRA LAYERS OF GEONET, 11.5' WIDE, BENEATH GEOCOMPOSITE WITH FLOW DIRECTION
- — PROPOSED SOLID LEAK DETECTION SUMP RISER PIPE
- PROPOSED SECONDARY COLLECTION SUMP

NOTES:

- THE BASE MAP WAS CREATED USING AN AERIAL SURVEY TAKEN IN 2020 BY WDI.
- GRADES, PIPING, AND GEOCOMPOSITE DEPICTED IN MC VI-G SUBCELLS G1-G2 REPRESENT AS-BUILT TOP OF SECONDARY LINER.

DATE: 05/17/21
 DESIGNED BY: BA
 DRAWN BY: WRG
 CHECKED BY: CAB
 APPROVED BY: XZ

CTI and Associates, Inc.
 2800 McArthur Blvd., Ste. 250
 Farmington Hills, MI 48334
 248.486.5100 (fax) 248.486.5050
 www.cticompanies.com

The drawings were prepared by CTI & Associates, Inc. (CTI) and are the property of CTI. No part of these drawings may be reproduced, stored in a retrieval system, or transmitted in any form or by any means, electronic, mechanical, photocopying, recording, or by any information storage and retrieval system, without the prior written permission of CTI.

REV	DATE	REVISION DESCRIPTION
1	05/17/21	F1-F4 REVISIONS AND RESPONSE TO EGLE COMMENTS
2	05/02/18	SUBCELLS G2 AND G3 REVISIONS
3	9/23/11	PER WDC COMMENTS
4	6/10/11	PHASING DESIGNATIONS

SECONDARY DIKE COORDINATE POINTS

Point #	Northing	Easting	Elevation
200	8685.01	3837.32	728.96
201	8685.01	5462.64	722.82
202	8618.14	3905.24	707.94
203	8652.04	4386.21	723.27
204	8652.53	4386.75	723.43
205	8652.48	4396.57	723.43
206	8599.03	4454.94	705.72
207	8583.37	4583.16	701.11
208	8605.29	4739.88	706.35

SECONDARY DIKE COORDINATE POINTS

Point #	Northing	Easting	Elevation
209	8605.60	4750.54	706.33
210	8584.93	4775.12	699.17
211	8573.40	4957.47	692.57
212	8599.30	5141.46	698.57
213	8441.11	3930.91	702.92
214	7961.13	3907.36	713.33
215	7960.81	5082.91	709.33
216	7949.91	3907.03	713.51
217	7949.59	5083.40	709.66

SECONDARY DIKE COORDINATE POINTS

Point #	Northing	Easting	Elevation
218	7924.24	3927.69	706.53
219	7904.34	5051.40	697.89
220	7842.87	3931.37	703.56
221	7842.87	5045.71	695.60
222	7697.85	3821.52	733.74
223	7712.50	3955.68	716.00
224	7670.78	3929.03	697.65
225	7647.54	5010.47	681.80
226	7641.99	5012.71	683.24

SECONDARY DIKE COORDINATE POINTS

Point #	Northing	Easting	Elevation
227	7597.85	3807.29	738.60
228	7591.06	5021.51	685.01
229	7570.29	4023.33	666.36
230	7561.67	5032.75	686.20
231	7498.71	5027.05	688.09
232	7349.00	5012.85	681.14
233	7338.74	4040.54	661.22
234	7275.80	5061.92	682.69
235	7179.18	5070.45	684.75

SECONDARY DIKE COORDINATE POINTS

Point #	Northing	Easting	Elevation
236	7127.83	4034.99	663.35
237	7083.28	3807.50	739.24
238	7043.49	5064.48	681.99
239	7042.34	3957.36	687.71
240	7039.01	5061.89	680.59
241	6983.28	3821.52	732.35
242	6686.99	3937.74	702.15
243	6636.62	3931.46	705.79
244	6437.59	5096.06	688.43

SECONDARY DIKE COORDINATE POINTS

Point #	Northing	Easting	Elevation
245	6425.35	3933.83	707.86
246	6383.34	5107.71	690.84
247	6353.82	5135.70	699.60
248	6316.02	3908.50	712.72
249	6308.86	4630.41	714.90
250	6305.63	4827.81	707.70
251	6304.21	4934.01	703.81
252	6295.30	4498.77	720.18
253	6290.14	4101.64	719.79

SECONDARY DIKE COORDINATE POINTS

Point #	Northing	Easting	Elevation
254	6278.55	4350.36	726.66
255	6270.50	4465.41	728.70
256	6270.26	4476.27	728.59
257	6255.28	4934.88	720.24
258	6237.90	3821.52	739.23
259	6235.55	4636.87	739.17
260	6229.43	4350.65	742.90
261	8266.19	3909.62	712.48
261	8266.19	3909.62	712.48

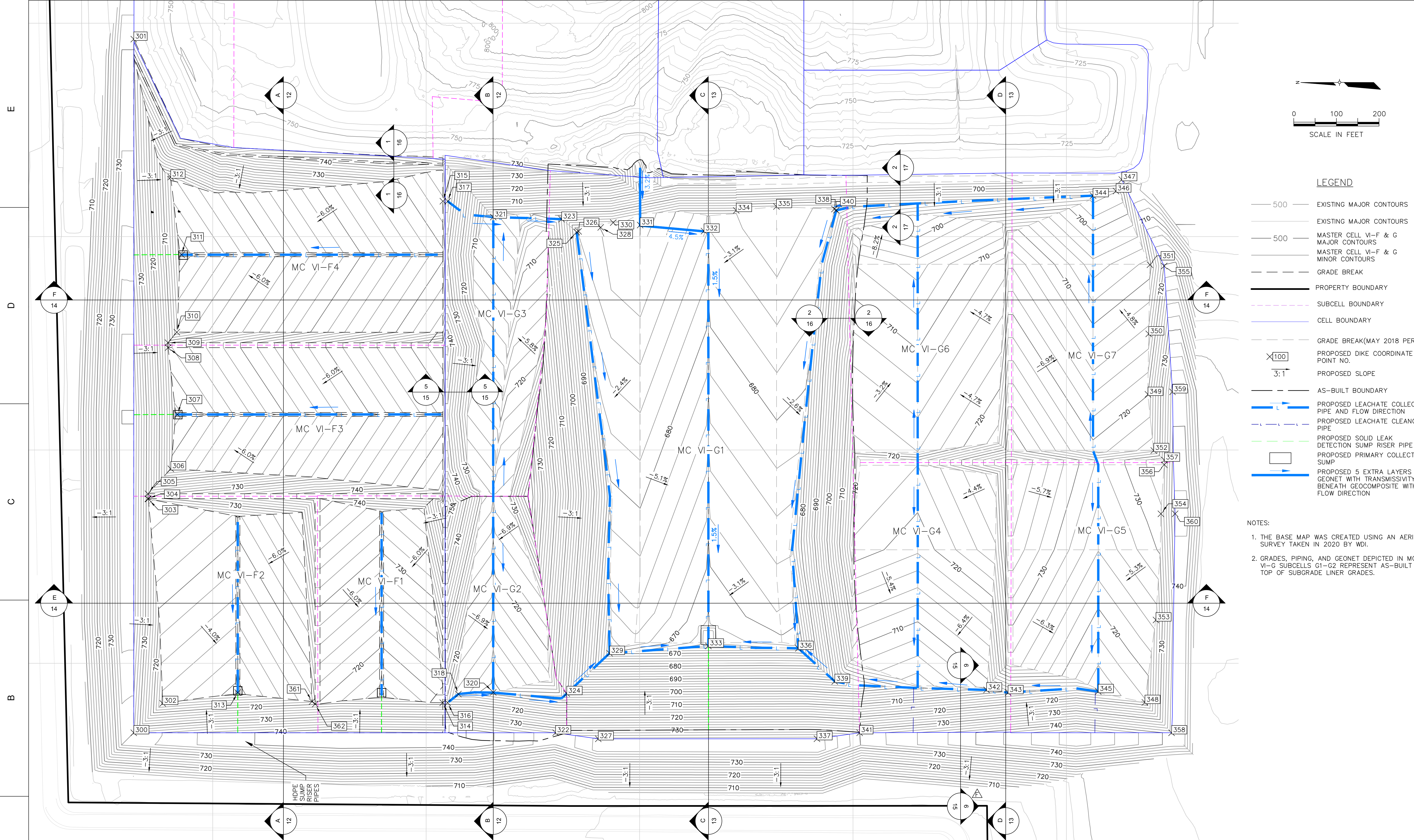
SECONDARY DIKE COORDINATE POINTS

Point #	Northing	Easting	Elevation
262	8259.28	3903.79	714.52
262	8259.28	3903.79	714.52
263	8248.62	3904.19	714.53
264	8104.44	3924.29	708.51
265	7991.35	3907.36	713.43

PROJECT NUMBER: 1208070039
 SCALE: 1" = 100'
 DRAWING NO: 05

WAYNE DISPOSAL, INC. SITE NO. 2 - MASTER CELL VI-F&G
 TOP OF SECONDARY LINER
 VAN BUREN TOWNSHIP, WAYNE COUNTY, MICHIGAN

TOP OF SECONDARY LINER GRADING PLAN



LEGEND

- 500 — EXISTING MAJOR CONTOURS
- 500 — EXISTING MAJOR CONTOURS
- 500 — MASTER CELL VI-F & G MAJOR CONTOURS
- 500 — MASTER CELL VI-F & G MINOR CONTOURS
- - - GRADE BREAK
- — — GRADE BREAK(MAY 2018 PERMIT)
- — — PROPERTY BOUNDARY
- - - SUBCELL BOUNDARY
- — — CELL BOUNDARY
- - - GRADE BREAK
- ⊗100 PROPOSED DIKE COORDINATE POINT NO.
- 3:1 PROPOSED SLOPE
- — — AS-BUILT BOUNDARY
- — — PROPOSED LEACHATE COLLECTION PIPE AND FLOW DIRECTION
- — — PROPOSED LEACHATE CLEANOUT PIPE
- — — PROPOSED SOLID LEAK DETECTION SUMP RISER PIPE
- — — PROPOSED PRIMARY COLLECTION SUMP
- — — PROPOSED 5 EXTRA LAYERS OF GEONET WITH TRANSMISSIVITY BENEATH GEOCOMPOSITE WITH FLOW DIRECTION

NOTES:

- THE BASE MAP WAS CREATED USING AN AERIAL SURVEY TAKEN IN 2020 BY WDI.
- GRADES, PIPING, AND GEONET DEPICTED IN MC VI-G SUBCELLS G1-G2 REPRESENT AS-BUILT TOP OF SUBGRADE LINER GRADES.

DATE: 05/17/21
 DESIGNED BY: BA
 DRAWN BY: WRC
 CHECKED BY: CAB
 APPROVED BY: XZ

CTI and Associates, Inc.
 2800 Cabot Drive, Ste. 250
 248.466.5100 (fax) 248.466.5050
 www.cticompanies.com

This drawing was prepared by CTI and Associates, Inc. (CTI) for the use of the client. It is the property of CTI and Associates, Inc. and shall not be used for any other project without the written consent of CTI. The client is responsible for the accuracy of the information provided to CTI. CTI does not warrant the accuracy or completeness of the information provided to CTI. The client is responsible for the accuracy of the information provided to CTI. The client is responsible for the accuracy of the information provided to CTI.

REV	DATE	PHASING DESIGNATIONS	REVISION DESCRIPTION
1	05/17/21	F1-F4 REVISIONS AND RESPONSE TO EGLE COMMENTS	
2	5/02/21	SUBCELLS G2 AND G3 REVISIONS	
3	9/23/21	PER WRC COMMENTS	
4	6/10/21		

PRIMARY DIKE COORDINATE POINTS

Point #	Northing	Easting	Elevation
300	8685.01	3837.32	734.39
301	8685.01	5462.64	728.25
302	8617.26	3906.14	713.09
303	8651.02	4385.09	728.36
304	8651.77	4385.91	728.60
305	8651.71	4397.41	728.61
306	8598.22	4455.83	710.88
307	8582.93	4583.16	706.44
308	8604.56	4739.88	711.53

PRIMARY DIKE COORDINATE POINTS

Point #	Northing	Easting	Elevation
309	8604.89	4751.38	711.52
310	8584.15	4776.05	704.33
311	8572.95	4957.47	697.90
312	8598.52	5139.51	703.64
313	8441.35	3931.41	708.19
314	7961.13	3907.79	718.62
315	7960.81	5082.91	714.76
316	7949.75	3907.70	718.61
317	7949.43	5082.91	714.76

PRIMARY DIKE COORDINATE POINTS

Point #	Northing	Easting	Elevation
318	7924.50	3928.02	711.75
319	7904.56	5051.05	703.11
320	7842.87	3931.97	708.82
321	7842.87	5045.77	700.84
322	7696.73	3837.32	733.74
323	7682.58	5040.91	697.50
324	7670.57	3929.29	702.88
325	7647.35	5010.49	687.00
326	7642.85	5012.25	688.18

PRIMARY DIKE COORDINATE POINTS

Point #	Northing	Easting	Elevation
327	7596.74	3823.09	738.60
328	7591.06	5021.51	690.24
329	7570.10	4023.55	671.56
330	7561.67	5032.75	691.59
331	7498.71	5027.05	693.52
332	7349.00	5012.85	686.42
333	7338.74	4040.74	666.42
334	7273.49	5061.28	687.73
335	7179.18	5070.45	689.94

PRIMARY DIKE COORDINATE POINTS

Point #	Northing	Easting	Elevation
336	7128.04	4035.19	668.55
337	7084.38	3823.30	739.24
338	7043.49	5064.48	687.10
339	7042.63	3957.62	692.90
340	7038.96	5061.69	685.79
341	6984.38	3837.32	732.35
342	6686.99	3937.74	0.00
343	6636.62	3931.46	0.00
344	6437.60	5095.87	693.63

PRIMARY DIKE COORDINATE POINTS

Point #	Northing	Easting	Elevation
345	6425.32	3934.02	713.06
346	6383.71	5106.68	695.89
347	6370.28	5133.49	704.60
348	6316.02	3908.50	717.88
349	6308.86	4630.41	720.03
350	6307.07	4772.00	714.72
351	6304.21	4934.01	709.18
352	6295.30	4498.77	725.35
353	6290.14	4101.68	724.99

PRIMARY DIKE COORDINATE POINTS

Point #	Northing	Easting	Elevation
354	6278.55	4350.36	731.79
355	6270.86	4931.07	720.24
356	6270.50	4465.41	733.79
357	6270.26	4476.27	733.80
358	6253.54	3837.32	739.23
359	6251.34	4636.24	739.17
360	6245.23	4350.52	742.90
361	8267.23	3910.50	717.60
361	8267.23	3910.50	717.60

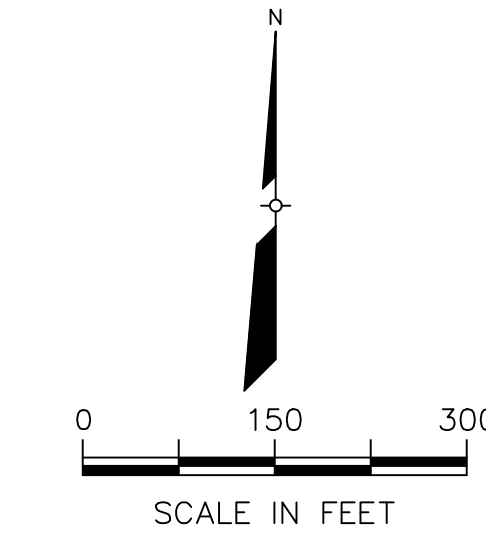
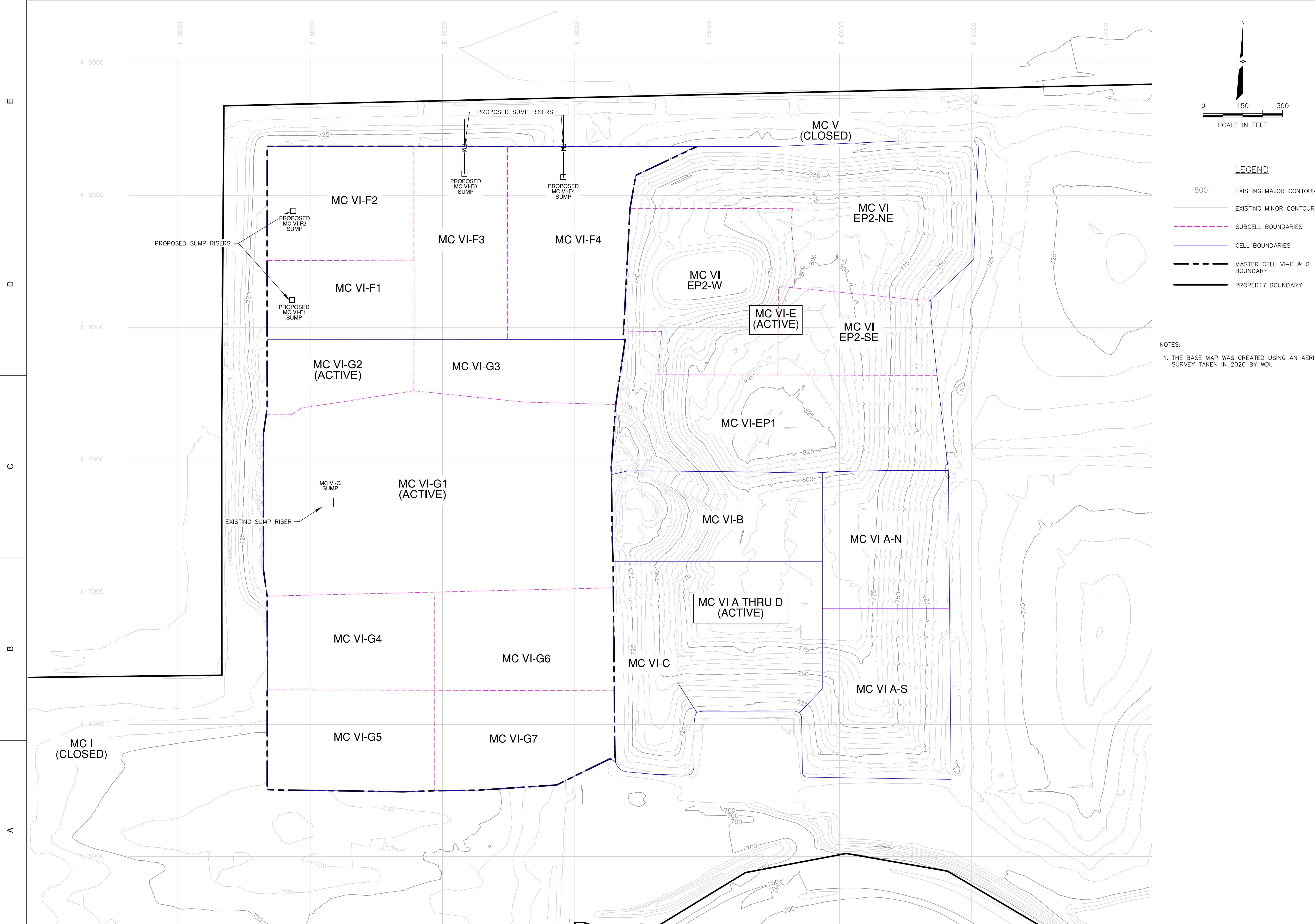
PRIMARY DIKE COORDINATE POINTS

Point #	Northing	Easting	Elevation
362	8260.12	3904.50	719.70
362	8260.12	3904.50	719.70
363	8248.62	3904.93	719.72
364	8104.44	3924.72	713.84
365	7990.81	3908.04	718.64

WAYNE DISPOSAL, INC. SITE NO. 2 - MASTER CELL VI-F&G
 TOP OF PRIMARY LINER
 VAN BUREN TOWNSHIP, WAYNE COUNTY, MICHIGAN

TOP OF PRIMARY LINER GRADING PLAN

PROJECT NUMBER: 1208070039
 SCALE: 1" = 100'
 DRAWING NO: 06

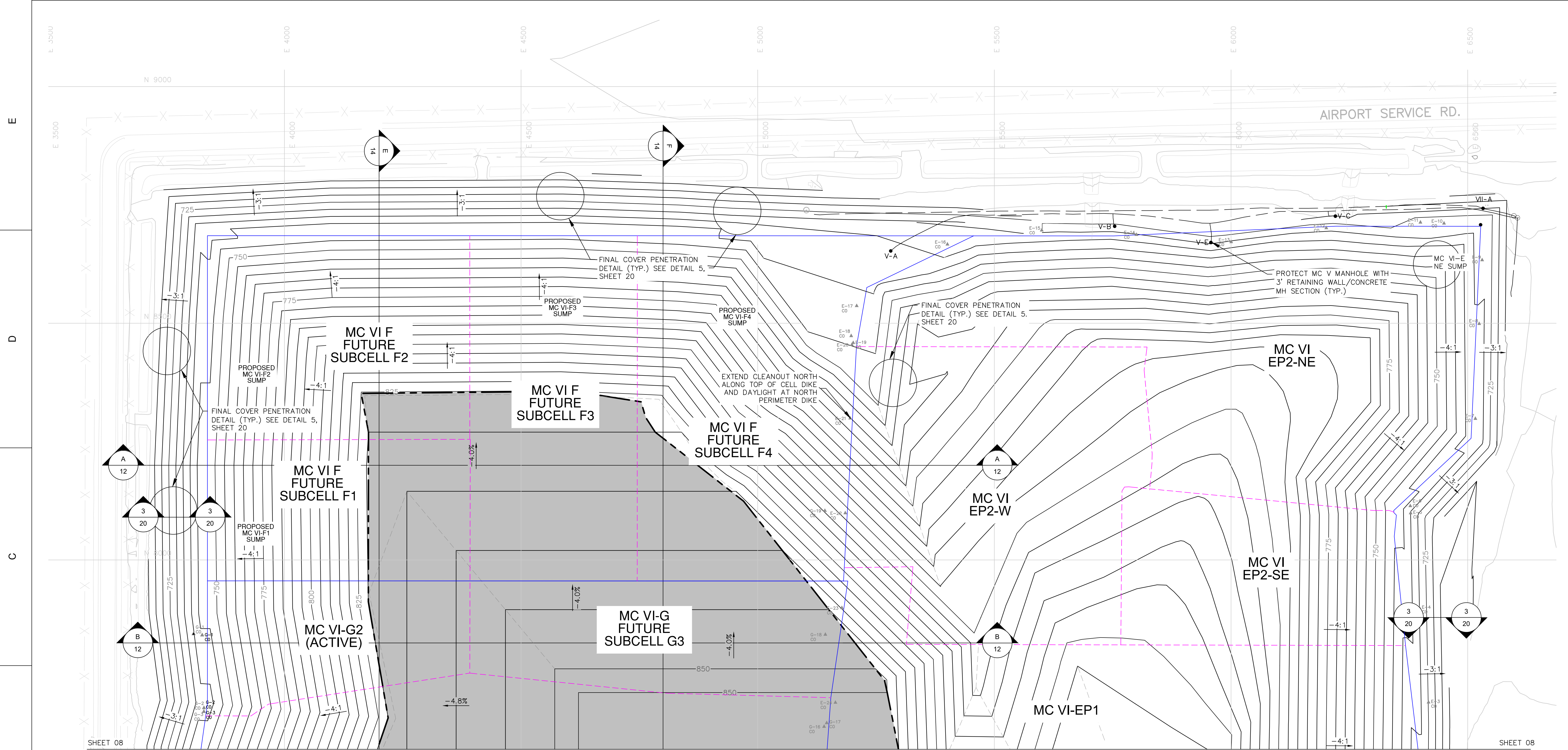


LEGEND

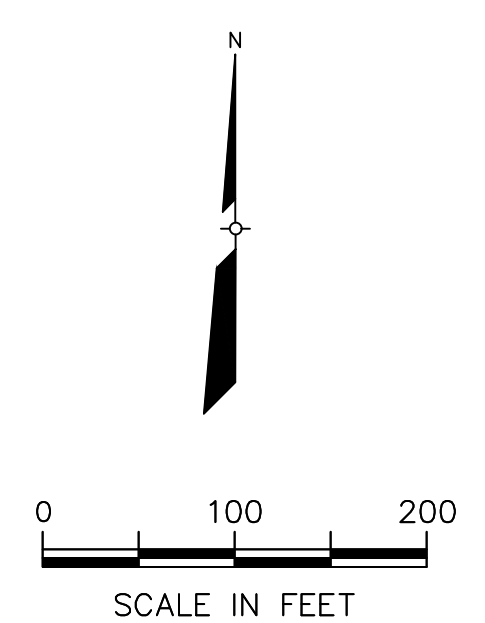
- 500 — EXISTING MAJOR CONTOURS
- — EXISTING MINOR CONTOURS
- - - - SUBCELL BOUNDARIES
- — CELL BOUNDARIES
- - - - MASTER CELL VI-F & G BOUNDARY
- — PROPERTY BOUNDARY

NOTES:
 1. THE BASE MAP WAS CREATED USING AN AERIAL SURVEY TAKEN IN 2020 BY WDI.

WAYNE DISPOSAL, INC. SITE NO. 2 - MASTER CELL VI-F&G LEACHATE MANAGEMENT PLAN VAN BUREN TOWNSHIP, WAYNE COUNTY, MICHIGAN		LEACHATE MANAGEMENT PLAN																									
PROJECT NUMBER 1208070039 SCALE 1" = 150' DRAWING NO <div style="font-size: 2em; font-weight: bold; text-align: right;">07</div>	<table border="1" style="width: 100%; border-collapse: collapse;"> <thead> <tr> <th>REV</th> <th>DATE</th> <th>PHASE/DESCRIPTION</th> <th>BY</th> <th>APP</th> </tr> </thead> <tbody> <tr> <td>F</td> <td>05/17/21</td> <td>FL-F4 REVISIONS AND RESPONSE TO EGLE COMMENTS</td> <td>WRG</td> <td>ZX</td> </tr> <tr> <td>A</td> <td>6/10/21</td> <td>PHASING DESIGNATIONS</td> <td>DRI</td> <td>APP</td> </tr> </tbody> </table>	REV	DATE	PHASE/DESCRIPTION	BY	APP	F	05/17/21	FL-F4 REVISIONS AND RESPONSE TO EGLE COMMENTS	WRG	ZX	A	6/10/21	PHASING DESIGNATIONS	DRI	APP	<table border="1" style="width: 100%; border-collapse: collapse;"> <tr> <td>DATE:</td> <td>05/17/21</td> </tr> <tr> <td>DESIGNED BY:</td> <td>BA</td> </tr> <tr> <td>DRAWN BY:</td> <td>WRG</td> </tr> <tr> <td>CHECKED BY:</td> <td>CAB</td> </tr> <tr> <td>APPROVED BY:</td> <td>XZ</td> </tr> </table> <p style="font-size: 0.8em;"> CTI and Associates, Inc. 2800 Cabot Drive, Ste. 250 Van Buren Township, Wayne County, Michigan 48156 (248) 486-5100 (Fax) 248-486-5050 www.cticompanies.com </p> <p style="font-size: 0.6em;"> This drawing was prepared by C.T.I. Associates, Inc. (CTI) and is the property of C.T.I. Associates, Inc. It is to be used only for the project and location specified. No part of this drawing may be reproduced or transmitted in any form or by any means, electronic, mechanical, photocopying, recording, or by any information storage and retrieval system, without the prior written permission of C.T.I. Associates, Inc. </p>	DATE:	05/17/21	DESIGNED BY:	BA	DRAWN BY:	WRG	CHECKED BY:	CAB	APPROVED BY:	XZ
REV	DATE	PHASE/DESCRIPTION	BY	APP																							
F	05/17/21	FL-F4 REVISIONS AND RESPONSE TO EGLE COMMENTS	WRG	ZX																							
A	6/10/21	PHASING DESIGNATIONS	DRI	APP																							
DATE:	05/17/21																										
DESIGNED BY:	BA																										
DRAWN BY:	WRG																										
CHECKED BY:	CAB																										
APPROVED BY:	XZ																										



LEGEND



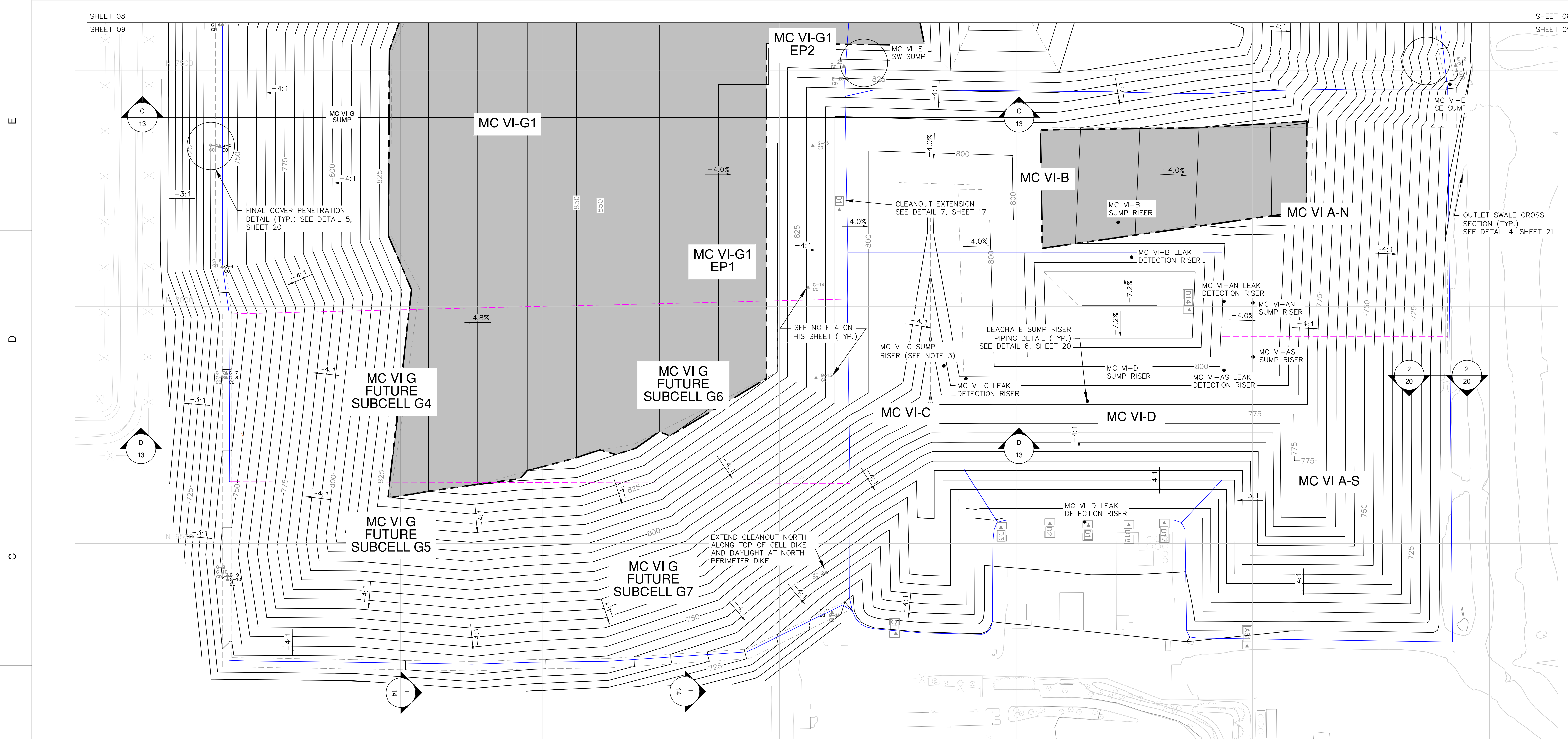
- 500 — EXISTING MAJOR CONTOURS
- — — EXISTING MINOR CONTOURS
- 500 — PERMITTED TOP OF FINAL COVER MAJOR CONTOURS
- — — PERMITTED TOP OF FINAL COVER MINOR CONTOURS
- - - - - EXISTING GRADE BREAKLINES
- - - - - EXISTING LEACHATE FORCEMAIN
- - - - - SUBCELL BOUNDARY
- — — CELL BOUNDARY
- — — PROPOSED GEOCOMPOSITE (TRANSMISSIVITY 5.0 X 10⁻⁴ M²/S)
- LEACHATE COLLECTION SYSTEM CLEANOUTS
- PROPOSED SUMP LOCATION AND COVER PENETRATION

- NOTES:**
1. THE BASE MAP WAS CREATED USING AN AERIAL SURVEY TAKEN IN 2020 BY WDI.
 2. INSTALL GAS MANAGEMENT SYSTEM IN ACCORDANCE WITH THE APPROVED CLOSURE PLAN.

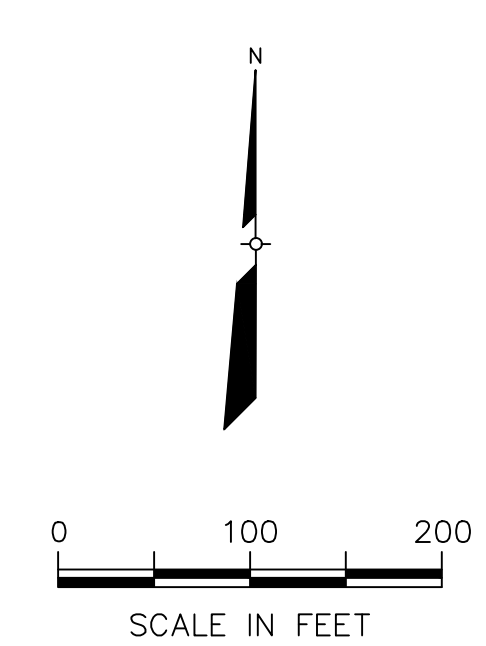
SHEET 08
SHEET 09

SHEET 08
SHEET 09

		DATE: 05/17/21 DESIGNED BY: BA DRAWN BY: WRG CHECKED BY: CAB APPROVED BY: XZ
CTI and Associates, Inc. 2800 Cabot Drive, Ste. 250 Farmington Hills, MI 48334 248.486.5100 (Tel) / 248.486.5050 (Fax) www.cticompanies.com		This drawing was prepared by CTI and Associates, Inc. (CTI) and is the property of CTI. It is to be used only for the project and site for which it was prepared. No part of this drawing may be reproduced or transmitted in any form or by any means, electronic or mechanical, including photocopying, recording, or by any information storage and retrieval system, without the prior written permission of CTI.
PROJECT NUMBER 1208070039	SCALE 1" = 100'	DRAWING NO 08
WAYNE DISPOSAL, INC. SITE NO. 2 - MASTER CELL VI-F&G FINAL COVER GRADING PLAN (1 OF 2) VAN BUREN TOWNSHIP, WAYNE COUNTY, MICHIGAN FINAL COVER GRADING PLAN (1 OF 2)		
REV F C 0 1 2 3	DATE 05/17/21 5/02/18	REVISION DESCRIPTION F1-F4 REVISIONS AND RESPONSE TO EGLE COMMENTS SUBCELLS G2 AND G3 REVISIONS



E
D
C
B
A



- LEGEND**
- 500 — EXISTING MAJOR CONTOURS
 - — — EXISTING MINOR CONTOURS
 - 500 — PERMITTED TOP OF FINAL COVER MAJOR CONTOURS
 - — — PERMITTED TOP OF FINAL COVER MINOR CONTOURS
 - ~~~~~ EXISTING VEGETATION
 - - - - - EXISTING GRADE BREAKLINES
 - — — EXISTING LEACHATE FORCEMAIN
 - - - - - SUBCELL BOUNDARY
 - — — CELL BOUNDARY
 - PROPOSED GEOCOMPOSITE (TRANSMISSIVITY 5.0 X 10⁻⁴ M²/S)
 - LEACHATE COLLECTION SYSTEM CLEANOUTS
 - PROPOSED SUMP LOCATION AND COVER PENETRATION

- NOTES:**
1. THE BASE MAP WAS CREATED USING AN AERIAL SURVEY TAKEN IN 2020 BY WDI.
 2. INSTALL GAS MANAGEMENT SYSTEM IN ACCORDANCE WITH THE APPROVED CLOSURE PLAN.
 3. CLEANOUTS IN MC VI-AN, AS, B, C, AND D ARE TO BE ABANDONED EXCEPT B1, C1, D1 THROUGH D3, D14, D17, D18, AND AS1.
 4. BEFORE PLACING WASTE AROUND MC VI-C SUMP RISER, A MONITORING PROGRAM SHOULD BE IMPLEMENTED TO MONITOR ITS FUNCTIONALITY.
 5. PRIOR TO PLACING WASTE AROUND CLEANOUTS E-22 THROUGH E-26 AND CLEANOUTS G-13 THROUGH G-19, THE CLEANOUTS SHOULD BE EVALUATED TO DETERMINE IF THE LEACHATE COLLECTION LINE CAN BE CLEANED BY A SINGLE ACCESS POINT. IF NOT, THE CLEANOUT SHOULD BE EXTENDED IN ACCORDANCE WITH DETAIL 7 ON SHEET 22 OR ALONG INTERIOR DIKE TO PERIMETER DIKE.

CTI

CTI and Associates, Inc.
2800 Cabot Drive, Ste. 250
Wayne, Michigan 48091
Tel: (313) 486-5100 Fax: (313) 486-5050
www.cticompanies.com

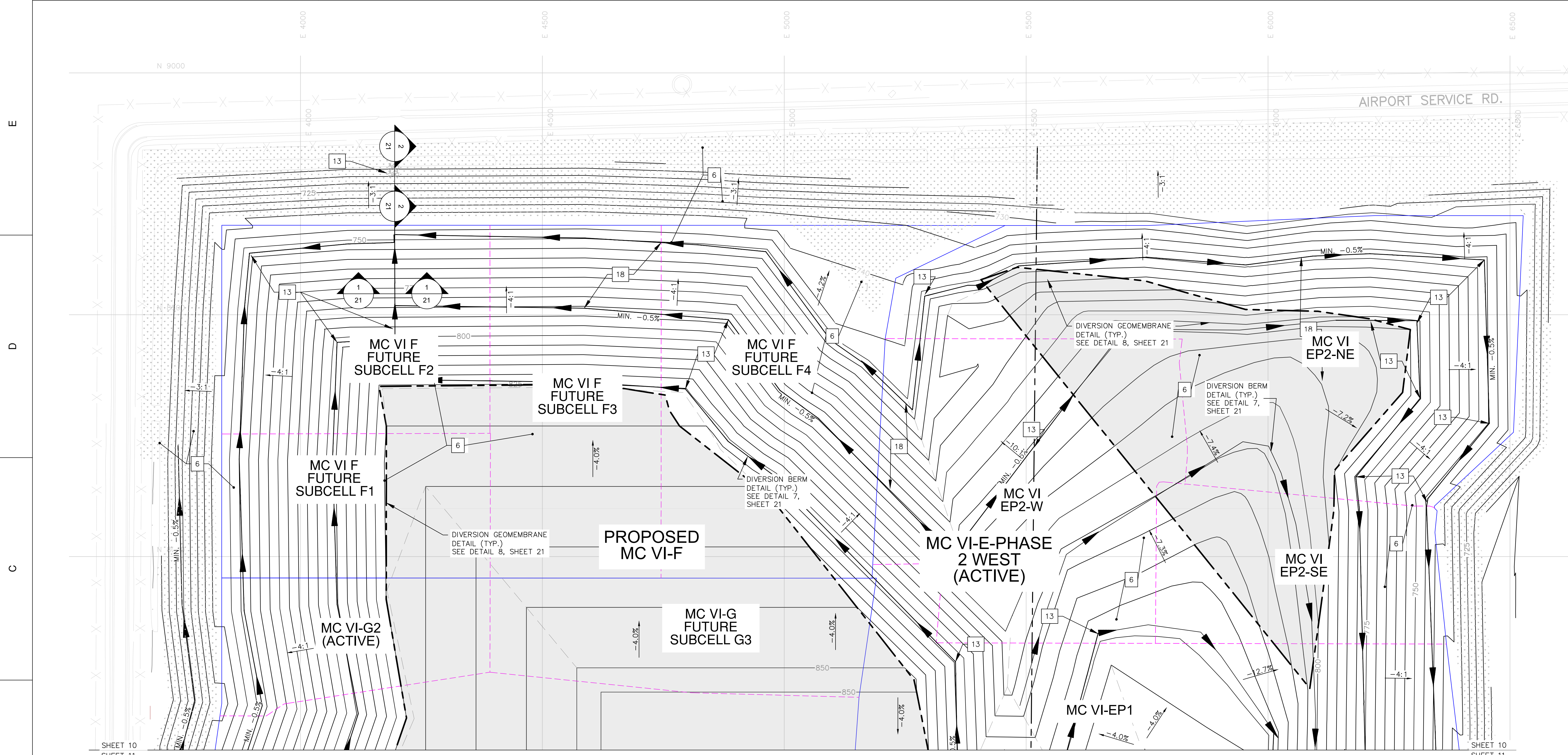
DATE: 05/17/21
DESIGNED BY: BA
DRAWN BY: WFG
CHECKED BY: CAB
APPROVED BY: XZ

PROJECT NUMBER: 1208070039
SCALE: 1" = 100'
DRAWING NO: 09

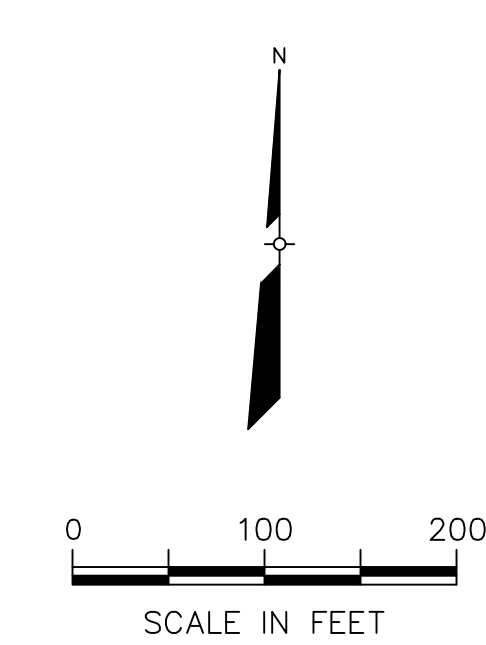
**WAYNE DISPOSAL, INC. SITE NO. 2 - MASTER CELL VI-F&G
FINAL COVER GRADING PLAN (2 OF 2)
VAN BUREN TOWNSHIP, WAYNE COUNTY, MICHIGAN**

FINAL COVER GRADING PLAN (2 OF 2)

REV	DATE	REVISION DESCRIPTION
F	05/17/21	F1-F4 REVISIONS AND RESPONSE TO EGLE COMMENTS
C	5/02/18	SUBCELLS G2 AND G3 REVISIONS

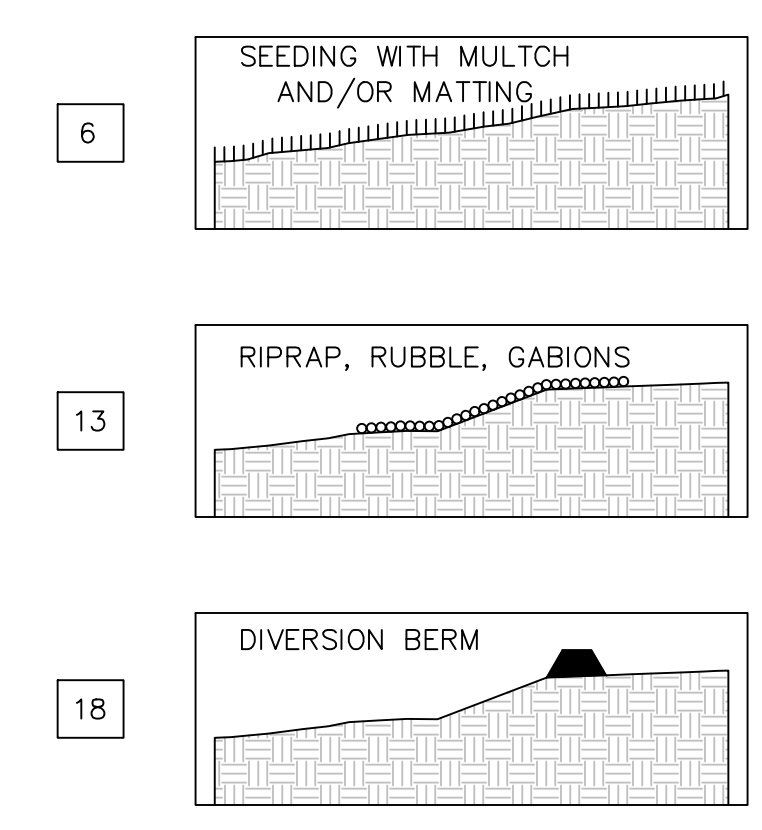


A
B
C
D
E



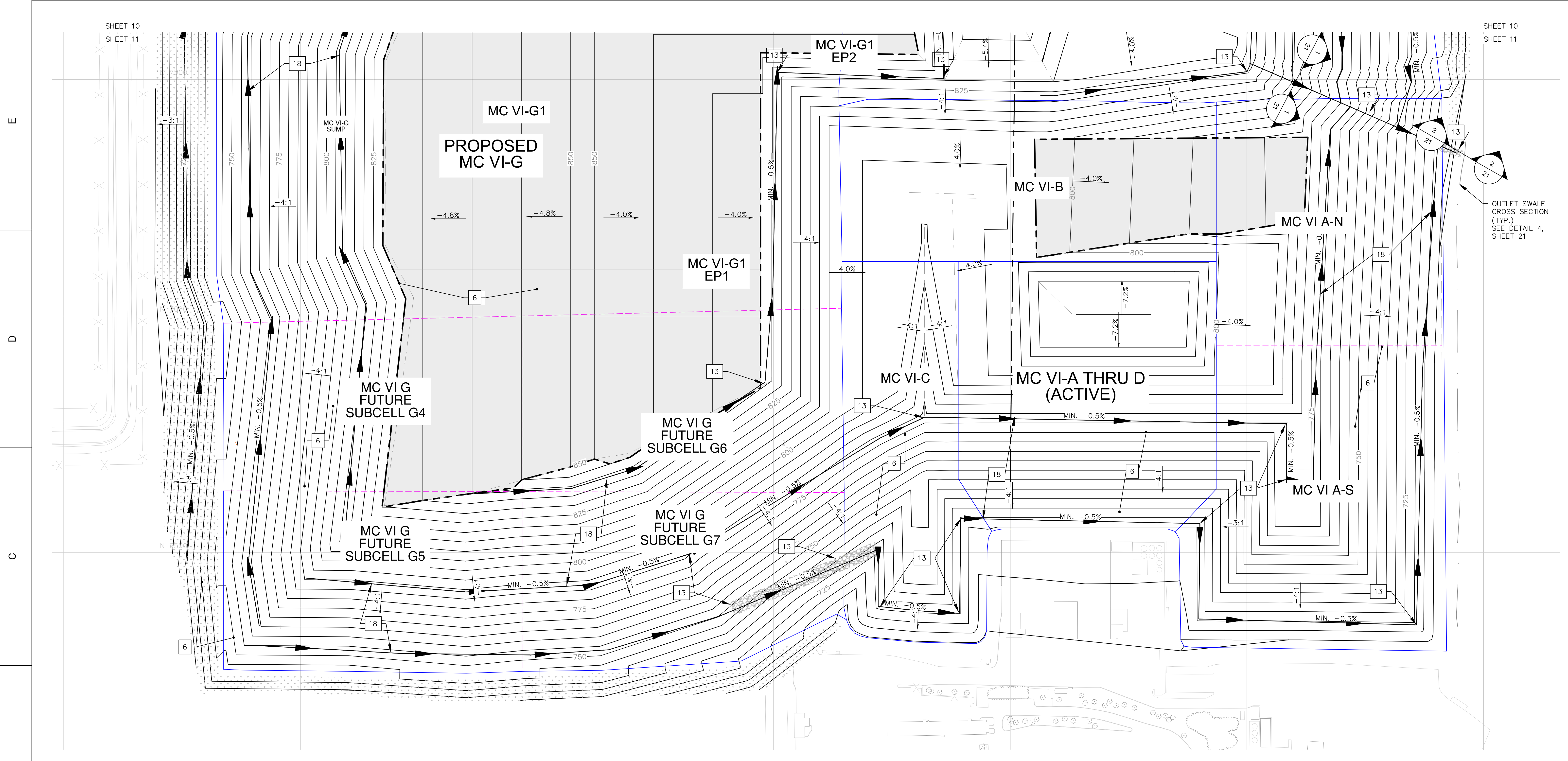
LEGEND

- 500 — EXISTING MAJOR CONTOURS
- — — EXISTING MINOR CONTOURS
- 500 — PERMITTED TOP OF FINAL COVER MAJOR CONTOURS
- — — PERMITTED TOP OF FINAL COVER MINOR CONTOURS
- ~~~~~ EXISTING VEGETATION
- - - - - PROPOSED GRADE BREAK
- - - - - EXISTING GRADE BREAK
- - - - - PROPOSED OUTLET SWALE
- - - - - PROPOSED DIVERSION GEOMEMBRANE
- - - - - SUBCELL BOUNDARY
- — — CELL BOUNDARY
- [Hatched Box] PROPOSED GEOCOMPOSITE (TRANSMISSIVITY 5.0 X 10⁻⁴ M²/S)
- [Riprap Box] PROPOSED RIP-RAP
- [Seeding Box] PROPOSED PERMANENT SEEDING-AT TIME OF DIKE CONSTRUCTION
- [Arrow] PROPOSED DIVERSION BERM

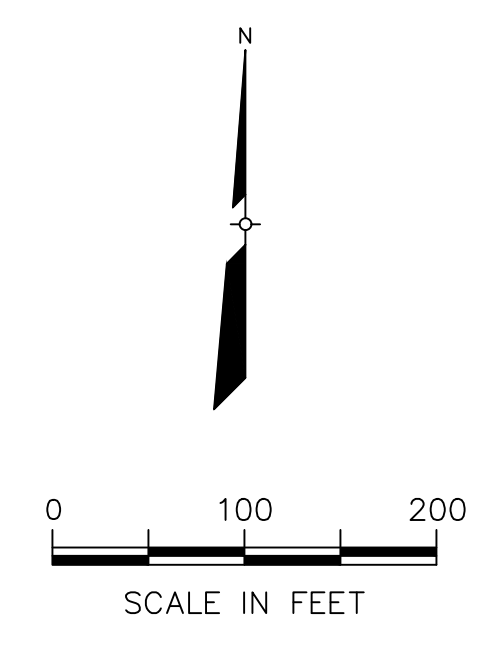


NOTES:
1. THE BASE MAP WAS CREATED USING AN AERIAL SURVEY TAKEN IN 2020 BY WDI.

		DATE: 05/17/21 DESIGNED BY: BA DRAWN BY: WFG CHECKED BY: CAB APPROVED BY: XZ
CTI and Associates, Inc. 2800 Cabot Drive, Ste. 250 Farmington Hills, MI 48334 (248) 486-5100 (Fax) 248-486-5050 www.cticompanies.com		This drawing was prepared by CTI and Associates, Inc. (CTI) and is the property of CTI. It is not to be used for any other project without the written consent of CTI. The user of this drawing is responsible for obtaining all necessary permits and approvals from the appropriate authorities. The user of this drawing is also responsible for ensuring that the drawing is used in accordance with the applicable laws and regulations.
PROJECT NUMBER 1208070039	SCALE 1" = 100'	DRAWING NO 10
WAYNE DISPOSAL, INC. SITE NO. 2 - MASTER CELL VI-F&G STORMWATER MANAGEMENT AND SEDIMENTATION PLAN (1 OF 2) VAN BUREN TOWNSHIP, WAYNE COUNTY, MICHIGAN STORMWATER MANAGEMENT AND SEDIMENTATION PLAN (1 OF 2)		
REV F E D C B A	DATE 05/17/21 05/17/21 05/17/21 05/17/21 05/17/21 05/17/21 05/17/21	REVISION DESCRIPTION F1-F4 REVISIONS AND RESPONSE TO EGLE COMMENTS WDG XZ DFN APP

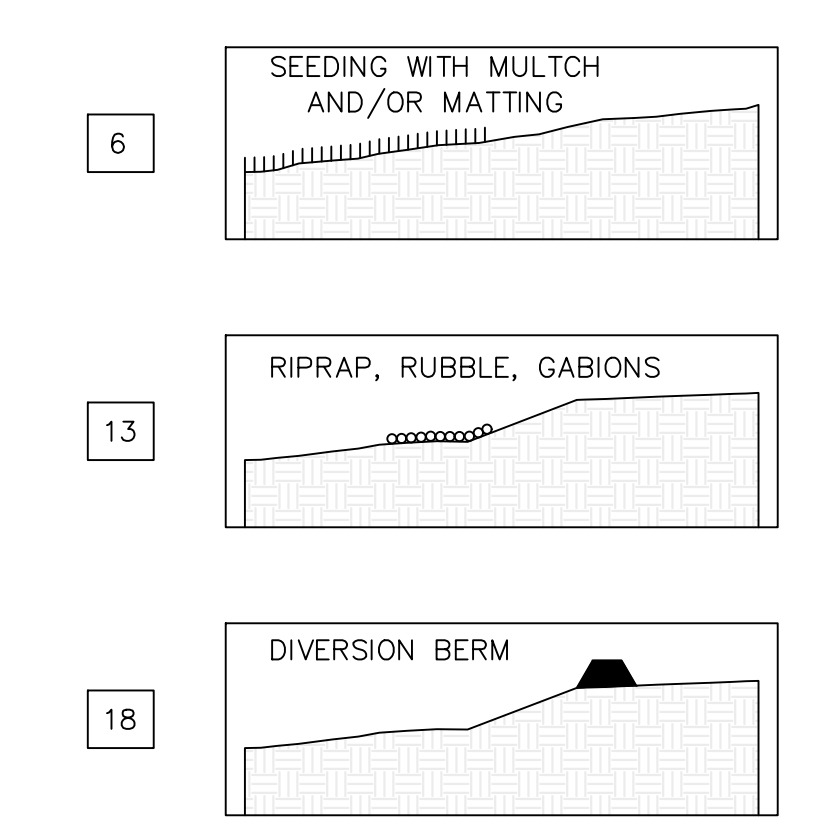


OUTLET SWALE
CROSS SECTION
(TYP)
SEE DETAIL 4,
SHEET 21



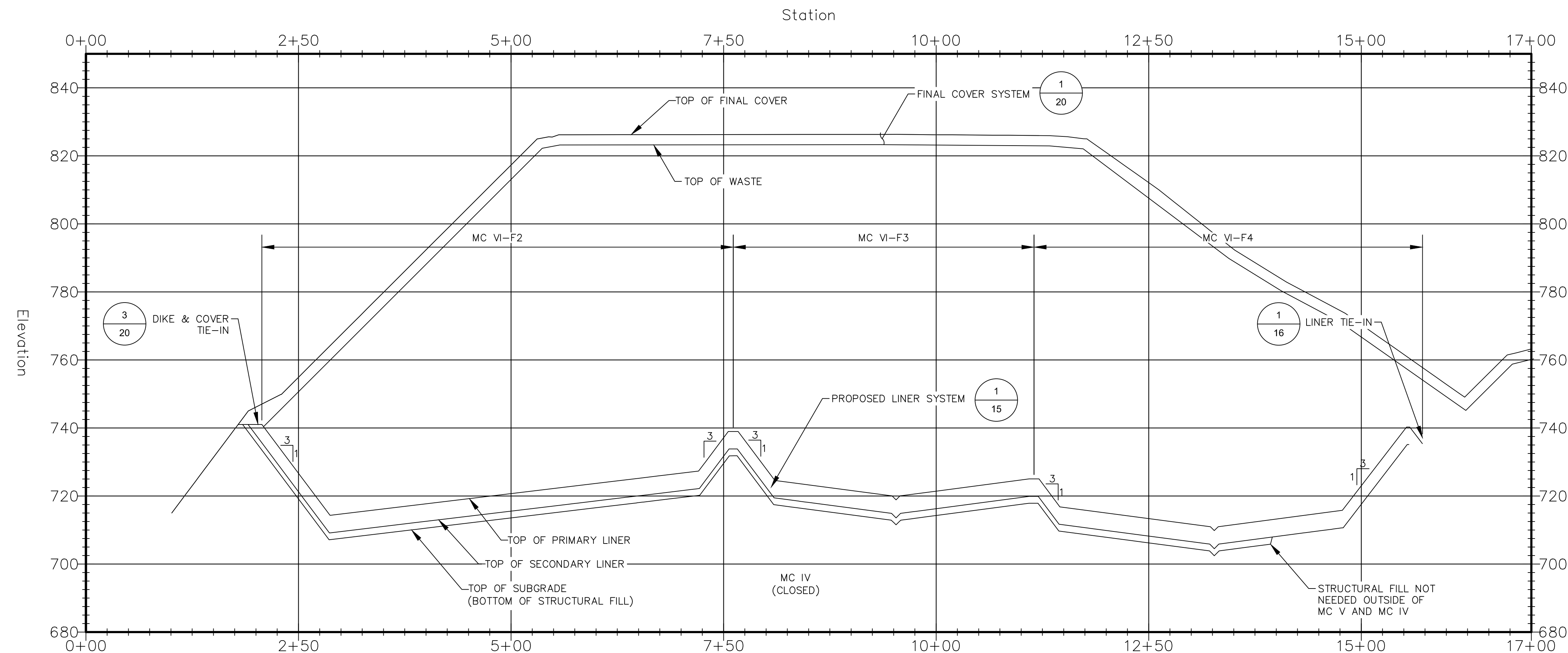
LEGEND

- 500 — EXISTING MAJOR CONTOURS
- — — EXISTING MINOR CONTOURS
- 500 — PERMITTED TOP OF FINAL COVER MAJOR CONTOURS
- — — PERMITTED TOP OF FINAL COVER MINOR CONTOURS
- ~~~~~ EXISTING VEGETATION
- - - - - PROPOSED GRADE BREAK
- - - - - EXISTING GRADE BREAK
- - - - - PROPOSED OUTLET SWALE
- - - - - PROPOSED DIVERSION GEOMEMBRANE
- - - - - SUBCELL BOUNDARY
- — — CELL BOUNDARY
- [Hatched Box] PROPOSED GEOCOMPOSITE (TRANSMISSIVITY 5.0 X 10⁻⁴ M²/S)
- [Stippled Box] PROPOSED RIP-RAP
- [Dotted Box] PROPOSED PERMANENT SEEDING-AT TIME OF DIKE CONSTRUCTION
- [Arrow] PROPOSED DIVERSION BERM

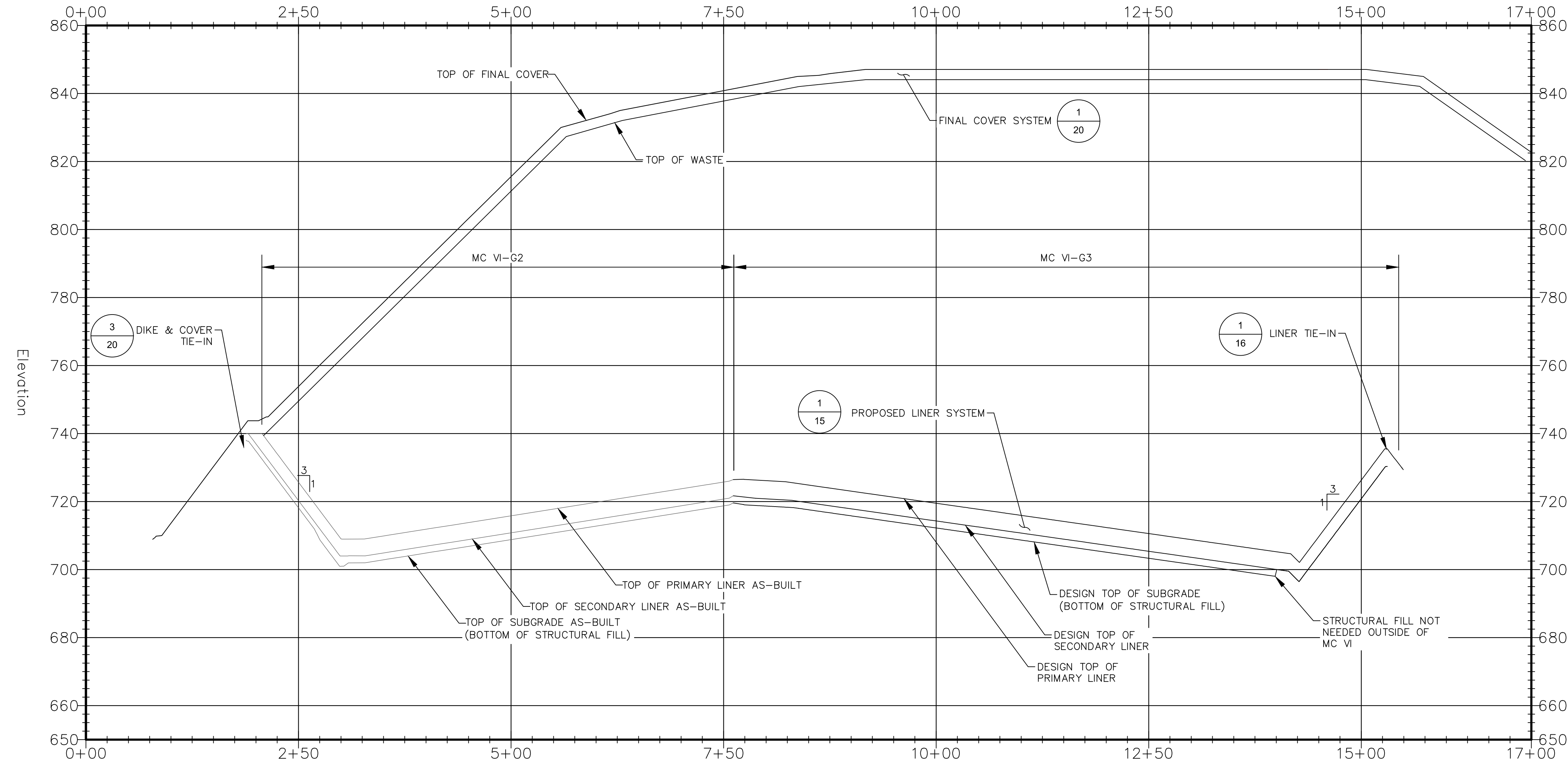


NOTES:
1. THE BASE MAP WAS CREATED USING AN AERIAL SURVEY TAKEN IN 2020 BY WDI.

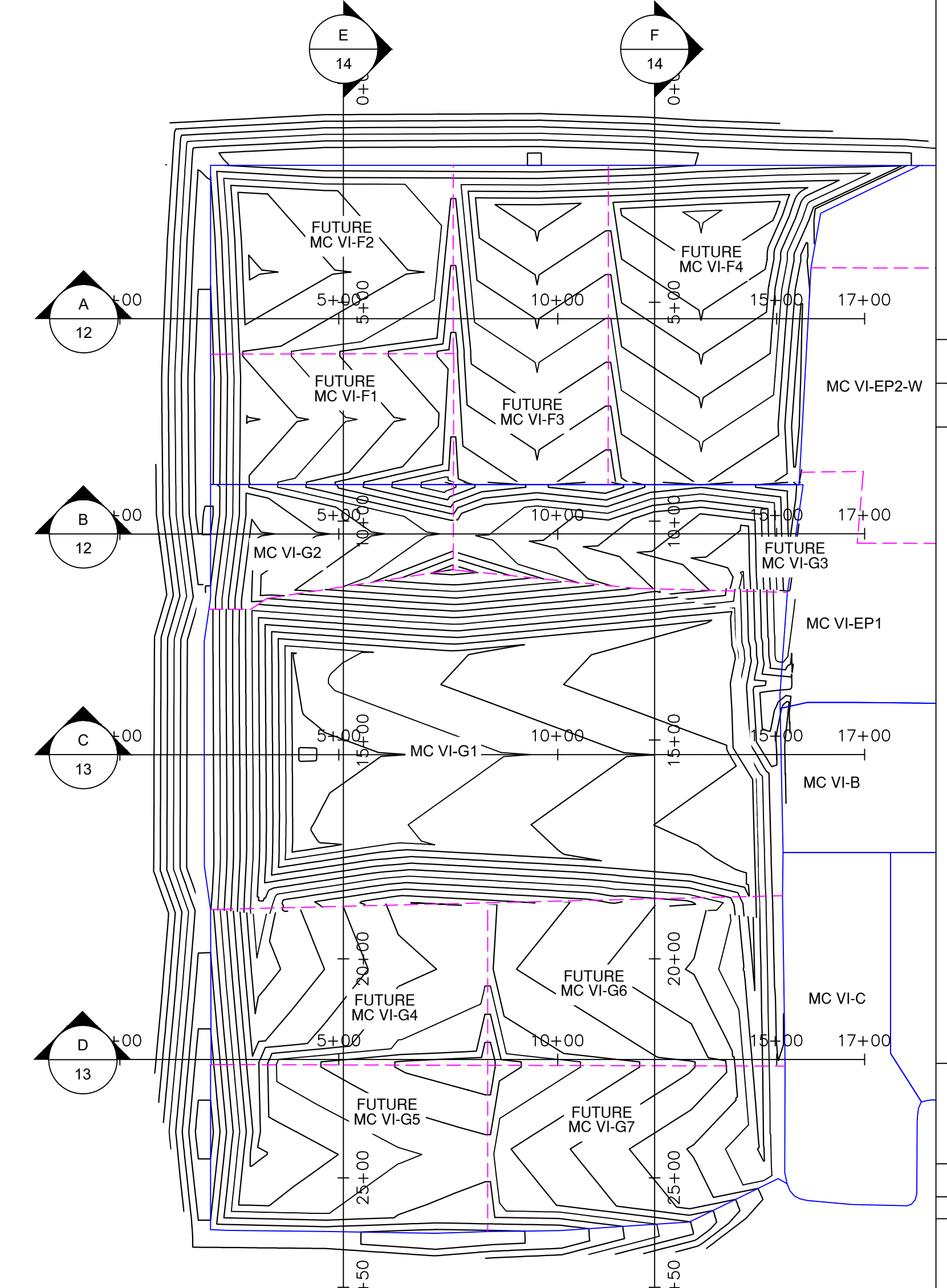
DATE: 05/17/21	DESIGNED BY: BA	DRAWN BY: WRC	CHECKED BY: CAB	APPROVED BY: XZ
CTI and Associates, Inc. 2800 Cabot Drive, Ste. 250 Farmington Hills, MI 48334 (248) 486-5100 (Fax) 248-486-5050 www.cticompanies.com				
This drawing was prepared by CTI and Associates, Inc. (CTI) and is the property of CTI. It is to be used only for the project and location specified. No part of this drawing may be reproduced or transmitted in any form or by any means, electronic, mechanical, photocopying, recording, or by any information storage and retrieval system, without the prior written permission of CTI.				
REV	DATE	REVISION DESCRIPTION		
F	05/17/21	F1-F4 REVISIONS AND RESPONSE TO EGLE COMMENTS		
E	05/17/21	F1-F4 REVISIONS AND RESPONSE TO EGLE COMMENTS		
D	05/17/21	F1-F4 REVISIONS AND RESPONSE TO EGLE COMMENTS		
C	05/17/21	F1-F4 REVISIONS AND RESPONSE TO EGLE COMMENTS		
B	05/17/21	F1-F4 REVISIONS AND RESPONSE TO EGLE COMMENTS		
A	05/17/21	F1-F4 REVISIONS AND RESPONSE TO EGLE COMMENTS		
WAYNE DISPOSAL, INC. SITE NO. 2 - MASTER CELL VI-F&G STORMWATER MANAGEMENT AND SEDIMENTATION PLAN (2 OF 2) VAN BUREN TOWNSHIP, WAYNE COUNTY, MICHIGAN				
STORMWATER MANAGEMENT AND SEDIMENTATION PLAN (2 OF 2)				
PROJECT NUMBER: 1208070039 SCALE: 1" = 100' DRAWING NO: 11				



A SECTION THROUGH MC VI-F
 SCALE: 1"=80' (HORIZONTAL), 1"=10' (VERTICAL)



B SECTION THROUGH MC VI-G
 SCALE: 1"=80' (HORIZONTAL), 1"=10' (VERTICAL)



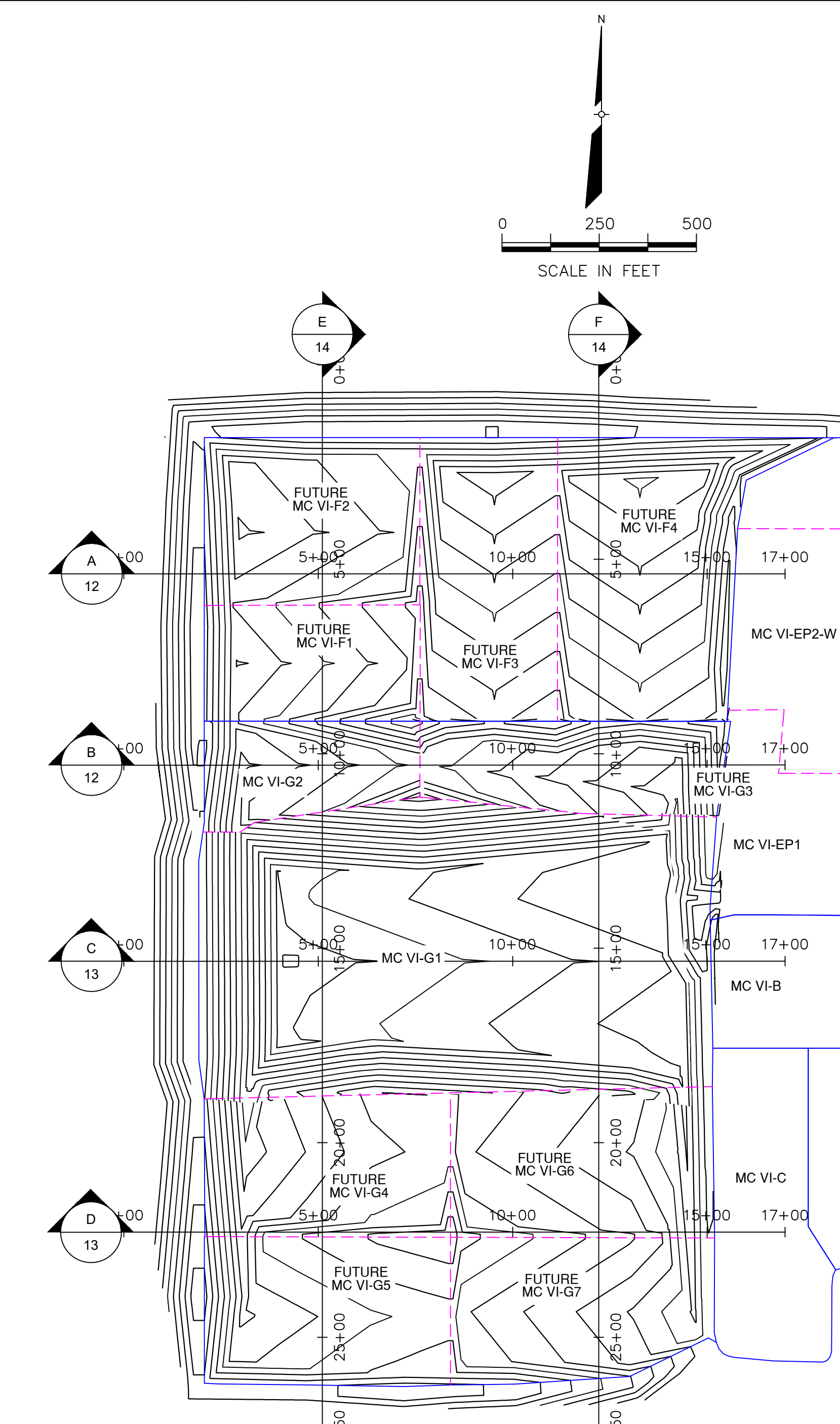
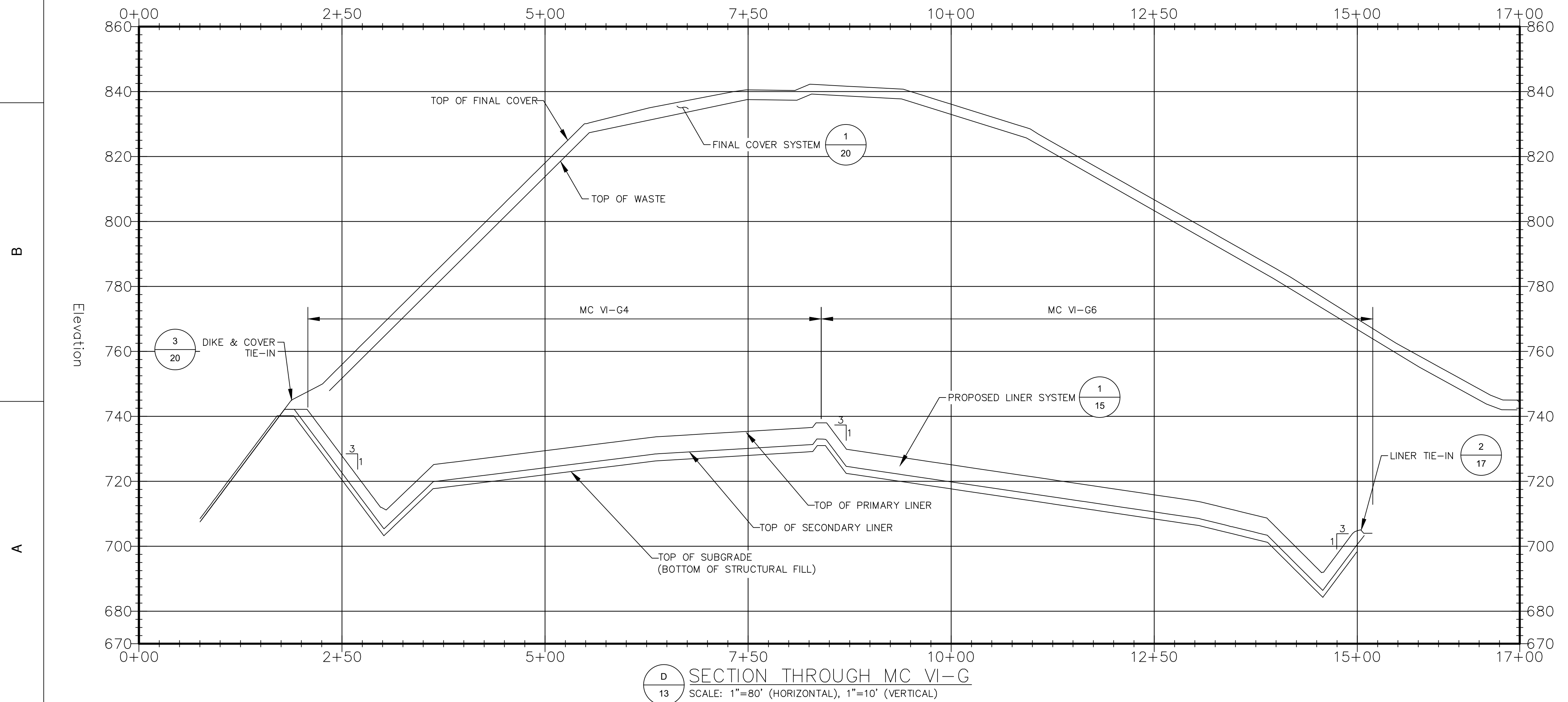
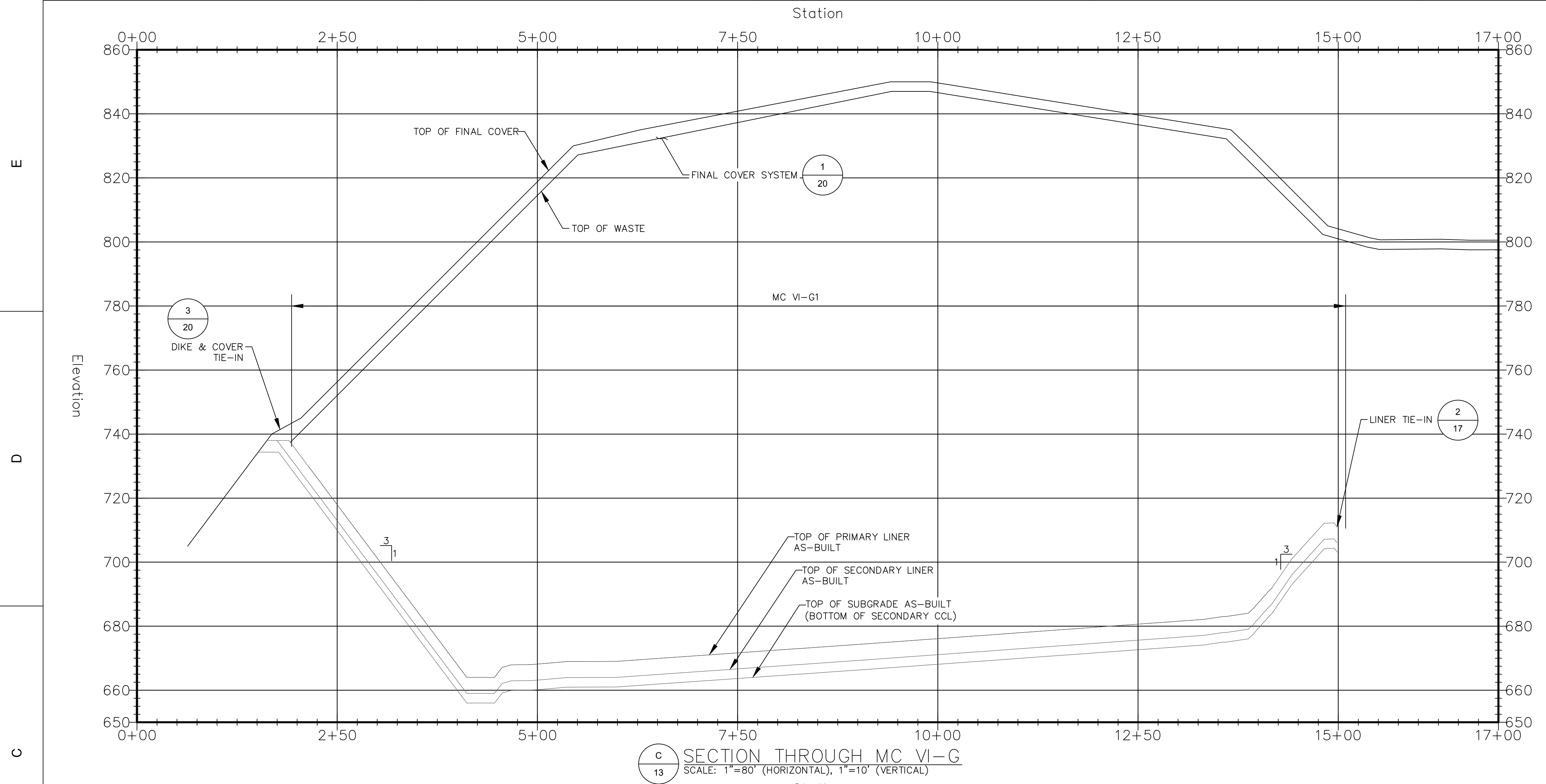
DATE: 05/17/21
 DESIGNED BY: BA
 DRAWN BY: WRG
 CHECKED BY: CAB
 APPROVED BY: XZ

CTI and Associates, Inc.
 2800 Cabot Drive, Ste. 250
 Van Buren Township, Michigan 48156
 (313) 486-5100 (Fax) 248.486.5050
 www.cticompanies.com

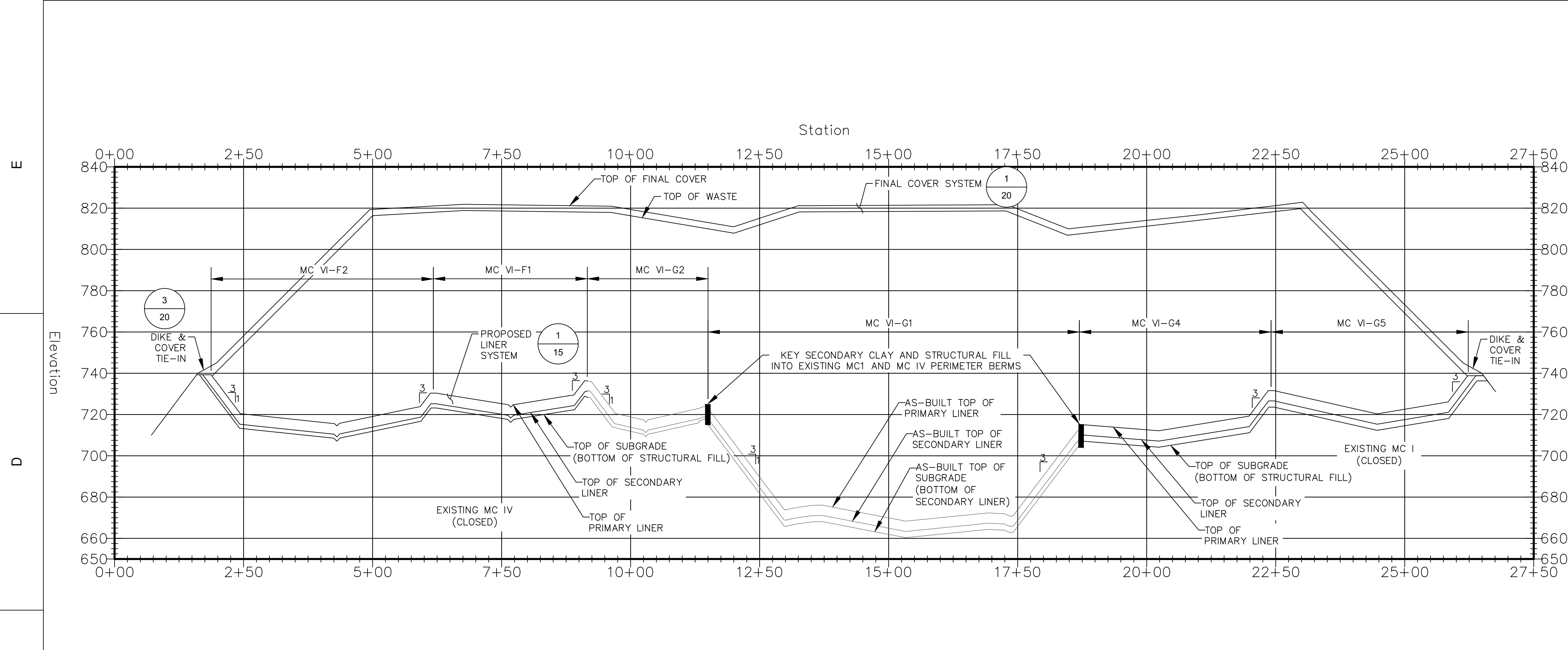
REV	DATE	REVISION DESCRIPTION
F	05/17/21	F1-F4 REVISIONS AND RESPONSE TO EGLE COMMENTS
C	5/02/18	SUBCELLS G2 AND G3 REVISIONS

WAYNE DISPOSAL, INC. SITE NO. 2 - MASTER CELL VI-F&G
 CROSS SECTIONS (1 OF 3)
 VAN BUREN TOWNSHIP, WAYNE COUNTY, MICHIGAN

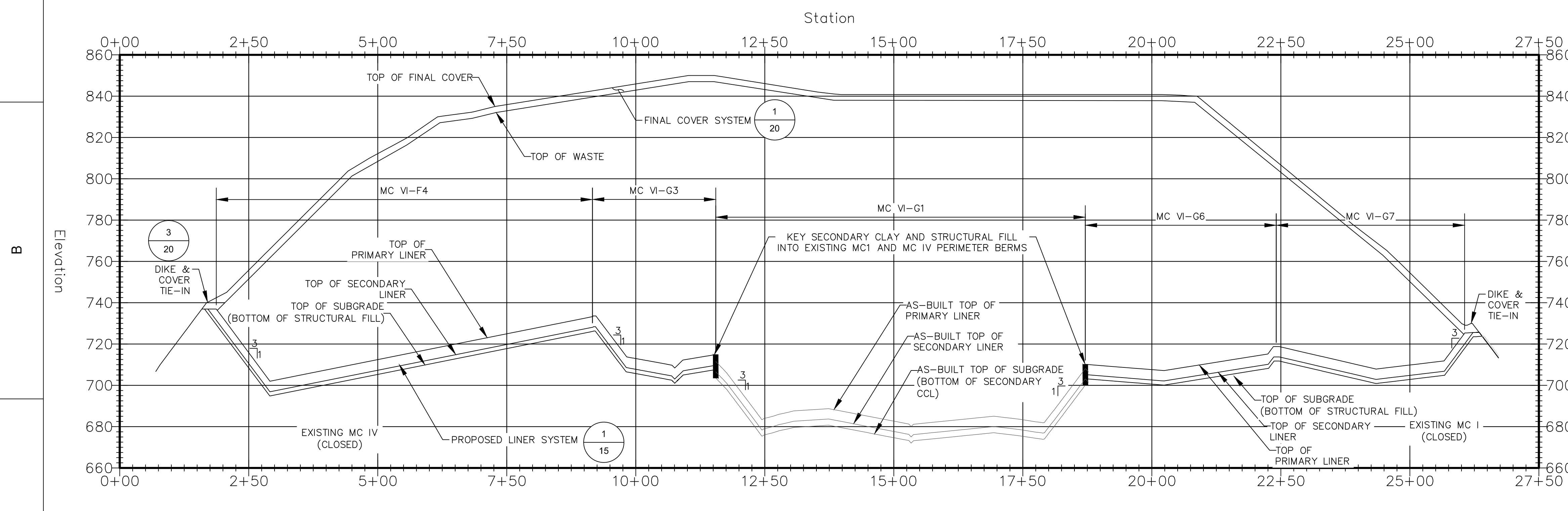
PROJECT NUMBER: 1208070039
 SCALE: AS SHOWN
 DRAWING NO: 12



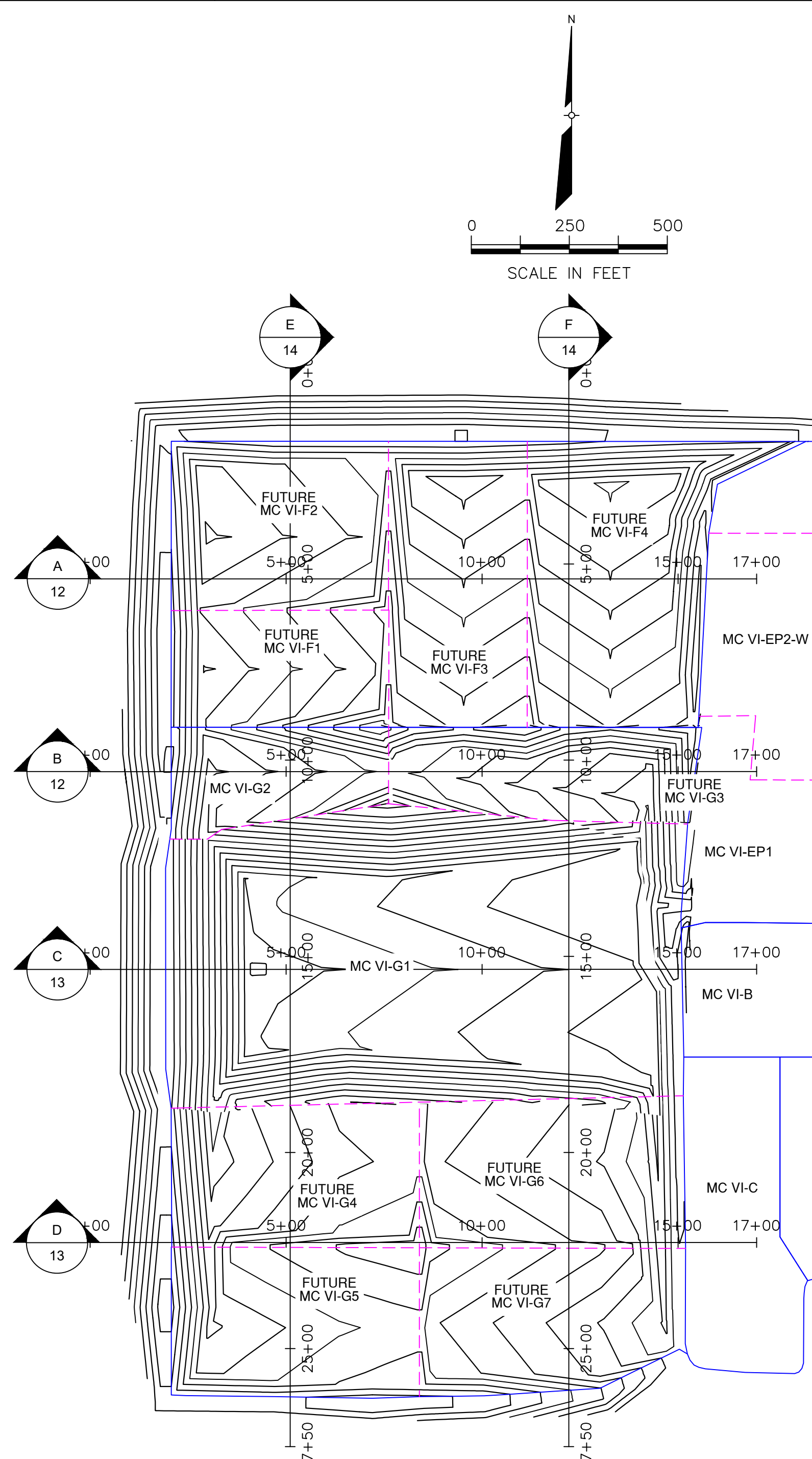
DATE:	05/17/21	DESIGNED BY:	BA	WRC	CAB	XZ
DRAWN BY:	WRC	CHECKED BY:	CAB	APPROVED BY:	XZ	
<p>CTI and Associates, Inc. 2800 Cabot Drive, Ste. 250 248.486.5100 (fax) 248.486.5050 www.cticompanies.com</p>						
<p>The information contained on this drawing is the property of CTI and Associates, Inc. (CTI) and shall not be used for any other project without the written consent of CTI. The user of this drawing shall be responsible for obtaining all necessary permits and approvals from the appropriate authorities and for ensuring that the drawing is used in accordance with the intended purpose. CTI and Associates, Inc. does not warrant the accuracy or completeness of the information contained on this drawing and shall not be held liable for any errors or omissions. The user of this drawing shall be responsible for obtaining all necessary permits and approvals from the appropriate authorities and for ensuring that the drawing is used in accordance with the intended purpose.</p>						
REV	DATE	REVISION DESCRIPTION	WRC	XZ	PAA	APP
F	05/17/21	F1-F4 REVISIONS AND RESPONSE TO EGLE COMMENTS				
C	5/02/18	SUBCELLS G2 AND G3 REVISIONS				
B	05/17/21	MC VI-G1 TO MC VI-G7				
A	05/17/21	MC VI-G1 TO MC VI-G7				
<p>WAYNE DISPOSAL, INC. SITE NO. 2 - MASTER CELL VI-F&G CROSS SECTIONS (2 OF 3) VAN BUREN TOWNSHIP, WAYNE COUNTY, MICHIGAN</p>						
PROJECT NUMBER		1208070039				
SCALE		AS SHOWN				
DRAWING NO		13				



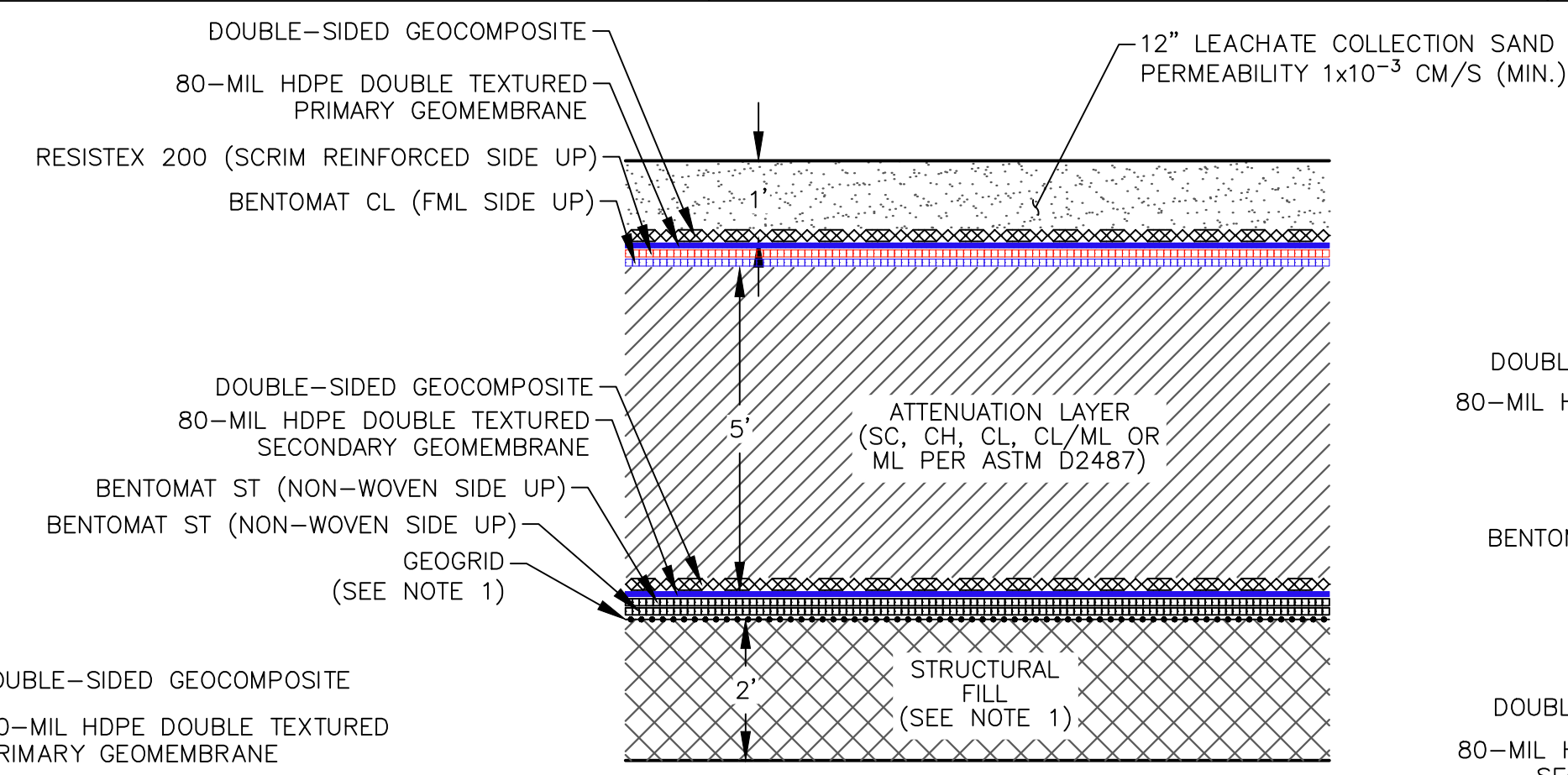
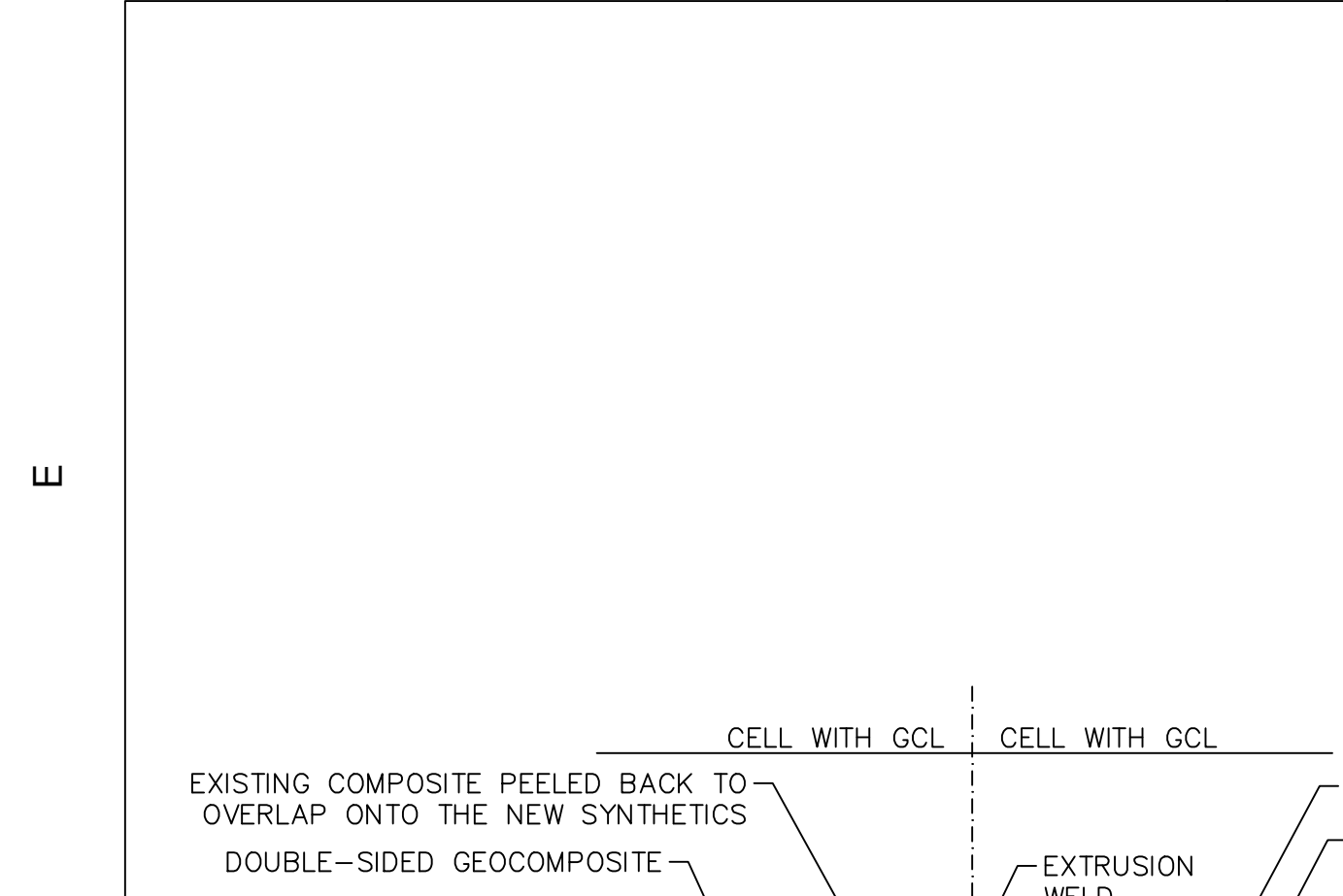
E SECTION THROUGH MC VI-F AND MC VI-G
 SCALE: 1"=125' (HORIZONTAL), 1"=10' (VERTICAL)



F SECTION THROUGH MC VI-F AND MC VI-G
 SCALE: 1"=125' (HORIZONTAL), 1"=10' (VERTICAL)

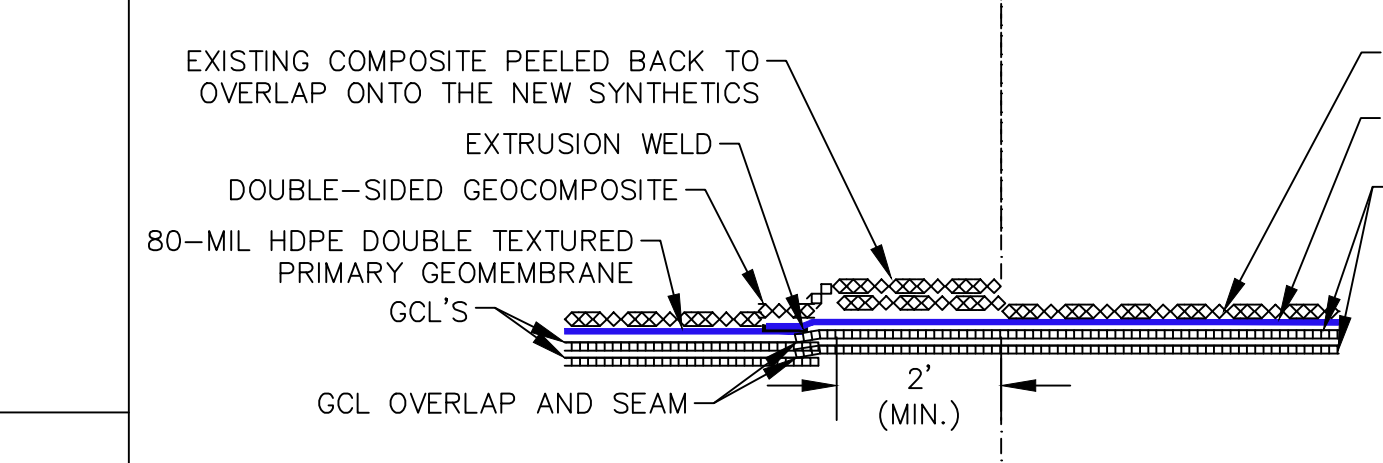


DATE:	05/17/21	DESIGNED BY:	BA	WRC	CAB	XZ
DRAWN BY:	WRC	CHECKED BY:	CAB	APPROVED BY:	XZ	
PROJECT NUMBER:	1208070039					
SCALE:	AS SHOWN					
DRAWING NO:	14					
PROJECT:	WAYNE DISPOSAL, INC. SITE NO. 2 - MASTER CELL VI-F&G					
CROSS SECTIONS (3 OF 3):	VAN BUREN TOWNSHIP, WAYNE COUNTY, MICHIGAN					
REV:	DATE:	DESCRIPTION:				
F	05/17/21	F1-F4 REVISIONS AND RESPONSE TO EGLE COMMENTS				
C	5/02/18	SUBCELLS G2 AND G3 REVISIONS				
B	9/23/11	PER MICRO COMMENTS				
A	6/10/11	PHASING DESIGNATIONS				



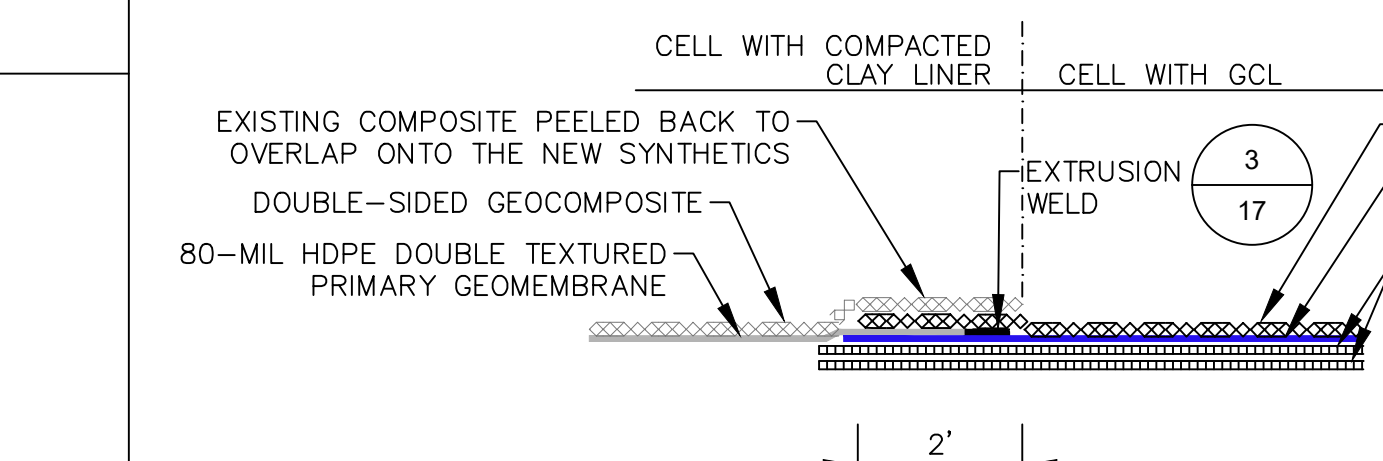
1
15
PROPOSED FLOOR LINER SYSTEM USING GCL
NOT TO SCALE

- NOTE:
- STRUCTURAL FILL AND GEOGRID NOT REQUIRED OUTSIDE OF MC I AND MC IV. SEE LIMITS ON SHEET 04
 - SEE DETAIL 4 SHEET 17 FOR GCL OVERLAP REQUIREMENT



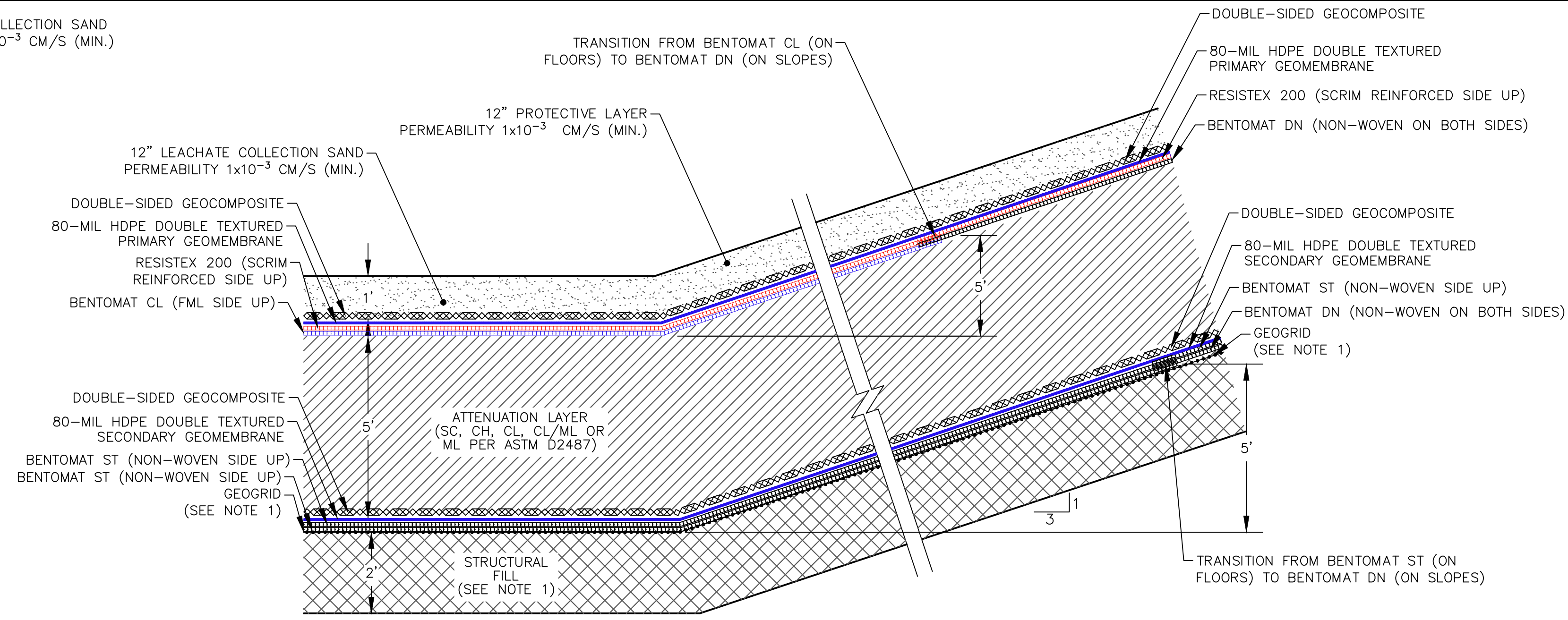
3
15
LINER TIE-IN DETAIL I
NOT TO SCALE

- NOTES:
- NEW AND EXISTING GEOCOMPOSITE LAYERS SHALL BE CONNECTED AS FOLLOWS:
- GEONET CORES SHALL BE JOINED BY PLASTIC FASTENERS.
- TOP GEOTEXTILE SHALL BE SEWN TOGETHER OR COVERED WITH EXTRA NON-WOVEN GEOTEXTILE (MINIMUM 24" WIDE) HEAT BONDED TO THE EXISTING GEOTEXTILE.
 - AT GCL SEAMS, DRY BENTONITE POWDER SHALL BE APPLIED PER MANUFACTURER'S INSTALLATION GUIDELINES.
 - SEAMS SHOULD BE CONSTRUCTED SUCH THAT THEY ARE SHINGLED IN THE DIRECTION OF THE GRADE TO PREVENT FLOW FROM ENTERING THE OVERLAP ZONE.



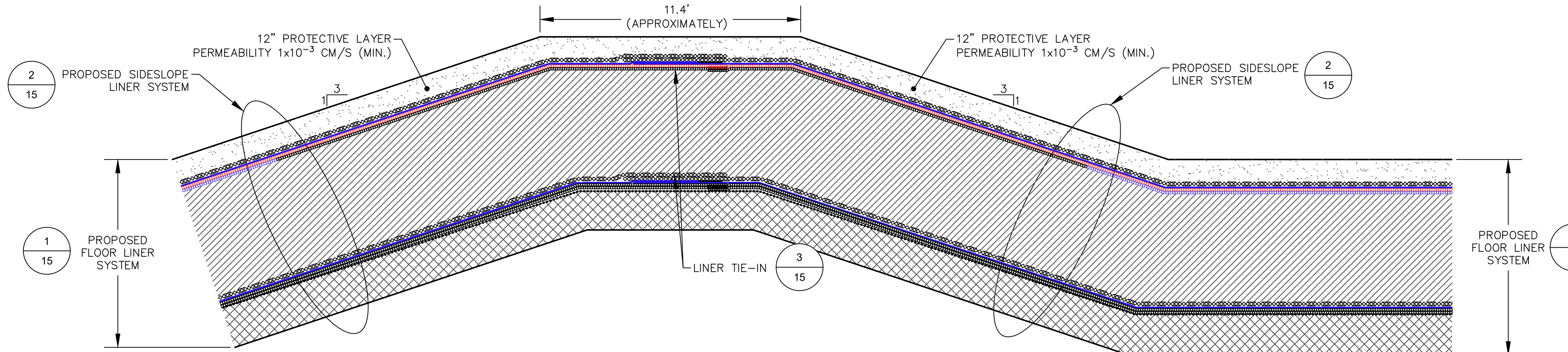
4
15
LINER TIE-IN DETAIL II
NOT TO SCALE

- NOTES:
- NEW AND EXISTING GEOCOMPOSITE LAYERS SHALL BE CONNECTED AS:
 - TOP GEOTEXTILE SHALL BE SEWN TOGETHER OR COVERED WITH EXTRA NON-WOVEN GEOTEXTILE (MINIMUM 24" WIDE) HEAT BONDED TO THE EXISTING GEOTEXTILE.



2
15
PROPOSED SIDESLOPE LINER SYSTEM USING GCL
NOT TO SCALE

- NOTE:
- STRUCTURAL FILL AND GEOGRID NOT REQUIRED OUTSIDE OF MC I AND MC IV. SEE LIMITS ON SHEET 04
 - SEE DETAIL 4 SHEET 17 FOR GCL OVERLAP REQUIREMENT



5
15
MC VI-F & G TIE-IN DETAIL
NOT TO SCALE

2
18

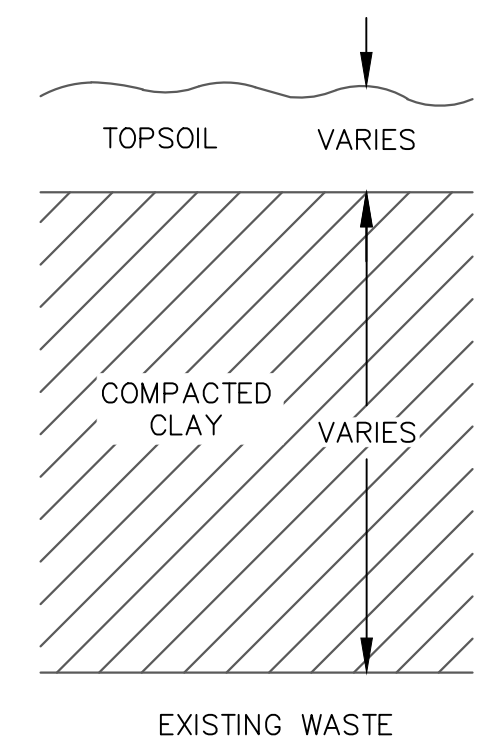
1
15

2
15

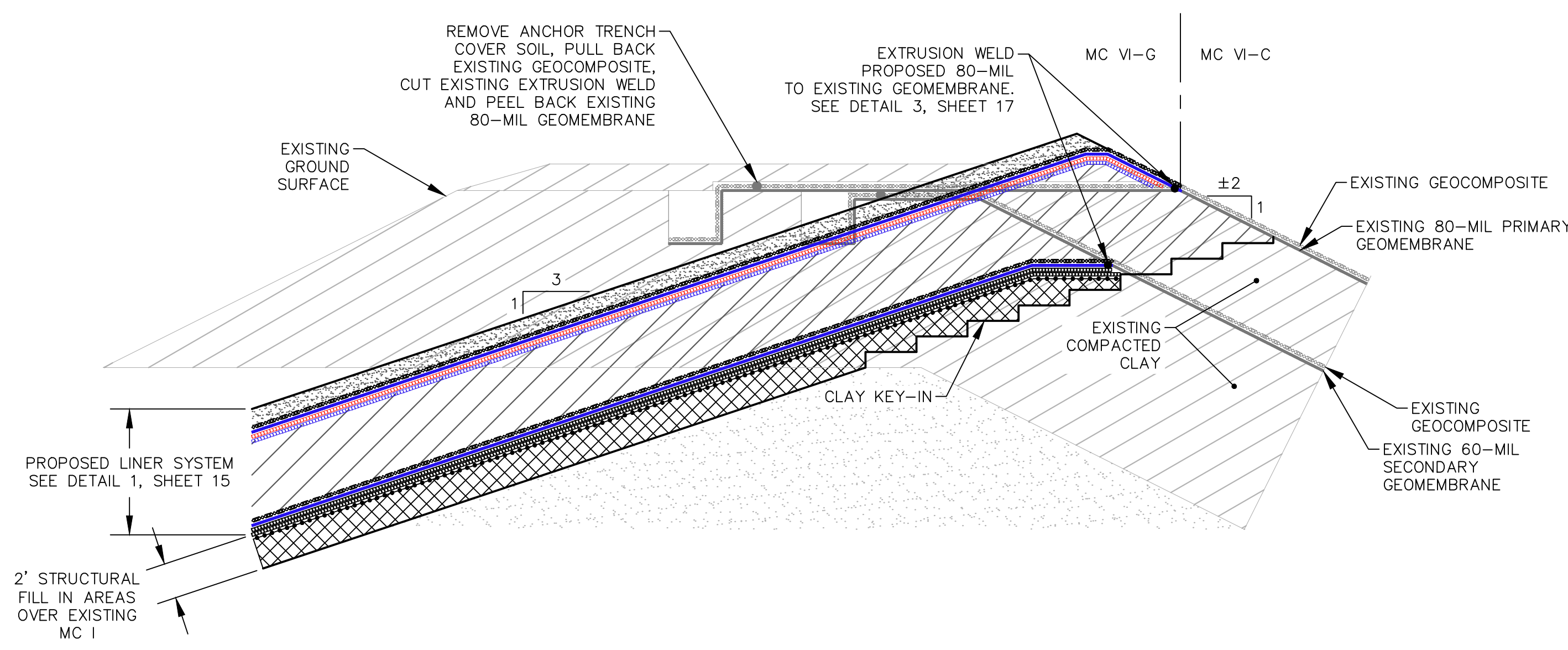
6
15
G CELLS WEST PERIMETER DIKE
NOT TO SCALE

DATE:	05/17/21	DESIGNED BY:	BA	DRAWN BY:	WRG	CHECKED BY:	CAB	APPROVED BY:	XZ
<p>CTI and Associates, Inc. 2800 Cabot Drive, Ste. 250 Livonia, MI 48150 248.486.5100 (fax) 248.486.5050 www.cticompanies.com</p> <p>This drawing was prepared by CTI and Associates, Inc. (CTI) and is the property of CTI. It is to be used only for the project and site for which it was prepared. No part of this drawing may be reproduced or transmitted in any form or by any means, electronic, mechanical, photocopying, recording, or by any information storage and retrieval system, without the prior written permission of CTI. The user of this drawing shall be responsible for obtaining all necessary permits and approvals from the appropriate authorities.</p>									
REV	DATE	DESCRIPTION							
F	05/17/21	F1-F4 REVISIONS AND RESPONSE TO EGLE COMMENTS							
E	5/29/18	ADDENDUM 1							
D	5/08/18	REVISIONS BASED ON MREG'S COMMENTS							
C	5/02/18	SUBCELLS C2 AND C3 REVISIONS							
<p>WAYNE DISPOSAL, INC. SITE NO. 2 - MASTER CELL VI-F&G LINER SYSTEM DETAILS (1 OF 3) VAN BUREN TOWNSHIP, WAYNE COUNTY, MICHIGAN</p> <p>LINER SYSTEM DETAILS (1 OF 3)</p>									
<p>PROJECT NUMBER 1208070039</p> <p>SCALE AS SHOWN</p> <p>DRAWING NO 15</p>									

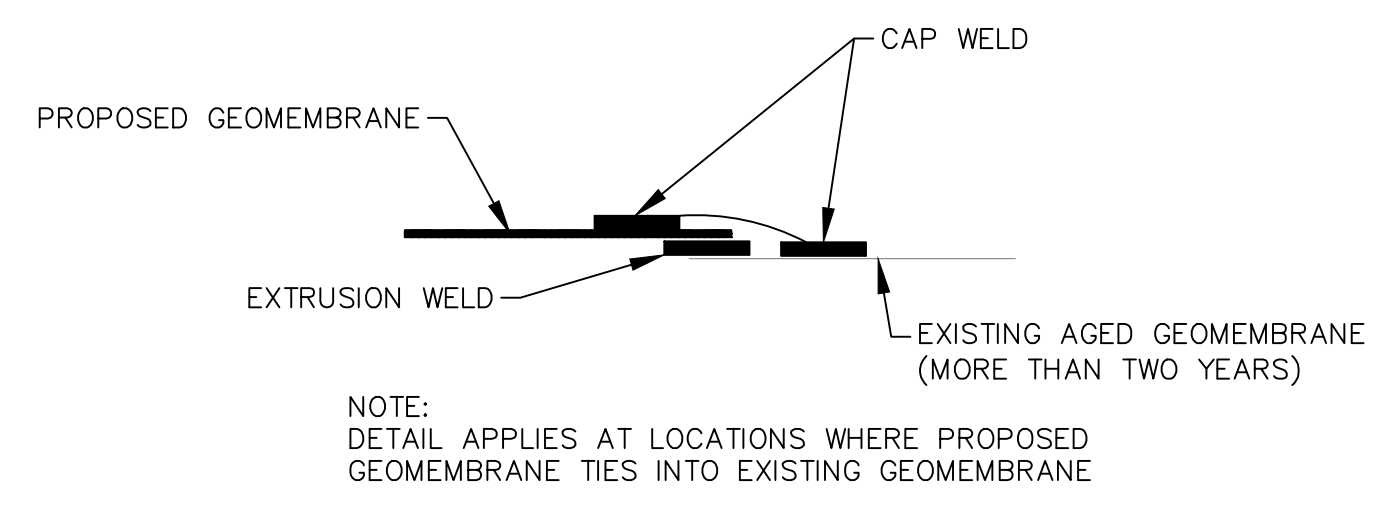
E
D
C
B
A



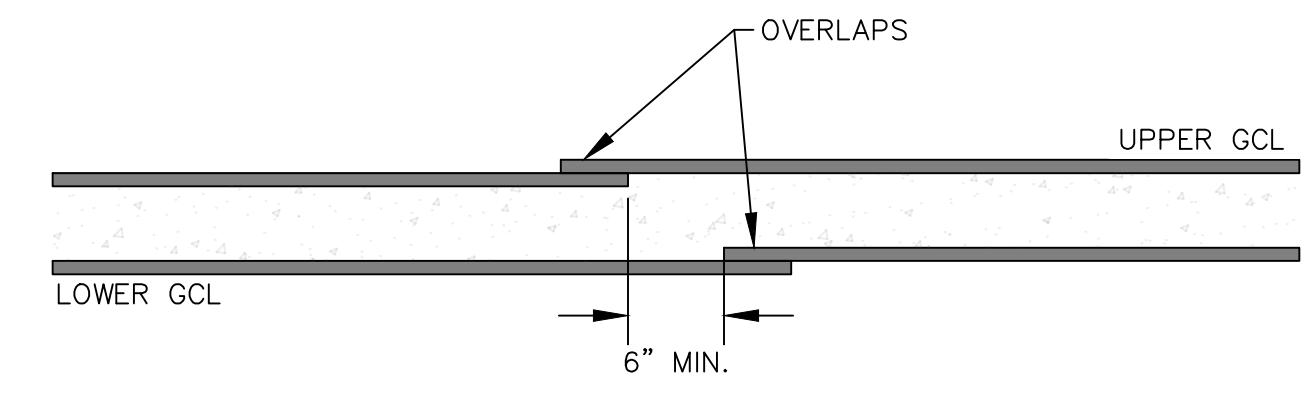
1
17
MC I & MC IV COVER DETAIL
NOT TO SCALE



2
17
MC VI-G6, MC VI-G7, & MC VI-C TIE-IN DETAIL
NOT TO SCALE

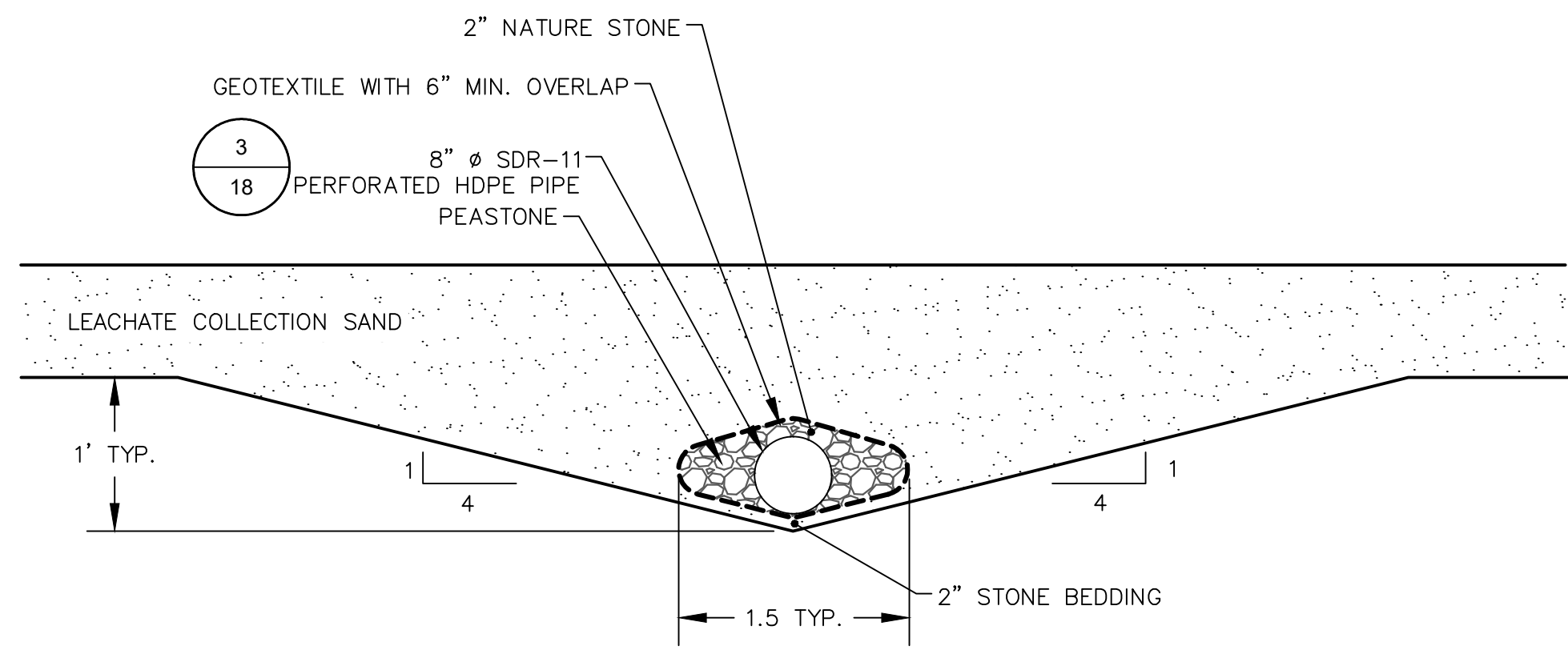


3
17
GEOMEMBRANE WELDING DETAIL
NOT TO SCALE

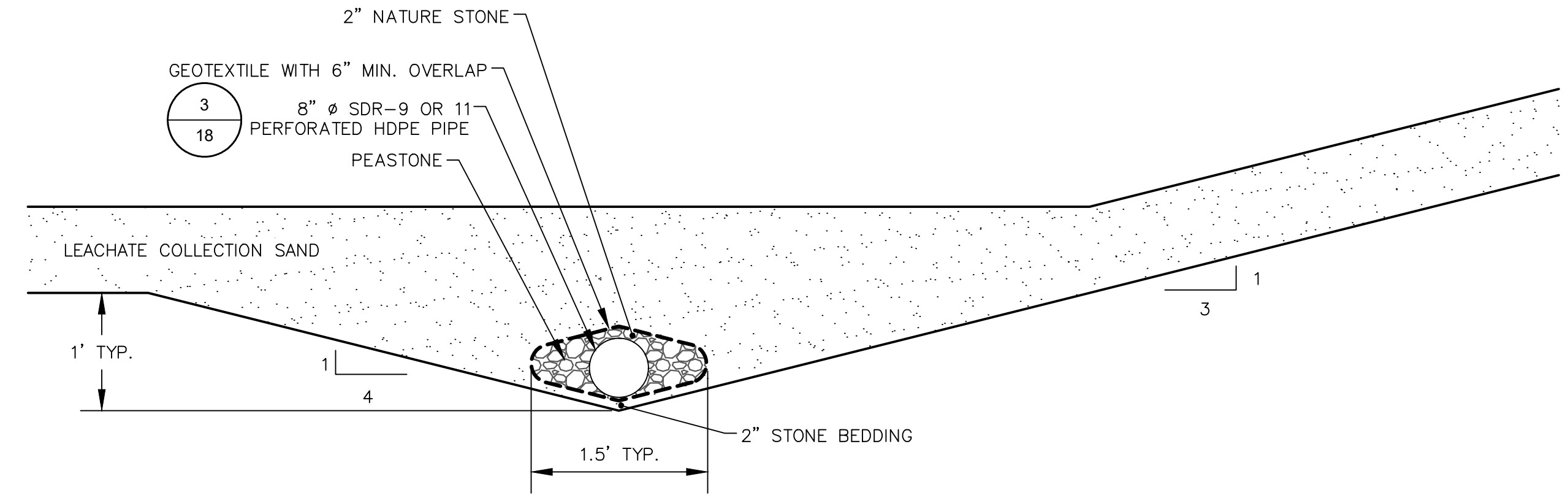


4
17
GCL OVERLAPS REQUIREMENT
NOT TO SCALE

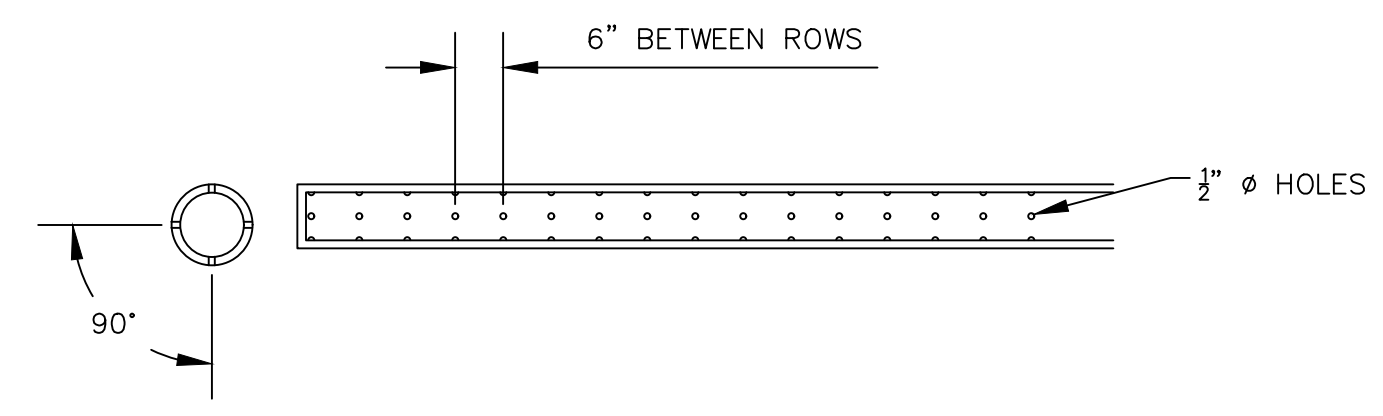
		CTI and Associates, Inc. 2800 Cabot Drive, Ste. 250 Farmington Hills, MI 48334 (248) 486-5100 (fax) 248 486-5050 www.cticompanies.com	DATE: 05/17/21 DESIGNED BY: BA DRAWN BY: WRG CHECKED BY: CAB APPROVED BY: XZ
WAYNE DISPOSAL, INC. SITE NO. 2 - MASTER CELL VI-F&G LINER SYSTEM DETAILS (3 OF 3) VAN BUREN TOWNSHIP, WAYNE COUNTY, MICHIGAN		PROJECT NUMBER: 1208070039 SCALE: AS SHOWN DRAWING NO: 17	
REV	DATE	DESCRIPTION	
F	05/17/21	F1-F4 REVISIONS AND RESPONSE TO EGLE COMMENTS	DRG
B	9/23/11	PER MDO COMMENTS	DRG
A	6/10/11	PHASING DESIGNATIONS	DRG
			DRN / APP



1
18 CELL FLOOR LEACHATE COLLECTION PIPE (TYP.)
NOT TO SCALE



2
18 TOE OF SLOPE LEACHATE COLLECTION PIPE (TYP.)
NOT TO SCALE



3
18 8" LEACHATE COLLECTION PIPE PERFORATION SPACING DETAIL
NOT TO SCALE

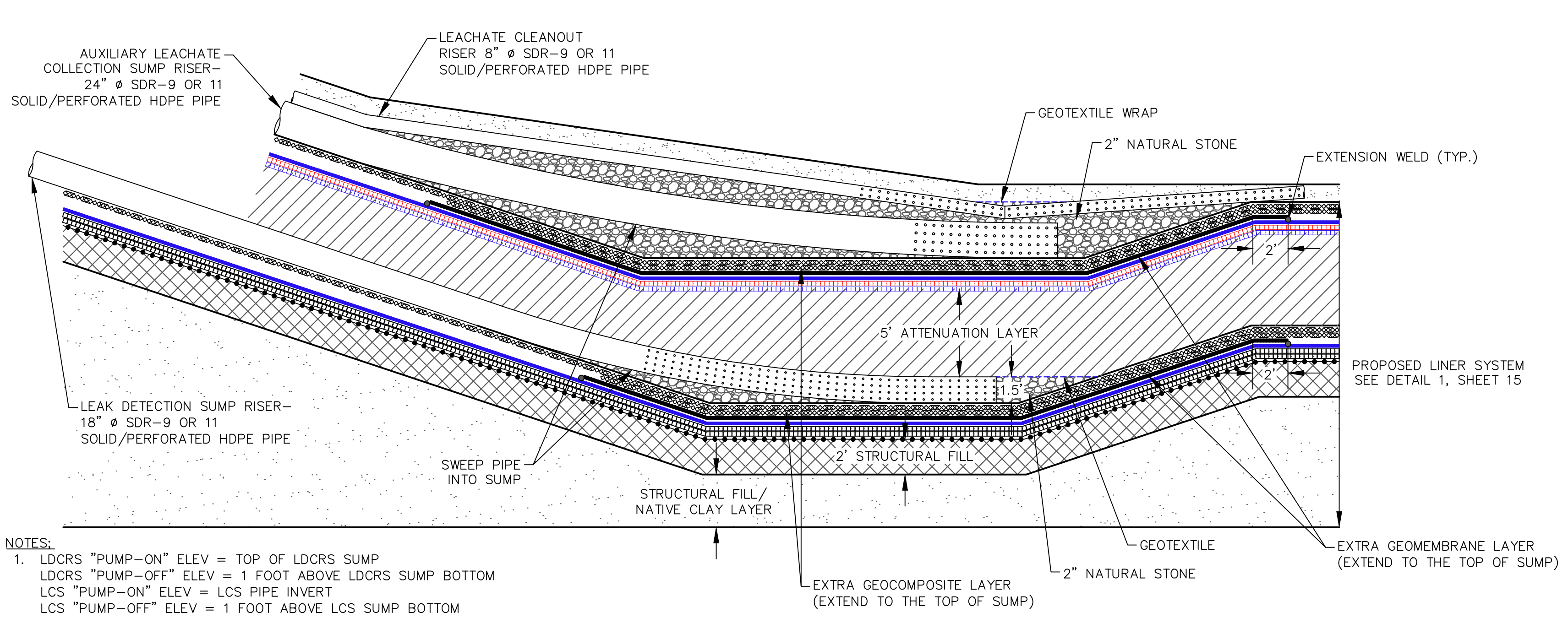
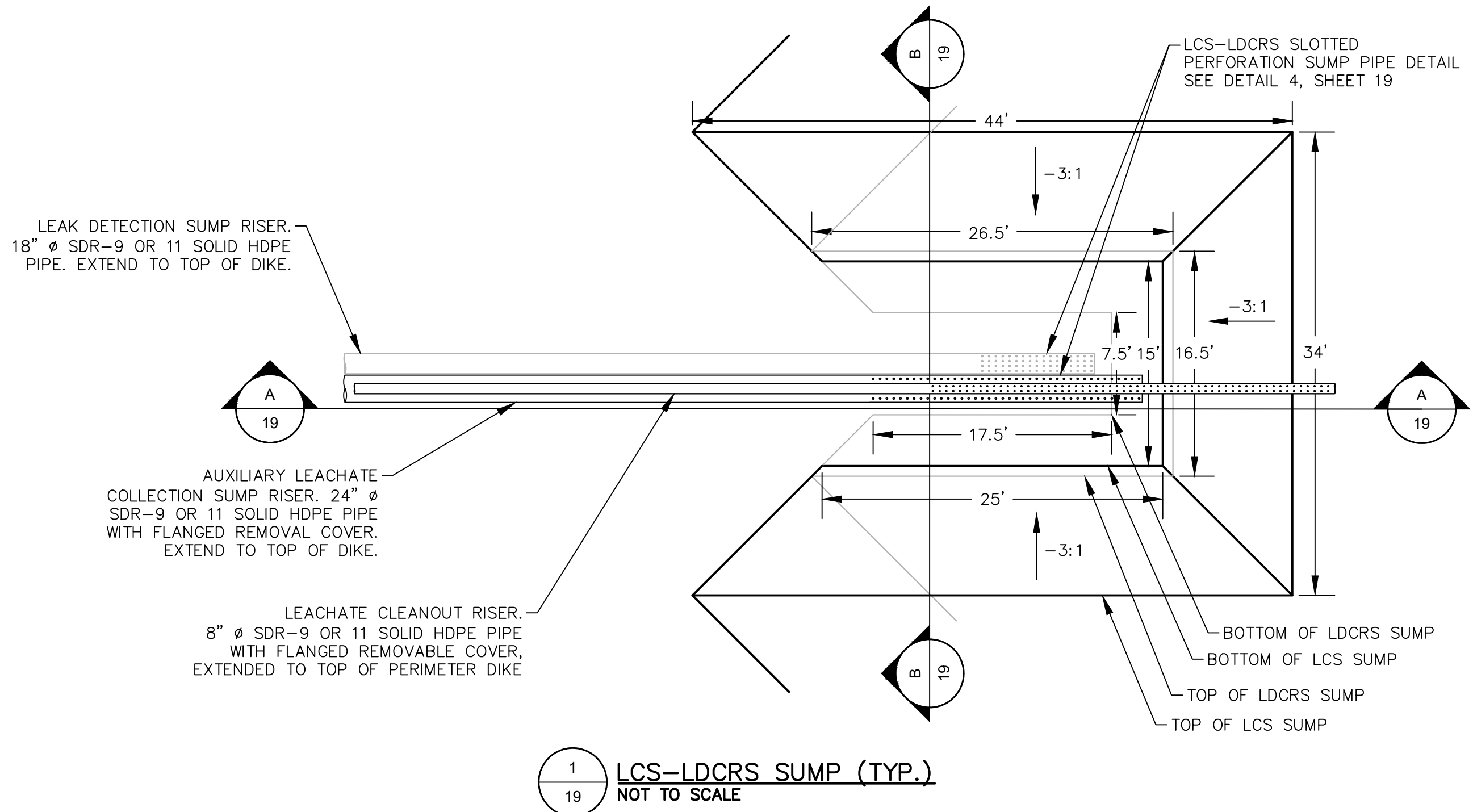
DATE:	05/17/21
DESIGNED BY:	BA
DRAWN BY:	WRG
CHECKED BY:	CAB
APPROVED BY:	XZ

CTI and Associates, Inc. 2800 Cabot Drive, Ste. 250 Farmington Hills, MI 48334 248.486.5100 (fax) 248.486.5050 www.cticompanies.com	
REV	DESCRIPTION
F	05/17/21 F1-F4 REVISIONS AND RESPONSE TO EGLE COMMENTS
E	5/29/18 ADDENDUM 1
D	5/08/18 REVISION BASED ON MDEQ'S COMMENTS
C	
B	
A	

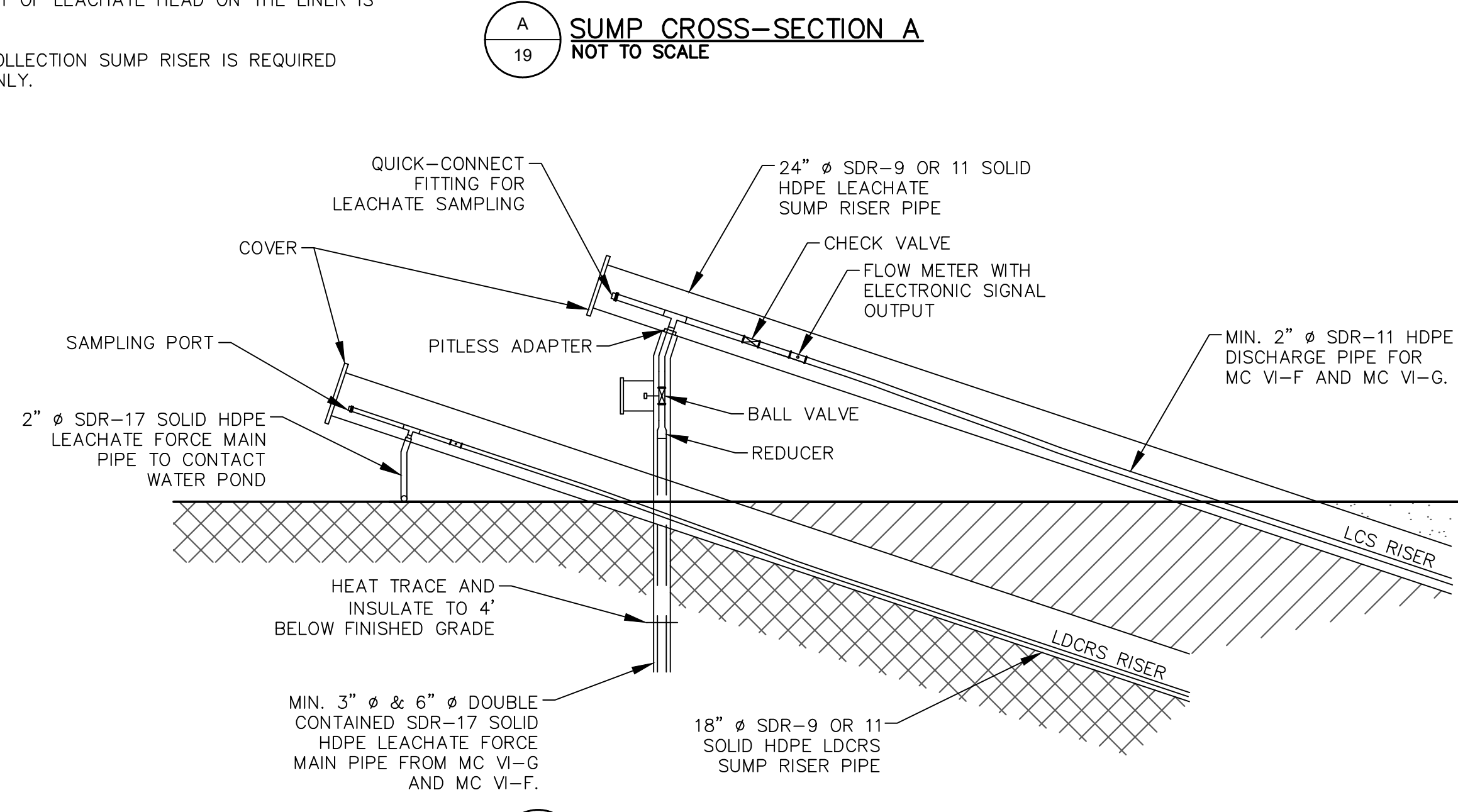
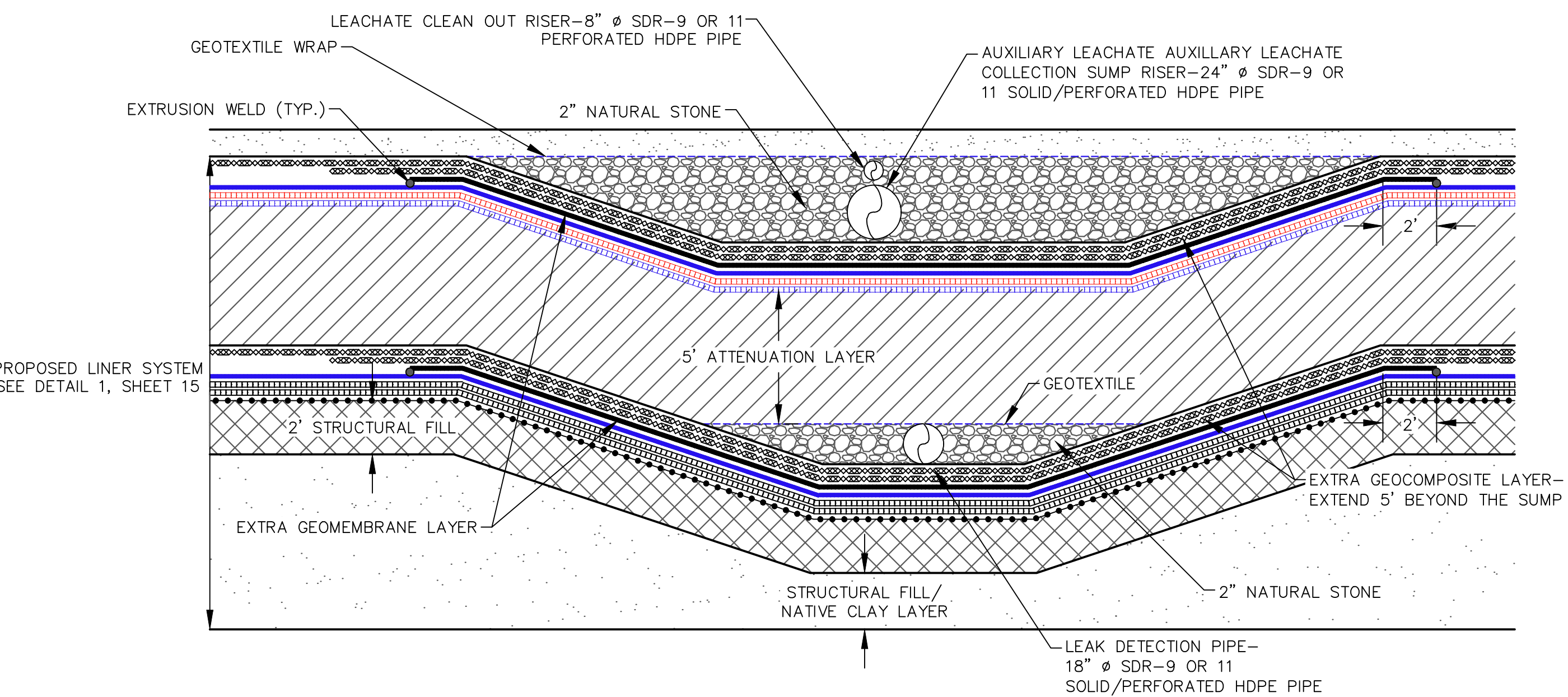
WAYNE DISPOSAL, INC. SITE NO. 2 - MASTER CELL VI-F&G
LEACHATE COLLECTION SYSTEM DETAILS (1 OF 2)
VAN BUREN TOWNSHIP, WAYNE COUNTY, MICHIGAN

LEACHATE COLLECTION SYSTEM DETAILS (1 OF 2)

PROJECT NUMBER	1208070039
SCALE	AS SHOWN
DRAWING NO.	18



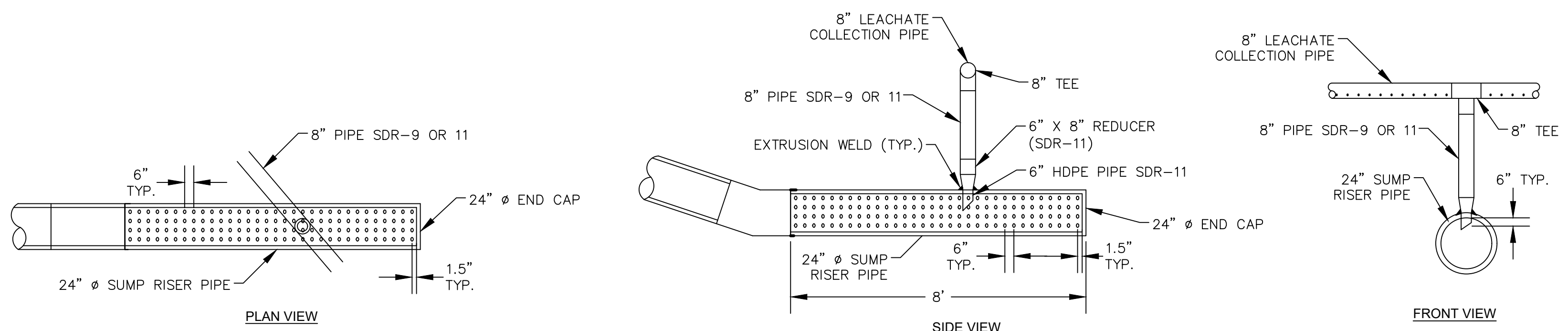
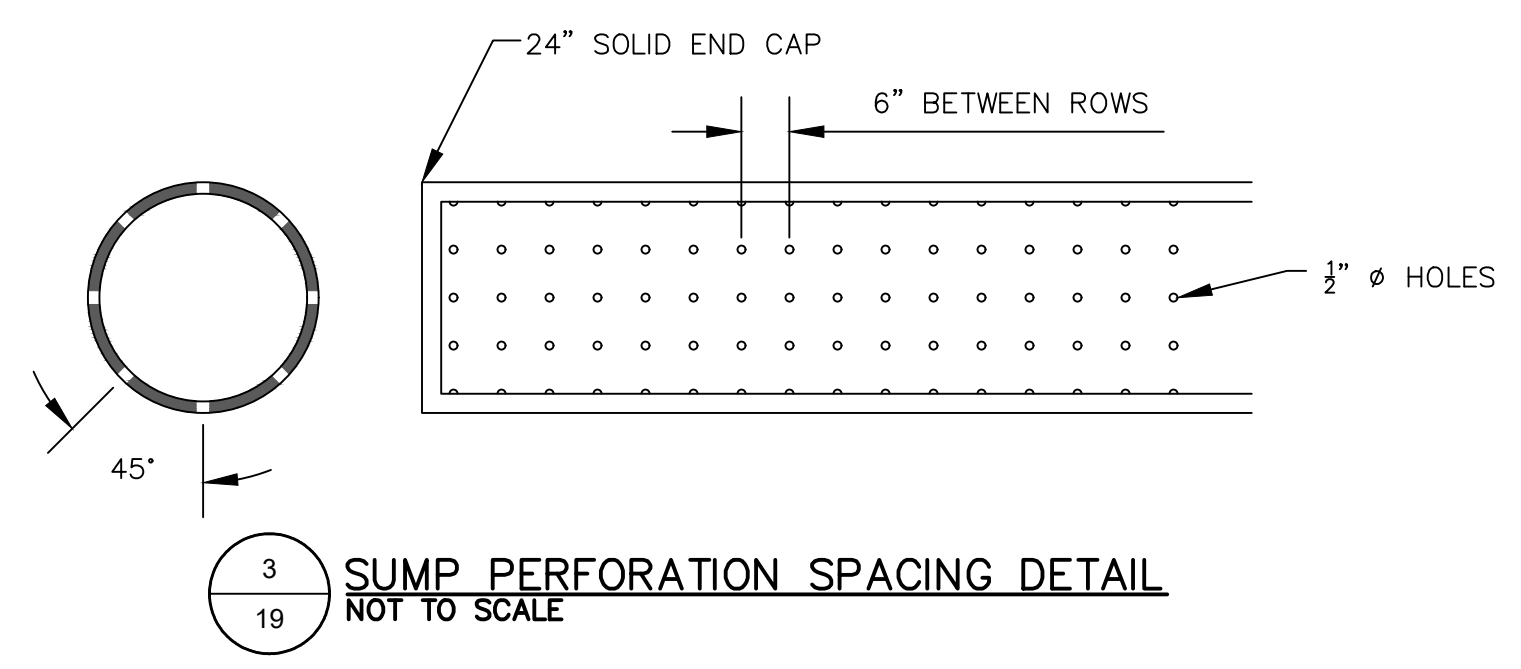
- NOTES:
- LDCRS "PUMP-ON" ELEV = TOP OF LDCRS SUMP
LDCRS "PUMP-OFF" ELEV = 1 FOOT ABOVE LDCRS SUMP BOTTOM
LCS "PUMP-ON" ELEV = LCS PIPE INVERT
LCS "PUMP-OFF" ELEV = 1 FOOT ABOVE LCS SUMP BOTTOM
 - OTHER "PUMP-ON"/"PUMP-OFF" CONTROLS MAY BE USED PROVIDED LESS THAN 1 FOOT OF LEACHATE HEAD ON THE LINER IS MAINTAINED
 - THE AUXILIARY LEACHATE COLLECTION SUMP RISER IS REQUIRED FOR THE MC VI-G1 SUMP ONLY.



Geosynthetic Materials

Material	Location	Description	Product	Additional Requirements
80-mil Geomembrane	Primary and secondary liners	80-mil HDPE, textured both sides	GSE HD textured, or equivalent	Interface friction requirements in CQA Plan
40-mil Geomembrane	Final cover	40-mil HDPE, textured both sides	GSE HD textured, or equivalent	Interface friction requirements in CQA Plan
Geosynthetic Clay Liner	Final cover and secondary liner	Sodium bentonite encapsulated between two geotextiles that are needle-punched or stitch-bonded together	CETCO Bentomat ST, or equivalent	Internal shear strength requirements in CQA Plan
Geosynthetic Clay Liner	Primary and secondary liners	Sodium bentonite encapsulated between two geotextiles that are needle-punched together	CETCO Bentomat DN, or equivalent	Internal shear strength requirements in CQA Plan
Geosynthetic Clay Liner	Primary liner	Sodium bentonite encapsulated between two geotextiles that are needle-punched and laminated to a geofilm	CETCO Bentomat CL, or equivalent	Internal shear strength requirements in CQA Plan
Geosynthetic Clay Liner	Primary Liner	Polymer-modified bentonite	CETCO Resistex 200 FLW9, or equivalent	Internal shear strength requirements in CQA Plan
Geocomposite	LCS and LDCRS	200-mil HDPE, bonded top and bottom to geotextile meeting requirements below	GSE FABRINET, or equivalent	Transmissivity and interface friction requirements in CQA Plan
Cover Geocomposite	Final cover	200-mil HDPE, bonded top and bottom to geotextile meeting requirements below	GSE FABRINET, or equivalent	Transmissivity and interface friction requirements in CQA Plan
Geonet	LCS and LDCRS sumps, and LDCRS collectors	200-mil HDPE	GSE HYPERNET, or equivalent	Transmissivity requirements in CQA Plan
Geotextile	All geocomposites, gravel/geotextile envelopes for LCS, and final cover perimeter drain	Nominal 8 oz/yd ² , needle-punched, non-woven polypropylene	Amoco 4508, Synthetic Industries Geotex 801, or equivalent	AASHTO M288-96 requirements for Drainage Geotextile (Class 2)
Geogrid	Above structural fill	Biaxial Polymeric Grid	Huesker Fortrac 80-80, or equivalent	None

LCS denotes leachate collection system
LDCRS denotes leak detection, collection, and removal system



CTI and Associates, Inc.
2800 Cabot Drive, Ste. 250
Livonia, MI 48150
248.486.5100 (fax) 248.486.5050
www.cticompanies.com

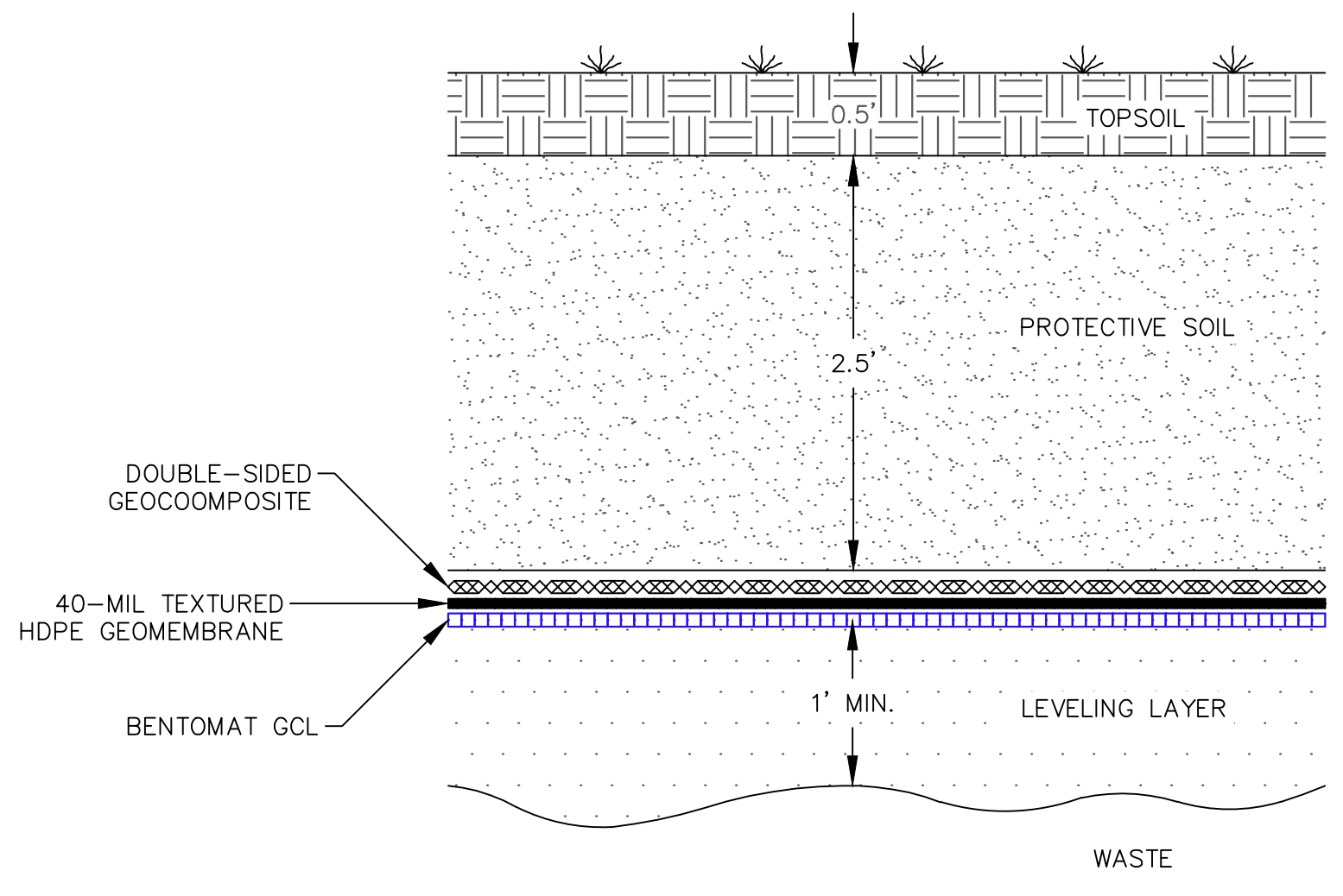
DATE: 05/17/21
DESIGNED BY: BA
DRAWN BY: WRG
CHECKED BY: CAB
APPROVED BY: XZ

PROJECT NUMBER: 1208070039
SCALE: AS SHOWN
DRAWING NO: 19

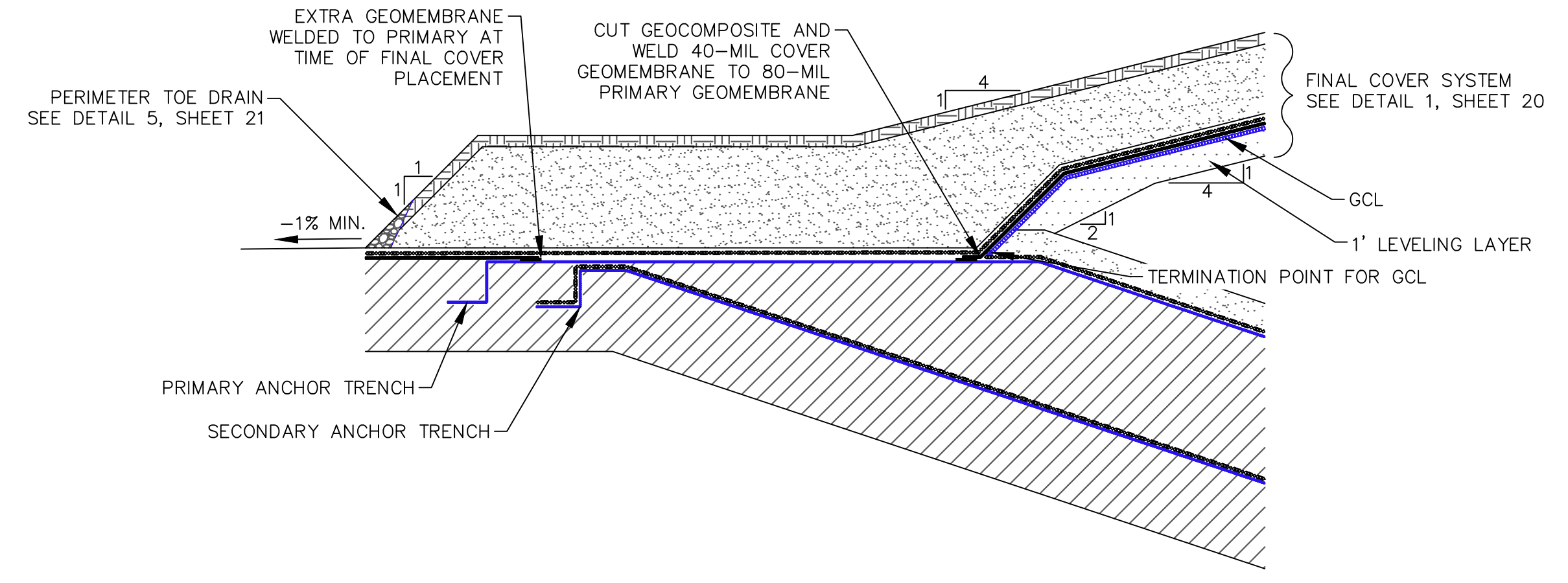
WAYNE DISPOSAL, INC. SITE NO. 2 - MASTER CELL VI-F&G
LEACHATE COLLECTION SYSTEM DETAILS (2 OF 2)
VAN BUREN TOWNSHIP, WAYNE COUNTY, MICHIGAN

LEACHATE COLLECTION SYSTEM DETAILS (2 OF 2)

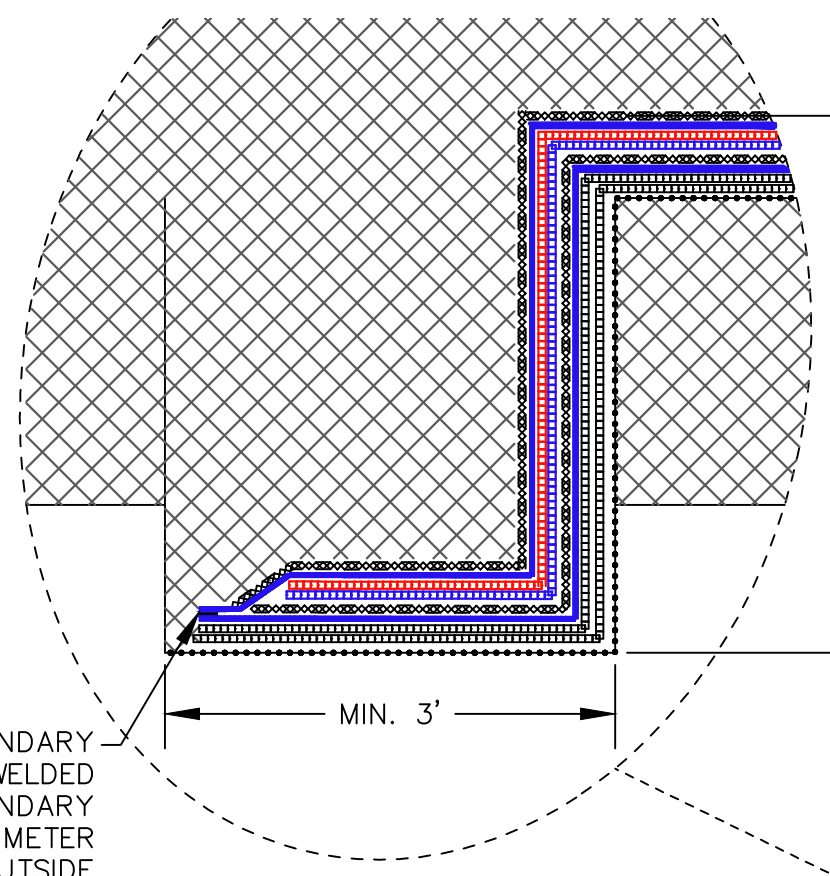
REV	DATE	DESCRIPTION
F	05/17/21	F1-F4 REVISIONS AND RESPONSE TO EGLE COMMENTS
B	9/23/11	PER MICRO COMMENTS
D		
W		
XZ		



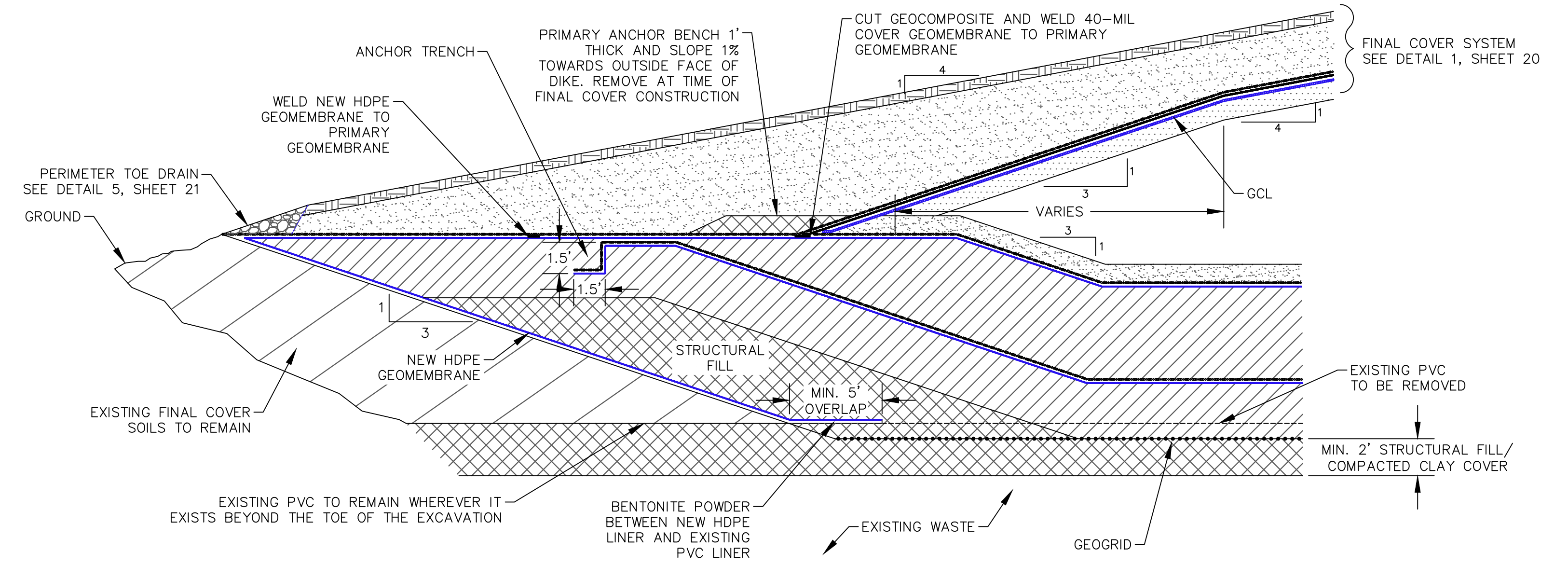
1
20
FINAL COVER SYSTEM
1'-2'



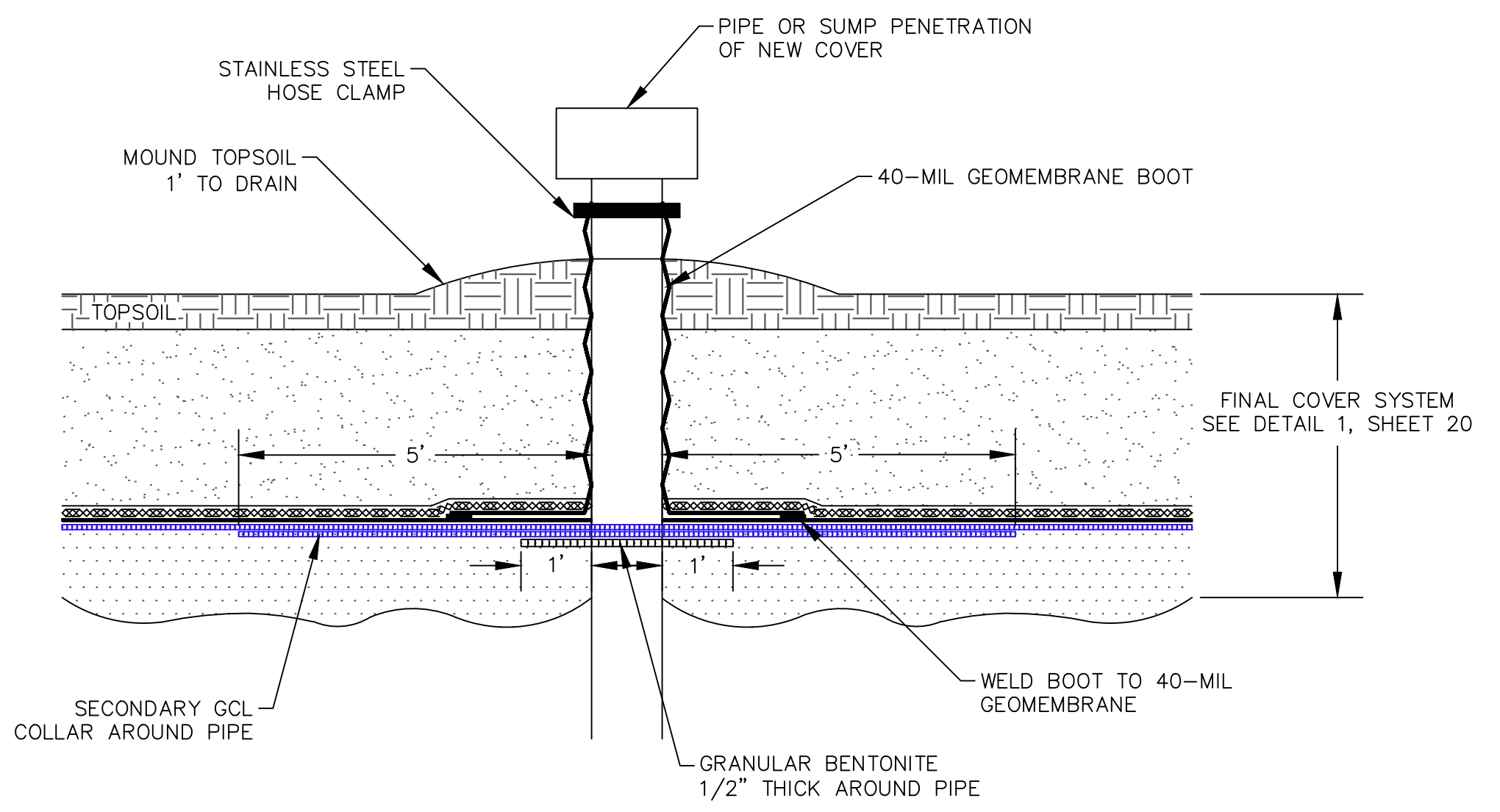
2
20
FINAL COVER TIE-IN DETAIL
MC VI-AN, AS, C & D
NOT TO SCALE



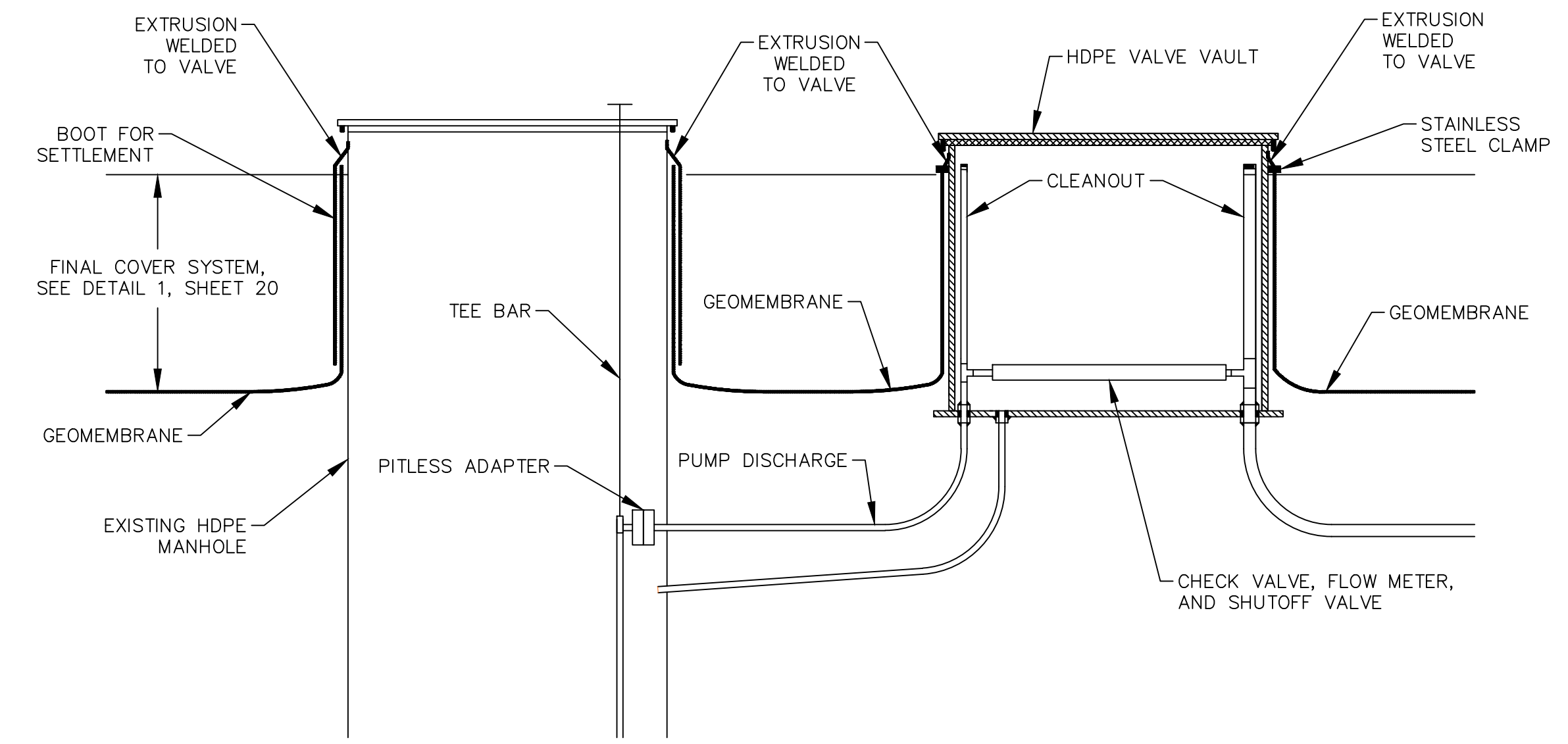
3
20
DIKE AND COVER TIE-IN DETAIL (TYP.)
MC VI-F, MC VI-G, & EAST SIDE OF MC VI-E
NOT TO SCALE



4
20
DIKE AND COVER TIE-IN DETAIL
NORTH SIDE OF MC VI-E
NOT TO SCALE

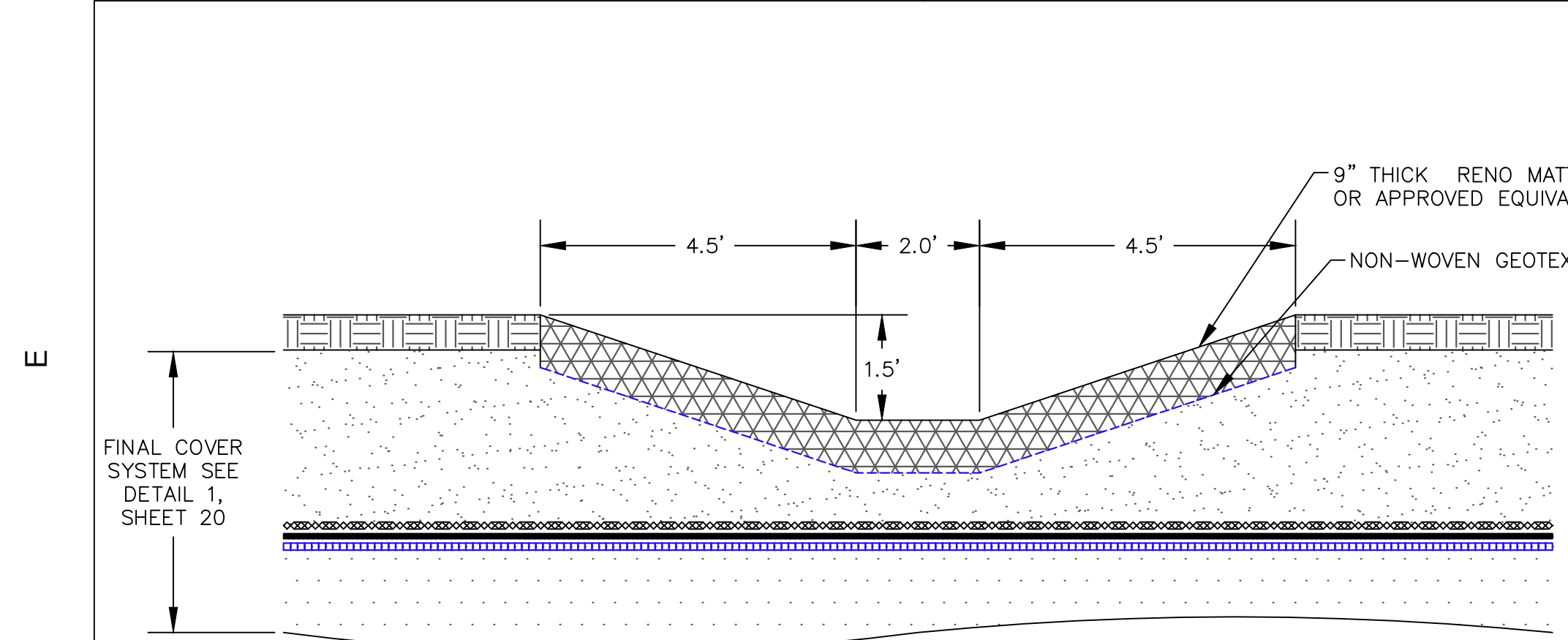


5
20
FINAL COVER PENETRATION DETAIL (TYP.)
NOT TO SCALE

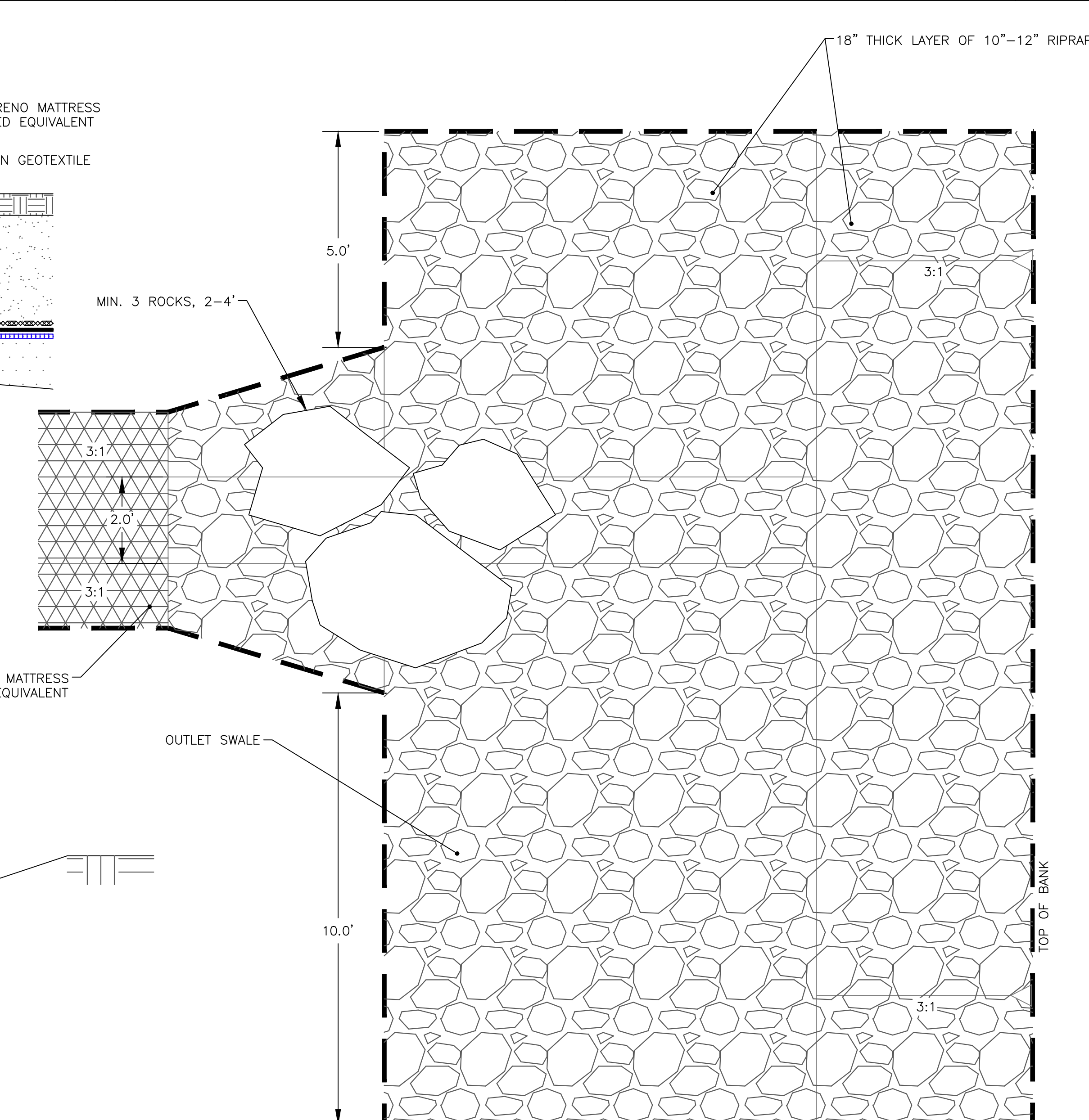


6
20
LEACHATE SUMP RISER PIPING DETAIL
(MC VI-AN, AS, B, C, & D RISERS)
NOT TO SCALE

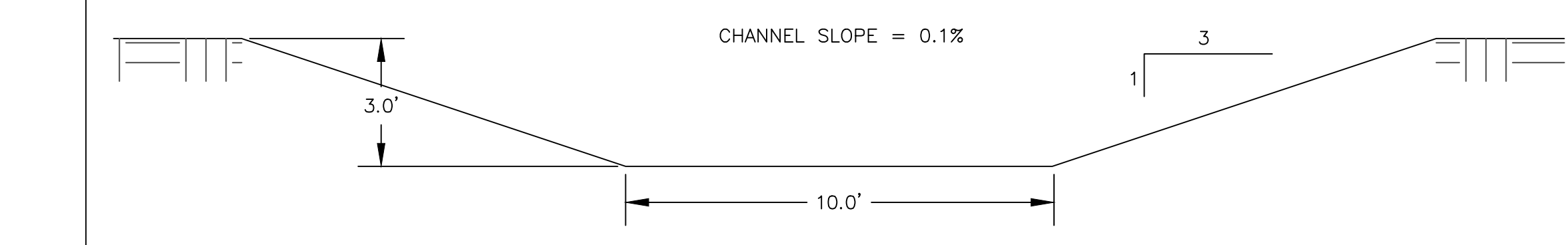
DATE:	05/17/21	
DESIGNED BY:	BA	
DRAWN BY:	WRG	
CHECKED BY:	CAB	
APPROVED BY:	XZ	
CTE and Associates, Inc. 28001 Cabot Drive, Ste. 250 248.486.5100 (fax) 248.486.5050 www.ctecompanies.com		
This drawing was prepared by CTE and Associates, Inc. (CTE) and is the property of CTE. It is to be used only for the project and location specified. CTE does not warrant the accuracy or completeness of the information provided. CTE is not responsible for any errors or omissions in this drawing. The user of this drawing shall be responsible for verifying the accuracy and completeness of the information provided. CTE is not responsible for any errors or omissions in this drawing. The user of this drawing shall be responsible for verifying the accuracy and completeness of the information provided.		
REV	DATE	DESCRIPTION
F	05/17/21	F1-F4 REVISIONS AND RESPONSE TO EGLE COMMENTS
E		
D		
C		
B		
A		
WAYNE DISPOSAL, INC. SITE NO. 2 - MASTER CELL VI-F&G FINAL COVER DETAILS VAN BUREN TOWNSHIP, WAYNE COUNTY, MICHIGAN		
PROJECT NUMBER 1208070039		
SCALE AS SHOWN		
DRAWING NO 20		



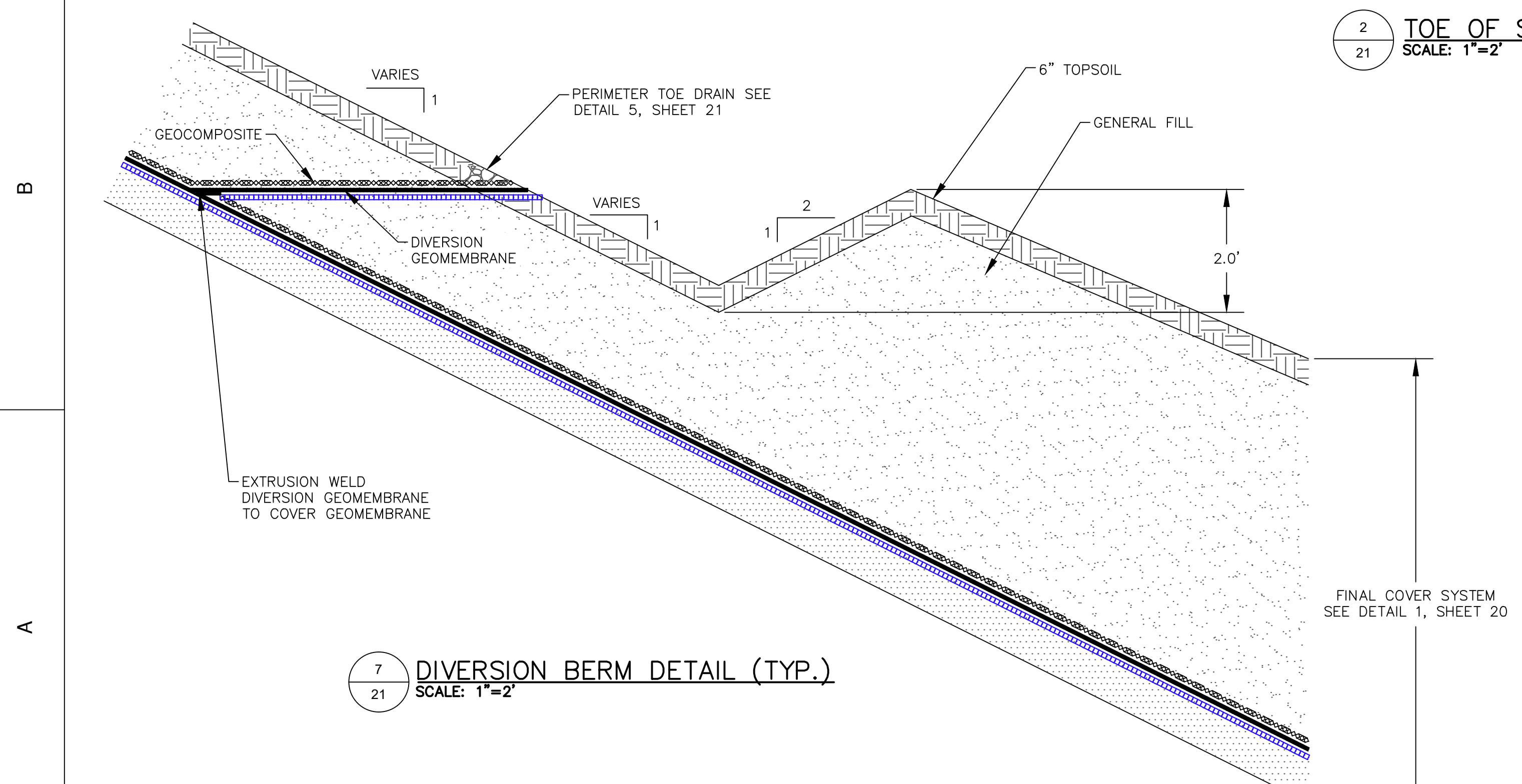
1 TYPICAL DOWNSLOPE SPILLWAY DETAIL
SCALE: 1"=2'



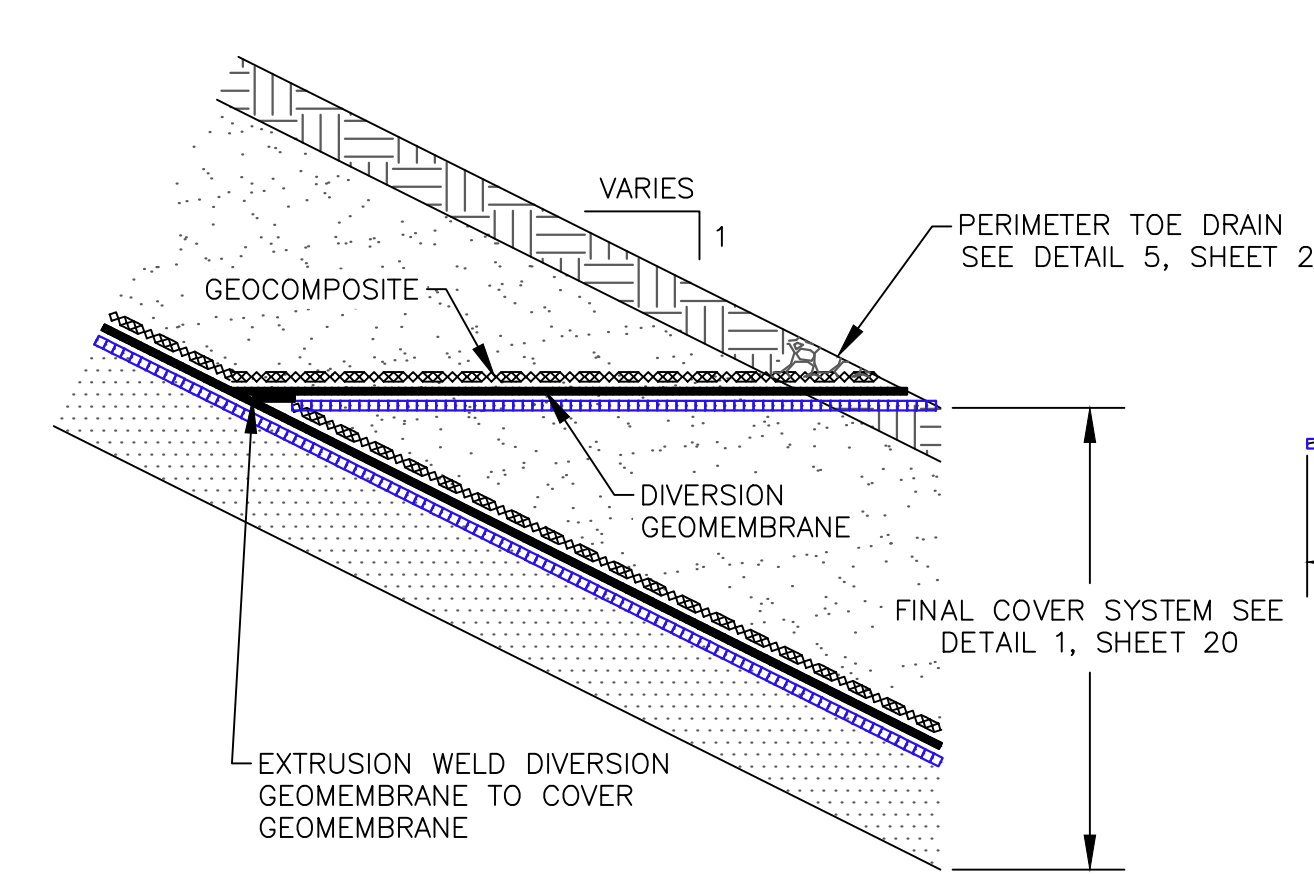
2 TOE OF SPILLWAY DOWNSLOPE CHANNEL
SCALE: 1"=2'



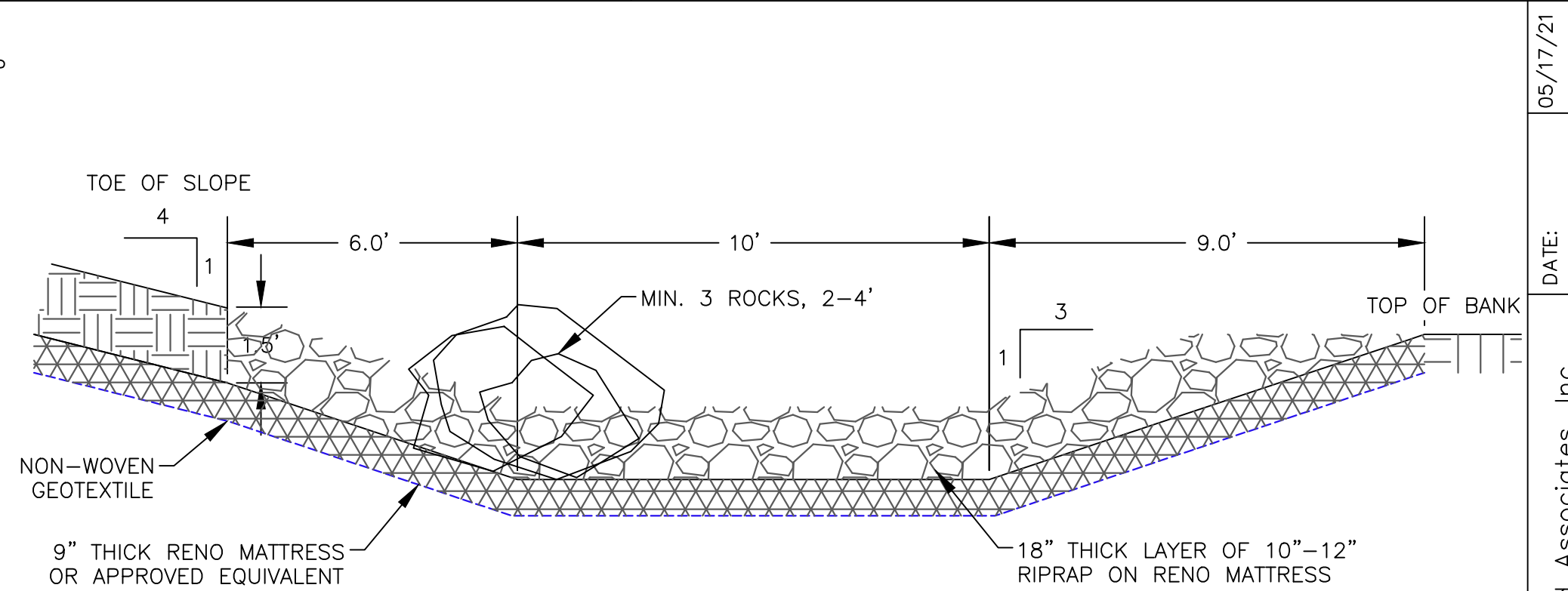
4 OUTLET SWALE CROSS SECTION (TYP.)
SCALE: 1"=3'



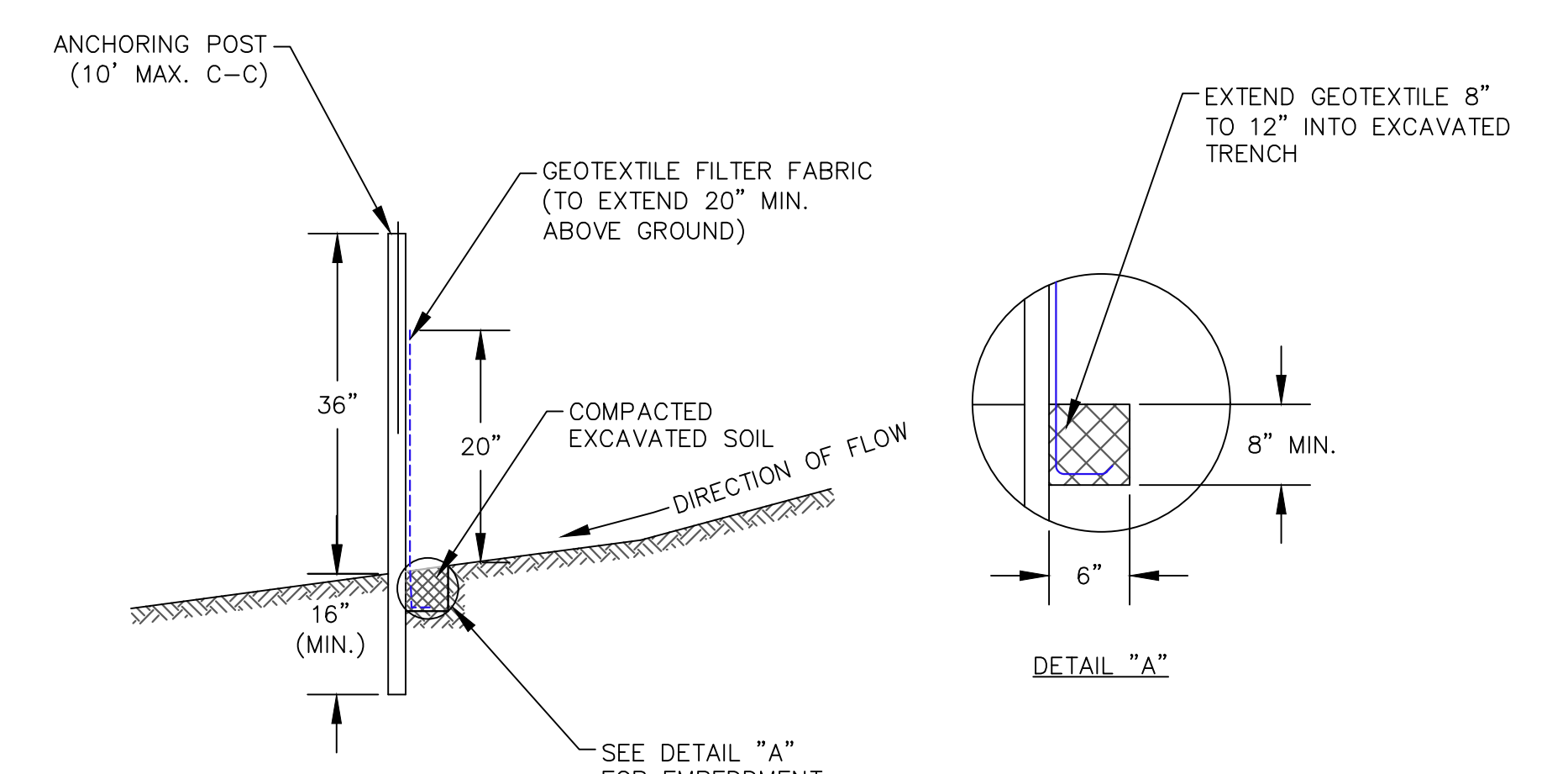
7 DIVERSION BERM DETAIL (TYP.)
SCALE: 1"=2'



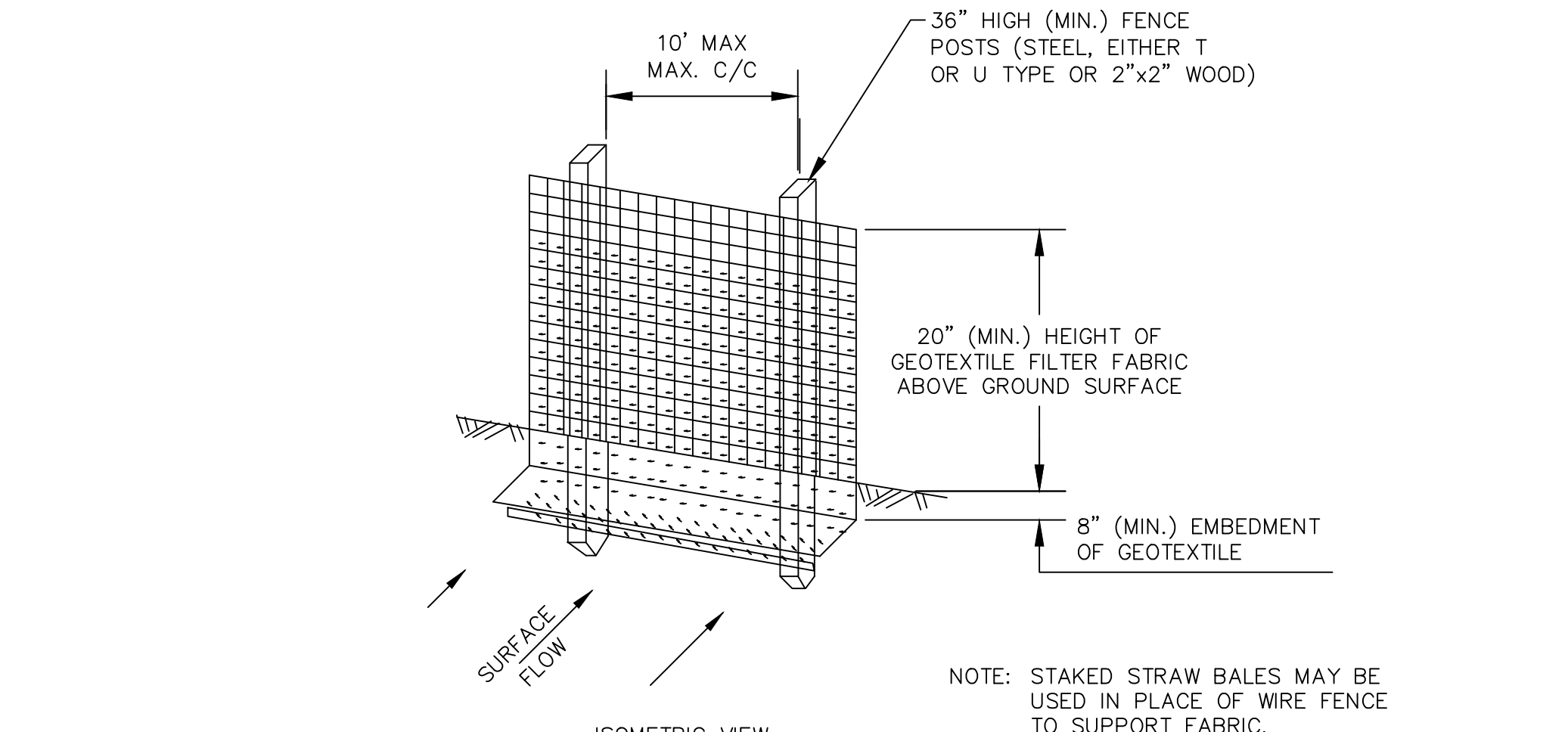
8 DIVERSION GEOMEMBRANE DETAIL (TYP.)
SCALE: 1"=2'



3 TOE OF SPILLWAY PROFILE
SCALE: 1"=3'



6 SILT FENCE DETAIL (TYP.)
SCALE: 1"=1'



5 PERIMETER TOE DRAIN
SCALE: 1"=1'

CTI and Associates, Inc.
2800 Cabot Drive, Ste. 250
Farmington Hills, MI 48334
248.486.5100 (fax) 248.486.5050
www.cticompanies.com

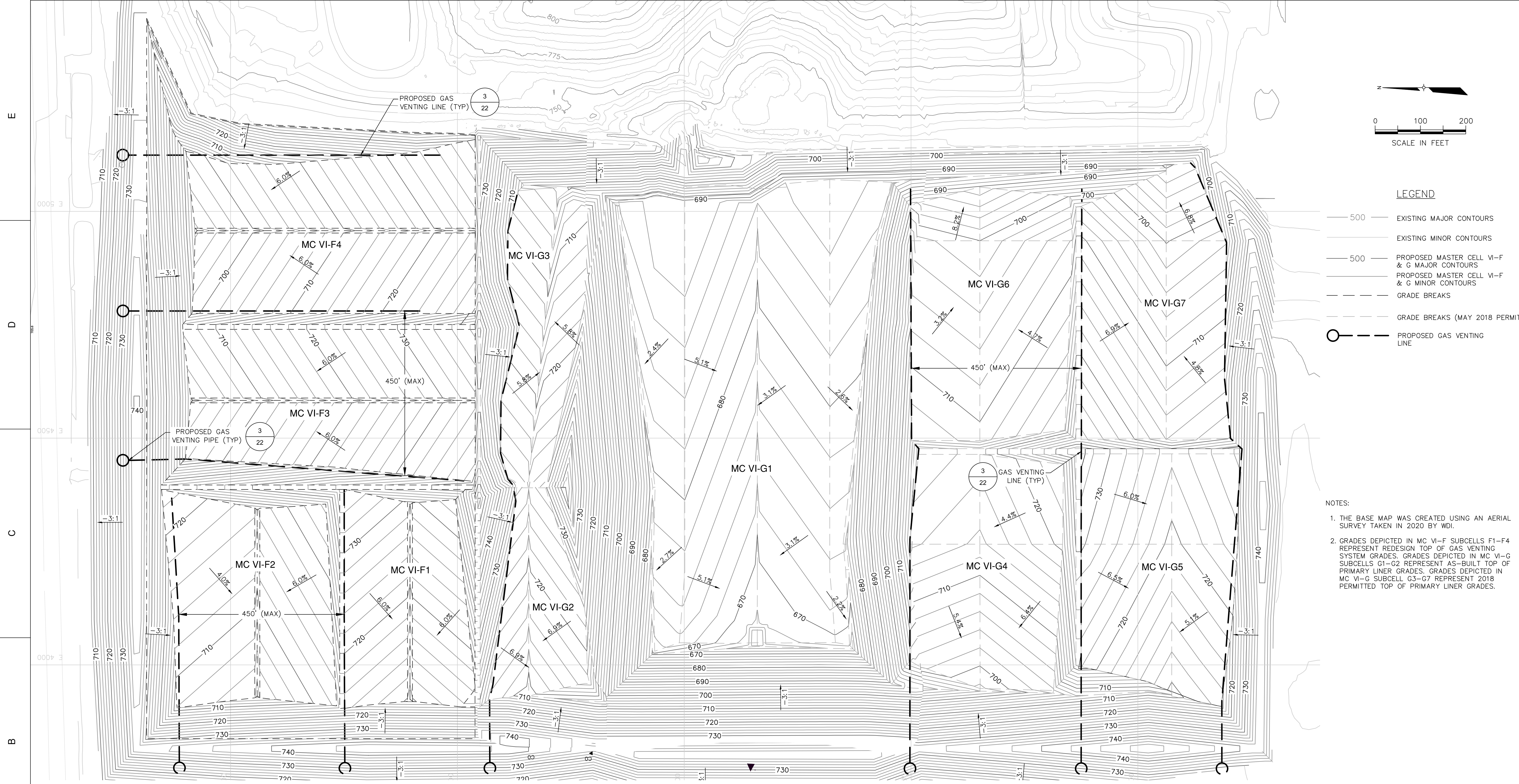
DATE: 05/17/21
DESIGNED BY: BA
DRAWN BY: WRG
CHECKED BY: CAB
APPROVED BY: XZ

PROJECT NUMBER: 1208070039
SCALE: AS SHOWN
DRAWING NO: 21

WAYNE DISPOSAL, INC. SITE NO. 2 - MASTERCELL VI-F&G
STORMWATER MANAGEMENT SYSTEM DETAILS
VAN BUREN TOWNSHIP, WAYNE COUNTY, MICHIGAN

STORMWATER MANAGEMENT SYSTEM DETAILS

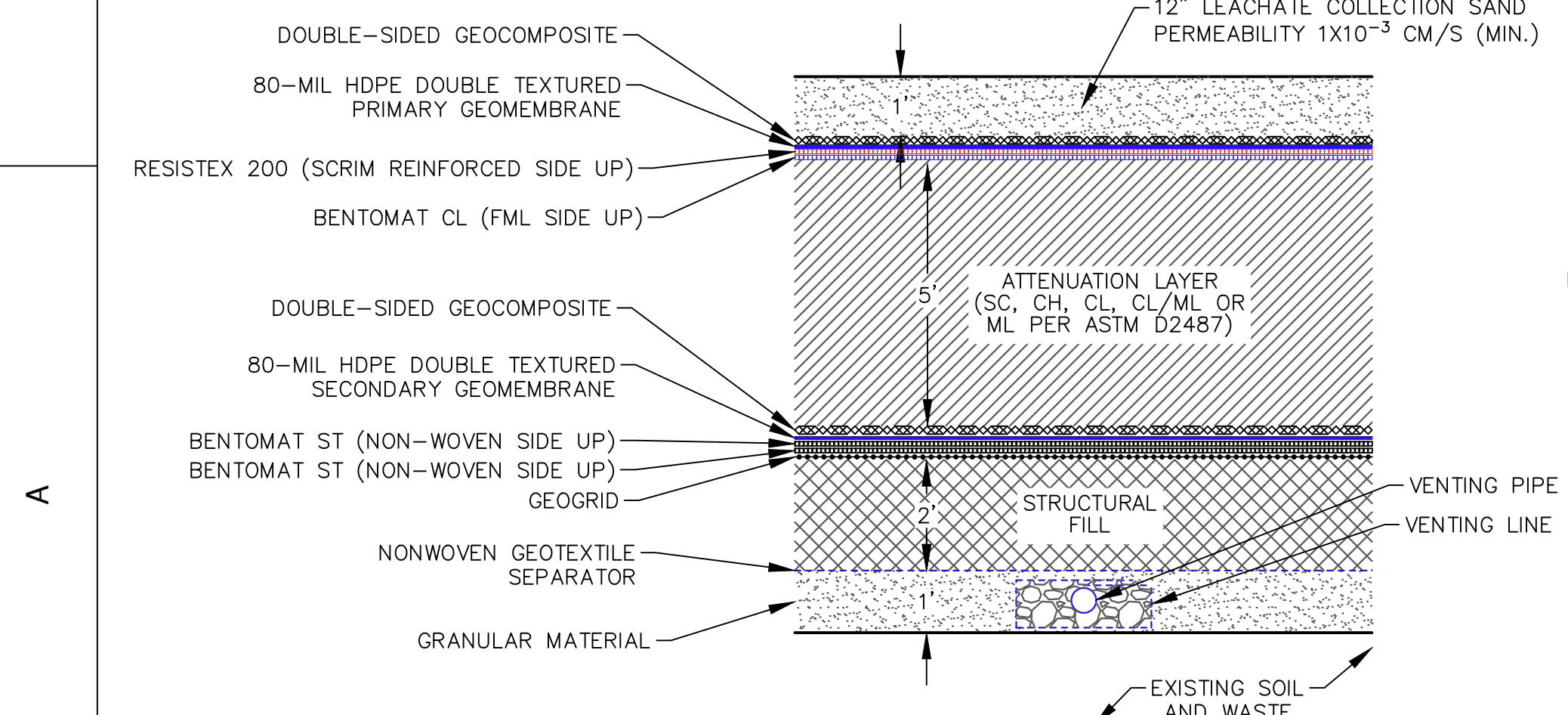
REV	DATE	DESCRIPTION
F	05/17/21	E1-F4 REVISIONS AND RESPONSE TO EGLE COMMENTS
DN		APP
WRG		XZ



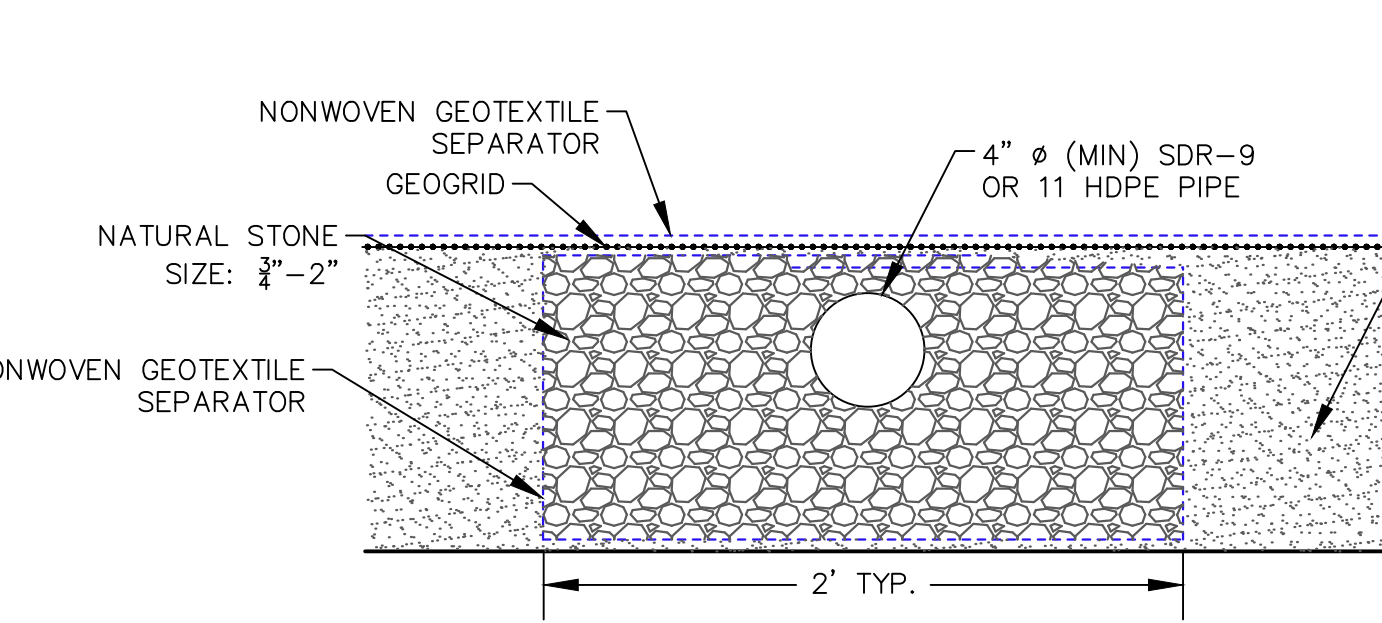
- LEGEND**
- 500 — EXISTING MAJOR CONTOURS
 - — EXISTING MINOR CONTOURS
 - 500 — PROPOSED MASTER CELL VI-F & G MAJOR CONTOURS
 - — PROPOSED MASTER CELL VI-F & G MINOR CONTOURS
 - - - GRADE BREAKS
 - - - GRADE BREAKS (MAY 2018 PERMIT)
 - - - - PROPOSED GAS VENTING LINE

- NOTES:**
- THE BASE MAP WAS CREATED USING AN AERIAL SURVEY TAKEN IN 2020 BY WDI.
 - GRADES DEPICTED IN MC VI-F SUBCELLS F1-F4 REPRESENT REDESIGN TOP OF GAS VENTING SYSTEM GRADES. GRADES DEPICTED IN MC VI-G SUBCELLS G1-G2 REPRESENT AS-BUILT TOP OF PRIMARY LINER GRADES. GRADES DEPICTED IN MC VI-G SUBCELLS G3-G7 REPRESENT 2018 PERMITTED TOP OF PRIMARY LINER GRADES.

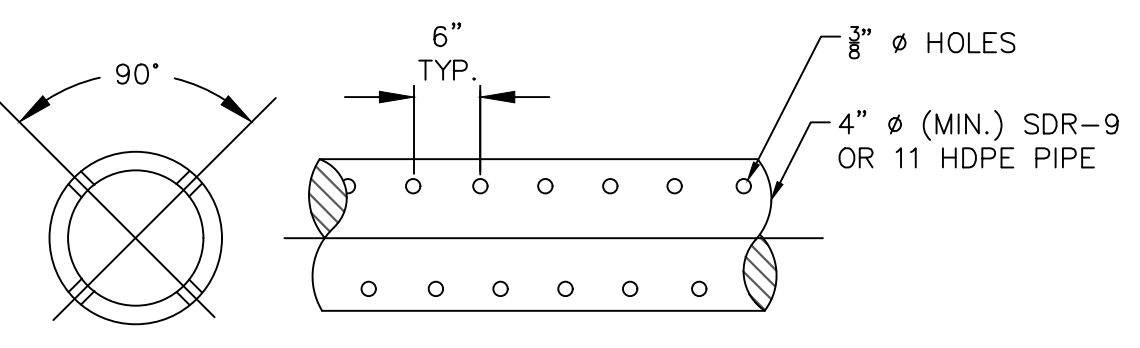
DATE:	05/17/21	DESIGNED BY:	BA
DRAWN BY:	WFG	CHECKED BY:	CAB
APPROVED BY:	XZ		
CTI and Associates, Inc. 2800 Cabot Drive, Ste. 250 248.486.5100 (fax) 248.486.5050 www.cticompanies.com			
<small>This drawing was prepared by C.T.I. Associates, Inc. (CTI) and is the property of C.T.I. Associates, Inc. It is to be used only for the project and location specified. No part of this drawing shall be reproduced, stored in a retrieval system, or transmitted in any form or by any means, electronic, mechanical, photocopying, recording, or by any information storage and retrieval system, without the prior written permission of C.T.I. Associates, Inc. The user of this drawing shall be responsible for obtaining all necessary permits and approvals from the appropriate authorities. The user shall indemnify and hold C.T.I. Associates, Inc. harmless from and against all claims, damages, and expenses, including reasonable attorneys' fees, arising from or due to the use of this drawing.</small>			
REV	DATE	REVISION DESCRIPTION	
F	05/17/21	F1-F4 REVISIONS AND RESPONSE TO EGLE COMMENTS	
E	5/29/18	ADDENDUM 1	
C	5/02/18	SUBCELLS G2 AND G3 REVISIONS	



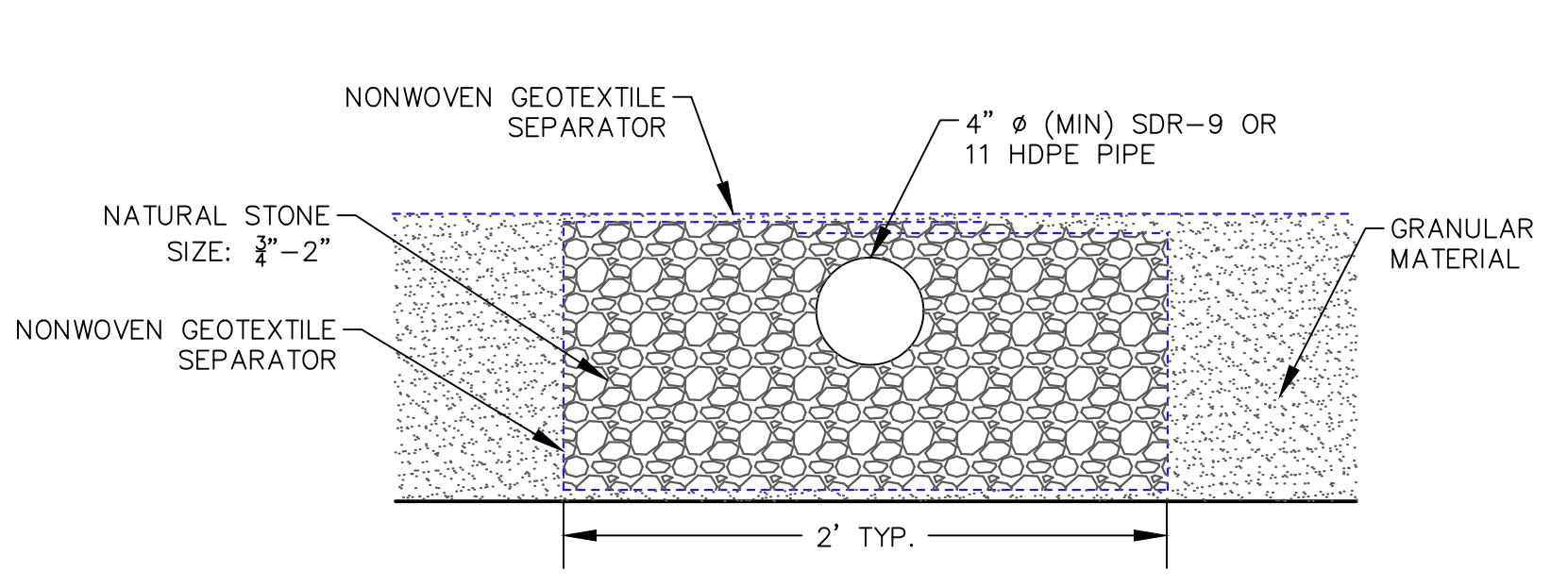
1 PROPOSED VENTING SYSTEM FOR SUBCELLS F1-4 AND G3-7
NOT TO SCALE



2A PROPOSED FLOOR LINER SYSTEM
NOT TO SCALE



3 VENTING PIPE DETAIL
NOT TO SCALE



2B VENTING LINE DETAIL FOR SUBCELLS F1-4 AND G3-7
NOT TO SCALE

WAYNE DISPOSAL, INC. SITE NO. 2 - MASTER CELL VI-F&G
CONCEPTUAL GAS VENTING SYSTEM
VAN BUREN TOWNSHIP, WAYNE COUNTY, MICHIGAN

PROJECT NUMBER
1208070039
SCALE
AS SHOWN
DRAWING NO.

Attachment 7

**Additional Information - Ladd (1991) Stability During Staged
Construction Terzaghi Lecture**

STABILITY EVALUATION DURING STAGED CONSTRUCTION

By Charles C. Ladd,¹ Fellow, ASCE

(The Twenty-Second Karl Terzaghi Lecture)

TABLE OF CONTENTS

1. Introduction
2. Background
 - 2.1 Stability Problems Classified According to Drainage and Loading Conditions
 - 2.2 Types of Limiting Equilibrium Stability Analyses
 - 2.3 Stability Analyses for Staged Construction: Historical Perspective
 - 2.4 Undrained Strength Analysis (USA)
 - 2.5 Definition of Undrained Shear Strength
3. Comparison of Effective Stress versus Undrained Strength Stability Analyses during Staged Construction
 - 3.1 Conventional Effective Stress Analysis
 - 3.2 Conceptual Comparison
 - 3.3 Methodology for Case Histories of Embankment Staged Construction
 - 3.4 Embankment on Connecticut Valley Varved Clay
 - 3.5 Embankment Dam on James Bay Sensitive Clay
 - 3.6 Upstream Tailings Dam
 - 3.7 Conclusions from Case Histories
 - 3.8 Overview of Current Practice
4. Soil Behavioral Issues
 - 4.1 Preconsolidation Pressure: Significance
 - 4.2 Preconsolidation Pressure: Evaluation
 - 4.3 Factors Affecting Consolidated–Undrained Strength Testing
 - 4.4 Sample Disturbance and Reconsolidation Techniques
 - 4.5 Time Effects
 - 4.6 Stress Systems for CK_0U Test Programs
 - 4.7 Components and Causes of Anisotropy
 - 4.8 Effects of Anisotropy
 - 4.9 Progressive Failure and Strain Compatibility
 - 4.10 Comparison of Field and Laboratory Strengths
 - 4.11 Strength Gain during Staged Construction
5. Recommended Methodology for Undrained Strength Analyses
 - 5.1 Overview
 - 5.2 Evaluation of Stress History and Consolidation Analyses
 - 5.3 Laboratory Strength Testing
 - 5.4 Stability Analyses
 - 5.5 Comments on Design Process

¹Prof. of Civ. Engrg., Massachusetts Inst. of Tech., Cambridge, MA 02139.

Note. Discussion open until September 1, 1991. To extend the closing date one month, a written request must be filed with the ASCE Manager of Journals. The manuscript for this paper was submitted for review and possible publication on September 9, 1990. This paper is part of the *Journal of Geotechnical Engineering*, Vol. 117, No. 4, April, 1991. ©ASCE, ISSN 0733-9410/91/0004-0540/\$1.00 + \$.15 per page. Paper No. 25705.

6. Alternative Approaches for Stability Analyses
 - 6.1 Stability Problems Classified According to Drainage Conditions and Definition of Factor of Safety
 - 6.2 QRS Methodology
 - 6.3 "Undrained" Effective Stress Analyses
 - 6.4 Some General Comments
7. Monitoring Field Performance
 - 7.1 Field Instrumentation
 - 7.2 Evaluating Consolidation Behavior
 - 7.3 Evaluating Foundation Stability
8. Summary and Conclusions
9. Acknowledgments
10. Appendix I. References
11. Appendix II. Notation

ENGINEERING SOCIETIES LIBRARY

MAR 26 1991

ABSTRACT: Staged construction uses controlled rates of load application to increase the foundation stability of structures founded on soft cohesive soils and to improve the slope stability of tailings dams. Because construction causes positive excess pore pressures and because actual failures usually occur without significant drainage, stability analyses should compute the factor of safety against an undrained failure as the most critical and realistic condition. This requires an undrained strength analysis (USA) that treats predicted or measured in situ effective stresses as equal to consolidation stresses in order to calculate variations in undrained shear strength during construction. The recommended USA methodology requires a detailed evaluation of changes in vertical stress history profiles, uses undrained strength ratios obtained from CK_0U tests to account for anisotropy and progressive failure, and is more rational than stability evaluations based on UU and CIU triaxial compression testing. Conventional effective stress analyses should not be used for staged construction because the computed factor of safety inherently assumes a drained failure that can give highly misleading and unsafe estimates of potential instability.

1. INTRODUCTION

This paper concerns techniques to assess stability under static loads for projects characterized as follows:

1. "Soft-ground" construction, meaning that the imposed *loading* is sufficiently large to stress the cohesive *foundation* soils beyond their preconsolidation pressure and hence well into the normally consolidated range. Examples include embankments for transportation facilities, flood-control levees, water-retention and tailings dams, refuse landfills, storage tanks, and offshore gravity platforms.
2. Tailings dams constructed for the purpose of storing cohesive waste products from mining operations, especially those using the more economical upstream method to contain the so-called "slimes" (Vick 1983).

Since these projects generate positive excess pore water pressures within the underlying foundation soils or within the slimes, the most critical stability condition occurs during actual construction. In other words, drainage due to consolidation after each load application will progressively strengthen the most highly stressed soils and hence increase the factor of safety against a shear induced failure.

In particular, the paper treats stability evaluation wherein the project design entails controlled rates of loading so that soil strengthening due to consolidation is sufficient to support the maximum required load safely. Such "staged construction" involves either a continuous, controlled rate of load application (e.g., during water testing of a storage tank or construction of a landfill or an upstream tailings dam) or construction in two or more stages (e.g., embankment filling over several seasons), or a combination of both. These projects may also include other techniques to improve stability during construction, prime examples being the installation of vertical drains to accelerate the rate of consolidation and the addition of temporary stability berms.

As will be demonstrated, considerable controversy and confusion exist concerning what type of stability analysis should be used for staged construction projects, both during the design process and later to check stability during actual construction. Stability evaluations to assess the safety of *existing* structures also face this same technical issue. The paper first reviews background material regarding stability problems classified according to their drainage conditions and describes three types of stability analysis: (1) The common "total stress analysis"; (2) the common "effective stress" analysis;

and (3) a hybrid of these called an “undrained strength” analysis. Two divergent approaches to evaluate stability during staged construction are then examined, where it will become evident that the real issue concerns the assumed (or implied) drainage condition during potential failure. Three case histories illustrate the practical importance of this critical assumption. The remaining parts of the paper then focus on soil behavioral issues related to predicting undrained strengths during staged construction, recommended techniques for executing “undrained strength analyses,” examination of alternative approaches (especially U.S. practice based on results from triaxial compression testing), and recommendations regarding field instrumentation to monitor construction.

2. BACKGROUND

2.1. Stability Problems Classified According to Drainage and Loading Conditions

Stability problems have historically been divided into three categories according to the drainage conditions that either exist or are considered critical during construction and during a potential failure. It is further useful to distinguish between *loading* versus *unloading* problems to differentiate construction that causes the total normal stresses acting within the soil mass to increase or decrease, respectively (Lambe and Whitman 1969). Staged construction projects inherently involve loading problems, whereas excavations entail unloading.

Case 1—Undrained (Also Called Short-Term or End-of-Construction)

This case denotes situations wherein both construction and failure occur rapidly enough to preclude significant drainage. Since there is negligible change in water content, the initial in situ undrained shear strength of the cohesive soil controls stability during construction. It represents the critical condition for loading problems since the factor of safety increases with time due to consolidation.

Case 2—Drained (Also Called Long-Term)

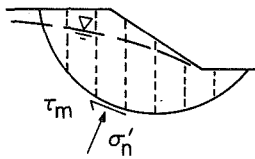
This case represents the opposite extreme, in that the excess pore pressures caused by loading (or unloading) have dissipated ($u_e = 0$) due to a slow rate of construction or sufficient time after construction, and the shear induced pore pressures are also zero ($u_s = 0$) due to a slow rate of shearing during failure. Stability is therefore controlled by the drained strength of the soil corresponding to equilibrium (long-term) pore pressures. This case represents the critical condition for unloading problems that generate negative excess pore pressures ($u_e < 0$) during construction (e.g., excavations in stiff clays) since the factor of safety decreases with time due to swelling.

Brinch-Hansen (1962) proposed renaming the short-term/long-term classifications as UU and CD failures because of their direct analogy to laboratory unconsolidated-undrained and consolidated-drained shear tests, respectively. The writer adopts that notation.

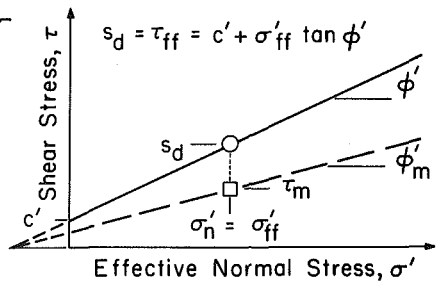
Case 3—Partially Drained (Also Called Intermediate)

This case applies to staged construction since loading problems produce positive excess pore pressures ($u_e > 0$) and hence decreases in water content

(a) EXCAVATION IN STIFF CLAY



(b) STRESSES AND SHEAR STRENGTH FOR AVERAGE ELEMENT



(c) DEFINITION OF FACTOR OF SAFETY (Bishop 1955; Janbu 1973)

$$FS = \frac{s_d}{\tau_m} = \frac{\tau_{ff}}{\tau_m} = \frac{\tan \phi'}{\tan \phi'_m}$$

FIG. 1. Conventional Effective Stress Analysis Applied to Critical CD Case for Unloading Problem

during construction. However, the types of analyses currently used to assess stability during staged construction make different assumptions regarding the drainage conditions during a potential failure. Specifically, will failure occur so slowly that it approaches a drained condition or will it occur so rapidly that it approaches an undrained condition? In other words, will the shear induced pore pressure be essentially zero ($u_s \rightarrow 0$) or significantly greater than zero? As later shown, this question basically entails treating staged construction either as a consolidated-drained or a consolidated-undrained failure, i.e., a CD case versus a CU case according to Brinch-Hansen's (1962) notation.

2.2. Types of Limiting Equilibrium Stability Analysis

This topic refers to the approach employed to compute the available shear strength and the resulting factor of safety for failure surfaces in cohesive soils when using a method of slices. Three types of analysis are considered here: (1) An effective stress analysis (ESA); (2) a total stress analysis (TSA); and (3) an undrained strength analysis (USA). The ESA and TSA types are first defined via their conventional application to unloading and loading problems, respectively. The paper then reviews common approaches for staged construction, leading to a description of an undrained strength analysis, which basically computes in situ undrained shear strengths as a function of the preshear effective (consolidation) stresses.

As illustrated in Fig. 1, a conventional effective stress analysis computes the available shear strength, $s_d = \tau_{ff}$, along a potential failure surface using

$$\tau_{ff} = c' + \sigma'_{ff} \tan \phi' \dots \dots \dots (1)$$

where c' and ϕ' define the Mohr-Coulomb effective stress failure envelope; and τ_{ff} and σ'_{ff} = the shear stress and effective normal stress on the failure plane at failure, respectively. In turn

$$\sigma'_{ff} = \sigma_{ff} - u = \sigma'_n = \sigma_n - u \dots \dots \dots (2)$$

where σ_{ff} and σ_n = the total normal stress; and u = the presumed pore pressure at failure. For the Fig. 1 excavation in stiff clay (and similar unloading problems in overconsolidated cohesive soils), the prudent value of u to use in Eq. 2 is the equilibrium, long-term pore pressure since this gives the drained strength, s_d , corresponding to the critical CD case.

Fredlund and Krahn (1977) compare commonly used methods of slices regarding: (1) The "side force" assumptions employed to estimate the magnitude of $\sigma'_{ff} = \sigma'_n$; (2) the differences in factors of safety (FS) computed based on force versus moment equilibrium; and (3) the relative costs for computer time. Those methods that have reasonable side force assumptions and that explicitly satisfy moment equilibrium when computing the factor of safety are recommended, such as Bishop (1955), Morgenstern and Price (1965), and Spencer (1967).

The commonly accepted definition of factor of safety as stated by Bishop (1955) is

$$FS = \frac{\text{available shear strength of soil}}{\text{shear stress required to maintain equilibrium}} \dots \dots \dots (3a)$$

$$FS = \frac{\tau_{ff} = c' + \sigma'_{ff} \tan \phi'}{\tau_m} \dots \dots \dots (3b)$$

which equals s_d/τ_m for the CD case illustrated in Fig. 1. The value of τ_m also represents the *mobilized* shear strength of the soil, i.e.

$$\tau_m = \frac{c' + \sigma'_{ff} \tan \phi'}{FS} \dots \dots \dots (3c)$$

If the degree of mobilization is the same for c' and $\tan \phi'$, as commonly assumed, then an alternate expression for the factor of safety becomes (Janbu 1973)

$$FS = \frac{\tan \phi'}{\tan \phi'_m} \dots \dots \dots (3d)$$

A conventional total stress analysis (TSA), as applied to the UU case, computes the available shear strength along a potential failure surface using

$$s = c + \sigma_{ff} \tan \phi \dots \dots \dots (4a)$$

where c and ϕ = the intercept and slope of a total stress failure envelope, respectively. Since saturated cohesive soils of interest behave as frictionless materials in terms of total stress, i.e., $\phi = 0$, Eq. 4a becomes (Skempton 1948a)

$$s_u = 0.5(\sigma_1 - \sigma_3)_f = q_f \dots \dots \dots (4b)$$

which equals the undrained shear strength of the soil. In turn, the factor of safety is defined as

$$FS = \frac{s_u}{\tau_m} \dots \dots \dots (5)$$

A total stress analysis (TSA) as described previously represents the traditional approach for assessing stability for loading problems, for which the UU case gives the minimum FS. The classic paper by Bishop and Bjerrum (1960) recommended unconsolidated-undrained triaxial compression (UUC) or field vane testing to obtain s_u , these implied to have an accuracy of $\pm 15\%$. Subsequent research has shown that measured field vane strengths need to be significantly reduced for highly plastic clays (Bjerrum 1972, 1973). However, much U.S. practice still often relies on measured UUC strengths [e.g., Peck et al. (1974); "Design and" (1978); "Slope Stability" (1982)]. Section 6.2 of the paper treats potential errors in using UUC strength data. In any case, the method of slices for a TSA mainly serves to compute τ_m in Eq. 5 since values of s_u are input directly for $\phi = 0$ materials.

2.3. Stability Analyses for Staged Construction:

Historical Perspective

The designer of staged construction projects such as previously described must estimate both the initial strength of the cohesive soil and its rate of increase with time due to consolidation under the applied loads. Total stress analyses (TSA) based on laboratory UU tests or field vane tests obviously cannot be used during design to predict the gain in strength due to dissipation of pore pressures and historically have been restricted to the end-of-construction UU case. On the other hand, Bishop and Bjerrum (1960) proposed that an effective stress analysis (ESA) "is a generally valid method for analysing any stability problem and is particularly valuable in revealing trends in stability which would not be apparent from total stress methods." They advocated its use for staged construction, noting that the greatest uncertainty lies in estimating the rate of pore pressure dissipation via consolidation theory and hence "field observations of pore pressure are advisable on important works."

Although others also realized the difficulty of making accurate pore pressure predictions during the design process [e.g., Peck and Lowe (1960)], the ESA attracted many followers, presumably since it could be readily used to check stability during construction based on *measured* pore pressures, whereas a TSA based on subsequent field vane testing or undisturbed sampling and UUC testing would be cumbersome at best. Moreover, all accept the premise that effective stresses control the strength of soil.

As will be demonstrated, a factor of safety computed via an ESA using *measured* (prefailure) pore pressures inherently assumes that the effective normal stress (σ'_{ff} in Eqs. 1 and 2) remains constant during a potential failure. In other words, this type of stability analysis basically treats staged construction as being equivalent to the consolidated-drained (CD) case. Bishop and Bjerrum (1960) realized this important fact since they noted the following: For factors of safety (FS) other than unity, the effective stress and total stress ($\phi = 0$) methods will not in general give equal values of FS; the former uses pore pressures under the actual loading conditions, and the value of FS "expresses the proportion of c' and $\tan \phi'$ then necessary for equilibrium" (i.e., Eq. 3); the latter, on the other hand, implicitly uses pore pressures related to those at failure in undrained shear. However, Bishop and Bjerrum (1960) apparently did not consider this to be a serious practical limitation since they essentially endorsed effective stress analyses whenever field pore-pressure data are available. However, others felt this approach to

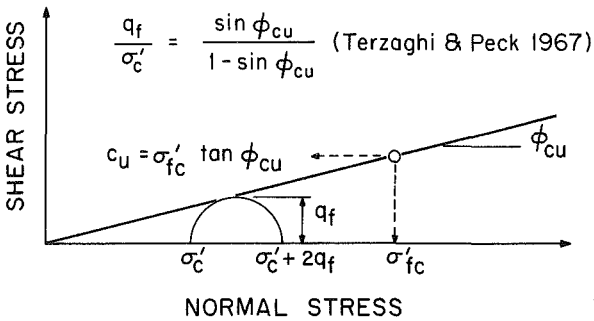


FIG. 2. Angle of Shearing Resistance ϕ_{cu} from Isotropically Consolidated-Undrained Triaxial Compression (CIUC) Tests as Defined by A. Casagrande

be dangerous (Brinch-Hansen 1962; Barron 1964), believing that staged construction should be treated as a consolidated-undrained (CU) case.

In particular, an entirely different approach for predicting strength gain with consolidation evolved in the United States from Arthur Casagrande's early research into the strength of clays, which explicitly assumes an undrained failure when calculating factors of safety during staged construction. Although it was adopted by major U.S. government agencies and many practitioners, the writer did not find a formal name for this methodology, henceforth called the *QRS* approach. In any case, *QRS* is referred to both as an "effective stress" and a "total stress" method, which is one reason for introducing a third type of analysis, the undrained strength analysis (USA). A more important reason lies in the fact that new techniques have been developed for estimating the in situ undrained strength of cohesive soils for both the UU and CU cases.

2.4. Undrained Strength Analysis (USA)

A USA basically treats the in situ effective stresses as consolidation stresses, which are then used to estimate the corresponding in situ undrained shear strength, denoted as c_u to differentiate it from the s_u associated with undrained strength measurements used for conventional total stress analyses. The most widespread, and perhaps earliest, application of a USA to staged construction is that developed by Arthur Casagrande as an outgrowth of his research in the early 1940s into the strength of clays as measured in UU, CU, and CD triaxial compression tests, which he first called quick (*Q*), consolidated-quick (*Q_c*), and slow (*S*), and later became *Q*, *R*, and *S* (Casagrande and Wilson 1960). Of particular interest to this paper is his manner of portraying results from isotropically consolidated-undrained triaxial compression ($R = CIUC$) tests as shown in Fig. 2 for a normally consolidated clay, where σ'_c equals the preshear consolidation stress. As quoted in Rutledge (1947), Casagrande states that the choice between using the UU or CU envelope for evaluating stability of a clay foundation "will depend on the thickness and consolidation characteristics of the clay and the rate at which load is applied to it." Moreover, the relationship

$$c_u = \sigma'_{fc} \tan \phi_{cu} \dots \dots \dots (6)$$

was adopted in design manuals for the U.S. Army Corps of Engineers (“Stability of” 1970; “Design and” 1978), wherein σ'_{fc} equals the effective normal (consolidation) stress acting on a potential failure surface, say from a method of slices. Since σ'_{fc} equals σ'_{ff} computed via a conventional ESA and since $\tan \phi'$ is significantly greater than $\tan \phi_{cu}$, this form of a USA will obviously give significantly lower factors of safety than a ESA (assuming that both analyses use measured prefailure pore pressures). Section 6.2 of the paper examines the *QRS* approach in more detail.

A second reason for introducing the USA occurred in the early 1970s with development of two new testing procedures for estimating the in situ undrained shear strength of clays, namely the Recompression technique developed at the Norwegian Geotechnical Institute (Bjerrum 1973) and the stress history and normalized soil engineering properties (SHANSEP) technique developed at MIT (Ladd and Foott 1974). Both attempt to minimize the adverse effects of sample disturbance (but in very different ways), recognize the importance of stress history, and consider the effects of undrained stress-strain-strength anisotropy by running K_0 consolidated-undrained (CK_0U) tests having different modes of failure. Although first applied mainly to stability problems falling under the UU case, these new techniques now enable a more rational and reliable form of a USA than the *QRS* approach for staged construction projects.

In essence, a USA using either the Recompression or SHANSEP technique will involve the following basic components, say for staged filling on a natural clay deposit:

1. Obtain the initial stress history of the soil, meaning the effective overburden stress (σ'_{v0}) and preconsolidation pressure (σ'_p).
2. Evaluate changes in stress history due to the proposed construction, using consolidation analyses for design and piezometers during construction.
3. Relate undrained shear strength to consolidation stresses via a laboratory program of CK_0U shear tests having different modes of failure.
4. Conduct stability analyses after inputting c_u profiles calculated from the aforementioned information.

Three case histories will illustrate these steps and also point out some of the simplifications used by the writer in executing a USA.

2.5. Definition of Undrained Shear Strength

Following the earlier work of Terzaghi (1936) and Skempton (1948a, 1948b, 1948c), Bishop and Bjerrum (1960) used an analysis of the *undrained* failure of a vertical cut in a homogeneous saturated clay to illustrate two fundamental points: (1) A TSA using $s_u = 0.5(\sigma_1 - \sigma_3)_f = q_f$ acting on a rupture surface inclined at $\alpha = 45^\circ$ to the horizontal (i.e., consistent with a $\phi = 0$ analysis) gives the same *failure height* as an effective stress analysis using $\tau_{ff} = q_f \cos \phi'$ acting on a surface inclined at $\alpha = 45 + \phi'/2$; and (2) the position of the critical rupture surface depends on the friction angle used in the analysis, and the closer it approximates the “true angle of internal friction” (meaning Hvorslev’s value), the “more realistic is the position of the failure surface.” (Note: The same conclusions also apply to Rankine active and passive earth pressures for isotropic strength parameters.) Because an undrained strength analysis should attempt to predict the available undrained

shear strength on the most realistic potential failure surface, the writer defines $c_u = \tau_{ff} = q_f \cos \phi'$. This approach should be correct when applied to active and passive wedges inclined at $\alpha = 45 \pm \phi'/2$. But it becomes more controversial when applied to the horizontal portion of a wedge or to a circular arc mode of failure. Nevertheless, others have used the same shear strength definition for undrained stability analyses [e.g., Lowe (1967); Johnson (1974); "Stability of" (1970)]. In essence, the real question concerns the actual location of the rupture surface during an undrained failure independent of how one estimates the available c_u . Also, if the $c_u = q_f \cos \phi'$ assumption is incorrect, the error will be on the safe side by 10–15% for typical values of $\cos \phi'$.

In summary, a total stress analysis (TSA) uses $s_u = q_f$ applied to a failure surface consistent with the $\phi = 0$ assumption whereas an undrained strength analysis (USA) uses $c_u = q_f \cos \phi'$ applied to the presumed actual location of the failure surface.

3. COMPARISON OF EFFECTIVE STRESS VERSUS UNDRAINED STRENGTH STABILITY ANALYSES DURING STAGED CONSTRUCTION

3.1. Conventional Effective Stress Analysis

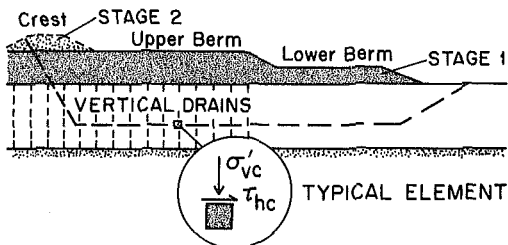
Effective stress analyses (ESA), as commonly used to assess stability during staged construction on natural cohesive deposits, typically proceed as follows (Bishop and Bjerrum 1960; Tavenas et al. 1978; "Slope Stability" 1982; Pilot et al. 1982; Murray and Symons 1984): (1) A method of slices is used to compute the distribution of total normal stress (σ_n) along the potential failure surface and the shear stress (τ_m) required for equilibrium; (2) measured pore pressures are obtained from piezometer data for determination of the existing effective normal stress (σ'_n) distribution; (3) σ'_n is assumed equal to σ'_{ff} in Eq. 1; (4) values of c' and ϕ' are determined from laboratory CD tests or from CU tests at maximum obliquity, which leads to estimates of the available shear strength ($s = \tau_{ff}$) along the potential failure surface; and (5) the resulting factor of safety is basically defined via Eq. 3 as $FS = \tau_{ff}/\tau_m = \tan \phi' / \tan \phi'_m$. This form of an effective stress analysis, i.e., using *measured* pore pressures and the aforementioned definition of factor of safety, represents a *conventional* ESA. The same approach also appears widespread for assessing stability during construction of tailings dams (Vick 1983; Stauffer and Obermeyer 1988).

After conceptually comparing the aforementioned form of a ESA with a corresponding undrained strength analysis (USA), the paper presents three case histories to further demonstrate the large practical differences in the safety implied by these two types of analyses.

3.2. Conceptual Comparison

Fig. 3(a) illustrates the staged construction of an embankment after installation of vertical drains under the upper berm. Since staged construction was necessary, the foundation clay under the upper berm becomes normally consolidated before stage 2 filling. Fig. 3(b) shows the stresses acting on a typical element for a horizontal failure surface, which can be simulated by a laboratory direct simple shear test (Bjerrum and Landva 1966). The value of the vertical consolidation stress (σ'_{vc}) is determined from estimates of the total vertical stress and from measurements of pore pressure, which would

(a) FIELD SITUATION FOR PARTIALLY OR FULLY CONSOLIDATED CLAY FOUNDATION



(b) STRENGTHS PREDICTED FROM ESA AND USA

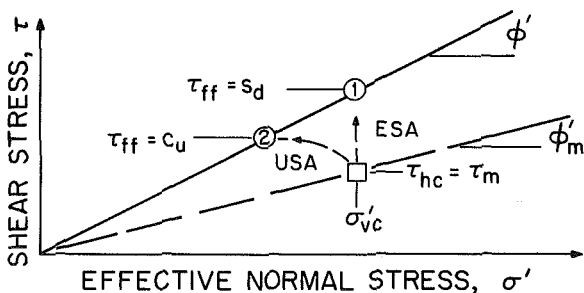


FIG. 3. Comparison of Effective Stress and Undrained Strength Analyses for Evaluating Stability during Staged Construction

typically be larger than hydrostatic. The value of the horizontal consolidation shear stress (τ_{hc}) will be equated to the mobilized shear stress (τ_m) as obtained from overall equilibrium via a method of slices.

A conventional ESA treats the existing effective normal stress as the effective normal stress at failure, i.e., $\sigma'_n = \sigma'_{vc} = \sigma'_{ff}$, and, hence, the computed available shear strength equals τ_{ff} at point 1. This represents the drained strength of the clay and the corresponding factor of safety becomes

$$FS = \frac{s_d}{\tau_m} = \frac{\tan \phi'}{\tan \phi'_m} \dots \dots \dots (7)$$

In other words, a ESA inherently assumes a slow failure with complete dissipation of shear induced pore pressures ($u_s = 0$) equivalent to the consolidated-drained (CD) case previously described. In contrast, a USA inherently assumes a rapid failure corresponding to the consolidated-undrained (CU) case. Since undrained shear of a normally consolidated clay will develop positive shear induced pore pressures ($u_s > 0$) and thus a lower effective normal stress at failure, the undrained shear strength ($\tau_{ff} = c_u$ at point 2) will be less than s_d . And the factor of safety

$$FS = \frac{c_u}{\tau_m} \dots \dots \dots (8)$$

will also be less than computed via a ESA.

The prime reason for conducting stability analyses during construction is

obviously to guard against an unexpected failure. What then might lead to instability when the FS computed by either Eq. 7 or 8 is reasonably greater than unity? Other than a significant error in the location of the presumed critical failure surface, the causes basically arise from an overestimate of the available resistance (s_d or c_u), an underestimate of the mobilized shear stress (τ_m), or a combination of both. Possible examples include localized lower σ'_{vc} due to malfunctioning vertical drains; τ_m too low due to error in fill weights or geometry; τ_m increased due to unauthorized filling or partial removal of a stability berm, etc.

Now consider whether the designer should assume that a failure will occur *so slowly* as to approach a drained (CD) condition or *so rapidly* as to approach an undrained (CU) condition. Although accurate predictions of rates of displacement and of rates of pore pressure dissipation during a failure are not possible, one can combine simple consolidation theory with field observations to obtain an idea of likely limits. Since staged construction will load the underlying soil into a normally consolidated condition, the coefficient of consolidation will range from about 0.05 m²/day to 0.003 m²/day for typical clays having liquid limits between 30% and 90%. For a "thin" rupture surface, as would be expected for a fairly "brittle" foundation soil (Section 7), having a drainage height of 5 cm, 50% pore pressure dissipation at the center will take from 30 minutes to 8 hours. But since large displacements usually occur during failures involving brittle soils within a time span of only seconds or minutes, an essentially undrained condition will prevail. For failures involving "ductile" foundation soils, the displacements are generally smaller and take longer to develop, say over a period of several hours or even days. But the size of the zone undergoing significant straining is also generally much larger, such that little pore pressure dissipation should be expected. Finally, undrained conditions certainly prevail during failures of tailings dams that lead to massive flow slides (Jeyapalan et al. 1983).

This reasoning should not imply that drainage may not occur during several hours or days preceding failure (although that may be true in most cases), but rather that undrained conditions will generally prevail during actual failures that entail significant displacements. Moreover, it should be emphasized that *whenever the average shear stress along a potential failure surface reaches the average available undrained shear strength existing at that time (i.e., $\tau_m \rightarrow c_u$), then an undrained failure will be initiated independent of the prior drainage conditions*. Hence, the prudent designer should always consider this possibility, especially for failures having the potential to cause extreme environmental damage or loss of life.

In summary, a conventional effective stress analysis that uses measured pore pressures, such as illustrated in Fig. 3, gives an "instantaneous" factor of safety corresponding to the effective stress-pore pressure conditions existing *prior to failure*. It inherently assumes that a potential failure will occur so slowly that the drained shear strength of the soil (s_d) will resist failure. In other words, a ESA a priori treats staged construction as a consolidated-drained (CD) case. The writer therefore concludes that the resulting factor of safety is potentially unsafe because it never considers the more critical possibility of an undrained shear failure and generally misleading because most failures during staged construction occur under essentially undrained conditions. In contrast, an undrained strength analysis (USA) inherently treats staged construction as a consolidated-undrained (CU) case wherein failure

occurs so rapidly as to preclude dissipation of shear induced pore pressures. And since the undrained shear strength (c_u) of normally consolidated soils is substantially less than the drained strength under field loading conditions, a USA will give both safer and more reliable estimates of the actual factor of safety.

3.3. Methodology for Case Histories of Embankment Staged Construction

The paper presents results from design studies made for two projects wherein the ESA-USA comparison was made for conditions corresponding to complete consolidation of all the foundation clays under the imposed loading. This "long-term" case was selected both to simplify computation of the consolidation stress profiles needed for the USA and to preclude argument regarding the correct pore pressure regime (i.e., hydrostatic values) for the ESA. The USA employed wedge-shaped failure surfaces [e.g., Fig. 3(a)] with anisotropic c_u values treated for the effects of progressive failure via the *strain compatibility* technique of Koutsoftas and Ladd (1985) as described later in Section 4.9. Computation of the increase in undrained shear strength (c_u) with consolidation involved two simplifications: (1) Changes in stress history being restricted to increases in the vertical consolidation stress (σ'_{vc}), which is less than the major principal consolidation stress (σ'_{1c}) except under the centerline; and (2) CK_0U test data used to relate c_u to σ'_{vc} for shearing in plane strain or triaxial compression and extension and in Geonor direct simple shear, whereas the in situ stresses obviously deviate from K_0 conditions. Section 4.11 of the paper indicates that these simplifications tend to underpredict the available strength, i.e., give too low factors of safety.

3.4. Embankment on Connecticut Valley Varved Clay

This example design problem was performed as part of an MIT research program sponsored by the Massachusetts Department of Public Works in cooperation with the U.S. Department of Transportation Federal Highway Administration (Ladd 1975; Ladd and Foott 1977). The 80-ft (24.4-m) thick deposit of medium to soft varved clay at the site (Fig. 4) required installation of vertical drains and staged construction with a stability berm and a surcharge to attain a 30-ft (9.15-m) net increase in grade and to minimize post-pavement settlements. Results from ESA and USA are compared for complete consolidation under the final embankment geometry. The USA used different stress history profiles for each of the five zones shown in Fig. 4. The site conditions are similar to those encountered in a 1972 MIT test program conducted at Amherst, Mass. The varved clay, deposited in glacial Lake Hitchcock during retreat of the late-Pleistocene ice sheet, has typical index properties as shown in Table 1.

Fig. 5(a) plots the initial stress history applicable to zone 1 and preconsolidation pressure data measured via constant rate of strain consolidation (CRSC) tests. The selected σ'_p profile assumed constant precompression below E1.100 and higher values above due to desiccation. The figure also shows final vertical consolidation stress profiles after complete pore pressure dissipation under the berm, slope, and crest (i.e., zones 2, 3, and 5, respectively), which account for a stress reduction due to settlement of the fill. Most of the underlying foundation clay becomes normally consolidated, except that zone 5 is slightly precompressed by 0.5 ± 0.1 ksf due to prior

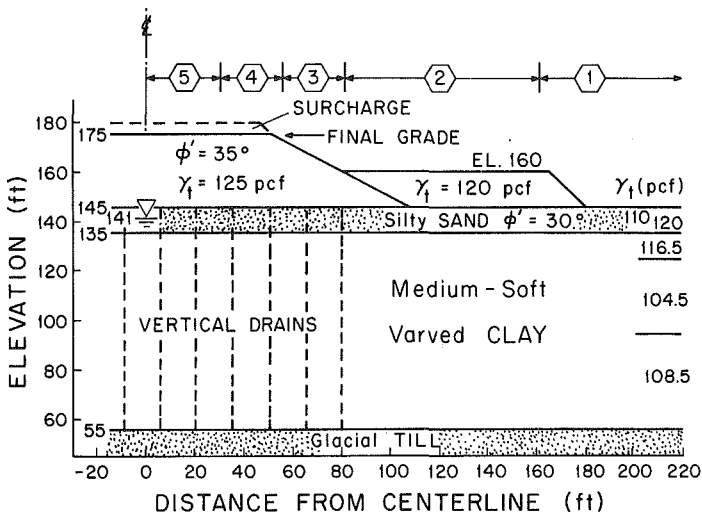


FIG. 4. Design Problem for Highway Embankment on Connecticut Valley Varved Clay (1 ft = 0.305 m; 1 pcf = 0.157 kN/m³)

consolidation under the 5-ft (1.5-m) thick surcharge fill (Fig. 4).

MIT studied the stress-strain-strength anisotropy of Connecticut Valley varved clays for several years, culminating in a doctoral thesis (Sambhandharaksa 1977). The program included block and 5-in. (127-mm) diameter Osterberg samples, both the Recompression and SHANSEP techniques and K_0 consolidated-undrained (CK_0U) tests sheared in compression, extension, and direct simple shear on specimens having different overconsolidation ratios. Application of the strain compatibility technique to the CK_0U stress-strain data resulted in anisotropic undrained strength parameters for wedge shaped failure surfaces corresponding to shear in plane strain compression (PSC), direct simple shear (DSS), and plane strain extension (PSE). These results can be approximated by the relationship

$$\frac{\tau}{\sigma'_{vc}} = S(\text{OCR})^m \dots \dots \dots (9)$$

where $\tau = c_u$ for a particular mode of failure; S = the normally consolidated value of τ/σ'_{vc} ; OCR = overconsolidation ratio = σ'_p/σ'_{vc} ; and m = the strength increase exponent. Table 2 presents the values of S and m that were used

TABLE 1. Typical Index Properties of Connecticut Valley Varved Clay

Component (1)	Natural water content, w_N (%) (2)	Liquid limit, w_L (%) (3)	Plasticity index, I_p (%) (4)
"Silt"	43	39	15
"Clay"	72	66	37
Bulk	60	54	27

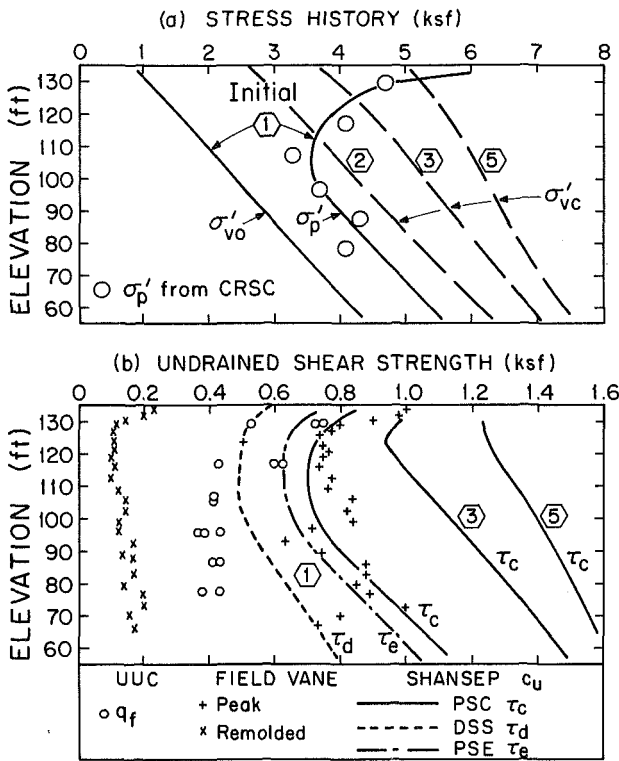


FIG. 5. Stress History and Undrained Strength Profiles for Connecticut Valley Varved Clay (1 ft = 0.305 m; 1 ksf = 47.9 kPa)

with the stress history profiles in Fig. 5(a) to calculate the SHANSEP c_u profiles plotted in Fig. 5(b). For the initial stress history in zone 1, σ'_{v0} equals σ'_{vc} in Eq. 9, whereas σ'_p becomes equal to σ'_{vc} for consolidation stresses that exceed the initial preconsolidation pressure of the varved clay deposit.

Comparison of the initial (zone 1) undrained shear strength data presented in Fig. 5(b) shows: (1) Significantly lower SHANSEP strengths for shearing parallel to the varves (τ_d) than for shearing across the varves in compression (τ_c) or in extension (τ_e); (2) peak strengths from Geonor field vane tests generally plotting above the SHANSEP values; and (3) a reversed trend for the laboratory UUC strengths, especially at depth in spite of using 5-in. (127-mm) diameter fixed piston samples. Fig. 5(b) also shows the computed gain in c_u due to full consolidation under the embankment loads via plots of the plane strain compression (PSC) τ_c for zones 3 and 5. Corresponding direct simple shear (DSS) strengths at E1.85 are $\tau_d = 0.74$ ksf in zone 2 and $\tau_d = 0.90$ ksf in zone 3.

The anisotropy of varved clays also causes substantial variations in the effective stress-strength parameters (Sambhandharaksa 1977): $c'/\sigma'_p = 0.01$ and $\phi' = 30^\circ$ for shear across the varves in CU and CD triaxial compression and CU triaxial extension tests; and $c'/\sigma'_p = 0.025$ and $\phi' = 20^\circ$ for shear

TABLE 2. Undrained Strength Parameters for Connecticut Valley Varved Clay and James Bay Sensitive Clay

Clay deposit (1)	MODE OF FAILURE					
	Compression		Direct Simple Shear		Extension	
	S (2)	m (3)	S (4)	m (5)	S (6)	m (7)
Connecticut Valley	0.21	0.83	0.15	0.775	0.20	0.74
James Bay Marine (1) Intact ^a	0.26 ±0.015	1.00	0.225 ±0.02	1.00	0.16 ±0.015	1.00
(2) Normally consolidated	0.26	—	0.225	—	0.16	—
James Bay Lacustrine (1) Intact ^b	0.225 ±0.03	1.00	0.19 ±0.00	1.00	0.14 ±0.01	1.00
(2) Normally consolidated	0.25 ^c	—	0.215	—	0.12 ^c	—

^aMean ± one standard deviation from five test series.

^bMean ± one standard deviation from two test series.

^cEstimated from data on other clays.

parallel to the varves in conventional CD direct shear tests and *CIUC* tests run on specimens trimmed at 45°. Although wedged-shaped failure surfaces would have been more appropriate for the ESA, the analyses used Bishop circular arcs with $\phi' = 25^\circ$ and $c' = 0$ (except for $c' = 0.05$ ksf within the top 10 ft of clay for zones 1 and 2).

Fig. 6 shows the embankment geometry after full consolidation ($\bar{U} = 100\%$), and having 8 ft of settlement under the crest. The ESA used hydrostatic pore

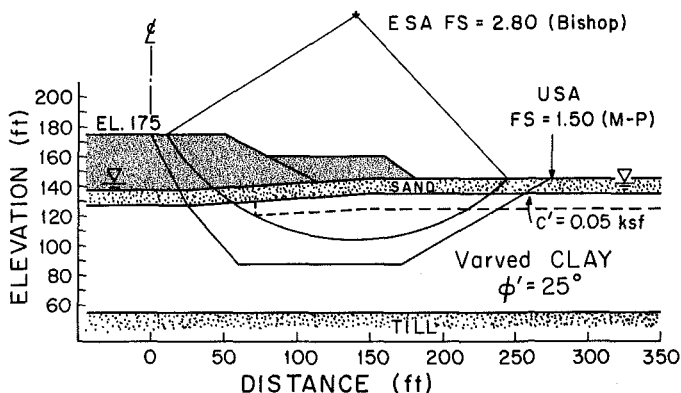


FIG. 6. ESA and USA Factors of Safety for Embankment on Connecticut Valley Varved Clay at $\bar{U} = 100\%$ [from Ladd and Foott (1977)] (1 ft = 0.305 m; 1 ksf = 47.9 kPa)

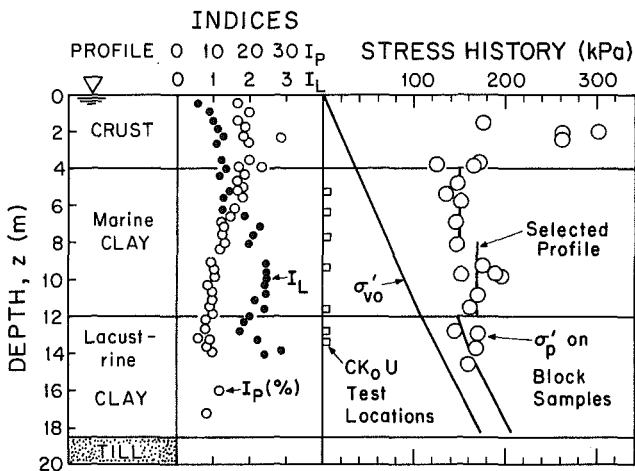


FIG. 7. Soil Profile, Index Properties, and Stress History at James Bay Site B-6 [from Ladd et al. (1983)]

pressures and gave a factor of safety (FS) = 2.8 for critical circles having a reasonable location within the foundation clay. The USA used anisotropic c_u values with the Morgenstern-Price (1965) method of slices having active and passive wedges inclined at 50° and 30° , respectively, within the varved clay. The most critical location (bottom of wedge at E1.86) gave FS = 1.50. Thus, the ESA, which assumes a slow drained failure, had a factor of safety almost double that from a USA corresponding to a rapid undrained failure of the foundation clay.

3.5. Embankment Dam on James Bay Sensitive Clay

This study was performed for Société d'Énergie de la Baie James (SEBJ) as part of the activities by a SEBJ "committee of specialists" to recommend techniques for designing embankment dams on soft sensitive clays for a hydroelectric project involving the Nottaway, Broadback, and Rupert rivers in northern Quebec. The Embankment Stability Subcommittee (Ladd et al. 1983) selected the site of the B-6 powerhouse, located 90 km up the Broadback River, for its example design problem. The final geometry entailed the following for a 21-m net increase in grade: (1) Installation of vertical drains to 80 m from the centerline; (2) stage 1 construction having 6-m and 12-m thick berms; and (3) stage 2 construction the following summer. Results from ESA and USA are compared for complete consolidation of the 18.5-m thick foundation under the final cross section (but without impoundment).

Fig. 7 shows the selected soil profile and related index properties. The 4-m crust has been weathered from freeze-thaw cycles. The next 8 m contain a relatively homogeneous, low plasticity marine clay having 75% clay size fraction, a high liquidity index ($I_L = 1.8 \pm 0.6$), and sensitivities increasing from about 30 to near 400 with depth. The properties of the underlying lacustrine clay are less well defined and also less homogeneous, with layers of silty sand. The actual site has a thin Muskeg cover, a thin transition zone

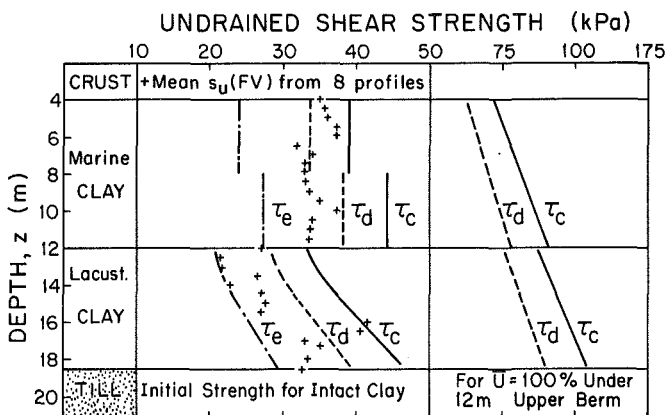


FIG. 8. Field Vane and Anisotropic Undrained Strength Profiles at James Bay Site B-6

between the marine and lacustrine clays, and till about 2 m deeper than selected for the problem.

The consolidation test program, run on block samples taken continuously down to 15 m with the Sherbrooke sampler (Lefebvre and Poulin 1979), gave the preconsolidation pressure data plotted in Fig. 7. The relatively constant σ'_p within the marine clay is believed to be caused by some kind of cementation (Lefebvre et al. 1983, 1988). The selected σ'_p profile for the lacustrine clay, which also considered field vane data, corresponds to a constant precompression of about 35 kPa. The σ'_{v0} profile accounts for downward seepage at the site.

The laboratory strength testing program included extensive CK_0U triaxial compression and extension and Geonor direct simple shear tests run using the Recompression technique. Specifically, one series of samples was tested with $\sigma'_{vc} = \sigma'_{v0}$ to obtain the initial undrained shear behavior of intact clay at the depths indicated in Fig. 7; and a second series was tested at σ'_{vc} increasing up to several times the in situ σ'_p to measure the gain in c_u with consolidation at two depths within both layers, but restricted to DSS testing for the lacustrine clay. Application of the strain compatibility technique to these data resulted in the anisotropic design strength parameters, selected at a shear strain of 2%, presented in Table 2. Intact clay denotes soil consolidated to stresses less than the preconsolidation pressure, and using $m = 1.00$ in Eq. 9 is equivalent to assuming a constant c_u/σ'_p , which ignores the small gain in c_u during recompression. The parameters selected for normally consolidated clay involved judgment, since S varied with consolidation stress level.

Fig. 8 plots the initial anisotropic c_u profiles for intact clay and those after complete consolidation under 12 m of fill. It also shows the mean peak strength from eight Nilcon field vane (FV) soundings run within a 5-m to 10-m radius from the block sample boring. The s_u (FV) within the marine clay remains nearly constant and agrees with the average c_u obtained from the CK_0U test program (Lefebvre et al. 1988). Vane strengths within the

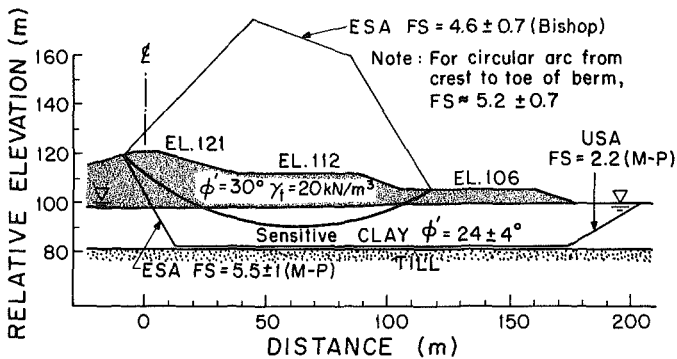


FIG. 9. ESA and USA Factors of Safety for Embankment Dam on James Bay Sensitive Clay at $\bar{U} = 100\%$ [from Ladd et al. (1983)]

lacustrine clay tend to increase with depth, but with significant scatter attributed to sandy layers.

Fig. 9 shows the final geometry for full consolidation ($\bar{U} = 100\%$) under the embankment loads. Anisotropic c_u profiles for the Morgenstern-Price analyses were calculated as follows: Boussinesq stress distribution used to obtain variations in σ'_{vc} throughout the foundation soils; values of c_u for intact clay (i.e., $\sigma'_{vc} < \sigma'_p$) taken equal to the τ_e and τ_d profiles plotted in Fig. 8; and values of τ_e and τ_d for normally consolidated clay calculated as σ'_{vc} times the corresponding S parameter in Table 2. The most critical wedge, shown in Fig. 9, gave a USA factor of safety (FS) = 2.2.

The effective stress analyses employed Bishop circles and Morgenstern-Price wedges with hydrostatic pore pressures since $\bar{U} = 100\%$. Most of the foundation soils become normally consolidated and $OCR = 1 CK_0UC$ tests on the marine clay gave $\phi' = 26 \pm 2^\circ$ at the peak strength and $\phi' = 33 \pm 4^\circ$ at maximum obliquity. The ESA used ϕ' values of 20° and 28° as a conservative lower-bound range compared to the measured data. Nevertheless, the resulting factors of safety in Fig. 9 were still very high. Taking $\phi' = 24^\circ$ as a lower limit, the ESA gives a FS of about 5.2 for an overall crest-to-toe failure.

3.6. Upstream Tailings Dam

The writer assisted Bromwell & Carrier, Inc. (BCI) of Lakeland, Florida during 1983–84 with the stability investigation of a tailings dam used to store slurried waste from processing of copper ore (Fig. 10). After construction of a starter dam and initial filling in 1969 to E1.85, subsequent raises employed the upstream method via cycloning the mine tailings to produce a sand beach that forms the shell and slope of the dam and contains the cohesive slimes that are discharged into the upstream pond. Significant filling occurred in 1973–74 to E1.155 and then more slowly since 1977 to reach E1.220 in late 1981. A nearby dam of similar geometry, but filled more rapidly, had failed the previous year.

A site investigation in 1983 included: measurement of in situ pore pressures via piezometer probes and additional piezometers; two Nilcon field vane soundings; and three borings with Osterberg fixed piston samples. In-

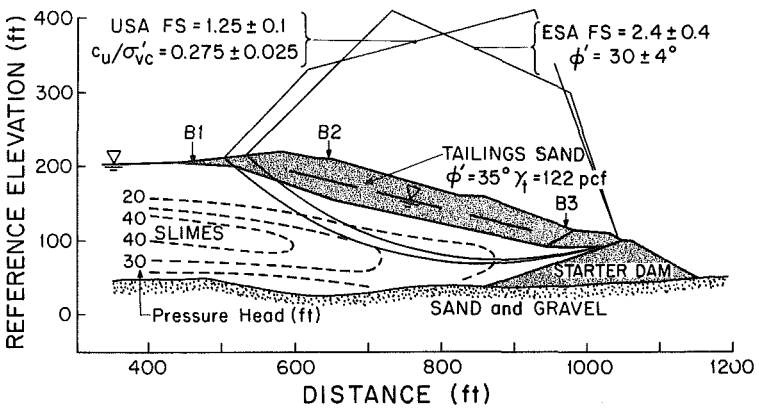


FIG. 10. ESA and USA Factors of Safety for Upstream Tailings Dam (from Bromwell & Carrier, Inc.) (1 ft = 0.305 m; 1 pcf = 0.157 kN/m³)

properties of the copper slimes obtained from borings B1 and B2 are: $w_L = 32 \pm 3\%$, $I_p = 10 \pm 3\%$, I_L decreasing from about 1.5 at E1.190 to 0.5 below E1.100, and γ_t increasing from 115 to 125 pcf (18.1 to 19.6 kN/m³).

Fig. 11 summarizes pond conditions measured at boring B1. The stress history data show pore pressures much less than hydrostatic, due to significant consolidation from downward seepage; and good agreement between the end-of-primary (EOP) oedometer σ'_{p0} and the measured $\sigma'_{v0} = \sigma_v - u$ within the "underconsolidated" slimes. BCI successfully modeled pore pressures within the pond using a one-dimensional finite strain consolidation analysis (Bromwell 1984), but measured much higher u values than predicted under the slope (see Fig. 10) and attributed this to significant horizontal flow. Fig. 11 also compares UUC and field vane strengths to c_u values computed as 0.25 and 0.30 times the measured vertical consolidation stress. The $s_u(FV)$ typically plot within this range and the sensitivity decreased with depth from about four to two. In contrast, $s_u(UUC)/\sigma'_{v0}$ averaged only 0.18.

The following summarizes CU test data obtained by R. S. Ladd in the Clifton, N.J. laboratory of Woodward-Clyde Consultants.

- Five CIUC with $\sigma'_c/\sigma'_{v0} > 1.5$:
Peak $q_f/\sigma'_c = 0.33 \pm 0.015$ at $\gamma = 14 \pm 2\%$ and $\phi' = 34 \pm 1^\circ$.
- Five CAUC with $\sigma'_{vc}/\sigma'_{v0} > 1.4$ and $K_c = \sigma'_{hc}/\sigma'_{vc} = 0.55 \pm 0.1$:
Peak $q_f/\sigma'_{vc} = 0.31 \pm 0.015$ at $\gamma = 0.25\%$ and $\phi' = 26 \pm 2^\circ$.
Maximum obliquity $q/\sigma'_{vc} = 0.27 \pm 0.015$ at $\gamma = 11.5 \pm 1.1\%$ and $\phi' = 33.5 \pm 1.0^\circ$.
- Four CK_0UDSS with $\sigma'_{vc}/\sigma'_{v0} > 1.5$:
Peak $\tau_h/\sigma'_{vc} = 0.225 \pm 0.002$ at $\gamma = 9.5 \pm 3.0\%$.

In addition, two DSS tests consolidated with $\tau_{hc}/\sigma'_{vc} = 0.1$ and 0.2 to better simulate the non- K_0 conditions existing under the slope of the dam gave peak $\tau_h/\sigma'_{vc} = 0.24$ and 0.28 at $\gamma = 4.4$ and 1.7%, respectively. After considering strain compatibility and the likely beneficial influence of three-dimensional

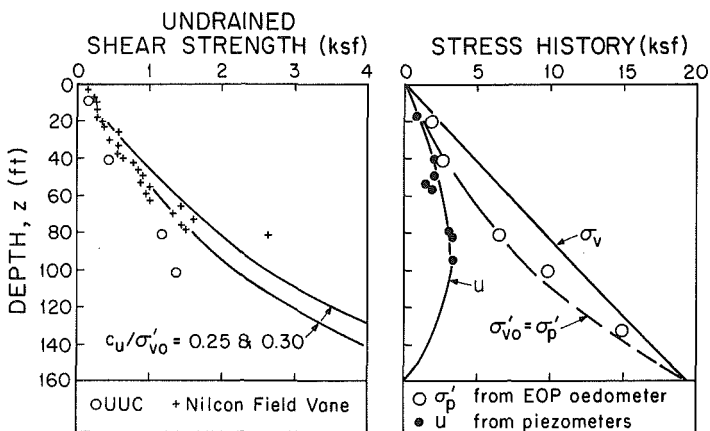


FIG. 11. Undrained Strength and Stress History Data at Boring B1 of Upstream Tailings Dam (from Bromwell & Carrier, Inc.) (1 ft = 0.305 m; 1 ksf = 47.9 kPa)

“end effects” during a potential failure (Azzouz et al. 1983), the writer selected $c_u/\sigma'_{v0} = 0.275 \pm 0.025$ as the best estimate and range of the in situ undrained shear strength ratio for the USA. As before, c_u was defined as $\tau = q \cos \phi'$ from triaxial tests and as τ_h from DSS tests. Both sets of triaxial tests gave the same friction angle at maximum obliquity ($\phi' = 34^\circ$), but anisotropic consolidation produced a much lower value ($\phi' = 26^\circ$) at the peak undrained strength due to the small strain at failure.

Fig. 10 shows results from Bishop circular arc analyses using pore pressure contours measured two years after the last filling in late 1981. BCI's program enabled direct computation of c_u as a fraction of the vertical effective stress for each slice and the circle having $FS = 1.25 \pm 0.1$ represents the critical location for the USA. The ESA used ϕ' varying in 5° increments over a wide range. The circle shown is typical of the critical location for $\phi' \leq 25^\circ$, whereas $\phi' \geq 30^\circ$ produced $FS \leq 2$ for failure of the starter dam (note: treatment of the tailings sand as an infinite slope gives $FS = 2.1$). Hence, the $FS = 2.4 \pm 0.4$ shown for the ESA corresponds to substantial failure through the slimes rather than minimum values for failures largely confined to granular soils. In any case, the USA results are more credible given the failure of a similar dam during construction and the lower pore pressures used for these analyses than existed at the end of filling two years earlier.

3.7. Conclusions from Case Histories

Table 3 summarizes the results from the three examples. Although both types of analyses require knowledge of the same prefailure effective stress conditions, they give large differences in the computed factor of safety, by a ratio of about two, due to differences in their definition of factor of safety. A conventional effective stress analysis inherently uses $FS(ESA) = s_d/\tau_m = \tan \phi' / \tan \phi'_m$ corresponding to a slow drained failure (CD case), whereas an undrained strength analysis uses $FS(USA) = c_u/\tau_m$ corresponding to a rapid undrained failure (CU case). Although an undrained failure is certainly

TABLE 3. Comparison of Effective Stress versus Undrained Strength Stability Analyses

Example (1)	Comparison for (2)	USA		ESA		FS(ESA)/ FS(USA) (7)	Remarks (8)
		Undrained strength (3)	FS (4)	Envelope (5)	FS (6)		
Embankment: varved clay	Long-term ($\bar{U} = 100\%$)	SHANSEP anisotropic c_u for wedge	1.50	$\phi' = 25^\circ$ best estimate	2.80	1.9	ESA gives shallow failure
Embankment: sensitive clay	Long-term ($\bar{U} = 100\%$)	Recompression anisotropic c_u for wedge	2.2	$\phi' = 24 \pm 4^\circ$ conservative	5.2 ± 0.7	2.35	For crest-toe failure; not ESA minimum
Upstream tailings dam	During staged construction	SHANSEP isotropic c_u	1.25 ± 0.1	$\phi' = 30 \pm 4^\circ$ best estimate	2.4 ± 0.4	1.9	For slimes failure; not ESA minimum

more critical (and, in the writer's opinion, also much more likely), one might still ask if the results in Table 3 are representative. In particular, would one expect smaller differences at lower factors of safety?

Comparison of ESA and USA results should ideally follow changes in FS during staged construction projects that eventually led to failures and had sufficient information regarding stress history, strength parameters, and measured pore pressures, etc., to enable detailed analyses. If both types of analysis were then made moments before an actual undrained failure, would they both calculate a FS near unity? Since such comparisons could not be found, the writer reviewed results from analyses of embankment failures that occurred during fairly rapid construction, i.e., failures falling under the UU case. This review focused on case histories with sufficient pore pressure data for meaningful effective stress analyses, with conclusions quite similar to those contained in Pilot et al. (1982). Although amazingly few definitive case histories exist in the literature, it would appear that ESA generally:

- Give reasonable FS values with clays of low plasticity, but tend to be unsafe with organic and highly plastic soils.
- Predict critical failure surfaces that tend to be significantly smaller than actually observed, i.e., they are too shallow.

The examples in Table 3 also agree with the second observation. In fact, the generally accepted hypothesis (Skempton 1948a; Bishop and Bjerrum 1960) that " $\phi = 0^\circ$ " circular arc analyses predict the wrong location of failure surfaces, in contrast to ESA, appears to be quite the opposite for field *loading* problems. It is not clear whether this serious problem with ESA occurs due to errors in pore pressure distribution, the selected c' - ϕ' values, the normal stress computed from a simplified Bishop (or comparable) method of slices, or a combination thereof. In any case, the writer concludes that even when staged construction exists at a near failure condition, a ESA may not provide a reliable prediction of an impending failure.

The three examples in Table 3 show similar ratios of factors of safety in spite of substantial differences in the computed FS(USA) for an undrained failure. A partial explanation for this apparent anomaly can be obtained from

quantifying the conceptual comparison in Fig. 3. Assume for simplicity that shear along the horizontal portion of the wedge fully controls stability. How then does the predicted stability vary with the level of shear stress required for equilibrium, i.e., the value of $\tau_{hc}/\sigma'_{vc} = \tau_m/\sigma'_{vc}$? From Eqs. 7 and 8:

$$\frac{\text{FS(ESA)}}{\text{FS(USA)}} = \frac{\frac{\tan \phi'}{\tan \phi'_m}}{\frac{c_u}{\tau_m}} = \frac{\frac{\tan \phi'}{\left(\frac{\tau_m}{\sigma'_{vc}}\right)}}{\left(\frac{c_u}{\sigma'_{vc}}\right)} = \frac{\tan \phi'}{\frac{c_u}{\sigma'_{vc}}} \dots \dots \dots (10)$$

Hence, the ratio is independent of FS provided that $\tan \phi'$ and c_u/σ'_{vc} remain constant. Taking $\phi' = 25 \pm 5^\circ$ and $\phi' = 29 \pm 5^\circ$ as typical for CK_0U triaxial compression tests at the peak undrained strength and maximum obliquity, respectively, and $c_u/\sigma'_{vc} = 0.23 \pm 0.04$ from CK_0U direct simple shear tests, one obtains mean FS(ESA)/FS(USA) ratios of 2.0 and 2.4, respectively.

The aforementioned calculation gives ratios strikingly similar to those in Table 3. But now look at the error resulting from the two simplifications described in Section 3.3 that were used to compute the undrained shear strength for the USA (as done previously and also for the embankment case histories). In essence, both of these simplifications tend to underestimate the available c_u at low factors of safety since c_u/σ'_{vc} generally increases with increasing $\tau'_m/\sigma'_{vc} = \tau_{hc}/\sigma'_{vc}$ (Section 4.11 presents data from so-called CAUDSS tests that quantify this beneficial effect). In other words, the simplified FS(USA) progressively errs on the safe side as the consolidated foundation clay approaches a failure condition. But even considering this error, the writer still expects FS(ESA)/FS(USA) ratios greater than about 1.5 for factors of safety encountered with typical staged construction projects that use *measured* pore pressures with realistic failure surfaces and strength parameters.

In summary, the writer concludes that conventional effective stress analyses employed to evaluate stability *during* staged construction based on *measured* prefailure pore pressures will generally give highly misleading and unsafe estimates of the factor of safety. This occurs because of the definition of FS used in a ESA, which inherently assumes a slow drained failure. In contrast, an undrained strength analysis makes a more critical (and generally more realistic) assumption of no drainage during a potential failure. Although some engineers may conduct ESA with “low” $c'-\phi'$ values and/or “high” u values in an attempt to guard against the possibility of an undrained failure, this approach should not be considered as a reliable replacement for a USA. Finally, a USA of the type used for the two embankment case histories does involve simplifications, but the resulting error tends to give safe rather than unsafe results. And more sophisticated USA can be made, such as used for the tailings dam case history, to remove undue conservatism.

3.8. Overview of Current Practice

As noted before, the use of effective stress analyses as proposed by Bishop and Bjerrum (1960) to check stability during staged construction attracted

many followers, both due to the known limitations of conventional total stress analyses and the ability of ESA to take ready advantage of field piezometer data [e.g., Section 31.4 of Lambe and Whitman (1969)]. Endorsements of this approach for embankment construction include Parry (1972), Rivard and Lu (1978), Tavenas and Leroueil (1980), Pilot et al. (1982), "Slope Stability" (1982), Murray and Symons (1984), and Section 5.1.3 of Wroth and Houlsby (1985). It appears widely used to assess the stability of tailings dams, even those containing cohesive slimes. And effective stress analyses are generally preferred on a conceptual basis by authors such as Janbu (1977, 1979) and Schmertmann (1975).

But as also previously noted, others have long believed that staged construction should be treated as a consolidated-undrained (CU) case. These include early papers on staged construction by Lobdell (1959) and Brinch-Hansen (1962) and, most importantly, the influence of Arthur Casagrande as evidenced by the adoption of his "QRS" approach in design manuals by the U.S. Army Corps of Engineers ("Stability of" 1970; "Design and" 1978) and the 1961–1971 versions of the NAVDOCKS/NAVFAC DM-7. For example, DM-7 ("Stability Analysis" 1971) (attributed to James Gould) makes the following statement regarding foundation stability both during and after (long-term) staged construction: "Where additional pore pressures are developed during shear of compressible impervious materials, utilize pore pressures . . . in effective stress analysis with strengths c and ϕ from CU tests." In essence, the " c and ϕ " denote values from *CIUC* tests interpreted as shown in Fig. 2 (i.e., $\phi = \phi_{cu}$) and the "effective stress analysis" means estimated or measured in situ *effective* stresses, which are treated as preshear consolidation stresses. The design manuals of the USACE make similar recommendations, but refer to Q , R , and S envelopes rather than total versus effective stress analyses. One major source of confusion lies in the fact that use of the ϕ_{cu} envelope in Fig. 2 is called an *effective stress* analysis by the Navy ("Stability Analysis" 1971), whereas Article 36 of Terzaghi and Peck (1967) refers to its use by the USACE as a *total stress* analysis.

In any case, the *QRS* approach treats staged construction as a CU case, has a long history, and has been widely adopted in the United States, at least for construction involving governmental agencies. Section 6 addresses its potential limitations, along with attempts to conduct "undrained" effective stress analyses. The paper also proposes a new classification of stability evaluations to help avoid future confusion regarding the assumed drainage conditions during construction and at failure and the corresponding strength parameters. First, basic soil behavioral issues affecting these parameters will be identified and summarized.

4. SOIL BEHAVIORAL ISSUES

Execution of an undrained strength analysis entails assessment of the initial in situ undrained shear strength (c_u) of the cohesive foundation soils and subsequent changes in c_u during staged construction. This process requires knowledge of the initial stress history of the deposit (σ'_{v0} and σ'_p), how it varies throughout construction, and, most importantly, the relationship between c_u and stress history. Section 4 of the paper treats the significance and evaluation of the initial preconsolidation pressure (Section 5 covers changes

in stress history) and then focuses on factors that should be considered in laboratory consolidated-undrained strength testing programs.

4.1. Preconsolidation Pressure: Significance

Although originally considered, and still often called, the “maximum past pressure” that acted on the clay, the profession now generally views σ'_p as representing a *yield stress* that separates small strain “elastic” behavior from large strains accompanied by plastic (irrecoverable) deformation during one-dimensional compression. This distinction has practical significance when attempting to select a σ'_p profile consistent with the geologic history of the deposit and in estimating the in situ state of stress. Examples cited in Table V of Jamiolkowski et al. (1985) include the following regarding four mechanisms that can cause overconsolidation ($\sigma'_p > \sigma'_{v0}$) within horizontal clay deposits with geostatic stresses.

1. *Mechanical*, due to overburden removal or lower water table: constant $\sigma'_p - \sigma'_{v0}$ versus depth; K_0 conditions.
2. *Desiccation*, due to evaporation or freezing: variable σ'_p decreasing with depth; probable deviations from K_0 .
3. *Aging* (secondary compression), due to drained creep: constant OCR versus depth; whether K_0 increases or remains essentially constant (writer's opinion) still controversial.
4. *Physico-chemical*, due to natural cementation and related phenomena: σ'_p probably variable; unknown effect on K_0 (Note: This mechanism may predominate in some sensitive, brittle deposits like the marine clay in Fig. 7).

For projects involving man-made deposits such as dredged materials and mineral processing wastes, the mechanical and desiccation mechanisms will usually dominate and the main practical problem often entails measurement of the degree of “underconsolidation,” i.e., the deposit is still consolidating with $\sigma'_{v0} = \sigma'_p$ (e.g., Fig. 11). But with natural deposits, the relative importance of the aforementioned mechanisms is often unclear and usually impossible to prove. For this reason, the writer feels that the distinction between normally consolidated “young” versus “aged” clays (Bjerrum 1973) may give a misleading impression of the actual preconsolidation mechanisms, i.e., the OCR of the latter may also include mechanical and physico-chemical effects. In any case, from a practical viewpoint, an accurate definition of the σ'_p profile is a major design issue since the initial stress history governs the initial in situ c_u within a fairly narrow range independent of the physical preconsolidation pressure mechanisms, and σ'_p represents the dividing line between recompression having relatively little increase in c_u and virgin compression causing substantial strengthening of the foundation soils.

4.2. Preconsolidation Pressure: Evaluation

Laboratory Tests

Laboratory consolidation tests constitute one of the most important components of the exploration and testing program. The following summarizes and updates pertinent conclusions from Jamiolkowski et al. (1985).

Sample Disturbance. Even though staged construction projects justify fixed-piston, thin-walled sampling of 70-mm–85-mm diameter, sample dis-

turbance may still affect the data adversely. Radiography can identify zones of excessive disturbance and is ideally suited to help select the most representative and best-quality soil for testing. Correlations of σ'_p with the measured strain at σ'_{v0} may prove useful (Lacasse et al. 1985; Holtz et al. 1986).

Test Equipment. Incremental oedometer tests using a load increment ratio ($\Delta P/P$) of unity are most common, except that $\Delta P/P$ should often be reduced to about 0.5 to obtain a better defined curve in the vicinity of σ'_p . The controlled gradient test (Lowe et al. 1969) and the constant rate of strain test (Smith and Wahls 1969; Wissa et al. 1971) give continuous data in much less time, but they require more sophisticated equipment and may seriously overestimate σ'_p if run too fast.

Interpretative Technique. The writer relies mainly on the method of Casagrande (1936), but also used Schmertmann's (1955) technique and now the work per unit volume technique of Becker et al. (1987) for soils having an ill-defined break in the compression curve.

Time Effects. Section 2.5 of Jamiolkowski et al. (1985) and subsequent "Discussion to Session 2" illustrate the divergent views regarding whether the time required to reach the end-of-primary consolidation (t_p) affects the location of the compression curve. In other words, does significant creep occur only *after* the dissipation of excess pore pressures (hypothesis A) or does it also occur *during* primary consolidation (hypothesis B). Leroueil (1988) summarizes field data for four extremely compressible (highly structured) clays that show in situ virgin compression curves and values of σ'_p that fall well below those obtained from laboratory end-of-primary compression curves, and concludes "that hypothesis A is not correct." But are those data representative of most soft clays? The writer believes that they probably represent a special case based on results in Lefebvre and LeBoeuf (1987) from CU triaxial tests sheared at different strain rates on block samples of three highly sensitive Canadian clays. For brittle *intact* ($OCR > 1$) specimens, the decrease in peak strength at slower strain rates was caused by a decrease in the effective stress failure (yield) envelope, with no change in pore pressure. For *destructured* ($OCR = 1$) specimens, the decrease in peak strength was caused by higher pore pressures, with no change in the failure envelope. Thus, a soil skeleton resistance produced by cementation bonds (i.e., the physico-chemical σ'_p mechanism described previously) can be very strain-rate dependent, which may explain the field observations reported by Leroueil (1988) for highly structured clays.

For more ordinary cohesive soils, the empirically developed end-of-primary uniqueness concept (Mesri and Choi 1985b) that forms the basis for hypothesis A still appears most reasonable for general practice. For incremental oedometer tests, this means using compression curves plotted at or shortly after the end-of-primary rather than at 24 hours (the latter typically reduces σ'_p by $10 \pm 10\%$). Constant rate of strain tests should be run with modest excess pore pressures [e.g., as recommended by Mesri (1985)] so as not to overestimate σ'_p . And controlled gradient tests are less desirable because they vary the strain rate (Leroueil et al. 1985).

Field Tests

Site characterization programs should include in situ testing as an economical means of soil profiling and to assess spatial variability in engineering properties, especially since laboratory data sometimes give mislead-

ing trends due to sample disturbance. Following are comments on three tests, with emphasis on their use to help interpolate and extrapolate laboratory preconsolidation pressure data.

Field Vane Test (FVT). For relatively homogeneous clay deposits (i.e., absence of shells, granular layers, varves, fibers, etc.), FVT data generally provide reasonable strengths for preliminary design [say $\pm 25\%$ with Bjerrum's (1972) correction factor] and therefore should reflect spatial variations in stress history. The data should be evaluated via log-log plots of undrained strength ratio versus overconsolidation ratio in order to use the relationship

$$\frac{s_u(\text{FV})}{\sigma'_{v0}} = S_{fv}(\text{OCR})^m \dots\dots\dots (11)$$

Chandler (1988) and Section 2.2.4 of Jamiolkowski et al. (1985) illustrate this approach. Since the values of S_{fv} and m vary significantly with soil type, quantitative estimates of σ'_p will require site-specific correlations.

Piezocene Penetration Test (CPTU). Baligh (1986a, 1986b) shows that universal correlations between penetration pore pressure–cone resistance data and stress history are not likely because the shear induced pore pressure, which varies with OCR, represents a small component of the total pore pressure measured either on the tip or behind the cone. Efforts to derive reliable undrained strengths from cone data also encounter problems (even after correction for the pore pressure–area ratio) and thus may require site-specific correlations. But the CPTU is ideally suited for rapid soil profiling and for estimating coefficients of consolidation (Campanella and Robertson 1988; Levadoux and Baligh 1986; and Section 3.4.5 of Jamiolkowski et al. 1985), provided that one uses well-designed equipment and pays careful attention to deairing and calibration.

Marchetti Dilatometer Test (DMT). Schmertmann (1986) presents a suggested standard for performing the DMT developed by Marchetti (1980) to provide a simple, inexpensive means both for identifying soil types and estimating certain engineering properties, such as the K_0 and OCR of cohesive deposits. Although the potential benefit of the OCR correlation is especially attractive, the empirical relationship developed by Marchetti (1980) for Italian clays has limitations [e.g., Lacasse and Lunne (1988)] and thus requires site-specific correlations for all major projects.

4.3. Factors Affecting Consolidated-Undrained Strength Testing

As previously stated, an undrained strength analysis (USA) requires predictions of the initial foundation strength and subsequent increases due to consolidation as functions of the initial stress history and how it changes during construction. Neither in situ nor laboratory UU-type tests have this capability, and, hence, the undrained strength-consolidation stress relationship must be obtained from laboratory consolidated-undrained (CU) strength testing. Rational selection of an appropriate CU test program should consider pertinent soil behavioral issues, as well as the practical limitations of available equipment. Consider, for example, the complex states of stress illustrated in Fig. 12. The clay foundation initially exists in a $K_0 < 1$ condition with the angle between the major principal stress and the vertical depositional direction being zero ($\delta = 0^\circ$). The initial undrained strength anisotropy governing stage 1 stability for the three elements on a wedge can be correctly

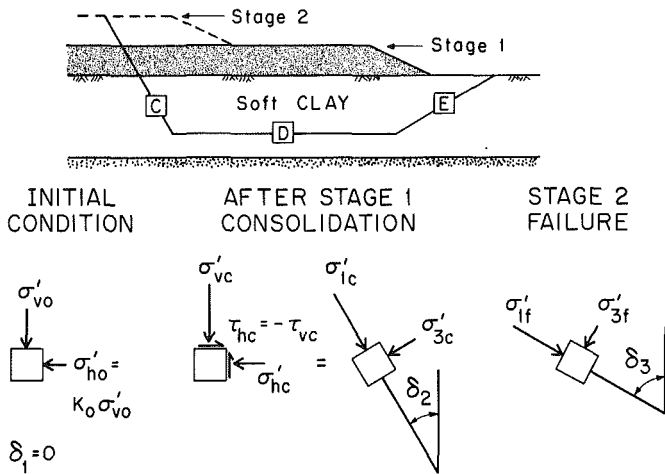


FIG. 12. Example of Complex States of Stress During Staged Construction for Element D

modeled in the laboratory via CK_0U plane strain compression (PSC), direct simple shear (DSS), and plane strain extension (PSE) tests. But subsequent consolidation under the stage 1 loading causes deviations from K_0 conditions, especially for element *D*. Accurate predictions of its strength for the stage 2 USA would require applying consolidation stresses having σ'_{1c} acting at angle δ_2 , followed by undrained shear with σ'_{1f} oriented at angle δ_3 . Test devices having this theoretical capability now exist, but only for research.

Since practical solutions clearly must simplify the real problem, one needs to appreciate the potential errors caused by various simplifications. For this purpose, the paper next summarizes aspects of CK_0U testing considered especially important: sample disturbance and consolidation stress history; time effects; intermediate principal stress; rotation of principal stresses (anisotropy); and progressive failure-strain compatibility. The paper then compares laboratory-derived strengths with those inferred from case histories of failures and evaluates potential errors from using CK_0U data to predict c_u after non- K_0 consolidation (i.e., for element *D* in Fig. 12).

4.4. Sample Disturbance and Reconsolidation Techniques

Although special large diameter samplers exist (Lefebvre and Poulin 1979; LaRochelle et al. 1981), most projects utilize more conventional tube sampling (preferably fixed piston) due to their lower cost and the need for deep samples. Baligh et al. (1987) show significant disturbance from the straining associated with common thin-walled tube sampling based on theoretical analyses using the strain path method (Baligh 1985) and experimental studies. This effect and other sources of disturbance (Table 7 of Jamiolkowski et al. 1985) alter the in situ soil structure, cause internal migration of water, frequently lead to substantial reductions in the effective stress of the sample (σ'_s), and often produce highly variable strengths from unconsolidated-undrained (UU) type testing. Hence, consolidated-undrained (CU) tests must

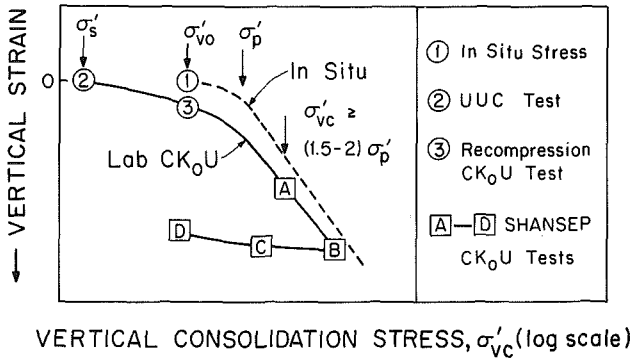


FIG. 13. Consolidation Procedures for Laboratory CK_0U Testing [after Ladd et al. (1977)]

be employed in order to minimize these adverse effects, where the two principal variables are the vertical consolidation stress, σ'_{vc} , and the consolidation stress ratio, $K_c = \sigma'_{hc}/\sigma'_{vc}$. The latter should approximate the in situ K_0 , both to help restore the in situ soil structure and to give more meaningful stress-strain-strength data. Therefore, *CIU* tests have little merit, unless K_0 is near unity, and attention will focus on the Recompression and SHANSEP reconsolidation techniques employed for CK_0U test programs.

These two techniques are illustrated in Fig. 13, which shows hypothetical in situ and laboratory K_0 compression curves for a slightly overconsolidated soft clay. Points 1 and 2 designate the in situ condition and the preshear effective stress for a UU test, respectively. Test specimens following the Recompression technique are reconsolidated to $\sigma'_{vc} = \sigma'_{vo}$ shown as point 3. Points A–D correspond to typical stresses used for SHANSEP.

Bjerrum (1973) presents the rationale underlying the Recompression technique long practiced by the Norwegian Geotechnical Institute. The companion paper by Berre and Bjerrum (1973) states: "Provided that the reduction in water content . . . [at point 3] . . . is not too large, the results . . . should give a fair representation of the behaviour of clay in the field." They quote typical volumetric strains of 1.5%–4% and conclude that destruction of natural bonding by sample disturbance more than offsets the strength gain due to the lower water content.

The SHANSEP technique, as described by Ladd and Foott (1974) and Ladd et al. (1977), entails the following basic steps (for a given layer and mode of failure): (1) Establish the initial stress history; (2) perform CK_0U tests on specimens consolidated well beyond the in situ σ'_p to measure the behavior of normally consolidated clay (points A and B in Fig. 13), and also on specimens rebounded to varying OCR to measure overconsolidated behavior (points C and D); (3) express the results in terms of log undrained strength ratio versus log OCR (e.g., to obtain values of S and m in Eq. 9); and (4) use these with the stress history to compute c_u profiles. Although originally developed based on the empirical observation that it yielded reasonable results, the rationale for the SHANSEP reconsolidation technique to minimize disturbance effects was predicated on the assumption that natural clays exhibit normalized behavior. Specifically, SHANSEP assumes me-

chanically overconsolidated behavior to represent all preconsolidation pressure mechanisms, and hence involves obvious errors with highly structured, sensitive clays and with naturally cemented deposits.

Although more research is needed to quantify the likely errors associated with using the Recompression and SHANSEP techniques for the wide range of sample qualities and soil types encountered in practice, the writer offers the following guidelines and comments for CK_0U test programs.

The Recompression technique:

1. Is clearly preferred when block quality samples are available.
2. Is more accurate for highly structured, brittle clays (say $S_t > 5-10$ and $I_L > 1-1.5$), such as typical of eastern Canada. But reliable stress-strain data also require high-quality samples (LaRochelle et al. 1981; Lacasse et al. 1985). SHANSEP may significantly underpredict peak triaxial strengths (Tavenas and Leroueil 1985) and probably gives somewhat conservative design strengths after considering anisotropy and strain compatibility.
3. Is preferred for strongly cemented soils (although often hard to identify), and for testing highly weathered and heavily overconsolidated crusts where SHANSEP is often difficult to apply.
4. Should not be used in truly normally consolidated soils ($OCR = 1$), such as encountered in tailings slimes, dredged materials, and recent deltaic deposits, since reconsolidation to $\sigma'_{v0} = \sigma'_p$ will clearly overestimate the in situ strength.
5. Should always be accompanied by a thorough evaluation of the in situ stress history in order to: estimate K_0 ; check the reasonableness of the measured c_u/σ'_{v0} values; and extrapolate and interpolate the "point" data versus OCR.

The SHANSEP technique:

1. Is strictly applicable only to mechanically overconsolidated and truly normally consolidated soils exhibiting normalized behavior.
2. Is probably preferred for testing conventional tube samples from low OCR deposits of "ordinary" clays, meaning a relatively low sensitivity and the preconsolidation pressure caused mainly by the mechanical-desiccation-aging mechanisms. SHANSEP may tend to underestimate strengths in deposits having significant physico-chemical effects and perhaps characterized by $m = 1$ in Eq. 9 leading to a constant c_u/σ'_p . On the other hand, Peck (1973) cautions that the Recompression technique "goes hand in hand with the most expert sampling" and when "samples of the necessary quality are not . . . obtained . . . the reconsolidation procedure will lead to serious errors."
3. Has the distinct advantage of forcing the user to assess the in situ stress history and of developing normalized strength parameters that are necessary for all staged construction projects.

The Recompression and SHANSEP techniques both involve K_0 consolidation, which is difficult and costly for triaxial testing without automation. Hence, many laboratories use a simplified technique via isotropic consolidation to $\sigma'_{hc} = K_0\sigma'_{vc}$, followed by drained loading to reach σ'_{vc} . This is reasonable, provided that the first step does not cross the "yield envelope" for isotropic consolidation (Germaine and Ladd 1988; Lacasse and Berre 1988). Both approaches also require shearing in different failure modes to assess stress-strain-strength anisotropy. Finally, it should be recognized, when

dealing with overconsolidated deposits, that Recompression *reloads* the soil and SHANSEP usually *unloads* the soil to the relevant OCR. Hence, the resulting undrained strength ratios may be different because of the hysteresis loop exhibited by one-dimensional unload-reload cycles.

In summary, both techniques should be considered for staged construction projects; have differing potentials for error, depending on the sample quality and soil type; and require relatively sophisticated CK_0U testing. Both also depend upon a careful assessment of the in situ history, explicitly for SHANSEP and implicitly for Recompression.

4.5. Time Effects

Two types of time effects influence the behavior of CK_0U tests: the time allowed for consolidation prior to shear; and the strain rate (or rate of load application) used during shear. The first type affects behavior due to the well-known fact that "aging" at constant effective stress (i.e., secondary compression equals one-dimensional drained creep) increases the stiffness and preconsolidation pressure (σ'_p) and hence the undrained strength of normally loaded soils. Mesri and Castro (1987) show a unique relationship between the rate of secondary compression and the slope of the one-dimensional compression curve during *both* recompression and virgin compression for any given soil. Aging effects are therefore most important with low OCR specimens, for which one should standardize the amount of aging in order to obtain consistent CK_0U data. The writer recommends one log cycle since: With $\log(t/t_p)$ much less than one, significant pore pressures may develop during undrained shear due to preventing secondary compression; a $\log(t/t_p)$ much greater than one will take too long and the c_u data will need a correction for the increased σ'_p .

Laboratory UU and CU tests on cohesive soils show higher strengths with increasing strain rate ($\dot{\epsilon}$) and hence decreasing time to failure (t_f). The effect can be expressed in terms of $\lambda = (\Delta c_u/c_{u0})/\Delta \log \dot{\epsilon}$, where c_{u0} is the reference strength, say at $\dot{\epsilon} = 1\%$ per hour. The thorough literature survey by Lacasse (1979) and subsequent research indicate the following trends: CIUC tests on OCR = 1 clays typically give $\lambda = 0.1 \pm 0.05$ for t_f ranging from several minutes to several hours; λ usually increases at very fast shearing rates; λ may be much larger in high OCR soils; and the mode of shearing affects λ , being higher for triaxial than for direct simple shear. The mechanisms responsible for this behavior are still poorly understood, and no proven framework exists to select strain rates for CK_0U testing. But general experience based on a balance between practicality and limited case histories has resulted in the following practice by many leading research-consulting laboratories: axial strain rate of 0.5%–1% per hour for triaxial tests; and shear strain rate of 5% per hour for direct simple shear tests.

4.6. Stress Systems for CK_0U Test Programs

When comparing shear devices available for CK_0U testing, two variables usually suffice to describe the basic differences in the applied stress system (applied state of stress): the relative magnitude of the intermediate principal stress as defined by $b = (\sigma_2 - \sigma_3)/(\sigma_1 - \sigma_3)$; and the direction of the applied major principal stress relative to the vertical (depositional) direction denoted by the δ angle (Fig. 12). Changes in the values of b and δ lead to different stress-strain responses due to the effects of σ_2 and anisotropy, respectively.

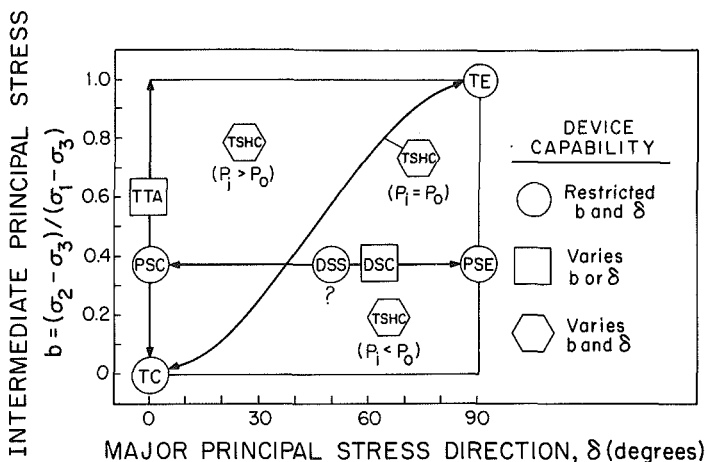


FIG. 14. Stress Systems Achievable by Shear Devices for CK_0U Testing [Modified from Germaine (1982)]

Ideally, CK_0U testing for staged construction projects should shear specimens at representative δ angles to measure the stress-strain-strength anisotropy of the soil. Such tests also should duplicate the in situ b value, which often approximates a plane strain condition (say with $b = 0.3-0.4$).

Fig. 14 illustrates the combinations of b and δ that can be achieved by laboratory shear devices. Comments regarding their usefulness for CK_0U testing in practice follow [Jamiolkowski et al. (1985) provide additional details and references].

Directional shear cell (DSC): The DSC has the unique ability to vary δ between 0° and 90° under plane strain conditions by application of normal and shear stresses to four sides of a cubical sample constrained between two rigid end platens (Arthur et al. 1981). Although ideally suited for detailed studies of anisotropy, this research device is not yet ready for use in practice.

Torsional shear hollow cylinder (TSHC): The apparatus developed at Imperial College (Hight et al. 1983) has the theoretical ability to cover much of the b -versus- δ space in Fig. 14, but its use to date has been restricted to tests on sand. TSHC tests that maintain equal inner and outer pressures ($P_i = P_o$) inherently cause b to increase from zero to unity as δ varies from 0° to 90° , which complicates interpretation of the data. Such tests have been run on conventional tube samples of clay (Saada and Townsend 1981).

True triaxial apparatus (TTA): Devices that can readily vary the principal stress magnitudes are well suited to study changes in b , but have very limited usefulness in practice regarding anisotropy (e.g., usually restricted to $\delta = 0^\circ$ as shown in Fig. 14).

Plane strain compression/extension (PSC/E): These devices can provide reliable CK_0U data for plane strain shearing at $\delta = 0^\circ$ and 90° (Vaid and Campanella 1974), but cannot achieve intermediate δ angles.

Direct simple shear (DSS): The Norwegian Geotechnical Institute (NGI) and MIT use the Geonor DSS (Bjerrum and Landva 1966) to simulate the horizontal

portion of a failure surface as part of their standard procedure for evaluating anisotropy via the Recompression and SHANSEP techniques. Its use in practice is increasing even though the failure values of $0.5 (\sigma_1 - \sigma_3)$ and δ in the DSS remain illusive due to nonuniform and incomplete stress-strain conditions [e.g., Ladd and Edgers (1972)].

Triaxial compression/extension (TC/E): Conventional CK_0U triaxial tests can shear samples only at $\delta = 0^\circ$ and 90° with $b = 0$ and i , respectively. Such testing should generally give conservative peak strengths for plane strain problems since Ladd et al. (1977) quote:

- At $\delta = 0^\circ$, $q_f(\text{TC})/q_f(\text{PSC}) = 0.92 \pm 0.05$ (several clays).
- At $\delta = 90^\circ$, $q_f(\text{TE})/q_f(\text{PSE}) = 0.82 \pm 0.02$ (only four clays).

In summary, essentially all available data for assessing the undrained stress-strain-strength anisotropy of natural clays, starting from K_0 conditions, have come from PSC or TC, DSS, and PSE or TE tests. The next sections review the nature of strength anisotropy and summarize typical results.

4.7. Components and Causes of Anisotropy

Initial anisotropy denotes changes in the stress-strain-strength response of a soil with variations in the applied σ_1 direction (δ angle) during monotonic shearing. For natural clays having a one-dimensional strain history (K_0 consolidation and rebound), the resulting cross-anisotropic behavior has two components. An *inherent* anisotropy arises from the “soil structure” developed at the microlevel (preferred particle orientations and interparticle forces) and also at the macrolevel for certain soils such as varved glacial-lake deposits. Clays also exhibit directionally dependent undrained strengths whenever shearing starts from a $K_0 \neq 1$ condition, as first predicted by Brinch-Hansen and Gibson (1949) and called *initial shear stress* anisotropy by Jamiolkowski et al. (1985). The combined effect of both components is of prime interest in practice, where the normalized undrained strength ratio for low OCR clays sheared in compression and extension can be expressed as follows:

$$\frac{q_f(C)}{\sigma'_{vc}} = \frac{[K_0 + (1 - K_0)A_f] \sin \phi'}{1 + (2A_f - 1) \sin \phi'} \dots \dots \dots (12a)$$

with $A_f = (\Delta u - \Delta\sigma_h)/(\Delta\sigma_v - \Delta\sigma_h)$ since $\Delta\sigma_h = \Delta\sigma_3$

$$\frac{q_f(E)}{\sigma'_{vc}} = \frac{[1 - (1 - K_0)A_f] \sin \phi'}{1 + (2A_f - 1) \sin \phi'} \dots \dots \dots (12b)$$

with $A_f = (\Delta u - \Delta\sigma_v)/(\Delta\sigma_h - \Delta\sigma_v)$ since $\Delta\sigma_v = \Delta\sigma_3$.

Assuming isotropic material properties with $K_0 = 1 - \sin \phi'$, Eq. 12 gives $K_s = q_f(E)/q_f(C) = 0.167/0.333 = 0.50$ for $\sin \phi' = 0.50$ and $A_f = 1.00$ and $K_s = 0.233/0.300 = 0.78$ for $\sin \phi' = 0.40$ and $A_f = 0.75$. Subsequent data show these values as being typical of the *initial* undrained strength anisotropy for lean and plastic OCR = 1 clays, respectively, even though $\sin \phi'$ and A_f also vary due to the effects of inherent anisotropy.

Ideally, one should also consider the influence of *evolving* anisotropy, which describes how the *initial* cross-anisotropic properties of a K_0 consolidated clay change due to plastic strains caused by stresses (both shear and consolidation) applied during staged construction. However, since common shear devices cannot realistically simulate complex principal stress rotations

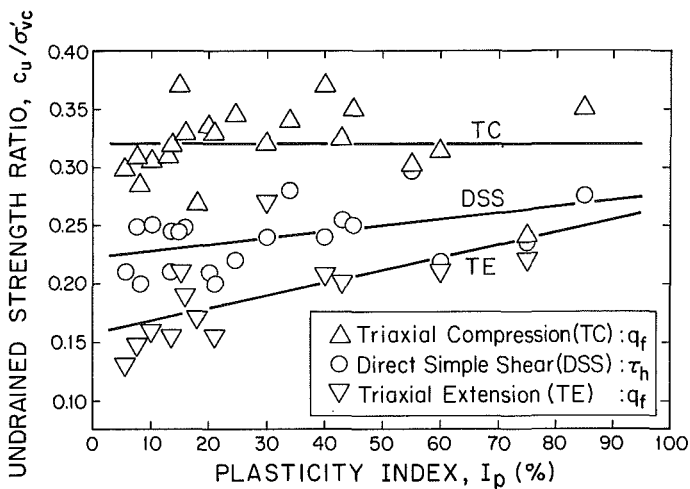


FIG. 15. Undrained Strength Anisotropy from CK_0U Tests on Normally Consolidated Clays and Silts [Data from Lefebvre et al. (1983); Vaid and Campanella (1974); and Various MIT and NGI Reports]

such as illustrated in Fig. 12, practice usually ignores evolving anisotropy except for special cases such as described in Section 4.11.

4.8. Effects of Anisotropy

Fig. 15 plots peak undrained strength ratios from CK_0U triaxial compression/extension, and Geonor direct simple shear tests run on various normally consolidated clays and silts (but excluding varved deposits). The data show: $q_f/\sigma'_{vc} = 0.32 \pm 0.03$ in TC and having no trend with I_p ; generally much lower DSS strengths that tend to decrease with lower plasticity; and even smaller ratios for shear in TE, especially at low I_p . Although triaxial testing tends to underestimate peak strengths for plane strain conditions (due to the b effect previously mentioned), these data and the literature clearly demonstrate that most $OCR = 1$ soils exhibit significant c_u anisotropy that generally becomes most important in lean clays, especially if also sensitive. Varved clays represent a special case wherein horizontal (DSS) shearing gives an unusually low peak τ_h/σ'_{vc} of only 0.16 ± 0.01 for northeastern U.S. deposits (Ladd 1987b).

Overconsolidated soils can also exhibit pronounced anisotropic behavior, as illustrated by the data in Fig. 16. The SHANSEP CK_0U test program run on the Atlantic Generating Station (AGS) moderately plastic marine clay ($I_p = 43 \pm 7\%$, $I_L = 0.6 \pm 0.1$) gives results considered representative of mechanically overconsolidated clays. Fig. 16(a) shows only slightly less c_u anisotropy with increasing OCR as measured in triaxial compression/extension and direct simple shear tests, and a very large increase in the shear strain at failure (γ_f) in going from TC to DSS to TE, especially at low OCR. Fig. 16(b) plots data from Recompression CK_0U tests performed on block samples of the marine clay for the James Bay case history (see Fig. 7) as representative of a highly sensitive, cemented lean clay. The OC (intact)

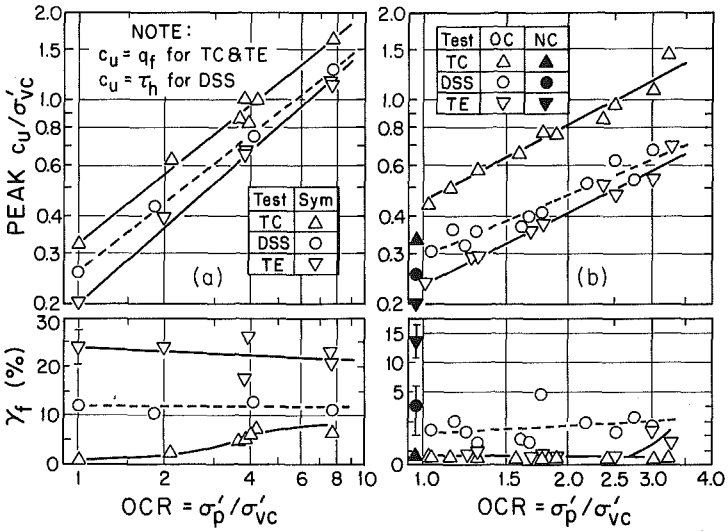


FIG. 16. OCR versus Undrained Strength Ratio and Shear Strain at Failure from CK_0U Tests: (a) AGS Plastic Marine Clay via SHANSEP (Koutsoftas and Ladd 1985); and (b) James Bay Sensitive Marine Clay via Recompression [B-6 Data from Le-febvre et al. (1983)]

data are from specimens consolidated to the in situ $OCR = 2.5 \pm 1$ and also up to the in situ preconsolidation pressure, whereas NC denotes results for σ'_{vc} ranging from 1.3 to 3 times the in situ σ'_p . For OC (intact) clay, Fig. 16(b) shows very high strengths in TC compared to DSS and TE and much smaller γ_f values compared to the AGS clay. For NC soil, wherein large consolidation strains presumably destroyed most of the cementation bonds, the solid symbols in Fig. 16(b) show somewhat less c_u anisotropy, but much greater differences in γ_f . Also note the lower NC c_u/σ'_{vc} values relative to those at OCR near unity for intact clay, which supports the view that SHANSEP yields conservative strengths for highly structured soils. Finally, the strength data for both soils in Fig. 16 closely follow straight lines on the log-log plot that define the S and m parameters used in Eq. 9.

4.9. Progressive Failure and Strain Compatibility

The paper now looks at how anisotropy affects undrained stress-strain behavior, rather than changes in peak strength, as illustrated by the results for $OCR = 1$ samples of the AGS plastic clay. Fig. 17 plots shear stress, defined as shown in the figure (with $\phi' = 35^\circ$), versus shear strain from CK_0U plane strain compression and extension and direct shear tests. For a wedge-shaped failure surface, τ_c represents the resistance of the active (compression) portion, τ_d simulates shear on the horizontal segment, and τ_e represents behavior within the passive (extension) zone. The τ_c curve has a small γ_f , followed by significant strain softening; τ_e starts from a negative value at consolidation and requires very large strains to reach its peak strength; and τ_d falls between these extremes. These data indicate that the compression portion of a failure wedge will be strained beyond its peak strength and lose

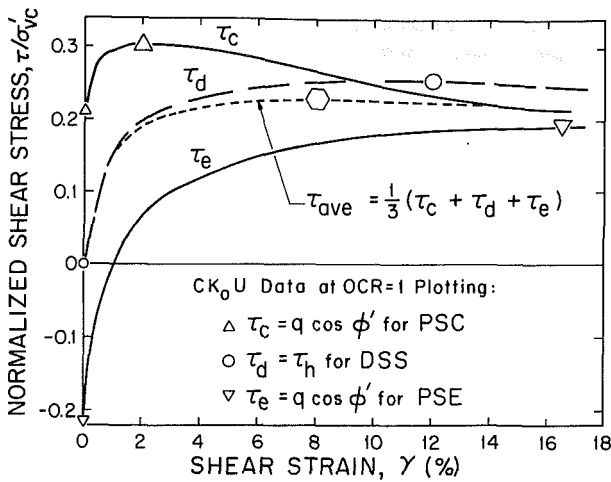


FIG. 17. Normalized Stress-Strain Data for AGS Marine Clay Illustrating Progressive Failure and the Strain Compatibility Technique [after Koutsoftas and Ladd (1985)]

resistance before the strengths along the horizontal surface and within the extension portion of the wedge can be fully mobilized. This phenomenon, called *progressive failure*, means that the in situ resistance that can be mobilized along an actual rupture surface will be less than the sum of the peak strengths for soils exhibiting strain softening.

Ladd (1975) developed the *strain compatibility* technique as an approximate methodology to account for progressive failure when conducting undrained strength analyses. As described in Koutsoftas and Ladd (1985), the technique assumes that the shear strain all along a potential failure surface will be uniform at the moment of actual failure, i.e., when the maximum average resistance is mobilized. Based on this premise, the average resistance that can be mobilized at any given strain equals $\tau_{ave} = 1/3 \times (\tau_c + \tau_d + \tau_e)$ for a rupture surface having equal contributions of τ_c , τ_d , and τ_e . The average resistance for the OCR = 1 clay in Fig. 17 reaches a maximum value of $\tau_{ave}/\sigma'_{vc} = 0.225$ at $\gamma = 8\%$, compared to an average of the peak strengths equal to $1/3 \times (0.305 + 0.255 + 0.19) = 0.25$. Thus, progressive failure reduces the available resistance in this case by 10%.

For a "rational" selection of the strain level at which to determine the corresponding design strengths, one ideally should consider the relative contributions of each failure mode and the in situ OCR for all design conditions. But such refinement is not practical, nor justified given the simplifying assumptions of the strain compatibility technique and typical uncertainties in the stress-strain and stress history data. Hence, the writer selects a design strain level for the foundation clays that gives τ_{ave} values near the collective maximum for stress histories representative of critical stability conditions, but also yields anisotropic strength ratios that appear reasonable, e.g., $\tau_c > \tau_d > \tau_e$. (Note: an error in the selected strain should give conservative parameters.)

TABLE 4. Normally Consolidated Undrained Strength Ratios from CK_0U Compression, Direct Simple Shear and Extension Tests Treated for Strain Compatibility

Number (1)	Soil (2)	Index Properties			Peak c_u/σ'_{vc}		Strain Compatibility c_u/σ'_{vc}					C/E testing ^b	Tests by (14)
		USC (3)	I_p (%) (4)	I_L (5)	Peak c_u/σ'_{vc}		γ^a (%) (8)	τ_c (9)	τ_d (10)	τ_e (11)	τ_{ave} (12)		
					q_f (TC) (6)	τ_h (DSS) (7)							
1	B2 marine clay	CL	8.5	2.6	0.31	0.23	1.5	0.26	0.22	0.09	0.19	TX	SEBJ
2	B6 marine clay	CL	13	1.9	0.33	0.24	2	0.26	0.225	0.16	0.215	TX	SEBJ
3	Resedimented BBC	CL	21	1.0	0.33	0.20	6	0.265	0.20	0.135	0.20	PS	MIT
4	Connecticut Valley varved clay	CL CH	12 39	—	0.25	0.16	6	0.21	0.15	0.20	0.185	PS	MIT
5	Great Salt Lake clay	CH	40	1.1	0.37	0.24	8	0.27	0.24	0.16	0.225	TX	MIT
6	AGS marine clay	CH	43	0.6	0.325	0.255	8	0.265	0.25	0.16	0.225	PS	MIT UBC
7	Omaha, Nebr. clay	CH	60	0.7	0.315	0.22	10	0.23	0.21	0.20	0.215	TX ^c	MIT
8	Arctic silt A	ML	15	0.3	0.37	0.245	12	0.305	0.24	0.18	0.24	TX	MIT
9	Arctic silt B	MH	30	0.7	0.32	0.24	12	0.27	0.24	0.20	0.235	TX	MIT
10	EABPL clay	CH	75	0.85	0.24	0.235	15	0.24	0.23	0.22	0.23	PS/TX ^d	MIT

^aDesign shear strain selected for strain compatibility.

^bTX = triaxial and PS = plane strain.

^cTriaxial τ_c increased by 5%.

^dApproximate mean of plane strain and triaxial data.

Table 4 presents undrained strength ratios at OCR = 1 obtained from applying the strain compatibility technique to 10 soils having widely varying index properties and moderate to extensive CK_0U data. The results are listed in order of increasing shear strain selected to obtain the strength parameters (which also considered overconsolidated data for soils 1–4 and 6) and range from a few percent in the two sensitive clays up to 10%–15% in the plastic clays and two Arctic silts. The average strengths fall within a narrow band, $\tau_{ave}/\sigma'_{vc} = 0.215 \pm 0.02$ SD (SD = standard deviation); they are $8 \pm 4\%$ less than the average of the peak strengths (data not shown); and those based on triaxial testing may err on the low side. The seven CL and CH clays (i.e., excluding the varved clay and two Arctic silts) show an amazingly consistent trend with plasticity index, with linear regression giving:

$$\frac{\tau_{ave}}{\sigma'_{vc}} = 0.20 + 0.045I_p, \quad r = 0.75 \text{ (see Fig. 18)}$$

$$K_s = \frac{\tau_e}{\tau_c} = 0.37 + 0.72I_p \quad r = 0.9$$

Hence, lean clays have pronounced undrained strength anisotropy even after considering strain compatibility. Such soils generally warrant wedge analyses using τ_c , τ_d , and τ_e , rather than circular arc analyses using τ_{ave} . The same applies to varved clays.

4.10. Comparison of Field and Laboratory Strengths

Larsson (1980) evaluated case histories of failures to obtain backcalculated

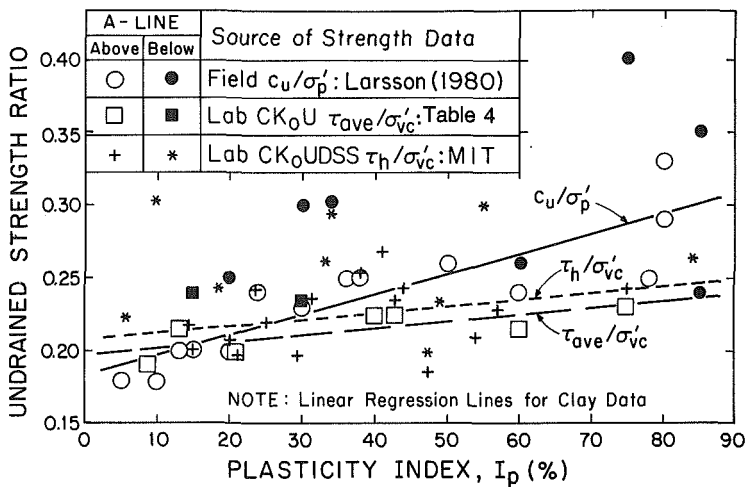


FIG. 18. Comparison of Field and Laboratory Undrained Strength Ratios for Nonvarved Sedimentary Soils (OCR = 1 for Laboratory CK₀U Testing)

average values of the in situ undrained strength divided by the preconsolidation pressure, c_u/σ'_p . Most of the cases involved UU failures of relatively low OCR soils. Fig. 18 plots his results for loading failures (embankments, tanks, load tests, etc.) of nonvarved soils versus plasticity index. In spite of potential errors in both c_u and σ'_p , the data show a reasonably consistent pattern:

- For inorganic clays (the Atterberg limits plot above Casagrande's A-line), $c_u/\sigma'_p = 0.235 \pm 0.04$ SD and strongly tends to increase with I_p based on 14 cases.
- For organic clays and silts (the Atterberg limits plot below the A-line), a higher $c_u/\sigma'_p = 0.30 \pm 0.06$ SD and having little trend with I_p based on seven cases.

Fig. 18 also plots τ_{ave}/σ'_{vc} values from Table 4, excluding the varved clay. The laboratory derived ratios for the inorganic clays have $\tau_{ave}/\sigma'_{vc} = 0.215 \pm 0.015$ SD and show less variation with I_p than the corresponding field data. These τ_{ave}/σ'_{vc} values presumably give the in situ c_u for infinitely long failures of OCR = 1 soils. For direct comparison with field-derived strengths, τ_{ave} should be increased by $10 \pm 5\%$ for typical "end effects" present in embankment failures (Azzouz et al. 1983) and reduced by $(OCR)^{m-1}$ to account for decreases in c_u due to "unloading," the latter being 10% at OCR = 2 with $m = 0.85$. Hence, the two ratios in Fig. 18 should, in theory, be nearly identical. Indeed, the laboratory data support a "practically constant field . . . $c_u/\sigma'_p = 0.22$ independent of plasticity index" that Mesri (1975) derived from Bjerrum's (1972) correlations of $s_u(FV)/\sigma'_{v0}$, σ'_p/σ'_{v0} and the field vane μ correction factor versus I_p .

Finally, Fig. 18 also presents the peak undrained strength ratio measured at MIT from Geonor CK₀UDSS tests on 25 OCR = 1 nonvarved soils, again

distinguishing between soils plotting above and below the A-line. Linear regression on 16 clays having $\tau_h/\sigma'_{vc} = 0.225 \pm 0.025$ SD gives a relationship 5% above that for τ_{ave}/σ'_{vc} . The data for nine silts and organic soils have $\tau_h/\sigma'_{vc} = 0.26 \pm 0.035$ SD and show no trend with I_p .

Based on the aforementioned results, the writer makes the following observations and conclusions.

1. For inorganic clays with $I_p = 25 \pm 15\%$, good agreement exists between strengths backcalculated from field failures and those obtained from comprehensive CK_0U tests treated for strain compatibility (τ_{ave}) and also from DSS tests (τ_h). For more plastic clays, Larsson's data infer higher strengths than measured via CK_0U tests, mainly based on two Swedish load tests. However, since three of the four τ_{ave} values (soils 5, 7, and 10 in Table 4) are supported by field observations, the writer places more credence in the laboratory relationship.

2. Silts and organic clays appear to have higher, and also more scattered, normalized strengths, as observed from a more limited number of field cases and laboratory CK_0U tests.

3. Section 5.3 of the paper will recommend three approaches for obtaining undrained strength ratios for use in stability analyses, namely complete CK_0U testing treated for strain compatibility; CK_0UDSS tests; and empirical correlations based on the data in Fig. 18.

4.11. Strength Gain during Staged Construction

As previously noted, estimates of the increases in c_u with consolidation for the two embankment case histories involved two simplifications: changes in consolidation stress being restricted to increases in σ'_{vc} , which are less than σ'_{ic} except under the center line; and CK_0U test data used to relate c_u to σ'_{vc} , whereas the actual consolidation stresses often deviate significantly from K_0 conditions. The error from these simplifications should become most important within normally consolidated soil under a berm, e.g., for element D in Fig. 12. The error can be approximately evaluated by comparing data from CK_0U versus CAU direct simple shear tests, the latter denoting tests wherein DSS specimens are consolidated with varying values of horizontal shear stress (τ_{hc}) prior to undrained shear.

Fig. 19(a) plots the increase in peak strength for three normally consolidated clays as a function of the preshear τ_{hc} , expressed as a fraction of the $c_u = \max \tau_h$ measured in conventional CK_0UDSS tests. The results show significant strengthening, e.g., by 15%–30% at a stress ratio of 0.8. There is also a marked reduction in the strain at failure and those CAU tests having large c_u increases also tend to exhibit more pronounced strain softening, as illustrated in Fig. 19(b) for Boston Blue Clay. Thus, staged construction leading to normally consolidated soil under berms can produce a stress-strain response to horizontal shearing approaching that for shear in compression, i.e., much stiffer and stronger than measured in conventional CK_0UDSS tests.

When stability analyses based on strengths derived from CK_0U data show marginal factors of safety, the writer recommends special CAUDSS testing to evaluate potentially higher undrained strength ratios for $OCR = 1$ soils encountered below embankment berms and under the slopes of tailings dams. If this had been done for the James Bay case history, the FS(USA) in Table 3 would probably have increased by at least 10% (assuming behavior similar to Boston Blue Clay). But the FS(USA) obtained for the embankment on

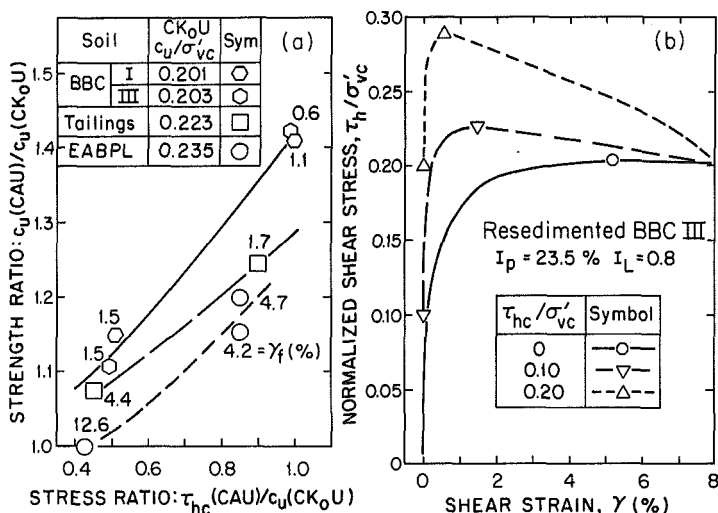


FIG. 19. Effect of Consolidation Shear Stress on Undrained Direct Simple Shear Behavior of Normally Consolidated Clay: (a) Increase in Peak Strength for Boston Blue Clay, Copper Tailings and Atchafalaya Clay; and (b) Shear Stress versus Shear Strain for Boston Blue Clay (Note: Copper Tailings Data by R. S. Ladd; Other Data by MIT)

varved clay would have remained unchanged since CAUDSS tests show no strength increase for this unusual soil type. And the mean c_u/σ'_{vc} ratio selected for the tailings dam case history did consider higher CAUDSS strengths because of its marginal stability.

5. RECOMMENDED METHODOLOGY FOR UNDRAINED STRENGTH ANALYSES

5.1. Overview

An undrained strength analysis (USA) denotes the use of limiting equilibrium analyses to obtain factors of safety wherein the available resistance against an undrained failure of cohesive soils is computed from knowledge of the current consolidation stresses and prior stress history combined with appropriate undrained strength-consolidation stress relationships. For the design of staged construction projects, such analyses would typically have the four steps shown in Table 5. Steps 1 and 2 evaluate stability for the stage 1 loading assuming no drainage during construction (the UU case), so that the initial stress history of the deposit (σ'_{v0} and σ'_p) governs the available undrained shear strength (c_u). Steps 3 and 4 refer to stability evaluations during subsequent construction at some time t_n wherein the combination of the applied loads and either partial or full consolidation has altered the initial stress history and increased the available resistance. Steps 3 and 4 fall under the CU case and would be repeated n times depending upon the project complexity.

Table 5 also illustrates the experimental and theoretical components needed

TABLE 5. Methodology for Conducting Undrained Strength Analyses During Design of Staged Construction Projects

Components (1)	Step No. 1: initial stress history and c_u (2)	Step No. 2: factor of safety for stage 1 (step No. 1 plus) (3)	Step No. 3: stress history and c_u at t_n (step No. 1 plus) (4)	Step No. 4: factor of safety at stage n (step No. 3 plus) (5)
Experimental analyses ^a				
E1—Initial state variables	X			
E2—Undrained strength parameters	X			
E3—Consolidation-flow parameters			X	
Theoretical Analyses				
T1—Stress distribution ^b			X	
T2—Consolidation ^b			X	
T3—Limiting equilibrium		X		X

^aObtained from combined evaluation of in situ and laboratory test data.

^bCombined results give σ'_{vc} profiles at time t_n .

for the previous steps. The initial state variables, listed as E1, refer to the soil profile (soil types and index properties and the ground-water conditions), the initial state of stress (σ'_{v0} and K_0) and the preconsolidation pressure (σ'_p). These, plus results from laboratory CU testing to obtain undrained strength ratios, furnish the information for step 1. The limiting equilibrium analyses of step 2 then use the initial c_u profile to compute factors of safety for stage 1 construction. Subsequent stability evaluations (steps 3 and 4) require knowledge of consolidation-flow parameters (e.g., permeability-compressibility properties) for use in theoretical stress distribution and consolidation analyses to predict vertical consolidation stress profiles at times t_n . The analyses would typically vary the loading geometry, rate of filling, and drainage conditions (e.g., with and without vertical drains to accelerate consolidation rates) as part of the iterative design process.

Section 5 focuses on technical recommendations regarding consolidation analyses to predict changes in stress history, laboratory CU test programs, and other approaches to obtain c_u versus stress history relationships, and selection of and input data for limiting equilibrium analyses. Section 7 treats the use of undrained strength analyses during construction monitoring.

5.2. Evaluation of Stress History and Consolidation Analyses

Evaluation of the initial stress history entails definition of the preconstruction in situ state of stress and the preconsolidation pressure. For natural clay deposits having a one-dimensional strain history, σ'_{v0} can be accurately obtained from measurements of unit weights and the ground-water conditions, whereas reliable estimates of $\sigma'_{h0} = K_0\sigma'_{v0}$ (required for realistic predictions of lateral deformations as described in Section 7 and also needed for Re-

compression CK_0U tests) are usually difficult. Proven techniques do not yet exist for directly measuring the in situ K_0 from laboratory testing, and Section 3.2 of Jamiolkowski et al. (1985) assesses the pros and cons of using various types of field devices to measure K_0 . For mechanically overconsolidated clay deposits, the empirical $K_0 = f(\phi', \text{OCR})$ relations given in Mayne and Kulhawy (1982) may suffice.

Evaluation of the initial σ'_p profile constitutes the single most important task on most projects since it basically governs both the initial c_u and the minimum stage 1 loading needed for substantial foundation strengthening. For natural deposits, Section 4.2 recommended using high-quality oedometer tests combined with in situ testing to assess spatial variability. Man-made deposits may warrant different techniques since these materials often exist in an "underconsolidated" state with $\sigma'_{v0} = \sigma'_p$ increasing with time due to self-weight consolidation. In both cases, the USA methodology requires explicit resolution of conflicts between the c_u profile developed in step 1 and values obtained from conventional in situ and laboratory strength testing.

Step 3 in Table 5 requires consolidation analyses to predict rates of pore pressure dissipation (increases in σ'_{vc}) during construction. These predictions often strongly impact the project feasibility, schedule, and costs during design on the one hand, and on the other also entail significant uncertainty. The following text makes recommendations and identifies problems regarding consolidation analyses during final design for vertical drainage of natural deposits, horizontal flow to installed vertical drains, and tailings dams.

One-Dimensional Consolidation of Natural Clays

Although practice often relies on chart solutions based on conventional Terzaghi theory, the assumption of constant values of the coefficient of consolidation (c_v) and compressibility ($m_v = d\epsilon_v/d\sigma'_{vc}$) will give poor estimates of pore pressures during consolidation for foundations with layers having different c_v and m_v values; moderately overconsolidated deposits (large changes in both c_v and m_v near σ'_p); and normally consolidated soils having highly stress-dependent parameters such sensitive clays. These situations may warrant numerical analyses that use a nonlinear model of soil behavior and that incorporate submergence and changes in loads and boundary pore pressures. As one example, the ILLICON program described by Mesri and Choi (1985a) models soils having linear e -log k and nonlinear e -log σ'_{vc} relationships. Experimental programs may also need more emphasis on direct measurements of permeability during incremental consolidation testing since values of k backcalculated from c_v and m_v can be erroneous (Tavenas et al. 1983).

Consolidation with Vertical Drains

Installation of vertical drains to accelerate the rate of consolidation introduces two additional problems regarding reliable predictions of pore pressures during staged construction: evaluation of the anisotropic permeability ratio, $r_k = k_h/k_v$, needed to estimate the coefficient of consolidation for horizontal flow, $c_h = r_k c_v$; and assessment of the likely effects of soil disturbance caused by drain installation (assuming high-quality drains having negligible resistance to flow of water into and then out of the drain). The value of r_k depends on four characteristics of the deposit: (1) Anisotropy at the microfabric level, which usually will be small, say $r_k = 1.0$ – 1.5 ; (2) regular layering at the macrolevel, as with varved clays where $r_k = 10 \pm 5$ might

be typical (Ladd 1987b); (3) *irregular* layering at the macrolevel due to permeable seams and lenses; and (4) the presence of occasional thick sand-silt layers. Proper laboratory testing can measure characteristics No. 1 and 2, whereas in situ testing with the piezocone, piezometers, etc., is better suited to evaluate characteristics No. 3 and 4.

Vertical drain technology has changed dramatically, first with the introduction in the late 1960s of moderate to negligible displacement sand drains (e.g., various augering and jetting techniques having typical diameters of 0.3 m–0.5 m) that could negate disturbance effects, and then in the 1970s with a wide variety of prefabricated wick drains that have essentially captured the market due to their very low cost. But installation and withdrawal of the mandrel causes severe disturbance to the soil surrounding wick drains, which can result in “effective” c_h values significantly less than the c_h for undisturbed soil. Attempts to predict this effect still largely rely on Barron’s (1948) theoretical treatment that incorporates an incompressible smear zone around the drain having a permeability less than that for undisturbed soil. Little information exists to guide the designer in selecting either the size of the smear zone or its reduced permeability. But a more basic problem lies in the unrealistic model used to represent the disturbed zone. For example, analysis of several case histories of drain performance (Ladd 1991) shows that the reduction in the effective c_h with decreasing drain spacing is much larger than can be predicted by Barron’s (1948) theory. In addition, the effective c_h can be less than the normally consolidated laboratory c_v at close drain spacings.

The writer does not suggest abandoning wick drains (although they may not be as cost effective as nondisplacement sand drains in highly sensitive or varved clays), but rather advocates the need for further experimental and theoretical research into disturbance effects caused by drain installation. Jamiolkowski et al. (1983), Rixner et al. (1986), “Placement and” (1987), and Ladd (1987a) provide added guidance and extensive references on consolidation with vertical drains.

Consolidation of Tailings (Slimes) Deposits

The writer refers the reader to *Sedimentation Consolidation* (1984), *Consolidation of* (1986), Morgenstern (1985), Schiffman et al. (1988), and Vick (1983) for empirical correlations, consolidation models, and field experience. As with consolidation of natural soils, the sophistication of the model should be consistent with the extent and reliability of the soils data and the complexity of the boundary conditions. In particular, nonlinear finite strain consolidation analyses may be needed for reasonable estimates of pore pressure dissipation rates within thick “underconsolidated” deposits.

5.3. Laboratory Strength Testing

This section recommends procedures to obtain undrained strength ratio versus stress history (c_u/σ'_{vc} versus OCR) relationships needed to calculate the initial c_u profile and subsequent increases due to consolidation (steps 1 and 3 in Table 5, respectively). The recommendations are divided into three levels of sophistication and expense depending on the degree of refinement required for the undrained strength analyses.

- Level A—For final design of all major projects and for sites where the foundation soils exhibit significant undrained stress-strain-strength anisot-

ropy or contain unusual features (fissuring, varved, highly organic, etc.) and for projects requiring predictions of lateral deformations during construction.

- Level B—For preliminary design and for final design of less important projects involving “ordinary” soils with low to moderate anisotropy.
- Level C—For preliminary feasibility studies and to check the reasonableness of initial strengths inferred from in situ and laboratory UU-type test programs.

Levels A and B require laboratory CU testing to provide anisotropic and isotropic (average c_u) input strengths, respectively, whereas level C relies on empirical correlations. The corresponding recommendations follow from the information presented in Section 4.

Programs to obtain anisotropic c_u/σ'_{vc} versus OCR relations at level A employ CK_0U tests having different modes of failure to provide stress-strain data suitable for application of the strain compatibility technique (Section 4.9). The CK_0U tests use either Recompression or SHANSEP consolidation procedures depending upon the soil type, in situ OCR, and sample quality (Section 4.4). Selection of the failure modes used to assess the effects of anisotropy on undrained stress-strain behavior depends on which shear devices are available (Fig. 14), their proven ability to provide reasonable data on natural soils, and the potential impact of changes in b . Based on current capabilities, the writer favors a program of direct simple shear (DSS) and plane strain compression/extension (PSE/E) tests, although the latter are usually replaced by triaxial compression/extension tests (triaxial data sometimes adjusted by increasing τ_c by 1.05–1.1 and τ_e by 1.1–1.2 for application of the strain compatibility technique).

The c_u/σ'_{vc} versus OCR relations obtained from properly executed and interpreted CK_0U data should “exactly” simulate the in situ response for stage 1 construction, but they involve errors on the safe side when used to compute strength increases during consolidation (Section 4.11). As illustrated in Fig. 19, CAU direct simple shear tests can be used to evaluate potentially higher c_u/σ'_{vc} values for OCR = 1 soils located below berms and slopes and are recommended when the CK_0U parameters give marginal factors of safety.

When the undrained strength data closely follow a linear log c_u/σ'_{vc} versus log OCR relationship, as is typical of many soils, the design parameters can be represented by Eq. 9 (in Section 3.4) with values of S and m corresponding to failure in compression (τ_c), direct simple shear (τ_d), and extension (τ_e). Note that S may vary with stress level for high structured clays. For example, the results in Fig. 16(b) show much higher values of S from tests on OC (intact) clay than from tests on NC (destructured) clay. In any case, the log-log plot is very useful in presenting and evaluating test data.

For level B programs, the writer recommends CK_0U direct simple shear testing to obtain c_u/σ'_{vc} versus OCR relations for stability analyses using *isotropic* strength profiles. The results in Fig. 18 indicate that the peak DSS strength should provide a reasonable estimate of the *average* undrained strength ratio along circular-arc or wedge-shaped failure surfaces for stage 1 construction on nonlayered sedimentary clays of low OCR. The writer further recommends the SHANSEP reconsolidation technique, rather than Recompression, since level B involves “ordinary” soils; use of log c_u/σ'_{vc} ver-

sus log OCR plots; and the addition of CAUDSS tests under conditions described for level A programs. He also favors the Geonor apparatus since it provided the data plotted in Fig. 18 and limited comparisons suggest that other DSS devices may tend to give somewhat higher, more scattered strengths.

An alternative program for level B can use CK_0U triaxial compression and extension tests to estimate the average c_u/σ'_{vc} versus OCR relationship. If the results are first treated for strain compatibility, the average strength should be reasonable based on the data contained in Table 4 (except for varved clays due to their very low DSS strength). However, CK_0U triaxial testing, compared to DSS testing, requires more soil and effort and a higher level of experience (hence greater costs) to obtain reliable data, especially for shear in extension.

Level B should not rely on isotropically consolidated triaxial compression testing since $CIUC$ strengths will greatly exceed the in situ average for most soils. Section 6.2 evaluates the use and interpretation of $CIUC$ data when employed as part of the QRS methodology for stability analyses.

Selection of strength parameters at level C uses empirical correlations, rather than CU testing, in the form of

$$\frac{c_u}{\sigma'_{vc}} = S(\text{OCR})^m \dots\dots\dots (13a)$$

which, for $m = 1$, becomes

$$\frac{c_u}{\sigma'_p} = S_p \dots\dots\dots (13b)$$

Based on the data in Fig. 18 and the related text in Section 4.10, the writer has concluded that: CL and CH clays tend to have lower, less scattered undrained strength ratios than soils plotting below the A-line; and the τ_{ave}/σ'_{vc} correlation line for clays is probably more reliable than the c_u/σ'_p line obtained from the case histories for highly plastic clays. In any case, the results in Fig. 18 can be used by readers to select values for S or S_p . When applying Eq. 13a, one also has to estimate m , which, according to the "critical state" concepts used to formulate the Modified Cam-Clay model of soil behavior, should equal $1 - C_s/C_c$, where C_s and C_c represent the slopes of the swelling and virgin compression lines, respectively (Roscoe and Burland 1968).

The writer's interpretation of Fig. 18 and other experience lead to the following recommendations (SD = standard deviation).

- Sensitive marine clays ($I_p < 30\%$, $I_L > 1$):
 $S_p = 0.20$, with nominal SD = 0.015
- Homogeneous CL and CH sedimentary clays of low to moderate sensitivity ($I_p = 20\% - 80\%$):
 $S = 0.20 + 0.05I_p$, or simply $S = 0.22$.
 $m = 0.88(1 - C_s/C_c) \pm 0.06$ SD, or simply $m = 0.8$.
- Northeastern U.S. varved clays:
 $S = 0.16$ (assumes DSS failure mode predominates).
 $m = 0.75$.
- Sedimentary deposits of silts and organic soils (Atterberg limits plot below

the A-line, but excluding peats) and clays with shells:

$$S = 0.25, \text{ with nominal SD} = 0.05.$$

$$m = 0.88 (1 - C_s/C_c) \pm 0.06 \text{ SD, or simply } m = 0.8.$$

The aforementioned m versus $(1 - C_s/C_c)$ relation is based on analysis of CK_0UDSS data on 13 soils having maximum OCR's of 5–10.

Levels A, B, and C all require a careful assessment of the stress history of the foundation soils. This fact, plus the observation that $c_u(\text{ave})/\sigma'_{vc}$ versus OCR for most soils (except varved clays) falls within a fairly narrow range, means that consolidation testing usually represents the single most important experimental component for the design of staged construction projects.

5.4. Stability Analyses

This section deals with some practical aspects of executing limiting equilibrium stability analyses (component T3 in Table 5), especially regarding input of undrained strengths. It is assumed that final design analyses will use a computerized method of slices that satisfies *moment equilibrium* in computing factors of safety for circular-arc or wedge-shaped failure surfaces as recommended in Section 2.2. The ability to search out the minimum FS automatically is obviously desirable, as commonly done for Bishop (1955) circular-arc and Janbu (1973) wedge-shaped surfaces. However, the latter results should be checked by a "generalized" method of slices that satisfies both force and moment equilibrium, e.g., Morgenstern and Price (1965) or Spencer (1967).

First consider analyses using *isotropic* strengths, either for preliminary design or to represent the average c_u for soils having low to moderate undrained strength anisotropy. For first stage construction, the c_u values obtained from step 1 in Table 5 can be used directly as input data, either as "zones" or continuous profiles depending upon the computer code. The same approach can also be followed for subsequent stages via the c_u values computed in step 3. But this process can get rather cumbersome, i.e., separate computations to obtain vertical consolidation stress (σ'_{vc}) profiles, then c_u values, and finally selection of input strengths. This was done for the two embankment case histories. For construction involving substantial portions of normally consolidated soil, a computer code that automatically calculates $c_u = S\sigma'_{vc}$ within OCR = 1 zones would greatly simplify the process. The required effort then becomes similar to a conventional effective stress analysis by replacing ϕ' and σ'_n with S and σ'_{vc} for applicable soils. Bromwell & Carrier, Inc. did this for the tailings dam case history. However, step 3 in Table 5 would still be needed for natural deposits to identify OCR = 1 soils and to calculate c_u values for σ'_{vc} less than σ'_p .

Analyses employing *anisotropic* strengths become significantly more complex, especially since most computer codes cannot automatically vary c_u with inclination of the failure surface. One notable exception is the three-dimensional slope stability program developed by Azzouz et al. (1981), although restricted to circular arcs. The writer's experience mainly involves embankment-type loadings, where wedge-shaped surfaces need evaluation. For the two embankment case histories (Figs. 6 and 9), with inclinations of the active and passive wedges being specified at $45 \pm \phi'/2$ degrees, the input strengths had to be changed for each change in the horizontal location of

the end wedges to correctly model τ_c and τ_e versus τ_d along the horizontal surface.

With either isotropic or anisotropic forms of an undrained strength analysis, there may be uncertainty about the drainage of some layers during a potential failure, e.g., shear induced pore pressures near zero. This might occur within partially saturated, heavily overconsolidated, and quite sandy-silty soils. In such cases, the writer would make runs treating these layers as both $c'-\phi'$ and c_u materials in order to quantify the resulting uncertainty in factor of safety.

The results in Azzouz et al. (1983) show that "end effects" typically increase the conventional two-dimensional (i.e., infinitely long failure) factor of safety by 1.1 ± 0.04 SD based on 17 case histories of embankment failures. For construction involving fairly uniform loading and foundation conditions and having marginal stability, the conventional factors of safety can therefore be increased by about 10% to take advantage of this beneficial effect. And with important projects having nonuniform geometries, three-dimensional stability analyses may be warranted.

5.5. Comments on Design Process

Undrained strength analyses constitute, of course, only one part of the overall design process. Another purely geotechnical aspect of staged construction projects would evaluate various foundation "stabilization" schemes, the most common being stability berms and lightweight fill materials to decrease the net driving moment; installation of vertical drains and longer construction times to increase the degree of consolidation and hence the available resisting moment; and surcharging to reduce postconstruction settlements, especially those caused by secondary compression. Mitchell (1981) and ASCE ("Placement and" 1987) provide useful guidance regarding other ground improvement techniques, including use of geotextiles and vertical reinforcement by stone columns and chemical admixtures. The iterative design process also must include costs analyses for alternative construction schemes, recommendations for monitoring construction (Section 7) and consideration of environmental and other legal issues affecting project feasibility and the consequences of a failure.

Controversy may arise about acceptable design factors of safety, especially when dealing with regulatory agencies. In the writer's view, acceptable FS values for staged construction projects can often be less than normal for single-stage loadings causing comparable potential damage for two reasons: (1) Multistage projects usually have a more detailed site characterization program, combined with more comprehensive stability evaluations; and (2) they often can employ the observational method (Peck 1969), i.e., the design can be altered based on observations made during construction. But how can these valid reasons for a reduced risk of failure be translated into recommendations for a lower design factor of safety? For this purpose, a *reliability analysis* can prove very helpful. In addition, this methodology enables one to quantify the collective effects of uncertainty in the loads, degree of consolidation, undrained strength ratios, etc., on the nominal probability of a failure. The Terzaghi Lecture by Whitman (1984) gives background information on this important topic.

6. ALTERNATIVE APPROACHES FOR STABILITY ANALYSES

The paper now evaluates three other approaches for conducting stability analyses: the "QRS" methodology developed by Arthur Casagrande; Moore's (1970) modification of conventional effective stress analyses to account for shear induced pore pressures ($u_s > 0$); and Janbu's use of "undrained" effective stress analyses. But a clearer description of the classes of stability problems and their corresponding definition of factor of safety are desirable before assessing these approaches.

6.1. Stability Problems Classified According to Drainage Conditions and Definition of Factor of Safety

Table 6 presents a proposed classification system for defining the three principal cases of practical interest. As previously suggested by Brinch-Hansen (1962), the first two cases are exactly analogous to laboratory unconsolidated-undrained and consolidated-drained shear tests. Hence, designation as the UU case and the CD case, respectively, provides a clearer definition, especially compared to "short-term" and "long-term." The appropriate definitions for FS (column 5) are also widely accepted as being the available undrained and drained strengths, respectively, divided by the mobilized shear stress (τ_m) required for equilibrium. Brinch-Hansen (1962) further designated the "intermediate" case 3 as the CU case "because of its similarity to a consolidated-undrained . . ." shear test, although Table 6 specifies that the soil can be either in a partially or fully consolidated state prior to an undrained failure.

TABLE 6. Stability Problems Classified According to Drainage Conditions and Definition of Factor of Safety

Case (1)	Common description (2)	Proposed description (3)	Proposed classification (4)	Definition of factor of safety ^a (5)
1	Undrained, short-term or end-of-construction	No consolidation of soil with respect to applied stresses and undrained failure	Unconsolidated-undrained = UU case	s_u/τ_m or c_u/τ_m (Eq. 5 or Eq. 8)
2	Drained or long-term	Full consolidation of soil with respect to applied stresses and drained failure ($u_s = 0$)	Consolidated-drained = CD case	$s_d/\tau_m = \tan \phi' / \tan \phi'_m$ (Eq. 7)
3	Partially drained or intermediate	Partial or full consolidation of soil with respect to applied stresses and undrained failure	Consolidated-undrained = CU case	c_u/τ_m (Eq. 8)

^a τ_m = mobilized shear stress required for equilibrium; s_u = undrained shear strength obtained from conventional testing associated with typical $\phi = 0$ analyses; c_u = undrained shear strength obtained from techniques recommended in Section 5; and s_d = drained shear strength defined in Eq. 1.

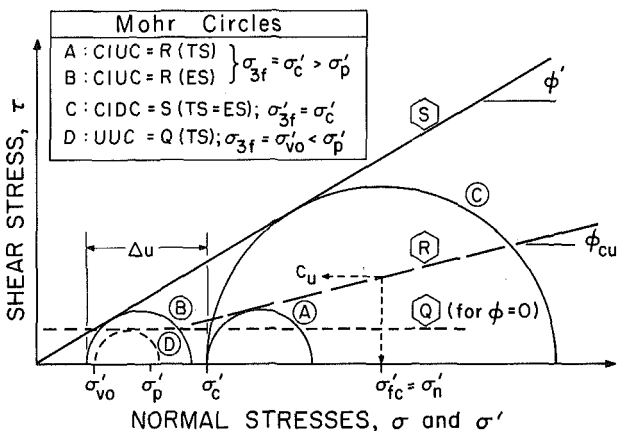


FIG. 20. Failure Envelopes from Q , R , and S Triaxial Compression Tests [Adapted from A. Casagrande's (1941) Harvard Report No. 3 as Abstracted by Rutledge (1947)]

As previously described in Section 3, the CU case is clearly the more critical and likely condition for staged construction projects, and, hence, defining $FS = c_u/\tau_m$ is also appropriate. Moreover, it is hard to envision a drained failure ($u_s = 0$) occurring *during* any type of construction when significant excess pore pressures still exist due to that construction. In reality, the UU and CD cases represent limiting conditions to the more *general* CU case (Brinch-Hansen 1962). For example, the UU case is the limiting critical condition for *loading* problems with soft soils and the CD case is the limiting critical condition for *unloading* problems with stiff soils.

6.2. QRS Methodology

As noted in Section 2, the QRS methodology treats staged construction as a CU case and evolved from research by Casagrande into the strength of clays as measured in laboratory triaxial compression tests. He used Mohr circles and failure envelopes similar to those drawn in Fig. 20 to illustrate the following concepts of his "working hypothesis." The excess pore pressure (Δu) developed at failure in a conventional $R = CIUC$ test run on normally consolidated soil is given by the difference between circle A (total stress) and circle B (effective stress). The "basic" effective stress failure envelope is unique, i.e., one obtains the same ϕ' from $CIUC$ and "slow" $= S = CIDC$ tests. For stability analyses, the available strength of soft clay foundations is determined by the Q envelope (obtained from UUC tests) for no consolidation and increases to the R envelope (defined by ϕ_{cu}) with consolidation.

As also noted earlier, major U.S. government agencies and many practitioners have used these envelopes when calculating factors of safety for staged construction on soft cohesive foundations. Based on information contained in design manuals of the U.S. Army Corps of Engineers ("Stability of" 1970; "Design and" 1978) and the Navy's DM-7 ("Stability Analysis" 1971), the writer interprets the "basic" QRS methodology when used to as-

sess foundation stability in conjunction with a method of slices and either estimated or measured pore pressures as follows.

1. Initial strengths usually obtained from UUC tests (perhaps supplemented by field and/or laboratory vane tests) to define the Q envelope.
2. $CIUC$ tests with σ'_c varying over the stress range of interest to define the R envelope, which can be represented by

$$c_u = c + \sigma'_{fc} \tan \phi_{cu} \dots \dots \dots (14)$$

where σ'_{fc} = the normal effective (consolidation) stress acting on the potential failure surface (note: In this regard, QRS stability analyses are identical to an effective stress analysis, but with c and ϕ_{cu} replacing c' and ϕ').

3. "Stability Analysis" (1971) recommends using Eq. 14 both during staged construction and for the long-term fully consolidated case, whereas the USACE appears to recommend Eq. 14 *during* construction of a "stable" embankment, but strengths falling midway between the R and S envelopes for the long-term case.

Potential problems associated with this methodology are now evaluated.

Reliance on UUC tests to obtain reasonable estimates of the initial undrained strength profile depends on a fortuitous compensation among three factors; namely the *increased strength* due to shearing at a very fast strain rate (60% per hour) and due to failure in triaxial compression (i.e., in situ shearing at $\delta > 0^\circ$ leads to lower strengths because of anisotropy) must be offset by a *strength reduction* due to sample disturbance. These compensating factors cannot be controlled, often produce large scatter, and may cause misleading trends with depth.

From the continued widespread use of UUC testing, it appears that many practicing engineers believe that sample disturbance will predominate, so that any net error in UUC strengths will always be conservative. However, the move in recent years to better sampling techniques can produce the opposite effect, as illustrated by four examples in Table 7 of Germaine and Ladd (1988). The writer concludes that UUC data can range from being unduly low to highly unsafe, say by 25%–50% or more in either direction. Thus, UUC data should always be compared to strengths predicted by Eq. 13 in order to judge if they are reasonable.

Now consider the use of Eq. 14 in conjunction with a method of slices to obtain the factor of safety for full or partial consolidation of the foundation soils under the stress increments imposed during staged construction. The values of c and ϕ_{cu} defining the R envelope presumably come from a series of $CIUC$ tests with σ'_c varying between the initial overburden stress (σ'_{vo}) and the maximum anticipated stress. It should be emphasized that this strength envelope is used with in situ *effective stresses*, not total stresses. Bishop and Bjerrum (1960) apparently failed to recognize this important fact when concluding that Eq. 14 will give unsafe results for foundation problems. However, the R envelope has been correctly criticized as having no rational basis and thus merits further examination. This will be done for normally consolidated soils so that Eq. 14 becomes $c_u = \sigma'_{fc} \tan \phi_{cu}$ (Fig. 2 and Eq. 6).

For a constant q_f/σ'_c from $CIUC$ tests on $OCR = 1$ soils, the slope of the R envelope represents an undrained strength ratio equal to

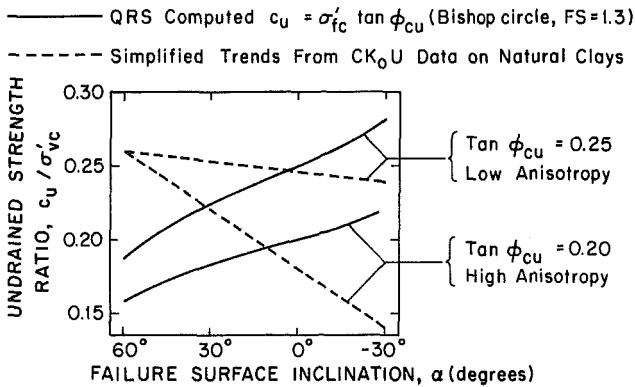


FIG. 21. Undrained Strength Ratios from QRS Methodology Compared to Trends from CK_0U Testing for Normally Consolidated Clay

$$\frac{c_u}{\sigma'_{fc}} = \tan \phi_{cu} = \frac{\frac{q_f}{\sigma'_c}}{\left(1 + \frac{2q_f}{\sigma'_c}\right)^{0.5}} \dots \dots \dots (15)$$

Based on the writer's files and results presented in Mayne (1980), representative $CIUC$ data on 30 natural clays and silts give $q_f/\sigma'_c = 0.33 \pm 0.05$ SD, which leads to $\tan \phi_{cu} = 0.255 \pm 0.03$ SD. These c_u/σ'_{fc} values are quite reasonable to slightly high compared to the ratios plotted in Fig. 18. However, Vick (1983) summarizes results for tailings slimes often having much higher ratios. These may reflect test consolidation stresses that were too low compared to the in situ preconsolidation pressure since $CIUC$ tests often need to be consolidated with $\sigma'_c/\sigma'_p > 3-4$ to achieve "truly" normally consolidated values.

The QRS methodology usually uses a method of slices to compute $\sigma'_{fc} = \sigma'_n =$ the normal effective (consolidation) stress acting on the potential failure surface with either predicted or measured pore pressures. For circular-arc analyses with the simplified Bishop (1955) method, the relation between normal and vertical effective stresses is given by

$$\frac{\sigma'_n}{\sigma'_v} = \frac{\sigma'_{fc}}{\sigma'_{vc}} = \frac{1}{1 + \frac{\tan \alpha \tan \phi_{cu}}{FS}} \dots \dots \dots (16)$$

where $\alpha =$ the inclination of the failure surface (positive and negative within the active and passive zones, respectively). Eq. 16 gives $\sigma'_{fc}/\sigma'_{vc}$ values less than one at positive α (say under the crest of the fill) and values greater than one at negative α (under the toe). Fig. 21 plots the computed undrained strength ratio versus α for two soils having $\tan \phi_{cu} = 0.20$ and 0.25 assuming $FS = 1.3$. Also shown for comparison are trends based on CK_0U test data for two clays exhibiting low and high degrees of anisotropy. Although the c_u/σ'_{vc} trends have been simplified via linear variation between compression

at $\alpha = +60^\circ$ and extension at $\alpha = -30^\circ$, the QRS approach obviously contradicts (inverts) real soil behavior.

Assessment of the potential errors in stability analyses based on the QRS methodology is difficult because both the location of the Q envelope derived from UUC tests and the computed strength variation along potential failure surfaces after consolidation can err in either direction. With projects where $\tan \phi_{cu}$ is near τ_{ave}/σ'_{vc} and when overall stability is largely governed by failure with positive α angles in OCR = 1 soil, it may underestimate the factor of safety. The tailings dam case history in Fig. 10 supports this opinion since QRS gave a FS = 1.1 for circular-arc analyses with $\tan \phi_{cu} = 0.256$ based on the measured CIUC q_f/σ'_c of 0.33. Although no comparisons were made for the two embankment case histories, QRS probably would have given unsafe results for deep wedge-shaped failure surfaces.

In summary, the QRS methodology has been widely used in the United States and is certainly preferable to a conventional effective stress analysis or to direct use of CIUC q_f/σ'_c ratios, both of which give unsafe results. But the accuracy of this empirical form of an undrained strength analysis does depend on compensating errors that are difficult to quantify. Moreover, QRS does not explicitly consider the stress history of the soil, which the writer feels should be a vital component of all stability evaluations.

6.3. "Undrained" Effective Stress Analyses

Proponents of an "effective stress" approach to stability problems often argue that it provides a more fundamental understanding of undrained behavior or that the very same factors that make it difficult to estimate shear induced pore pressures accurately also affect accurate predictions of undrained shear strength (e.g., p. 473 of Lambe and Whitman 1969). However, few persons have actually developed an effective stress based technique suitable for practical application to staged construction. Two such attempts are reviewed.

Moore (1970) correctly emphasized that a conventional effective stress analysis does not account for shear induced pore pressures and then developed equations to adjust results from such analyses in order to obtain the factor of safety against an undrained failure, defined as $FS = c_u/\tau_m$. His approach requires knowledge of Skempton's pore pressure parameter A_f for highly complex stress conditions (e.g., element D in Fig. 12) and inherently assumes that the principal stress directions do not change during failure. The writer is therefore uncertain about its accuracy.

Janbu and his colleagues at the University of Trondheim, Norway, have long advocated and used an "undrained effective stress approach," (UESA) (Janbu 1973; Janbu 1979; Svano 1981). In contrast to Moore (1970), they developed techniques to predict prefailure conditions along a potential rupture surface for undrained or partially drained conditions starting from the initial state of stress in the ground. Based on the writer's understanding of how Janbu would conduct stability analyses during the design of a staged construction project, it appears that a typical UESA involves the following simplifications: isotropic initial state of stress ($K_0 = 1$); basic soil parameters (c', ϕ', A) derived from triaxial compression tests; and a constant *degree of mobilization*, defined as $f = \tan \phi'_m/\tan \phi'$, all along the potential failure surface. The last assumption is of particular concern since the corresponding factor of safety will be defined as $FS = 1/f = \tan \phi'/\tan \phi'_m$, which is

identical to that used for a conventional ESA. Hence, to obtain a $FS = c_u/\tau_m$ against an undrained failure, the UESA must be carried one step further by somehow predicting the *additional* changes in effective stress during undrained shear to failure while maintaining the *same* loading conditions. This additional step, which was attempted by Moore (1970), is very complex and probably involves more uncertainty than an undrained strength analysis of the type proposed in Section 5.

6.4. Some General Comments

All of the techniques described thus far for stability evaluations make simplifying assumptions and entail an artificial separation of stress distribution-consolidation analyses on the one hand and limiting equilibrium analyses on the other. The availability of a realistic *generalized soil model* for use in numerical analyses such as the finite element method would provide a more rational approach and fewer limitations. The set of constitutive equations used by such a model can predict soil behavior for different stress paths and for both undrained and drained conditions. The highly innovative Modified-Cam Clay model (Roscoe and Burland 1968) has been used to predict foundation performance during staged construction in spite of the fact that it neglects soil-behavioral features such as stress-strain-strength anisotropy and strain softening and is further restricted to low OCR clays. Recent research by Whittle (1987, 1991) has successfully removed these major limitations, but his model still ignores creep effects that may be important with some projects. In any case, adoption of this new approach in general practice first requires additional theoretical research and detailed evaluation via case histories of field performance.

Meanwhile, practitioners must still evaluate and select types of stability analyses from those now available, and also deal with conflicting terminology. For example, use of the R envelope in Fig. 20 is called a *total stress* approach by Terzaghi and Peck (1967) and an *effective stress* approach by NAVFAC ("Stability Analysis" 1971). To help clarify the process, the writer suggests the following.

1. Clearly identify which stability case is being evaluated (UU, CD, or CU in Table 6) and make sure that the selected type of analysis uses an appropriate definition for its factor of safety. For example, it is inconsistent to apply Janbu's undrained effective stress approach to the UU and CU cases since it inherently uses $FS = \tan \phi'/\tan \phi'_m$ corresponding to a drained failure.

2. Retain the conventional total stress analysis (TSA), mainly for historical perspective, to denote stability analyses wherein the available undrained strength for the UU case is literally computed as a function of the in situ total stresses.

3. The other types of analyses discussed in this paper require knowledge of the prefailure (equilibrium) in situ *effective stresses* and the basic difference between them is the assumed drainage conditions *during* failure. Hence, one should refer to them as either drained or undrained strength analyses.

4. If one accepts the aforementioned, then a conventional effective stress analysis (ESA) would be called a drained strength analysis since it inherently computes the available resistance as being equal to the drained strength of the soil. As such, it is applicable only to the fully drained CD case.

5. In contrast, an undrained strength analysis (USA) treats the same in situ effective stresses as consolidation stresses in order to compute the available re-

sistance against an undrained failure. As such, it can be applied to both the UU and CU cases and should be used to evaluate stability during staged construction. The QRS approach is fairly simple to apply in practice, but its empirical nature involves errors of unknown magnitude and direction. The USA methodology recommended in Section 5 requires more sophisticated engineering, but it should provide more reliable factors of safety.

7. MONITORING FIELD PERFORMANCE

Staged construction always involves the risk of a stability failure since it requires significant strengthening of the foundation soils in order to achieve the design objectives. When used with precompression to reduce postconstruction settlements (e.g., for buildings, tanks, highways, etc.), the risk of excessive long-term deformations also exists. Both risks occur due to uncertainties in the initial soil conditions, in the soil compressibility and subsequent gain in strength, in the rates of loading and consolidation, and in the methods of stability and settlement analysis. For these conditions, adoption of the *observational method* (Peck 1969) often permits maximum economy and assurance of satisfactory performance, provided that the design can be modified as construction progresses. As Peck emphasizes, successful application of this approach also entails the following items:

- That the designer select appropriate quantities to be monitored during construction; make predictions of their magnitudes based on the working hypothesis adopted for design (i.e., the most probable conditions) and also for the most unfavorable likely conditions; and develop suitable actions or modifications to handle all significant deviations from the design hypothesis.
- That the field instrumentation provide reliable, timely measurements of the quantities to be observed.
- That the engineer evaluate these data to ascertain the actual conditions and have the ability to implement corrective actions *during* construction.

To illustrate the advantages of the observational method, consider situations that arise during construction of a project such as shown in Fig. 22. Precompression for a bridge approach embankment uses wick drains to accelerate the rate of consolidation and a stage 1 filling with a stability berm, a stage 2 loading the next year with a surcharge fill to reduce long-term secondary compression settlements, and paving the third year after removal of the surcharge. Field performance data would be needed to reach the following decisions: reduction in the stage 1 design fill elevation, or addition of a temporary berm, if stability proved worse than expected; changes in the design consolidation period after stage 1 or stage 2; and changes in the design surcharge thickness due to revised estimates of soil compressibility.

7.1. Field Instrumentation

All staged construction projects that could result in undesirable performance should include field instrumentation, even if the design did not formally adopt the observational method. Besides providing data essential for any meaningful assessment of foundation stability (which includes rates of consolidation) needed for routine construction control, Dunnycliff (1988) lists

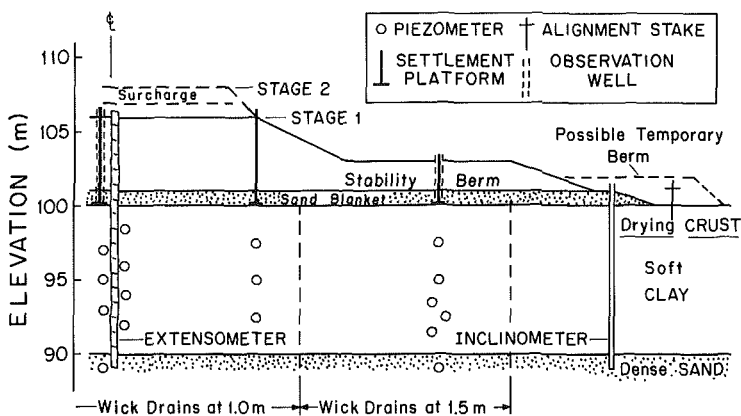


FIG. 22. Possible Layout of Instrumentation for Staged Construction of Embankment with Vertical Drains

other potential benefits as follows: measurements of fill quantities (for payment); effects of construction on adjacent property (legal protection); enhanced public relations; and advancing the state of the art of geotechnical engineering.

Peck (1988) states that "every instrument installed on a project should be selected and placed to assist in answering a specific question," but also in sufficient number "to provide a meaningful picture of the scatter in results . . ." and "to allow for inevitable losses resulting from malfunction and damage . . ." The instrumentation shown in Fig. 22 illustrates one possible layout for use with the observational method as part of construction monitoring. Some requirements for the instrumentation are:

1. Detailed measurements of settlement (an extensometer is a multipoint settlement gauge) and pore pressure versus depth under the centerline, plus observation wells in the sand blanket and piezometers in the underlying sand to obtain boundary pore pressures. The resulting data can be used to obtain in situ compression curves and rates of consolidation.

2. Settlement platforms as backup to the extensometer, to assess scatter in stage 1 settlements, and to define the embankment profile (note: These platforms can have internal rods anchored in the dense sand to serve as convenient bench marks).

3. Piezometer groups under the slope and berm to use with stress distribution analyses to obtain σ'_{vc} profiles needed for undrained strength analyses and to measure rates of pore pressure dissipation.

4. All piezometer groups include some redundancy, and at least half of the gauges should be placed before the wick drains to measure both the initial groundwater conditions and any excess pore pressures caused by drain installation. Special effort should be made to install the piezometers near the midpoint between the drains in order to obtain representative pore pressures.

5. An inclinometer to measure lateral deformations beneath the toe of the fill. Alignment stakes might be placed at intermediate intervals for construction on "ductile" foundation clays.

Dunnicliff (1988) gives detailed guidance regarding selection and installation of specific types of instrumentation to measure settlements, pore pressures, and lateral displacements. He also correctly emphasizes that the designer should have ultimate control (either directly or via designated parties) over procuring, installing, reading, and interpreting the field instrumentation. An essential, but too often neglected, part of the overall monitoring program must also include continuous field inspection with detailed records of construction activities (especially fill elevations and, if used, lengths of vertical drains), accurate measurements of fill unit weights, and periodic site visits by the designer.

The next sections of the paper offer guidance regarding interpretation of data from field instrumentation to evaluate consolidation behavior and to assess foundation stability.

7.2. Evaluating Consolidation Behavior

Evaluation of the field consolidation behavior has two principal objectives: (1) To obtain in situ pore pressure distributions in order to compute profiles of vertical consolidation stress ($\sigma'_{vc} = \sigma_v - u$) as part of undrained strength analyses to assess foundation stability; and (2) to determine actual consolidation characteristics for comparison with those used for design in order to make improved predictions of future performance. The latter includes boundary drainage and pore pressure conditions and the compressibility-flow-stress history properties of the foundation soils. This information is also needed to extend the measured piezometer data throughout the foundation soils as part of the first objective.

Techniques based on the Barron (1948) theory of consolidation for evaluating piezometer and settlement data in order to backcalculate the "effective" coefficient of consolidation (c_h) for horizontal flow to vertical drains are now considered. These techniques apply, at best, only to field behavior during periods of constant load for *normally consolidated* soil having a reasonably linear strain versus $\log \sigma'_{vc}$ curve.

Johnson (1970) describes the conventional approach for calculating field c_h values from piezometers located at the midpoint between vertical drains. It requires knowledge of the initial excess pore pressure (u_0) in order to compute changes in the degree of consolidation ($U_h = 1 - u_e/u_0$) with time, where u_e equals the measured excess pore pressure. The technique of Orleach (1983) avoids the resultant errors in c_h due to uncertainties in both u_0 and the actual piezometer tip location by plotting $\log u_e$ versus time. This plot should give a *linear* relationship for constant boundary conditions and c_h and negligible vertical drainage. Field coefficients of consolidation based on rates of pore pressure dissipation can then be calculated using

$$c_h(u) = \frac{d_e^2 F_n}{8} \frac{\ln \left(\frac{u_{e1}}{u_{e2}} \right)}{(t_2 - t_1)} \dots \dots \dots (17)$$

where d_e = the equivalent drain spacing; and F_n = the drain spacing factor ($F_n = 0.9-2.5$). Besides being very simple, nonlinear $\log u_e$ versus t portions of the data will identify errors in u_e or changes in $c_h(u)$, boundary pore pressures, applied loads, etc.

The conventional approach for analyzing field settlement data with vertical drains to obtain $c_h(s)$ requires knowledge of changes in the average degree of consolidation with time. Section 3.4.6 of Jamiolkowski et al. (1985) describes practical problems with this approach, which include errors due to uncertainties in both the "initial" settlement (i.e., that caused by undrained shear deformations) and the final consolidation settlement. Both of these errors can be eliminated for the case of radial drainage only (with constant c_h , loading, etc.) by using the Asaoka (1978) method of analysis, which can also predict final settlements. However, this technique tends to overestimate $c_h(s)$ since it ignores the effect of vertical drainage on rates of settlement. This may explain why field values of $c_h(s)$ often exceed $c_h(u)$ obtained from piezometers located within the central portion of foundation clays. In any case, predictions of consolidation rates for stability evaluations during subsequent loading should use $c_h(u)$ since consolidation stresses, rather than settlements, govern increases in undrained shear strength.

The Asaoka (1978) technique can also be used to obtain c_v values from piezometer and settlement data during consolidation with vertical drainage only, but only for conditions adhering to Terzaghi's original assumptions. Since uniform layers with well-defined drainage boundaries seldom occur (compared to the simpler case of foundations with vertical drains), realistic evaluations of field consolidation behavior will often need some type of numerical analysis. This may be especially true regarding pore pressure dissipation rates in cases involving construction on initially overconsolidated or highly structured clays, and consolidation of thick slimes (see Section 5.2).

Now consider the use of field data to assess the *yield* characteristics of the foundation clay. Yield denotes the transition from "elastic" (recoverable) to "plastic" (irrecoverable) behavior and the locus of stress states causing yield defines the *yield envelope*. In particular, plots of excess pore pressure (u_e) versus applied stress are frequently used to infer when yielding first occurs and to derive undrained shear strengths and preconsolidation pressures for comparison with design values. However, evaluation of the same data has often led to quite different conclusions regarding in situ behavior, as described herein.

Plots of u_e versus the applied major principal stress increment ($\Delta\sigma_1$) for piezometers located beneath embankment fills typically show the following pattern during *initial* loading (for overconsolidated clay and no vertical drains or berms). The value of $\bar{B} = u_e/\Delta\sigma_1$ starts off being relatively small, but then increases significantly such that the incremental \bar{B} is near unity. Hoeg et al. (1969) and D'Appolonia et al. (1971) interpreted such field data as representing undrained shear behavior with Skempton's *A* parameter being fairly low, followed by local yielding (failure) and the formation of a zone of *contained plastic flow*. Within this zone, the in situ shear stress equals the undrained shear strength, and further filling causes $\Delta u_e = \Delta\sigma_1$ (or $\Delta u_e > \Delta\sigma_1$ if strain softening occurs).

In contrast, Tavenas and Leroueil (1980) cite the extensive study by Leroueil et al. (1978) to support their view that the high coefficient of consolidation of overconsolidated clays leads to significant pore pressure dissipation during initial loading "in all types of clays and for all rates of embankment construction" (the latter paper quoted a midclay depth $\bar{B} = 0.58 \pm 0.12$ SD for embankments without drains). They further hypothesize that subsequent increases in the incremental \bar{B} to near unity "is not due to the

development of confined failure . . . , as suggested by Hoeg et al. (1969), but merely to the passage of the clay to a normally consolidated state.”

The writer believes that the aforementioned picture of field behavior cannot be universally true for the following reasons:

- Rates of pore pressure dissipation during initial construction can vary within very wide limits, with \bar{B} often being a poor indicator of actual degrees of drainage [e.g., Mesri and Choi (1981); Folkes and Crooks (1985)].
- One would expect significant zones of contained plastic flow due to local overstressing (shear failure) at factors of safety (FS = 1.2–1.5) typically associated with staged construction.
- Abrupt changes from overconsolidated to normally consolidated field behavior are probably restricted to highly structured clays having a sharp break in the compression curve at σ'_p .

Hence, the ability to detect and interpret properly the physical significance of changes in excess pore pressure versus applied stress during initial construction is a complex task that varies with the loading geometry and piezometer locations, the degree of drainage, the soil type (meaning brittle versus ductile behavior) and disturbance due to drain installation, and the conditions causing “yield,” which can range from an undrained shear failure to consolidation beyond the yield envelope.

Although u_e versus $\Delta\sigma_1$ or $\Delta\sigma_v$ plots should be evaluated and may prove useful, in situ compression curves (ϵ_v versus $\log \sigma'_{vc}$) should give a more direct check on the design σ'_p profile, plus compressibility characteristics for comparison with laboratory oedometer data. This process needs detailed measurements throughout construction of the strains and pore pressures within “uniform” layers and reliable estimates of total vertical stress, which may justify numerical analyses to account for embankment rigidity and varying foundation stiffnesses. Ladd et al. (1972) and Pelletier et al. (1979) compare field and laboratory compression curves for two projects having vertical drains, with resultant differences attributed to disturbance of the oedometer test specimens. In contrast, Leroueil (1988) summarizes data for several highly structured clays (without vertical drains) wherein “strain rate” effects during primary consolidation were used to explain field settlements much larger than predicted from end-of-primary laboratory curves (but also see Section 4.2). Unfortunately, little experience exists to predict the relative importance of disturbance, rate effects, non- K_0 stress conditions (including undrained shear deformations), soil type, etc., on potential differences between laboratory and field compression curves. Theoretical research using realistic “generalized” models of soil behavior could clarify some of these issues.

7.3. Evaluating Foundation Stability

The most important part of the field monitoring program for staged construction projects concerns foundation stability (including tailings slimes), which can be assessed by two general approaches. One employs limiting equilibrium stability analyses to obtain a quantitative measure of safety. The other uses the field instrumentation data, usually in a more qualitative manner, to infer (un)satisfactory performance during periods of actual loading. Both approaches should be used, as neither ensures success. The following offers some guidance and comments on their relative merits.

The limiting equilibrium analyses should calculate the factor of safety against an *undrained* failure since the CU case (Table 6) is the most critical and likely condition. Section 5 presents recommendations for doing this via undrained strength analyses (USA), which basically use vertical consolidation stresses and undrained strength ratios (c_u/σ'_{vc}) to compute c_u profiles throughout the foundation. But these analyses entail considerable effort, which preclude them as a routine means of assessing (un)satisfactory field performance during periods of rapid loading. Moreover, they apply only to specific locations and, even then, may give misleading answers due to uncertainties in the computational techniques and input parameters. Hence, the monitoring program also should continuously use “graphical” interpretation of the field data to help detect potential foundation instability.

Although piezometer data are essential for undrained strength analyses and to evaluate field consolidation behavior, they seldom provide a direct warning of foundation instability since the *yield* phenomenon described in Section 7.2 typically occurs at factors of safety well above those used for design, and dramatic pore pressure increases occur (if at all) only just prior to or during actual failures. The real question therefore concerns the usefulness of vertical and horizontal movements, specifically those resulting from undrained shear deformations rather than consolidation. The answer depends to an important degree on the stress-strain characteristics of the foundation soil. For this purpose, the writer modified Vaughan’s (1972) field brittleness index developed to describe differing clay *embankment* behavior in order to distinguish between clay *foundations* having *brittle* versus *ductile* responses. The revised definition for the foundation brittleness index (FBI) is

$$FBI = \frac{\bar{c}_u - \bar{c}_r}{\bar{c}_u} \dots\dots\dots (18)$$

where \bar{c}_u = average undrained strength mobilized along the failure surface at failure; and \bar{c}_r = the average undrained shear stress at large strains after failure has occurred. The value of FBI approaches unity for highly sensitive clays and approaches zero for insensitive soils.

Following Vaughan’s (1972) logic (but now applied to natural rather than compacted clays), the writer would expect the soil characteristics and resultant response of foundations having limiting values of the foundation brittleness index as presented in Table 7. Case histories of embankments on *brittle* clays, such as encountered in eastern Canada, show little prior warning of very abrupt failures having large displacements along well-defined rupture surfaces. Shear deformations *during* loading are small and difficult to measure and may not accelerate until only hours before failing [e.g., Dascal et al. (1972); Ladd (1972); LaRochelle et al. (1974)]. For these soils, measurements of settlement and horizontal displacements may not detect an impending failure unless made very accurately, and also with loading rates sufficiently slow to allow “undrained” creep deformations.

In contrast, field instrumentation can provide clear evidence of foundation instability for construction on *ductile* soils. The overall deformation magnitudes will be much larger, such that even visual observations of alignment stakes may detect problem areas. However, definition of failure becomes more nebulous as it reflects excessive deformations within a zone, rather than on a distinct surface, that continue with time, perhaps with the for-

TABLE 7. Expected Soil Characteristics and Resultant Foundation Response for Limiting Values of Foundation Brittleness Index (FBI)

Value of FBI = $(\bar{c}_u - \bar{c}_v)/\bar{c}_u$ (1)	Undrained stress-strain behavior and typical soil type (2)	Foundation Response	
		During loading (3)	During failure (4)
Near Unity (Brittle Behavior)	<ul style="list-style-type: none"> • Small strain at failure, high modulus and pronounced postpeak strain softening • Clays of high sensitivity (often lean and/or cemented) 	<ul style="list-style-type: none"> • Small undrained shear deformations due to high E_u/c_u, even at low FS having large zone of contained plastic flow • Little warning prior to well-defined failure 	<ul style="list-style-type: none"> • Very abrupt and large displacements due to large strength reduction along distinct rupture surface • Large pore pressure increases along rupture surface
Near Zero (Ductile Behavior)	<ul style="list-style-type: none"> • Large strain at failure, low modulus and little postpeak strain softening • Organic and plastic clays of low sensitivity 	<ul style="list-style-type: none"> • Large undrained shear deformations due to low E_u/c_u, especially at low FS having large zone of contained plastic flow • Ample warning prior to ill-defined failure 	<ul style="list-style-type: none"> • Relatively small but continuing deformations occurring within zone rather than along rupture surface • Small changes in pore pressure

mation of cracks and a modest scarp in the fill [e.g., Foott and Ladd (1977); Simons (1976)]. The remaining text discusses the use of settlement and horizontal displacement data for relatively ductile foundations via a case history of staged construction, followed by an overview of correlations between vertical and horizontal deformations.

The case history involves the rectangular Fore River Test (FRT) section built on a tidal mud flat in Portland, Maine for the purpose of evaluating different types of vertical sand drains (Fig. 23). Ladd et al. (1969) and Simon et al. (1974) summarize the properties of the soft organic silty clay ($I_p = 33\%$, $I_L \approx 1$) that had a constant initial strength [$c_u = 250$ psf (12 kPa)] and slightly decreasing preconsolidation pressure with depth. Foundation instability during stage 1 construction to E1.10 over a 240-ft (73-m) square area led to flattening of the slopes, removal of fill to E1.8, and added instrumentation. After installing augured, jetted, and driven sand drains within the central 120-ft (36.5-m) square portion of the test area, the stage 2 filling continued until large cracks developed along the easterly portion of FRT at E1.18.5. Construction then stopped after removing some fill.

Fig. 24 plots settlement data during stage 1 filling to E1.10 and Ladd et al. (1969) describe the unexpected North slope failure, which initially caused displacements of several feet that approximately doubled during the next two weeks. Although not evaluated during construction, the high settlement rates of the North (N) and Northeast (NE) settlement platforms (SP) relative to

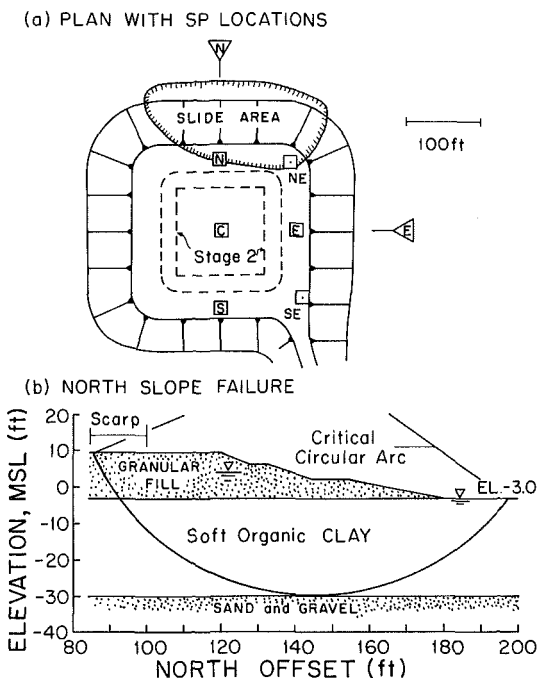


FIG. 23. Stage 1 Construction of Fore River Test Section (1 ft = 0.305 m) [after Ladd et al. (1969)]

the center show obvious signs of excessive undrained shear deformations nearly one week before the failure. The settlement behavior along the East and South slopes similarly indicates instability problems before the development of noticeable cracking. Moreover, the slope flattening caused an immediate reduction in settlement rates to values consistent with one-dimensional consolidation.

The aforementioned results demonstrate that settlement data can warn of impending failures if they reflect much larger movements, compared to ordinary consolidation settlements, that are caused by excessive undrained shear deformations within the foundation. This condition, besides requiring ductile soil behavior, is highly dependent on the geometry of the problem and the relative magnitude of the consolidation settlements. For example, settlement data during the FRT stage 2 filling did not show evidence of foundation distress (Ladd et al. 1969), which is probably typical for embankments having wide stability berms. Foundations with vertical drains also tend to negate monitoring based only on settlement data since fast rates of consolidation settlement mask vertical movements caused by undrained shear deformations.

Measurements of horizontal displacements generally show the clearest evidence of foundation instability since they directly reflect deformations caused by undrained shear and are less affected by consolidation than settlement data. Fig. 25 summarizes horizontal displacements (h) measured for the East

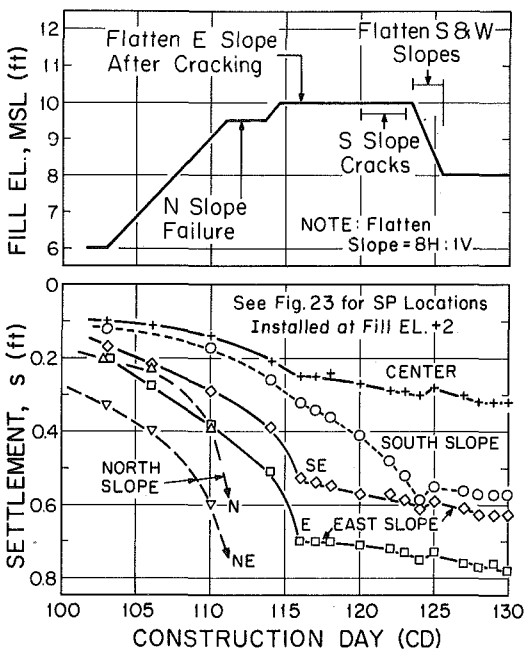


FIG. 24. Settlement versus Time During FRT Stage 1 Filling (1 ft = 0.305 m) [after Ladd et al. (1969)]

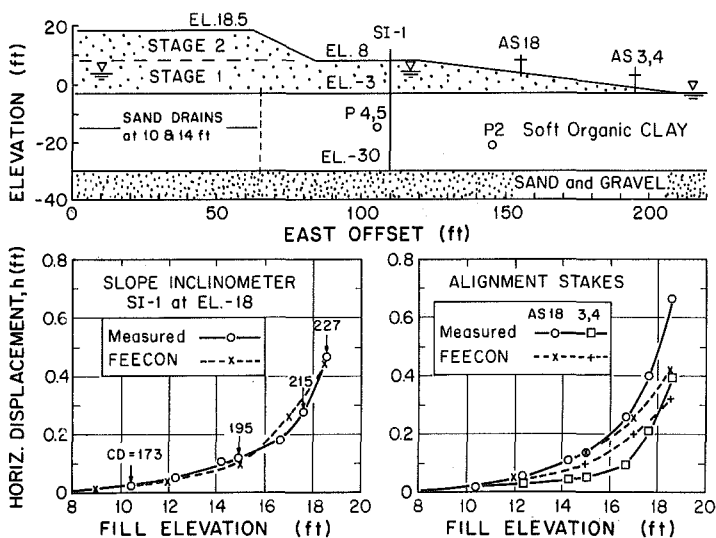


FIG. 25. Horizontal Displacements During FRT Stage 2 Filling (1 ft = 0.305 m) [after Simon et al. (1974)]

slope of FRT during stage 2 filling. After reaching E1.18.5 at construction day 221, the slope inclinometer sheared off on CD230 and fill was removed on CD235 after large cracks appeared. The plots of h versus fill elevation for the inclinometer and the alignment stakes both show significant changes in shape near E1.17 having a computed FS(USA) about 10% higher than at maximum grade. The displacement rates at constant load also increased significantly due to undrained creep, providing further evidence of very marginal stability some two weeks before cracks appeared in the fill.

As part of the aforementioned *observational method*, one should make predictions of undrained shear deformations, both to help select appropriate field instrumentation and for comparisons during construction monitoring. As an example, for the inclinometer in Fig. 25 one would want to predict overall displacement magnitudes, the shape of h versus depth (e.g., the effects of weaker zones and local yielding), and expected changes in h versus fill elevation for varying degrees of foundation consolidation and hence overall stability. The results in Fig. 25 show that finite element analyses can make reasonable predictions, in this case via FEECON, which considers initial shear stress and undrained strength anisotropy and used a bilinear stress-strain curve (Simon et al. 1974). However, even this type C1 analysis (Lambe 1973) had problems due to uncertainties in K_0 , strength, and modulus throughout the foundation soils. FEECON also cannot account for undrained creep and strain softening or for increases in strength, stiffness, etc., from consolidation during loading periods. Very sophisticated "generalized soil models" are required to predict the effects of these important, but complex, aspects of soil behavior. In the meantime, the writer suggests:

- As a minimum, elastic analyses to predict general magnitudes of undrained horizontal displacements, but realizing that E_u/c_u can vary from less than 200 to over 2,000 with soil type and stress level (Foott and Ladd 1981).
- For major projects, nonlinear finite element analyses that consider the effects of initial shear stress and undrained strength anisotropy [e.g., Simon et al. (1974)].

Tavenas et al. (1979) demonstrate that correlations between horizontal displacements and vertical settlements can provide useful insight regarding the relative importance of undrained versus drained deformations within embankment foundations. For 21 case histories involving simple loading geometries (see sketch in Fig. 26), they analyzed the relationship between the maximum horizontal displacement (h_m) measured by inclinometers at the toe of the fill and the maximum (circa centerline) settlement (s). In particular, they evaluated changes in the h_m versus s slope observed during and after construction and the shape of the horizontal displacement versus depth curves (h versus z) to arrive at several important conclusions. For convenience, the h_m versus s slope will be called the deformation ratio, $DR = dh_m/ds$.

The following summarizes principal conclusions from Tavenas et al. (1979). During single stage construction of about 15 embankments without vertical drains on overconsolidated deposits:

1. Significant drainage during initial loading (due to high OC c_v values) causes horizontal displacements much less than predicted from undrained analyses; resultant $DR = dh_m/ds = 0.18 \pm 0.09$ SD.

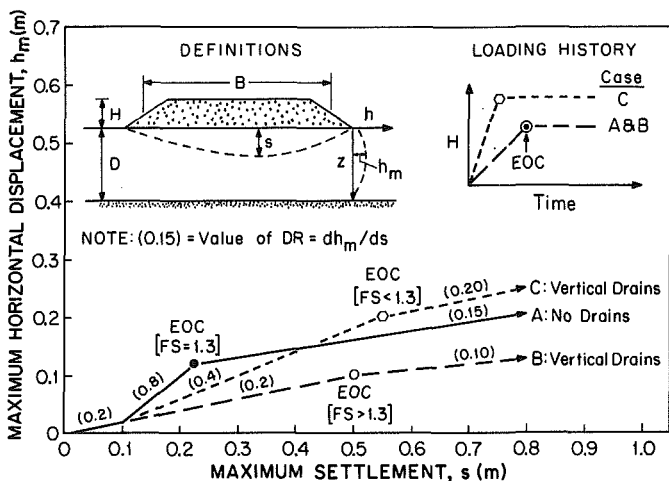


FIG. 26. Schematic Relationships Between Maximum Horizontal Displacement and Maximum Settlement for First-Stage Embankment Construction

2. Then a relatively abrupt increase in horizontal displacements occurs when a significant zone of the foundation becomes "normally consolidated," such that undrained shear deformations now dominate behavior; $DR = 0.9 \pm 0.2$ during this phase.

3. The maximum displacement of the h versus z curve more or less coincides with the location of the minimum undrained strength within the foundation.

During subsequent consolidation over several years for 12 embankments having B/D ranging from 0.9 to almost 10:

1. The maximum horizontal displacement continues to increase linearly with settlement; $DR = 0.16 \pm 0.07$ and can be affected by small changes in slope geometry.

2. The h versus z shape remains approximately constant, unless the thickness of normally consolidated soil increases with time.

This behavior has produced long-term lateral displacements several times larger than measured at the end of construction. Although the mechanisms causing this phenomenon are unclear, the writer feels that continued shear distortions due to (or similar to) undrained creep may be an important factor.

Since staged construction often employs vertical drains to accelerate the rate of strength gain from consolidation, their possible effect on h_m versus s correlations is of interest. The schematic relationships presented in Fig. 26 attempt to do this for an overconsolidated ductile foundation based on the Palavas site in Tavenas et al. (1979), the writer's analysis of several wick drain projects, and considerable judgment. Case A represents construction *without* drains having the essential features described by Tavenas et al. (1979), i.e., partially drained and then undrained behavior during filling, followed by consolidation having a deformation ratio (DR) of 0.15. Case B has an

identical loading history, but the vertical drains now cause significant drainage *throughout* filling (much larger s and slightly smaller h_m at the end of construction). More rapid consolidation also reduces DR after loading due to smaller effects of “undrained” creep. Case C places more fill in less time, resulting in a much larger DR = 0.4 during filling (an approximate upper limit for stable foundations with vertical drains reviewed by the writer); and also a larger ratio during consolidation due to higher rates of creep.

It should be emphasized that significant deviations from the schematic results in Fig. 26 can be expected since they are based on rather limited field evidence for simple loading geometries, and the processes governing combined consolidation and creep behavior are poorly understood, especially within foundations having large zones of contained plastic flow. Therefore, one cannot now predict the effects on h_m versus s relationships of changes in geometry (especially with berms), brittle versus ductile foundations, second versus first stage loadings, etc. Nevertheless, plots like Fig. 26 may still prove useful.

In conclusion, interpretation of field *deformation* data to warn of foundation instability requires considerable experience and judgement and the use of different plots depending upon the particular problem. Besides maintaining detailed records of time versus fill height (H), settlement (s), and horizontal displacement (h), the writer suggests plotting the following for monitoring foundation stability:

1. Periodic h versus depth to detect weaker zones and to locate the maximum value (h_m).
2. s and h_m versus H , with h_m generally providing much clearer evidence of potential problems.
3. h_m versus s to help detect partially drained versus undrained response and for comparison with prior behavior.
4. During periods at *constant load* (highly recommended whenever stability becomes critical), evaluation of changes in dh_m/ds and dh_m/dt as a function of H and time. Since dh_m/dt should gradually decrease with time if controlled by consolidation, an increasing rate may imply excessive undrained shear deformations and impending failure.

8. SUMMARY AND CONCLUSIONS

Staged construction uses controlled rates of loading to enable soil strengthening via consolidation in order to increase the foundation stability of dams, embankments, landfills, and tanks founded on soft cohesive soils. It is also used for the operation of many tailings waste storage dams. This paper treats the controversial issue of what *type* of stability analysis to use for the design of staged construction projects and to check stability during actual construction. Stability evaluations to assess the safety of *existing* structures also face the same issue.

Classification of Stability Problems

The factor of safety (FS) obtained from limiting equilibrium stability analyses is commonly defined as

$$FS = \frac{\text{Available shear strength of the soil}}{\tau_m} \dots \dots \dots (19)$$

where τ_m = the mobilized shear stress required for equilibrium. Since τ_m remains constant for a given failure surface, the selected type of stability analysis should use (or compute) a shear strength consistent with the most likely drainage conditions during a potential failure. The paper recommends the following classification system, which is analogous to the three basic types of laboratory shear tests.

1. UU case (replaces “undrained,” “short-term,” etc.):
 - No *consolidation* of soil with respect to the applied stresses and *undrained failure*.
 - $FS = c_u/\tau_m$, where c_u is the *initial* in situ undrained strength prior to construction.
2. CD case (replaces “drained,” “long-term”):
 - *Full consolidation* of soil with respect to the applied stresses and *drained failure* with zero shear induced pore pressures.
 - $FS = s_d/\tau_m$, where s_d is the available drained strength at the in situ effective stresses = $c' + \sigma'_{ff} \tan \phi'$.
3. CU case (replaces “partially drained,” “intermediate”):
 - *Partial or full consolidation* of soil with respect to the applied stresses and *undrained failure*.
 - $FS = c_u/\tau_m$, where c_u is the new undrained strength corresponding to the current in situ consolidation stress history.

Note that the UU and CD cases represent limiting conditions to the more general CU case.

Since staged construction produces positive excess pore pressures and *since actual failures of cohesive soils usually occur without significant dissipation of shear induced pore pressures*, stability evaluations should select the CU case as representing the most critical and realistic condition. The selected type of stability analysis therefore should compute the factor of safety against an undrained failure.

Stability Analyses for Staged Construction

Current practice commonly uses a method of slices (with either predicted or measured pore pressures) to compute factors of safety by one of the following two types of analysis.

1. A *conventional* effective stress analysis (ESA) that:
 - Treats the in situ effective stresses as equal to the effective stresses that will act on a potential failure surface at failure.
 - Computes $s_d = c' + \sigma'_{ff} \tan \phi'$.
 - Defines $FS(ESA) = s_d/\tau_m = \tan \phi' / \tan \phi'_m$.
 - Therefore inherently assumes a *drained* failure corresponding to the CD case.
 - Would be better described as a drained strength analysis.
2. A so-called undrained strength analysis (USA) that:
 - Treats the in situ effective stresses as equal to consolidation stresses.
 - Uses these consolidation stresses to compute the available undrained strength within the foundation.
 - Defines $FS(USA) = c_u/\tau_m$.
 - Therefore inherently assumes an *undrained* failure corresponding to the CU case.

Section 3 presents a conceptual comparison of ESA and USA factors of safety (Fig. 3) and detailed results from three case histories (Table 3 and Figs. 4–11), which show FS(ESA)/FS(USA) ratios of about two. Although the undrained strength analyses (USA) involved simplifying assumptions that tend to err on the safe side, the writer concludes that conventional effective stress analyses (ESA) based on realistic strength parameters (c' and ϕ') and measured pore pressures can give highly misleading and unsafe estimates of actual factors of safety for staged construction. This results from the inherent ESA assumption of a drained, rather than an undrained, failure. Janbu's "undrained effective stress" approach to stability analyses has the same inherent problem (Section 6.3).

Methodology for Undrained Strength Analyses

Undrained strength analyses (USA) require estimates of the initial in situ undrained shear strength (c_u) of the cohesive foundation soils and subsequent increases in c_u during staged construction. The recommended approach for doing this evolved during the past 20 years from the important recognition of the close correlation between the in situ undrained strength ratio (c_u/σ'_{vc}) and the overconsolidation ratio ($OCR = \sigma'_p/\sigma'_{vc}$) of cohesive soils and with the development of new laboratory strength testing procedures. The latter use K_0 consolidated-undrained (CK_0U) tests to minimize the adverse effects of sample disturbance and to evaluate stress-strain-strength anisotropy.

The recommended approach has four basic components:

1. Establish the initial stress history of the deposit (profiles of σ'_{v0} and σ'_p), which requires high-quality laboratory oedometer tests, supplemented by in situ testing to help assess spatial variability.
2. Establish changes in the vertical stress history during staged construction via consolidation analyses for design and piezometers during construction.
3. Develop c_u/σ'_{vc} versus OCR relationships for the foundation soils as described herein.
4. Use these relationships and the stress history profiles from the first and second components to compute c_u values for USA.

There are three levels of sophistication to obtain c_u/σ'_{vc} versus OCR relationships:

- Level A— CK_0U compression, direct simple shear, and extension tests using either the Recompression (Bjerrum 1973) or the SHANSEP (Ladd and Foott 1974) recompression technique and treated for *strain compatibility* (Section 4.9). This level enables anisotropic stability analyses, i.e., with c_u/σ'_{vc} varying with inclination of the failure surface.
- Level B— CK_0U direct simple shear tests using SHANSEP.
- Level C—Use $c_u/\sigma'_{vc} = S(OCR)^m$, with values of S and m obtained from correlations presented in Section 5.3. For example, $S = 0.22 \pm 0.03$ for homogeneous sedimentary clays plotting above Casagrande's A-line; $S = 0.25 \pm 0.05$ for silts and organic clays plotting below the A-line; and $m = 0.88(1 - C_s/C_c)$, where C_s and C_c equal the slope of the swelling and virgin compression lines, respectively.

The recommended USA methodology simplifies the real problem by only considering changes in vertical consolidation stress (σ'_{vc}) and by using c_u/σ'_{vc}

ratios obtained from CK_0U test data. The resultant errors, which should be on the safe side, can be reduced by the special direct simple shear testing described in Section 4.11.

The recommended USA methodology differs significantly from that developed for staged construction by Arthur Casagrande in the 1940s. This so called *QRS* approach uses *UU* and *CIU* triaxial compression test data in an empirical manner such that its accuracy depends on compensating errors that are difficult to quantify (Section 6.2).

Monitoring Field Performance

Section 7 summarizes the advantages of using the *observational method* (Peck 1969) during staged construction and recommendations for successful field instrumentation. It suggests new techniques for backcalculating field c_h values for projects with vertical drains and describes how *brittle* versus *ductile* stress-strain characteristics of the foundation soil affect the use of field instrumentation to warn of impending failures. Correlations between horizontal displacements and vertical settlements can be used to evaluate the relative importance of undrained versus drained deformations within embankment foundations.

Research Needs

Current capabilities for assessing foundation stability make simplifying assumptions and entail an artificial separation of stress distribution-consolidation analyses on the one hand and limiting equilibrium analyses on the other. The availability of a realistic *generalized soil model* for use in numerical analyses would provide a more rational approach. Such analyses could also clarify the effects of partial drainage during loading and of contained plastic flow during consolidation on pore pressures and deformations within clay foundations. While constitutive relationships capable of modeling soil behavioral features such as anisotropy and strain softening have recently been developed, other important aspects such as "rate effects" are still poorly understood.

9. ACKNOWLEDGMENTS

The ESA-USA stability comparisons for the three case histories were made possible by the support of the Massachusetts Department of Public Works and the U.S. Federal Highway Administration for the varved clay site; the Société d'Énergie de la Baie James (SEBJ) of Montreal, Canada for the James Bay site; and Bromwell and Carrier, Inc. for the tailings dam. Key persons who helped with analyses, other than those cited in the references, include L. G. Bromwell, S. M. Lacasse, and J.-J. Pare. The field performance data presented in Section 7 were obtained for Haley and Aldrich, Inc., geotechnical consultant for the project. J. P. Gould kindly provided background material on the early work by A. Casagrande leading to the *QRS* methodology; W. F. Marcuson III and L. McAnear did likewise regarding its use by the U.S. Army Corps of Engineers. The writer is indebted to a former doctoral student, Don J. DeGroot, for pertinent references and help in developing soil behavior correlations. Detailed comments on the first (1988) draft by L. G. Bromwell, J. Dunnycliff, M. Jamiolkowski, S. M. Lacasse,

G. Mesri, and S. G. Vick are greatly appreciated; and likewise for J. T. Christian on the final version.

10. APPENDIX I. REFERENCES

- Arthur, J. R. F., Bekenstein, S., Germaine, J. T., and Ladd, C. C. (1981). "Stress path tests with controlled rotation of principal stress directions." *Symp. on Laboratory Shear Strength of Soil*, ASTM, STP 740, 516–540.
- Asaoka, A. (1978). "Observational procedure of settlement prediction." *Soils and Foundations*, Japan, 18(4), 87–101.
- Azzouz, A. S., Baligh, M. M., and Ladd, C. C. (1981). "Three-dimensional stability analysis of four embankment failures." *Proc. 10th Int. Conference on Soil Mech. and Found. Engrg.*, Stockholm, Sweden, 3, 343–346.
- Azzouz, A. S., Baligh, M. M., and Ladd, C. C. (1983). "Corrected field vane strength for embankment design." *J. Geotech. Engrg.*, ASCE, 109(5), 730–734.
- Baligh, M. M. (1985). "Strain path method." *J. Geotech. Engrg.*, ASCE, 111(9), 1108–1136.
- Baligh, M. M. (1986a). "Undrained deep penetration, I: Shear stresses." *Geotechnique*, London, England, 36(4), 471–485.
- Baligh, M. M. (1986b). "Undrained deep penetration, II: Pore pressures." *Geotechnique*, London, England, 36(4), 487–501.
- Baligh, M. M., Azzouz, A. S., and Chin, C.-T. (1987). "Disturbance due to 'ideal' tube sampling." *J. Geotech. Engrg.*, ASCE, 113(7), 739–757.
- Barron, R. A. (1948). "Consolidation of fine-grained soils by drain wells." *Trans.*, ASCE, 113, 718–754.
- Barron, R. A. (1964). Discussion of "Stability coefficients for earth slopes," by A. W. Bishop and N. R. Morgenstern. *Geotechnique*, London, England, 14(4), 360–361.
- Becker, D. E., Crooks, J. H. A., Been, K., and Jefferies, M. G. (1987). "Work as a criterion for determining in situ and yield stresses in clays." *Canadian Geotech. J.*, 24(4), 549–564.
- Berre, T., and Bjerrum, L. (1973). "Shear strength of normally consolidated clays." *Proc. 8th Int. Conference on Soil Mech. and Found. Engrg.*, Moscow, U.S.S.R., 1.1, 39–49.
- Bishop, A. W. (1955). "The use of the slip circle in the stability analysis of slopes." *Geotechnique*, London, England, 5(1), 7–17.
- Bishop, A. W., and Bjerrum, L. (1960). "The relevance of the triaxial test to the solution of stability problems." *Proc. Res. Conference on Shear Strength of Cohesive Soils*, ASCE, 437–501.
- Bjerrum, L. (1972). "Embankments on soft ground: SOA Report." *Proc. Speciality Conference on Performance of Earth and Earth-Supported Structures*, ASCE, 2, 1–54.
- Bjerrum, L. (1973). "Problems of soil mechanics and construction on soft clays: SOA Report." *Proc. 8th Int. Conference on Soil Mech. and Found. Engrg.*, Moscow, U.S.S.R., 3, 111–159.
- Bjerrum, L., and Landva, A. (1966). "Direct simple shear tests on a Norwegian quick clay." *Geotechnique*, London, England, 16(1), 1–20.
- Brinch-Hansen, J. (1962). "Relationship between stability analyses with total and effective stress." *Sols-Soils*, (3), 28–41.
- Brinch-Hansen, J., and Gibson, R. E. (1949). "Undrained shear strengths of anisotropically consolidated clays." *Geotechnique*, London, England, 1(3), 189–204.
- Bromwell, L. G. (1984). "Consolidation of mining wastes." *Proc. Symp. on Sedimentation-Consolidation Models: Predictions and Validation*, ASCE, 275–295.
- Campanella, R. G., and Robertson, P. K. (1988). "Current status of the piezocone test." *Proc. 1st Int. Symp. on Penetration Testing*, A. A. Balkema Publishing, 1, 93–116.
- Casagrande, A. (1936). "The determination of the pre-consolidation load and its practical significance." *Proc. 1st Int. Conference on Soil Mech. and Found. Engrg.*, Cambridge, Mass., 3, 60–64.

- Casagrande, A., and Wilson, S. D. (1960). "Testing equipment, techniques and errors: Moderators' Report, Session 2," *Proc. Res. Conference on Shear Strength of Cohesive Soils*, ASCE, 1123-1130.
- Chandler, R. J. (1988). "The in-situ measurement of the undrained shear strength of clays using the field vane: SOA paper." *Vane Shear Strength Testing in Soils: Field and Laboratory Studies*, ASTM, STP 1014, 13-44.
- Consolidation of soils: Testing and evaluation.* (1986). *ASTM STP 892*, R. N. Yong and F. C. Townsend, eds., ASTM.
- D'Appolonia, D. J., Lambe, T. W., and Poulos, H. G. (1971). "Evaluation of pore pressures beneath an embankment." *J. Soil Mech. and Found. Div.*, ASCE, 97(6), 881-897.
- Dasal, O., Tournier, J. P., Tavenas, F., and LaRochelle, P. (1972). "Failure of a test embankment on sensitive clay." *Proc. Specialty Conference on Performance of Earth and Earth-Supported Structures: Part 1*, ASCE, 1, 129-158.
- "Design and construction of levees." (1978). U.S. Army Corps of Engineers, *Engineer Manual EM 1110-2-1913*, Office of the Chief of Engineers, Washington, D.C.
- Dunnicliff, J. (1988). *Geotechnical instrumentation for monitoring field performance*. John Wiley and Sons, Inc., New York, N.Y.
- Folkes, D. J., and Crooks, J. H. A. (1985). "Effective stress paths and yielding in soft clays below embankments." *Canadian Geotech. J.*, 22(3), 357-374.
- Foott, R., and Ladd, C. C. (1977). "Behaviour of Atchafalaya levees during construction." *Geotechnique*, London, England, 27(2), 137-160.
- Foott, R., and Ladd, C. C. (1981). "Undrained settlement of plastic and organic clays." *J. Geotech. Engrg. Div.*, ASCE, 107(8), 1079-1094.
- Fredlund, D. G., and Krahn, J. (1977). "Comparison of slope stability methods of analysis." *Canadian Geotech. J.*, 14(3), 429-439.
- Germaine, J. T. (1982). "Development of the directional shear cell for measuring cross-anisotropic clay properties," thesis presented to the Massachusetts Institute of Technology, at Cambridge, Massachusetts, in partial fulfillment of the requirements for the degree of Doctor of Science.
- Germaine, J. T., and Ladd, C. C. (1988). "Triaxial testing of saturated cohesive soils: SOA paper." *Advanced Triaxial Testing of Soil and Rock*, ASTM STP 977, 421-459.
- Hight, D. W., Gens, A., and Symes, M. J. (1983). "The development of a new hollow cylinder apparatus for investigating the effects of principal stress rotation in soils." *Geotechnique*, London, England, 33(4), 355-384.
- Hoeg, K., Andersland, O. B., and Rolfsen, E. N. (1969). "Undrained behaviour of quick clay under load tests at Asrum." *Geotechnique*, London, England, 19(1), 101-115.
- Holtz, R. D., Jamiolkowski, M. B., and Lancellotta, R. (1986). "Lessons from oedometer tests on high quality samples." *J. Geotech. Engrg.*, ASCE, 112(8), 768-776.
- Jamiolkowski, M., Ladd, C. C., Germaine, J. T., and Lancellotta, R. (1985). "New developments in field and laboratory testing of soils: Theme Lecture 2." *Proc. 11th Int. Conference on Soil Mech. and Found. Engrg.*, San Francisco, 1, 57-153.
- Jamiolkowski, M., Lancellotta, R., and Wolski, W. (1983). "Precompression and speeding up consolidation: General report speciality session 6." *Proc. 8th European Conference on Soil Mech. and Found. Engrg.*, Helsinki, 3, 1201-1226.
- Janbu, N. (1973). "Slope stability computations." *Embankment-dam engineering*, R. C. Hirschfeld and S. Poulos, eds., John Wiley and Sons, New York, N.Y., 47-86.
- Janbu, N. (1977). "Slopes and excavations in normally and lightly overconsolidated clays: SOA Report." *Proc. 9th Int. Conference on Soil Mech. and Found. Engrg.*, Tokyo, 2, 549-566.
- Janbu, N. (1979). "Design analysis for gravity platform foundations." *Proc. 2nd Int. Conference on Behaviour of Offshore Structures*, London, 1, 407-426.
- Jeyapalan, J. K., Duncan, J. M., and Seed, H. B. (1983). "Analysis of flow failures

- of mine tailings dams." *J. Geotech. Engrg.*, ASCE, 109(2), 150-171.
- Johnson, S. J. (1970). "Foundation precompression with vertical sand drains." *J. Soil Mech. and Foundations Div.*, ASCE, 96(1), 145-175.
- Johnson, S. J. (1974). "Analysis and design relating to embankments." *Proc. Conference on Analysis and Design in Geotech. Engrg.*, ASCE, 2, 1-48.
- Koutsoftas, D. C., and Ladd, C. C. (1985). "Design strengths for an offshore clay." *J. Geotech. Engrg.*, ASCE, 111(3), 337-355.
- Lacasse, S. M. (1979). "Effect of load duration on undrained behavior of clay and sand-literature survey." *Internal Report 40007-1*, Norwegian Geotech. Inst.
- Lacasse, S., and Berre, T. (1988). "Triaxial testing methods for soils: SOA paper." *Advanced Triaxial Testing of Soil and Rock*, ASTM STP 977, 264-289.
- Lacasse, S., Berre, T., and Lefebvre, G. (1985). "Block sampling of sensitive clays." *Proc. 11th Int. Conference on Soil Mech. and Found. Engrg.*, 2, 887-892.
- Lacasse, S., and Lunne, T. (1988). "Calibration of dilatometer correlations." *Proc. 1st Int. Symp. on Penetration Testing*, Orlando, A. A. Balkema Publishing, 1, 539-548.
- Ladd, C. C. (1972). "Test embankment on sensitive clay." *Proc. Speciality Conference on Performance of Earth and Earth-Supported Structures: Part 1*, ASCE, 1, 101-128.
- Ladd, C. C. (1975). "Foundation design of embankments constructed on Connecticut Valley varved clays." *Research Report R75-7*, Dept. of Civil Engrg., MIT, Cambridge, MA, 439 p.
- Ladd, C. C. (1987a). "Use of precompression and vertical drains for stabilization of foundation soils." *GeoConsult lecture series on soft ground construction*, GeoConsult, San Juan, Puerto Rico.
- Ladd, C. C. (1987b). "Characteristics and engineering properties of Northeastern varved clays." *Notes for Foundations and Soil Mechanics Group*, Metropolitan Section of ASCE, New York, N.Y.
- Ladd, C. C. (1991). "Effects of disturbance on the performance of vertical drains." *J. Geotech. Engrg.*, ASCE (In preparation).
- Ladd, C. C., Aldrich, H. P., and Johnson, E. G. (1969). "Embankment failure on organic clay." *Proc. 7th Int. Conference on Soil Mech. and Found. Engrg.*, Mexico City, 2, 627-634.
- Ladd, C. C., Dascal, O., Law, K. T., Lefebvre, G., Lessard, G., Mesri, G., and Tavenas, F. (1983). "Report of the embankment stability subcommittee." *Committee of Specialists on Sensitive Clays on the NBR Complex*, SEBJ, Montréal, Canada, Annexe II.
- Ladd, C. C., and Edgers, L. (1972). "Consolidated-undrained direct simple shear tests on saturated clays." *Research Report R72-82*, Dept. of Civ. Engrg., MIT, Cambridge, Mass.
- Ladd, C. C., and Foott, R. (1974). "New design procedure for stability of soft clays." *J. Geotech. Engrg. Div.*, ASCE, 100(7), 763-786.
- Ladd, C. C., and Foott, R. (1977). "Foundation design of embankments constructed on varved clays." *FHWA TS-77-214*, U.S. Dept. of Transp., Washington, D.C.
- Ladd, C. C., Foott, R., Ishihara, K., Schlosser, F., and Poulos, H. G. (1977). "Stress-deformation and strength characteristics: SOA report." *Proc. 9th Int. Conference on Soil Mech. and Found. Engrg.*, 2, 421-494.
- Ladd, C. C., Rixner, J. J., and Gifford, D. C. (1972). "Performance of embankments with sand drains on sensitive clay." *Proc. Speciality Conference on Performance of Earth and Earth-Supported Structures: Part 1*, ASCE, 1, 211-242.
- Lambe, T. W. (1973). "Predictions in soil engineering: 13th Rankine Lecture." *Geotechnique*, London, England, 23(2), 149-202.
- Lambe, T. W., and Whitman, R. V. (1969). *Soil mechanics*. 1st Ed., John Wiley and Sons, Inc., New York, N.Y.
- LaRochele, P., Sarrailh, J., Tavenas, F., Roy, M., and Leroueil, S. (1981). "Causes of sampling disturbance and design of a new sampler for sensitive soils." *Canadian Geotech. J.*, 18(1), 52-66.
- LaRochele, P., Trak, B., Tavenas, F., and Roy, M. (1974). "Failure of a test em-

- bankment on a sensitive Champlain clay deposit." *Canadian Geotech. J.*, 11(1), 142–164.
- Larsson, R. (1980). "Undrained shear strength in stability calculation of embankments and foundations on soft clays." *Canadian Geotech. J.*, 17(4), 591–602.
- Lefebvre, G., Ladd, C. C., Mesri, G., and Tavenas, F. (1983). "Report of the testing subcommittee." *Committee of Specialists on Sensitive Clays on the NBR Complex*, SEBJ, Montréal, Canada, Annexe I.
- Lefebvre, G., Ladd, C. C., and Pare, J.-J. (1988). "Comparison of field vane and laboratory undrained shear strengths in soft sensitive clays." *Vane Shear Strength Testing in Soils: Field and Laboratory Studies*, ASTM STP 1014, 233–246.
- Lefebvre, G., and LeBoeuf, D. (1987). "Rate effects and cyclic loading of sensitive clays." *J. Geotech. Engrg.*, ASCE, 113(5), 476–489.
- Lefebvre, G., and Poulin, C. (1979). "A new method of sampling in sensitive clay." *Canadian Geotech. J.*, 16(1), 226–233.
- Leroueil, S. (1988). "Tenth Canadian Geotechnical Colloquium: Recent developments in consolidation of natural clays." *Canadian Geotech. J.*, 25(1), 85–107.
- Leroueil, S., Kabbaj, M., Tavenas, F., and Bouchard, R. (1985). "Stress-strain-strain rate relation for the compressibility of sensitive natural clays." *Geotechnique*, London, England, 35(2), 159–180.
- Leroueil, S., Tavenas, F., Mieussens, C., and Peignaud, M. (1978). "Construction pore pressures in clay foundations under embankments. Part II: Generalized behaviour." *Canadian Geotech. J.*, 15(1), 66–82.
- Levadoux, J.-N., and Baligh, M. M. (1986). "Consolidation after undrained piezocone penetration, I: prediction." *J. Geotech. Engrg.*, ASCE, 112(7), 707–728.
- Lobdell, H. L. (1959). "Rate of constructing embankments on soft foundation soils." *J. Soil Mech. and Found. Div.*, ASCE, 85(5), 61–76.
- Lowe, J., III, (1967). "Stability analysis of embankments." *J. Soil Mech. and Found. Div.*, ASCE, 93(4), 1–33.
- Lowe, J., III, Jonas, E., and Obrician, V. (1969). "Controlled gradient consolidation test." *J. Soil Mech. and Found. Div.*, ASCE, 95(1), 77–97.
- Marchetti, S. (1980). "In situ tests by flat dilatometer." *J. Geotech. Engrg. Div.*, ASCE, 106(3), 299–321.
- Mayne, P. W. (1980). "Cam-clay predictions of undrained strength." *J. Geotech. Engrg. Div.*, ASCE, 106(11), 1219–1242.
- Mayne, P. W., and Kulhawy, F. H. (1982). " K_0 -OCR relationships in soil." *J. Geotech. Engrg. Div.*, ASCE, 108(6), 851–872.
- Mesri, G. (1975). Discussion of "New design procedure for stability of soft clays," by C. C. Ladd and R. Foott. *J. Geotech. Engrg. Div.*, ASCE, 101(4), 409–412.
- Mesri, G. (1985). "Discussion, Session 2 on laboratory testing-new procedures and data acquisition techniques." *Proc. 11th Inter. Conf. on Soil Mech. and Foundation Engrg.*, San Francisco, 5, 2689–2690.
- Mesri, G., and Castro, A. (1987). " $C\alpha/C_c$ concept and K_0 during secondary compression." *J. Geotech. Engrg.*, ASCE, 113(3), 230–247.
- Mesri, G., and Choi, Y. K. (1981). Discussion of "The behaviour of embankments on clay foundations," by F. Tavenas and S. Leroueil. *Canadian Geotech. J.*, 18(3), 460–462.
- Mesri, G., and Choi, Y. K. (1985a). "Settlement analysis of embankments on soft clays." *J. Geotech. Engrg.*, ASCE, 111(4), 441–464.
- Mesri, G., and Choi, Y. K. (1985b). "The uniqueness of the end-of-primary (EOP) void ratio-effective stress relationship." *Proc. 11th Int. Conference on Soil Mech. and Found. Engrg.*, 2, 587–590.
- Mitchell, J. K. (1981). "Soil improvement: SOA report." *Proc. 10th Int. Conference on Soil Mech. and Found. Engrg.*, 4, 509–565.
- Moore, P. J. (1970). "The factor of safety against undrained failure of a slope." *Soils and Foundations*, Japan, 10(3), 81–91.
- Morgenstern, N. R. (1985). "Geotechnical aspects of environmental control: Theme Lecture 3." *Proc. 11th Int. Conference on Soil Mech. and Found. Engrg.*, San Francisco, 1, 155–185.
- Morgenstern, N. R., and Price, V. E. (1965). "An analysis of the stability of general

- slip surfaces." *Geotechnique*, London, England, 15(1), 79–93.
- Murray, R., and Symons, I. F. (1984). "Settlement and stability of embankments on soft subsoils." *Ground movements and their effects on structures*, Surrey University Press, 321–352.
- Orleach, P. (1983). "Techniques to evaluate the field performance of vertical drains," thesis presented to the Massachusetts Institute of Technology, at Cambridge, Massachusetts, in partial fulfillment of the requirements for the degree of Master of Science.
- Parry, R. H. G. (1972). "Stability analysis for low embankments on soft clays." *Proc. Roscoe Memorial Symp. on Stress-Strain Behaviour of Soils*, Cambridge, Univ., Cambridge, England, 643–668.
- Peck, R. B. (1969). "Advantages and limitations of the observational method in applied soil mechanics: 9th Rankine Lecture." *Geotechnique*, London, England, 19(2), 171–187.
- Peck, R. B. (1973). "Discussion in Main Session 4." *Proc. 8th Int. Conference on Soil Mech. and Found. Engrg.*, Moscow, U.S.S.R., 4.2, 99–100.
- Peck, R. B. (1988). Foreword to *Geotechnical instrumentation for monitoring field performance*, by J. Dunncliff. John Wiley and Sons, Inc., New York, N.Y., vii–ix.
- Peck, R. B., Hanson, W. E., and Thornburn, T. H. (1974). *Foundation engineering*. John Wiley and Sons, Inc., New York, N.Y.
- Peck, R. B., and Lowe, J., III, (1960). "Shear strength of undisturbed cohesive soils: Moderators' report, session 4." *Proc. Res. Conference on Shear Strength of Cohesive Soils*, ASCE, Boulder, 1137–1140.
- Pelletier, J. H., Olson, R. E., and Rixner, J. J. (1979). "Estimation of consolidation properties of clay from field observations." *Geotech. Testing J.*, 2(1), 34–43.
- Pilot, G., Trak, B., and LaRoche, P. (1982). "Effective stress analysis of the stability of embankments on soft soils." *Canadian Geotech. J.*, 19(4), 433–450.
- "Placement and improvement of soils: Committee Reports." (1987). *Soil improvement—A ten year update*, J. S. Welsh, ed., ASCE, GSP No. 12, 1–135.
- Rivard, P. J., and Lu, Y. (1978). "Shear strength of soft fissured clays." *Canadian Geotech. J.*, 15(3), 382–390.
- Rixner, J. J., Kraemer, S. R., and Smith, A. D. (1986). "Prefabricated vertical drains, Vol. I, engineering guidelines." *FHWA/RD-86/168*, Federal Highway Admin., Washington, D.C.
- Roscoe, K. H., and Burland, J. B. (1968). "On the generalized stress-strain behaviour of 'wet' clay." *Engineering plasticity*, Cambridge University Press, Cambridge, England, 535–609.
- Rutledge, P. C. (1947). "Review of the cooperative triaxial shear research program of the Corps of Engineers." *Soil Mechanics Fact Finding Survey, Progress Report*, U.S. Waterways Experiment Station, Vicksburg, Miss., 1–178.
- Saada, A. S., and Townsend, F. C. (1981). "State-of-the-art: Laboratory strength testing of soils." *Symp. on Lab. Shear Strength of Soil*, ASTM STP 740, 7–77.
- Sambhandharaksa, S. (1977). "Stress-strain-strength anisotropy of varved clays," thesis presented to the Massachusetts Institute of Technology, at Cambridge, Massachusetts, in partial fulfillment of the requirements for the degree of Doctor of Science.
- Schiffman, R. L., Vick, S. G., and Gibson, R. E. (1988). "Behavior and properties of hydraulic fills." *Proc. Specialty Conference on Hydr. Fill Structures*, ASCE, GSP No. 21, 166–202.
- Schmertmann, J. H. (1955). "The undisturbed consolidation of clay." *Trans.*, ASCE, 120, 1201–1233.
- Schmertmann, J. H. (1975). "Discussion on measurement of in situ shear strength." *Proc. Specialty Conference on In Situ Measurement of Soil Properties*, ASCE, 2, 175–179.
- Schmertmann, J. H. (1986). "Suggested method for performing the flat dilatometer test." *Geotech. Testing J.*, ASTM, 9(2), 93–101.
- Sedimentation consolidation models: Predictions and validation.* (1984). R. N. Yong and F. C. Townsend, eds., ASCE.
- Simon, R. M., Christian, J. T., and Ladd, C. C. (1974). "Analysis of undrained

- behavior of loads on clay." *Proc. Conference on Analysis and Design in Geotech. Engrg.*, ASCE, 1, 51–84.
- Simons, N. E. (1976). "Field studies of the stability of embankments on clay foundations." *Laurits Bjerrum Memorial Volume*, Norwegian Geotechnical Institute, Oslo, 183–209.
- Skempton, A. W. (1948a). "The $\phi = 0$ analysis for stability and its theoretical basis." *Proc. 2nd Int. Conference on Soil Mech. and Found. Engrg.*, Rotterdam, 1, 72–78.
- Skempton, A. W. (1948b). "A study of the immediate triaxial test on cohesive soils." *Proc. 2nd Int. Conference on Soil Mech. and Found. Engrg.*, Rotterdam, 1, 192–196.
- Skempton, A. W. (1948c). "A study of the geotechnical properties of some post-glacial clays." *Geotechnique*, London, England, 1(1), 7–22.
- "Slope stability and protection." (1982). *Design Manual 7.1: Soil mechanics*, Naval Facilities Engrg. Command, Dept. of the Navy, Washington, D.C., Table 2, 7.1–312.
- Smith, R. E., and Wahls, H. E. (1969). "Consolidation under constant rates of strain." *J. Soil Mech. and Found. Div.*, ASCE, 95(2), 519–539.
- Spencer, E. (1967). "A method of analysis of the stability of embankments assuming parallel inter-slice forces." *Geotechnique*, 17(1), 11–26.
- "Stability analysis." (1971). *Design manual 7: Soil mechanics, foundations, and earth structures*, Chapter 7, Naval Facilities Engrg. Command, Dept. of the Navy, Washington, D.C.
- "Stability of earth and rock fill dams." (1970). U.S. Army Corps of Engineers, *Engineer Manual EM 1110-2-1902*, Office of the Chief of Engineers, Washington, D.C.
- Stauffer, P. A., and Obermeyer, J. R. (1988). "Pore water pressure conditions in tailings dams." *Proc. Speciality Conference on Hydr. Fill Structures*, ASCE, GSP No. 21, 924–939.
- Svano, G. (1981). "Undrained effective stress analyses," thesis presented to the Norwegian Institute of Technology, at Trondheim, Norway, in partial fulfillment of the requirements for the degree of Doctor of Engineering.
- Tavenas, F., Blanchet, R., Garneau, R., and Leroueil, S. (1978). "The stability of stage-constructed embankments on soft clays." *Canadian Geotech. J.*, 15(2), 283–305.
- Tavenas, F., Leblond, P., Jean, P., and Leroueil, S. (1983). "The permeability of natural soft clays, Part I: Methods of laboratory measurement." *Canadian Geotech. J.*, 20(4), 629–644.
- Tavenas, F., and Leroueil, S. (1980). "The behaviour of embankments on clay foundations." *Canadian Geotech. J.*, 17(2), 236–260.
- Tavenas, F., and Leroueil, S. (1985). Discussion of "New developments in field and laboratory testing of soils," by Jamiolkowski et al., *Proc. 11th Int. Conference on Soil Mech. and Found. Engrg.*, San Francisco, 5, 2693–2694.
- Tavenas, F., Mieussens, C., and Bourges, F. (1979). "Lateral displacements in clay foundations under embankments." *Canadian Geotech. J.*, 16(3), 532–550.
- Terzaghi, K. (1936). "The shearing resistance of saturated soils and the angle between the planes of shear." *Proc. 1st Int. Conference on Soils Mech. and Found. Engrg.*, Cambridge, Mass., 1, 54–56.
- Terzaghi, K., and Peck, R. B. (1967). *Soil Mechanics in Engineering Practice*. 2nd Ed., John Wiley and Sons, Inc., New York, N.Y.
- Vaid, Y. P., and Campanella, R. G. (1974). "Triaxial and plane strain behavior of natural clay." *J. Geotech. Engrg. Div.*, ASCE, 100(3), 207–224.
- Vaughan, P. R. (1972). "Undrained failure of clay embankments." *Proc. Roscoe Memorial Symp. on Stress-Strain Behaviour of Soils*, Cambridge Univ., 683–691.
- Vick, S. G. (1983). *Planning, Design and Analysis of Tailings Dams*. John Wiley and Sons, Inc., New York, N.Y.
- Whitman, R. V. (1984). "Evaluating calculated risk in geotechnical engineering: 17th Terzaghi Lecture." *J. Geotech. Engrg.*, ASCE, 110(2), 145–188.
- Whittle, A. J. (1987). "A constitutive model for overconsolidated clays with appli-

- cation to the cyclic loading of friction piles," thesis presented to the Massachusetts Institute of Technology, at Cambridge, Massachusetts, in partial fulfillment of the requirements for the degree of Doctor of Science.
- Whittle, A. J. (1991). "Evaluation of a model for predicting the behaviour of over-consolidated clays." *Geotechnique*, London, England (in Press).
- Wissa, A. E. Z., Christian, J. T., Davis, E. H., and Heiberg, S. (1971). "Consolidation at constant rate of strain." *J. Soil Mech. and Found. Div.*, ASCE, 97(10), 1393-1413.
- Wroth, C. P., and Houlsby, G. T. (1985). "Soil mechanics-property characterization and analysis procedures: Theme Lecture 1." *Proc. 11th Int. Conference on Soil Mech. and Found. Engrg.*, San Francisco, 1, 1-55.

11. APPENDIX II. NOTATION

The following symbols are used in this paper:

- b = $(\sigma_2 - \sigma_3)/(\sigma_1 - \sigma_3)$;
- C = compression;
- CD = consolidated-drained;
- CIU = isotropically consolidated-undrained shear test;
- CIUC = isotropically consolidated-undrained TC test;
- CK₀U = K_0 consolidated-undrained shear test;
- CU = consolidated-undrained;
- c' = cohesion intercept in terms of effective stress;
- c_h = coefficient of consolidation for horizontal drainage;
- c_u = undrained shear strength;
- c_v = coefficient of consolidation for vertical drainage;
- DSS = direct simple shear;
- E = extension;
- E_u = undrained Young's modulus;
- ESA = effective stress analysis;
- h = horizontal displacement;
- I_L = liquidity index;
- I_p = plasticity index;
- K_c = ratio of horizontal to vertical consolidation stress;
- K_0 = coefficient of earth pressure at rest;
- m = strength rebound exponent;
- PSC = plane-strain compression;
- PSE = plane-strain extension;
- QRS = Casagrande's notation for UU, CU, and CD shear tests;
- q = $0.5(\sigma_v - \sigma_h)$ or $0.5(\sigma_1 - \sigma_3)$;
- q_f = q at failure;
- S = undrained strength ratio at OCR = 1;
- S_t = sensitivity = s_u (undisturbed)/ s_u (remolded);
- SD = standard deviation;
- s = vertical settlement;
- s_d = drained shear strength;
- s_u = undrained shear strength from UU-type tests;
- TC = triaxial compression;
- TE = triaxial extension;
- TSA = total stress analysis;
- \bar{U} = average degree of consolidation;
- USA = undrained strength analysis;

UU	=	unconsolidated-undrained;
UUC	=	UU triaxial compression test;
u	=	pore (water) pressure;
u_e	=	excess pore pressure;
u_s	=	shear induced pore pressure;
w_L	=	liquid limit;
w_N	=	natural water content;
w_p	=	plastic limit;
δ	=	angle between direction of σ_{1f} and vertical;
γ	=	shear strain;
γ_f	=	shear strain at failure;
γ_t	=	total unit weight;
μ	=	field vane correction factor;
σ'_c	=	isotropic consolidation stress;
σ'_{fc}	=	consolidation stress on failure plane;
σ'_{ff}	=	effective stress on failure plane at failure;
σ'_h	=	horizontal effective stress;
σ'_{hc}	=	horizontal consolidation stress;
σ'_n	=	effective normal stress;
σ'_p	=	preconsolidation pressure;
σ'_v	=	vertical effective stress;
σ'_{vc}	=	vertical consolidation stress;
σ'_{v0}	=	in situ initial vertical effective stress;
$\sigma_1, \sigma_2, \sigma_3$	=	major, intermediate, minor principal stresses;
σ_{1f}	=	major principal stress at failure;
τ	=	shear stress;
τ_{ave}	=	$1/3 \times (\tau_c + \tau_d + \tau_e)$;
τ_c	=	τ for shear in compression;
τ_d	=	τ for shear along horizontal failure surface;
τ_e	=	τ for shear in extension;
τ_{ff}	=	τ on failure plane at failure;
τ_h	=	horizontal τ or τ in DSS test;
τ_{hc}	=	horizontal τ at consolidation;
τ_m	=	mobilized shear stress required for equilibrium;
ϕ	=	friction angle in terms of total stresses;
ϕ_{cu}	=	ϕ from <i>CIUC</i> tests plotted as per Fig. 2;
ϕ'	=	friction angle in terms of effective stresses; and
ϕ'_m	=	mobilized value of ϕ' .

Attachment 8
Additional Information - Response to Comments
August 18, 2021

Additional Information Response to Comments – August 18, 2021

Comment:

TRC has reviewed CTI’s response to comments and the provided paper. CTI’s response clarifies why the undrained soil parameters were used in the drained condition analyses in Attachment B-1 Slope Stability scenarios 8 through 11. CTI states that undrained shear strength parameters used in the analyses are lower than shear strength values under drained conditions. TRC concurs with using the more conservative strength parameters to model the stability of the proposed landfill, and requests that CTI provide the strength envelopes comparing the undrained and drained strengths for the upper clay, middle clay, and lower clay soils referenced in the stability analyses.

Response:

The following figures present the requested information. Additionally, CTI offers the following context to aid in the interpretation of test data and the corresponding strength parameters used in design:

- The depositional environment at WDI is coarse-grained lacustrine deposits that formed at the delta of a glacial outwash watercourse (see Figure 1). Accordingly, the occurrence and properties of the clay layers present at the site vary significantly from place to place across the site. The generalized soil profile that has been used historically at the site to analyze the stability of MC VI-F Cells therefore conservatively assigns strength parameters from a subset of lower strength values assessed from soil borings within and near MC VI-F.

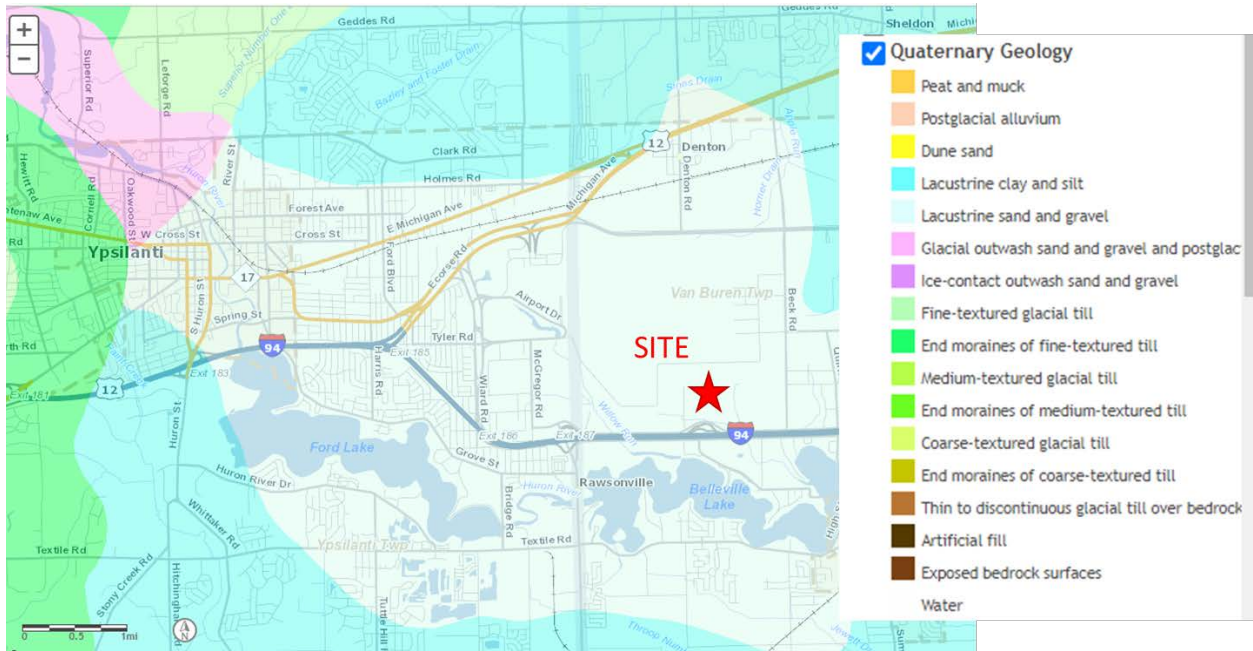


Figure 1. Map of Quaternary Geology at WDI and surrounding area. Source: <http://www.deq.state.mi.us/geowebface/#>.

- Slope stability analyses presented in support of previous permit applications made use of a generalized soil profile that distinguished between upper, middle, and lower clay layers. The basis for this discretization of the soil profile was a series of unconfined compressive strength

tests and hand penetrometer tests used historically to quantify the in-situ soil consistency. CTI has chosen to continue using this generalized profile. Additionally, CTI performed soil borings in winter 2020-2021 to obtain additional samples for laboratory strength testing. As part of this sampling activity, new hand penetrometer measurements were taken. The resulting undrained shear strength profile, aggregated over the entire WDI footprint, is presented in Figure 2. Figure 2 also shows the generalized soil profile for comparison.

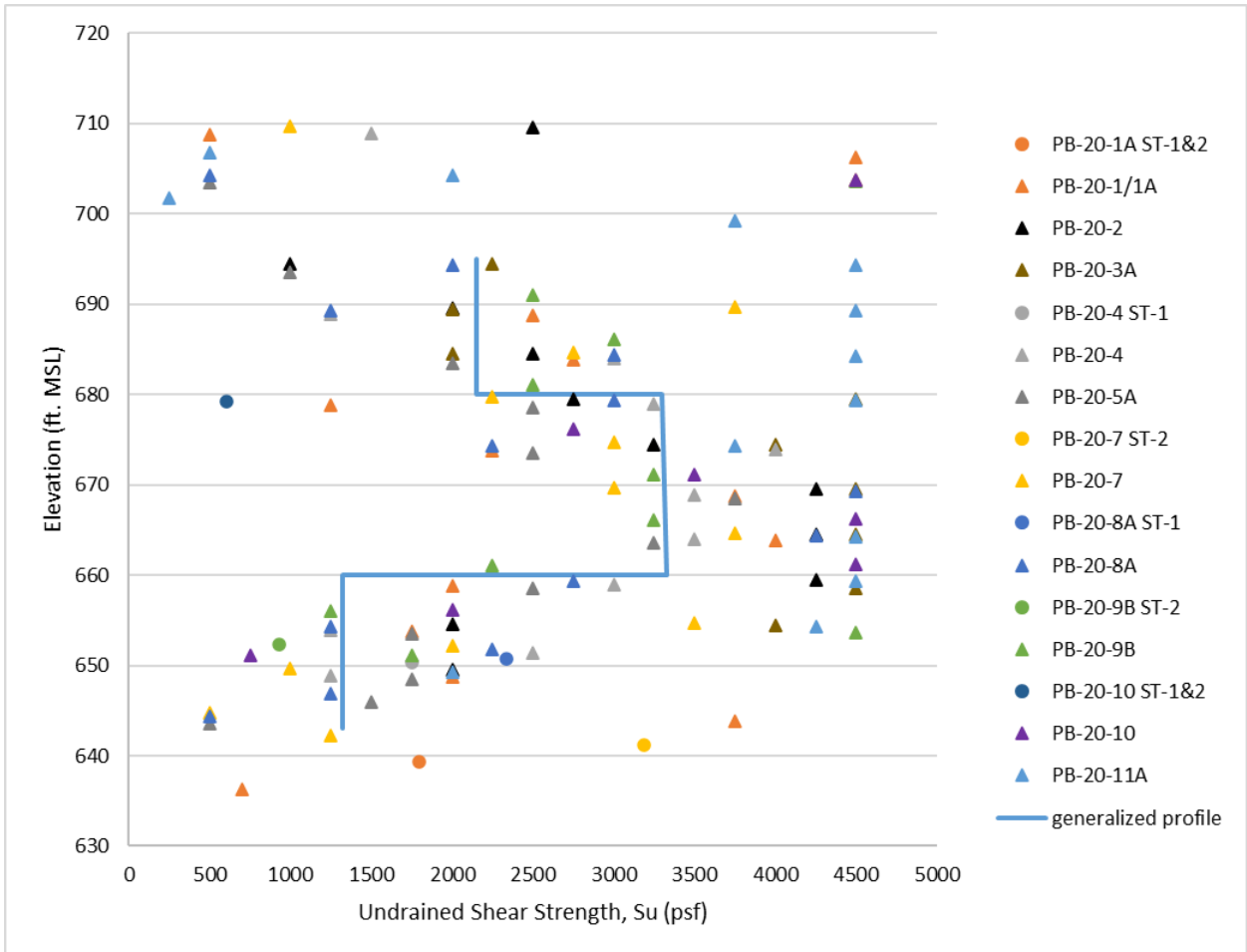


Figure 2. Plot of Undrained Shear Strength Values Estimated from Hand Penetrometer Testing and Consolidated-Undrained Triaxial Testing on Samples from 2020-2021 Soil Borings.

- Previous analyses of the lower soft clay used a undrained shear strength-to-effective vertical stress ratio (s_u/σ'_v) of 0.22 to analyze the stability of the lower clay under different overburden stresses. A ratio of 0.22 was selected from literature values recommending this value for clays with the same Liquid Limit as that measured for clays at WDI. CTI has conservatively continued using this value of s_u/σ'_v . However, recent strength testing, as discussed below, suggests that a higher value may be more representative of the soils on site.

- Consolidated-Undrained Triaxial tests (TX-CU) were performed on Shelby tube samples recovered during the 2020-2021 soil borings. The confining stresses applied during these tests varied over a range of values that represented both pre-construction conditions as well as the vertical overburden pressures anticipated during the life of the site. To allow a direct comparison of shear strength values obtained from the lab to those representative of the state of stress in the ground, the laboratory TX-CU effective confining stresses were converted to an equivalent vertical effective stress using $K_0 = 0.5$, corresponding to a saturated clay. Figure 3 plots the values of shear strength obtained in the TX-CU tests vs. the corresponding vertical effective stress values. Also plotted in Figure 3 are the strength envelopes used for stability analyses of the upper, middle, and lower clay layers assigned from the generalized soil profile.

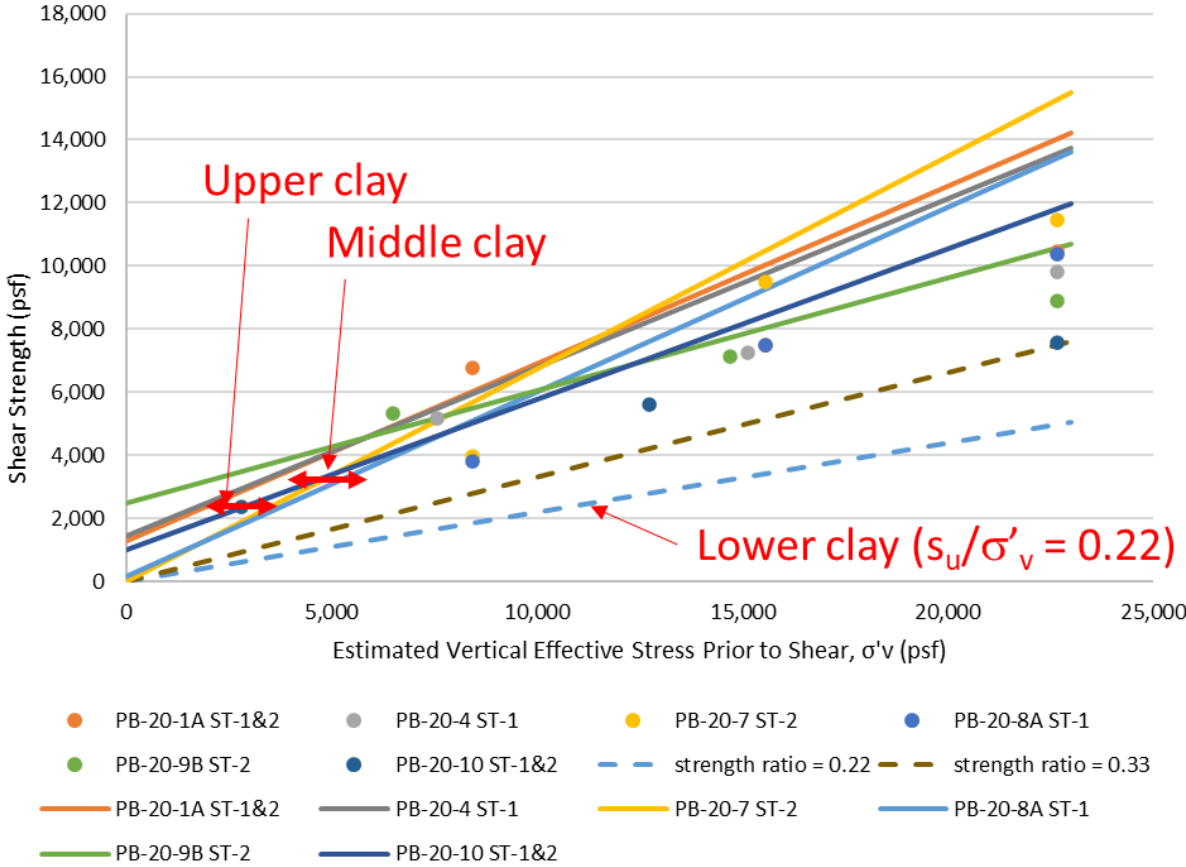


Figure 3. Comparison of Soil Shear Strength Parameters Used for Slope Stability Analysis with Strength Envelopes Obtained from Consolidated-Undrained Triaxial (TX-CU) Testing on Samples from 2020-2021 Soil Borings. Dots indicate individual values of undrained shear strength from TX-CU tests, plotted vs. σ'_v prior to shear. Dashed lines indicate undrained shear strength ratios (0.22 used for analysis, 0.33 suggested by recent testing). Solid Lines show the drained strength envelopes obtained from the same TX-CU tests (shear strength vs. effective stress at failure). Red arrows show constant values of undrained shear strength used for analysis of upper and middle clay layers.